GENOMICS AND EPIGENOMICS OF ALCOHOLISM

EDITED BY: Feng C. Zhou and Kristin Hamre
PUBLISHED IN: Frontiers in Genetics

frontiers Research Topics

frontiers

ISSN 1664-8714
ISBN 978-2-88974-137-3
DOI 10.3389/978-2-88974-137-3

About Frontiers

Frontiers is more than just an open-access publisher of scholarly articles: it is a pioneering approach to the world of academia, radically improving the way scholarly research is managed. The grand vision of Frontiers is a world where all people have an equal opportunity to seek, share and generate knowledge. Frontiers provides immediate and permanent online open access to all its publications, but this alone is not enough to realize our grand goals.

Frontiers Journal Series

The Frontiers Journal Series is a multi-tier and interdisciplinary set of open-access, online journals, promising a paradigm shift from the current review, selection and dissemination processes in academic publishing. All Frontiers journals are driven by researchers for researchers; therefore, they constitute a service to the scholarly community. At the same time, the Frontiers Journal Series operates on a revolutionary invention, the tiered publishing system, initially addressing specific communities of scholars, and gradually climbing up to broader public understanding, thus serving the interests of the lay society, too.

Dedication to Quality

Each Frontiers article is a landmark of the highest quality, thanks to genuinely collaborative interactions between authors and review editors, who include some of the world's best academicians. Research must be certified by peers before entering a stream of knowledge that may eventually reach the public - and shape society; therefore, Frontiers only applies the most rigorous and unbiased reviews.
Frontiers revolutionizes research publishing by freely delivering the most outstanding research, evaluated with no bias from both the academic and social point of view. By applying the most advanced information technologies, Frontiers is catapulting scholarly publishing into a new generation.

What are Frontiers Research Topics?

Frontiers Research Topics are very popular trademarks of the Frontiers Journals Series: they are collections of at least ten articles, all centered on a particular subject. With their unique mix of varied contributions from Original Research to Review Articles, Frontiers Research Topics unify the most influential researchers, the latest key findings and historical advances in a hot research area! Find out more on how to host your own Frontiers Research Topic or contribute to one as an author by contacting the Frontiers Editorial Office: frontiersin.org/about/contact

GENOMICS AND EPIGENOMICS OF ALCOHOLISM

Topic Editors:
Feng C. Zhou, Indiana University Bloomington, United States
Kristin Hamre, University of Tennessee Health Science Center (UTHSC), United States

Citation: Zhou, F. C., Hamre, K., eds. (2022). Genomics and Epigenomics of Alcoholism. Lausanne: Frontiers Media SA. doi: 10.3389/978-2-88974-137-3

Table of Contents

frontiers in Genetics

ORIGINAL RESEARCH
published: 08 February 2018
doi: 10.3389/fgene.2018.00032

Heavy Chronic Intermittent Ethanol Exposure Alters Small Noncoding RNAs in Mouse Sperm and Epididymosomes

*Gregory R. Rompala[1], Anais Mounier[2], Cody M. Wolfe[2], Qishan Lin[3], Iliya Lefterov[2] and Gregg E. Homanics[1,4,5,6]**

[1] Center for Neuroscience, University of Pittsburgh, Pittsburgh, PA, United States, [2] Department of Environmental and Occupational Health, University of Pittsburgh, Pittsburgh, PA, United States, [3] Mass Spectrometry Facility, Center for Functional Genomics, University at Albany, Rensselaer, NY, United States, [4] Department of Anesthesiology, University of Pittsburgh, Pittsburgh, PA, United States, [5] Department of Pharmacology and Chemical Biology, University of Pittsburgh, Pittsburgh, PA, United States, [6] Department of Neurobiology, University of Pittsburgh, Pittsburgh, PA, United States

While the risks of maternal alcohol abuse during pregnancy are well-established, several preclinical studies suggest that chronic preconception alcohol consumption by either parent may also have significance consequences for offspring health and development. Notably, since isogenic male mice used in these studies are not involved in gestation or rearing of offspring, the cross-generational effects of paternal alcohol exposure suggest a germline-based epigenetic mechanism. Many recent studies have demonstrated that the effects of paternal environmental exposures such as stress or malnutrition can be transmitted to the next generation via alterations to small noncoding RNAs in sperm. Therefore, we used high throughput sequencing to examine the effect of preconception ethanol on small noncoding RNAs in sperm. We found that chronic intermittent ethanol exposure altered several small noncoding RNAs from three of the major small RNA classes in sperm, tRNA-derived small RNA (tDR), mitochondrial small RNA, and microRNA. Six of the ethanol-responsive small noncoding RNAs were evaluated with RT-qPCR on a separate cohort of mice and five of the six were confirmed to be altered by chronic ethanol exposure, supporting the validity of the sequencing results. In addition to altered sperm RNA abundance, chronic ethanol exposure affected post-transcriptional modifications to sperm small noncoding RNAs, increasing two nucleoside modifications previously identified in mitochondrial tRNA. Furthermore, we found that chronic ethanol reduced epididymal expression of a tRNA methyltransferase, *Nsun2*, known to directly regulate tDR biogenesis. Finally, ethanol-responsive sperm tDR are similarly altered in extracellular vesicles of the epididymis (i.e., epididymosomes), supporting the hypothesis that alterations to sperm tDR emerge in the epididymis and that epididymosomes are the primary source of small noncoding RNAs in sperm. These results add chronic ethanol to the growing list of paternal exposures that can affect small noncoding RNA abundance and nucleoside modifications in sperm. As small noncoding RNAs in sperm have been shown to causally induce heritable phenotypes in offspring, additional research is warranted to understand the potential effects of ethanol-responsive sperm small noncoding RNAs on offspring health and development.

Keywords: ethanol, noncoding RNA, sperm, epididymosomes, epigenetics

OPEN ACCESS

Edited by:
Feng C. Zhou,
School of Medicine, Indiana University Bloomington, United States

Reviewed by:
Richard S. Lee,
Johns Hopkins University, United States
Robert Philibert,
University of Iowa, United States

***Correspondence:**
Gregg E. Homanics
homanicsge@anes.upmc.edu

Specialty section:
This article was submitted to Behavioral and Psychiatric Genetics, a section of the journal Frontiers in Genetics

Received: *06 December 2017*
Accepted: *24 January 2018*
Published: *08 February 2018*

Citation:
Rompala GR, Mounier A, Wolfe CM, Lin Q, Lefterov I and Homanics GE (2018) Heavy Chronic Intermittent Ethanol Exposure Alters Small Noncoding RNAs in Mouse Sperm and Epididymosomes. Front. Genet. 9:32. doi: 10.3389/fgene.2018.00032

INTRODUCTION

Studies examining the cross generational effects of alcohol have primarily focused on maternal alcohol abuse during pregnancy given the severe risk of inducing developmental deficits that typify fetal alcohol syndrome in offspring. Given the long-held belief that fathers only contribute genomic information through the germline, the preconception health of the father has historically been viewed as inconsequential to offspring development. However, a surge of recent preclinical research has triggered a growing interest in how various paternal factors such as stress, diet, and alcohol prior to conception can also affect the offspring phenotype, presumably via epigenetic mechanisms in sperm (Finegersh et al., 2015b; Stuppia et al., 2015; Schagdarsurengin and Steger, 2016).

Various forms of chronic ethanol treatment in male rodents prior to conception have been found to directly affect diverse phenotypes such as body weight, cortical thickness, and even behavioral sensitivity to drugs like amphetamine in the next generation (reviewed in Finegersh et al., 2015b). Recently, we added to this evidence, showing that males exposed intermittently to vapor ethanol over 5 weeks produce male offspring with reduced ethanol drinking behavior, increased ethanol sensitivity and attenuated stress responsivity (Finegersh and Homanics, 2014; Rompala et al., 2016, 2017). Since these studies were performed using isogenic sires that played no role in offspring rearing and development, paternal preconception ethanol may be driving unique changes in offspring behavior through nongenomic mechanisms in sperm. Therefore, greater emphasis should be put on understanding the consequences of paternal alcohol abuse prior to conception and identifying potential epigenetic mechanisms in the germline.

Although sperm DNA is densely packed in the nucleus, sperm are not solely passive carriers of genetic material, but also feature a complex epigenetic machinery. As most histones in sperm are exchanged for protamines during spermatogenesis, and sperm DNA loses most of its methylation at fertilization, identifying sperm-based mechanisms of epigenetic inheritance has been challenging (Heard and Martienssen, 2014). However, in addition to chromatin, sperm have a unique RNA profile enriched with diverse small noncoding RNA species (Ostermeier et al., 2002; Krawetz et al., 2011). These include well-described small RNA classes like microRNA and piRNA as well as under-studied groups like tRNA- and mitochondria-derived small RNAs that are overrepresented in sperm (Peng et al., 2012; Schuster et al., 2016b). As the sperm genome is thought to be transcriptionally quiescent (Kierszenbaum and Tres, 1975), these small noncoding RNAs may instead function during the earliest stages of embryogenesis. Indeed, sperm RNA is delivered to the oocyte (Ostermeier et al., 2004) and recent studies have found that sperm-derived small noncoding RNAs are required for normal embryonic development (Liu et al., 2012; Yuan et al., 2016; Guo et al., 2017).

The earliest evidence for RNA-mediated inheritance demonstrated that a mutation-induced white tail color phenotype in mice could be transmitted to wild type offspring via altered sperm RNA (Rassoulzadegan et al., 2006). Since then, numerous studies have found that sperm small noncoding RNAs are sensitive to various paternal environmental factors including stress, diet and exercise (Rodgers et al., 2013; Gapp et al., 2014; Chen et al., 2016a; de Castro Barbosa et al., 2016; Sharma et al., 2016; Short et al., 2016, 2017). Moreover, in humans, alterations in sperm small noncoding RNAs have been associated with obesity (Donkin et al., 2016) and smoking history (Marczylo et al., 2012). Finally, recent intergenerational studies have shown that cross generational effects of stress and diet can be recapitulated in offspring derived from embryos injected with stress- or diet- altered sperm RNAs, respectively, suggesting a causal role in paternal epigenetic inheritance (Gapp et al., 2014; Grandjean et al., 2015; Rodgers et al., 2015; Chen et al., 2016a).

Ethanol has deleterious effects on several measures of sperm quality in mice such as sperm count, circulating testosterone levels, and overall fertility, and similar effects have been found in alcoholic men (reviewed in La Vignera et al., 2013). Additionally, ethanol has been shown to impact epigenetic mechanisms in sperm. For instance, DNA methylation at imprinting gene loci is reduced in chronic ethanol-treated mice (Knezovich and Ramsay, 2012; Finegersh and Homanics, 2014; Liang et al., 2014) and men with alcohol use disorder (Ouko et al., 2009). However, whether ethanol directly affects small noncoding RNAs in sperm is entirely unknown. This is an important question given the prevalence of alcohol use disorder and the implication of small noncoding RNAs as a causal factor in paternally-linked epigenetic inheritance of complex behavior. Therefore, given the evidence that paternal preconception ethanol exposure has intergenerational effects, we hypothesized that ethanol causes epigenetic reprogramming of sperm small noncoding RNAs.

RESULTS

Chronic Ethanol Exposure Shifts the Small Noncoding RNA Profile in Sperm

Adult male C57BL/6J mice were exposed to vapor ethanol or room air conditions for 8 h/day, 5 days/week over 5 weeks. This chronic ethanol exposure induced an average blood ethanol concentration of ∼160 mg/dl and there was no effect of chronic ethanol on body weight at the end of the 5-week exposure (**Figure 1A**) as previously reported (Finegersh and Homanics, 2014; Rompala et al., 2016). Twenty-four hours following the final ethanol or control exposure, motile sperm were collected from each cauda epididymis for small RNA sequencing. First, we analyzed the various small RNA classes present in mouse sperm. Consistent with other studies in mice (Peng et al., 2012; Sharma et al., 2016), we found the majority (>60%) of 15–45 nucleotide (nt) sequencing reads were transfer RNA (tRNA)-derived small RNAs (tDR) in sperm from both control and ethanol-treated mice while the remaining reads were classified as mitochondrial small RNA (mitosRNA), piRNA, microRNA (miRNA), ribosomal RNA (rRNA), small nucleolar RNA (snoRNA) and small nuclear RNA (snRNA) (**Figure 1B**). The vast majority of tDR are ∼30–35 nt halves (**Figure 1C**) cleaved from the 5′ end of whole length tRNA at or near the anticodon loop (**Supplementary Figure 1**). Interestingly, there was a significant interaction between chronic

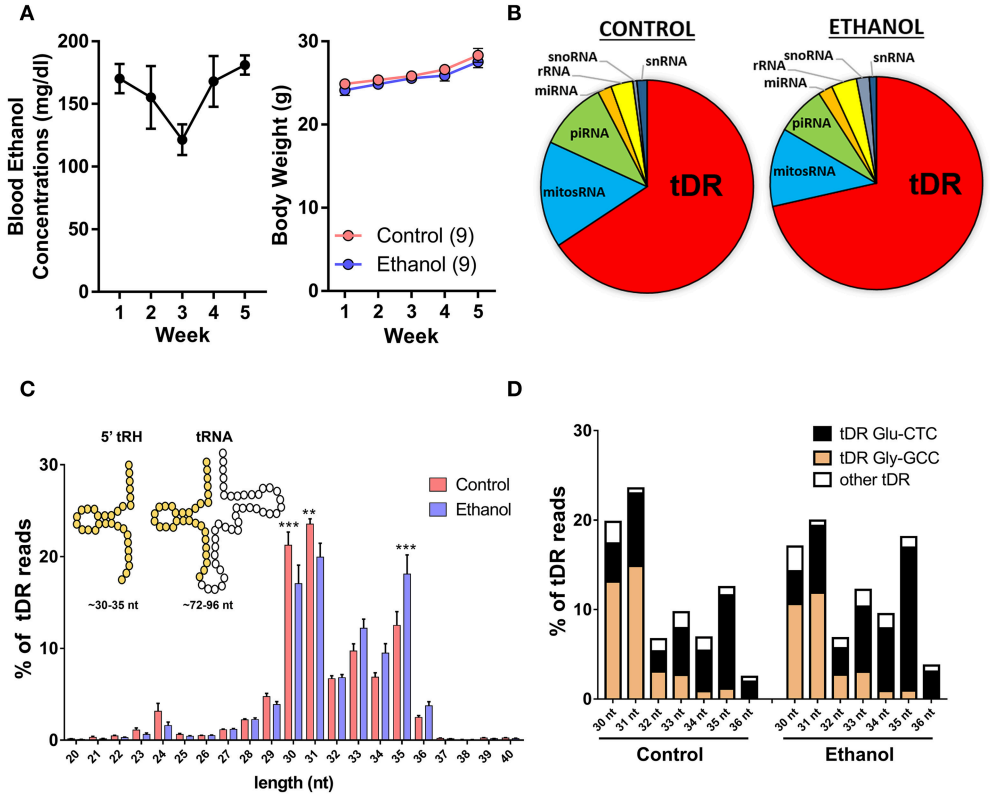

FIGURE 1 | Chronic ethanol shifts the tDR profile of sperm small noncoding RNA. **(A)** Chronic intermittent ethanol vapor exposure (left panel) induced an average blood ethanol concentration of 159.2 ± 9.2 mg/dl [mean (μ) ± standard error of the mean (SEM)] over its 5 week duration. There was no effect of chronic ethanol on body weight (right panel) compared to the control group ($p > 0.05$). **(B)** Pie charts displaying the percentage of each small RNA class represented in sperm from control and ethanol treatment groups. **(C)** Most tDR are 30–35 nt 5′-derived tRNA halves (5′-tRH) (see insert) and chronic ethanol significantly altered the percentage of 30, 31, and 35 nt tDR reads. **(D)** Most 30–36 nt tDR reads map to Glu-CTC and Gly-GCC relative to all other tDR species. Data in bar graphs presented as μ ± SEM. $N = 9$/treatment in all panels. $^{**}p < 0.01$. $^{***}p < 0.001$.

ethanol exposure and the size distribution of tDR reads [$F_{(20, 336)} = 4.2$; $p < 0.001$]. *Post-hoc* analysis revealed that chronic ethanol exposure reduced 30 ($p < 0.001$) and 31 nt tDR ($p < 0.01$) while increasing 35 nt tDR ($p < 0.001$) (**Figure 1C**). When we sorted tDR by their parent tRNA amino acid and anticodon sequence, two tDR species, Gly-GCC and Glu-CTC, accounted for >70% of all tDR sequencing reads as previously reported (Peng et al., 2012; Chen et al., 2016a; Cropley et al., 2016; Sharma et al., 2016). Notably, the 30–31 nt tDR were dominated by Gly-GCC while Glu-CTC accounted for the majority of 33–35 nt reads (**Figure 1D**).

Chronic Ethanol Exposure Alters Expression of Several Small Noncoding RNA Species

When we examined the effect of chronic ethanol exposure on the four major small noncoding RNA types in sperm, small RNA sequencing revealed 15 tDRs (**Figure 2A**), 8 miRNAs (**Figure 2B**), 5 mitosRNAs (**Figure 2C**), and 0 piRNA (**Supplementary Figure 2**) that were significantly affected by ethanol after false discovery rate adjustment ($q < 0.1$, **Figure 2D**, **Supplementary Table 1**). Subsequently, several altered small noncoding RNAs with high endogenous expression were chosen for RT-qPCR validation in an independent cohort of mice. Here, we found that five of the six analyzed small noncoding RNAs were significantly altered by chronic ethanol exposure [increased: tDR Glu-CTC, $t_{(14)} = 2.33$, $p < 0.05$; tDR His-GTG, $t_{(14)} = 3.14$, $p < 0.01$; miR-10a, $t_{(18)} = 2.41$, $p < 0.05$; miR-99b, $t_{(20)} = 2.79$, $p < 0.05$; decreased: tDR Ser-AGA, $t_{(14)} = 2.08$, $p < 0.05$; no change: tDR Pro-AGG, $p > 0.05$] (**Figure 2E**), supporting the validity of the sequencing results.

Predicting the Functional Significance of Ethanol-Responsive Sperm Small Noncoding RNAs

Given the evidence that sperm miRNA and tDR have been causally-linked to paternal epigenetic inheritance, we performed target prediction and gene ontology analysis on these ethanol-responsive small noncoding RNAs to infer functional significance at fertilization. The primary function attributed to miRNAs is RNA silencing through post-transcriptional regulation of the 3′-untranslated region (UTR). Thus, we

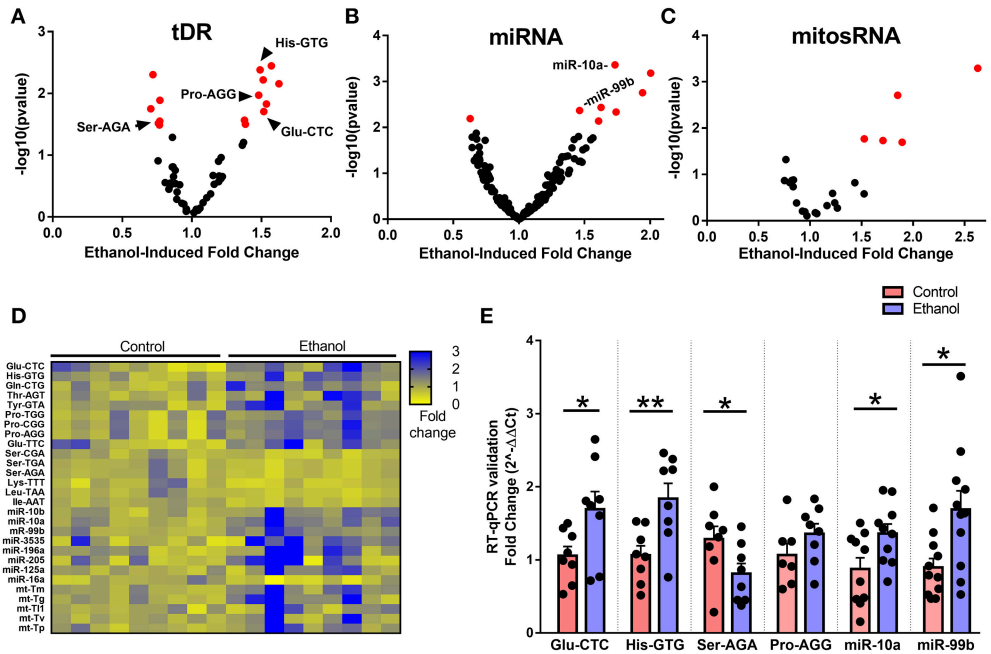

FIGURE 2 | Chronic ethanol alters abundance of several tDR, miRNA, and mitosRNA species in sperm. Volcano plots depicting fold change and log-transformed *p*-value for sperm (**A**) tDR, (**B**) miRNA, and (**C**) mitosRNA. Red dots indicate significance ($q \leq 0.1$). **(D)** Heat map of differentially expressed sperm small noncoding RNAs representing fold change in normalized counts for each small RNA sequencing sample represented by each column. **(E)** RT-qPCR validation of sequencing results revealed a significant effect of chronic ethanol on sperm tDRs Glu-CTC ($p < 0.05$), His-GTG ($p < 0.01$), Ser-AGA ($p < 0.05$), with no change in Pro-AGG ($p > 0.05$) and significantly increased miR-10a ($p < 0.05$) and miR-99b ($p < 0.05$), $N = 7$–11/treatment. RT-qPCR data presented as $\mu \pm$ SEM with black dots representing biological replicates (one mouse/replicate). $^{*}p < 0.05$, $^{**}p < 0.01$.

analyzed the predicted 3′-UTR targets of the 7 miRNA that were increased by chronic ethanol exposure for common targets (**Supplementary Table 2**). This revealed 37 genes targeted by at least 3 ethanol-enriched miRNAs and 3 genes (*Lcor*, *Nr6a, Rora*) that were targeted by ≥ 4 (**Figure 3A**). Gene ontology analysis of the predicted 3′-UTR targets of ≥ 3 sperm miRNA revealed enrichment for activators (i.e., transcription factors), transcription-regulators, and Ubl conjugation genes ($q < 0.01$, **Figure 3B**, **Supplementary Table 3**).

Although many studies have found that some tDR species can play a similar role to miRNA in post-transcriptional regulation of gene expression (Keam and Hutvagner, 2015), the specific mechanisms involved are unknown. Recent studies that employed rigorous target prediction analysis for all tDR species suggest that most tDR are more likely to act on the 5′-UTR of transcripts through complementary sequence-based gene regulation (Schuster et al., 2016a,b). Consistently, when we examined the predicted targets of all ethanol-responsive tDR, we found that each tDR examined had a greater number of genes with predicted 5′-UTR targets relative to the coding and 3′-UTR regions (**Figure 3C**, **Supplementary Table 4**). Strikingly, the number of genes with predicted 5′-UTR targets was more than 14 times greater for one tDR, Glu-CTC, relative to all other ethanol-responsive tDR examined (**Figure 3C**, **Supplementary Table 4**). Given the extreme enrichment of tDR Glu-CTC reads (**Figure 1D**), in addition to the surfeit of predicted targets, we performed gene ontology on genes with predicted 5′-UTR targets of tDR Glu-CTC, focusing on high confidence results. This revealed enrichment for gene targets associated with signal transduction (i.e., phosphoproteins, acetylation), alternative splicing, and the cytoplasm ($q < 0.01$, **Figure 3D**, **Supplementary Table 5**).

Chronic Ethanol Exposure Alters Select Sperm Small Noncoding RNA Modifications

Recent evidence suggests a functional role for post-transcriptional nucleoside modifications on small noncoding RNAs in sperm, particularly on tDR, as tRNA is the most heavily modified RNA class (Kirchner and Ignatova, 2015). For instance, whereas native sperm tDR is stable in the fertilized oocyte for several hours, synthetic tDR lacking endogenous nucleoside modifications are rapidly degraded (Chen et al., 2016a). Thus, we directly examined if chronic ethanol exposure (see **Supplementary Figure 3** for average blood ethanol concentrations and body weights) affects nucleoside modifications in the tDR-enriched ∼30–40 nt fraction of sperm RNA using ultra performance liquid chromatography tandem mass spectrometry (UHPLC-MS/MS) (Basanta-Sanchez et al., 2016). We focused our analysis on 22 post-transcriptional modifications previously identified in eukaryotic species (**Supplementary Table 6**) (Machnicka et al., 2013). This revealed two significantly increased nucleoside modifications: the

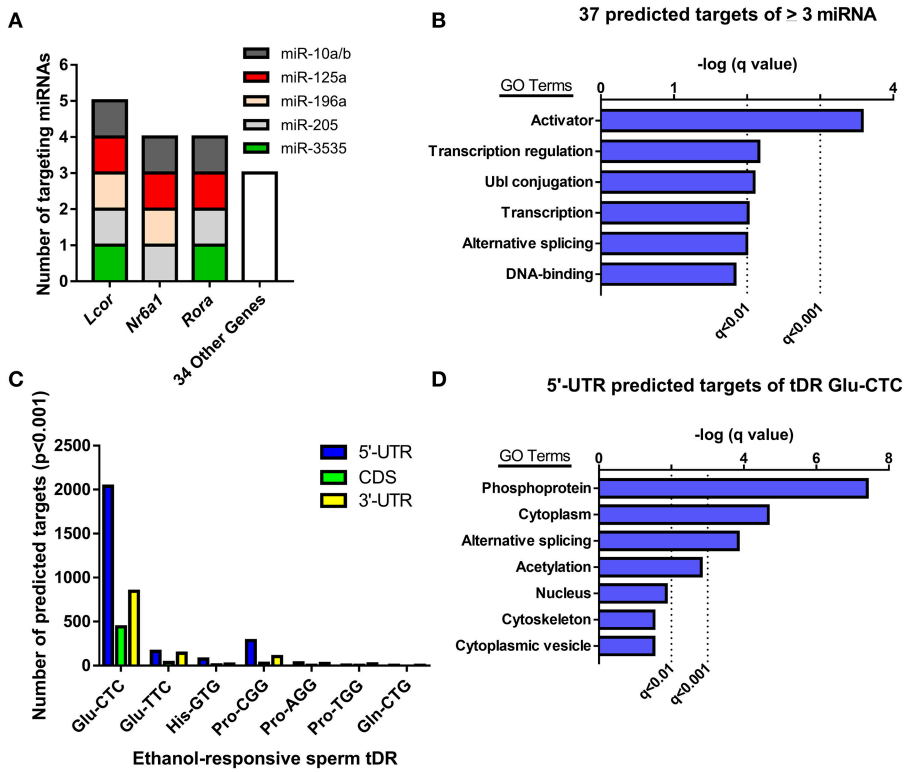

FIGURE 3 | Analyzing predicted gene targets of ethanol-responsive sperm miRNA and tDR Glu-CTC. **(A)** Genes with 3′-UTRs targeted by three or more miRNAs. **(B)** Gene ontology analysis of predicted target genes of ≥ 3 miRNA. **(C)** Number of genes with predicted 5′-UTR, coding, or 3′-UTR targets of ethanol-responsive sperm tDR. (**D**) Gene ontology analysis for genes with predicted 5′-UTR targets of tDR Glu-CTC.

uridine modification, 5′-methylaminomethyl-2-thiouridine (mnm^5s^2U) ($q < 0.1$; **Figure 4A**) and the cytidine modification, formylcytidine (f^5C) ($q < 0.01$; **Figure 4B**). There were no alterations to adenosine (**Figure 4C**) or guanosine (**Figure 4D**) base modifications.

Effects of Chronic Ethanol on Sperm tDR Are Reflected in Epididymosomes

Following spermatogenesis in the testis, newly developed spermatozoa enter the epididymis, gaining motility while migrating from the caput to cauda segment where mature sperm are stored prior to ejaculation. Interestingly, when we observed sperm isolated from the caput segment, there was no effect of chronic ethanol exposure on the tDR species altered by ethanol in cauda sperm (**Figure 5A**), suggesting the tDR alterations in mature sperm emerge during epidydimal transit or storage. This is consistent with recent evidence suggesting that sperm tDR are nearly absent in testis and become the dominant small RNA type through interactions with tDR-enriched extracellular vesicles or "epididymosomes" in the epididymal lumen (Reilly et al., 2016; Sharma et al., 2016). Supporting those findings, we found that immature sperm from testis were enriched for tDR species following coincubation with epididymosomes *in vitro* (**Supplementary Figures 4A,B**). Remarkably, when we isolated cauda epididymosomes from control and ethanol-treated mice (**Figure 5B**) after 2- and 5-week exposure times and used RT-qPCR to examine the same tDR species that were altered in cauda sperm, tDR Glu-CTC was increased at 2 weeks ethanol treatment [$t_{(18)} = 2.41$, $p < 0.05$; **Figure 5C**] and tDR His-GTG was increased at 5 weeks [$t_{(13)} = 2.20$, $p < 0.05$; **Figure 5D**] with no change in tDR Ser-AGA ($p > 0.05$) at either time point. Expression of each tDR was not correlated between cauda sperm and cauda epididymosomes at 5 weeks (**Supplementary Figures 5A–C**, $p > 0.05$), although there was a significant positive correlation at 2 weeks for tDR Glu-CTC in the ethanol group (**Supplementary Figure 5D**, $p < 0.05$).

Chronic Ethanol Reduces Epididymal Expression of *Nsun2* Gene Involved in tDR Biogenesis

Although the specific mechanisms in sperm and epididymis are unknown, loss of the tRNA cytosine-5 methyltransferases *Nsun2* or *Dnmt2* increases angiogenin-dependent cleavage of tRNA into 5′-derived tRNA halves (Schaefer et al., 2010; Blanco et al., 2014), the primary tDR subtype in sperm. Interestingly, we found that chronic ethanol exposure reduced expression of *Nsun2* [$t_{(13)} = 2.2$, $p < 0.05$] with no effect on *Dnmt2* ($p > 0.05$) in cauda epididymis (**Figure 6**).

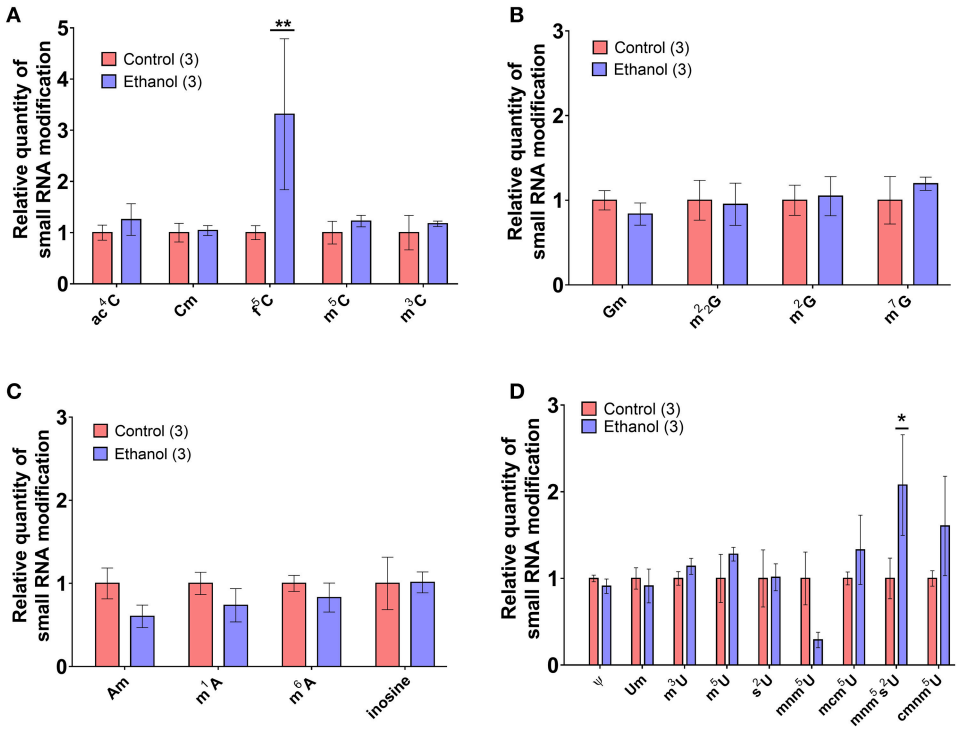

FIGURE 4 | Chronic ethanol alters select RNA modifications in sperm small noncoding RNA. UHPLC-MS/MS was performed on the ~30–40 nt fraction of sperm RNA from chronic ethanol and control exposed groups. Post-transcriptional modifications were examined for each of the parent nucleosides, **(A)** uridine, **(B)** cytidine, **(C)** adenosine, and **(D)** guanosine. Chronic ethanol increased the uridine modification, 5-methylaminomethyl-2-thiouridine (mnm^5s^2U) ($q < 0.1$) and the cytidine modification formylcytidine (f^5C) ($q < 0.01$). Data presented as $\mu \pm$ SEM bars. $N = 3$ pooled samples/group. *$q < 0.1$, **$q < 0.01$.

DISCUSSION

Several studies suggest that small noncoding RNAs are functional epigenetic regulators in sperm, capable of directing gene expression in the early embryo and ultimately impacting offspring behavior into adulthood. The current study is the first to our knowledge to examine the effects of ethanol on small noncoding RNAs in sperm. We found that chronic intermittent ethanol exposure altered the expression of several sperm tDR, mitosRNAs, and miRNAs. In addition, chronic ethanol increased specific posttranscriptional nucleoside modifications on sperm small noncoding RNAs. Gene ontology analysis of predicted ethanol-responsive miRNA and tDR targets revealed enrichment for gene sets involved in diverse biological functions, most robustly transcriptional factors and phosphoproteins. Finally, in the epididymis, we found that ethanol-responsive sperm tDR were similarly affected in extracellular vesicles (i.e., epididymosomes) and chronic ethanol exposure reduced expression of a tRNA methyltransferase, *Nsun2*, directly involved in tDR biogenesis (Blanco et al., 2014), suggesting a somatic origin to altered small noncoding RNAs in the male germline.

Many psychiatric and addiction disorders including alcohol use disorder have long been faced with what's been termed the "missing heritability" problem. That is, while alcohol use disorder has ~50% heritability (Prescott and Kendler, 1999; Young-Wolff et al., 2011; Ystrom et al., 2011), putative genetic variants associated with alcoholism account for only a minor fraction of that heritability (Treutlein and Rietschel, 2011). This suggests a significant role for non-genomic germline mechanisms of inheritance. The finding that chronic ethanol exposure alters sperm small noncoding RNAs adds to a growing literature demonstrating that a diverse range of paternal preconception exposures with cross-generational effects are associated with altered small noncoding RNAs in sperm (Rodgers et al., 2013; Gapp et al., 2014; Chen et al., 2016a; de Castro Barbosa et al., 2016; Sharma et al., 2016; Short et al., 2016, 2017). Remarkably, recent studies identified a causal relationship between altered small noncoding RNA and intergenerational phenotypes (Gapp et al., 2014; Grandjean et al., 2015; Rodgers et al., 2015; Chen et al., 2016a). We have shown previously that chronic preconception ethanol exposure alters complex behaviors in male offspring including ethanol drinking preference and stress responsivity (Finegersh and Homanics, 2014; Rompala et al., 2016, 2017). Here we found the same chronic ethanol exposure induces differential expression of several small noncoding RNA species in sperm. Thus, additional studies are needed to directly test the role of ethanol-responsive sperm small noncoding RNAs in the heritable effects of paternal preconception chronic ethanol exposure.

Among the different small noncoding RNA types, we found that tDR were most affected by chronic ethanol treatment. Given the abundance of tDR in sperm and emerging evidence

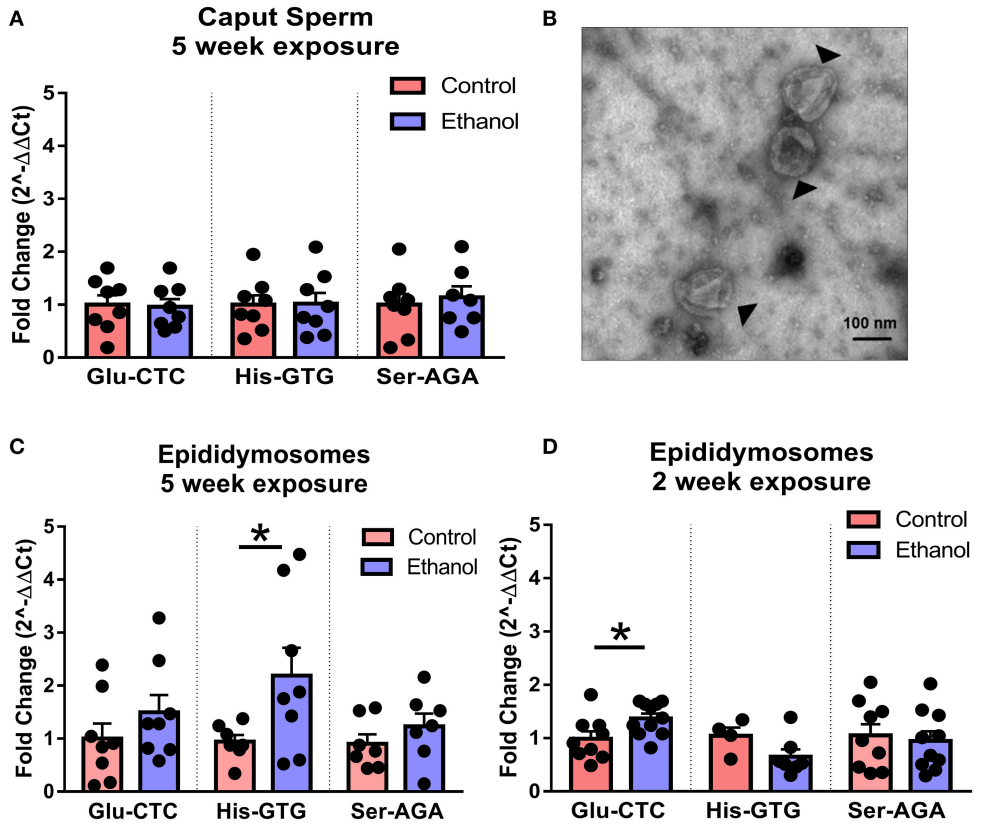

FIGURE 5 | Effects of chronic ethanol on sperm tDR are reflected in epididymosomes. **(A)** RT-qPCR showing no effect of chronic ethanol on tDR Glu-CTC, His-GTG, and Ser-AGA in caput epididymal sperm ($p > 0.05$). (**B**) Transmission electron microscopy image of epididymosomes (arrows) isolated from adult mouse cauda epididymis. **(C)** RT-qPCR reveled a significant effect of chronic ethanol on tDR Glu-CTC with no change in His-GTG or Ser-AGA with 2 weeks of ethanol exposure. **(D)** RT-qPCR showing increased tDR His-GTG with no change in Glu-CTC or Ser-AGA with 5 weeks ethanol exposure. $N = 4$–11/treatment. Data presented as $\mu \pm$ SEM with black dots representing biological replicates (one mouse/replicate). $^*p < 0.05$.

of their role in gene expression regulation, tDR have become a major focus as a potential causal mechanism for paternally-linked epigenetic inheritance. Low protein diet, high fat diet, and increased exercise have all been shown to directly confer changes in sperm tDR (Chen et al., 2016a; Sharma et al., 2016; Short et al., 2017) while obesity and vinclozolin exposure affect sperm tDRs transgenerationally (Cropley et al., 2016; Schuster et al., 2016a). Remarkably, one recent study found that the effects of paternal high fat diet on glucose tolerance in offspring were recapitulated in mice derived from fertilized embryos injected with sperm tDR, but not when the embryos were injected with all other sperm RNA classes except tDR (Chen et al., 2016a). This illustrates a specific causal role for tDR in RNA-mediated epigenetic inheritance.

In addition to affecting tDR, chronic ethanol exposure increased several of the second most abundant small noncoding RNA type, mitosRNA. While little is known about these small noncoding RNAs, they are derived from mitochondrial genes for rRNA and tRNA and have been shown to increase the expression of their parent genes *in vitro* (Ro et al., 2013). Given that mitosRNA are enriched in total sperm and yet barely detected in the sperm head (Schuster et al., 2016b), they are likely confined to the sperm mitochondrial sheath. Several parameters of mitochondrial function appear critical for sperm motility and fertilization capacity, including control of reactive oxygen species production, apoptotic pathways, and calcium homeostasis (Amaral et al., 2013). As chronic ethanol has been shown to affect several measures of sperm quality including reduced motility and increased apoptosis (Rahimipour et al., 2013), it is possible that ethanol directly affects sperm mitochondrial function. While paternal mitochondria do enter the oocyte at fertilization, the mitochondria and its DNA are rapidly degraded (Politi et al., 2014). It is unknown whether the mitochondrial RNA and mitosRNAs are similarly degraded or if they may serve some function in the early embryo.

While less expressed in sperm relative to other small noncoding RNA species, miRNA have been found to play a critical role in fertilization and preimplantation development (Liu et al., 2012; Yuan et al., 2016). Furthermore, altered sperm miRNA have been associated with the greatest range of environmental factors (although this may be due to the greater use of miRNA-specific analysis strategies such as microarray). Most notable among these studies, chronic variable stress was shown to increase nine sperm miRNAs and offspring of stressed

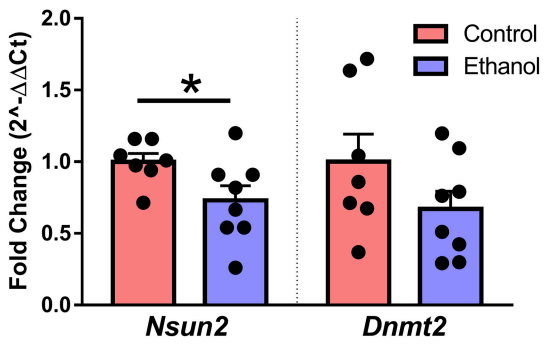

FIGURE 6 | Effect of chronic ethanol on epididymal expression of genes regulating tDR biogenesis. RT-qPCR in cauda epididymal tissue revealed a significant effect of chronic ethanol on the tRNA methyltransferase *Nsun2* ($p < 0.05$) with no change in *Dnmt2* ($p > 0.5$). $N = 7$–8/treatment. Data presented as $\mu \pm$ SEM with black dots representing biological replicates (one mouse/replicate). $^*p < 0.05$.

sires have a blunted stress responsivity phenotype (Rodgers et al., 2013). That same phenotype could be elicited in mice derived from control fertilized embryos injected with the nine stress-enriched miRNAs, suggesting a causal role for environmentally-responsive sperm miRNA (Rodgers et al., 2015). Interestingly, although we previously found that our chronic ethanol exposure similarly blunted stress responsivity in male offspring (Rompala et al., 2016), none of the stress-enriched miRNAs were affected in the current study, suggesting the intergenerational effects of the current chronic ethanol exposure are likely conferred through a different constellation of small noncoding RNAs or an alternative epigenetic pathway.

Although the specific function of sperm small noncoding RNAs is unknown, the two species directly implicated in intergenerational inheritance, miRNA and tDR, are both associated with post-transcriptional regulation of gene expression and are hypothesized to exert their epigenetic effects by regulating transcriptional cascades in the fertilized oocyte (Chen et al., 2016b). As miRNA have been found to predominantly target the 3′-UTR of mRNAs, we used sequence homology target prediction to identify common 3′-UTRs targeted by ethanol-responsive sperm miRNAs. Gene ontology analysis of common targets revealed enrichment for transcription factors and transcriptional regulators. Three genes, *Lcor*, *Nr6a1*, and *Rora*, were targeted by four or more of the seven ethanol-enriched miRNAs. *Lcor* binds with various steroid receptors including estrogen, progesterone, and glucocorticoid receptors (Palijan et al., 2009). It has been found to directly attenuate progesterone regulated gene expression (Fernandes et al., 2003) and is highly expressed in two-cell embryos (Fernandes et al., 2003), suggesting a critical role in steroid-hormone receptor mediated gene expression during embryogenesis. In addition, loss of *Nr6a1*, also known as germ cell nuclear factor, results in lethality during embryonic development (Wang and Cooney, 2013). Thus, future studies are warranted to investigate the effects of paternal chronic ethanol exposure on predicted targets of ethanol-responsive miRNA during embryogenesis.

While the specific role of sperm tDR is unknown, most evidence suggests tDR act similarly to miRNA via post-transcriptional regulation of mRNA. Notably, while miRNA function is primarily associated with regulation at 3′-UTRs, tDR are more likely to target 5′-UTRs (Schuster et al., 2016a,b). Remarkably, we found that the number of predicted 5′-UTR targets was substantially greater for one tDR, Glu-CTC, relative to all other analyzed species. This was striking considering it is also enriched several hundred-fold relative to nearly all other small noncoding RNAs in sperm. Gene ontology analysis of predicted 5′-UTR targets of tDR Glu-CTC revealed greatest enrichment for genes related to phosphoprotein, alternative splicing, cytoplasm, and acetylation. Therefore, Glu-CTC is well-positioned to be functionally significant in the fertilized oocyte. Supporting this notion, one study found that expression of approximately half of the predicted mRNA targets of tDR Glu-CTC was reduced more than two-fold from the oocyte to four cell-stage of embryonic development (Cropley et al., 2016). Furthermore, injecting the other equally-enriched tDR species in sperm, Gly-GCC, into fertilized oocytes dramatically altered gene expression while an equal amount of endogenously less-expressed sperm tDRs were comparatively ineffective (Sharma et al., 2016), suggesting a potentially greater role for sperm small RNAs with robust endogenous expression such as Glu-CTC. Future studies will need to examine the effect of ethanol-sensitive tDR Glu-CTC on gene expression in the early embryo.

There is growing interest in the role of post-transcriptional nucleoside modifications in RNA function. Small noncoding RNAs also feature these modifications which are important for stability in the oocyte and even the ability of small noncoding RNAs to induce intergenerational phenotypes (Chen et al., 2016a). When we used HPLC-MS/MS to examine the tDR enriched ∼30–40 nt sperm RNA fraction directly for nucleoside modifications, we found a significant effect of chronic ethanol exposure on two modifications, f^5C and mnm^5s^2U. Each of these nucleoside modifications have been identified previously on intact mitochondrial-encoded tRNAs at the wobble position of the anticodon loop (Yan and Guan, 2004; Machnicka et al., 2013; Nakano et al., 2016), critical to tRNA structure and codon recognition. Two pathogenic point mutations have been associated with the inability to form f^5C modifications (Nakano et al., 2016), suggesting functional significance. Whether these nuceloside modifications reflect alterations to the parent mitochondrial tRNA in sperm or if they also serve a specific function on mitosRNA such as stability or target recognition is unknown. Interestingly, f^5C is found on mt-Tm, the mitochondrial tRNA for methionine (Nakano et al., 2016), and mitosRNAs mapping to mt-Tm were increased by chronic ethanol exposure (**Figure 2D**). Increased f^5C may be a consequence of increased mt-Tm small noncoding RNAs or it is also possible that f^5C stabilizes mt-Tm-mapping mitosRNAs. Overall, these findings further support the notion that in addition to sperm small RNA abundance, post-transcriptional modifications are sensitive to environmental insults such as chronic ethanol exposure.

Given that DNA in sperm is condensed by highly alkaline protamines, there is minimal transcriptional activity in mature sperm. Thus, environmentally-induced changes to the sperm RNA profile are likely driven by extracellular factors. Supporting this notion, the epididymis is enriched with principal secretory cells that release extracellular vesicles (i.e., epididymosomes) capable of fusing with the sperm membrane. Many studies have characterized epididymosome-mediated protein exchange with sperm (reviewed in Sullivan, 2016). More recently, it was found that epididymosomes carry a tDR-enriched small RNA milieu that is similar to sperm (Sharma et al., 2016) and epididymosomes can directly transfer small noncoding RNAs to immature sperm *in vitro* (Reilly et al., 2016; Sharma et al., 2016). Here, we found that caput sperm did not have the same ethanol-induced changes to sperm tDR seen in cauda sperm, suggesting ethanol-sensitive sperm tDRs are altered during epididymal transit. Indeed, when we examined RNA from epididymosomes, we found that the effects of chronic ethanol exposure on sperm tDRs Glu-CTC and His-GTG were reflected in epididymosomes. While we only found a correlation between tDR and epididymosomes for tDR Glu-CTC and only following two, but not 5 weeks of ethanol exposure, several factors may contribute to differences between the RNA cargo of epididymosomes vs. sperm stored in the cauda epididymis at a given time point. For instance, after epididymal transit, mature rodent sperm are estimated to remain motile in the cauda epididymis for 1 month (Jones, 1999). Moreover, the majority of epididymosomes have been found to target dead sperm while a subtype of CD9-positive epididymosomes show increased preference for live sperm (Caballero et al., 2013). Thus, a better understanding of the temporal and subtype-specific dynamics of *in vivo* epididymosome to sperm RNA transfer is needed in future investigations of this novel soma to germline mechanism.

In other tissues, the production of 5′-derived tRNA halves results from cellular stress-induced cleavage at the anticodon loop by the RNase angiogenin (Fu et al., 2009). This tRNA cleavage is increased in the absence of cytosine-5 methylation (Tuorto et al., 2012). The major cytosine-5 tRNA methyltransferase enzymes are *Nsun2* and *Dnmt2* and chronic ethanol exposure reduced expression of *Nsun2* in cauda epididymis. Loss of *Nsun2*-dependent tRNA methylation results in dramatically increased cleavage of tRNAs into ∼30–35 nt halves by angiogenin (Blanco et al., 2014). Although it is unclear whether angiogenin-mediated cleavage and tRNA cytosine-5 methylation similarly regulate tDR production in epididymis and sperm, *Nsun2* and *Dnmt2* are highly expressed in both testis and epididymis and *Nsun2* is critical for proper germ cell differentiation (Hussain et al., 2013). Furthermore, a recent study found that maternal and paternal *Dnmt2* expression is essential in two separate animal models of RNA-mediated inheritance (Kiani et al., 2013). Thus, tRNA cytosine-5 methyltransferase activity may be important for sperm tDR biogenesis and RNA-mediated epigenetic inheritance. More studies are needed to investigate the mechanistic role of tRNA cytosine-5 methyltransferase enzymes specifically in sperm tDR production and function.

While the emerging evidence suggesting a causal role for small noncoding RNA in inheritance of paternal preconception environment is intriguing, it is important to acknowledge the limitations and remaining challenges to discerning functional significance. For instance, the sperm RNA payload is minuscule (100 fg in rodents) and even the contribution of sperm-enriched tDR and miRNA is negligible relative to the amount of pre-existing copies in the oocyte (Yang et al., 2016). Therefore, studies to date examining the function of specific RNAs in fertilized embryos may not reflect physiological conditions. It is possible that sperm RNAs acquire unique functionality by forming as-yet unidentified protein-RNA effector complexes or through RNA modifications (Kiani et al., 2013). In addition, if the RNA cargo from epididymosomes adhering to the sperm exterior is also trafficked to the embryo cytoplasm, this would greatly increase the paternal RNA contribution (Sharma and Rando, 2017). Finally, sperm-derived RNAs may be reverse-transcribed and amplified in the early embryo as transcriptionally-competent cDNA (Spadafora, 2017). Undoubtedly, additional studies are needed to uncover potential mechanisms of RNA-mediated inheritance.

In summary, our findings provide the first evidence that chronic ethanol exposure alters small noncoding RNA abundance and nucleoside modifications in sperm. Additionally, we provide evidence that ethanol directly alters the same small noncoding RNAs in epididymosomes, further supporting the hypothesis that alterations to sperm RNA may be downstream of environmentally-induced changes to extracellular vesicles in the epididymal lumen. Given the prevalence of alcohol use disorder in men, these findings have significant public health implications. Future studies are needed to directly interrogate the effects of ethanol-sensitive small noncoding RNAs in sperm on embryo and offspring development.

METHODS

All experiments were approved by the Institutional Animal Care and Use Committee of the University of Pittsburgh and conducted in accordance with the National Institutes of Health Guidelines for the Care and Use of Laboratory Animals. Seven-week-old, ethanol-naïve, specific pathogen free C57BL/6J mice were purchased from the Jackson Laboratory (Bar Harbor, ME). Mice were habituated to the University of Pittsburgh animal facility for at least 1 week prior to initiation of experiments. Mice were housed under 12 h light/dark cycles and had *ad libitum* access to food (irradiated 5P76 ProLab IsoPro RMH 3000, [LabDiet, St.Louis, MO]) and water.

Chronic Intermittent Ethanol Inhalation

Chronic intermittent ethanol inhalation was performed as previously described (Finegersh and Homanics, 2014; Finegersh et al., 2015a; Rompala et al., 2016, 2017). Briefly, 8-week-old male C57BL/6J mice were randomly assigned to one of two treatments. Half the mice were treated in ethanol inhalation chambers in the home cage with water and food for 5 weeks from 09:00 to 17:00 over five consecutive day blocks with 2 days in between blocks. The other half of mice were assigned controls that were exposed

to identical chamber conditions without ethanol vapor. Animals were group-housed throughout the exposure and cages, food, and water were all changed routinely after the final exposure of each week. Blood ethanol concentration was measured after the final exposure of each week by extracting tail vein blood using heparin-coated capillary tubes (Drummond, Broomall, PA) and running plasma samples (extracted from blood by centrifugation at 2,300 × g for 10 min) on an Analox EtOH analyzer (AM1, Analox Instruments, London, UK). Tail blood was drawn from all groups to control for the extraction procedure. Ethanol content in the ethanol inhalation chambers was monitored using a custom sensor generously provided by Brian McCool and flow rates in the chambers were adjusted weekly based on blood ethanol concentration measurements made during the preceding week. Importantly, animals do not lose significant body weight (defined as >10%). In addition, the effects of ethanol vapor on lungs, heart, and liver are comparable to those associated with other chronic ethanol exposure models (Mouton et al., 2016).

Epididymis Collection and Sperm Isolation

Sperm samples were isolated from adult male mice sacrificed ∼16–19 h following the final ethanol or room air exposure during the light cycle (08:00–11:00). Briefly, after euthanasia by CO2 asphyxiation, left and right cauda epididymides were dissected into 1.5 ml of EmbryoMax Human Tubal Fluid (HTF) (Sigma-Aldrich, St. Louis, MO) at 37°C. Several small cuts were made in each epididymis to release the sperm into solution. The sperm solution was then transferred to a 1.5 ml Eppendorf tube and motile sperm dispersed in media for 20 min at 37°C. The top 1.2 ml supernatant was carefully collected for further processing while the settled epididymal tissue was stored at −80°C for later RNA extraction. Next, the supernatant was centrifuged at 2,000 × g for 5 min to pellet the sperm. The supernatant from this step was saved for epididymosome isolation and the pelleted sperm was then gently resuspended by pipetting in 1.0 ml of somatic cell lysis buffer (0.1% SDS, 0.5% Triton-X) which was put on ice for 20 min. This step is also critical for lysis and removal of adherent RNA-containing extracellular vesicles (Sharma et al., 2016). Next, the sperm was re-pelleted and washed twice with ice cold 1X PBS. After the final wash, the sperm pellet was lysed in 1.0 ml Trizol (Thermo Fisher, Waltham, MA) supplemented with 200 mM β-mercaptoethanol (Sigma-Aldrich) to facilitate lysis of disulfide-bond enriched sperm cells. Samples were lysed using a 2.0 ml Dounce glass tissue homogenizer to break up the sperm pellet and further homogenized with a mechanical homogenizer on ice followed by brief heating at 65°C for 5 min before being moved back to ice. Complete lysis of the sperm nucleus was confirmed with light microscopy.

Caput sperm were extracted from caput epididymis into 1.5 ml HTF at 37°C. Since caput sperm are not fully motile, sperm were centrifuged at 300 × g for 3 min to discard larger tissue pieces (while the partially motile sperm remained in suspension) and treated with somatic cell lysis buffer for 30 min to enrich for caput sperm and remove adherent epididymosomes. Sperm were then re-centrifuged at 2,000 × g for 5 min and washed twice with 1X PBS. Sample purity was confirmed using light microscopy.

RNA Extraction

All samples were lysed in Trizol (note the additional steps used for sperm described above) using phenol-chloroform separation. The aqueous phase was then processed with Zymo RNA Clean and Concentrator Kit with DNAse1 on-column treatment (Zymo Research, Irving, CA). Final sperm RNA concentrations were determined with Qubit RNA HS assay (Thermo Fisher) and RNA Analysis ScreenTape (Agilent, Santa Clara, CA) was used to confirm absence of 18S and 28S ribosomal peaks that are indicative of somatic cell contamination.

Small RNA Sequencing

Barcoded small RNA libraries were prepared from 100 ng total RNA from individual mice using NEBNext Small RNA for Illumina Kit (New England Biolabs, Ipswich, MA) per manufacturer's instructions. Samples were selected for sequencing ($N = 9$/treatment) by randomly selecting 3 mice from each of 3 cages of 4 mice per treatment group. To prevent carry over of adapter dimers and nonspecific amplicons into the sequencing run, cDNA libraries were size-selected using 2% agarose gel electrophoresis with a Pippin Prep system (Sage Science, Beverley, MA). cDNA libraries were multiplexed and sequenced to an average depth of 9 million reads/sample on a NextSeq500 (Illumina, San Diego, CA) at the John G. Rangos Sr. Research Center at Children's Hospital of Pittsburgh of UPMC (Pittsburgh, PA). Investigators were blinded to treatment for both library preparation and sequencing.

Sequencing Analysis and Bioinformatics

Small RNA sequencing fastq files were filtered for read quality and trimmed with Cutadapt (Martin, 2011) which removed library preparation adapters and sequences outside the 15–45 nt range. For alignment to the mouse genome (GRCm38/mm10 assembly), Bowtie2 (Langmead and Salzberg, 2012) was used with standard parameters (–n 1, –l 18, –e 70). Mapped reads were annotated to small noncoding RNA features provided at spermbase.org (Schuster et al., 2016b) and summated with FeatureCounts (Liao et al., 2014). Final normalized counts were extracted and analyzed for differential expression analysis using DESeq2 (Love et al., 2014). For tDR analysis, all sized fragments mapping to a single species (e.g., tDR Glu-CTC) were summed to a single data point. The program tDRmapper (Selitsky and Sethupathy, 2015) was used to determine the size distribution of tDR reads and to further classify tDR species by type of fragmentation (e.g., 5′-tRH).

To predict genes with 3′-UTR targeted by miRNAs, we used TargetScan Mouse Custom ver. 5.2 (Lewis et al., 2005). For an unbiased prediction of genes with 5′UTR, coding or 3′UTR regions targeted by tDR, we used RNAhybrid (Kruger and Rehmsmeier, 2006) with established parameters (Schuster et al., 2016a). Gene ontology analysis was performed on all predicted target gene lists using DAVID Bioinformatics Resources ver. 6.8 (Huang da et al., 2009).

Reverse-Transcription Quantitative PCR (RT-qPCR)

For cDNA preparation of tDRs and mRNAs, cDNA was produced using total RNA from individual mice with RevertAid First Strand cDNA Synthesis Kit (Thermo Fisher, Waltham, MA) with gene-specific RT primers (see: Kramer, 2011 for stem-loop primer design methods) for tDR and oligo-dT RT primers for mRNA. For miRNA, cDNA was produced using miScript II RT Kit (Qiagen, Valencia, CA). Diluted cDNA was used for qPCR with iScript SYBR green (BioRad, Hercules, CA) on a BioRad iCycler. Expression was calculated using the $2^{-\Delta\Delta Ct}$ method. Small RNAs and mRNAs were normalized to U6 and β-Actin, respectively. All qPCR amplicons were validated by melt curve analysis, electrophoresis, and, for tDRs, additionally with Sanger sequencing. See Supplementary Materials for a full list of RT-qPCR oligos (**Supplementary Table 7**).

Ultra-High-Performance Liquid Chromatography Tandem Mass Spectrometry (UHPLC-MS/MS) Analysis of Sperm Small Noncoding RNA Modifications

Sperm total RNA was pooled from 4 to 8 mice (3 pooled samples/group), loaded (∼1 μg/lane) on Novex TBE-Urea 15% polyacrylamide gels (Thermo Fisher) and electrophoresed at 180 V for 1 h. Under UV light, the ∼30–40 nt band of RNA was recovered using ZR small-RNA PAGE Recovery Kit (Zymo Research). For each sample, 100 ng of the recovered small RNA was digested and prepared for UHPLC-MS/MS at the University at Albany RNA Mass Spectrometry Core (Albany, NY) using established methods (Basanta-Sanchez et al., 2016). Briefly, prior to UHPLC-MS/MS analysis, each sample was diluted to 10 ng/μl in 10 μl volume prior to enzymatic hydrolysis. This process involved the use of two enzymes. Nuclease P1 at 37°C overnight first followed by the addition of bacterial alkaline phosphatase at 37°C for 2-h. Resultant nucleoside mixtures were lyophilized and reconstitute to final concentration of 1 ng/μl in RNase-free water, 0.1% formic acid for subsequent UHPLC-MS/MS analysis. A total of 3 instrument replicates were processed per sample. To quantify RNA modified nucleosides, calibration curves were prepared for 42 modified nucleosides including adenosine, cytidine, guanosine and uridine. [13C15N]-Guanosine was used as an internal standard. Several processing software scaffolds including MassLynx and Targetlynx (Waters, Milford, MA) were used for the post processing of UHPLC-MS/MS data. Python script / Production of calibration curves and the Originlab software suite (Northampton, MA) were used to quantify RNA modified nucleosides. Investigators were blinded to treatment throughout UHPLC-MS/MS procedures and analysis.

Epididymosome Isolation

Following the pelleting of motile cauda sperm (described above), epididymosomes were isolated from the supernatant by filtration and ultracentrifugation. First, the epididymosome-containing media was centrifuged at 10,000 × g for 30 min at 4°C before being passed through a 0.2 μm syringe filter. Finally, epididymosomes were pelleted in a table top ultracentrifuge at 120,000 × g for 2 h at 4°C, washed once with ice cold 1.5 ml PBS to remove excess protein aggregates, centrifuged again at 120,000 × g for 2 h at 4°C and snap frozen with liquid nitrogen.

Epididymosome-Sperm Coincubation

The methods used for the coincubation were adapted from previously established methods (Reilly et al., 2016; Sharma et al., 2016). Briefly, for each paired sample, three 20-month-old adult male mice were sacrificed and each testis was dissected by removing the tunica and placing the seminiferous tubules in 3 ml HTF media at 37°C. The tissue was next finely minced and gently pipetted up and down to release spermatozoa and spermatogenic cells. After incubating further for 15 min at 37°C, sperm cells were run through a 100 μm cell strainer and centrifuged for 3 min at 200 × g to pellet somatic cells while leaving primarily immature sperm cells in suspension. This testicular spermatozoa-enriched preparation was pelleted at 1,000 × g and washed once in PBS. The sperm pellet was resuspended in 600 μl HTF (supplemented with 1 mM $ZnCl_2$ and pH adjusted to 6.5) and half the sample was incubated for 3 h at 37°C with epididymosomes isolated from the whole epididymis of one mouse and the other half with an equal volume (50 μl) of epididymosome-depleted media from ultracentrifugation. Following coincubation, sperm were washed twice at 2,000 × g with PBS and immediately processed for RNA extraction.

Electron Microscopy

Exosome microscopy was performed with a JEOL JEM-1011 transmission electron microscope at Center for Biological Imaging at the University of Pittsburgh (Pittsburgh, PA) using negative staining procedures.

Statistical Analysis

Unpaired two-way student's *t*-tests were used to compare control and ethanol group means [body weight and all RT-qPCR experiments] and paired two-way *t*-tests were used for the sperm-epididymosome coincubation experiment. Two-way analysis of variance (ANOVA) was used to analyze distribution of tDR reads between control and ethanol groups for effects of ethanol or ethanol × tDR size. Bonferroni *post-hoc* tests were used to analyze specific group effects in the event of a significant ethanol × tDR size interaction. Analysis of nucleoside modifications was performed using multiple comparisons analysis (accounting for all 22 assessed nucleoside modifications in a single analysis) with false discovery rate adjustment using the two-stage step up method ($q < 0.1$) (Benjamini et al., 2006). Sequencing data was corrected for false discovery rate ($q \leq 0.1$). Pearson's *r* was used to analyze all correlations between sperm and epididymosome tDRs for control and ethanol groups.

Archiving Sequencing Data

Sequencing data was deposited to NCBI's Sequencing Read Archive with the accession: PRJNA414349.

ETHICS STATEMENT

This study was carried out in accordance with the recommendations of the National Institutes of Health Guidelines for the Care and Use of Laboratory Animals and Institutional Animal Care and Use Committee of the University of Pittsburgh. The protocol was approved by the Institutional Animal Care and Use Committee of the University of Pittsburgh.

AUTHOR CONTRIBUTIONS

GR, IL, and GH designed the experiments. GR, AM, and QL performed the experiments. GR, QL, CW, IL, and GH analyzed the data. GR and GH wrote the manuscript.

FUNDING

This work was supported by NIH/NIAAA grants awarded to GH (AA010422 & AA020889) and GR (AA024670).

ACKNOWLEDGMENTS

The authors would like to acknowledge the technical support of Carolyn Ferguson and Florent Letronne and bioinformatic support from Dario Boffelli. We thank Brian McCool of Wake Forest University for his generous donation of the ethanol vapor sensor utilized in this study.

SUPPLEMENTARY MATERIAL

The Supplementary Material for this article can be found online at: https://www.frontiersin.org/articles/10.3389/fgene.2018.00032/full#supplementary-material

Supplementary Figure 1 | Most tDR are 5′-derived tRNA halves. Graph showing the percentage of different tDR subtypes in chronic ethanol and control groups, classified by how each subtype is cleaved from the mature tRNA: 5′-derived tRNA halves (5′tRH), 5′-derived tRNA fragments (5′-tRF), 3′-derived tRNA halves (3′-tRH), 3′-derived tRNA fragments (3′-tRF), or undefined. Data presented as $\mu \pm$ SEM.

Supplementary Figure 2 | Effect of chronic ethanol on sperm piRNA. Volcano plot depicting fold change and log-transformed *p*-values for all piRNAs detected with small RNA sequencing. No piRNA species were significantly altered by chronic ethanol ($q \leq 0.1$).

Supplementary Figure 3 | Effect of chronic ethanol on blood ethanol concentration and body weights in sperm RNA modification analysis cohort. The average blood ethanol concentration (left panel) over the 5-week chronic ethanol exposure was 158.2 ± 6.8 mg/dl ($\mu \pm$ SEM). Body weights (right panel) were not significantly altered by chronic ethanol exposure ($p > 0.05$). Data presented as $\mu \pm$ SEM. $N = 12$/treatment.

Supplementary Figure 4 | Epididymosomes transfer tDRs to immature testis sperm *in vitro*. Each testis sperm suspension was equally divided and half of the sample was incubated for 3 h with epididymosomes while the other half was incubated with epididymosome-depleted media to examine the effect of epididymosome *in vitro* coincubation on sperm tDRs **(A)** Gly-GCC and **(B)** Glu-CTC. Data presented as fold change from control values with lines indicating paired samples. $^*p < 0.05$.

Supplementary Figure 5 | Relationship between sperm tDR and epididymosome tDR RT-qPCR expression. Scatterplots showing no correlation for levels of tDRs **(A)** Glu-CTC, **(B)** His-GTG, and **(C)** Ser-AGA expression between cauda sperm and cauda epididymosomes at 5 weeks and **(D)** a significant correlation at 2 weeks for tDR Glu-CTC in the ethanol group. Plotted lines for control and ethanol groups represent linear regression analysis. $^*p < 0.05$.

Supplementary Table 1 | Differential expression analysis of sperm small noncoding RNA sequencing results ($n = 9$/group).

Supplementary Table 2 | Predicted 3′-UTR targets of miRNAs altered in sperm by chronic ethanol exposure.

Supplementary Table 3 | Gene ontology analysis of > 3 sperm miRNA that were increased by chronic ethanol exposure.

Supplementary Table 4 | Predicted 5′-UTR, coding, and 3′-UTR targets of ethanol-responsive sperm tDR.

Supplementary Table 5 | Gene ontology analysis for top predicted 5′-UTR targets of tDR Glu-CTC.

Supplementary Table 6 | List of RNA modifications examined with UHPLC-MS/MS.

Supplementary Table 7 | List of RT-qPCR oligos.

REFERENCES

Amaral, A., Lourenco, B., Marques, M., and Ramalho-Santos, J. (2013). Mitochondria functionality and sperm quality. *Reproduction* 146, R163–R174. doi: 10.1530/REP-13-0178

Basanta-Sanchez, M., Temple, S., Ansari, S. A., D'Amico, A., and Agris, P. F. (2016). Attomole quantification and global profile of RNA modifications: epitranscriptome of human neural stem cells. *Nucleic Acids Res.* 44, e26. doi: 10.1093/nar/gkv971

Benjamini, Y., Kreiger, A. M., and Yekutieli, D. (2006). Adaptive linear step-up procedures that control the false discovery rate. *Biometrika* 93, 491–507. doi: 10.1093/biomet/93.3.491

Blanco, S., Dietmann, S., Flores, J. V., Hussain, S., Kutter, C., Humphreys, P., et al. (2014). Aberrant methylation of tRNAs links cellular stress to neuro-developmental disorders. *EMBO J.* 33, 2020–2039. doi: 10.15252/embj.201489282

Caballero, J. N., Frenette, G., Belleannee, C., and Sullivan, R. (2013). CD9-positive microvesicles mediate the transfer of molecules to Bovine Spermatozoa during epididymal maturation. *PLoS ONE* 8:e65364. doi: 10.1371/journal.pone.0065364

Chen, Q., Yan, M., Cao, Z., Li, X., Zhang, Y., Shi, J., et al. (2016a). Sperm tsRNAs contribute to intergenerational inheritance of an acquired metabolic disorder. *Science* 351, 397–400. doi: 10.1126/science.aad7977

Chen, Q., Yan, W., and Duan, E. (2016b). Epigenetic inheritance of acquired traits through sperm RNAs and sperm RNA modifications. *Nat. Rev. Genet.* 17, 733–743. doi: 10.1038/nrg.2016.106

Cropley, J. E., Eaton, S. A., Aiken, A., Young, P. E., Giannoulatou, E., Ho, J. W., et al. (2016). Male-lineage transmission of an acquired metabolic phenotype induced by grand-paternal obesity. *Mol. Metab.* 5, 699–708. doi: 10.1016/j.molmet.2016.06.008

de Castro Barbosa, T., Ingerslev, L. R., Alm, P. S., Versteyhe, S., Massart, J., Rasmussen, M., et al. (2016). High-fat diet reprograms the epigenome of rat spermatozoa and transgenerationally affects metabolism of the offspring. *Mol. Metab.* 5, 184–197. doi: 10.1016/j.molmet.2015.12.002

Donkin, I., Versteyhe, S., Ingerslev, L. R., Qian, K., Mechta, M., Nordkap, L., et al. (2016). Obesity and bariatric surgery drive epigenetic variation of spermatozoa in humans. *Cell Metab.* 23, 369–378. doi: 10.1016/j.cmet.2015.11.004

Fernandes, I., Bastien, Y., Wai, T., Nygard, K., Lin, R., Cormier, O., et al. (2003). Ligand-dependent nuclear receptor corepressor LCoR functions by histone

deacetylase-dependent and -independent mechanisms. *Mol. Cell* 11, 139–150. doi: 10.1016/S1097-2765(03)00014-5

Finegersh, and Homanics, G. E. (2014). Paternal alcohol exposure reduces alcohol drinking and increases behavioral sensitivity to alcohol selectively in male offspring. *PLoS ONE* 9:e99078. doi: 10.1371/journal.pone.0099078

Finegersh, A., Ferguson, C., Maxwell, S., Mazariegos, D., Farrell, D., and Homanics, G. E. (2015a). Repeated vapor ethanol exposure induces transient histone modifications in the brain that are modified by genotype and brain region. *Front. Mol. Neurosci.* 8:39. doi: 10.3389/fnmol.2015.00039

Finegersh, A., Rompala, G. R., Martin, D. I., and Homanics, G. E. (2015b). Drinking beyond a lifetime: new and emerging insights into paternal alcohol exposure on subsequent generations. *Alcohol* 49, 461–470. doi: 10.1016/j.alcohol.2015.02.008

Fu, H., Feng, J., Liu, Q., Sun, F., Tie, Y., Zhu, J., et al. (2009). Stress induces tRNA cleavage by angiogenin in mammalian cells. *FEBS Lett.* 583, 437–442. doi: 10.1016/j.febslet.2008.12.043

Gapp, K., Jawaid, A., Sarkies, P., Bohacek, J., Pelczar, P., Prados, J., et al. (2014). Implication of sperm RNAs in transgenerational inheritance of the effects of early trauma in mice. *Nat. Neurosci.* 17, 667–669. doi: 10.1038/nn.3695

Grandjean, V., Fourre, S., De Abreu, D. A., Derieppe, M. A., Remy, J. J., and Rassoulzadegan, M. (2015). RNA-mediated paternal heredity of diet-induced obesity and metabolic disorders. *Sci. Rep.* 5:18193. doi: 10.1038/srep18193

Guo, L., Chao, S. B., Xiao, L., Wang, Z. B., Meng, T. G., Li, Y. Y., et al. (2017). Sperm-carried RNAs play critical roles in mouse embryonic development. *Oncotarget* 8, 67394–67405. doi: 10.18632/oncotarget.18672

Heard, E., and Martienssen, R. A. (2014). Transgenerational epigenetic inheritance: myths and mechanisms. *Cell* 157, 95–109. doi: 10.1016/j.cell.2014.02.045

Huang da, W., Sherman, B. T., and Lempicki, R. A. (2009). Systematic and integrative analysis of large gene lists using DAVID bioinformatics resources. *Nat. Protoc.* 4, 44–57. doi: 10.1038/nprot.2008.211

Hussain, S., Tuorto, F., Menon, S., Blanco, S., Cox, C., Flores, J. V., et al. (2013). The mouse cytosine-5 RNA methyltransferase NSun2 is a component of the chromatoid body and required for testis differentiation. *Mol. Cell. Biol.* 33, 1561–1570. doi: 10.1128/MCB.01523-12

Jones, R. C. (1999). To store or mature spermatozoa? the primary role of the epididymis. *Int. J. Androl.* 22, 57–67. doi: 10.1046/j.1365-2605.1999.00151.x

Keam, S. P., and Hutvagner, G. (2015). tRNA-derived fragments (tRFs): emerging new roles for an ancient RNA in the regulation of gene expression. *Life* 5, 1638–1651. doi: 10.3390/life5041638

Kiani, J., Grandjean, V., Liebers, R., Tuorto, F., Ghanbarian, H., Lyko, F., et al. (2013). RNA-mediated epigenetic heredity requires the cytosine methyltransferase Dnmt2. *PLoS Genet.* 9:e1003498. doi: 10.1371/journal.pgen.1003498

Kierszenbaum, A. L., and Tres, L. L. (1975). Structural and transcriptional features of the mouse spermatid genome. *J. Cell Biol.* 65, 258–270. doi: 10.1083/jcb.65.2.258

Kirchner, S., and Ignatova, Z. (2015). Emerging roles of tRNA in adaptive translation, signalling dynamics and disease. *Nat. Rev. Genet.* 16, 98–112. doi: 10.1038/nrg3861

Knezovich, J. G., and Ramsay, M. (2012). The effect of preconception paternal alcohol exposure on epigenetic remodeling of the h19 and rasgrf1 imprinting control regions in mouse offspring. *Front. Genet.* 3:10. doi: 10.3389/fgene.2012.00010

Kramer, M. F. (2011). Stem-loop RT-qPCR for miRNAs. *Curr. Protoc. Mol. Biol.* Chapter 15, Unit 15 10. doi: 10.1002/0471142727.mb1510s95

Krawetz, S. A., Kruger, A., Lalancette, C., Tagett, R., Anton, E., Draghici, S., et al. (2011). A survey of small RNAs in human sperm. *Hum. Reprod.* 26, 3401–3412. doi: 10.1093/humrep/der329

Kruger, J., and Rehmsmeier, M. (2006). RNAhybrid: microRNA target prediction easy, fast and flexible. *Nucleic Acids Res.* 34, W451–454. doi: 10.1093/nar/gkl243

Langmead, B., and Salzberg, S. L. (2012). Fast gapped-read alignment with Bowtie 2. *Nat. Methods* 9, 357–359. doi: 10.1038/nmeth.1923

La Vignera, S., Condorelli, R. A., Balercia, G., Vicari, E., and Calogero, A. E. (2013). Does alcohol have any effect on male reproductive function? a review of literature. *Asian J. Androl.* 15, 221–225. doi: 10.1038/aja.2012.118

Lewis, B. P., Burge, C. B., and Bartel, D. P. (2005). Conserved seed pairing, often flanked by adenosines, indicates that thousands of human genes are microRNA targets. *Cell* 120, 15–20. doi: 10.1016/j.cell.2004.12.035

Liang, F., Diao, L., Liu, J., Jiang, N., Zhang, J., Wang, H., et al. (2014). Paternal ethanol exposure and behavioral abnormities in offspring: associated alterations in imprinted gene methylation. *Neuropharmacology* 81, 126–133. doi: 10.1016/j.neuropharm.2014.01.025

Liao, Y., Smyth, G. K., and Shi, W. (2014). Featurecounts: an efficient general purpose program for assigning sequence reads to genomic features. *Bioinformatics* 30, 923–930. doi: 10.1093/bioinformatics/btt656

Liu, W. M., Pang, R. T., Chiu, P. C., Wong, B. P., Lao, K., Lee, K. F., et al. (2012). Sperm-borne microRNA-34c is required for the first cleavage division in mouse. *Proc. Natl. Acad. Sci. U.S.A.* 109, 490–494. doi: 10.1073/pnas.1110368109

Love, M. I., Huber, W., and Anders, S. (2014). Moderated estimation of fold change and dispersion for RNA-seq data with DESeq2. *Genome Biol.* 15, 550. doi: 10.1186/s13059-014-0550-8

Machnicka, M. A., Milanowska, K., Osman Oglou, O., Purta, E., Kurkowska, M., Olchowik, A., et al. (2013). MODOMICS: a database of RNA modification pathways—2013 update. *Nucleic Acids Res.* 41, D262–D267. doi: 10.1093/nar/gks1007

Marczylo, E. L., Amoako, A. A., Konje, J. C., Gant, T. W., and Marczylo, T. H. (2012). Smoking induces differential miRNA expression in human spermatozoa: a potential transgenerational epigenetic concern? *Epigenetics* 7, 432–439. doi: 10.4161/epi.19794

Martin, M. (2011). Cutadapt removes adapter sequences from high-throughput sequencing reads. *EMBnet J.* 17, 10–12. doi: 10.14806/ej.17.1.200

Mouton, A. J., Maxi, J. K., Souza-Smith, F., Bagby, G. J., Gilpin, N. W., Molina, P. E., et al. (2016). Alcohol vapor inhalation as a model of alcohol-induced organ disease. *Alcohol. Clin. Exp. Res.* 40, 1671–1678. doi: 10.1111/acer.13133

Nakano, S., Suzuki, T., Kawarada, L., Iwata, H., Asano, K., and Suzuki, T. (2016). NSUN3 methylase initiates 5-formylcytidine biogenesis in human mitochondrial tRNA(Met). *Nat. Chem. Biol.* 12, 546–551. doi: 10.1038/nchembio.2099

Ostermeier, G. C., Dix, D. J., Miller, D., Khatri, P., and Krawetz, S. A. (2002). Spermatozoal RNA profiles of normal fertile men. *Lancet* 360, 772–777. doi: 10.1016/S0140-6736(02)09899-9

Ostermeier, G. C., Miller, D., Huntriss, J. D., Diamond, M. P., and Krawetz, S. A. (2004). Reproductive biology: delivering spermatozoan RNA to the oocyte. *Nature* 429, 154. doi: 10.1038/429154a

Ouko, L. A., Shantikumar, K., Knezovich, J., Haycock, P., Schnugh, D. J., and Ramsay, M. (2009). Effect of alcohol consumption on CpG methylation in the differentially methylated regions of H19 and IG-DMR in male gametes: implications for fetal alcohol spectrum disorders. *Alcohol. Clin. Exp. Res.* 33, 1615–1627. doi: 10.1111/j.1530-0277.2009.00993.x

Palijan, A., Fernandes, I., Verway, M., Kourelis, M., Bastien, Y., Tavera-Mendoza, L. E., et al. (2009). Ligand-dependent corepressor LCoR is an attenuator of progesterone-regulated gene expression. *J. Biol. Chem.* 284, 30275–30287. doi: 10.1074/jbc.M109.051201

Peng, H., Shi, J., Zhang, Y., Zhang, H., Liao, S., Li, W., et al. (2012). A novel class of tRNA-derived small RNAs extremely enriched in mature mouse sperm. *Cell Res.* 22, 1609–1612. doi: 10.1038/cr.2012.141

Politi, Y., Gal, L., Kalifa, Y., Ravid, L., Elazar, Z., and Arama, E. (2014). Paternal mitochondrial destruction after fertilization is mediated by a common endocytic and autophagic pathway in Drosophila. *Dev. Cell* 29, 305–320. doi: 10.1016/j.devcel.2014.04.005

Prescott, C. A., and Kendler, K. S. (1999). Genetic and environmental contributions to alcohol abuse and dependence in a population-based sample of male twins. *Am. J. Psychiatry* 156, 34–40. doi: 10.1176/ajp.156.1.34

Rahimipour, M., Talebi, A. R., Anvari, M., Sarcheshmeh, A. A., and Omidi, M. (2013). Effects of different doses of ethanol on sperm parameters, chromatin structure and apoptosis in adult mice. *Eur. J. Obstet. Gynecol. Reprod. Biol.* 170, 423–428. doi: 10.1016/j.ejogrb.2013.06.038

Rassoulzadegan, M., Grandjean, V., Gounon, P., Vincent, S., Gillot, I., and Cuzin, F. (2006). RNA-mediated non-mendelian inheritance of an epigenetic change in the mouse. *Nature* 441, 469–474. doi: 10.1038/nature04674

Reilly, J. N., McLaughlin, E. A., Stanger, S. J., Anderson, A. L., Hutcheon, K., Church, K., et al. (2016). Characterisation of mouse epididymosomes reveals a complex profile of microRNAs and a potential mechanism for modification of the sperm epigenome. *Sci. Rep.* 6:31794. doi: 10.1038/srep31794

Ro, S., Ma, H. Y., Park, C., Ortogero, N., Song, R., Hennig, G. W., et al. (2013). The mitochondrial genome encodes abundant small noncoding RNAs. *Cell Res.* 23, 759–774. doi: 10.1038/cr.2013.37

Rodgers, A. B., Morgan, C. P., Bronson, S. L., Revello, S., and Bale, T. L. (2013). Paternal stress exposure alters sperm microRNA content and reprograms offspring HPA stress axis regulation. *J. Neurosci.* 33, 9003–9012. doi: 10.1523/JNEUROSCI.0914-13.2013

Rodgers, A. B., Morgan, C. P., Leu, N. A., and Bale, T. L. (2015). Transgenerational epigenetic programming via sperm microRNA recapitulates effects of paternal stress. *Proc. Natl. Acad. Sci. U.S.A.* 112, 13699–13704. doi: 10.1073/pnas.1508347112

Rompala, G. R., Finegersh, A., and Homanics, G. E. (2016). Paternal preconception ethanol exposure blunts hypothalamic-pituitary-adrenal axis responsivity and stress-induced excessive fluid intake in male mice. *Alcohol* 53, 19–25. doi: 10.1016/j.alcohol.2016.03.006

Rompala, G. R., Finegersh, A., Slater, M., and Homanics, G. E. (2017). Paternal preconception alcohol exposure imparts intergenerational alcohol-related behaviors to male offspring on a pure C57BL/6J background. *Alcohol* 60, 169–177. doi: 10.1016/j.alcohol.2016.11.001

Schaefer, M., Pollex, T., Hanna, K., Tuorto, F., Meusburger, M., Helm, M., et al. (2010). RNA methylation by Dnmt2 protects transfer RNAs against stress-induced cleavage. *Genes Dev.* 24, 1590–1595. doi: 10.1101/gad.586710

Schagdarsurengin, U., and Steger, K. (2016). Epigenetics in male reproduction: effect of paternal diet on sperm quality and offspring health. *Nat. Rev. Urol.* 13, 584–595. doi: 10.1038/nrurol.2016.157

Schuster, A., Skinner, M. K., and Yan, W. (2016a). Ancestral vinclozolin exposure alters the epigenetic transgenerational inheritance of sperm small noncoding RNAs. *Environ. Epigenet.* 2:dvw001. doi: 10.1093/eep/dvw001

Schuster, A., Tang, C., Xie, Y., Ortogero, N., Yuan, S., and Yan, W. (2016b). Spermbase: a database for sperm-borne RNA contents. *Biol. Reprod.* 95, 99. doi: 10.1095/biolreprod.116.142190

Selitsky, S. R., and Sethupathy, P. (2015). tDRmapper: challenges and solutions to mapping, naming, and quantifying tRNA-derived RNAs from human small RNA-sequencing data. *BMC Bioinformatics* 16:354. doi: 10.1186/s12859-015-0800-0

Sharma, U., Conine, C. C., Shea, J. M., Boskovic, A., Derr, A. G., Bing, X. Y., et al. (2016). Biogenesis and function of tRNA fragments during sperm maturation and fertilization in mammals. *Science* 351, 391–396. doi: 10.1126/science.aad6780

Sharma, U., and Rando, O. J. (2017). Metabolic Inputs into the Epigenome. *Cell Metab.* 25, 544–558. doi: 10.1016/j.cmet.2017.02.003

Short, A. K., Fennell, K. A., Perreau, V. M., Fox, A., O'Bryan, M. K., Kim, J. H., et al. (2016). Elevated paternal glucocorticoid exposure alters the small noncoding RNA profile in sperm and modifies anxiety and depressive phenotypes in the offspring. *Transl. Psychiatry* 6, e837. doi: 10.1038/tp.2016.109

Short, A. K., Yeshurun, S., Powell, R., Perreau, V. M., Fox, A., Kim, J. H., et al. (2017). Exercise alters mouse sperm small noncoding RNAs and induces a transgenerational modification of male offspring conditioned fear and anxiety. *Transl. Psychiatry* 7, e1114. doi: 10.1038/tp.2017.82

Spadafora, C. (2017). Sperm-mediated transgenerational inheritance. *Front. Microbiol.* 8:2401. doi: 10.3389/fmicb.2017.02401

Stuppia, L., Franzago, M., Ballerini, P., Gatta, V., and Antonucci, I. (2015). Epigenetics and male reproduction: the consequences of paternal lifestyle on fertility, embryo development, and children lifetime health. *Clin. Epigenetics* 7, 120. doi: 10.1186/s13148-015-0155-4

Sullivan, R. (2016). Epididymosomes: role of extracellular microvesicles in sperm maturation. *Front. Biosci.* 8, 106–114. doi: 10.2741/s450

Treutlein, J., and Rietschel, M. (2011). Genome-wide association studies of alcohol dependence and substance use disorders. *Curr. Psychiatry Rep.* 13, 147–155. doi: 10.1007/s11920-011-0176-4

Tuorto, F., Liebers, R., Musch, T., Schaefer, M., Hofmann, S., Kellner, S., et al. (2012). RNA cytosine methylation by Dnmt2 and NSun2 promotes tRNA stability and protein synthesis. *Nat. Struct. Mol. Biol.* 19, 900–905. doi: 10.1038/nsmb.2357

Wang, Q., and Cooney, A. J. (2013). Revisiting the role of GCNF in embryonic development. *Semin. Cell Dev. Biol.* 24, 679–686. doi: 10.1016/j.semcdb.2013.08.003

Yan, Q., and Guan, M. X. (2004). Identification and characterization of mouse TRMU gene encoding the mitochondrial 5-methylaminomethyl-2-thiouridylate-methyltransferase. *Biochim. Biophys. Acta* 1676, 119–126. doi: 10.1016/j.bbaexp.2003.11.010

Yang, Q., Lin, J., Liu, M., Li, R., Tian, B., Zhang, X., et al. (2016). Highly sensitive sequencing reveals dynamic modifications and activities of small RNAs in mouse oocytes and early embryos. *Sci. Adv.* 2:e1501482. doi: 10.1126/sciadv.1501482

Young-Wolff, K. C., Enoch, M. A., and Prescott, C. A. (2011). The influence of gene-environment interactions on alcohol consumption and alcohol use disorders: a comprehensive review. *Clin. Psychol. Rev.* 31, 800–816. doi: 10.1016/j.cpr.2011.03.005

Ystrom, E., Reichborn-Kjennerud, T., Aggen, S. H., and Kendler, K. S. (2011). Alcohol dependence in men: reliability and heritability. *Alcohol. Clin. Exp. Res.* 35, 1716–1722. doi: 10.1111/j.1530-0277.2011.01518.x

Yuan, S., Schuster, A., Tang, C., Yu, T., Ortogero, N., Bao, J., et al. (2016). Sperm-borne miRNAs and endo-siRNAs are important for fertilization and preimplantation embryonic development. *Development* 143, 635–647. doi: 10.1242/dev.131755

Conflict of Interest Statement: The authors declare that the research was conducted in the absence of any commercial or financial relationships that could be construed as a potential conflict of interest.

frontiers in Genetics

ORIGINAL RESEARCH
published: 27 August 2018
doi: 10.3389/fgene.2018.00323

Distinct Roles for Two Chromosome 1 Loci in Ethanol Withdrawal, Consumption, and Conditioned Place Preference

*Laura B. Kozell, Deaunne L. Denmark, Nicole A. R. Walter and Kari J. Buck**

Department of Behavioral Neuroscience, Portland Veterans Affairs Medical Center and School of Medicine, Oregon Health and Science University, Portland, OR, United States

OPEN ACCESS

Edited by:
Kristin Hamre, University of Tennessee Health Science Center, United States

Reviewed by:
Camron D. Bryant, School of Medicine, Boston University, United States
Juko Ando, Keio University, Japan

***Correspondence:**
Kari J. Buck
buckk@ohsu.edu

Specialty section:
This article was submitted to Behavioral and Psychiatric Genetics, a section of the journal Frontiers in Genetics

Received: *07 May 2018*
Accepted: *30 July 2018*
Published: *27 August 2018*

Citation:
Kozell LB, Denmark DL, Walter NAR and Buck KJ (2018) Distinct Roles for Two Chromosome 1 Loci in Ethanol Withdrawal, Consumption, and Conditioned Place Preference. Front. Genet. 9:323. doi: 10.3389/fgene.2018.00323

We previously identified a region on chromosome 1 that harbor quantitative trait loci (QTLs) with large effects on alcohol withdrawal risk using both chronic and acute models in mice. Here, using newly created and existing QTL interval-specific congenic (ISC) models, we report the first evidence that this region harbors two distinct alcohol withdrawal QTLs (*Alcw1*$_1$and *Alcw1*$_2$), which underlie 13% and 3–6%, respectively, of the genetic variance in alcohol withdrawal severity measured using the handling-induced convulsion. Our results also precisely localize *Alcw1*$_1$ and *Alcw1*$_2$ to discreet chromosome regions (syntenic with human 1q23.1–23.3) that encompass a limited number of genes with validated genotype-dependent transcript expression and/or non-synonymous sequence variation that may underlie QTL phenotypic effects. ISC analyses also implicate *Alcw1*$_1$and *Alcw1*$_2$ in withdrawal-induced anxiety-like behavior, representing the first evidence for their broader roles in alcohol withdrawal beyond convulsions; but detect no evidence for *Alcw1*$_2$ involvement in ethanol conditioned place preference (CPP) or consumption. Our data point to high-quality candidates for *Alcw1*$_2$, including genes involved in mitochondrial respiration, spatial buffering, and neural plasticity, and to *Kcnj9* as a high-quality candidate for *Alcw1*$_1$. Our studies are the first to show, using two null mutant models on different genetic backgrounds, that *Kcnj9* $^{-/-}$ mice demonstrate significantly less severe alcohol withdrawal than wildtype littermates using acute and repeated exposure paradigms. We also demonstrate that *Kcnj9* $^{-/-}$ voluntarily consume significantly more alcohol (20%, two-bottle choice) than wildtype littermates. Taken together with evidence implicating *Kcnj9* in ethanol CPP, our results support a broad role for this locus in ethanol reward and withdrawal phenotypes. In summary, our results demonstrate two distinct chromosome 1 QTLs that significantly affect risk for ethanol withdrawal, and point to their distinct unique roles in alcohol reward phenotypes.

Keywords: quantitative trait locus (QTL), anxiety, convulsions, consumption, GIRK

INTRODUCTION

Abuse of alcohol, prescription and other sedative-hypnotic drugs is among the top five health problems identified in the U.S. (Office of National Drug Control Policy, 2004). Alcohol dependence (alcoholism) and abuse affect up to 30% of Americans (Hasin et al., 2007) and complicate most chronic illnesses. Alcohol dependence is also among the most highly heritable addictive disorders (Goldman et al., 2005). However, alcoholism is a heterogeneous disorder with a complex interaction between genetic and environmental factors, making conclusive identification of genetic determinants difficult to elucidate (Ducci and Goldman, 2012). This continues to hamper development of effective therapeutic and prevention strategies.

Although animal models cannot duplicate alcoholism, models for specific factors (e.g., withdrawal and reward phenotypes) have proven useful for identifying potential determinants of liability in humans. Withdrawal is a hallmark of alcohol physiological dependence, and constitutes a motivational force that can maintain the cycle of use and abuse (Little et al., 2005). The handling-induced convulsion (HIC) is a robust measure of CNS hyperexcitability in mice, and a sensitive measure of alcohol withdrawal using acute, repeated, and chronic alcohol exposure models (Goldstein and Pal, 1971; Kosobud and Crabbe, 1986; Crabbe et al., 1991; Metten et al., 2007; Chen et al., 2008). Alcohol withdrawal convulsions occur in all species tested, including humans (Friedman, 1980), and have a clear genetic contribution (Goldstein, 1973; Metten and Crabbe, 1999; Lutz et al., 2006). We previously mapped significant quantitative trait loci (QTLs) with large effects on predisposition to physiological dependence and associated withdrawal convulsions following chronic and acute alcohol exposure in mice (Buck et al., 1997, 2002) to a broad region of chromosome 1.

High resolution QTL mapping is crucial to progress toward identification of the genes that underlie QTL phenotypic effects and, just as importantly, to assess potential pleiotropic effects. One of the most powerful strategies to precisely map a QTL employs interval-specific congenic (ISC) models (Darvasi, 1997; Fehr et al., 2002; Shirley et al., 2004). Because of the near elimination of genetic "noise" from loci elsewhere in the genome, comparisons between congenic and wildtype (WT) animals are invaluable to elucidate QTL actions. Using this strategy, we previously confirmed and mapped a QTL for acute alcohol withdrawal (*Alcw1*) to a maximal 1.7 Mb interval of chromosome 1, and also localized a QTL affecting chronic alcohol withdrawal (*Alcdp1*) to the same 1.7 Mb interval (Kozell et al., 2008). We also mapped a QTL (*Pbw1*) proven to affect both pentobarbital and zolpidem withdrawal to a distinct 0.44 Mb interval of chromosome 1 (Kozell et al., 2009). However, currently, it is unproven whether one, two, or possibly even more distinct QTLs within this QTL rich region in fact affect alcohol withdrawal risk. The present studies report the creation of an ISC model (R3), analyses of which proved invaluable to confirm that at least two distinct alcohol withdrawal QTLs on chromosome 1 (now termed $Alcw1_1$ and $Alcw1_2$) exist within the original broad *Alcw1* region (Buck et al., 1997), and we demonstrate that each significantly affects alcohol withdrawal risk.

While some withdrawal signs are genetically correlated with HIC severity (i.e., Kosobud and Crabbe, 1986; Belknap et al., 1987; Feller et al., 1994; tremors, hypoactivity, emotionality), others are not (i.e., tail stiffness; Kosobud and Crabbe, 1986). Thus, assessment of HICs can inform analyses for signs correlated to alcohol withdrawal, but represent only part of a complex syndrome. Furthermore, we and others have noted that the chromosomal region focused on in the present studies is a hotbed for confirmed and putative QTLs for a variety of phenotypes relevant to alcohol actions and many others (Kerns et al., 2005; Denmark and Buck, 2008), including for phenotypes shown to be significantly genetically correlated with risk for alcohol withdrawal convulsions, e.g., ethanol consumption (Metten et al., 2014). Therefore, the present studies also expand upon previous analyses and include additional measures of withdrawal (i.e., anxiety-like behavior) and reward phenotypes (i.e., alcohol self-administration and ethanol conditioned place preference [CPP]) to begin to assess the potential broader actions of $Alcw1_1$ and $Alcw1_2$. In summary, our results confirm two alcohol withdrawal QTLs on chromosome 1, and also begin to elucidate their distinct broader roles in alcohol withdrawal and reward behaviors.

MATERIALS AND METHODS

Animals

C57BL/6J (B6) and DBA/2J (D2) inbred strain breeders were purchased from the Jackson Laboratory. The four chromosome 1 congenic models were all created in our colony at the Veterinary Medical Unit of the Portland VA Medical Center, and include: a newly created D2.B6 ISC (R3), a recently created D2.B6 ISC (R2; Walter et al., 2017), D2.B6$^{-D1Mit206}$ (Kozell et al., 2008), and a reciprocal (B6.D2) ISC (R8; Kozell et al., 2008). To maintain our congenic models on an inbred (D2 or B6) genetic background, congenic heterozygotes were backcrossed to background strain animals from the Jackson Laboratory every third generation. *Kcnj9* encodes the G protein-coupled inwardly-rectifying potassium channel subunit 3 (GIRK3). One of the two *Kcnj9* null mutant models (inbred B6 genetic background; Torrecilla et al., 2002) was originally generously provided by Dr. Kevin Wickman, and has been used extensively and maintained in our colony for over 20 generations using a heterozygote (B6-*Kcnj9*$^{+/-}$) x B6-*Kcnj9*$^{+/-}$ breeding strategy, and backcrossing to B6 strain mice every third generation as is required to maintain integrity. The other null mutant *Kcnj9*$^{-/-}$ model [inbred D2 genetic background; Kozell et al., 2009] used in these studies was created and maintained in our colony as above. A total of 1192 mice were behaviorally tested, with males and females used in approximately equal numbers: 670 congenic and appropriate WT animals, and 526 *Kcnj9*$^{-/-}$, *Kcnj9*$^{+/-}$ and WT littermates. Animals were group housed 2–4 per cage by sex. Mouse chow (Purina #5001) and water were available *ad libitum*, and lights were on from 6:00 to 18:00 with the room temperature maintained at 22.0 ± 1.0°C. All procedures were approved by the VA Medical Center and Oregon Health and Science University Institutional Animal Care and Use Committees in accordance

with United States Department of Agriculture and United States Public Health Service guidelines.

Development of D2.B6 ISC Strains

We previously showed that a QTL affecting acute withdrawal severity (*Alcw1*) was captured within the introgressed interval of a chromosome 1 congenic strain, D2.B6$^{-D1Mit206}$ (Kozell et al., 2008). Genotypic analyses delimited its maximal introgressed interval to 151.6-177.5 Mb. Here, we used D2.B6$^{-D1Mit206}$ as our point of departure to create a novel D2.B6 ISC model (R3). D2.B6$^{-D1Mit206}$ congenics were crossed to D2 inbred strain mice to yield F_1 (D2.B6$^{-D1Mit206}$ X D2) animals, which were then backcrossed to D2 mice. Individual progeny were genotyped using *D1Mit* and single nucleotide polymorphism (SNP) markers within or flanking the acute and chronic alcohol withdrawal QTLs on chromosome 1 (Buck et al., 1997, 2002; http://www.informatics.jax.org/searches/marker_report.cgi) to identify recombinant mice, thereby defining the boundaries of introgressed intervals. Individual recombinants were again backcrossed to D2 strain mice, resulting in multiple offspring with the same recombination. A final intercross used performed to isolate the donor homozygotes, which constitute a finished ISC strain. Congenic and appropriate WT animals are compared in phenotypic analyses to test for QTL "capture" within the differential introgressed congenic interval, as in our previous work (Kozell et al., 2008).

Alcohol Withdrawal HIC Phenotypic Analyses

Physiological dependence is operationally defined as the manifestation of physical disturbances (withdrawal symptoms) after alcohol administration is suspended. Handling-induced convulsions (HICs), a sensitive index of withdrawal severity (Crabbe et al., 1991; Goldstein and Pal, 1971), were used initially to monitor genetic variation in alcohol withdrawal severity.

Acute Alcohol Model

(McQuarrie and Fingl, 1958) first demonstrated a state of withdrawal CNS hyperexcitability after a single hypnotic dose of ethanol (4 g/kg, p.o.). Details of the acute alcohol withdrawal procedure and HIC scoring system used in our work have been published (Metten et al., 1998; Kozell et al., 2008). Mice were scored twice for baseline (pre-ethanol) HICs 20 min apart, followed by a single hypnotic dose of ethanol (4 g/kg, i.p., in 20% w/v in saline) and then scored hourly between 2 and 12 h post-ethanol administration. To create an index of alcohol withdrawal independent of potential individual and/or genetic model differences in baseline HIC scores, post-ethanol HIC scores were corrected for individual baseline scores as in previous work (Kozell et al., 2008). Acute alcohol withdrawal severity was calculated as the area under the curve (i.e., the sum of the post-ethanol HIC scores) from 2 to 12 h post-ethanol.

Repeated Alcohol Model

Some animals were tested using an established repeated alcohol exposure paradigm (Chen et al., 2008). Animals were moved into a procedure room at least 1 h prior to beginning the experiment. Body weights were recorded before each ethanol injection. Baseline HICs were measured twice (20 min apart), immediately followed by a first dose of ethanol (4 g/kg) at 0 h, with alcohol administration repeated 8 and 20 h later, for a total of three doses. HIC testing began at 22 h and continued hourly through 32 h. Alcohol withdrawal severity was indexed as described above. Acute alcohol withdrawal severity was calculated as the area under the curve (i.e., the sum of the post-ethanol HIC scores) from 2 to 12 h post-ethanol.

Anxiety-Like Behavior in the Elevated Zero Maze (EZM) Using Alcohol Withdrawn and Control Animals

The EZM apparatus and procedure used to assess anxiety-like behavior were based on previous studies (Kliethermes et al., 2004; Milner and Crabbe, 2008; Barkley-Levenson and Crabbe, 2015). The apparatus has an external diameter of 45 cm and consists of four proportional arms, two open and two closed, with a black acrylic floor (5.5 cm across) elevated 46 cm above the floor and placed in a large cob bedding filled tub to prevent potential fall-related injuries. Closed arm walls are 11 cm tall clear acrylic, with a small (3 mm) lip along the inner and outer edges of open arms to prevent falls. All testing occurred under dim lighting (15–20 lux) and was videotaped from above with camcorders. Mice were tested on two sets of two mazes concurrently with an opaque barrier between mazes, and mice were placed onto an open arm facing a closed arm at the start of a test. Before each subject was placed in the apparatus, the floor and walls were sprayed with 10% isopropanol and wiped with clean paper towels to eliminate odors.

Habituation

Mice were habituated to the apparatus for three days (prior to beginning ethanol dependence induction), and moved into the procedure room at least 1 h prior to the first habituation session. On each daily habituation, mice were removed from home cages and placed onto the open arm portion at the beginning of each 10 min session. Arm and placement remained the same throughout, and animals remained in the procedure room until transfer to inhalation chambers.

Alcohol Dependence Induction

Details of the chronic ethanol exposure method used to induce physical dependence have been published, and involve a standard paradigm in which adult mice are continuously exposed to ethanol vapor for 72 h (Terdal and Crabbe, 1994). Mice were weighed and scored twice (20 min apart) for baseline HICs prior to receiving either saline (air-control group) or a loading dose of ethanol (1.5 g/kg ethanol, i.p., 20% in saline). In addition, all mice received daily injections of pyrazole-hydrochloride (68 mg/kg, i.p.; alcohol dehydrogenase inhibitor) to stabilize blood and brain ethanol levels. Levels of ethanol in vapor (typically 6-8 mg ethanol/liter air) were selected to achieve approximately equal blood ethanol concentration (BEC) values across individuals and genetic models. After 24 and 48 h of ethanol vapor exposure, blood samples (20 μl) were drawn from 20 mice by tail nicking with a capillary tube, serving as an additional check

on inhalation procedure efficacy in each pass and allowing minor adjustments to ethanol flow rates to maintain BEC values near the desired blood level (∼1.5 mg/ml). At 72 h, all mice were removed from inhalation chambers. Blood samples were drawn from the ethanol-exposed mice for BEC analysis, and control animals were tail-nicked, but no blood was collected. Blood samples were analyzed soon after collection using headspace gas chromatography exactly as previously published (Finn et al., 2007).

EZM Testing

Animals were moved into the procedure room at least 1 h prior to the testing session. Ethanol-dependent and control animals were tested in the EZM (10 min sessions) 24 and 48 h after removal from the chambers. Some genotypes (R2) were also tested 7 h after removal from chambers. Locomotor activity (distance traveled), time spent in open arms, and entries into arms were measured using Ethovision 8.5 XT video-tracking software (Noldus Information Technology, Inc.). Head dips in the same video clip were scored by an observer blinded to experimental treatment.

Ethanol CPP

R3 congenic and WT animals (D2 genetic background) were tested using an established apparatus and paradigm (Cunningham, 2014). R8 congenic and WT animals (B6 genetic background) were tested using a slightly modified protocol (Tipps et al., 2015). CPP chambers (San Diego Instruments) are housed in illuminated, ventilated, and sound-attenuating chambers (AccuScan Instruments Inc) and consist of clear plastic walls 30 L × 15 W × 15 H cm equipped with exchangeable floor panels, which are themselves two textured interchangeable halves. The "grid" floor is constructed of 2.3 mm stainless steel rods mounted 6.4 mm apart, and the "hole" floor a stainless steel panel with 6.4 mm round holes aligned with 9.5 mm staggered centers. Horizontal activity and animal location are measured using photocell beam interruptions recorded by a fully automated, computer-connected system. The protocol involves three phases: habituation (1 session), conditioning (8–16 sessions) and testing (1–4 sessions). Animals were randomly assigned to conditioning groups and the groups counter-balanced. Chamber and floors were wiped down with a damp sponge after each animal. Sessions were conducted 5 days a week with a 2 day break between the first four and final four conditioning sessions for R3 congenic and WT littermate testing. Testing for R8 congenic and background strain animals was similar, but without breaks. Each animal was handled, weighed, and injected (i.p.) with saline (20 ml/kg) or ethanol (2 g/kg; 12.5% ethanol in saline) just before placement into the apparatus for each session. During the entire experiment the orientation of the floors remained the same for individual animals (i.e., if the grid floor was on the left side for habituation, it was on the left side for conditioning and test sessions).

On the habituation day, animals were injected with saline and placed immediately in CPP chambers with a hole floor on one side and grid floor on the other, with free access to both sides of the chamber. Habituation sessions lasted for 30 and 5 min, respectively, for R3 and R8 analyses. On four alternating days, animals were then conditioned using ethanol or saline during 5 min sessions with a single floor type (grid or hole), blocked by a clear acrylic divider from the other side of the chamber. R3 animals had 2 days off followed by another 4 conditioning sessions, for a total of 8 conditioning sessions (4 ethanol and 4 saline sessions). For R8 analyses, no breaks occurred between the sessions; instead, testing was performed after every 4 conditioning trials, for a total of 4 tests and 16 conditioning trials. Conditioning sessions were 5 min for R3 and WT littermates, and 15 min for R8 and WT animals. On the final test day, mice were injected with saline (no drug on board) and placed in the CPP apparatus for 30 min (R3 and WT) or 15 min (R8 and WT), with both floor types (grid and hole) available. Amount of time spent on the ethanol-paired floor (hole or grid) was the primary dependent variable measured.

Two-Bottle Choice Drinking

Two-bottle choice drinking was tested using a well-established paradigm (Phillips et al., 1994). All animals tested were acclimated to single housing in standard shoebox housing with paper bedding and a wire-top lid for at least 1 week prior to start of the experiment.

Ethanol Consumption and Preference

R8 congenic and WT animals received 24 h access to two 25 ml bottles containing tap water for 4 days, prior to exposure to 24 h access to ethanol (3, 6, 10, and 20%, 4 days each) or tap water. In a separate study, *Kcnj9*$^{-/-}$ (B6 background) and WT littermates were assessed for ethanol consumption and preference using the same procedure. Ethanol consumption (expressed in g/kg/day) of each ethanol solution was calculated as the average of the 2nd and 4th day the solution was presented, and was analyzed as previously described (Phillips et al., 1994). Ethanol preference compared to tap water was calculated as volume ethanol/total fluid consumed in g/kg/day, as in our previous work (Milner et al., 2015).

Tastants (Saccharin, Quinine, and KCl)

Following a 4–5 day washout period (water exposure only), mice from the studies above were assessed for tastant consumption and preference. Animals had 24 h access to saccharin (0.033 and 0.066%), quinine (15 and 30 μM) and KCl (100 and 200 mM) for 4 days each. Consumption was calculated as the average of 2nd and 4th days of solution presentation, and expressed as mg/kg/day. Tastant preference compared to tap water was calculated as volume tastant/volume total fluid consumed in g/kg/day.

Genotype Analyses

DNA was extracted from ear punch tissue using the QuickExtract™ DNA Extraction Solution (Lucigen) according to manufacturer instructions. PCR amplification and gel electrophoresis was performed using SNP and simple sequence length polymorphism markers from the *D1Mit* series for mouse chromosome 1 (www.informatics.jax.org). *Kcnj9*$^{-/-}$, *Kcnj9*$^{-/+}$, and WT littermates were differentiated using a PCR-based

assay with a common forward primer (G3com) and two reverse primers (G3WT and G3KO). Null mutant and wildtype animals produce 500 and 645 bp PCR products, respectively, and a heterozygote produces both. All PCR reactions are performed using Qiagen HotStar under standard conditions with a 55°C annealing temperature. The primer sequences are as follows: G3com (GATACTAGACTAGCGTAACTCTGGAT), G3WT (GATAAAGAGCACAGACTGGGTGTCG), G3KO (CAAAGCTGAGACATCTCTTTGGCTCTG).

Alcw1$_1$ and *Alcw1*$_2$ Candidate Genes

Protein coding genes and non-coding RNAs within the maximal QTL interval were identified using Ensembl database for the reference B6 genome. (www.ensembl.org, GRCm38.p5). EMBL-EBI (https://www.ebi.ac.uk/gxa/home) was searched for evidence of brain expression in mouse or other species. Sequence variation was queried for non-synonymous coding region changes in any annotated transcript for each gene using MGI (Jackson Labs) database, specifically for B6 vs. D2 SNPs (single nucleotide polymorphisms). Gene expression analyses in our chromosome 1 congenics vs. background strain animals were from our previous publications of microarray and/or QPCR data (Denmark and Buck, 2008; Kozell et al., 2009; Walter et al., 2017).

Data Analyses

For analyses of normally distributed data (based on a nonsignificant Shapiro-Wilks test), we performed analysis of variance (ANOVA) followed by a post-hoc (Tukey) test. For comparisons in which data were not normally distributed, analyses using a non-parametric Kruskal-Wallis ANOVA on ranks, which generates a U statistic for two groups and an H statistic for more than 2 groups, followed by a post hoc Conover-Inman Test (Systat 13; Systat Systems, Inc.) were performed. Anxiety-like behavior was analyzed using an ANOVA followed by a one-tailed post-hoc Tukey's test, as in previous work showing heightened anxiety in alcohol-withdrawn animals compared to controls (Kliethermes et al., 2004). Ethanol CPP was assessed using a one sample t-test with the mean set to 0.5 (no preference). Data throughout are presented as the mean ± SEM, with significance ($p < 0.05$) indicated based on two-tailed analyses (unless one-tailed is specified). Percentage of total variance attributable to each R2 and R3 congenic strain for acute alcohol withdrawal was calculated based on R^2-values from a one-way ANOVA by strain ($SS_{betweenstrains}/SS_{total}$) (Belknap et al., 1996).

RESULTS

R3 Congenic Interval Captures an Alcohol Withdrawal QTL on Chromosome 1 (*Alcw1*$_2$)

We report the creation of a novel D2.B6 ISC model, R3. Genotypic analyses of R3 determined the minimal introgressed interval to be 7.2 Mb (164.30–171.35 Mb; maximal 164.17–171.36 Mb; build GRCm38). As shown in **Figure 1**, we tested for QTL capture by phenotypic comparisons of R3 congenic and WT animals using the same robust behavioral phenotype (acute alcohol withdrawal severity measured by the HIC) used to initially detect and confirm an alcohol withdrawal QTL to a large region of chromosome 1 (Buck et al., 1997). A main effect of sex is apparent ($p = 1.5 \times 10^{-4}$), but with no genotype x sex interaction ($p > 0.2$, NS), HIC data for both sexes were collapsed to increase statistical power of the analyses. A main effect of treatment was evident, with R3 congenics demonstrating significantly less severe withdrawal compared to background strain animals (withdrawal severity scores = 17.2 ± 0.8, and 21.8 ± 1.6, respectively; $F_{(1,142)} = 12.5$, $p = 0.001$, **Figure 1B**). Our results confirm that a gene(s) affecting alcohol withdrawal is captured within the R3 introgressed interval.

Comparison of R3 and R2 ISCs Delineates a Second QTL With a Larger Effect Size on Risk for Alcohol Withdrawal (*Alcw1*$_1$)

We recently created a second D2.B6 ISC (R2) with a larger introgressed interval (minimal 10.2 Mb, 164.3–174.5 Mb; maximal 164.1–174.6 Mb; Build GRCm38; Walter et al., 2017), which spans entirely and extends beyond the R3 introgressed interval (**Figure 2**). Our data clearly show that the effect size accounted for in the R2 congenic is significantly greater than that accounted for by R3, contributing 16 and 3%, respectively, of the genetic variance in acute alcohol withdrawal severity. Taken together, our results confirm the existence of an alcohol withdrawal QTL within the R3 introgressed interval (contributing 3% of the genetic variance), and point to the existence of an additional alcohol withdrawal QTL also within the larger R2 introgressed interval (which, by subtraction, we estimate contributes 13% of the genetic variance). Given the larger effect size of the latter, these two QTLs are termed *Alcw1*$_2$ and *Alcw1*$_1$, respectively. The minimal *Alcw1*$_1$ interval is 3.11 Mb (171.37–174.47 MB), and maximal 3.28 Mb (171.35–174.63 Mb), which includes proximal (0.02 Mb) and distal (0.16 Mb) boundary regions.

Comparison of R3 and R8 ISC Models Suggest More Precise Localization of *Alcw1*$_2$

Our previous analyses comparing R8 congenic and background strain (B6) animals confirmed capture of a locus/loci affecting alcohol withdrawal severity using both acute and chronic models, and contributes 6% of the genetic variance in acute alcohol withdrawal severity (Kozell et al., 2008). As illustrated in **Figure 2**, the small R8 introgressed interval (1.2–1.7 Mb; minimal 170.9–172.1 Mb, maximal 170.4–172.1 Mb; Build GRCm38p5; Kozell et al., 2008) largely overlaps that of R3. Furthermore, given the comparable QTL effect size accounted for by these two congenic models (6 and 3%, respectively), *Alcw1*$_2$is likely captured in both R8 and R3. If so, *Alcw1*$_2$ would now be localized to a very narrow 405-923 Kb interval (minimal 170.94–171.35 Mb, maximal 170.44–171.37 Mb). Arguably even more importantly, the creation of R3 and R8 *Alcw1*$_2$ congenic models with different inbred D2 and B6 genetic backgrounds, respectively, are invaluable genetic tools to begin to test

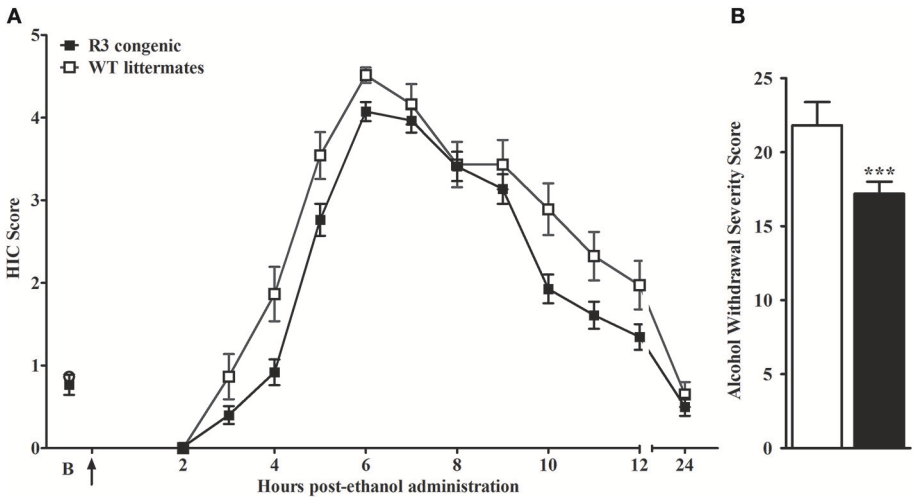

FIGURE 1 | R3 congenic animals demonstrate a modest but significant reduction in alcohol withdrawal severity compared to WT animals. **(A)** HIC time course before and after ethanol administration (4 g/kg, i.p., indicated by the arrow) for R3 congenic and WT animals ($n = 110$ and 37, respectively). HICs were scored at baseline ("B", i.e., pre-ethanol) and then hourly from 2 to 12 h post-ethanol and then again at 24 h. Baseline HIC scores did not differ between genotypes [$F_{(1, 143)} = 0.1$, $p = 0.78$, NS]. As ethanol is metabolized, HIC scores increase above baseline beginning about 4 h post-ethanol, indicating a state of withdrawal hyperexcitability, which peaks approximately 6–7 h post-ethanol exposure. **(B)** Alcohol withdrawal severity, calculated as the mean AUC12 ± SEM (from 2 to 12 h, and corrected for baseline scores), was significantly reduced in the R3 congenic compared to WT background strain animals (***$p = 0.001$).

potential pleiotropic *Alcw1*$_2$ effects on diverse phenotypes, including behavioral tests limited by genetic background (below).

Alcw1$_1$ and *Alcw1*$_2$ Interval Resident Genes With Validated Expression in the Brain

The R2 congenic introgressed interval spans the R3 interval and extends distally another 3.28 Mb, (maximal interval; See **Figure 2**). *Alcw1*$_1$ is defined as that part of the R2 interval that does *not* overlap with the R3 interval. The minimal *Alcw1*$_1$ interval contains 77 protein coding genes and an additional 3 coding genes lie within the maximal boundaries. Within the maximal interval, there are also 29 pseudogenes 10 long noncoding RNAs, and 9 short noncoding RNAs annotated. A total of 48 coding genes have confirmed expression in the brain and are presented in **Table 1**. Twenty-five have at least one B6 vs. D2 nonsynonymous coding SNP, and 20 have evidence of differential mRNA expression between congenic and background strain mice, indicating *cis*-regulation.

The *Alcw1*$_2$ interval as shown in **Figure 2** is defined as donor region that is common to the reciprocal R8 and R3 congenic strains. The minimal region contains 19 protein coding genes with an additional 9 in the boundary regions. All of these exhibit some evidence of brain expression and are listed in **Table 2**. Thirteen have at least one B6 vs. D2 nonsynonymous coding SNP, and 15 have evidence of differential mRNA expression between congenic and background strain mice, indicating *cis*-regulation. Within the maximal interval, there are also 5 pseudogenes, 4 long noncoding RNAs, and 7 short noncoding RNAs annotated. Two coding genes (*Pfdn2* and *Klhdc9*) are within the shared boundary region (i.e., *Alcw1*$_2$ distal boundary and proximal *Alcw1*$_1$ boundary).

Anxiety-Like Behavior in *Alcw1*$_1$ and *Alcw1*$_2$ Congenic Models in Alcohol Dependent and Control Animals

To begin to assess the potential broader effects of *Alcw1*$_1$ beyond alcohol withdrawal enhanced HICs, we tested ISC (R3 and R2) and appropriate WT background strain animals for withdrawal-induced anxiety-like behavior in the EZM. We initially employed the acute alcohol withdrawal paradigm, but were unable to reliably detect any anxiety-like behavior using the B6.D2 R8 congenic (not shown). Thus, we report here results for the chronic alcohol withdrawal protocol in which animals are rendered alcohol-dependent by continuous (72 h) exposure to ethanol vapor in an inhalation chamber and compared to appropriate controls (adjacent air control chambers). R3 congenic and WT littermates were tested 24 and 48 h after removal from chambers. R2 congenic and WT littermates were tested at 7 (see **Supplementary Figure 1**), 24 and 48 h after removal from the chambers. Main effects of treatment (ethanol withdrawn vs. air control) and genotype (R2 vs. WT, R3 vs. WT), as well as potential genotype X treatment (GXT) interactions were assessed (below).Genotype-dependent differences in BEC values were not detected after 24, 48, or 72 h continuous ethanol vapor exposure (**Supplementary Table 1**; all $p > \sim 0.3$, NS). We applied an EZM habituation procedure shown to be crucial to detecting alcohol withdrawal associated anxiety-like behavior in dependent mice (Kliethermes et al., 2004): all animals were placed in the EZM apparatus for 10 min on three sequential days of the week prior to vapor chamber testing. Across habituation

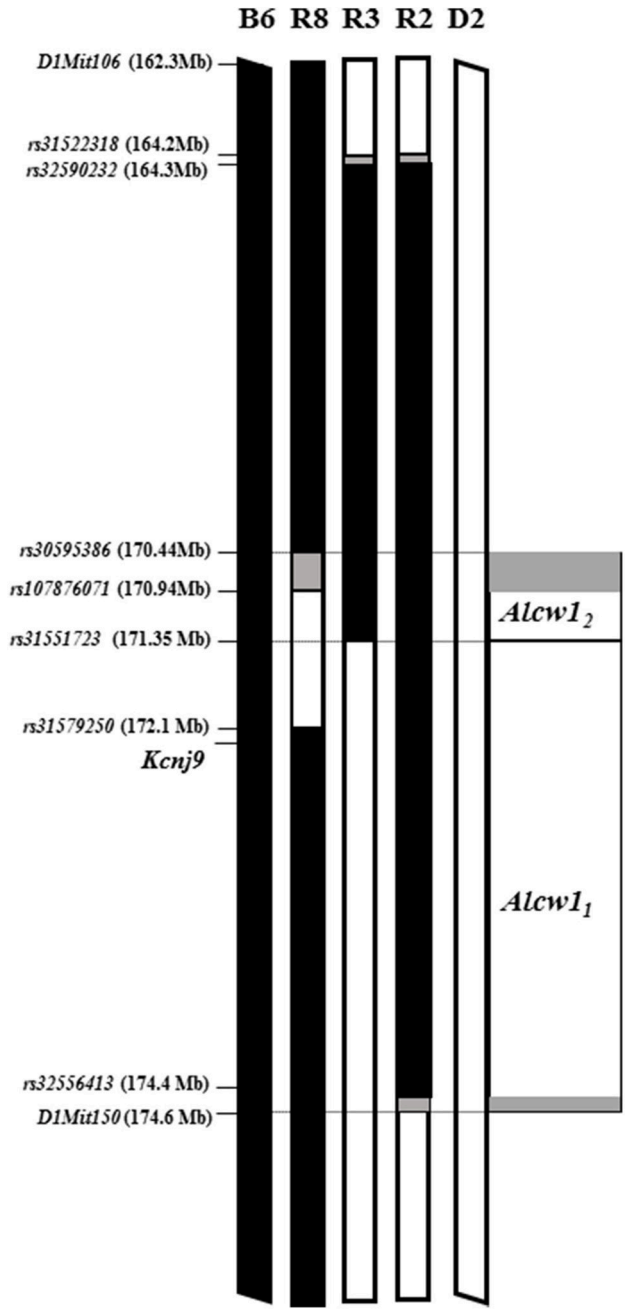

FIGURE 2 | *Alcw1*$_1$ and *Alcw1*$_2$ localization using multiple, reciprocal ISC genetic models**.** Allelic status at genetic markers across the region of chromosome 1 that spans *Alcw1*$_1$ and *Alcw1*$_2$ is illustrated for the two progenitor strains (B6 and D2), two D2.B6 congenic strains (R3; and R2, Walter et al., 2017), and one B6.D2 congenic strain (R8; Kozell et al., 2008). The genetic markers used to establish the introgressed interval boundaries are indicated, with their locations also given. Chromosomal regions homozygous for the B6 strain allele are shown in black. Chromosomal regions homozygous for the D2 strain allele are shown in white. The boundary regions, within which the precise transition exists but is not currently known, are shown in gray. In some cases the boundary region is so small that it is not visible. The *Alcw1*$_2$ interval as shown is defined as donor region that is common to the reciprocal R8 and R3 congenic strains. The *Alcw1*$_1$ interval as shown is defined as that region of the R2 congenic introgressed interval that excludes the *Alcw1*$_2$ interval.

TABLE 1 | *Alcw1*$_1$ interval protein coding genes.

	Congenic vs. WT	
Gene	**ΔSeq**	**ΔExp**
Pfdn2	0	+
Klhdc9	2	+
Nectin4	0	nd
Arhgap30	5	–
Usf1	0	+
Tstd1	0	+
F11r	0	–
Alyref2	3	nd
Cd244	14	–
Slamf7	4	+
Cd48	3	–
Slamf1	0	–
Cd84	2	–
Gm10521	0	nd
Slamf6	1	–
Vangl2	1	+
Nhlh1	0	–
Ncstn	3	+
Copa	2	+
Pex19	2	+
Dcaf8	0	+
Pea15a	0	–
Casq1	0	+
Atp1a4	4	+
Igsf8	2	+
Atp1a2	0	–
Kcnj9	0	+
Kcnj10	5	+
Pigm	1	–
Slamf9	3	+
Igsf9	4	+
Tagln2	0	–
Cfap45	0	–
Vsig8	2	+
Slamf8	3	–
Fcrl6	6	nd
Dusp23	0	–
Crp	1	–
Apcs	0	–
Fcer1a	2	–
Ackr1	0	nd
Cadm3	1	+
Aim2	0	–
Pydc3	0	nd
Mnda	0	nd
Ifi203	0	–
Spta1	0	nd
Fmn2	2	+

The Alcw1$_1$ *interval protein coding genes with demonstrated expression in whole brain are listed in order of location, from most proximal to most distal, including those within the minimal distal boundary region (gray shaded;* ***Figure 2****). The number of validated non-synonymous SNPs (ΔSeq) between the two progenitor strains are indicated. Genes showing significant differential mRNA expression (ΔExp) between congenic and background strain animals are indicated (+), as is the absence of detected DE (-); (nd) indicates no current data comparing chromosome 1 congenic and background strain animals. Other protein coding genes not shown include olfactory receptor genes, interferon activated genes, and four genes (Ly9, Mptx2, Mptx1 and Mnda1) which lack evidence of brain expression. Additionally, there are many pseudogenes and noncoding RNAs within this Alcw1*$_1$ *interval that are not shown.*

TABLE 2 | *Alcw1*$_2$ interval protein coding genes.

	Congenic vs. WT	
Gene	**ΔSeq**	**ΔExp**
Nos1ap	0	+
Olfml2b	0	nd
Atf6	1	+
Dusp12	3	–
Gm26620	0	nd
Fcr1b	0	nd
Fcrla	0	nd
Fcgr2b	0	–
Fcgr4	0	–
Fcgr3	4	+
Cfap126	2	–
Sdhc	3	+
Mpz	1	–
Pcp4l1	0	nd
Nrli3	1	–
Tomm40l	0	+
Apoa2	0	+
Fcer1g	5	–
Ndufs2	1	+
Adamts4	2	+
B4galt3	0	+
Ppox	0	+
Usp21	1	+
Ufc1	0	+
Dedd	0	–
Nit1	1	+
Pfdn2	0	+
Klhdc9	2	+

The Alcw1$_2$ *interval protein coding genes with demonstrated expression in whole brain are listed in order of location, from most proximal to most distal, including those within the minimal distal boundary region (grey shaded;* ***Figure 2****). The number of validated non-synonymous SNPs (ΔSeq) between the two progenitor strains are indicated. Genes showing significant differential mRNA expression (ΔExp) between congenic and background strain animals are indicated (+), as is the absence of detected DE (-); (nd) indicates no current data comparing chromosome 1 congenic and background strain animals. Additionally, there are many pseudogenes and noncoding RNAs within the Alcw1*$_2$ *interval that are not included in the table.*

days, we observed significant decreases in distance traveled, time spent in open arms, open arm entries and head dips within subjects (**Supplementary Tables 2**, **3**; $p < 0.05$), and a main effect of genotype on distance traveled in R2 vs. WT [$F_{(2,43)} = 10.3$, $p = 0.003$], with R2 traveling less distance than WT littermates. However, no treatment or GXT interactions (all $p > 0.7$ and $p > 0.2$, respectively, NS) were detected. Because no differences due to treatment nor GXT interactions were apparent during habituation days, differences in activity and measures of anxiety detected post-ethanol exposure are not likely explained by potential strain-dependent apparatus habituation.

Percent Time in the Open Arms

The percent time spent in the open arms is a well-established measurement of anxiety-like behavior in the EZM (Milner and Crabbe, 2008; Barkley-Levenson and Crabbe, 2015), and for which ethanol withdrawal-induced anxiety-like behavior has been observed (Kliethermes et al., 2004). As shown in **Figure 3**, no main effect of treatment (all $p > 0.18$; **Figures 3A,C**) genotype were detected (all $p > 0.37$, NS). A significant GXT interaction was evident at 24 h [$F_{(1,42)} = 5.2$, $p = 0.028$], but not 48 h [$F_{(1,42)} = 1.9$, $p = 0.17$] post-ethanol. Ethanol withdrawn WT animals spent less time in the open arms compared to air-control WT at 24 h post-ethanol ($p = 0.028$, 1-tailed). Ethanol withdrawn R2 animals did not differ from air-control animals in time spent in the open arms at 24 or 48 h (both $p > 0.8$, NS). Although R2 and WT air control animals did not differ in percent time spent in the open arm at 24 h ($p = 0.23$) or 48 h ($p = 1.0$), it is possible that these non-significant differences may also contribute to the significant GXT interactions identified. Overall, these results are consistent with the conclusion that WT animals show more robust and longer lasting withdrawal-induced anxiety like behavior than R2 congenic animals.

In contrast, in the R3 congenic and WT analyses, no main effect of treatment was detected at either time point assessed (24 and 48 h post-ethanol, both $p > 0.5$, **Figures 3B,D**). No main effect of genotype detected at either time point tested (both $p > 0.6$, NS), and no GXT interactions detected (both $p > 0.5$, NS). Taken together, these results suggest that a gene(s) within the R2 interval significantly affects alcohol withdrawal-induced anxiety-like behavior (and with the same direction of effect as for alcohol withdrawal enhanced HIC severity).

Number of Open Arm Entries

The number of open arm entries is another well-established measurement of anxiety-like behavior in the EZM (Milner and Crabbe, 2008; Barkley-Levenson and Crabbe, 2015), and for which ethanol withdrawal-induced anxiety-like behavior has been observed (Kliethermes et al., 2004). As shown in **Figure 5**, a main effect of treatment was evident at the 24 h withdrawal time point, with ethanol withdrawn R2 congenic and WT animals exhibiting a robust reduction in open arm entries [$F_{(1, 41)} = 10.6$, $p = 0.002$, **Figure 4A**], but not maintained 48 h post-ethanol [$F_{(1, 42)} = 0.25$, $p > 0.6$, **Figure 4C**]. No main effect of genotype was detected ($p > 0.3$). A trend for a GXT interaction was detected at 24 h [$F_{(1, 41)} = 2.7$, $p = 0.055$, one-tailed], with ethanol withdrawn R2 animals not differing from air-control R2 animals ($p > 0.6$, NS), while ethanol withdrawn WT animals made fewer entrances into the open arms compared to air-control WT animals ($p = 0.007$). There were no GXT interactions at 48 h [$F_{(1, 42)} = 1.1$, $p = 0.29$; **Figure 4C**] post-ethanol.

In the R3 and WT comparison, a significant main effect of treatment was evident 24 h post-ethanol, with ethanol withdrawn R3 and WT animals exhibiting a robust reduction in open arm entries compared to air-control animals [$F_{(1, 50)} = 10.8$, $p = 0.002$, **Figure 4B**]; but was not maintained 48 h post-ethanol [$F_{(1, 50)} = 1.1$, $p > 0.29$, NS, **Figure 4D**]. No main effect of genotype was detected (both $p > 0.27$, NS). However, a significant GXT interaction was apparent 24 h post-ethanol [$F_{(1, 50)} = 3.7$, $p = 0.03$, 1-tailed] comparison, with ethanol withdrawn WT littermates making fewer entrances into the open arms compared to their air-controls ($p = 0.006$), while ethanol withdrawn R3

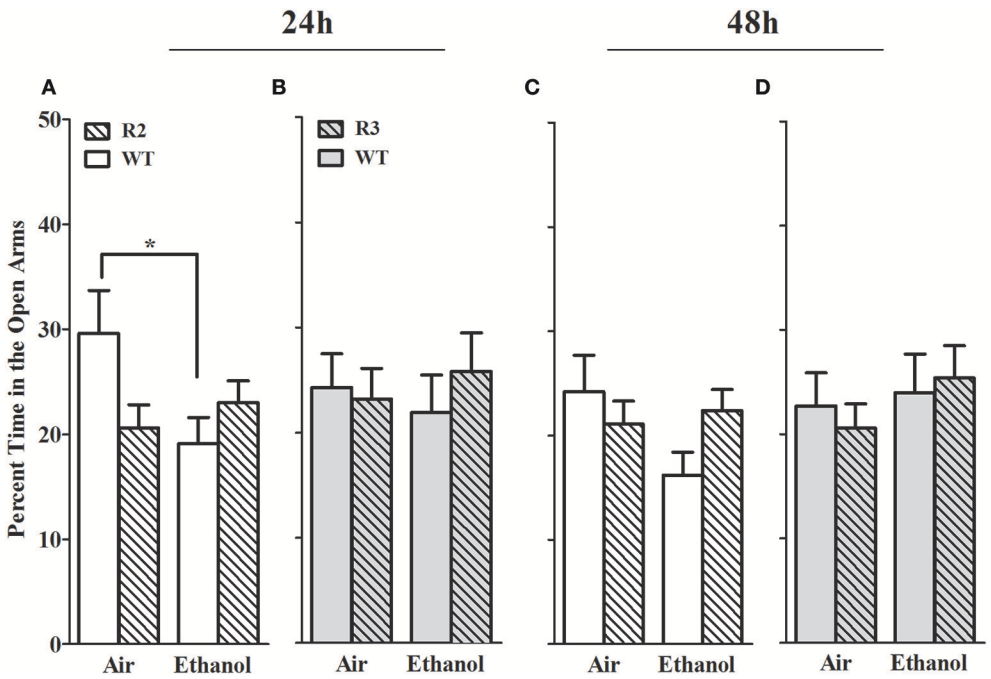

FIGURE 3 | Percent time in the open arms of the EZM in withdrawn (24 and 48 h after cessation of chronic ethanol exposure) and control (air-pyrazole) animals: R2 congenic vs. WT and R3 congenic vs. WT comparisons. Panels show the percentage of time (mean ± SEM) animals spent in the open arm of the EZM during a 10 min test. **(A)** R2 vs. WT (24 h): No main effects of genotype ($p = 0.37$) or treatment ($p = 0.18$) are detected. Nonetheless, there was a significant GXT interaction ($p < 0.03$), with withdrawn WT (but not R2 congenic) animals spending less time in the open arms compared to air-control animals (*$p = 0.028$, one-tailed). **(B)** R3 vs. WT (24 h): No main effects of treatment, genotype, or GXT interaction were detected (all $p > 0.5$). **(C)** R2 vs. WT (48 h): No main effects of treatment ($p = 0.4$), genotype ($p = 0.2$, NS) or GXT interaction is apparent ($p = 0.17$). **(D)** R3 vs. WT (48 h): there were no effects of ethanol withdrawal on percent open arm time in the R3 mice compared to WT littermate for treatment, genotype, or GXT interaction (all $p > 0.5$). *$p < 0.05$, GXT *post hoc* analysis, withdrawn significantly different from air-controls.

congenic animals did not differ from their air-controls ($p > 0.7$, NS). Finally, there was a GXT significant interaction at 48 h [$F_{(1, 50)} = 3.7$, $p = 0.048$, 1-tailed] but there were no differences between ethanol withdrawn R3 or WT and their respective air-controls (both $p > 0.29$; NS). These results indicate that a gene(s) within the R3 introgressed interval has a significant effect on alcohol withdrawal-induced anxiety-like behavior (and with the same direction of effect as for alcohol withdrawal enhanced HIC severity). Given the modest effect size in the R3 vs. WT analyses compared to the R2 vs. WT analyses, our results may also suggest the influence of a second locus within the R2 interval (distinct from the R3 interval) that also affects alcohol withdrawal-induced anxiety-like behavior (again, with the same direction of effect as for alcohol withdrawal enhanced HIC severity). Although R3 and WT air control animals did not differ in open arm entries at 24 h ($p = 0.32$) or 48 h ($p = 0.30$), it is possible that these non-significant differences may also contribute to the significant GXT interactions found.

Head Dips

Head dips over the side of the apparatus are a measurement of exploratory behavior, and furthermore, animals exhibiting anxiety-like behavior are also significantly less likely to scan over the side of the apparatus and thus demonstrate fewer head dips than control animals (Weiss et al., 1998; Morgan et al., 2018). We therefore also measured head dips in the open arms. In the R2 congenic and WT analyses, a main effect of treatment was evident at all the withdrawal time points tested, with ethanol withdrawn R2 and WT animals exhibiting a robust reduction in head dips compared to air-controls at 24 h, [$F_{(1, 41)} = 12.5$, $p = 0.001$; **Figure 5A**] and 48 h post-ethanol [$F_{(1, 43)} = 9.9$, $p = 0.003$; **Figure 5C**]. No main effect of genotype was detected (all $p > 0.27$). No GXT interaction was detected at 24 h post-ethanol [$F_{(1, 41)} = 0.73$, $p = 0.40$; **Figure 6A**] or 48 h [$F_{(1, 43)} = 1.0$, $p = 0.33$; **Figure 5C**].

In the R3 and WT analyses, a robust main effect of treatment was evident 24 h [$F_{(1, 50)} = 11.4$, $p = 0.001$; **Figure 5B**] but not 48 h [$F_{(1, 50)} = 1.6$, $p = 0.17$; **Figure 5D**] post-ethanol. Although no main effect of genotype was detected (all $p > 0.24$), significant GXT interactions were apparent both 24 h [$F_{(1, 50)} = 5.8$, $p = 0.02$; **Figure 5B**] and 48 h [$F_{(1, 51)} = 4.8$, $p = 0.033$; **Figure 5D**] post-ethanol. At 24 h ethanol withdrawn WT animals made significantly fewer head dips than their air controls ($p = 0.002$) while at 48 h there was a trend for fewer head dips in the ethanol withdrawn WT compared to air controls ($p = 0.11$). These results indicate that a gene(s) within the R3 introgressed interval significantly affects alcohol withdrawal-induced exploratory/anxiety-like behavior. Here, R3 and WT air control animals show a trend for a difference in the number of head dips at 24 h ($p = 0.12$) and 48 h ($p = 0.15$), so it is

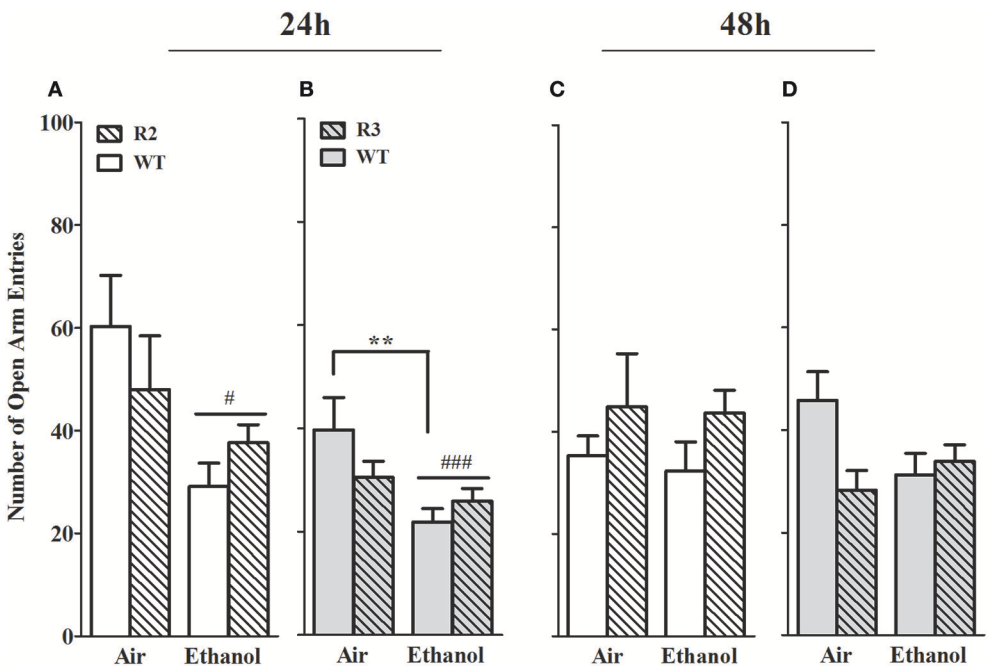

FIGURE 4 | Number of open arm entries in the EZM using withdrawn (24 and 48 h after cessation of chronic ethanol exposure) and air-control animals: comparison of R2 congenic and WT analyses and R3 congenic and WT analyses. These data represent the number of entrances into the open arms (mean ± SEM) during the 10 min test. **(A)** R2 vs. WT (24 h): a main effect of treatment is evident ($p = 0.002$) but no main effect of genotype ($p = 0.77$). A trend for a GXT interaction is detected ($p = 0.055$, one-tailed). **(B)** R3 vs. WT (24 h): a significant main effect of treatment is apparent ($p = 0.002$) but no main effect of genotype ($p = 0.41$). However, a trend for a GXT interaction is detected ($p = 0.035$, one-tailed), with WT withdrawn mice making fewer entries into open arms than air-exposed mice (**$p = 0.007$). **(C)** R2 vs. WT (48 h): no main effects of treatment ($p = 0.62$) or genotype ($p = 0.31$), or GXT interaction ($p = 0.29$) were detected. **(D)** R3 vs. WT (48 h): no main effect of treatment is evident ($p = 0.30$). A trend for a main effect of genotype is detected ($p = 0.078$), and a significant GXT interaction ($p = 0.02$), with ethanol-withdrawn WT littermates showing a trend to spend less time in the open arms than air-control animals ($p = 0.055$, one-tailed). $^{\#}p < 0.05$, $^{\#\#\#}p < 0.001$, main effect of treatment. $^{*}p < 0.05$, GXT *post hoc* analysis, withdrawn significantly different from air-controls.

possible that these non-significant differences may contribute to the significant GXT interaction identified. However, R2 and WT air-controls exhibit comparable numbers of head dips and demonstrate a significant GXT interaction, suggesting that a difference between the congenic and WT air-control groups is not required to observe a significant GXT interaction.

Distance Traveled

To appropriately interpret EZM results, important primary and control behaviors were assessed, including total distance traveled. *Furthermore, alcohol withdrawal has been shown to be associated with reduced activity in the EZM* (Kliethermes et al., 2004), *and may represent an additional measure of alcohol withdrawal. However, it should be kept in mind that the extent to which this phenotype may (or not) be centrally mediated is not known.* As shown in **Figures 6A,C**, a main effect of treatment was evident: ethanol-withdrawn R2 and WT animals show less distance traveled compared to control (air) animals at 24 h [$F_{(1, 42)} = 3.7$, $p = 0.03$, one-tailed] post-ethanol, though not at 48 h [$F_{(1, 43)} = 0.34$, $p = 0.5$, NS]. No main effect of genotype was detected (all $p > 0.4$), but trends for a GXT interaction were detected at 24 h [$F_{(1, 42)} = 2.7$, $p = 0.11$] and 48 h [$F_{(1, 43)} = 2.3$, $p = 0.14$].

As shown in **Figures 6B,D**, a main effect of treatment was also evident using R3 and WT animals, with ethanol-withdrawn animals exhibiting a significant reduction in distance traveled both 24 and 48 h post-ethanol [$F_{(1, 51)} = 20.4$, $p < 5 \times 10^{-5}$, and $F_{(1, 51)} = 4.7$, $p = 0.002$, respectively]. No main effect of genotype (all $p > 0.3$), nor GXT interaction at 24 h ($p > 0.75$) was detected. However, a small but significant GXT interaction was apparent between R3 and WT [$F_{(1, 51)} = 4.8$, $p = 0.03$, **Figure 6D**], with a slight withdrawal-induced reduction in distance traveled still evident in WT littermates 48 h post-ethanol ($p = 0.02$), but no longer detected in R3 animals ($p = 0.99$). Importantly, this GXT interaction between R3 and WT littermates indicates that WT animals are affected by this alcohol withdrawal symptom to a greater extent than $Alcw1_2$ congenic animals, consistent with the direction of effect for alcohol withdrawal enhanced HICs).

Kcnj9$^{-/-}$ (D2 Genetic Background) Animals Demonstrate Significantly Less Severe Acute Alcohol Withdrawal Than WT Littermates

Our previous work identified a QTL for pentobarbital withdrawal (*Pbw1*, Buck et al., 1999), with our subsequent work precisely localizing *Pbw1* (Kozell et al., 2009) to a region within

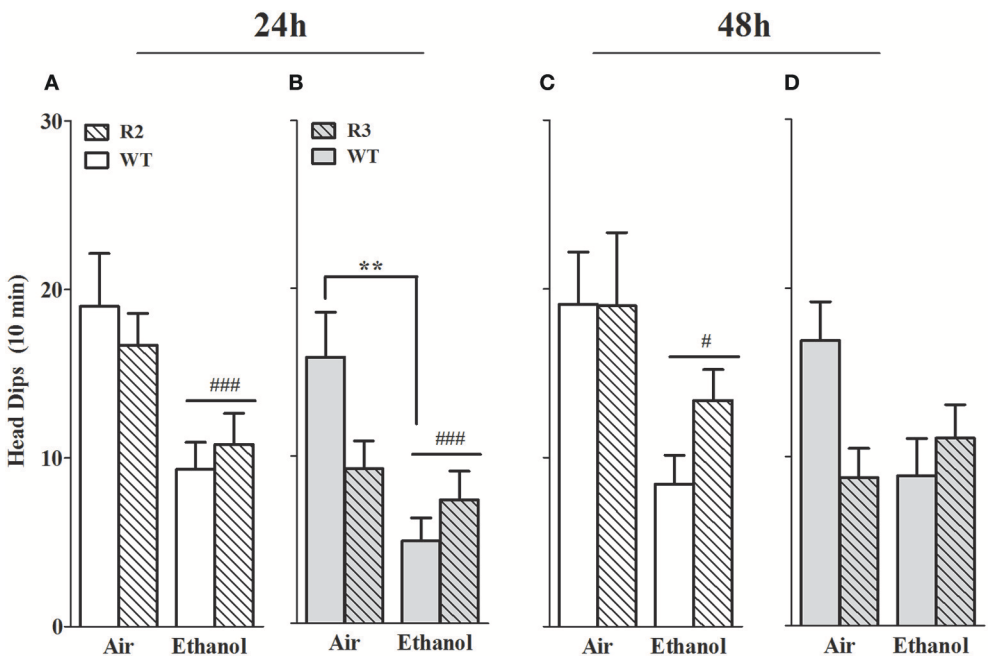

FIGURE 5 | Head dips measured in the EZM using ethanol withdrawn (24 and 48 h post-ethanol) and control animals: R2 congenic vs. WT and R3 congenic vs. WT comparisons. Panels show the number of head dips over the side of the open arms of the EZM apparatus during a 10 min test. **(A)** R2 and WT (24 h): ethanol withdrawn mice made fewer head dips than air-controls ($p = 0.001$). No main effect of genotype ($p = 0.27$) nor GXT interaction ($p = 0.4$) were detected. **(B)** R3 and WT (24 h): no main effects due to genotype ($p = 0.27$) were detected. Both a main effect of treatment ($p = 0.001$) and a GXT interaction ($p = 0.02$) are evident, with ethanol-withdrawn WT littermates making significantly fewer head dips than their air-controls (**$p = 0.002$). **(C)** R2 and WT (48 h): no main effect of genotype ($p = 0.35$) or GXT interaction ($p = 0.33$) were detected. However, a main effect of treatment is apparent ($p = 0.003$). **(D)** R3 and WT (48 h): no main effects of genotype ($p = 0.24$) or treatment ($p = 0.17$) were detected. A significant GXT interaction is apparent ($p = 0.033$), with withdrawn WT showing a trend for fewer head dips compared to WT air-control animals ($p = 0.055$, one-tailed). #$p < 0.05$; ###$p < 0.001$, main effect of treatment. **$p < 0.01$, GXT *post hoc* analysis, withdrawn significantly different from air-controls.

chromosomal region *Alcw1*$_1$ (**Figure 2**) and identify *Kcnj9* as a high quality candidate gene (QTG) to underlie its phenotypic effects. Here, we report our results using two *Kcnj9*$^{-/-}$ knockout models (with two different, inbred genetic backgrounds). Because no main effect of sex ($p > 0.15$) or sex × genotype interaction (SXG; $p > 0.20$; $n = 17$ to 22 sex/genotype) were detected, the data for both sexes were combined for the subsequent analyses. As shown in **Figure 7**, using D2.*Kcnj9*$^{-/-}$ model previous created by us (Kozell et al., 2009), a significant main effect of genotype is apparent [$H_{(2,\ 153)} = 28.7$, $p < 6 \times 10^{-7}$, $n =$ 119, 59 and 51, respectively], with alcohol withdrawal was less severe in *Kcnj9*$^{-/-}$ compared to both D2-*Kcnj*$^{+/-}$ and WT littermates ($p = 7 \times 10^{-7}$ and $p = 3 \times 10^{-5}$ respectively, **Figure 7B**).

Kcnj9$^{-/-}$ (B6 Genetic Background) Mice Demonstrate Reduced Withdrawal Severity Compared to WT Littermates Using a Repeated Alcohol Withdrawal Paradigm

We initially employed the acute alcohol withdrawal model, but were unable reliably detect withdrawal enhanced HIC severity above baseline scores using B6 background *Kcnj9*$^{-/-}$ or WT genetic models (not shown), and thus did not replicate results of Herman et al. (2015) who reported a significant genotype effect at 8 h post-ethanol using male B6 background *Kcnj9*$^{-/-}$ mice. Therefore, the present studies use mice tested using a repeated alcohol withdrawal model which can yield more robust withdrawal (Chen et al., 2008). B6 background *Kcnj9*$^{-/-}$, *Kcnj9*$^{-/+}$ and WT received three doses of ethanol (4 g/kg), at 0, 8 and 20 h, as this has previously been shown to result in enhanced withdrawal HICs in B6 strain and B6-derived genetic models (Chen et al., 2008), followed by HIC scoring from 22 to 32 h (**Figure 8A**). Because no main effect of sex ($p > 0.6$,) or SXG interaction ($p > 0.9$; n = 16–26 sex/genotype) were detected, the data for both sexes were combined for the subsequent analyses. We observed a robust main effect of genotype on ethanol withdrawal severity [$H_{(2,\ 128)} = 9.6$, $p = 0.008$; $n = 43$, 35 and 48, respectively], with *Kcnj9*$^{-/-}$ and *Kcnj9*$^{+/-}$ both demonstrating significantly less severe withdrawal than WT littermates ($p = 0.009$ and $p = 0.006$, respectively; **Figure 8B**).

Ethanol Drinking and Preference in *Alcw1*$_2$ Congenic (R8) and WT Animals

Using a two-bottle, free-choice protocol in which mice could choose either water or an ascending series of ethanol concentrations, ethanol consumption was measured in female B6 genetic background congenic (R8) and WT background

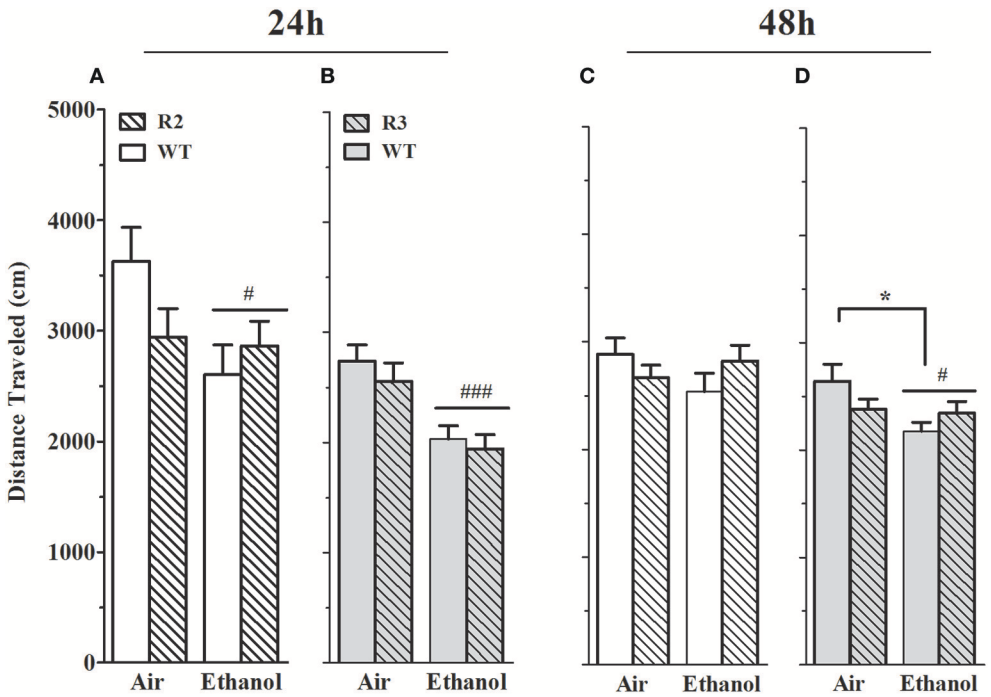

FIGURE 6 | Distance traveled on EZM is reduced in alcohol withdrawn R2, R3 and WT mice compared to air-control animals. Panels show the total distance traveled (mean ± SEM) on the EZM during a 10 min test. **(A)** R2 vs. WT (24 h): a main effect of treatment ($p = 0.03$, one-tailed) is apparent, with alcohol withdrawn mice traveling less distance than air-controls. Although there is no main effect of genotype ($p = 0.4$), a trend for a GXT interaction is detected ($p = 0.06$, one-tailed). **(B)** R3 vs. WT (24 h): a main effect of treatment is evident, with ethanol withdrawn animals traveling significantly less distance than the air-controls ($p < 4\text{x}10^{-6}$). There is no main effect of genotype ($p = 0.4$) or GXT interaction ($p = 0.8$). **(C)** R2 vs. WT (48 h): no main effects of treatment, genotype, or interaction are detected (all $p > 0.1$). (**D**) R3 vs. WT (48 h): a main effect of treatment ($p = 0.02$), with ethanol withdrawn animals traveling significantly less distance than air-controls. There is also a significant GXT interaction ($p = 0.03$), with ethanol withdrawn WT (but not R3) animals moving significantly less than their air-control group ($^{*}p = 0.02$). $^{\#}p < 0.05$, $^{\#\#\#}$ $p < 0.001$, main effect of treatment; $^{*}p < 0.05$, GXT *post hoc* analysis, withdrawn significantly different from air-control group.

strain animals. As shown in **Figure 9**, R8 and WT animals showed comparable consumption of 3, 10, and 20% ethanol solutions [all $t_{(1, 26)} < 0.3$ and $p > 0.7$, NS], with a trend detected for R8 to potentially drink more of the 6% ethanol solution than WT littermates [$t_{(1, 26)} = 1.6$, $p = 0.13$]. R8 and WT animals preferred 3, 6, and 10% ethanol (preference ratios >0.5), but not 20% ethanol (preference ratio <0.5), compared to tap water (data not shown); with no difference between R8 and WT detected [all $t_{(1, 26)} < 1.3$, $p > 0.2$, NS]. One week after the ethanol drinking study, the same mice were tested for saccharin intake (selected for its sweet taste), quinine (bitter taste), and potassium chloride (salty taste). These substances are non-caloric and are not known for confounding pharmacological effects. Consumption and preference did not differ between R8 and WT animals for any of the tastants (all $p > 0.1$, **Supplementary Figure 2**), though R8 animals showed a trend to drink more 0.066% saccharin than WT [$t_{(1, 26)} = 2.0$, $p = 0.054$]. There were no differences in water consumption or in total volume of fluid consumed [all $t_{(1, 26)} < 1.6$, $p > 0.1$, NS]. In summary, our results are consistent with the conclusion that *Alcw1*$_2$ does not affect alcohol consumption (or preference drinking), and thus does not contribute to the known genetic relationship between this phenotype and alcohol withdrawal in mice (Metten et al., 1998).

Ethanol Drinking and Preference (Two Bottle Choice) in *Kcnj9*$^{-/-}$ and WT Littermates

Using the same two-bottle, free-choice protocol as described above, ethanol consumption was measured in B6 background *Kcnj9*$^{-/-}$ and WT littermates. A main effect of sex was apparent for each ethanol concentration (3%, $p = 0.024$; 6%, $p < 2.4 \times 10^{-11}$; 10%, $p < 2.2 \times 10^{-11}$; 20%, $p < 2.51 \times 10^{-11}$). However, no GXT interactions were detected (all $p > 0.3$; $n = 17$–22 sex/genotype), therefore the data for both sexes were collapsed to increase statistical power of the analyses. As shown in **Figure 10**, *Kcnj9*$^{-/-}$ and WT littermates animals showed comparable consumption of 3%, and 10% ethanol solutions [all $t_{(1, 78)} < 1.4$ and $p > 0.5$, NS], with a trend for *Kcnj9*$^{-/-}$animals to drink more 6% ethanol than littermates detected [$t_{(1, 78)} = 1.4$, $p = 0.16$]. *Kcnj9*$^{-/-}$ animals drank significantly more 20% ethanol than WT littermates [$t_{(1, 77)} = 2.3$, $p = 0.024$]. *Kcnj9*$^{-/-}$ and WT littermates preferred 3, 6, and 10% ethanol (all preference ratios >0.5), but not 20% ethanol (preference ratio not different from 0.5), compared to tap water (data not shown); with no difference between *Kcnj9*$^{-/-}$ and WT animals detected for alcohol preference [all $t_{(1, 79)} < 1.5$ and $p > 0.15$, NS]. One week after completion of the ethanol preference drinking

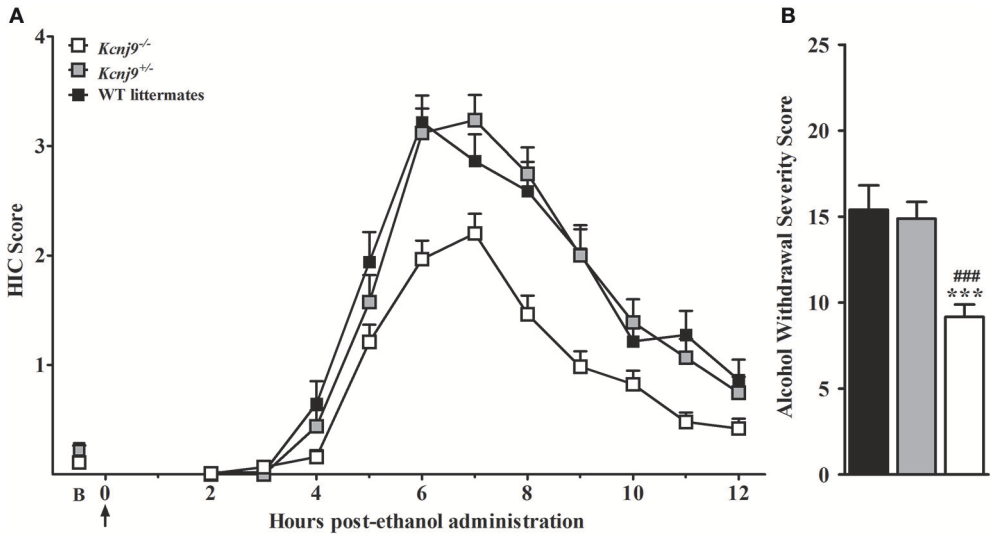

FIGURE 7 | *Kcnj9*$^{-/-}$ null mutant homozygotes (D2 background) demonstrate less severe alcohol withdrawal convulsions (acute model) than *Kcnj9*$^{+/-}$ heterozygote and WT littermates. **(A)** HIC time course before and after ethanol administration (4 g/kg, i.p., indicated by the arrow) using *Kcnj9*$^{-/-}$, *Kcnj9*$^{+/-}$ and WT littermates ($n = 119$, 59 and 51, respectively). HICs were scored at baseline ("B", i.e., pre-ethanol) and then hourly from 2 to 12 h post-ethanol. Baseline HIC scores did not differ among genotypes [$F_{(2,144)} = 1.2$, $p = 0.3$]. As ethanol is metabolized, HIC scores increase above baseline, indicating a state of withdrawal hyperexcitability, which peaks approximately 6–7 h post-ethanol exposure. **(B)** Alcohol withdrawal severity, which was calculated as the AUC ± SEM from 2 to 12 h (corrected for baseline scores), and was significantly different among genotypes ($p < 4 \times 10^{-7}$). *Post hoc* analysis indicated that ethanol withdrawal severity was attenuated in *Kcnj9*$^{-/-}$ compared to *Kcnj9*$^{+/-}$ and WT littermates (###$p = 8.1 \times 10^{-6}$ and ***$p = 1.5 \times 10^{-5}$, respectively).

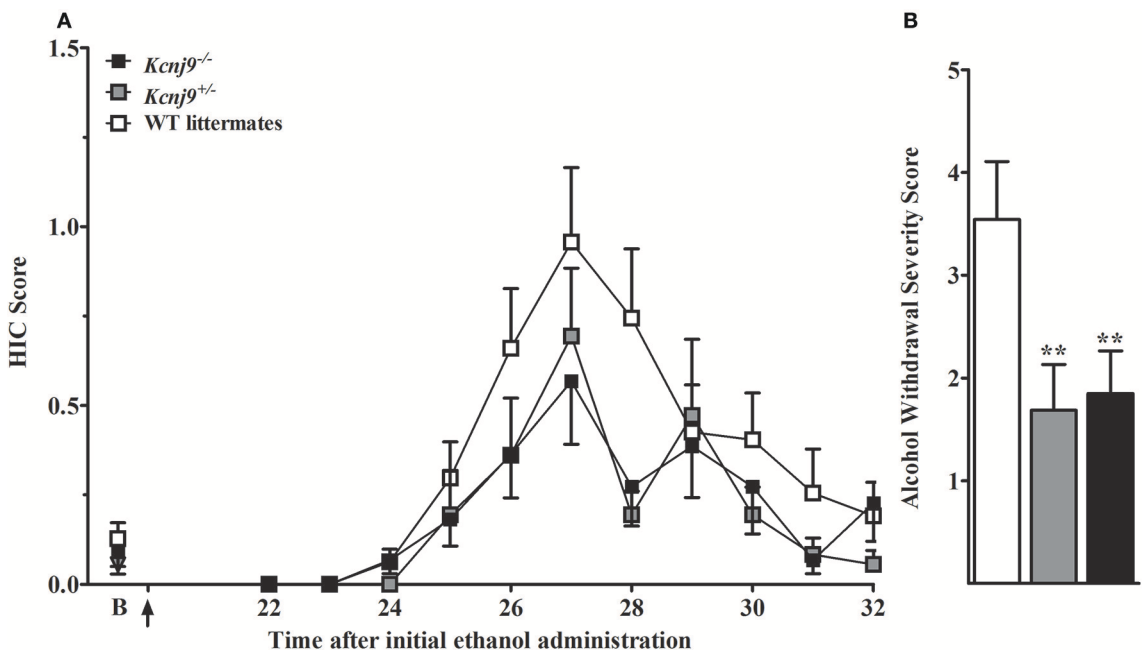

FIGURE 8 | *Kcnj9*$^{-/-}$ null mutant homozygotes (B6 background) show less severe alcohol withdrawal (repeated ethanol model) than WT littermates. **(A)** HIC time course before and after ethanol administration (4 g/kg, i.p., alcohol administered at 0, 8, and 20 h). The last of three ethanol injections is indicated by arrow (at 20 h). Baseline HICs did not differ among genotypes [$F_{(2,124)} = 0.8$, $p = 0.4$]. HICs were scored at baseline (indicated by "B") and hourly from 22 h until 32 h. As alcohol is metabolized, HIC scores increase above baseline, indicating a state of withdrawal hyperexcitability. **(B)** Repeated episodes of alcohol intoxication and withdrawal significantly enhanced alcohol withdrawal severity, which was indexed as the AUC ± SEM (corrected for baseline scores). There was a significant difference in ethanol withdrawal severity among genotypes ($p = 0.008$; $n = 43$, 35 and 48, respectively). *Post hoc* analyses indicated that *Kcnj9*$^{-/-}$ or *Kcnj9*$^{+/-}$ had significantly less severe alcohol withdrawal compared WT littermates (**$p = 0.009$ and **$p = 0.006$, respectively, compared to WT littermates).

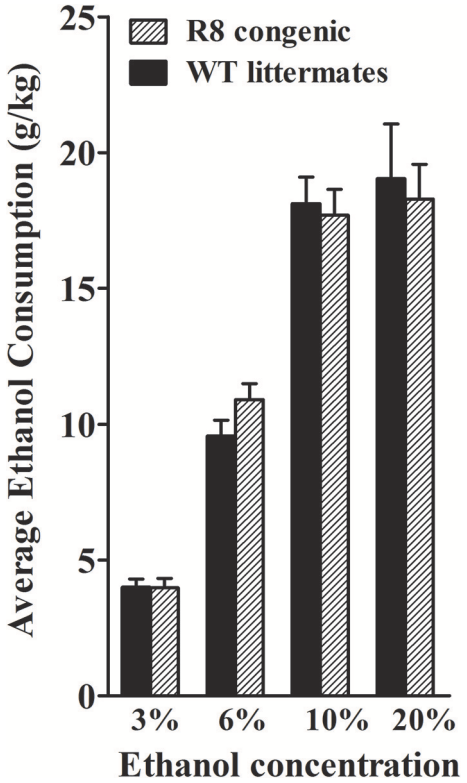

FIGURE 9 | Ethanol consumption does not differ between R8 congenic and WT background strain animals. Ethanol consumption (mean ± SEM) is plotted vs. ethanol concentration offered. There were no differences in the amount of 3, 10, and 20% ethanol consumed between R8 and B6 background strain mice (all p's > 0.7), but there was a trend for R8 mice to drink more 6% ethanol than B6 mice ($p = 0.13$).

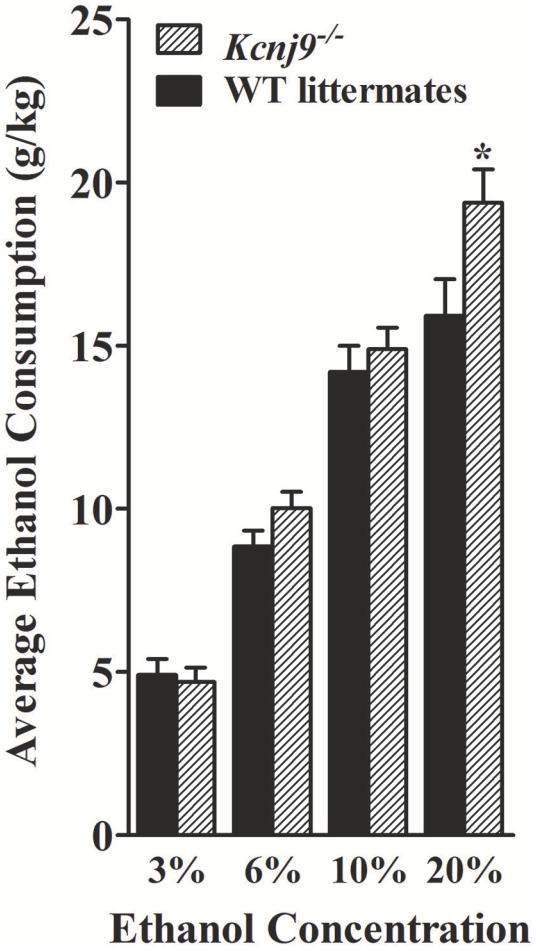

FIGURE 10 | *Kcnj9*$^{-/-}$ mice voluntarily drink more than their *Kcnj9*$^{+/+}$ littermates. Ethanol consumption (mean ±SEM) is plotted vs. ethanol concentration offered. There were no genotype differences between *Kcnj9*$^{-/-}$ and *Kcnj9*$^{+/+}$ mice in 3 or 10% ethanol consumption ($p = 0.71$ and 0.39, respectively) and a trend at 6% ($p = 0.13$). However at 20% ethanol, *Kcnj9*$^{-/-}$ mice drank significantly more ethanol ($p = 0.014$) than WT littermates. *$p < 0.05$ compared to WT littermates.

studies, the same mice were tested for saccharin, quinine and potassium chloride intake (**Supplementary Figure 3**). No differences between *Kcnj9*$^{-/-}$ and WT littermates were detected for saccharin consumption or preference at either concentration tested, for quinine consumption at either concentration tested, or for KCl consumption or preference at either concentration tested between genotypes (all $p > 0.3$, NS). Total water consumption and the total volume of fluid consumed also did not differ between *Kcnj9*$^{-/-}$ and WT littermates (both $p > 0.18$, NS).

Ethanol CPP

Our recent studies implicate *Kcnj9* as importantly involved in ethanol CPP (Tipps et al., 2016). Therefore, in the present studies, we also assessed this translational phenotype using $Alcw1_2$ (R3 and R8) congenic and WT animals. Ethanol (2 g/kg, i.p.) induced CPP was robust in R3 congenic and WT littermates [$t_{(1, 30)} = 4.0$, $p < 5 \times 10^{-5}$, after 8 total conditioning trials, **Figure 11A**]. This is consistent with work demonstrating significant induction of CPP by 2 g/kg ethanol in D2 strain and D2 genetic background animals (Cunningham et al., 1992; Cunningham, 1995, 2014). Notably, our results show that females exhibited more robust ethanol CPP than males [$F_{(1, 27)} = 6.3$, $p = 0.018$; **Figure 11B**; $n = 7$–8 sex/genotype]. However, no difference between R3 congenic and WT littermates in ethanol CPP was detected [$F_{(1, 27)} = 0.0$, $p = 0.94$, NS].

B6 genetic background R8 congenic and background strain animals were tested in a separate study. Here, even after 16 conditioning trials and 4 test days, we were unable to detect ethanol CPP (all tests $p > 0.28$, NS, **Figure 11C**), with comparable results in males and females (all tests $p > 0.1$, NS; $n = 7$–9 sex/genotype). Although a small difference between R8 and WT animals was detected on the pretest day [$F_{(1, 28)} = 5$, $p = 0.034$, with R8 spending less time on the drug-paired floor prior to the conditioning trials], repeated measures ANOVA across the pretest and test days indicated no difference between R8 and WT animals [$F_{(1, 108)} = 0.34$, $p = 0.55$, NS]. Taken together, our results using R3 and R8 $Alcw1_1$ congenic models are consistent with the conclusion that $Alcw1_1$ is not involved in ethanol CPP, at least at under the experimental conditions in the present studies.

Table 3 summarizes the alcohol withdrawal and reward phenotypes that have been tested in our genetic models and

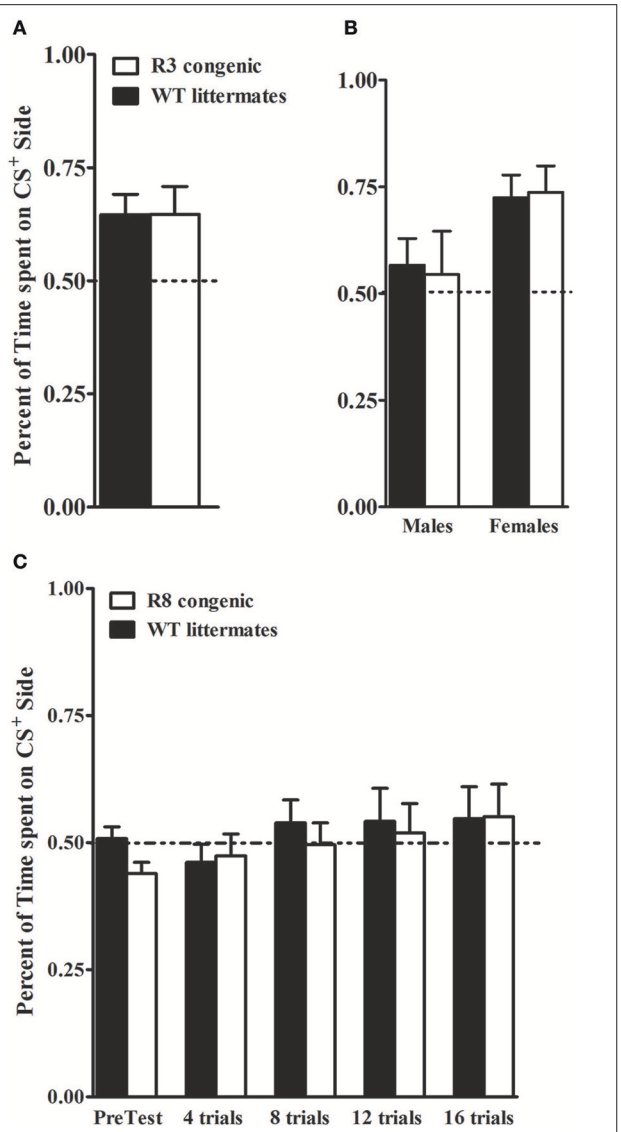

FIGURE 11 | Ethanol CPP in *Alcw1*$_2$ congenic and WT littermates. **(A,B)** R3 and WT littermates: on the test day, R3 and WT littermates spent more time on the CS^+ side than on the CS^- side of the testing apparatus with robust ethanol CPP detected in both genotypes ($p = 0.03$ and $p = 0.005$, respectively). Preference is indicated by mice spending > 50% time on the CS^+ side of the test apparatus. No main effect of genotype ($p = 0.94$) or GXT interaction ($p = 0.82$) were detected. However, a significant difference between males and females is apparent, with females showing robust CPP compared to males ($p = 0.018$; **B**). **(C)** R8 and WT littermates: ethanol CPP was not evident in R8 and WT littermates. The mean time spent on the CS^+ vs. CS^- side of the apparatus did not differ during pretest or during preference tests after 4, 8, 12, or 16 trials (all $p > 0.27$). No main effect of genotype in the time spent on the CS^+ side (all $p > 0.23$, NS) was detected.

evidence for a significant role for *Alcw1*$_1$ and/or *Alcw1*$_2$ is indicated.

DISCUSSION

Our data show that two distinct alcohol withdrawal QTLs (*Alcw1*$_1$and *Alcw1*$_2$) exist on chromosome 1, which account for 13 and 3–6%, respectively, of the genetic variance in acute alcohol withdrawal severity measured using the HIC. Our data also implicate *Alcw1*$_1$and *Alcw1*$_2$ in withdrawal-induced anxiety-like behavior in alcohol dependent animals, representing the first evidence for their broader roles beyond withdrawal convulsions. Further, we show that this effect is not due to general differences in BEC values. Our data also implicate *Alcw1*$_1$ in ethanol consumption and ethanol CPP, but detect no evidence for *Alcw1*$_2$ involvement in these reward phenotypes. Our data also point to *Kcnj9* as a high-quality QTG candidate for *Alcw1*$_1$. Here, for the first time, we demonstrate using two *Kcnj9*$^{-/-}$ (D2 and B6 background) genetic models, that *Kcnj9*$^{-/-}$ exhibit a robust reduction in alcohol withdrawal severity compared to WT littermates. Additionally, using a B6 background *Kcnj9*$^{-/-}$ genetic model, we demonstrate a modest increase in voluntary alcohol (20%) consumption compared to WT littermates. Thus, our results support a broad role for *Alcw1*$_1$/*Kcnj9* in ethanol withdrawal (convulsions and anxiety-like behavior) as well as reward phenotypes. Additionally, our results localize *Alcw1*$_2$ to a small 405–923 Kb interval and point to genes involved in mitochondrial respiration as compelling QTG candidates. Thus, our results demonstrate the existence of *Alcw1*$_1$and *Alcw1*$_2$ as two significant QTLs for alcohol withdrawal convulsions, implicate both in withdrawal-induced anxiety-like behavior, and demonstrate their distinct roles in ethanol-induced CPP and alcohol consumption.

Withdrawal-Induced Anxiety-Like Behavior

Anxiety and anxiety-like behaviors are well-established symptoms of alcohol withdrawal in humans (Driessen et al., 2001) and animal models (Metten et al., 2018), and are thought to affect risk for relapse to alcohol abuse and dependence. Ethanol vapor inhalation has long been used as a tool to induce physical dependence in rodents. In dependent animals, withdrawal-induced anxiety-like behavior can be assessed using a variety of behavioral tests including the open field activity, EZM, elevated plus maze, light-dark box (for review see Kliethermes, 2005) and nesting building (Greenberg et al., 2016). In the present studies animals were tested in the EZM, allowing data collection on multiple measures that interrogate primary and anxiety-like behaviors.

Overall, and particularly for the phenotype percent time in the open arms, our data are consistent with the conclusion that alcohol dependent R2 congenic animals exhibit significantly less severe (and, plausibly, for that reason, shorter duration) withdrawal-induced anxiety-like behavior compared to WT animals. This demonstrates that a gene(s) within the R2 introgressed interval significantly affects withdrawal-induced anxiety-like behavior. Furthermore, the direction of effect is the same direction as for withdrawal convulsions (Walter et al., 2017), supporting the conclusion that the gene(s) affecting withdrawal-induced anxiety-like behavior is, plausibly, the same as that underlying *Alcw1*$_1$ or/and *Alcw1*$_2$ phenotypic effects on withdrawal convulsions. These data are in agreement and build upon previous work indicating a significant genetic correlation

TABLE 3 | Summary of alcohol phenotypes tested in *Kcnj9/Alcw1*$_1$ and *Alcw1*$_2$ genetic models.

Alcohol phenotype	Genetic model	Different vs. WT	*Evidence for role of*	
			Alcw1$_1$	*Alcw1*$_2$
Withdrawal (acute or repeated ethanol exposure models)	R3	++	Yes	
	[a]R8	+++	Yes	
Enhanced HIC severity	[b]R2	+++		Yes
Withdrawal (chronic model)			-	
Reduced locomotor activity	R2	(+)	(Yes)	
	R3	+		Yes
Anxiety-like behaviors (EZM)				
Percent time in Open Arms	R2	+	Yes	
	R3	–		No
Number of Open Arm Entries	R2	+	No	
	R3	–		Yes
Number of head dips	R2	(+)	(Yes)	
	R3	+		Yes
Alcohol-induced CPP	R3	–	No	
	R8	–	No	
	[c]*Kcnj9*$^{-/-}$	+		Yes
Alcohol consumption (2 bottle choice)	R8	–	No	
	Kcnj9$^{-/-}$	+		Yes

The alcohol withdrawal and reward phenotypes tested, and the genetic models tested and compared to appropriate WT animals, are indicated. Significant differences between the genetic models tested (R3, R2, or R8 congenic and Kcnj9$^{-/-}$null mutants) and appropriate WT animals are indicated bold and by: +, ++, +++ (for $p < 0.05$, $p < 0.01$, and $p < 0.001$, respectively), with trends ($p \sim 0.1$) indicated by (+). Evidence for a significant role one or both chromosome 1 QTLs is also indicated as Yes, with trends indicated as (Yes); and evidence indicating no significant role as No. Some of these data are given in detail in recent publications: [a](Walter et al., 2017); [b](Kozell et al., 2008); [c](Tipps et al., 2016). The bolded values indicate that there is a significant difference between genotypes.

between alcohol withdrawal convulsions and alcohol withdrawal-induced anxiety-like behavior (Metten et al., 2018).

Not surprisingly, given the smaller effect size for withdrawal convulsions apparent in R3 congenic animals, our data using this genetic model are less robust than in the R2 model for withdrawal-induced anxiety-like behavior. Nonetheless, overall, and particularly for phenotypes of numbers of open arm entries and head-dips, our results are consistent with the conclusion that a gene(s) in the smaller R3 introgressed interval is significantly involved in withdrawal-induced anxiety-like behavior. Here again, the direction of effect is the same direction as for withdrawal convulsions, supporting the conclusion that the gene(s) affecting withdrawal-induced anxiety-like behavior is, plausibly, the same as that underlying *Alcw1*$_2$ phenotypic effects on withdrawal convulsions. Given that anxiety-like behavioral tests do not necessarily address the same underlying construct (see Milner and Crabbe, 2008), future studies using other anxiety measures to rigorously assess the roles of *Alcw1*$_1$ and *Alcw1*$_2$in withdrawal-induced anxiety-like behaviors will be important.

Ethanol CPP

The neural mechanisms that underlie the rewarding effects of ethanol are highly complex. CPP is a widely used measure of drug reward (Sanchis-Segura and Spanagel, 2006). The present studies tested CPP in order to assess the potential role of *Alcw1*$_2$in ethanol's rewarding and motivational properties in *Alcw1*$_2$congenic and WT animals. Our data show that *Alcw1*$_2$congenic and WT animals do not differ in ethanol CPP, and thus do not support a role for *Alcw1*$_2$in ethanol CPP. In contrast, our recent data using *Alcw1*$_1$ QTG candidate targeted models (*Kcnj9*$^{-/-}$ and WT littermates) show significantly enhanced ethanol CPP compared to WT littermates (Tipps et al., 2016). Further, enhanced ethanol CPP in *Kcnj9*$^{-/-}$ compared to WT littermates is not due to general differences in BECs, the development of ethanol tolerance/sensitization, or the ability of ethanol to alter learning and memory (Tipps et al., 2016). Thus, our data are in agreement and build upon work demonstrating a significant genetic correlation between ethanol CPP and withdrawal (Cunningham, 2014), and also support the involvement of *Alcw1*$_1$*/Kcnj9,* but not *Alcw1*$_2$,in this genetic relationship.

Ethanol Consumption

The fact that alcohol consumption is a prerequisite for the development of alcoholism is self-evident. In a meta-analysis, Metten et al. (1998) found that low voluntary ethanol consumption using a two bottle choice paradigm is significantly genetically correlated with severe ethanol withdrawal convulsions (using both chronic and acute ethanol exposure models), and *vice versa*, when tested independently in separate animals, suggesting that ethanol consumption and withdrawal may share specific (but anonymous) genetic contributions. Here, we tested the potential role of *Alcw1*$_1$and *Alcw1*$_2$in ethanol consumption using the two-bottle choice paradigm using female *Alcw1*$_2$congenic (R8) and WT animals as well as using male and female *Alcw1*$_1$ QTG candidate genetic models (B6 background *Kcnj9*$^{-/-}$ and WT littermates). Our data for ethanol consumption and preference in the WT mice were consistent with levels normally seen in the B6 inbred strain (Belknap et al., 1993; Melo et al., 1996). Overall, our data do

not show a role for *Alcw1*$_2$ in ethanol consumption using this drinking paradigm. However, our data do indicate that *Kcnj9*$^{-/-}$ mice show a modest increase in ethanol consumption (20%) compared to WT littermates. Our results build upon, but are not entirely consistent with, those of Herman et al. (2015) who reported a significant difference in ethanol consumption using a limited access paradigm, with *Kcnj9*$^{-/-}$ mice consuming more ethanol than WT littermates, but detected no difference using a 15% ethanol two-bottle choice paradigm. However, there are several methodological differences between the two-bottle choice drinking studies. First, Herman et al. (2015) used a single ethanol concentration (15%) and assessed drinking for 6 days, whereas our study used ascending concentrations of ethanol (3, 6, 10, and 20%) for 4 days each. Our study assessed consumption in males and females, whereas Herman et al. (2015) tested only males. We switched sides for presentation of ethanol and water tubes every other day, and use consumption data from days two and four to assess ethanol consumption (Phillips et al., 1994), whereas Herman et al. (2015) switched sides for presentation of ethanol and water daily and did not specify which data was used to assess ethanol consumption. Overall, our data and that of other laboratories indicates a modest but significant difference in ethanol consumption between *Kcnj9*$^{-/-}$ and WT animals.

Neuronal Circuitry Activation Affected in an *Alcw1* Dependent Manner

Our data using c-Fos induction as a high-resolution marker of neuronal activation show that mice congenic for a region spanning *Alcw1*$_1$ and *Alcw1*$_2$ demonstrate significantly ($p < 0.05$) less alcohol withdrawal associated activation than background strain mice in the prelimbic cortex, basolateral amygdala, nucleus accumbens shell, dorsolateral striatum, and caudal substantia nigra pars reticulata (Buck et al., 2017). These data elucidate circuitry by which *Alcw1*$_1$ and/or *Alcw1*$_2$ influence alcohol withdrawal behaviors. The relative effect sizes for *Alcw1*$_1$ and *Alcw1*$_2$ suggest a greater influence of *Alcw1*$_1$ compared to *Alcw1*$_2$ on the brain regions implicated. The prelimbic cortex plays an important role in the inhibition of hypothalamo-pituitary-adrenal (HPA) responses to emotional stress *via* influences on neuroendocrine effector mechanisms (Figueiredo et al., 2003; Radley et al., 2006) and is thought to be involved in ethanol withdrawal behaviors including anxiety-like behavior. Ongoing studies implicate *Kcnj9*/GIRK3 actions in the basolateral amygdala as crucial to alcohol withdrawal-enhanced fear conditioned behavior (Buck and Tipps, unpublished results). Lesions of caudolateral substantia nigra pars reticulata attenuate ethanol withdrawal convulsions and support a role of this brain region in withdrawal convulsions (Chen et al., 2008), with RNA interference (RNAi) analyses demonstrating a role for expression of a different proven alcohol withdrawal QTG (*Mpdz*) on alcohol withdrawal convulsions (Kruse et al., 2014).

Alcw1$_2$Points to a Mechanism Involving Oxidative Homeostasis

Taken together, our analyses using reciprocal R3 and R8 congenic models localize *Alcw1*$_2$ to a minimal 405 Kb (maximal 923 Kb) interval on mouse chromosome 1. This region (and the syntenic region in humans) is known for an exceptional gene density, containing 4-5 times more than estimated averages genome wide (Waterston et al., 2002). Moreover, regulation of the expression of genes within this region, as well as mediated by a gene(s) in this region, is complex, involving *cis* and *trans*-regulation (Mozhui et al., 2008; Walter et al., 2017). The present studies finely map *Alcw1*$_2$, within which we now delineate eleven genes (*Fcgr3, Tomm40l, Apoa2, Adamts4, B4galt3, Usp21, Nit1, Sdhc*, *Ndufs2, Ppox,* and *Ufc1*) in the minimal interval that demonstrate *cis*-regulation based on published data (Denmark and Buck, 2008; Walter et al., 2017). Strikingly, three of these genes (*Sdhc, Ndufs2* and *Ppox*) encode proteins involved in mitochondrial oxidative phosphorylation (OXPHOS) pathways (Denmark and Buck, 2008). Furthermore, recent weighted gene coexpression network analyses (WGCNA) using complementary R8 and R2 ISC models implicate an OXPHOS-enriched network module affected by *Alcw1* genotype, and identify *Sdhc* and *Ndufs2* as candidate quantitative trait genes in the OXPHOS co-expression network (Walter et al., 2017). R8 and WT animals differ significantly in ethanol withdrawal severity, but not pentobarbital withdrawal (Kozell et al., 2009), so it is noteworthy that alcohol significantly impacts brain oxidative homeostasis *via* alcohol metabolic by-products which drive OXPHOS and impair the actions of antioxidants (Sun and Sun, 2001; Bailey, 2003), whereas barbiturate exposure has neutral or anti-oxidative actions (Smith et al., 1980; Ueda et al., 2007). Alcohol-induced oxidative damage is well-established, but oxidative status during alcohol withdrawal have been less studied. Nonetheless, rodent studies show increased brain reactive oxygen species for several hours after ethanol exposure (Dahchour et al., 2005) and this correlates well with withdrawal seizure severity (Vallett et al., 1997). Our recent data also demonstrate that N-acetylcysteine, an FDA-approved antioxidant, significantly reduces severity of alcohol withdrawal seizures in mice (Walter et al., 2017). Finally, expression changes for a number of oxidative stress and mitochondrial genes are hallmarks of the human alcoholic brain (Flatscher-Bader et al., 2006; Liu et al., 2006). Thus, although additional genes remain in the *Alcw1*$_2$ interval, in our opinion the mounting evidence elevates the status of *Ndufs2, Sdhc,* and *Ppox* as compelling QTG candidate genes.

Ndufs2 encodes a core Complex I protein (NADH dehydrogenase [ubiquinone] Fe-S protein 2) which is crucial for mitochondrial respiration. *Ndufs2* is significantly DE in reciprocal congenic vs. respective background strains (Walter et al., 2017). Its mRNA content is regulated by ethanol in the amygdala (Most et al., 2015), which is a region implicated in *Alcw1* actions (Buck et al., 2017). In our genetic models, *Ndufs2* also contains a single coding region nonsynonymous SNP that is predicted to be functionally relevant (Denmark and Buck, 2008). Mutation in the *Caenorhabditis elegans* ortholog (*gas-1*) causes oxidative stress (Kayser et al., 2003) and ethanol hypersensitivity (Morgan and Sedensky, 1995), whereas mutations in human *NDUFS2* leads to increased seizure susceptibility (Ugalde et al., 2004). Interestingly, recent data implicates genetic differences in respiratory supercomplex organization, and specifically supercomplexes containing Complex I, in risk for alcohol withdrawal (Buck et al., 2014),

suggesting an intriguing mechanism for *Ndufs2* involvement in alcohol withdrawal.

Ppox encodes protoporphyrin oxidase (PPOX), which catalyzes the final step of heme biosynthesis, the prosthetic group required for the cytochrome function central to electron transport chain (ETC) activity. Interestingly, there is a mutation in human PPOX (González-Arriaza and Bostwick, 2003) with seizures as a primary symptom. This would be consistent with *Ppox* as a plausible QTG candidate for withdrawal convulsions.

Sdhc encodes succinate dehydrogenase complex subunit C (SDHC), a membrane-anchoring subunit that is required for the proper assembly of Complex II in the ETC. *Sdhc* contains multiple functionally critical SNPs between B6/D2 strains (Denmark and Buck, 2008). It shows significant DE between $Alcw1_2$ congenic and WT animals (Walter et al., 2017), and as noted above for *Ndufs2*, its expression is also regulated by ethanol in the amygdala (Most et al., 2015). *Sdhc* is contained in a significant OXPHOS module in mouse lines selected for the dual traits of alcohol consumption and withdrawal (Metten et al., 2014). In work implicating genetic differences in respiratory supercomplex organization as contributing to differences in alcohol withdrawal risk, Complex II involvement was not apparent (Buck et al., 2014). However, given that Complex II is a convergence point where substrate metabolism is coupled to ATP-generating OXPHOS, *Sdhc* should be considered a high-quality QTG candidate.

Plausible Mechanism Involving *Kcnj9*/GIRK3

Our analyses identify *Kcnj9* (GIRK3) as a promising high-quality QTG candidate to underlie $Alcw1_1$phenotypic effects on alcohol withdrawal symptoms and more. GIRK3 is widely expressed in brain where it contributes to heteromeric GIRK2/3 and GIRK1/3 channels (Torrecilla et al., 2002; Koyrakh et al., 2005; Labouèbe et al., 2007; Ciruela et al., 2010). It is not understood whether GIRK3-containing channels show altered sensitivity to ethanol compared to other GIRK channel subtypes, but GIRK2/3 channels do in fact show reduced sensitivity to Gβγ activation (Jelacic et al., 2000). If GIRK2/3 channels are also less sensitive to activation by ethanol, then the effect of reduced GIRK3 expression could be an enhancement of ethanol's ability to modulate GIRK signaling. Thus, GIRK signaling in $Kcnj9^{-/-}$ mice may be more sensitive to modulation by ethanol. Alternatively, reduced GIRK3 expression could affect channel trafficking and thus the adaptation of cells to ethanol exposure. GIRK3 subunits associate with sorting nexin 27 (SNX27), which regulates GIRK channel expression by targeting GIRK3-containing channels to early endosomes. This reduces both cell surface expression of GIRK3-containing channels and GIRK currents (Lunn et al., 2007; Balana et al., 2013). SNX27 itself has also been implicated in the rewarding effects of drugs of abuse (Munoz and Slesinger, 2014), suggesting that the regulation of GIRK signaling *via* this mechanism is an important adaptation to drug exposure. While the effects of ethanol on channel trafficking via SNX27 are unknown, it is possible that this mechanism could play a role in adapting to ethanol exposure and might contribute to the altered dopamine signaling observed following repeated ethanol exposure (Perra et al., 2011; Herman et al., 2015). Future investigations into these possibilities may help address the question of how reduced *Kcnj9* expression and the loss of GIRK3 can alter ethanol responses. Nevertheless, our data and findings from other laboratories support the hypothesis that GIRK channels play an important role in ethanol actions, and suggest that GIRK-based therapeutics, particularly those targeted to specific GIRK subunits, could be effective treatments for alcohol addiction and relapse (Sugaya et al., 2012; Bodhinathan and Slesinger, 2014; Herman et al., 2015; Munoz et al., 2016; Glaaser and Slesinger, 2017).

Human Relevance of QTLs/QTGs Identified in Mice

Our studies precisely localize $Alcw1_1$ and $Alcw1_2$ to a region syntenic with human 1q23.1-23.3. Several studies have identified markers on human 1q associated with alcoholism (reviewed by Ehlers et al., 2010) that, while localized to large regions, are potentially syntenic. However, homology to human remains to be proven. It is worth noting that human studies have generally sought markers associated with the diagnosis and endophenotypes (maximum drinks, metabolism, brain oscillations) rather than withdrawal risk or other phenotypes studied in our animal studies. Two human studies have identified alcohol dependence QTLs (LODs > 3) on the q-arm of human chromosome 1 (Dick et al., 2002; Hill et al., 2004). A third human QTL for tobacco usage has been identified in this same region (Ehlers and Wilhelmsen, 2006) and a fourth on 1q for heavy drinking (Guerrini et al., 2005). Finally, there is evidence from a family-based association study (Hill et al., 2013) for an alcohol dependence QTL on 1q. A recent genome-wide association study (GWAS) by Zuo et al. (2012) also detected variants associated with alcohol dependence on 1q, and depending on what correction method they used, alcohol dependence was associated with variants in or very near the $Alcw1_1$/$Alcw1_2$ syntenic interval, just missing the cutoff threshold. This group identified KIAA0040 as a plausible candidate. However, the majority of the subjects were co-dependent on nicotine, and nearly half were co-dependent on cocaine and marijuana. Further, the same group finds that this same locus is significantly associated with nicotine-alcohol co-dependence (Zuo et al., 2012), suggesting that its influence may not be specific (or even related) to alcohol dependence. Furthermore, the authors state that nearly half of the subjects were co-dependent on cocaine and marijuana. Interestingly, a recent publication (Han et al., 2013) that examined the protein interaction networks associated with alcohol dependence [using the same SAGE and COGA datasets used by Zuo et al. (2012)] also finds hits on 1q are just shy of the cutoff threshold used, and may be syntenic to $Alcw1_1$/$Alcw1_2$. Thus, while it is true that the relevance of $Alcw1_1$ and $Alcw1_2$ to alcohol dependence in humans is not certain, the currently available data do not imply evidence against it either.

Summary

We have now confirmed five significant ethanol withdrawal QTLs, i.e., two on chromosome 1 ($Alcw1_1$ and $Alcw1_2$), one

on chromosome 4 (*Alcw2*, for which we have identified *Mpdz* as a causal QTG; Milner et al., 2015; Kruse et al., 2014), one on chromosome 11 (*Alcw3*; Buck et al., 1997; Hood et al., 2006), and one on chromosome 19 (Buck et al., 2002). At least three of these ($Alcw1_1$, $Alcw1_2$, and *Alcw2*/*Mpdz*) are now implicated as having distinct broader roles in alcohol actions, including reward phenotypes [Milner et al., 2015, and unpublished results]. Interestingly, our data may also point to synergistic mechanisms involving oxidative homeostasis and GABA receptor function. Ongoing work using *Mpdz* genetic models points to its actions affecting $GABA_B$ receptor function (Kruse and Buck, unpublished results) and OXPHOS (Walter and Buck, unpublished results) and thus might act synergistically with $Alcw1_1$/*Kcnj9* and/or $Alcw1_2$. The possibility that the genes underlying $Alcw1_1$ and $Alcw1_2$ may play an important role in distinct translational responses makes them important targets.

AUTHOR CONTRIBUTIONS

DD, NW, LK, and KB participated in writing and revising the manuscript. NW, LK, and KB participated in the concept and design of these studies. LK acquired and analyzed the data. DD, NW, and LK were involved in interpretation of the data.

FUNDING

This work was supported by a VA Merit grant BX00022 (KB) and National Institute of Health grants R01AA011114 (KB), P60AA01760, and R24AA020245 (KB).

ACKNOWLEDGMENTS

We are grateful to Dr. Denesa Lockwood (previously Oberbeck) for her assistance in manuscript preparation. We are grateful to Mr. Jordan Thacker-Feist, Mr. Gregory Auger and Ms. Maarvi Khawaja for their technical assistance.

SUPPLEMENTARY MATERIAL

The Supplementary Material for this article can be found online at: https://www.frontiersin.org/articles/10.3389/fgene.2018.00323/full#supplementary-material

REFERENCES

Bailey, S. M. (2003). A review of the role of reactive oxygen and nitrogen species in alcohol-induced mitochondrial dysfunction. *Free Radic. Res.* 37, 585–596. doi: 10.1080/1071576031000091711

Balana, B., Bahima, L., Bodhinathan, K., Taura, J. J., Taylor, N. M., Nettleton, M. Y., et al. (2013). Ras-association domain of sorting Nexin 27 is critical for regulating expression of GIRK potassium channels. *PLoS ONE* 8:e59800. doi: 10.1371/journal.pone.0059800

Barkley-Levenson, A. M., and Crabbe, J. C. (2015). Genotypic and sex differences in anxiety-like behavior and alcohol-induced anxiolysis in high drinking in the dark selected mice. *Alcohol* 49, 29–36. doi: 10.1016/j.alcohol.2014.07.022

Belknap, J. K., Crabbe, J. C., and Young, E. R. (1993). Voluntary consumption of ethanol in 15 inbred mouse strains. *Psychopharmacology* 112, 503–510. doi: 10.1007/BF02244901

Belknap, J. K., Laursen, S. E., and Crabbe, J. C. (1987). Ethanol and nitrous oxide produce withdrawal-induced convulsions by similar mechanisms in mice. *Life Sci.* 41, 2033–2040. doi: 10.1016/0024-3205(87)90477-2

Belknap, J. K., Mitchell, S. R., O'Toole, L. A., Helms, M. L., and Crabbe, J. C. (1996). Type, I., and type II error rates for quantitative trait loci (QTL) mapping studies using recombinant inbred mouse strains. *Behav. Genet.* 26, 149–160. doi: 10.1007/BF02359892

Bodhinathan, K., and Slesinger, P. A. (2014). Alcohol modulation of G-protein-gated inwardly rectifying potassium channels: from binding to therapeutics. *Front. Physiol.* 5:76. doi: 10.3389/fphys.2014.00076

Buck, K., Metten, P., Belknap, J., and Crabbe, J. (1999). Quantitative trait loci affecting risk for pentobarbital withdrawal map near alcohol withdrawal loci on mouse chromosomes 1, 4, and 11. *Mamm. Genome* 10, 431–437. doi: 10.1007/s003359901018

Buck, K. J., Chen, G., and Kozell, L. B. (2017). Limbic circuitry activation in ethanol withdrawal is regulated by a chromosome 1 locus. *Alcohol* 58, 153–160. doi: 10.1016/j.alcohol.2016.09.030

Buck, K. J., Metten, P., Belknap, J. K., and Crabbe, J. C. (1997). Quantitative trait loci involved in genetic predisposition to acute alcohol withdrawal in mice. *J. Neurosci.* 17, 3946–3955. doi: 10.1523/JNEUROSCI.17-10-03946.1997

Buck, K. J., Rademacher, B. S., Metten, P., and Crabbe, J. C. (2002). Mapping murine loci for physical dependence on ethanol. *Psychopharmacology* 160, 398–407. doi: 10.1007/s00213-001-0988-8

Buck, K. J., Walter, N. A., and Denmark, D. L. (2014). Genetic variability of respiratory complex abundance, organization and activity in mouse brain. *Genes Brain Behav.* 13, 135–143. doi: 10.1111/gbb.12101

Chen, G., Kozell, L. B., Hitzemann, R., and Buck, K. J. (2008). Involvement of the limbic basal ganglia in ethanol withdrawal convulsivity in mice is influenced by a chromosome 4 locus. *J. Neurosci.* 28, 9840–9849. doi: 10.1523/JNEUROSCI.1713-08.2008

Ciruela, F., Fernández-Dueñas, V., Sahlholm, K., Fernández-Alacid, L., Nicolau, J. C., Watanabe, M., et al. (2010). Evidence for oligomerization between GABAB receptors and GIRK channels containing the GIRK1 and GIRK3 subunits. *Eur. J. Neurosci.* 32, 1265–1277. doi: 10.1111/j.1460-9568.2010.07356.x

Crabbe, J. C., Merrill, C. D., and Belknap, J. K. (1991). Effects of convulsants on handling-induced convulsions in mice selected for ethanol withdrawal severity. *Brain Res.* 550, 1–6. doi: 10.1016/0006-8993(91)90397-E

Cunningham, C. L. (1995). Localization of genes influencing ethanol-induced conditioned place preference and locomotor activity in BXD recombinant inbred mice. *Psychopharmacology* 120, 28–41. doi: 10.1007/BF02246142

Cunningham, C. L. (2014). Genetic relationship between ethanol-induced conditioned place preference and other ethanol phenotypes in 15 inbred mouse strains. *Behav. Neurosci.* 128, 430–445. doi: 10.1037/a0036459

Cunningham, C. L., Niehus, D. R., Malott, D. H., and Prather, L. K. (1992). Genetic differences in the rewarding and activating effects of morphine and ethanol. *Psychopharmacology* 107, 385–393. doi: 10.1007/BF02245166

Dahchour, A., Lallemand, F., Ward, R. J., and De Witte, P. (2005). Production of reactive oxygen species following acute ethanol or acetaldehyde and its reduction by acamprosate in chronically alcoholized rats. *Eur. J. Pharmacol.* 520, 51–58. doi: 10.1016/j.ejphar.2005.07.012

Darvasi, A. (1997). Interval-specific congenic strains (ISCS): an experimental design for mapping a QTL into a 1-centimorgan interval. *Mamm. Genome* 8, 163–167. doi: 10.1007/s003359900382

Denmark, D. L., and Buck, K. J. (2008). Molecular analyses and identification of promising candidate genes for loci on mouse chromosome 1 affecting alcohol physical dependence and associated withdrawal. *Genes Brain Behav.* 7, 599–608. doi: 10.1111/j.1601-183X.2008.00396.x

Dick, D. M., Nurnberger, J. Jr., Edenberg, H. J., Goate, A., Crowe, R., Rice, J., et al. (2002). Suggestive linkage on chromosome 1 for a quantitative alcohol-related phenotype. *Alcohol. Clin. Exp. Res.* 26, 1453–1460. doi: 10.1111/j.1530-0277.2002.tb02443.x

Driessen, M., Meier, S., Hill, A., Wetterling, T., Lange, W., and Junghanns, K. (2001). The course of anxiety, depression and drinking behaviours after completed detoxification in alcoholics with and without comorbid anxiety and depressive disorders. *Alcohol Alcohol.* 36, 249–255. doi: 10.1093/alcalc/36.3.249

Ducci, F., and Goldman, D. (2012). The genetic basis of addictive disorders. *Psychiatr. Clin. North Am.* 35, 495–519. doi: 10.1016/j.psc.2012.03.010

Ehlers, C. L., Walter, N. A., Dick, D. M., Buck, K. J., and Crabbe, J. C. (2010). A comparison of selected quantitative trait loci associated with alcohol use phenotypes in humans and mouse models. *Addict. Biol.* 15, 185–199. doi: 10.1111/j.1369-1600.2009.00195.x

Ehlers, C. L., and Wilhelmsen, K. C. (2006). Genomic screen for loci associated with tobacco usage in Mission Indians. *BMC Med. Genet.* 7:9. doi: 10.1186/1471-2350-7-9

Fehr, C., Shirley, R. L., Belknap, J. K., Crabbe, J. C., and Buck, K. J. (2002). Congenic mapping of alcohol and pentobarbital withdrawal liability loci to a <1 centimorgan interval of murine chromosome 4: identification of Mpdz as a candidate gene. *J. Neurosci.* 22, 3730–3738. doi: 10.1523/JNEUROSCI.22-09-03730.2002

Feller, D. J., Bassir, J. M., Crabbe, J. C., and Le Fevre, C. A. (1994). Audiogenic seizure susceptibility in WSP and WSR mice. *Epilepsia* 35, 861–867. doi: 10.1111/j.1528-1157.1994.tb02524.x

Figueiredo, H. F., Bodie, B. L., Tauchi, M., Dolgas, C. M., and Herman, J.P. (2003). Stress integration after acute and chronic predator stress: differential activation of central stress circuitry and sensitization of the hypothalamo-pituitary-adrenocortical axis. *Endocrinology* 144, 5249–5258. doi: 10.1210/en.2003-0713

Finn, D.A., Snelling, C., Fretwell, A. M., Tanchuck, M. A., Underwood, L., Cole, M., et al. (2007). Increased drinking during withdrawal from intermittent ethanol exposure is blocked by the CRF receptor antagonist D-Phe-CRF(12-41). *Alcohol. Clin. Exp. Res.* 31, 939–949. doi: 10.1111/j.1530-0277.2007.00379.x

Flatscher-Bader, T., van der Brug, M. P., Landis, N., Hwang, J.W., Harrison, E., and Wilce, P.A. (2006). Comparative gene expression in brain regions of human alcoholics. *Genes Brain Behav.* 5(Suppl. 1), 78–84. doi: 10.1111/j.1601-183X.2006.00197.x

Friedman, H. J. (1980). "Assesment of physical dependence on and withdrawal from ethanol in animals," in *Alcohol Tolerance and Dependence,* eds H. Rigter, and Crabbe, J.C. (Amsterdam: Elsevier), 93–121.

Glaaser, I. W., and Slesinger, P. A. (2017). Dual activation of neuronal G protein-gated inwardly rectifying potassium (GIRK) channels by cholesterol and alcohol. *Sci. Rep.* 7:4592. doi: 10.1038/s41598-017-04681-x

Goldman, D., Oroszi, G., O'Malley, S., and Anton, R. (2005). COMBINE genetics study: the pharmacogenetics of alcoholism treatment response: genes and mechanisms. *J. Stud. Alcohol Suppl.* 56–64, discussion 33. doi: 10.15288/jsas.2005.s15.56

Goldstein, D. B. (1973). Alcohol withdrawal reactions in mice: effects of drugs that modify neurotransmission. *J. Pharmacol. Exp. Ther.* 186, 1–9.

Goldstein, D. B., and Pal, N. (1971). Alcohol dependence produced in mice by inhalation of ethanol: grading the withdrawal reaction. *Science* 172, 288–290. doi: 10.1126/science.172.3980.288

González-Arriaza, H. L., and Bostwick, J. M. (2003). Acute porphyrias: a case report and review. *Am. J. Psychiatry* 160, 450–459. doi: 10.1176/appi.ajp.160.3.450

Greenberg, G. D., Huang, L. C., Spence, S. E., Schlumbohm, J. P., Metten, P., Ozburn, A. R., et al. (2016). Nest building is a novel method for indexing severity of alcohol withdrawal in mice. *Behav. Brain Res.* 302, 182–190. doi: 10.1016/j.bbr.2016.01.023

Guerrini, I., Cook, C. C., Kest, W., Devitgh, A., McQuillin, A., Curtis, D., et al. (2005). Genetic linkage analysis supports the presence of two susceptibility loci for alcoholism and heavy drinking on chromosome 1p22.1-11.2 and 1q21.3-24.2. *BMC Genet.* 6:11. doi: 10.1186/1471-2156-6-11

Han, S., Yang, B. Z., Kranzler, H. R., Liu, X., Zhao, H., Farrer, L. A., et al. (2013). Integrating GWASs and human protein interaction networks identifies a gene subnetwork underlying alcohol dependence. *Am. J. Hum. Genet.* 93, 1027–1034. doi: 10.1016/j.ajhg.2013.10.021

Hasin, D. S., Stinson, F. S., Ogburn, E., and Grant, B. F. (2007). Prevalence, correlates, disability, and comorbidity of DSM-IV alcohol abuse and dependence in the United States: results from the national epidemiologic survey on alcohol and related conditions. *Arch. Gen. Psychiatry* 64, 830–842. doi: 10.1001/archpsyc.64.7.830

Herman, M. A., Sidhu, H., Stouffer, D. G., Kreifeldt, M., Le, D., Cates-Gatto, C., et al. (2015). GIRK3 gates activation of the mesolimbic dopaminergic pathway by ethanol. *Proc. Natl. Acad. Sci. U.S.A.* 112, 7091–7096. doi: 10.1073/pnas.1416146112

Hill, S. Y., Jones, B. L., Zezza, N., and Stiffler, S. (2013). Family-based association analysis of alcohol dependence implicates KIAA0040 on chromosome 1q in multiplex alcohol dependence families. *Open J. Genet.* 3, 243–252. doi: 10.4236/ojgen.2013.34027

Hill, S. Y., Shen, S., Zezza, N., Hoffman, E. K., Perlin, M., and Allan, W. (2004). A genome wide search for alcoholism susceptibility genes. *Am. J. Med. Genet. B Neuropsychiatr. Genet.* 128B, 102–113. doi: 10.1002/ajmg.b.30013

Hood, H. M., Metten, P., Crabbe, J. C., and Buck, K. J. (2006). Fine mapping of a sedative-hypnotic drug withdrawal locus on mouse chromosome 11. *Genes Brain Behav.* 5, 1–10. doi: 10.1111/j.1601-183X.2005.00122.x

Jelacic, T. M., Kennedy, M. E., Wickman, K., and Clapham, D. E. (2000). Functional and biochemical evidence for G-protein-gated inwardly rectifying K+ (GIRK) channels composed of GIRK2 and GIRK3. *J. Biol. Chem.* 17, 36211–36216. doi: 10.1074/jbc.M007087200

Kayser, E. B., Hoppel, C. L., Morgan, P. G., and Sedensky, M. M. (2003). A mutation in mitochondrial complex I increases ethanol sensitivity in *Caenorhabditis elegans*. *Alcohol. Clin. Exp. Res.* 27, 584–592. doi: 10.1111/j.1530-0277.2003.tb04394.x

Kerns, R. T., Ravindranathan, A., Hassan, S., Cage, M. P., York, T., Sikela, J. M., et al. (2005). Ethanol-responsive brain region expression networks: implications for behavioral responses to acute ethanol in DBA/2J versus C57BL/6J mice. *J. Neurosci.* 25, 2255–2266. doi: 10.1523/JNEUROSCI.4372-04.2005

Kliethermes, C. L. (2005). Anxiety-like behaviors following chronic ethanol exposure. *Neurosci. Biobehav. Rev.* 28, 837–850. doi: 10.1016/j.neubiorev.2004.11.001

Kliethermes, C. L., Cronise, K., and Crabbe, J. C. (2004). Anxiety-like behavior in mice in two apparatuses during withdrawal from chronic ethanol vapor inhalation. *Alcohol. Clin. Exp. Res.* 28, 1012–1019. doi: 10.1097/01.ALC.0000131976.40428.8F

Kosobud, A., and Crabbe, J. C. (1986). Ethanol withdrawal in mice bred to be genetically prone or resistant to ethanol withdrawal seizures. *J. Pharmacol. Exp. Ther.* 238, 170–177.

Koyrakh, L., Luján, R., Colón, J., Karschin, C., Kurachi, Y., Karschin, A., et al. (2005). Molecular and cellular diversity of neuronal G-protein-gated potassium channels. *J. Neurosci.* 25, 11468–11478. doi: 10.1523/JNEUROSCI.3484-05.2005

Kozell, L., Belknap, J. K., Hofstetter, J. R., Mayeda, A., and Buck, K. J. (2008). Mapping a locus for alcohol physical dependence and associated withdrawal to a 1.1 Mb interval of mouse chromosome 1 syntenic with human chromosome 1q23.2-23.3. *Genes Brain Behav.* 7, 560–567. doi: 10.1111/j.1601-183X.2008.00391.x

Kozell, L. B., Walter, N. A., Milner, L. C., Wickman, K., and Buck, K. J. (2009). Mapping a barbiturate withdrawal locus to a 0.44 Mb interval and analysis of a novel null mutant identify a role for Kcnj9 (GIRK3) in withdrawal from pentobarbital, zolpidem, and ethanol. *J. Neurosci.* 29, 11662–11673. doi: 10.1523/JNEUROSCI.1413-09.2009

Kruse, L. C., Walter, N. A., and Buck, K. J. (2014). Mpdz expression in the caudolateral substantia nigra pars reticulata is crucially involved in alcohol withdrawal. *Genes Brain Behav.* 13, 769–776. doi: 10.1111/gbb.12171

Labouèbe, G., Lomazzi, M., Cruz, H. G., Creton, C., Luján, R., Li, M., et al. (2007). RGS2 modulates coupling between GABAB receptors and GIRK channels in dopamine neurons of the ventral tegmental area. *Nat. Neurosci.* 10, 1559–1568. doi: 10.1038/nn2006

Little, H. J., Stephens, D. N., Ripley, T. L., Borlikova, G., Duka, T., Schubert, M., et al. (2005). Alcohol withdrawal and conditioning. *Alcohol. Clin. Exp. Res.* 29, 453–464. doi: 10.1097/01.ALC.0000156737.56425.E3

Liu, J., Lewohl, J. M., Harris, R. A., Iyer, V. R., Dodd, P. R., Randall, P. K., et al. (2006). Patterns of gene expression in the frontal cortex discriminate alcoholic from nonalcoholic individuals. *Neuropsychopharmacology* 31, 1574–1582. doi: 10.1038/sj.npp.1300947

Lunn, M. L., Nassirpour, R., Arrabit, C., Tan, J., McLeod, I., Arias, C. M., et al. (2007). A unique sorting nexin regulates trafficking of potassium channels via a PDZ domain interaction. *Nat. Neurosci.* 10, 1249–1259. doi: 10.1038/nn1953

Lutz, U. C., Batra, A., Kolb, W., Machicao, F., Maurer, S., and Köhnke, M. D. (2006). Methylenetetrahydrofolate reductase C677T-polymorphism and its association with alcohol withdrawal seizure. *Alcohol. Clin. Exp. Res.* 30, 1966–1971. doi: 10.1111/j.1530-0277.2006.00242.x

McQuarrie, D. J., and Fingl, E. (1958). Effects of single doses and chronic administration of ethanol on experimental seizures in mice. *J. Pharmacol. Exp. Ther.* 124, 264–271.

Melo, J. A., Shendure, J., Pociask, K., and Silver, L. M. (1996). Identification of sex-specific quantitative trait loci controlling alcohol preference in C57BL/ 6 mice. *Nat. Genet.* 13, 147–153. doi: 10.1038/ng0696-147

Metten, P., Belknap, J. K., and Crabbe, J. C. (1998). Drug withdrawal convulsions and susceptibility to convulsants after short-term selective breeding for acute ethanol withdrawal. *Behav. Brain Res.* 95, 113–122. doi: 10.1016/S0166-4328(97)00216-7

Metten, P., Buck, K. J., Merrill, C. M., Roberts, A. J., Yu, C. H., and Crabbe, J. C. (2007). Use of a novel mouse genotype to model acute benzodiazepine withdrawal. *Behav. Genet.* 37, 160–170. doi: 10.1007/s10519-006-9094-3

Metten, P., and Crabbe, J. C. (1999). Genetic determinants of severity of acute withdrawal from diazepam in mice: commonality with ethanol and pentobarbital. *Pharmacol. Biochem. Behav.* 63, 473–479. doi: 10.1016/S0091-3057(99)00017-9

Metten, P., Iancu, O. D., Spence, S. E., Walter, N. A., Oberbeck, D., Harrington, C. A., et al. (2014). Dual-trait selection for ethanol consumption and withdrawal: genetic and transcriptional network effects. *Alcohol. Clin. Exp. Res.* 38, 2915–2924. doi: 10.1111/acer.12574

Metten, P., Schlumbohm, J. P., Huang, L. C., Greenberg, G. D., Hack, W. R., Spence, S. E., et al. (2018). An alcohol withdrawal test battery measuring multiple behavioral symptoms in mice. *Alcohol* 68, 19–35. doi: 10.1016/j.alcohol.2017.08.014

Milner, L. C., and Crabbe, J. C. (2008). Three murine anxiety models: results from multiple inbred strain comparisons. *Genes Brain Behav.* 7, 496–505. doi: 10.1111/j.1601-183X.2007.00385.x

Milner, L. C., Shirley, R. L., Kozell, L. B., Walter, N. A., Kruse, L. C., Komiyama, N. H., et al. (2015). Novel MPDZ/MUPP1 transgenic and knockdown models confirm Mpdz's role in ethanol withdrawal and support its role in voluntary ethanol consumption. *Addict. Biol.* 20, 143–147. doi: 10.1111/adb.12087

Morgan, J. A., Singhal, G., Corrigan, F., Jaehne, E.J., Jawahar, M. C., and Baune, B.T. (2018). The effects of aerobic exercise on depression-like, anxiety-like, and cognition-like behaviours over the healthy adult lifespan of C57BL/6 mice. *Behav. Brain Res.* 337, 193–203. doi: 10.1016/j.bbr.2017.09.022

Morgan, P. G., and Sedensky, M. M. (1995). Mutations affecting sensitivity to ethanol in the nematode, *Caenorhabditis elegans*. *Alcohol. Clin. Exp. Res.* 19, 1423–1429. doi: 10.1111/j.1530-0277.1995.tb01002.x

Most, D., Ferguson, L., Blednov, Y., Mayfield, R. D., and Harris, R. A. (2015). The synaptoneurosome transcriptome: a model for profiling the emolecular effects of alcohol. *Pharmacogenomics J.* 15, 177–188. doi: 10.1038/tpj.2014.43

Mozhui, K., Ciobanu, D. C., Schikorski, T., Wang, X., Lu, L., and Williams, R. W. (2008). Dissection of a QTL hotspot on mouse distal chromosome 1 that modulates neurobehavioral phenotypes and gene expression. *PLoS Genet.* 4:e1000260. doi: 10.1371/journal.pgen.1000260

Munoz, M. B., Padgett, C. L., Rifkin, R., Terunuma, M., Wickman, K., Contet, C., et al. (2016). A role for the GIRK3 subunit in methamphetamine-induced attenuation of GABAB receptor-activated GIRK currents in VTA dopamine neurons. *J. Neurosci.* 16, 3106–3114. doi: 10.1523/JNEUROSCI.1327-15.2016

Munoz, M. B., and Slesinger, P. A. (2014). Sorting nexin 27 regulation of G protein-gated inwardly rectifying K(+) channels attenuates *in vivo* cocaine response. *Neuron* 82, 659–669. doi: 10.1016/j.neuron.2014.03.011

Office of National Drug Control Policy (2004). *The Economic Costs of Drug Abuse in the United States, 1992–2002.* Washington, DC: Executive Office of the President (Publication No. 207303).

Perra, S., Clements, M. A., Bernier, B. E., and Morikawa, H. (2011). *In vivo* ethanol experience increases D(2) autoinhibition in the ventral tegmental area. *Neuropsychopharmacology* 36, 993–1002. doi: 10.1038/npp.2010.237

Phillips, T. J., Crabbe, J. C., Metten, P., and Belknap, J. K. (1994). Localization of genes affecting alcohol drinking in mice. *Alcohol. Clin. Exp. Res.* 18, 931–941. doi: 10.1111/j.1530-0277.1994.tb00062.x

Radley, J. J., Arias, C. M., and Sawchenko, P. E. (2006). Regional differentiation of the medial prefrontal cortex in regulating adaptive responses to acute emotional stress. *J. Neurosci.* 26, 12967–12976. doi: 10.1523/JNEUROSCI.4297-06.2006

Sanchis-Segura, C., and Spanagel, R. (2006). Behavioural assessment of drug reinforcement and addictive features in rodents: an overview. *Addict. Biol.* 11, 2–38. doi: 10.1111/j.1369-1600.2006.00012.x

Shirley, R. L., Walter, N. A., Reilly, M. T., Fehr, C., and Buck, K. J. (2004). Mpdz is a quantitative trait gene for drug withdrawal seizures. *Nat. Neurosci.* 7, 699–700. doi: 10.1038/nn1271

Smith, D. S., Rehncrona, S., and Siesjö, B. K. (1980). Barbiturates as protective agents in brain ischemia and as free radical scavengers *in vitro*. *Acta Physiol. Scand. Suppl.* 492, 129–134.

Sugaya, N., Ogai, Y., Kakibuchi, Y., Senoo, E., and Ikeda, K. (2012). Influence of GIRK channel inhibition on relapse risk in Japanese alcohol-dependent inpatients. *Nihon Shinkei Seishin Yakurigaku Zasshi* 32, 165–167.

Sun, A. Y., and Sun, G. Y. (2001). Ethanol and oxidative mechanisms in the brain. *J. Biomed. Sci.* 8, 37–43. doi: 10.1007/BF02255969

Terdal, E. S., and Crabbe, J. C. (1994). Indexing withdrawal in mice: matching genotypes for exposure in studies using ethanol vapor inhalation. *Alcohol. Clin. Exp. Res.* 18, 542–547. doi: 10.1111/j.1530-0277.1994.tb00907.x

Tipps, M. E., Raybuck, J. D., Buck, K. J., and Lattal, K. M. (2015). Acute ethanol withdrawal impairs contextual learning and enhances cued learning. *Alcohol. Clin. Exp. Res.* 39, 282–290. doi: 10.1111/acer.12614

Tipps, M. E., Raybuck, J. D., Kozell, L. B., Lattal, K. M., and Buck, K. J. (2016). G Protein-gated inwardly rectifying potassium channel subunit 3 knock-out mice show enhanced ethanol reward. *Alcohol. Clin. Exp. Res.* 40, 857–864. doi: 10.1111/acer.13012

Torrecilla, M., Marker, C. L., Cintora, S. C., Stoffel, M., Williams, J. T., and Wickman, K. (2002). G-protein-gated potassium channels containing Kir3.2 and Kir3.3 subunits mediate the acute inhibitory effects of opioids on locus ceruleus neurons. *J. Neurosci.* 22, 4328–4334. doi: 10.1523/JNEUROSCI.22-11-04328.2002

Ueda, Y., Doi, T., Nagatomo, K., and Nakajima, A. (2007). Protective role of pentobarbital pretreatment for NMDA-R activated lipid peroxidation is derived from the synergistic effect on endogenous anti-oxidant in the hippocampus of rats. *Neurosci. Lett.* 417, 46–49. doi: 10.1016/j.neulet.2007.02.031

Ugalde, C., Janssen, R. J., van den Heuvel, L. P., Smeitink, J. A., and Nijtmans, L. G. (2004). Differences in assembly or stability of complex I and other mitochondrial OXPHOS complexes in inherited complex I deficiency. *Hum. Mol. Genet.* 13, 659–667. doi: 10.1093/hmg/ddh071

Vallett, M., Tabatabaie, T., Briscoe, R. J., Baird, T. J., Beatty, W. W., Floyd, R. A., et al. (1997). Free radical production during ethanol intoxication, dependence, and withdrawal. *Alcohol. Clin. Exp. Res.* 21, 275–285. doi: 10.1111/j.1530-0277.1997.tb03761.x

Walter, N. A., Denmark, D. L., Kozell, L. B., and Buck, K. J. (2017). A systems approach implicates a brain mitochondrial oxidative homeostasis co-expression network in genetic vulnerability to alcohol withdrawal. *Front. Genet.* 7:218. doi: 10.3389/fgene.2016.00218

Waterston, R. H., Lander, E. S., and Sulston, J. E. (2002). On the sequencing of the human genome. *Proc. Natl. Acad. Sci. U.S.A.* 99, 3712–3716. doi: 10.1073/pnas.042692499

Weiss, S. M., Wadsworth, G., Fletcher, A., and Dourish, C. T. (1998). Utility of ethological analysis to overcome locomotor confounds in elevated maze models of anxiety. *Neurosci. Biobehav. Rev.* 23, 265–271. doi: 10.1016/S0149-7634(98)00027-X

Zuo, L., Gelernter, J., Zhang, C. K., Zhao, H., Lu, L., Kranzler, H. R., et al. (2012). Genome-wide association study of alcohol dependence implicates KIAA0040 on chromosome 1q. *Neuropsychopharmacology* 37, 557–566. doi: 10.1038/npp.2011.229

Conflict of Interest Statement: The authors declare that the research was conducted in the absence of any commercial or financial relationships that could be construed as a potential conflict of interest. The contents of this publication do not represent the views of the U.S. Department of Veterans Affairs or the United States Government.

frontiers in Genetics

ORIGINAL RESEARCH
published: 28 August 2018
doi: 10.3389/fgene.2018.00300

Regional Differences and Similarities in the Brain Transcriptome for Mice Selected for Ethanol Preference From HS-CC Founders

Alexandre M. Colville[1†], Ovidiu D. Iancu[1], Denesa R. Lockwood[1], Priscila Darakjian[1], Shannon K. McWeeney[2], Robert Searles[3], Christina Zheng[2,4] and Robert Hitzemann[1]*

[1] Department of Behavioral Neuroscience, Oregon Health & Science University, Portland, OR, United States, [2] Department of Medical Informatics and Clinical Epidemiology, Oregon Health & Science University, Portland, OR, United States, [3] Integrated Genomics Laboratory, Oregon Health & Science University, Portland, OR, United States, [4] Knight Cancer Institute, Oregon Health & Science University, Portland, OR, United States

The high genetic complexity found in heterogeneous stock (HS-CC) mice, together with selective breeding, can be used to detect new pathways and mechanisms associated with ethanol preference and excessive ethanol consumption. We predicted that these pathways would provide new targets for therapeutic manipulation. Previously (Colville et al., 2017), we observed that preference selection strongly affected the accumbens shell (SH) genes associated with synaptic function and in particular genes associated with synaptic tethering. Here we expand our analyses to include substantially larger sample sizes and samples from two additional components of the "addiction circuit," the central nucleus of the amygdala (CeA) and the prelimbic cortex (PL). At the level of differential expression (DE), the majority of affected genes are region-specific; only in the CeA did the DE genes show a significant enrichment in GO annotation categories, e.g., neuron part. In all three brain regions the differentially variable genes were significantly enriched in a single network module characterized by genes associated with cell-to-cell signaling. The data point to glutamate plasticity as being a key feature of selection for ethanol preference. In this context the expression of *Dlg2* which encodes for PSD-93 appears to have a key role. It was also observed that the expression of the clustered protocadherins was strongly associated with preference selection.

Keywords: RNA-Seq, collaborative cross, nucleus accumbens shell, central nucleus of amygdala (CeA), prelimbic cortex, network analysis

OPEN ACCESS

Edited by:
Feng C. Zhou,
Indiana University Bloomington, United States

Reviewed by:
Susan E. Bergeson,
Texas Tech University Health Sciences Center, United States
Richard Lowell Bell,
Indiana University Bloomington, United States

***Correspondence:**
Denesa R. Lockwood
denesaruth@gmail.com

[†] *Deceased*

Specialty section:
This article was submitted to Behavioral and Psychiatric Genetics, a section of the journal Frontiers in Genetics

Received: *01 May 2018*
Accepted: *17 July 2018*
Published: *28 August 2018*

Citation:
Colville AM, Iancu OD, Lockwood DR, Darakjian P, McWeeney SK, Searles R, Zheng C and Hitzemann R (2018) Regional Differences and Similarities in the Brain Transcriptome for Mice Selected for Ethanol Preference From HS-CC Founders. Front. Genet. 9:300. doi: 10.3389/fgene.2018.00300

INTRODUCTION

Beginning with Lewohl et al. (2000) there are now more than 200 studies using some form of genome-wide profiling to examine the relationships among alcohol effects, excessive alcohol consumption and the brain transcriptome. Contet (2012) reviewed the existing literature and noted that the genes associated with the risk of excessive consumption and/or the effects of excessive consumption had regionally specific effects on gene expression. Subsequent studies have confirmed and extended the "region" effect (e.g., Melendez et al., 2012; Osterndorff-Kahanek et al., 2015; Smith et al., 2016; Mulligan et al., 2017). It is important to note that these studies also by and large confirmed earlier observations (e.g., Kimpel et al., 2007) that regional differences in gene expression are generally far greater than the effects of treatment, strain or line (e.g., Mulligan et al., 2017). From a somewhat different perspective we have also observed

that the regional transcriptional network signature is largely independent of genetic diversity (Iancu et al., 2010).

In the current study we explore at the regional level how selection for ethanol preference affects the transcriptome. The regions compared (nucleus accumbens shell [SH], central nucleus of the amygdala [CeA], and prelimbic cortex [PL]) are components of the addiction circuit (Koob and Volkow, 2010, 2016). A previous study (Dhaher et al., 2008) suggested that the CeA but not the SH has a more significant role in preference (2-bottle choice) consumption. The short-term selection of the High and Low ethanol preference lines from heterogeneous stock-collaborative cross (HS-CC) founders has been described elsewhere (Colville et al., 2017). After three generations of bidirectional selection, the difference in the ethanol preference ratio was 0.49 vs. 0.15 in the High and Low lines, respectively. Sixty-five percent of the High females and 37% of the High males had a preference ratio of >0.5 compared with 6.5% of the Low females and 2.3% of the Low males. The HS-CC founders (formed from five laboratory and three wild-derived strains) provide substantially more genetic diversity than would be available in F_2 intercrosses or HS animals formed solely from inbred laboratory mouse strains (Roberts et al., 2007). It is estimated that the HS-CC founder strains encompass >90% of *Mus musculus* genetic diversity (Churchill et al., 2004).

Colville et al. (2017) used RNA-Seq to examine how High/Low line selection affected the SH transcriptome. The data analysis emphasized the effects of selection on gene networks. Networks were constructed using the weighted gene coexpression network analysis (WGCNA) (Zhang and Horvath, 2005). Selection targeted one of the network coexpression modules that were significantly enriched in genes associated with receptor signaling activity, including *Chrna7, Grin2a, Htr2a,* and *Oprd1*. Connectivity in the module as measured by changes in the hub nodes was significantly reduced in the low preference line. The current study expands on these observations by asking what features are regionally specific or non-specific. For this purpose, sample sizes have been substantially increased from Colville et al. (2017) to insure the high quality of network structures across brain regions (see Langfelder et al., 2011).

MATERIALS AND METHODS

Husbandry

The short term selection lines (Colville et al., 2017) were obtained from the colony at the Portland VA Medical Center, an AAALAC approved facility. All procedures were in accordance with the VA Institutional Animal Care and Use Committee and were performed according to NIH Guidelines for the Care and Use of Laboratory Animals. Mice were maintained at 21 ± 1°C in plastic cages (19 cm × 31 cm × 13 cm) on Eco-Fresh bedding (Absorption Corp.) with tap water and Purina 5001 chow (PMI Nutrition International, Brentwood, MO, United States) given *ad libitum*. Pups were weaned and housed with same-sex litter mates at postnatal day 21.

Selection

Selection details are found in Colville et al. (2017). Briefly, HS-CC founders (Iancu et al., 2010) were selected for breeding based on their preference for 10% ethanol vs. water. Beginning with 200 founders, the 20 males and 20 females with the highest preference values were paired, with brother-sister matings avoided, to create a "High" preference line; similarly, the 40 mice with the lowest preference scores were paired to create a "Low" line. ∼200 pups from each generation were weaned and tested at adulthood as above for three subsequent generations; active selection concluded at S_3. S_4 alcohol-naive pups were used for genetic analyses.

Dissection of Tissue and Extraction of RNA

At 8 weeks of age, naive S_4 mice, balanced for sex and line, were euthanized, the brains removed and immediately frozen on dry ice. Frozen brains were sliced in 55 micron coronal sections on a freezing microtome at −13°C and slices containing the nucleus accumbens, the amygdala, and the medial prefrontal cortex were mounted on PEN slides. Mounted slices were lightly thionin-stained under RNAse-free conditions and dehydrated in increasing concentrations of ethanol diluted in RNAse free water (50, 70, 95, and 100%) for 30 s each and then air-dried. The shell of the accumbens (SH), the CeA and the PL were dissected bilaterally on a Leica LMD-6000 using known anatomical landmarks (Franklin and Paxinos, 2008). Dissected tissue was processed with the ARCTURUS PicoPure kit. RNA quality was assessed using the Caliper LabChip GX and RNA Quality Scores (RQS). Only samples with RQS scores of >7 and >100 ng of total RNA were used for library formation. Sample numbers were as follows: SH-71; CeA-67; and PL-54. For reasons that were not clear, the percentage of extractions from the PL for high quality RNA was significantly lower.

RNA-Seq

Library formation (polyA+, stranded) and sequencing were all performed according to Illumina's specifications at the OHSU Massively Parallel Sequencing Shared Resource. Libraries were multiplexed six per lane, yielding approximately 25–30 million totals read per sample. FastQC was used for quality checks on the raw sequence data. Sequence data were then aligned using STAR [Spliced Transcripts Alignment to a Reference (Dobin et al., 2013)] allowing for a maximum of three mismatches per 100 bp read. For all samples >85% of the reads uniquely aligned. Using the featureCounts suite (Liao et al., 2014), reads were aligned to known genomic features to generate counts at the gene level. Gene expression data were imported into the R application environment; upper-quartile normalization was performed using the edgeR Bioconductor package (Robinson et al., 2010). The gene read density threshold for inclusion in the network analyses was an average of >1 count per million (CPM). Network connectivity for coexpression was calculated as described elsewhere (Colville et al., 2017). The

expression data have been deposited to NCBI's Gene Expression Omnibus[1].

Differential Expression (DE), Differential Variability (DV), and Differential Wiring (DW) Analyses

Differential expression was determined using edgeR, with the option of "tagwise" dispersion. Adjustment for multiple comparisons was performed using the SGOF procedure (de Uña-Alvarez, 2012). The threshold for significance was set at adjusted p-value < 0.05, although for module enrichment we utilized unadjusted p-values < 0.01. For gene differentially variable (DV), we utilized the "var.test" procedure in the R "stats" package; the threshold for significance was also set at adjusted p-value < 0.05. To mitigate the computational load for detecting differential wiring (DW), we restricted the search to Pearson correlations between individual genes that differed by ≥ 0.5. This general procedure has been used to quantify network rewiring in both genomic (Gill et al., 2010) and neural imaging studies (Hosseini et al., 2012). Using this procedure, we identified for each gene, the number of changed edges and then inquired as to whether some genes had a disproportionately high number of changing edges. For the latter, the binomial test was used with the following parameters. The average incidence of changing edges (the rate of the binomial test) was computed by dividing the number of changing edges ($p < 0.01$) by the total number of network edges. The number of trials (for each gene) was equal to the number of edges. The number of "successes" was equal to the number of changing edges.

Coexpression Network Construction

The coexpression network was constructed by means of the WGCNA (Langfelder and Horvath, 2008; Iancu et al., 2012). We started by constructing adjacency network matrices independently for each region by computing the Pearson correlation between all gene pairs. These values were raised to a power $\beta = 6$ for all regions, which was chosen such that the network approaches a scale-free structure (exponential distribution of node connectivity).

Given that biological mechanisms of network components are best captured by the most connected genes, we restricted the size of the network to genes that were in the top 80% with regards to connectivity. This also reduces the overall network size and decreases the computational load while preserving scale-free topology. The resulting networks contained ∼6,500 genes in the three networks (see **Supplementary Tables**).

We clustered the adjacency matrices utilizing average linkage and the WGCNA cuttreeHybrid function with the following parameters: cutHeight = 0.9995, minClusterSize = 100, and deepSplit = 4. The resulting clusters (denoted as modules) are uniquely identified by arbitrarily chosen colors which are independently generated for each brain region.

To determine the extent to which modules are preserved across brain regions we employed two complementary procedures. First we utilized the WGCNA modulePreservation function to check whether modules detected in one region show increased coexpression/connectivity in the other regions, recognizing that they might be distributed across different modules even if preserved. A second measure of module preservation was computed based on the gene overlap between all module pairs in all three regions, which is denoted as tabulation-based module preservation in the modulePreservation WGCNA function (Langfelder et al., 2011).

Coexpression Module Characterization

Module enrichment in DE, DV, and DW genes was used to assess the effects of selection on network structure. We considered a module "enriched" based on overlap between module genes and DE/DV/DW genes, using Fisher's exact test with Bonferroni correction for number of modules. The Gorilla algorithm (Eden et al., 2009) was used to provide a visual representation of GO annotation enrichment. To implement a ranking procedure we integrated differential network results at the module and gene summarization level into a comprehensive gene screening procedure. Modules enriched in gene or edge changes were the primary focus of further annotations. At the individual gene level, we focused on module hubs with normalized intramodular connectivity above 0.8 (see Colville et al., 2017; Iancu et al., 2018).

RESULTS

Summary of Gene Expression Data in the SH, CeA, and PL

The average gene expression levels across the three brain regions are presented in **Supplementary Table S1**; data are provided for the Ensembl annotated "genes" (N = 42,282). In all regions approximately 15,000 "genes" met the threshold of one CPM reads. Genes showing at least a 10-fold difference in expression between two regions are also found in **Supplementary Table S1**. Some expected examples include the high expression of *Adora2, Penk*, and *Drd2* in the CeA and SH and the high expression of *Bdnf* and *Cck* in the PL.

Gene Coexpression Networks

Gene networks were constructed using the WGCNA as described elsewhere (Colville et al., 2017). Initially all genes meeting the expression criteria of one CPM were entered into the analysis using a consensus module approach (Iancu et al., 2010). The number of genes in each network was then culled to include only those genes that contribute >80% of the total network connectivity. It was these reduced sets of genes (∼6,500/region) that were entered into subsequent analyses. Modules were color coded arbitrarily within or across regions. **Supplementary Table S2** also provides annotation for which network modules were significantly enriched in genes associated with neurons, astrocytes, and oligodendrocytes (Cahoy et al., 2008). We investigated the interaction subnetwork of *Dlg2*, a gene affected by selection and well-connected in the network. Utilizing the GeneMANIA (Warde-Farley et al., 2010) software as

[1] http://www.ncbi.nlm.nih.gov/geo/query/acc.cgi?acc=GSE65950

implemented in the associated Cytoscape (Shannon et al., 2003) plugin, we found a number of non-transcriptional mechanisms by which *Dlg2* interacts with other members of the glutamate family (**Figure 1**).

Module Preservation and Affected Gene Module Distribution Across Regions

Utilizing the tabulation-based module preservation procedure, we quantified the extent to which modules overlap across regions. The vast majority of modules were preserved across regions (Z summary $>$ 2), as described in Langfelder et al. (2011). There were a few exceptions: the CeA modules cyan, greenyellow, midnightblue, and yellow were either not preserved or only mildly preserved (2 $<$ Z summary $<$ 3) in both SH and PL. The SH modules grey60 and lightgreen were not preserved in either CeA or PL; additionally SH lightcyan was not preserved in CeA. The PL module midnightblue was not preserved in the CeA. The rest of the modules were either preserved (2 $<$ Z summary $<$ 10) or in most cases highly preserved (Z summary $>$ 10). These results illustrate that transcriptional network organization is overall preserved across brain regions, although the strength of interaction varies.

We also utilized a complementary module preservation measure which is tabulation-based and uses the Fisher exact test. This measure evaluates whether the intersection of two modules originating from different brain regions is greater than what can be expected by chance. We found that in most cases each module has one or at most 2–3 counterparts in different brain regions (**Figure 2**). When overlaying the DE/DV/DW information on the module overlap, a complex picture emerges. We have examples of counterpart modules being affected across region, for example the DW CeA blue module having a very strong counterpart in the DE SH lightgreen module (**Figure 2A**). Another example of concordance across regions includes the DE, DV, and DW SH magenta module having a strong counterpart in the DV, DW PL brown module (**Figure 2C**). The clearest example of lack of concordance is the DE, DV, DW SH magenta module with no counterpart in the CeA (**Figure 2A**).

Differential Expression (DE) Across Regions

There were 398, 302, and 183 genes showing significant (adjusted p-value $<$ 0.05) DE between the High and Low selected lines in the CeA, SH, and PL, respectively (**Supplementary Table S3**). The overlap in DE is illustrated in **Figure 3**. Only five genes (*5730455P16Rik, Gdi2, Skiv2, Tsr1*, and *Glod4*), all with increased expression in the High line, showed common DE. The overlap for DE was highest between the SH and CeA (N = 31). Genes in all the overlapping categories are listed in **Supplementary Table S3**. Only one gene showed a difference in the direction of DE between regions; *Doc2b* showed increased/decreased expression in the High line (PL vs. SH). GO annotation of the CeA DE genes revealed a significant enrichment in genes associated with the neurononal component (FDR $< 3 \times 10^{-5}$), structural constituent of myelin sheath

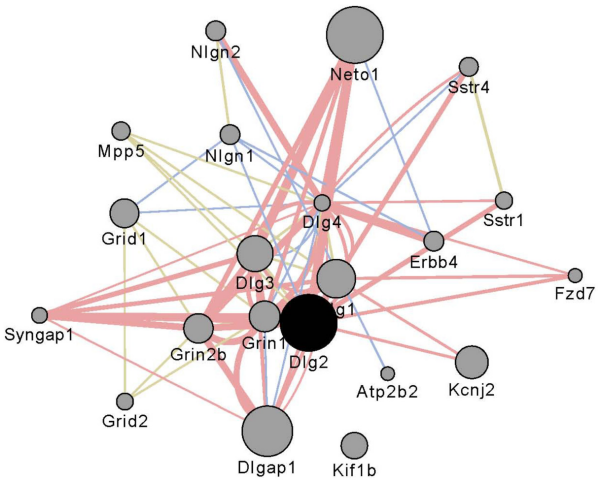

FIGURE 1 | Interaction partners for *Dlg2* extracted using Gene Mania (Warde-Farley et al., 2010) which was accessed as a Cytoscape plugin with default settings. Depicted are top 20 genes related to *Dlg2* through physical interactions, colocalizations, or sharing protein domains. *Dlg2* which encodes for PSD93, interacts with a number of genes and gene products associated with glutamate receptor activity including *Dlg4, Syngap1, Neto, Grin1, Grin2b, Dlgap1*, and *Dlg3*.

(FDR $< 4 \times 10^{-3}$) and axon ensheathment (FDR $< 7 \times 10^{-3}$) (**Supplementary Table S4**). Genes in the neuron part category included *Adora1, Chrna4, Crhr1, Drd1a, Gabbr2, Gabrd, Gal, Htr1a, Htr2a, Htr7, Pde1b, Reln, Syt2*, and *Tac1*. The CeA DE genes were significantly (corrected $p < 8 \times 10^{-7}$) enriched in the yellow network module (**Supplementary Table S2**). The yellow module was enriched in annotations associated with plasma membrane (FDR $< 5 \times 10^{-4}$), regulation of nervous system development (FDR $< 4 \times 10^{-4}$) and structural constituent of myelin sheath (FDR $< 9 \times 10^{-3}$; **Supplementary Table S4**). The average relative intramodular connectivity (full scale – 0.0 to 1.0) for the yellow module DE genes in the Low and High lines was 0.30 and 0.31, respectively (see **Supplementary Table S3**). Five of the 109 DE yellow module genes were hub nodes (relative connectivity $>$0.80 in either the High or Lines or both lines). These genes were *Rbm24, Dock10, Prkcd, Rap1gap*, and *Spg2*.

There was no significant enrichment in any GO annotation for the DE genes in the SH. Similarly, this group of genes was not enriched in any of the SH network modules. The average relative intramodular connectivity for these DE genes in the Low and High lines was 0.41 and 0.39, respectively.

There was no significant enrichment in any GO annotation for the DE genes in the PL. This group of genes was however, significantly enriched ($p < 4 \times 10^{-5}$) in the PL turquoise network module. This module was enriched in genes with the Rho GTPase binding annotation (FDR $< 6 \times 10^{-3}$). The average relative intramodular connectivity for these DE genes in the Low and High lines was 0.43 and 0.32, respectively ($p < 0.003$). Five of the 83 DE turquoise module genes were hub nodes. These genes were *Mapk7, Pcgf2, Leng2, Col5a3*, and *Pabpn1*.

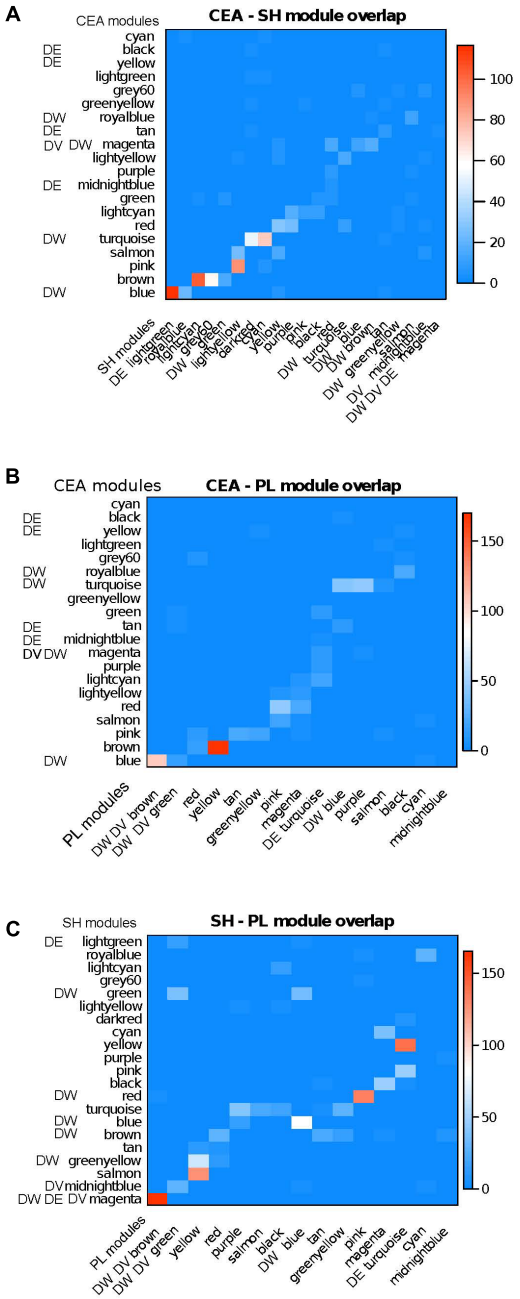

FIGURE 2 | Module overlap across brain regions together with enrichment of modules in DE/DV/DW genes. Color from blue to red is proportional to –log10(p) of overlap between module membership (Fisher exact test). A majority of modules have strong counterparts across regions. The affected modules also have an affected counterpart in a majority of cases, although we also find region specific affected modules. **(A)** CeA – SH; **(B)** CeA – PL; **(C)** SH – PL.

Differential Variability (DV) Across Regions

There were 424, 479, and 236 genes showing significant (adjusted p-value < 0.05) DV between the High and Low selected lines in the CeA, SH, and PL, respectively (**Supplementary Table S5**). The overlap in DV is illustrated in **Figure 3C**. Thirty genes were common to all three regions and this grouping was significantly (FDR $< 3 \times 10^{-3}$) enriched in genes associated with cell-to-cell signaling. Genes with this GO annotation included *Dlg2, Egr3, Gabbr2, Lnpep, Pcdhgb2, Pcdhac2, Sstr4*, and *Syt10*. The overlap in genes ($N = 44$) between the PL and SH showed a significant enrichment in genes with the GO annotation of neuron projection (FDR $< 6 \times 10^{-3}$). Genes with this GO annotation included *Bace1, Cpeb3, Fzd3, Igf1r, Igsf9, Kcna3, Kcnb1, Kcnma1, Slc8a1, Sv2c, Tenm1*, and *Tenm3*. In all three regions the direction of the DV was High line $>>$ Low line.

GO annotation of the CeA DV genes revealed a significant enrichment in genes associated with cell-to-cell signaling (FDR $< 3 \times 10^{-4}$; **Supplementary Table S7**). Genes in this category and not already noted above included *Chat, Gabrg3, Glra3, Gpr88, Ntrk2, Pten, Sdcbp*, and five additional protocadherins. The CeA DV genes were significantly (1×10^{-8}) enriched in a single network module, blue. Annotations for the blue module included synaptic membrane (FDR $< 5 \times 10^{-2}$) and cell-to-cell signaling (FDR $< 2 \times 10^{-7}$; **Supplementary Table S6**). The blue module contained most of the cell-to-cell signaling genes noted above and included *Chrm5, Chrna7, Chrnb2, Grid1, Grik3, Grin2a, Grin2b, Htr5a*, and *Sv2c;* the module was also associated with 16 protocadherin genes. For the blue module DV genes, intramodular connectivity was significantly different between the Low and High lines (0.32 vs. 0.48, $p < 1 \times 10^{-16}$). The most prominent change in connectivity for non-hub to hub status was seen for *Ntrk2* (0.197 vs. 0.821; Low vs. High line). *Nrtk2* encodes TrkB, a receptor for Bdnf.

GO annotation of the SH DV genes revealed a significant enrichment in genes associated with cell-to-cell signaling (FDR $< 2 \times 10^{-4}$; **Supplementary Table S6**) and neuron projection (FDR $< 7 \times 10^{-3}$). The signaling genes ($N = 33$) in addition to the common DV genes noted above included *Chat, Chrna7, Grik2, Grin2b Htr1b, Htr2a, Oprd1, Sv2c*, and 10 protocadherins. The SH DV genes were enriched ($p < 2 \times 10^{-21}$) in a single network module, magenta; 187 or the 231 members of the magenta module were significantly DV between the High and Low selected lines. The magenta module was enriched in genes associated with cell-to-cell signaling ($p < 3 \times 10^{-11}$) and neuron part ($p < 4 \times 10^{-5}$; **Supplementary Table S6**). The magenta module signaling genes overlapped with those noted above, e.g., *Chrna7* and *Grin2b*, and included 12 protocadherins. Focusing on the DV genes within the magenta module, average intramodular connectivity increased from 0.34 to 0.73 (Low vs. High; $p < 1 \times 10^{-63}$). Genes showing large changes (non-hub to hub status; Low vs. High) included *Pde4d, Adra1a, Pcdhga8&6*, and *Ncam2*.

GO annotation of the PL DV genes revealed a significant enrichment in genes associated with signal transduction (FDR $< 1 \times 10^{-6}$), cell to cell signaling (FDR $< 1 \times 10^{-4}$) and neuron part (FDR $< 8 \times 10^{-9}$) (**Supplementary Table S6**). The signaling genes overlap with those noted above but also include *Nos1* and *Gm3*. The PL DV genes were enriched ($p < 3 \times 10^{-10}$) in a single network module, brown. GO annotations for the brown module included neuron part (FDR $< 5 \times 10^{-11}$), PDZ

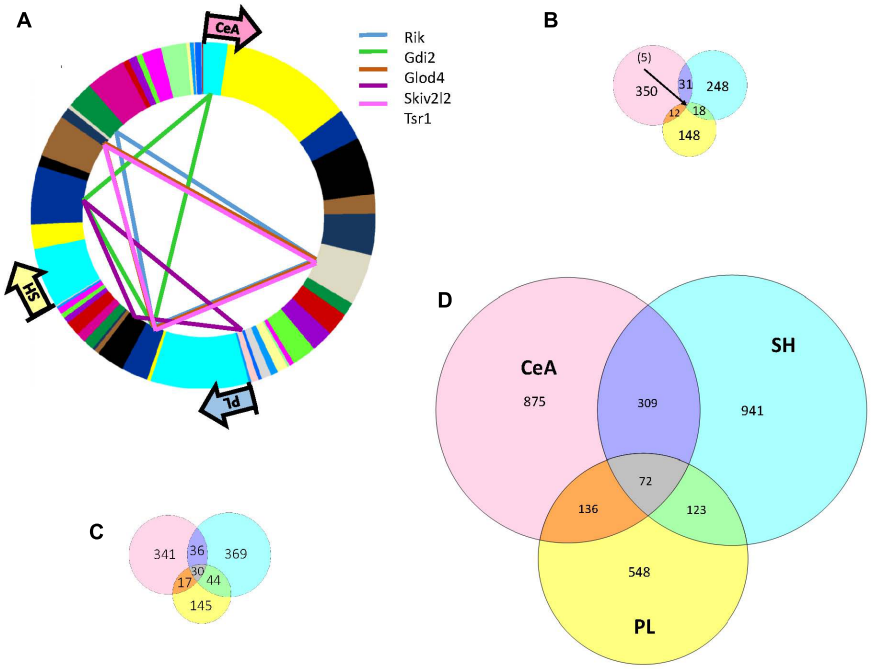

FIGURE 3 | Overlap of selection associated DE, DV, and DW genes across three brain regions: CeA, SH, and PL. **(A)** As indicated in the Venn diagram **(B)** there was only 5 DE genes common to all three brain regions: *5730455P16Rik,Gdi2, Skiv2, Tsr1,* and *Glod4*. The region and module distribution of these genes is illustrated. The greatest overlap was between the CeA and SH ($N = 31$). Only annotation of the CeA DE genes revealed a significant enrichment in GO categories that included neuron part, structural constituent of myelin sheath and axon ensheathment. Genes in the neuron part category included *Adora1, Chrna4, Crhr1, Drd1a,Gabbr2, Gabrd, Gal, Htr1a, Htr2a, Htr7, Pde1b, Reln, Syt2*, and *Tac1*. **(C)** Overlap of selection associated DV genes across three brain regions: CeA, SH, and PL. There were 30 significant DV genes common to all three brain regions and this grouping was significantly enriched (FDR $< 3 \times 10^{-3}$) in genes associated with the GO annotation of cell to cell signaling. Genes with this GO annotation included *Dlg2, Egr3, Gabbr2, Lnpep, Pcdhgb2, Pcdhac2, Sstr4*, and *Syt10*. The significant DV genes unique to each brain region also showed an enrichment in genes associated with cell to cell signaling. **(D)** Overlap of selection associated DW genes across three brain regions: CeA, SH, and PL. There were 72 significant DW genes common to all three brain regions and this grouping was significantly enriched (FDR $< 5 \times 10^{-3}$) in genes associated with the GO annotation of post-synapse. Genes with this GO annotation included *Chrna7, Als2, Pppir9a, Strn, Kcna4, Kif1a*, and *Slc1a2*. Genes showing unique DW to each of the three brain regions were enriched in genes associated with the GO annotation synapse or synapse part.

domain signaling (FDR $< 1 \times 10^{-2}$) and cell to cell signaling (FDR $< 7 \times 10^{-11}$). The signaling genes ($N = 49$) largely overlap the signaling genes in the blue and magenta modules noted above and include a large number ($N = 18$) of protocadherins, also seen prominently in the SH results. Focusing on the brown module DV genes, average intramodular connectivity differed between the High vs. Low lines (0.72 vs. 0.40; $p < 5 \times 10^{-20}$). Genes showing large differences in hub status (High $>>$ Low) included *Syt10, Dgkh, Grin2a*, and *Adra1a*.

Differential Wiring (DW) Across Regions

There were 1,392, 1,445, and 879 genes showing significant (adjusted p-value < 0.05) DW between the High and Low selected lines in the CeA, SH, and PL, respectively (**Supplementary Table S7**). The overlap in DW is illustrated in **Figure 3D**. Seventy-two genes were common to all three regions and this grouping was significantly (FDR $< 5 \times 10^{-3}$) enriched in genes associated with the post-synaptic component. Genes with this GO annotation included *Chrna7, Als2, Pppir9a, Strn, Kcna4, Kif1a*, and *Slc1a2* (**Supplementary Table S8**). The overlap in genes between the PL and SH ($N = 123$) showed a significant (FDR $< 2 \times 10^{-2}$) enrichment in genes with the synaptic membrane annotation; these genes included *Arrb1, Itgb1, Cpd, Akap5, Rim1, Shank3, Ptprz1, Gm3, Ank2, Gm1*, and *Cntmap2*. There was no annotation enrichment in the overlapping genes between the PL and CeA. The overlapping genes between the CeA and the SH ($N = 309$) showed a significant (FDR $< 2 \times 10^{-3}$) enrichment in genes associated with the neuronal component (**Supplementary Table S8**); genes in this category ($N = 60$) included *Calm1, Gad2, Nlg1, Oprd1, Pten, Rab10*, and *Sv2a*.

GO annotation of the CeA DW genes revealed a significant enrichment (FDR $< 4 \times 10^{-7}$) in genes ($N = 118$) associated with the synaptic component (**Supplementary Table S8**); genes in this category included *Cnr1, Dlg1, Gabra4, Gabrb3, Gabrg3, Gphn, Gria2, Grid2, Grik3, Grin2b, Grm5, Slc1a2&3, Stx1b,2&3*, and *Syap1*. The CeA DW genes were enriched in three modules: blue, magenta, and turquoise (**Supplementary Table S8**). The blue CeA module is described above. The magenta module did not have a significant enrichment in any GO category. The turquoise module was enriched in the categories macromolecule metabolic process (FDR $< 1 \times 10^{-8}$), ubiquitin–protein transferase activity (FDR $< 2 \times 10^{-4}$) and membrane-bound organelle (FDR $< 1 \times 10^{-9}$). It also should be noted that for six modules, the number of DW genes was significantly less than

expected; these modules were significantly conserved in response to selection. For the DW genes in the blue, magenta, and turquoise modules, intramodular connectivity (Low vs. High; 0.26 vs. 0.55) was significantly different ($p < 1 \times 10^{-95}$). Large changes (>0.5 in relative connectivity) were noted for the genes *Cab39, Nrtk2, Ankrd10,* and *Mov10;* all of these genes increased relative connectivity from the Low to the High line. Additional details for *Nrtk2* are noted above.

GO annotation of the SH DW genes revealed a significant enrichment (FDR $< 4 \times 10^{-12}$) in genes ($N = 137$) associated with the synaptic component (**Supplementary Table S8**); genes in this category and not noted previously included *Adam10, Arrb1, Epha4, Grm4&7, Homer1, P2ry1, Snap25&29, Synpo,* and *Synpr*. The SH DW genes were enriched in five network modules, most prominently in the green module ($p < 4 \times 10^{-9}$). The green module was significantly enriched in genes associated with the synaptic component ($p < 2 \times 10^{-8}$), nervous system development ($p < 1 \times 10^{-4}$) and enzyme binding ($p < 2 \times 10^{-2}$). For nine modules, the number of DW genes was significantly less than expected. For the green module DW genes, intramodular connectivity on average showed no change between the Low and High lines (0.61 vs. 0.62, respectively).

GO annotation of the PL DW genes revealed a significant enrichment in genes ($N = 75$) associated with the synaptic component (FDR $< 2 \times 10^{-8}$) and in genes ($N = 282$) associated with development (FDR $< 2 \times 10^{-4}$; **Supplementary Table S8**). Genes in the synapse category and not noted previously included *Cadm1&2, Dmd, Kcna2&4, Phactr1, Snph, Sntb1, and Tln1.* The PL DW genes were significantly enriched in two network modules, brown and green. The brown module is described above. The green module was enriched in genes associated with regulation of cellular localization (FDR $< 2 \times 10^{-2}$) and in genes associated with the neuronal component (FDR $< 6 \times 10^{-4}$). Different from the CeA and SH, only one PL module (yellow) showed significant conservation (corrected $p < 0.05$). For the brown module DW genes, relative intramodular connectivity increased in the High vs. Low line (0.59 vs. 0.24; $p < 6 \times 10^{-56}$). Genes moving from non-hub status (Low line) to hub status (High line) included *Sox6, Egr3, Soga3, Pcdhgb5, Pcdhga8, Senp5,* and *Prkg1*. For the green module DW genes, relative intramodular connectivity increased in the High vs. Low line (0.52 vs. 0.21; $p < 2 \times 10^{-37}$). Genes moving from non-hub status (Low line) to hub status (High line) included *Ncoa4, Edem3, Xpr1,* and *Necab1*.

DISCUSSION

We recognize that there are many strategies available for analyzing complex datasets, such as those presented here, and each will emphasize somewhat different aspects of the data. The approach taken here is one that we have used previously (Colville et al., 2017; Iancu et al., 2018). The key metrics; DE, DV, and DW, are computationally straightforward and can be easily replicated. The WGCNA has greatly matured since its introduction (Zhang and Horvath, 2005) and has been used in more than 300 publications. In the current study we have focused our investigations on those genes that contribute to at least 80% of network connectivity. This thresholding reduced the number of genes considered for further analyses from ∼15,000 to ∼6,500 in each of the three brain regions. The genes culled are "leaf" nodes with low connectivity. While selection will have significant effects on some of these culled genes, none will be hub nodes. We also note that the sample sizes used in the current study were sufficient to produce networks of high quality (Langfelder and Horvath, 2008). The selection of the High and Low ethanol preference lines from HS-CC founders has been described elsewhere (Colville et al., 2017). The HS-CC was derived from eight mouse strains, including three wild-derived strains; the genetic diversity captured is ∼90% of that available in *M. musculus* (Roberts et al., 2007). The preference lines were bred using a short-term selective breeding protocol (Belknap et al., 1997; Metten et al., 2014) that minimizes the stochastic fixation of alleles unrelated to the phenotype of interest, here 2-bottle choice ethanol preference. From the perspective of ethanol preference and consumption, the HS-CC are of interest in that ∼25% of the animals show a preference for ethanol; this differs from a <5% preference found in our HS/NPT mice (unpublished observation) that were derived from eight laboratory mouse strains (Hitzemann et al., 2014).

Contet (2012) surveyed the existing literature and noted that multiple functional categories were associated with a "predisposition" to excessive ethanol consumption and in most cases each of the categories have been supported by multiple publications (see Table 2 in Contet, 2012). Some regional specificity for each of the functional categories was also noted; however, the regional differences in gene expression were generally larger than those associated with selection for preference or binge drinking (Kimpel et al., 2007; Mulligan et al., 2011). Subsequent studies have confirmed and extended the "region" effect (e.g., Melendez et al., 2012; Osterndorff-Kahanek et al., 2015; Smith et al., 2016; Mulligan et al., 2017). The data in **Supplementary Table S1** again confirm marked differences in regional gene expression. Fifty or more genes in each of the three regions show a 10-fold higher expression when compared with at least one other region. In no region was selection associated with a change in expression of >2-fold and in most cases, selection was associated with small changes in expression (<30%) among the genes included in the DE analyses (see above). The number of significantly DE genes, common to all three regions was small ($N = 5$) and the genes appear to have no common function(s). Only in the CeA, did the analyses reveal that the DE genes were associated with significant GO annotations (neuron part, structural constituent of myelin sheath and axon ensheathment). Among the genes in the neuron part category were several that have been implicated in excessive ethanol consumption, including *Adora1, Crhr1, Gal,* and *Syt2* (Belfer et al., 2006; Enoch et al., 2013; Barbier et al., 2015; Clark et al., 2017). However, in the CeA as well as the SH and PL, the DE genes had on average a low intramodular connectivity, i.e., these genes were "leaf" nodes. This observation is consistent with the observation that the degree of DE was generally quite small and to detect such small changes requires that the variance for these genes must be relatively low. Connectivity requires

sufficient variance to accurately detect gene–gene correlations (see below). Overall, we conclude that DE is not a key selection feature for preference lines derived from genetically diverse HS-CC founders and when viewed in a network context. A similar conclusion was reached on a smaller SH sample (Colville et al., 2017).

The relationship(s) between network connectivity and gene variability are not entirely clear. However, if the variance is "biological" and not technical or simply stochastic, it follows that variance and connectivity will increase in tandem; for the moderate sample sizes of most gene expression studies, gene–gene correlations and hence connectivity will be more easily detected. Colville et al. (2017) observed that selection for the High and Low preference lines was associated with a cluster of DV genes that were highly enriched in a single network module (greenyellow). The module was highly enriched in genes associated with receptor signaling (e.g., *Chrna7*, *Grin2a*, *Htr2a*, and *Oprd1*) but also included a large number of genes associated with cell adhesion. Cadherins and protocadherins were particularly enriched in the greenyellow module. Expanding the SH sample size from Colville et al. (2017) by ∼50% did not perceptually change the results. In the SH, the DV genes were highly enriched in a single module (magenta) that was similar to the greenyellow module (again remembering that module color has no meaning and is randomly assigned). The magenta and greenyellow modules are of a similar size (231 vs. 227 genes, respectively); 98 genes overlap between the modules (**Supplementary Table S9**). The modules share 37 hub nodes; including *Oprd1, Dlg2, Gabrb2, Pcdhgb2, Pcdhga6, and Pcdhga7*, i.e., a measure of core connectivity is unchanged. The differences between the modules are largely found in the less connected nodes.

The CeA and PL DV genes also were enriched in single network modules, blue and brown, respectively. Annotation of these modules was similar to that for the SH magenta module, e.g., a significant enrichment in genes associated with cell to cell signaling. The SH magenta, the CeA blue and the PL brown modules were significantly different in size (231, 773, and 593 genes, respectively). However, 183 (79%) the genes in the SH module are also found in the CeA and PL modules. This grouping of module core genes is found in **Supplementary Table S9**. This core grouping contains several receptors including *Adra1a, Chrna7, Grin2b, Htr2a, Oprd1,* and *Sstr4;* this core group also contains 17 protocadherins including 14 of the 22 known γ protocadherins. Thirty significant DV genes were identified as common to all three regions (see **Figure 2**); 25 genes of this group are found in the core module grouping. Within the core module grouping, we identified the 18 genes that were hub nodes across all three regions; we next aligned these genes with the 25 common DV genes found in the core module. Our rationale for this step was to identify high priority hub nodes, that could be targeted in future studies. Six genes were identified: *Dlg2, Gatad2b, Pcdhac2, Tnks, Usp29,* and *Usp9x. Dlg2* encodes for post-synaptic density protein 93 (PSD-93), *Gatad2b* encodes for transcriptional repressor p66-beta, *Pcdhac2* encodes for protocadherin αc2, *Tnks* encodes for Tankyrase-1, *Usp29* encodes for ubiquitin specific protease 29 and *Usp9x* encodes for ubiquitin specific protease 9, X-linked. That two ubiquitin-related genes are in this group cannot be unexpected, given the long standing observations that ubiquitination is associated with chronic ethanol exposure in both animals and humans (see Sokolov et al., 2003; Liu et al., 2006; Contet, 2012; Melendez et al., 2012; Widagdo et al., 2017). Our data link ubiquitination to risk for excessive consumption. The precise mechanisms are unknown but we note here that ubiquitination has a key role in glutamate receptor trafficking (Widagdo et al., 2017). The functions of Tankyrase-1 (Tank-1) in the brain have not been investigated. However, Tank-1 is a member of a large family of poly (ADP-ribose) polymerases (PARPs). PARP-1 is thought to have key role(s) in the neuroinflammatory cascade associated with binge ethanol consumption (Tajuddin et al., 2018). To our knowledge, Pcdhαc2 has no function remarkably different from the other members of the αPcdh family; however relatively little is known about functions of the individual gene products. What the data presented previously (Colville et al., 2017) and again confirmed here clearly illustrates that selection for ethanol preference engages a large number of the clustered protocadherins. Again with a focus on glutamate neurotransmission, Suo et al. (2012) have shown that both the α and γ protocadherin clusters are involved in the inhibition of Pyk2 (protein tyrosine kinase 2), which results in the disinhibition of Rac1 (Ras-related C3 botulinum toxin substrate 1) that in turn can facilitate the proper assembly of dendritic spines (see Figure 8 in Suo et al., 2012). Mutations and deletions in *Gatad2b* have been associated with intellectual disabilities (e.g., Tim-Aroon et al., 2017). Perhaps more pertinent for the current study, the ENIGMA consortium has found that SNPs associated with both *Gatad2b* and *Dlg2* are associated with differences in putamen size (Chen et al., 2017). The coexpression and physical interaction partners for *Dlg2* are shown in **Figure 1**. Key partners include a number of genes encoding glutamate receptor subunits (e.g., *Grin2b* and *Grid1*) and genes encoding glutamate associated membrane proteins (e.g., *Dlg1, Dlg4*, and *Dlgap1*). Bell et al. (2016) have reviewed the literature associated with ethanol risk, ethanol effects and glutamate reward circuitry; importantly, these authors noted when comparing the P and NP rats, there were a number of differences in glutamate signaling genes that predate ethanol exposure. Clinical studies have shown that in family history positive (FHP) individuals there is an altered response to both alcohol and the NMDA antagonist ketamine, suggesting a genetic link between alcoholism and NMDA receptor function (Petrakis et al., 2004; Joslyn et al., 2010).

Differential wiring which is necessarily related to DV, provided a measure of how selection affects the interaction (connectivity) of each gene with the entire coexpression network. Similar to our previous results (Colville et al., 2017; Iancu et al., 2018), we observed that selection has marked effects on DW and this was true across all regions, with the effects somewhat more prominent in the CeA and SH than the PL. The large DW effect associated with selection is largely silent in most analyses of coexpression data, even though the data illustrate here that the rewiring of the coexpression system is perhaps the most profound change in the transcriptome. There were 71 common DW genes across the three brain regions and this core group was significantly

enriched in genes associated with the post-synaptic membrane. The genes in this category included *Chrna7, Als2, Ppp1r9a, Strn, Kcna4, Kif1a, and Slc1a2. Slc1a2,* which encodes for the excitatory amino acid transporter 2 (EAAT2) and is the principal transporter within the brain for glutamate, is of interest given the focus on excitatory neurotransmission above and evidence that inhibition of EAAT2 reduces ethanol consumption (Sari et al., 2016). Other members of this group appear to have some role(s) in regulating glutamatergic receptor function. For example, the deletion of *Chrna7* leads to the loss of NMDA receptors (Lin et al., 2014). Interestingly, the deletion of *Chrna7* is also associated with increased sensitivity to several ethanol-induced behaviors (Bowers et al., 2005). *Als2* encodes for alsin which has been shown to protect neurons from glutamate-associated neurotoxicity (Lai et al., 2006; Kwak and Weiss, 2006; Cai et al., 2008). *Strn* which encodes for striatin, is highly enriched in dendritic spines; this localization is reduced by NMDA receptor stimulation which appears to have a key role in synaptic plasticity (see Chen et al., 2012 and references therein). *Kcna4* which encodes potassium voltage-gated channel subfamily A member four, is recruited to the synapse by PSD95, where it is phosphorylated (Wong and Schlichter, 2004). *Kif1a* encodes a kinsin family three member which is also known as axonal transporter of synaptic vesicles. Mutations in the *Drosophila* homolog unc-104, have revealed the importance of the protein product in glutamate spontaneous release and in post-synaptic density organization (Zhang et al., 2017).

In each of the three brain regions, the DW genes unique to that region were highly enriched in synapse-associated genes. This effect was particularly dramatic in the CeA where a large number of both GABA and glutamate receptor subunits were affected. DW genes were distributed across several network modules, making the distribution of the DW genes more diffuse than that for the DV genes. It was also observed in both the CeA and SH that a number of network modules were largely preserved from the effects of selection on wiring. Many of these preserved modules had annotations associated with ATP metabolic processes, DNA replication, rRNA cellular respiration and so on. One purpose of using a short-term selective breeding protocol is to minimize genetic drift and focus the analysis on only those alleles associated with the phenotype of interest, here ethanol preference. Clearly, the DW data illustrates that even three rounds of selection had marked and extensive effects on the brain transcriptome.

Our discussion has largely focused on those changes in gene expression that are similar across the three brain regions. Our argument for taking this perspective is that these changes are the "broad" targets for manipulation. Included in these broad targets are core genes, including hub nodes, associated with glutamate receptor signaling and synaptic plasticity. We have also confirmed (see Colville et al., 2017) that selection for ethanol preference in HS-CC mice involves a large cohort of clustered protocadherins. This differs from selection for binge ethanol consumption where we have observed that selection for "drinking in the dark" involves numerous extra-cellular matrix genes such as collagens and matrix metalloproteases (Iancu et al., 2018). "Narrow" sense targets for manipulations will include those selection based changes that are regionally unique. For example, we observed that in the CeA, the expression of *Nrtk2* which encodes TrkB, a receptor for Bdnf, moves from non-hub status in the Low selected line to hub status in the High line. Numerous studies have linked the regulation of ethanol consumption to the regulation of Bdnf function; Darcq et al. (2016) have found in the rat dorsolateral striatum the Bdnf-TrkB system is essential to maintaining moderate ethanol intake. Our data suggest that manipulating this system in the CeA will likely have marked effects on ethanol preference.

AUTHOR CONTRIBUTIONS

AC performed all of the dissections and RNA extractions as well as the post-sequencing data analysis and preparation of the manuscript. OI conducted data analysis and manuscript and figure preparation. DL performed the behavioral selection to derive the mice used and helped prepare the manuscript. PD contributed to data analysis. SM contributed to experimental design, data analysis, and manuscript preparation. RS performed the sequencing and contributed to experimental design. CZ contributed to data analysis. RH was the PI for this project and oversaw all components, also contributing to data analysis and manuscript preparation.

FUNDING

This work was supported in part by National Institutes of Health (AA11034, AA13484, and AA10760).

ACKNOWLEDGMENTS

AC passed away unexpectedly in August 2015. The data presented here was part of his Ph.D. dissertation, which was presented posthumously in June 2016. All authors were involved either in the acquisition of the data and/or in the data analysis and manuscript preparation.

SUPPLEMENTARY MATERIAL

The Supplementary Material for this article can be found online at: https://www.frontiersin.org/articles/10.3389/fgene.2018.00300/full#supplementary-material

TABLE S1 | Gene expression (RNA-Seq) in the CeA, SH, and PL expressed as counts (reads) per million (CPM) – average data (N = 67, 71, and 54, respectively).

TABLE S2 | Annotation of how the network modules in each of the brain regions were significantly enriched in genes associated with neurons, astrocytes, and oligodendrocytes.

TABLE S3 | Differential expression (DE) between the High and Low selected lines in the CeA, SH, and PL (FDR < 0.05).

TABLE S4 | Gene Ontology (GO) annotation for DE genes.

TABLE S5 | List of genes found to be differentially variable (DV) in the CeA, SH, and PL (FDR < 0.05).

TABLE S6 | GO annotation of overlapping DV genes between brain regions.

TABLE S7 | List of differentially wired (DW) genes in the CeA, SH, and PL (FDR < 0.05).

TABLE S8 | GO annotation of overlapping DW genes between brain regions.

TABLE S9 | Comparison of data taken from this study with that of previous work from our laboratory.

REFERENCES

Barbier, E., Tapocik, J. D., Juergens, N., Pitcairn, C., Borich, A., Schank, J. R., et al. (2015). DNA methylation in the medial prefrontal cortex regulates alcohol-induced behavior and plasticity. *J. Neurosci.* 35, 6153–6164. doi: 10.1523/JNEUROSCI.4571-14.2015

Belfer, I., Hipp, H., McKnight, C., Evans, C., Buzas, B., Bollettino, A., et al. (2006). Association of galanin haplotypes with alcoholism and anxiety in two ethnically distinct populations. *Mol. Psychiatry* 11, 301–311. doi: 10.1038/sj.mp.4001768

Belknap, J. K., Richards, S. P., O'Toole, L. A., Helms, M. L., and Phillips, T. J. (1997). Short-term selective breeding as a tool for QTL mapping: ethanol preference drinking in mice. *Behav. Genet.* 27, 55–66. doi: 10.1023/A:1025615409383

Bell, R. L., Hauser, S. R., McClintick, J., Rahman, S., Edenberg, H. J., Szumlinski, K. K., et al. (2016). Ethanol-associated changes in glutamate reward neurocircuitry: a minireview of clinical and preclinical genetic findings. *Prog. Mol. Biol. Transl. Sci.* 137, 41–85. doi: 10.1016/bs.pmbts.2015.10.018

Bowers, B. J., McClure-Begley, T. D., Keller, J. J., Paylor, R., Collins, A. C., and Wehner, J. M. (2005). Deletion of the alpha7 nicotinic receptor subunit gene results in increased sensitivity to several behavioral effects produced by alcohol. *Alcohol. Clin. Exp. Res.* 29, 295–302. doi: 10.1097/01.ALC.0000156116.40817.A2

Cahoy, J. D., Emery, B., Kaushal, A., Foo, L. C., Zamanian, J. L., Christopherson, K. S., et al. (2008). A transcriptome database for astrocytes, neurons, and oligodendrocytes: a new resource for understanding brain development and function. *J. Neurosci.* 28, 264–278. doi: 10.1523/JNEUROSCI.4178-07.2008

Cai, H., Shim, H., Lai, C., Xie, C., Lin, X., Yang, W. J., et al. (2008). ALS2/alsin knockout mice and motor neuron diseases. *Neurodegener. Dis.* 5, 359–366. doi: 10.1159/000151295

Chen, C.-H., Wang, Y., Lo, M.-T., Schork, A., Fan, C.-C., Holland, D., et al. (2017). Leveraging genome characteristics to improve gene discovery for putamen subcortical brain structure. *Sci. Rep.* 7:15736. doi: 10.1038/s41598-017-15705-x

Chen, Y.-K., Chen, C.-Y., Hu, H.-T., and Hsueh, Y.-P. (2012). CTTNBP2, but not CTTNBP2NL, regulates dendritic spinogenesis and synaptic distribution of the striatin-PP2A complex. *Mol. Biol. Cell* 23, 4383–4392. doi: 10.1091/mbc.E12-05-0365

Churchill, G. A., Airey, D. C., Allayee, H., Angel, J. M., Attie, A. D., Beatty, J., et al. (2004). The collaborative cross, a community resource for the genetic analysis of complex traits. *Nat. Genet.* 36, 1133–1137. doi: 10.1038/ng1104-1133

Clark, S. L., McClay, J. L., Adkins, D. E., Kumar, G., Aberg, K. A., Nerella, S., et al. (2017). Deep sequencing of 71 candidate genes to characterize variation associated with alcohol dependence. *Alcohol. Clin. Exp. Res.* 41, 711–718. doi: 10.1111/acer.13352

Colville, A. M., Iancu, O. D., Oberbeck, D. L., Darakjian, P., Zheng, C. L., Walter, N. A. R., et al. (2017). Effects of selection for ethanol preference on gene expression in the nucleus accumbens of HS-CC mice. *Genes Brain Behav.* 16, 462–471. doi: 10.1111/gbb.12367

Contet, C. (2012). Gene expression under the influence: transcriptional profiling of ethanol in the brain. *Curr. Psychopharmacol.* 1, 301–314. doi: 10.2174/2211556011201040301

Darcq, E., Morisot, N., Phamluong, K., Warnault, V., Jeanblanc, J., Longo, F. M., et al. (2016). The neurotrophic factor receptor p75 in the rat dorsolateral striatum drives excessive alcohol drinking. *J. Neurosci.* 36, 10116–10127. doi: 10.1523/JNEUROSCI.4597-14.2016

de Uña-Alvarez, J. (2012). The Beta-Binomial SGoF method for multiple dependent tests. *Stat. Appl. Genet. Mol. Biol.* 11:14. doi: 10.1515/1544-6115.1812

Dhaher, R., Finn, D., Snelling, C., and Hitzemann, R. (2008). Lesions of the extended amygdala in C57BL/6J mice do not block the intermittent ethanol vapor-induced increase in ethanol consumption. *Alcohol. Clin. Exp. Res.* 32, 197–208. doi: 10.1111/j.1530-0277.2007.00566.x

Dobin, A., Davis, C. A., Schlesinger, F., Drenkow, J., Zaleski, C., Jha, S., et al. (2013). STAR: ultrafast universal RNA-seq aligner. *Bioinformatics* 29, 15–21. doi: 10.1093/bioinformatics/bts635

Eden, E., Navon, R., Steinfeld, I., Lipson, D., and Yakhini, Z. (2009). GOrilla: a tool for discovery and visualization of enriched GO terms in ranked gene lists. *BMC Bioinformatics* 10:48. doi: 10.1186/1471-2105-10-48

Enoch, M.-A., Baghal, B., Yuan, Q., and Goldman, D. (2013). A factor analysis of global GABAergic gene expression in human brain identifies specificity in response to chronic alcohol and cocaine exposure. *PLoS One* 8:e64014. doi: 10.1371/journal.pone.0064014

Franklin, K., and Paxinos, G. (2008). *The Mouse Brain in Sterotaxic Coordinates*, 3rd Edn. Oxford: Elsevier.

Gill, R., Datta, S., and Datta, S. (2010). A statistical framework for differential network analysis from microarray data. *BMC Bioinformatics* 11:95. doi: 10.1186/1471-2105-11-95

Hitzemann, R., Bottomly, D., Iancu, O., Buck, K., Wilmot, B., Mooney, M., et al. (2014). The genetics of gene expression in complex mouse crosses as a tool to study the molecular underpinnings of behavior traits. *Mamm. Genome* 25, 12–22. doi: 10.1007/s00335-013-9495-6

Hosseini, S. M. H., Hoeft, F., and Kesler, S. R. (2012). GAT: a graph-theoretical analysis toolbox for analyzing between-group differences in large-scale structural and functional brain networks. *PLoS One* 7:e40709. doi: 10.1371/journal.pone.0040709

Iancu, O. D., Colville, A., Walter, N. A. R., Darakjian, P., Oberbeck, D. L., Daunais, J. B., et al. (2018). On the relationships in rhesus macaques between chronic ethanol consumption and the brain transcriptome. *Addict. Biol.* 23, 196–205. doi: 10.1111/adb.12501

Iancu, O. D., Darakjian, P., Walter, N. A. R., Malmanger, B., Oberbeck, D., Belknap, J., et al. (2010). Genetic diversity and striatal gene networks: focus on the heterogeneous stock-collaborative cross (HS-CC) mouse. *BMC Genomics* 11:585. doi: 10.1186/1471-2164-11-585

Iancu, O. D., Kawane, S., Bottomly, D., Searles, R., Hitzemann, R., and McWeeney, S. (2012). Utilizing RNA-Seq data for de novo coexpression network inference. *Bioinformatics* 28, 1592–1597. doi: 10.1093/bioinformatics/bts245

Joslyn, G., Ravindranathan, A., Brush, G., Schuckit, M., and White, R. L. (2010). Human variation in alcohol response is influenced by variation in neuronal signaling genes. *Alcohol. Clin. Exp. Res.* 34, 800–812. doi: 10.1111/j.1530-0277.2010.01152.x

Kimpel, M. W., Strother, W. N., McClintick, J. N., Carr, L. G., Liang, T., Edenberg, H. J., et al. (2007). Functional gene expression differences between inbred alcohol-preferring and -non-preferring rats in five brain regions. *Alcohol* 41, 95–132. doi: 10.1016/j.alcohol.2007.03.003

Koob, G. F., and Volkow, N. D. (2010). Neurocircuitry of addiction. *Neuropsychopharmacology* 35, 217–238. doi: 10.1038/npp.2009.110

Koob, G. F., and Volkow, N. D. (2016). Neurobiology of addiction: a neurocircuitry analysis. *Lancet Psychiatry* 3, 760–773. doi: 10.1016/S2215-0366(16)00104-8

Kwak, S., and Weiss, J. H. (2006). Calcium-permeable AMPA channels in neurodegenerative disease and ischemia. *Curr. Opin. Neurobiol.* 16, 281–287. doi: 10.1016/j.conb.2006.05.004

Lai, C., Xie, C., McCormack, S. G., Chiang, H.-C., Michalak, M. K., Lin, X., et al. (2006). Amyotrophic lateral sclerosis 2-deficiency leads to neuronal degeneration in amyotrophic lateral sclerosis through altered AMPA receptor trafficking. *J. Neurosci.* 26, 11798–11806. doi: 10.1523/JNEUROSCI.2084-06.2006

Langfelder, P., and Horvath, S. (2008). WGCNA: an R package for weighted correlation network analysis. *BMC Bioinformatics* 9:559. doi: 10.1186/1471-2105-9-559

Langfelder, P., Luo, R., Oldham, M. C., and Horvath, S. (2011). Is my network module preserved and reproducible? *PLoS Comput. Biol.* 7:e1001057. doi: 10.1371/journal.pcbi.1001057

Lewohl, J. M., Wang, L., Miles, M. F., Zhang, L., Dodd, P. R., and Harris, R. A. (2000). Gene expression in human alcoholism: microarray analysis of frontal cortex. *Alcohol. Clin. Exp. Res.* 24, 1873–1882. doi: 10.1111/j.1530-0277.2000.tb01993.x

Liao, Y., Smyth, G. K., and Shi, W. (2014). FeatureCounts: an efficient general purpose program for assigning sequence reads to genomic features. *Bioinformatics* 30, 923–930. doi: 10.1093/bioinformatics/btt656

Lin, H., Hsu, F.-C., Baumann, B. H., Coulter, D. A., and Lynch, D. R. (2014). Cortical synaptic NMDA receptor deficits in α7 nicotinic acetylcholine receptor gene deletion models: implications for neuropsychiatric diseases. *Neurobiol. Dis.* 63, 129–140. doi: 10.1016/j.nbd.2013.11.021

Liu, W., Thielen, R. J., and McBride, W. J. (2006). Effects of repeated daily treatments with a 5-HT3 receptor antagonist on dopamine neurotransmission and functional activity of 5-HT3 receptors within the nucleus accumbens of Wistar rats. *Pharmacol. Biochem. Behav.* 84, 370–377. doi: 10.1016/j.pbb.2006.06.002

Melendez, R. I., McGinty, J. F., Kalivas, P. W., and Becker, H. C. (2012). Brain region-specific gene expression changes after chronic intermittent ethanol exposure and early withdrawal in C57BL/6J mice. *Addict. Biol.* 17, 351–364. doi: 10.1111/j.1369-1600.2011.00357.x

Metten, P., Iancu, O. D., Spence, S. E., Walter, N. A. R., Oberbeck, D., Harrington, C. A., et al. (2014). Dual-trait selection for ethanol consumption and withdrawal: genetic and transcriptional network effects. *Alcohol. Clin. Exp. Res.* 38, 2915–2924. doi: 10.1111/acer.12574

Mulligan, M. K., Mozhui, K., Pandey, A. K., Smith, M. L., Gong, S., Ingels, J., et al. (2017). Genetic divergence in the transcriptional engram of chronic alcohol abuse: a laser-capture RNA-seq study of the mouse mesocorticolimbic system. *Alcohol* 58, 61–72. doi: 10.1016/j.alcohol.2016.09.001

Mulligan, M. K., Rhodes, J. S., Crabbe, J. C., Mayfield, R. D., Harris, R. A., and Ponomarev, I. (2011). Molecular profiles of drinking alcohol to intoxication in C57BL/6J mice. *Alcohol. Clin. Exp. Res.* 35, 659–670. doi: 10.1111/j.1530-0277.2010.01384.x

Osterndorff-Kahanek, E. A., Becker, H. C., Lopez, M. F., Farris, S. P., Tiwari, G. R., Nunez, Y. O., et al. (2015). Chronic ethanol exposure produces time- and brain region-dependent changes in gene coexpression networks. *PLoS One* 10:e0121522. doi: 10.1371/journal.pone.0121522

Petrakis, I. L., Limoncelli, D., Gueorguieva, R., Jatlow, P., Boutros, N. N., Trevisan, L., et al. (2004). Altered NMDA glutamate receptor antagonist response in individuals with a family vulnerability to alcoholism. *Am. J. Psychiatry* 161, 1776–1782. doi: 10.1176/ajp.161.10.1776

Roberts, A., Pardo-Manuel de Villena, F., Wang, W., McMillan, L., and Threadgill, D. W. (2007). The polymorphism architecture of mouse genetic resources elucidated using genome-wide resequencing data: implications for QTL discovery and systems genetics. *Mamm. Genome* 18, 473–481. doi: 10.1007/s00335-007-9045-1

Robinson, M. D., McCarthy, D. J., and Smyth, G. K. (2010). edgeR: a Bioconductor package for differential expression analysis of digital gene expression data. *Bioinformatics* 26, 139–140. doi: 10.1093/bioinformatics/btp616

Sari, Y., Toalston, J. E., Rao, P. S. S., and Bell, R. L. (2016). Effects of ceftriaxone on ethanol, nicotine or sucrose intake by alcohol-preferring (P) rats and its association with GLT-1 expression. *Neuroscience* 326, 117–125. doi: 10.1016/j.neuroscience.2016.04.004

Shannon, P., Markiel, A., Ozier, O., Baliga, N. S., Wang, J. T., Ramage, D., et al. (2003). Cytoscape: a software environment for integrated models of biomolecular interaction networks. *Genome Res.* 13, 2498–2504. doi: 10.1101/gr.1239303

Smith, M. L., Lopez, M. F., Archer, K. J., Wolen, A. R., Becker, H. C., and Miles, M. F. (2016). Time-course analysis of brain regional expression network responses to chronic intermittent ethanol and withdrawal: implications for mechanisms underlying excessive ethanol consumption. *PLoS One* 11:e0146257. doi: 10.1371/journal.pone.0146257

Sokolov, B. P., Jiang, L., Trivedi, N. S., and Aston, C. (2003). Transcription profiling reveals mitochondrial, ubiquitin and signaling systems abnormalities in postmortem brains from subjects with a history of alcohol abuse or dependence. *J. Neurosci. Res.* 72, 756–767. doi: 10.1002/jnr.10631

Suo, L., Lu, H., Ying, G., Capecchi, M. R., and Wu, Q. (2012). Protocadherin clusters and cell adhesion kinase regulate dendrite complexity through Rho GTPase. *J. Mol. Cell. Biol.* 4, 362–376. doi: 10.1093/jmcb/mjs034

Tajuddin, N., Kim, H.-Y., and Collins, M. A. (2018). PARP inhibition prevents ethanol-induced neuroinflammatory signaling and neurodegeneration in rat adult-age brain slice cultures. *J. Pharmacol. Exp. Ther.* 365, 117–126. doi: 10.1124/jpet.117.245290

Tim-Aroon, T., Jinawath, N., Thammachote, W., Sinpitak, P., Limrungsikul, A., Khongkhatithum, C., et al. (2017). 1q21.3 deletion involving GATAD2B: an emerging recurrent microdeletion syndrome. *Am. J. Med. Genet. A* 173, 766–770. doi: 10.1002/ajmg.a.38082

Warde-Farley, D., Donaldson, S. L., Comes, O., Zuberi, K., Badrawi, R., Chao, P., et al. (2010). The GeneMANIA prediction server: biological network integration for gene prioritization and predicting gene function. *Nucleic Acids Res.* 38, W214–W220. doi: 10.1093/nar/gkq537

Widagdo, J., Guntupalli, S., Jang, S. E., and Anggono, V. (2017). Regulation of AMPA Receptor Trafficking by Protein Ubiquitination. *Front. Mol. Neurosci.* 10:347. doi: 10.3389/fnmol.2017.00347

Wong, W., and Schlichter, L. C. (2004). Differential recruitment of Kv1.4 and Kv4.2 to lipid rafts by PSD-95. *J. Biol. Chem.* 279, 444–452. doi: 10.1074/jbc.M304675200

Zhang, B., and Horvath, S. (2005). A general framework for weighted gene co-expression network analysis. *Stat. Appl. Genet. Mol. Biol.* 4:17. doi: 10.2202/1544-6115.1128

Zhang, Y. V., Hannan, S. B., Kern, J. V., Stanchev, D. T., Koç, B., Jahn, T. R., et al. (2017). The KIF1A homolog Unc-104 is important for spontaneous release, postsynaptic density maturation and perisynaptic scaffold organization. *Sci. Rep.* 7:38172. doi: 10.1038/srep38172

Conflict of Interest Statement: The authors declare that the research was conducted in the absence of any commercial or financial relationships that could be construed as a potential conflict of interest.

The reviewer RB and handling Editor declared their shared affiliation.

frontiers in Genetics

ORIGINAL RESEARCH
published: 30 August 2018
doi: 10.3389/fgene.2018.00346

Stable Histone Methylation Changes at Proteoglycan Network Genes Following Ethanol Exposure

David P. Gavin[1,2†], Joel G. Hashimoto[3,4†], Nathan H. Lazar[3], Lucia Carbone[3], John C. Crabbe[3,4] and Marina Guizzetti[3,4]*

[1] Jesse Brown Veterans Affairs Medical Center, Chicago, IL, United States, [2] Department of Psychiatry, Center for Alcohol Research in Epigenetics, University of Illinois at Chicago, Chicago, IL, United States, [3] Department of Behavioral Neuroscience, Oregon Health and Science University, Portland, OR, United States, [4] VA Portland Health Care System, Portland, OR, United States

OPEN ACCESS

Edited by:
Kristin Hamre, University of Tennessee Health Science Center, United States

Reviewed by:
Sarven Sabunciyan, Johns Hopkins University, United States
Robert Philibert, University of Iowa, United States

***Correspondence:**
Marina Guizzetti
guizzett@ohsu.edu

† These authors have contributed equally to this work

Specialty section:
This article was submitted to Behavioral and Psychiatric Genetics, a section of the journal Frontiers in Genetics

Received: *01 March 2018*
Accepted: *09 August 2018*
Published: *30 August 2018*

Citation:
Gavin DP, Hashimoto JG, Lazar NH, Carbone L, Crabbe JC and Guizzetti M (2018) Stable Histone Methylation Changes at Proteoglycan Network Genes Following Ethanol Exposure. Front. Genet. 9:346. doi: 10.3389/fgene.2018.00346

Alcohol use disorder (AUD) is a chronic mental illness in which patients often achieve protracted periods of abstinence prior to relapse. Epigenetic mechanisms may provide an explanation for the persisting gene expression changes that can be observed even after long periods of abstinence and may contribute to relapse. In this study, we examined two histone modifications, histone 3 lysine 4 tri-methylation (H3K4me3) and histone 3 lysine 27 tri-methylation (H3K27me3), in the prefrontal cortex of Withdrawal Seizure Resistant (WSR) mice 21 days after 72 h of ethanol vapor exposure. These histone modifications were selected because they are associated with active promoters (H3K4me3) and repressed gene expression in a euchromatic environment (H3K27me3). We performed a genome-wide analysis to identify differences in H3K4me3 and H3K27me3 levels in post-ethanol exposure vs. control mice by ChIP-seq. We detected a global reduction in H3K4me3 peaks and increase in H3K27me3 peaks in post-ethanol exposure mice compared to controls, these changes are consistent with persistent reductions in gene expression. Pathway analysis of genes displaying changes in H3K4me3 and H3K27me3 revealed enrichment for genes involved in proteoglycan and calcium signaling pathways, respectively. Microarray analysis of 7,683 genes and qPCR analysis identified eight genes displaying concordant regulation of gene expression and H3K4me3/H3K27me3. We also compared changes in H3K4me3 and/or H3K27me3 from our study with changes in gene expression in response to ethanol from published literature and we found that the expression of 52% of the genes with altered H3K4me3 binding and 40% of genes with H3K27me3 differences are altered by ethanol exposure. The chromatin changes associated with the 21-day post-exposure period suggest that this period is a unique state in the addiction cycle that differs from ethanol intoxication and acute withdrawal. These results provide insights into the enduring effects of ethanol on proteoglycan and calcium signaling genes in the brain.

Keywords: alcohol withdrawal, alcohol dependence, calcium signaling, ChIP-seq, histone methylation, proteoglycans

INTRODUCTION

Alcohol use disorder (AUD) is a chronic condition where sufferers may relapse even after periods of protracted abstinence (Olive, 2010). Gene expression and epigenetic changes following acute and chronic ethanol use and acute withdrawal have begun to be characterized (Gavin et al., 2016; Pandey et al., 2017). However, the mediators of persisting changes to gene expression caused by 72-h ethanol exposure have not been fully explored. The stable nature of some epigenetic marks could provide mechanisms to account for lasting changes in gene expression that mediate relapse to ethanol use following protracted abstinence (Wiren et al., 2006).

In this study, we examine changes in two durable histone modifications, histone 3 lysine 4 and lysine 27 trimethylation (H3K4me3 and H3K27me3). Histones have a half-life of months, and there is evidence that H3K4 and H3K27 methylation are mitotically inherited (Commerford et al., 1982; Chen and Dent, 2014). These two marks serve countervailing roles with H3K4me3 being present at active promoters and H3K27me3 being associated with repression of transcript elongation (Strahl et al., 1999; Schubeler et al., 2004; Guenther et al., 2007). We decided to focus on these histone modifications because they have the stability to encode changes in gene expression over a prolonged period (Robison and Nestler, 2011).

There is a growing literature regarding the association between histone modifications and ethanol. Studies of patients with alcohol dependence have identified ethanol-induced changes to histone modifications in the brain (Zhou et al., 2011; Ponomarev et al., 2012). In the rat amygdala, acute ethanol increases global and prodynorphin and pronociceptin promoter histone acetylation levels (Pandey et al., 2008; D'Addario et al., 2013), and reduces prodynophin and pronociceptin H3K27me3 binding (D'Addario et al., 2013). Moreover, in the hippocampus, ethanol-induced histone H3 acetylation and H3K4me3 have been found to regulate expression of brain derived neurotrophic factor (BDNF) exons (Stragier et al., 2015). Finally, acute ethanol withdrawal leads to decreased histone acetylation in the rat amygdala (Pandey et al., 2008; Sakharkar et al., 2012; Moonat et al., 2013).

A state of alcohol dependence must be inferred in rodents by the emergence of withdrawal signs when alcohol is discontinued. Most laboratory rodents will not voluntarily drink sufficient alcohol to become physically dependent (Crabbe, 2014). Even when exposure to drinking solutions is extended for months, blood alcohol values rarely reach intoxicating levels (Wahlstrom, 1987). A very common procedure used to produce chronic dependence is to expose animals continuously to vaporized alcohol (Goldstein and Pal, 1971; Rogers et al., 1979; Becker, 2014). Following vapor inhalation exposure to intoxicating blood levels, the subsequent withdrawal signs in rodents parallel those in human alcoholics very closely (Friedman, 1980). For example, depending on the vapor concentration, withdrawal from 72 h exposure to ethanol vapor can be lethal in mice (Goldstein, 1972). We have selectively bred Withdrawal Seizure-Prone (WSP) and -Resistant (WSR) mouse lines to display severe or mild withdrawal handling-induced convulsions, respectively, following 72 h continuous vapor exposure (Kosobud and Crabbe, 1986), and have characterized their withdrawal extensively (Metten and Crabbe, 1996). WSP and WSR mice both show many withdrawal signs, but differ on some due to their genetic constitutions. WSP mice show tremors, seizures, enhanced sensitivity to chemical convulsants, anxiety-like behavior and reduced activity, while WSR mice display enhanced backward walking, Straub tail (Kosobud and Crabbe, 1986) and a tendency to engage in relapse drinking (Hashimoto et al., 2011). In the current study, we exposed WSR to 72 h of ethanol vapor and measured the genome-wide distribution of H3K4me3 and H3K27me3 marks in the prefrontal cortex using chromatin immunoprecipitation followed by sequencing (ChIP-seq) 21 days after ethanol exposure. The prefrontal cortex is a critical site of ethanol's rewarding effects, wherein it mediates approach/avoidant behavior through its communications with multiple brain regions, such as the nucleus accumbens, ventral tegmental area, and amygdala (Chandler et al., 1993; Harper and Matsumoto, 2005).

This study identifies, for the first time, the locations of differential H3K4me3 and H3K27me3 peaks in mice 21 days after ethanol exposure compared to control mice. We find that genes related to proteoglycans are enriched in H3K4me3 peaks and that genes related to calcium signaling are enriched in H3K27me3 binding, suggesting that these gene networks are differentially epigenetically regulated during protracted withdrawal and may have a role in relapse.

MATERIALS AND METHODS

Animal Subjects and Ethanol Intoxication

The Withdrawal Seizure Resistant (WSR-1, -2) mice, derived from heterogeneous HS/Ibg mice by phenotypic selection for resistance to chronic ethanol withdrawal seizures (Crabbe and Kosobud, 1986), were used for this study. We have previously shown altered signaling of genes related to epigenetic regulation following chronic ethanol exposure and increased relapse drinking in these mice (Hashimoto et al., 2011, 2017). WSR-1 was used for the chromatin-immunoprecipitation followed by massively parallel DNA sequencing (ChIP-seq) experiments, and WSR-1 and -2 were used for microarray expression analysis. Mice were maintained with a lights-on and lights-off cycle at 6 a.m. and 6 p.m., respectively, and a room temperature of 22 $\pm$ 1°C. Purina Lab Diet chow and water were available *ad libitum* throughout routine husbandry and during experimentation. All animal procedures were in accordance with the US NIH guide for the care and use of laboratory animals and were approved by the Portland Oregon VAMC IACUC.

Four adult WSR-1 male mice per group (control and ethanol) were used for ChIP-seq analyses (H3K4me3 and H3K27me3 ChIP-seq analyses were carried out on the same animals). Four additional adult WSR-1 male mice per group were used in validation ChIP-qPCR experiments; the animals used in ChIP-seq and the animals used in ChIP-qPCR studies were from the same ethanol exposure studies.

Eight adult WSR-1 and -2 male mice per group (control and ethanol) were used for microarray experiments. For each array hybridization, the RNA from two animals from the same selected line and treatment group was pooled; the number of replicates (n) per treatment group is therefore 4. Four additional adult WSR-1 and -2 male mice per group were used in qPCR validation experiments; the animals used in microarray studies and the animals used in qPCR studies were from the same ethanol exposure studies.

Exposure to ethanol vapor was carried out as previously described (Wilhelm et al., 2014). Briefly, mice were injected i.p. with 1.5 g/kg ethanol and 68.1 mg/kg pyrazole HCl (to maintain elevated blood ethanol concentrations, BECs, by inhibiting alcohol dehydrogenase) immediately before being placed in the ethanol chambers. Control animals were injected with 68.1 mg/kg pyrazole HCl and placed in chambers identical to the ethanol chambers but with ambient air circulated instead of vaporized ethanol. Each day, mice were briefly removed from the chambers to record weights, administer 68.1 mg/kg pyrazole HCl, and to obtain a blood sample. BECs were monitored daily by sampling 20 μL of blood from the tail vein with ethanol concentrations determined by gas chromatography (Beadles-Bohling and Wiren, 2006). The WSR line and alcohol exposure paradigm used here has been found to induce dependence as documented in several prior publications (Kosobud and Crabbe, 1986; Hashimoto et al., 2011). After 72 h of ethanol exposure, all animals were returned to normal mouse cages for 21 days with daily monitoring of overall health but no further experimental manipulations.

ChIP-seq Library Generation, Sequencing, and Analysis

Twenty-one days after cessation of ethanol vapor or control exposure, mice were euthanized and the prefrontal cortex was rapidly isolated, snap-frozen in liquid nitrogen, and stored at −80°C as previously described (Hashimoto et al., 2017) until processing. Each prefrontal cortex was homogenized in a 10 mL Dounce homogenizer in RPMI buffer, cross-linked with a final concentration of 1.6% formaldehyde, and fragmented by sonication using a Bioruptor-Pico (Diagenode, Denville, NJ, United States) to achieve fragment sizes ranging from ∼100 to 500 bp. Protein A/G PLUS-Agarose Beads were used to pre-clear the fragmented chromatin samples for 2 h at 4°C with slow end-over-end rotation. Primary antibody [Millipore Anti-Trimethyl-Histone H3 (Lys4), Cat# 07-473; or Millipore Anti-Trimethyl-Histone H3 (Lys27), Cat# 07-449] was added to supernatant after clearing along with fresh agarose beads and incubated overnight at 4°C with gentle end-over-end rotation. The following day, beads were washed with low salt buffer, high salt buffer, lithium chloride buffer, and TE buffer followed by elution from the beads and DNA isolation using the ChIP DNA Clean and Concentrator Kit (Zymo Research, Irvine, CA, United States). DNA was quantitated using the Quant-iT PicoGreen dsDNA Assay Kit (Thermo Fisher Scientific, Waltham, MA, United States) according to the manufacturers protocol. Sequencing libraries were prepared using the NEBNext ChIP-seq Library Prep Master Mix Set and Multiplex Oligos for Illumina Index Primer Set 1 according to the manufacturer's protocol using 10 ng of ChIP DNA and size selection for 150 bp inserts (New England Biolabs, Ipswich, MA, United States). Short read sequencing assays were performed by the OHSU Massively Parallel Sequencing Shared Resource.

Sequencing results consisting of 75 bp single-ended reads from the prefrontal cortex of 8 WSR-1 mice (four control and four ethanol-treated) and the pooled reads from the input material from all eight samples were obtained. Adapter sequences were removed using trimmomatic (v0.35) (Bolger et al., 2014), exact read copies were removed using fastx collapser (v0.0.13) (Hannon Lab, 2010), and reads were mapped to the GRCm38/mm10 mouse genome assembly with BWA-mem (v0.7.9.a) (Li and Durbin, 2009). After removing reads with mapping scores below 30 we used the R SPP package (Kharchenko et al., 2008) to calculate strand cross-correlation measures and all samples were exceeding or near recommended thresholds set by ENCODE. Two H3K4me3 samples (one control and one ethanol) were removed from further analysis because they contain a large fraction of duplicated reads compared to the other samples.

For the H3K4me3 and H3K27me3 ChIP-seq analysis, we counted the number of mapped reads, the number of unique mapping positions and estimated the library complexity using the non-redundant fraction (Landt et al., 2012). For genomic tracks of read coverage, we extended reads to the fragment length (150 bp) and computed the Pearson correlation coefficient between the mapping profiles of each pair of samples after removing 'blacklisted' regions obtained from the ENCODE consortium (Consortium, 2012). To identify peaks above background we used the irreproducibility discovery rate (IDR) analysis detailed by Li et al. (2011) with an IDR cutoff of 0.01. We then performed a differential binding analysis on the H3K4me3 data using the DiffBind package (v3.2) to run EdgeR (Robinson et al., 2010) with an FDR cutoff of 0.1. Finally, we associated all peaks with RefSeq (Pruitt et al., 2005) genes noting the distance to the nearest gene.

Because H3K27me3 ChIP-seq produces broad peaks that cover larger areas of the genome instead of the narrow peaks seen with H3K4me3 marks, we sequenced an additional Illumina lane of 75 base-pair single-ended reads and combined these reads for each sample. Peaks were called using MACS2 (Zhang et al., 2008; Feng et al., 2012) and the IDR analysis was not performed as this method is not applicable to broad peaks. Instead we used stringent overlap criteria requiring that peaks were found to overlap in all four samples of one condition and zero samples of the other condition.

RNA Isolation and Microarray Processing

Twenty-one days after cessation of ethanol vapor or control exposure, mice were euthanized and the prefrontal cortex was rapidly isolated, snap-frozen in liquid nitrogen, and stored at −80°C as previously described (Hashimoto et al., 2017) until processing. Total RNA was isolated using RNA STAT-60 (Tel Test Inc., Friendswood, TX, United States) with genomic DNA removal using the DNA-Free RNA Kit (Zymo Research) as described previously (Hashimoto et al., 2017) and RNA integrity was determined using a 1% agarose gel stained with SYBR Gold

(Thermo Fisher Scientific, Waltham, MA, United States) and quantitated by UV spectroscopy.

Microarrays were purchased from the National Institute on Aging microarray facility which includes 16,897 features corresponding to 7,683 unique GenBank Gene IDs (Nadon et al., 2005). Complex probe was generated by linear synthesis with 33P-dCTP using SuperScript II Reverse Transcriptase (Thermo Fisher, Waltham, MA, United States) as previously described (Nadon et al., 2005). Complex probes were purified using Biospin P-30 columns (Bio-Rad, Hercules, CA, United States) and labeling efficiency determined using a Bioscan QC-4000 XER (Bioscan, Inc., Washington, DC, United States) and hybridized to arrays overnight with gentle mixing. Probe hybridization was measured using a Cyclone Phosphorimager and OptiQuant version 4.0 (Packard Instrument Company, Downers Grove, IL, United States). Spot identification and intensity measurements were carried out on exported data from OptiQuant using Array-Pro Analyzer 4.5 (MediaCybernetics, Rockville, MD, United States).

Spot hybridization intensities were analyzed using R. The microarray data presented here are part of a larger gene expression study to be published at a later date, which includes 62 total array hybridizations including samples derived from the two sexes of multiple mouse lines at 0 h, 8 h, and 21 days after ethanol exposure. In this study, we present the results from eight arrays that corresponded to the ChIP-seq experiments (i.e., WSR male mice prefrontal cortices 21 days after ethanol exposure). Clones with hybridization intensities below background on more than 10% of the arrays were excluded and batch effects were removed using the 'sva' package (Leek et al., 2012). Ethanol regulated genes were determined using the empirical Bayes function of the 'LIMMA' package (McCarthy and Smyth, 2009; Ritchie et al., 2015).

Bioinformatic Analysis of ChIP-seq and Gene Expression

Genes showing differential peaks of H3K4me3 or H3K27me3 in ChIP-seq analysis or identified as differentially regulated by post-ethanol were analyzed separately for Gene Ontology (GO) and pathway enrichment using The Database for Annotation, Visualization and Integrated Discovery (DAVID) v6.8 (Huang et al., 2009). The KEGG pathway schematic with ChIP-seq data integrated into a simplified pathway was created in Cytoscape (3.5.1) using the CytoKegg (1.0.1) application (Shannon et al., 2003). Sequencing data was visualized using the Integrated Genomics Viewer (IGV, 2.4.5).

Confirmation of ChIP-seq and Microarray Results

Peak regions identified in the ChIP-seq analyses were used in the design of primers using the NCBI Primer-BLAST on-line tools (Ye et al., 2012). Quantitative PCR (qPCR) was run on ChIP DNA using the SsoAdvanced Universal SYBR Green Supermix and CFX96 Real-Time System (Bio-Rad, Hercules, CA, United States) and data is presented as percent of input. Gene expression changes were measured by qRT-PCR using the iTaq Universal SYBR Green One-Step Kit (Bio-Rad, Hercules, CA, United States) using RNA from independent animals from the same studies as those used for the microarray experiment described here. Primers were designed using Primer-BLAST (Ye et al., 2012) for *Alk* and were down-loaded from PrimerBank (Wang et al., 2012) for *Wnt5a*, *Camk2a*, *Dgkb*, and *Ezr*. For each set of qPCR and qRT-PCR primers, primer efficiency was between 90 and 110% and resulted in a discreet single peak during melt analysis.

RESULTS

ChIP-seq Analysis

Our analysis of the H3K4me3 ChIP-seq data identified 445 differentially bound peaks between the post-ethanol and control mice of which 271 (61%) were located within regulatory regions or gene bodies of 294 unique genes (**Supplementary Table 1**). Seven genes had multiple peaks associated (*1700011I03Rik, Gm10921, Gm13152, Gm14345, Gm14346, Gm38437, Soga1*). Furthermore, 29 peaks had two genes associated, and 4 peaks had three genes associated. We found that 92 (30%) of the gene-associated peaks were located within 100 bp of the transcription start site (TSS; 33 peaks) or proximal promoter region (59 peaks) defined here as 2,000 bp upstream of the TSS and 200 bp into the gene. **Figure 1** shows representative examples of differential Integrative Genomics Viewer (IGV) tracks of H3K4me3 peaks associated with the TSS of two genes in control and post-ethanol mice. Of the genes showing differential H3K4me3 distribution, 52% (159 genes) have been previously shown to be differentially regulated by ethanol (Ponomarev et al., 2012; Wilhelm et al., 2014; Farris et al., 2015; Smith et al., 2016; van der Vaart et al., 2017). The majority of these gene-associated peaks (196, 64%) reported here showed decreased H3K4me3 in the post-ethanol samples compared to control, consistent with prevalent downregulation of gene expression (**Table 1**).

To further our understanding of ethanol dysregulation of histone marks during this 21-day post-ethanol exposure period we also performed ChIP-seq for H3K27me3. H3K27me3 generally produces broad peaks often encompassing several kilobases of DNA, which makes analysis with traditional statistical approaches challenging, requiring a different strategy than the one described above for H3K4me3. We first looked at peaks present in all four samples of each group and found 35,710 peaks in the ethanol treatment group and 29,883 peaks in the control group. A large portion of the peaks identified completely or partially overlapped in the control and ethanol-treatment samples (**Figure 2**). To avoid false-positive results, we used a very stringent method for calling differential H3K27me3 peaks between control and post-ethanol samples. Only when peaks are present in all four replicates of one treatment group with no corresponding peaks present in any of the four replicate samples of the other treatment group do we identify them as differential H3K27me3 peaks. We identified 771 peaks that were present in one condition but not in the other. 640 peaks were present in all four post-ethanol samples but in none of the control samples; 131 peaks were present in all the control samples but in none of the post-ethanol samples (**Figure 2**). Two hundred forty of

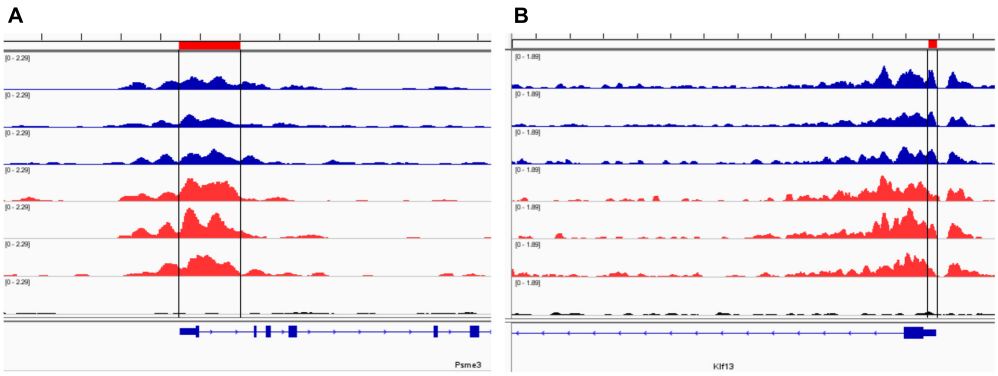

FIGURE 1 | Representative Integrative Genomics Viewer (IGV) browser tracks of H3K4me3 peaks near the TSS following ethanol exposure. For each panel, blue tracks are from control animals, red tracks are from ethanol-treated animals, and black track is the input signal. All IGV tracks in a given comparison have the same scaling factor for the *y*-axis as indicated in the upper left hand region of each track. The region of the genome identified as differentially bound is indicated near the top of each panel in red and with black lines through the tracks. The RefSeq gene map is presented in blue at the bottom of each panel showing the overall gene structure. **(A)** *Psme3* shows increased H3K4me3 in ethanol treated samples. **(B)** *Klf13* shows decreased H3K4me3 in ethanol treated samples at one of the primary peaks at the gene TSS.

TABLE 1 | Matrix of the changes in H3K4me3, H3K27me3, and microarray gene expression and their overlap during ethanol withdrawal in comparison to control.

	H3K27me3/array no change	H3K27me3 peaks present only post-ethanol	H3K27me3 peaks present only in controls	Array increase	Array decrease	Total H3K4me3 changes
H3K4me3/array no change	–	204	36	–	–	
H3K4me3 increase	110	0	0	2		112
H3K4me3 decrease	192	3	0	0	1	196
Array decrease	–	2	0			
Total H3K27me3 changes		209	36			

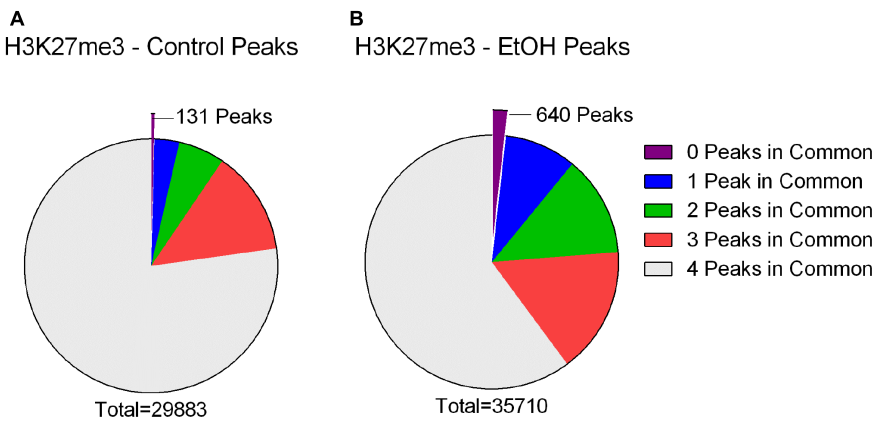

FIGURE 2 | H3K27me3 peaks called in control and ethanol samples. **(A)** Out of a total of 29,883 peaks called in all four Control samples, 23,072 were also present in all four ethanol treated samples (77.21%), 3,972 were present in three of the ethanol treated samples (13.29%), 1,769 were present in two of the ethanol treated samples (5.92%), 939 were present in one of the ethanol treated samples (3.14%), and 131 were present in 0 of the ethanol-treated samples (0.44%). **(B)** Out of a total of 35,710 peaks called in all four ethanol samples, 21,477 were also present in all four Control samples (60.14%), 5,755 were present in three of the control samples (16.12%), 4,570 were present in two of the control samples (12.80%), 3,268 were present in one of the Control samples (9.15%), and 640 were present in 0 of the Control samples (1.79%).

these differential peaks were associated with 231 unique genes. Five peaks were associated with two genes. Ten genes had two peaks present (*Drd3, Gm5134, Gpr39, Rora, Sorcs2, Svep1, Syt9, Tspan18, Wwox, 2310007B03Rik*), two genes (*Alk, Sncaip*) had three peaks. **Supplementary Table 2** shows the list of the 245 genes associated with H3K27me3 differential peaks (genes with two or three peaks are listed duplicated in the table) and the gene region where the differential peak is located. Eight peaks are

associated with the promoter region, eight are in the TSS region, and 229 are associated with the gene body. Of the 245 genes with differentially bound peak regions 85% (209) had H3K27me3 peaks only in the post-ethanol samples compared to control. These results, similarly to the results found for post-ethanol changes on H3K4me3 and described in the previous paragraph, are consistent with prevalent down-regulation of gene expression during the 21-day post-ethanol period (**Table 1**). **Figure 3** shows representative examples of differential IGV tracks of H3K27me3 peaks associated with the TSS of two genes in control and post-ethanol mice. Comparison of our H3K27me3 ChIP-seq data with previously published ethanol data showed 40% (98 genes) of genes identified in this study have been previously identified as regulated by ethanol (Ponomarev et al., 2012; Wilhelm et al., 2014; Farris et al., 2015; Smith et al., 2016; van der Vaart et al., 2017).

Three genes had differential H3K4me3 and H3K27me3 peaks, *Trp63* (transformation related protein 63); *Wnt5a* (wingless-type MMTV integration site family, member 5A); and *Lhfpl3* (lipoma HMGIC fusion partner-like 3). All three genes had reduced H3K4me3 in the ethanol samples and the presence of H3K27me3 peaks in the post-ethanol samples suggesting expression of these genes is repressed during protracted ethanol withdrawal (**Table 1** and **Supplementary Tables 1**, **2**).

Pathway and Gene Ontology Analyses

Next we performed pathway and GO analyses on the genes showing differential histone marks. For H3K4me3, the top KEGG pathways identified were "proteoglycans in cancer," "viral carcinogenesis," and "viral myocarditis" (**Table 2**). The top GO categories were "dendrite," "synapse," and "cell junction" (**Table 3**). Interestingly, four genes that are part of the top KEGG pathway for H3K4me3, "proteoglycans in cancer," were identified in the H3K27me3 analysis suggesting dysregulation of this pathway through multiple epigenetic mechanisms (**Table 2** and **Figure 4**). For H3K27me3, the top KEGG pathways identified were "calcium signaling pathway" and "nicotinate and nicotinamide metabolism" (**Table 2**). We observed an additional six genes in the "calcium signaling pathway" in our H3K4me3 analysis suggesting an important role of calcium signaling during this post-ethanol period (**Table 2**). The top GO categories for H3K27me3 were "calcium ion binding," "receptor complex," and "transcriptional activator activity, RNA polymerase II core promoter proximal region sequence-specific binding" (**Table 3**).

Gene Expression Analysis

Additionally, we carried out gene expression array analysis of the PFC of control and post-ethanol exposure mice. We found that 21 d after ethanol exposure 86 of the 7,683 genes present in the microarray platform were differentially expressed, with an unadjusted p-value < 0.01, 40% of the differentially expressed genes were downregulated and 60% were upregulated (**Table 3**). Notably, DNA methyltransferase 3A (*Dnmt3a*) was down-regulated during protracted withdrawal from alcohol and has been previously identified as dysregulated following ethanol exposure (Smith et al., 2016; van der Vaart et al., 2017). We then subjected the differentially expressed genes to pathway and GO analyses. The top KEGG pathway identified was "cell adhesion molecules." The top GO categories were "protein binding," "nucleoplasm," and "coronary vasculature development." The microarray platform used for this experiment contained 49% of the genes that showed changes in H3K4me3 and 18% of the genes that showed changes in H3K27me3. Five genes displaying changes in H3K4me3 or H3K27me3 also showed differential expression; in all five cases, the expression profile of the genes matched the predicted expression based on histone methylation with increased H3K4me3 associated with increased expression and increased H3K27me3 associated with decreased expression. Specifically, we found that genes *Pard3* and *Plagl1* showed increased H3K27me3 in ethanol

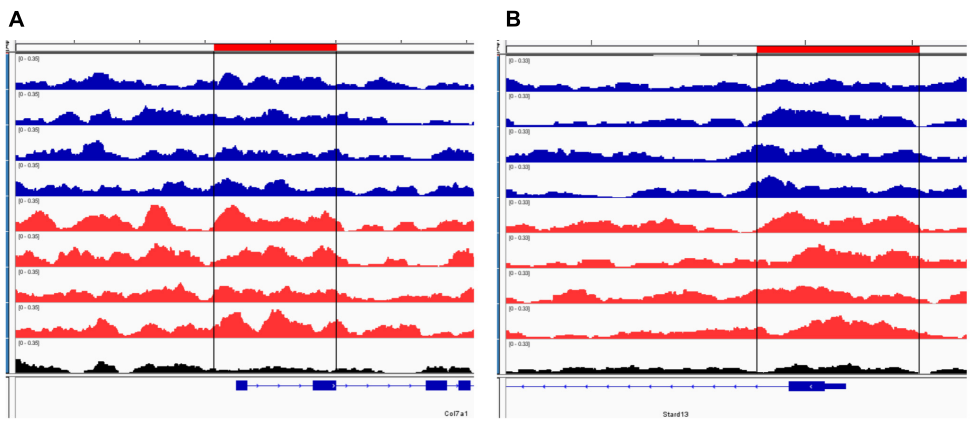

FIGURE 3 | Representative IGV browser tracks of H3K27me3 peaks near the TSS following ethanol exposure. For each panel, the blue tracks are from control animals, red tracks are from ethanol-treated animals, and black track is the input signal. All IGV tracks in a given comparison have the same scaling factor for the y-axis as indicated in the upper left hand region of each track. The region of the genome identified as differentially bound is indicated near the top of each panel in red and with black lines through the tracks. The RefSeq gene map is presented in blue at the bottom of each panel showing the overall gene structure. **(A)** *Col7a1* shows increased H3K27me3 in ethanol treated samples. **(B)** *Stard13* shows increased H3K27me3 in ethanol treated samples.

TABLE 2 | Enriched KEGG pathways in genes with post-ethanol-induced changes in H3K4me3 and H3K27me3.

KEGG identity	Count	*P*-Value	Genes	Count	*P*-Value	Genes
Proteoglycans in cancer	5	0.0869	Erbb3, Itgb5, Wnt5a, Itpr3	10	0.0009	Ddx5, Hpse2, Wnt5a, Rps6kb2, Camk2a, Grb2, Mapk14, Ezr, Wnt1, Ank1
Calcium signaling pathway	7	0.0100	Htr7, Erbb3, Erbb4, Itpr3, Mylk, Plcd4, Ryr1	6	0.0503	Pde1c, Camk2a, Atp2b2, Cacna1e, Ntsr1, Grin1
Gastric acid secretion	3	0.0542	Slc26a7, Itpr3, Mylk	9	0.0110	Ep300, Jak1, Tradd, Casp8, Ccnd2, Grb2, H2-T23, H2-T9, H2-Bl
Wnt signaling pathway	2	0.4898	Wnt5a, Nfatc1	6	0.0186	Ccnd2, Ctbp1, Wnt5a, Camk2a, Ep300, Wnt1
Phosphatidylinositol signaling system	2	0.3130	Itpr3, Plcd4	4	0.0566	Inpp4b, Dgkb, Pi4k2a, Pik3c2b
Taste transduction	4	0.0157	Scnn1b, Itpr3, Htr3b, Pkd1l3	1	0.7082	Pde1c
Long-term potentiation	1	0.5361	Itpr3	4	0.0162	Gria1, Camk2a, Ep300, Grin1
Prolactin signaling pathway				4	0.0216	Ccnd2, Grb2, Mapk14, Socs7
Thyroid hormone synthesis	3	0.0490	Pax8, Itpr3, Creb5	1	0.8267	Ep300

Gene names in red indicate decreased gene expression would be predicted based on the histone modification and green indicate increased gene expression would be predicted based on the histone modification.

TABLE 3 | Enriched GO categories in genes with post-ethanol-induced changes in H3K4me3 and H3K27me3.

GO term	H3K27me2		H3K4me3	
	Count	*P*-Value	Count	*P*-Value
Membrane (GO:0016020)	–	–	124	0.0000
Positive regulation of transcription from RNA polymerase II promoter (GO:0045944)	22	0.0010	12	0.3556
Cell junction (GO:0030054)	–	–	27	0.0000
Calcium ion binding (GO:0005509)	22	0.0000	4	0.0000
Dendrite (GO:0030425)	–	–	24	0.0000
Synapse (GO:0045202)	–	–	23	0.0000
Chromatin binding (GO:0003682)	–	–	20	0.0000
Transcriptional activator, RNA polymerase II core promoter proximal region sequence-specific binding (GO:0001077)	11	0.0004	3	0.3832
Receptor complex (GO:0043235)	10	0.0000	2	0.5332
Neuronal cell body (GO:0043025)	2	0.3173	7	0.0006
Z disk (GO:0030018)	7	0.0015	1	0.6353

samples and decreased expression compared to controls; the gene *Calu* displayed reduced H3K4me3 binding and reduced gene expression; genes *Ezr* and *Dgkb* had increased H3K4me3 and increased gene expression (**Tables 1**, **4** and **Supplementary Tables 1**, **2**).

Validation Experiments

We validated some of the changes observed in H3K4me3 and/or H3K27me3 analysis using ChIP followed by qPCR analysis of immunoprecipitated DNA in four additional samples per condition. Furthermore, we used qRT-PCR to validate differential expression detected by microarray and measure RNA expression of two genes (*Alk* and *Camk2a*) not present in the microarray platform but displaying H3K4me3 and/or H3K27me3 changes by ChIP-seq.

The five genes selected for validation were: *Alk*, *Wnt5a, Camk2a, Ezr, and Dgkb. Alk* was selected for validation as several previous studies have implicated this gene in modulating alcohol-drinking behavior (Heberlein et al., 2010; Lasek et al., 2011; Dutton et al., 2017); *Wnt5a*, *Camk2a,* and *Ezr* were selected for validation because components of the "Proteoglycans in Cancer" pathway identified as significantly altered by ethanol withdrawal by KEGG pathway analysis of our ChIP-seq results (**Figure 4**). In addition, *Wnt5* displayed a concordant increase in H3K27me3 and decrease in H3K4me3 while *Ezr* and *Dgkb* displayed a concordant increase in H3K4me3 and in gene expression (**Table 4**).

We performed ChIP-qPCR for two regions of the *Alk* gene showing H3K27me3 differential peaks (region 1 at 538 kb downstream from the TSS and region 2 located 520 kb upstream of the TSS) but only found a significant difference for one of the regions (**Figure 5A**, left and middle). Consistent with the presence of the repressive mark, qRT-PCR revealed that *Alk* expression is reduced by ethanol withdrawal (**Figure 5A**, right). The ChIP-qPCR results of *Wnt5a* confirmed the ChIP-seq results, displaying increased H3K27me3 and decreased H3K4me3 (**Figure 5B**, left and middle) and its expression was decreased by ethanol, in agreement with its chromatin state (**Figure 5B**, right). In agreement with the ChIP-seq results, we observed a decrease in *Camk2a* H3K4me3, associated with a decrease in *Camk2a* gene expression measured by qRT-PCR (**Figure 5C**). Finally, we validated the increase in H3K4me3 in the *Ezr* and *Dgkb* genes associated with increased expression (**Figures 5D,E**), in agreement with ChIP-seq and microarray results.

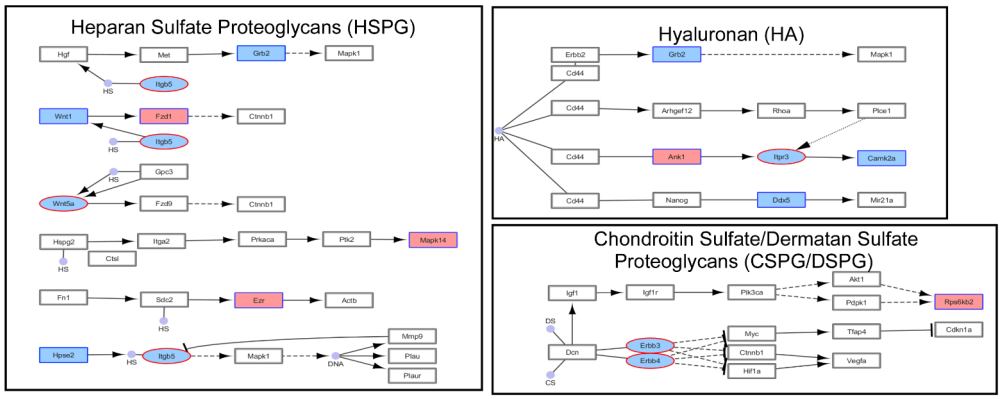

FIGURE 4 | Simplified KEGG pathway "Proteoglycans in Cancer" with H3K4me3 and H3K27me3 enriched genes. The KEGG pathway was down-loaded into Cytoscape (3.5.1) using the CytoKegg (1.0.1) application. ChIP-seq data was overlaid on the pathway with H3K4me3 results shown in blue rectangles and H3K27me3 results shown in red ovals. Blue filled nodes indicate a predicted down-regulation with ethanol based on the ChIP-seq results and pink filled nodes indicate a predicted up-regulation. Proteoglycans play several crucial roles in modulating neuronal migration, axonal regeneration, and synaptic plasticity.

DISCUSSION

The current study examined stable changes in H3K4me3 and H3K27me3 following protracted withdrawal from ethanol. We performed ChIP-seq experiments in the prefrontal cortex of animals that 21 days previously had been exposed to ethanol. We found 445 H3K4me3 peaks and 771 H3K27me3 peaks that differed between control and ethanol treated mice, indicating persistent changes in chromatin state 21 days following high dose ethanol treatment. In particular, we observed that 64% of the H3K4me3 peaks that differed between the treatment group and the controls were reduced while 85% of the H3K27me3 peaks were increased, indicating a global repression of gene expression. Three genes showed simultaneous reduction of H3K4me3 and appearance of H3K27me3 in the ethanol-withdrawn samples: *Trp63*, *Wnt5a*, and *Lhfpl3*. We also found that five genes that were differentially expressed in our microarray analysis also displayed changes in H3K4me3 or H3K27me3 (**Tables 1**, **4**). All changes in expression were in the direction that would be predicted based on the histone modifications.

We also compared changes in H3K4me3 and H3K27me3 to prior studies that examined gene expression and, interestingly, found that 52% (159 genes) of our differentially tri-methylated H3K4 and 40% (98 genes) of our differentially tri-methylated H3K27 genes have been previously identified as regulated by ethanol (Ponomarev et al., 2012; Wilhelm et al., 2014; Farris et al., 2015; Smith et al., 2016; van der Vaart et al., 2017). For example, we find H3K27me3 peaks following treatment in Glial cell line-derived neurotrophic factor (*Gdnf*) and Anaplastic lymphoma kinase (*Alk*) genes, and increased H3K4me3 peaks in the ethanol samples at the Glutamate Receptor, Ionotropic, AMPA 1 (*Gria1*) gene. These genes have been reported to be dysregulated by ethanol exposure (Carnicella et al., 2009; Heberlein et al., 2010; Lasek et al., 2011; Wolen et al., 2012; Reynolds et al., 2015; Dutton et al., 2017). With regard to H3K4me3 analysis, there is 0.004% chance of observing this level of overlap with the literature findings by chance using a hypergeometric test, suggesting a high level of correlation between H3K4me3 and gene expression. Notably, this overlap is despite myriad different models and ethanol exposure paradigms used in these prior studies. For example, the Ponomarev et al. (2012) and Farris et al. (2015) studies were conducted using human post-mortem samples, while Smith et al. (2016) used mice exposed to chronic intermittent ethanol exposure and measured gene expression 0 h, 8 h, 72 h, and 7 days post-treatment. On the other hand, we found that there is a high chance of randomly observing the level of overlap seen in the H3K27me3 analysis (58%).

We found that "proteoglycans in cancer" and "calcium signaling pathways" emerged as networks affected by ethanol during protracted withdrawal in the ChIP-seq analysis of H3K4me3 and H3K27me3, respectively. Ethanol and its metabolites, such as acetaldehyde have been shown to interfere with the synthesis, stability, and degradation of glycoconjugates, including proteoglycans in the brain and periphery (Waszkiewicz et al., 2012). Proteoglycans serve essential roles in the brain as part of the extracellular matrix (ECM). Most of the cells in the brain secrete ECM proteins, which provide structural support but can also activate or inhibit cell signaling involved in neuronal plasticity. The ECM can be divided into three main compartments: the basement membrane, the neural interstitial matrix, and perineuronal nets (PNs) (Lau et al., 2013; Lasek, 2016). The basement membrane is a component of the blood brain barrier, and the interstitial matrix and PNs help stabilize neural circuits and diffusion rates of membrane receptors, neurotransmitters, and ions (Celio et al., 1998; Yamaguchi, 2000; Pizzorusso et al., 2002; Gogolla et al., 2009; Dityatev et al., 2010; Gundelfinger et al., 2010; McRae and Porter, 2012). Several recent studies have indicated an important role for ECM factors in alcoholism (Zhang et al., 2014; Lasek, 2016).

Prior to the current study the status of ECM components and regulatory factors during protracted ethanol withdrawal were not well characterized. In the current study, we found *Wnt5a*, *Wnt1*, and *Grb2*, and integrin protein *Itgb5* had histone

TABLE 4 | Post-ethanol-induced gene expression differences in the PFC of male WSR mice.

Symbol	Gene ID	Log FC	*p*-Value	Symbol	Gene ID	Log FC	*p*-Value
Pard3	93742	−0.302	0.0084	Lmbrd2	320506	0.154	0.0098
Acbd5	74159	−0.298	0.0078	Erc2	238988	0.157	0.0060
Col4a5	12830	−0.288	0.0009	Psph	100678	0.159	0.0006
Cbln1	12404	−0.273	0.0045	Rbbp8	225182	0.160	0.0016
Smg5	229512	−0.242	0.0061	Ndst2	17423	0.164	0.0072
Pcif1	228866	−0.223	0.0003	Ccno	218630	0.166	0.0071
Mrps18b	66973	−0.215	1.4E-05	Ccpg1	72278	0.168	0.0088
Cul1	26965	−0.197	0.0074	Cdc7	12545	0.171	0.0027
Folr4	64931	−0.194	0.0093	Vps29	56433	0.172	0.0056
Fgf22	67112	−0.192	0.0032	Sri	109552	0.172	0.0027
Dnmt3a	13435	−0.190	0.0019	Emilin1	100952	0.173	0.0018
Jam2	67374	−0.189	0.0021	Gna14	14675	0.174	0.0087
Tnfaip1	21927	−0.189	0.0050	Chd4	107932	0.178	0.0099
Srrt	83701	−0.187	0.0084	Def8	23854	0.179	0.0092
Scp2	20280	−0.184	0.0098	Lars	107045	0.180	0.0030
Plagl1	22634	−0.180	0.0067	Fbxo8	50753	0.182	0.0089
Lyst	17101	−0.179	0.0003	Icosl	50723	0.182	0.0051
Ccdc122	108811	−0.174	0.0020	Arl1	104303	0.187	0.0026
Adam19	11492	−0.173	0.0023	Prpsap1	67763	0.193	0.0025
Calu	12321	−0.166	0.0053	Med13	327987	0.194	0.0040
Pnpla7	241274	−0.164	0.0072	Usp16	74112	0.198	0.0066
Jam3	83964	−0.155	0.0066	Lasp1	16796	0.201	0.0017
Lsr	54135	−0.153	0.0045	Il17rc	171095	0.204	0.0003
Rps15	20054	−0.152	0.0016	Fam195b	192173	0.205	0.0031
Smarca4	20586	−0.152	0.0021	Kif7	16576	0.205	0.0007
Cd34	12490	−0.151	0.0025	**Ezr**	22350	0.208	0.0003
Efna5	13640	−0.147	0.0039	Reep5	13476	0.210	0.0002
Kif16b	16558	−0.143	0.0035	Tsen15	66637	0.210	0.0049
Trmt2a	15547	−0.135	0.0035	Usp9x	22284	0.213	0.0096
Lgals1	16852	−0.135	0.0024	Hat1	107435	0.218	0.0040
Casp8ap2	26885	−0.133	0.0055	Clk2	12748	0.223	0.0003
Bach2	12014	−0.131	0.0093	Lrp1	16971	0.227	0.0014
Mettl16	67493	−0.129	0.0052	Sf3a2	20222	0.233	0.0031
Hspd1	15510	−0.119	0.0059	Rnaseh1	19819	0.233	0.0072
Ripply3	170765	0.108	0.0069	Zfp229	381067	0.236	0.0002
Psmd2	21762	0.110	0.0088	Ildr1	106347	0.242	0.0004
Olfr976	258364	0.136	0.0086	Alas1	11655	0.245	0.0008
Irak1	16179	0.142	0.0099	Ntrk2	18212	0.259	0.0014
Wbp7	75410	0.147	0.0059	Osbp	76303	0.265	0.0009
Bok	51800	0.147	0.0035	Uck2	80914	0.269	0.0044
Phip	83946	0.149	0.0037	Ndufb7	66916	0.270	0.0035
Eef1b2	55949	0.151	0.0039	**Dgkb**	217480	0.325	0.0017
Heatr5b	320473	0.153	0.0032	Exosc5	27998	0.459	0.0012

Genes with altered expression after 72-h vapor ethanol exposure followed by 21 days without ethanol in the PFC of male WSR mice. Genes in bold were also identified in ChIP-seq analysis as enriched in either control or ethanol treated samples.

modifications consistent with reduced gene expression. WNT signaling pathway is of particular interest considering the important role it plays in neuritogenesis (Ille and Sommer, 2005). In relation to the ECM, WNT1 has been shown to positively regulate a key component of PNs, aggrecan, in human adipose stem cell culture (Wang and Fawcett, 2012; Luo et al., 2013). In accord with an increase in H3K27me3 at *Wnt5a* reported here, ethanol treatment of neural stem cells reduced *Wnt5a* expression (Vangipuram and Lyman, 2012; Mandal et al., 2015a). WNT5A has been shown to induce the expression of the γ2 subunit of laminin, an important ECM protein in the brain parenchyma and in the epithelial basement membrane (Yamamoto et al., 2009). On the other hand, WNT1 and WNT5A promote the expression of enzymes that degrade the ECM, such as matrix metalloproteinases (MMPs) (Wu et al., 2007; Huang et al., 2017). The epidermal growth factor receptor adapter protein

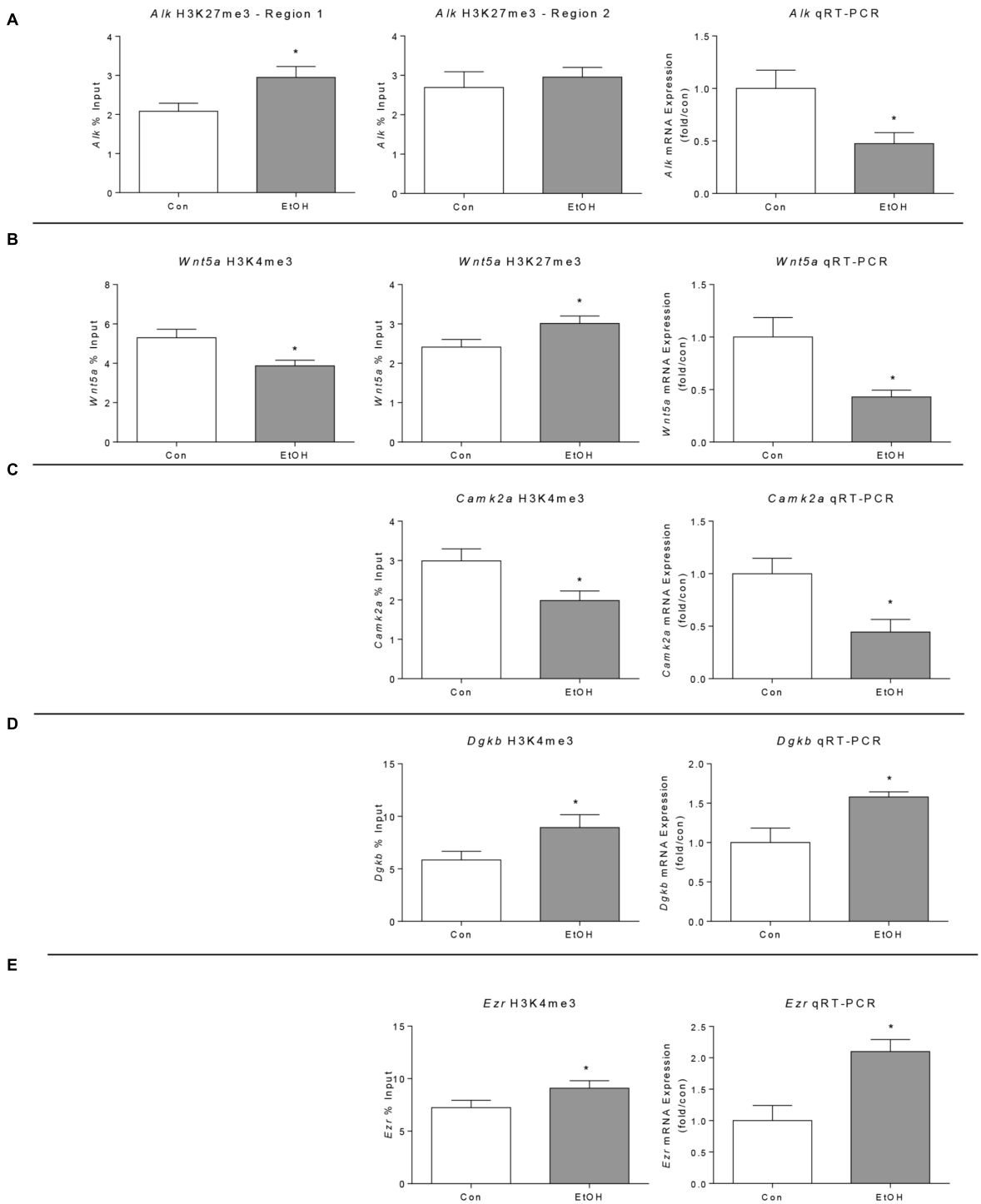

FIGURE 5 | Validation of selected ChIP-seq and microarray results in the prefrontal cortex of WSR male rats 21 days after ethanol exposure by ChIP and qPCR analyses. **(A)** *Alk* genomic region 1 was significantly enriched for H3K27me3 in ethanol samples but region 2 was not significantly enriched. *Alk* gene expression was down-regulated by ethanol exposure as predicted by the H3K27me3 ChIP-seq analysis (*Alk* was not present in the microarray platform used in this study). **(B)** *Wnt5a* H3K4me3 was significantly decreased and H3K27me3 was significantly increased by ChIP-qPCR, in agreement with the ChIP-seq findings. In addition, expression analysis showed decreased *Wnt5a* expression. **(C)** *Camk2a* H3K4me3 was reduced by alcohol confirming ChIP-seq results; in agreement with this modification, its expression was also reduced (*Camk2a* was not present in the microarray platform used in this study). **(D)** *Dgkb* H3K4me3 and gene expression were increased in alcohol withdrawal samples analyzed by ChIP-qPCR and qPCR respectively, confirming the ChIP-seq and microarray results. **(E)** *Ezr* H3K4me3 and gene expression were increased in alcohol withdrawal samples analyzed by ChIP-qPCR and qPCR respectively, confirming the ChIP-seq and microarray results. $^*p < 0.05$ by Student's *t*-test.

GRB2 also induces MMP expression (Crampton et al., 2009). In addition, we found an increase in H3K4me3 at the *Mapk14* gene. MAPK14 promotes interstitial matrix component fibronectin mRNA expression in hepatic stem cells (Gu et al., 2016). Prior studies indicated that acute or chronic ethanol, for the most part, promote ECM degradation (Guizzetti et al., 2010; Giordano et al., 2011), in part perhaps due to increases in MMP-9 activity (Wright et al., 2003). A reduction of *Wnt* and *Grb2* expression, together with increased *Mapk14*, as indicated by histone modifications found here, would be consistent with the notion that protracted ethanol withdrawal constitutes a period of ECM repair and growth.

Calcium signaling emerged as an overrepresented pathway in our pathway analyses of H3K4me3 and H3K27me3. Blocking certain types of calcium channel signaling has been shown to reduce rodent ethanol consumption (De Beun et al., 1996; Walter and Messing, 1999). In an ethanol exposure paradigm similar to the one used in this study in which rats were exposed to intermittent ethanol and their prefrontal cortex was analyzed 21 days after the last exposure, ion channels, including those that influence neurotransmitter release through effects on membrane potentials and calcium flux, emerged as one of the top GO categories in a miRNA and a DNA methylation study (Tapocik et al., 2013; Barbier et al., 2015). Calcium signaling also emerged as an important pathway following maternal binge-like ethanol doses in embryonic day 18 fetuses in a microarray study (Mandal et al., 2015b). Our results therefore further indicate an important role for calcium signaling in AUD, and suggest epigenetic mechanisms may encode persisting alterations in this pathway.

Some prior studies have examined H3K4me3 and H3K27me3 in relation to ethanol intake. Similar to our results, these studies have indicated that protracted withdrawal from ethanol produces global reductions in H3K4me3 levels (Govorko et al., 2012; Bekdash et al., 2013), although in these studies exposure was done *in utero* and measurements were done in the adult brain. In neonatal mice ethanol was found to increase H3K27me2 levels between 4 and 24 h following treatment (Subbanna et al., 2013). In contrast to our results, one study found that early post-natal ethanol exposure increased H3K4me3 and decreased H3K27me3 at adulthood (Chater-Diehl et al., 2016), and another reported a global increase in H3K4me3 6 h following a single ethanol exposure in adult mice (Finegersh and Homanics, 2014). Additionally, H3K4me3 levels were increased in postmortem human brain samples of subjects with alcoholism (Ponomarev et al., 2012). In light of these previous studies, our results suggest that protracted withdrawal is a unique state differing from controls, ethanol intoxication, and acute withdrawal, in which H3K4me3 remains low and H3K27me3 is high following high-dose ethanol exposure. Our results help clarify the dynamic changes in histone methylation in adulthood caused by ethanol as a function of time after exposure.

We found that differences in H3K4me3 and H3K27me3 in many cases did not lead to differences in gene expression. However, all changes in expression that did occur were in the direction that would be predicted based on the type(s) of chromatin modifications. For instance, we found two genes (*Pard3* and *Plagl1*) with both an H3K27me3 peak in the ethanol-exposed mice and a decrease in expression based on microarray analysis. Moreover, one gene (*Calu*) showed a reduction in H3K4me3 and a decrease in mRNA expression, and two genes (*Ezr* and *Dgkb*) showed an increase in H3K4me3 and mRNA expression. In addition, we decided to validate H3K27me3 and H3K4me3 peaks identified by ChIP-seq in *Alk* and *Camk2a* genes, respectively, and because these two genes were not included in the microarray, we carried out qRT-PCR analysis and found a decreased expression of both genes, as expected by the increased H3K27me3 in *Alk* and the decreased H3K4me3 in *Camk2a*. One reason for the lack of overlap was a methodological limitation of our study as 51% of the genes in which there were H3K4me3 differences and 82% of the genes in which there were H3K27me3 differences were not present in the microarray platform used. A second reason may be inherent to the nature of the relationship between histone modifications and gene expression. In fact, a lack on concordance between H3K4me3 or H3K27me3 and gene expression has been reported by others (Zhou et al., 2011; Chater-Diehl et al., 2016). Specifically, Henikoff and Shilatifard (2011) argued that histone modifications reflect rather than drive transcriptional activity. This explanation is supported by observations that global loss of H3K4me3 does not cause an overall decline in gene expression. In addition, H3K4me3 is not required for transcription in *in vitro* models. Also, there are many instances in which H3K4me3 levels peak after gene expression has already begun (Pavri et al., 2006; Borde et al., 2009; Clouaire et al., 2012; Kuang et al., 2014). Based on these observations there is evidence that the function of some histone marks is to stabilize gene expression over the long term. Certain histone modifications may mark genes for faster or slower induction of gene expression upon re-exposure to a stimulus or at genes that require frequent or infrequent reactivation (Muramoto et al., 2010; Ding et al., 2012; Mosesson et al., 2014). Therefore, the lack of overlap between histone modifications and gene expression reported here is in fact an interesting observation in itself and its further investigation may contribute to the understanding of the role of histone modifications in gene expression.

CONCLUSION

Ours is the first study to examine enduring epigenetic changes following protracted withdrawal in adult mice. These results indicate that even in the fully mature brain prior heavy ethanol exposure can produce enduring changes in chromatin structure. Our results indicate an overall reduction in H3K4me3 and increase in H3K27me3. Several of the genes affected by these changes have been previously implicated in AUD. Finally, our results strongly point to alterations in proteoglycans and calcium channel signaling as persisting changes following ethanol exposure. Roles for ECM-related factors, such as proteoglycans, and calcium signaling in AUD have recently gained prominence due to several recent reports.

DATA AVAILABILITY STATEMENT

The datasets generated for this study can be found in the Sequence Read Archive (SRP156323) and the Gene Expression Omnibus (GSE117925).

AUTHOR CONTRIBUTIONS

MG and JH designed the study. DG, JH, NL, LC, JC, and MG analyzed the data and/or interpreted the results. JC developed the mouse strain and provided the expertise related to ethanol administration. JH prepared ChIP samples. NL and LC performed the initial sequencing data analysis. DG and JH performed the downstream pathway analyses. DG, JH, and MG wrote the manuscript. All authors reviewed the manuscript.

FUNDING

This work was supported by the Department of Veterans Affairs Merit Review Awards BX001819 (MG) and BX000313 (JC) and BX004091 (DG), National Institutes of Health (R01AA021468), (R01AA022948) (MG), (R01AA025035) (DG), R24AA020245, U01AA013519 (JC), and National Library of Medicine (LM007088) (NL).

ACKNOWLEDGMENTS

We thank the OHSU ExaCloud Cluster Computational Resource, which allowed us to perform the intensive large-scale data workflows. Short read sequencing assays (ChIP-seq analysis) were performed by the OHSU Massive Parallel Sequencing Shared Resource. The contents do not represent the views of the United States Department of Veterans Affairs or the United States Government.

SUPPLEMENTARY MATERIAL

The Supplementary Material for this article can be found online at: https://www.frontiersin.org/articles/10.3389/fgene.2018.00346/full#supplementary-material

REFERENCES

Barbier, E., Tapocik, J. D., Juergens, N., Pitcairn, C., Borich, A., Schank, J. R., et al. (2015). DNA methylation in the medial prefrontal cortex regulates alcohol-induced behavior and plasticity. *J. Neurosci.* 35, 6153–6164. doi: 10.1523/JNEUROSCI.4571-14.2015

Beadles-Bohling, A. S., and Wiren, K. M. (2006). Anticonvulsive effects of kappa-opioid receptor modulation in an animal model of ethanol withdrawal. *Genes Brain Behav.* 5, 483–496. doi: 10.1111/j.1601-183X.2005.00200.x

Becker, H. C. (2014). "Alcohol dependence, withdrawal and relapse," in *Neurobiology of Alcohol Dependence*, eds A. B. C. Noronha, C. Cui, R. A. Harris, and J. C. Crabbe (San Diego, CA: Academic Press), 337–410.

Bekdash, R. A., Zhang, C., and Sarkar, D. K. (2013). Gestational choline supplementation normalized fetal alcohol-induced alterations in histone modifications, DNA methylation, and proopiomelanocortin (POMC) gene expression in beta-endorphin-producing POMC neurons of the hypothalamus. *Alcohol. Clin. Exp. Res.* 37, 1133–1142. doi: 10.1111/acer.12082

Bolger, A. M., Lohse, M., and Usadel, B. (2014). Trimmomatic: a flexible trimmer for Illumina sequence data. *Bioinformatics* 30, 2114–2120. doi: 10.1093/bioinformatics/btu170

Borde, V., Robine, N., Lin, W., Bonfils, S., Geli, V., and Nicolas, A. (2009). Histone H3 lysine 4 trimethylation marks meiotic recombination initiation sites. *EMBO J.* 28, 99–111. doi: 10.1038/emboj.2008.257

Carnicella, S., Amamoto, R., and Ron, D. (2009). Excessive alcohol consumption is blocked by glial cell line-derived neurotrophic factor. *Alcohol* 43, 35–43. doi: 10.1016/j.alcohol.2008.12.001

Celio, M. R., Spreafico, R., De Biasi, S., and Vitellaro-Zuccarello, L. (1998). Perineuronal nets: past and present. *Trends Neurosci.* 21, 510–515. doi: 10.1016/S0166-2236(98)01298-3

Chandler, L. J., Newsom, H., Sumners, C., and Crews, F. (1993). Chronic ethanol exposure potentiates NMDA excitotoxicity in cerebral cortical neurons. *J. Neurochem.* 60, 1578–1581. doi: 10.1111/j.1471-4159.1993.tb03326.x

Chater-Diehl, E. J., Laufer, B. I., Castellani, C. A., Alberry, B. L., and Singh, S. M. (2016). Alteration of gene expression, DNA methylation, and histone methylation in free radical scavenging networks in adult mouse hippocampus following fetal alcohol exposure. *PLoS One* 11:e0154836. doi: 10.1371/journal.pone.0154836

Chen, T., and Dent, S. Y. (2014). Chromatin modifiers and remodellers: regulators of cellular differentiation. *Nat. Rev. Genet.* 15, 93–106. doi: 10.1038/nrg3607

Clouaire, T., Webb, S., Skene, P., Illingworth, R., Kerr, A., Andrews, R., et al. (2012). Cfp1 integrates both CpG content and gene activity for accurate H3K4me3 deposition in embryonic stem cells. *Genes Dev.* 26, 1714–1728. doi: 10.1101/gad.194209.112

Commerford, S. L., Carsten, A. L., and Cronkite, E. P. (1982). Histone turnover within nonproliferating cells. *Proc. Natl. Acad. Sci. U.S.A.* 79, 1163–1165. doi: 10.1073/pnas.79.4.1163

Consortium, E. P. (2012). An integrated encyclopedia of DNA elements in the human genome. *Nature* 489, 57–74. doi: 10.1038/nature11247

Crabbe, J. C. (2014). "Use of animal models of alcohol-related behavior," in *Alcohol and the Nervous System*, eds E. V. Sullivan and A. Pfefferbaum (Cambridge, MA: Elsevier), 71–86.

Crabbe, J. C., and Kosobud, A. (1986). Sensitivity and tolerance to ethanol in mice bred to be genetically prone or resistant to ethanol withdrawal seizures. *J. Pharmacol. Exp. Ther.* 239, 327–333.

Crampton, S. P., Wu, B., Park, E. J., Kim, J. H., Solomon, C., Waterman, M. L., et al. (2009). Integration of the beta-catenin-dependent Wnt pathway with integrin signaling through the adaptor molecule Grb2. *PLoS One* 4:e7841. doi: 10.1371/journal.pone.0007841

D'Addario, C., Caputi, F. F., Ekstrom, T. J., Di Benedetto, M., Maccarrone, M., Romualdi, P., et al. (2013). Ethanol induces epigenetic modulation of prodynorphin and pronociceptin gene expression in the rat amygdala complex. *J. Mol. Neurosci.* 49, 312–319. doi: 10.1007/s12031-012-9829-y

De Beun, R., Schneider, R., Klein, A., Lohmann, A., and De Vry, J. (1996). Effects of nimodipine and other calcium channel antagonists in alcohol-preferring AA rats. *Alcohol* 13, 263–271. doi: 10.1016/0741-8329(95)02054-3

Ding, Y., Fromm, M., and Avramova, Z. (2012). Multiple exposures to drought 'train' transcriptional responses in Arabidopsis. *Nat. Commun.* 3:740. doi: 10.1038/ncomms1732

Dityatev, A., Schachner, M., and Sonderegger, P. (2010). The dual role of the extracellular matrix in synaptic plasticity and homeostasis. *Nat. Rev. Neurosci.* 11, 735–746. doi: 10.1038/nrn2898

Dutton, J. W. III, Chen, H., You, C., Brodie, M. S., and Lasek, A. W. (2017). Anaplastic lymphoma kinase regulates binge-like drinking and dopamine receptor sensitivity in the ventral tegmental area. *Addict. Biol.* 22, 665–678. doi: 10.1111/adb.12358

Farris, S. P., Harris, R. A., and Ponomarev, I. (2015). Epigenetic modulation of brain gene networks for cocaine and alcohol abuse. *Front. Neurosci.* 9:176. doi: 10.3389/fnins.2015.00176

Feng, J., Liu, T., Qin, B., Zhang, Y., and Liu, X. S. (2012). Identifying ChIP-seq enrichment using MACS. *Nat. Protoc.* 7, 1728–1740. doi: 10.1038/nprot.2012.101

Finegersh, A., and Homanics, G. E. (2014). Acute ethanol alters multiple histone modifications at model gene promoters in the cerebral cortex. *Alcohol. Clin. Exp. Res.* 38, 1865–1873. doi: 10.1111/acer.12465

Friedman, H. J. (1980). "Assessment of physical dependence on and withdrawal from ethanol in animals," in *Alcohol Tolerance and Dependence*, eds H. Rigter and J. C. Crabbe (Amsterdam, NL: Elsevier), 93–121.

Gavin, D. P., Kusumo, H., Zhang, H., Guidotti, A., and Pandey, S. C. (2016). Role of growth arrest and DNA damage-inducible, beta in alcohol-drinking behaviors. *Alcohol. Clin. Exp. Res.* 40, 263–272. doi: 10.1111/acer.12965

Giordano, G., Guizzetti, M., Dao, K., Mattison, H. A., and Costa, L. G. (2011). Ethanol impairs muscarinic receptor-induced neuritogenesis in rat hippocampal slices: role of astrocytes and extracellular matrix proteins. *Biochem. Pharmacol.* 82, 1792–1799. doi: 10.1016/j.bcp.2011.08.014

Gogolla, N., Caroni, P., Luthi, A., and Herry, C. (2009). Perineuronal nets protect fear memories from erasure. *Science* 325, 1258–1261. doi: 10.1126/science.1174146

Goldstein, D. B. (1972). Alcohol dependence produced in mice by inhalation of ethanol: grading the withdrawal reaction. *Science* 172, 288–290. doi: 10.1126/science.172.3980.288

Goldstein, D. B., and Pal, N. (1971). Relationship of alcohol dose to intensity of withdrawal signs in mice. *J. Pharmacol. Exp. Ther.* 180, 203–215.

Govorko, D., Bekdash, R. A., Zhang, C., and Sarkar, D. K. (2012). Male germline transmits fetal alcohol adverse effect on hypothalamic proopiomelanocortin gene across generations. *Biol. Psychiatry* 72, 378–388. doi: 10.1016/j.biopsych.2012.04.006

Gu, L., Tao, X., Xu, Y., Han, X., Qi, Y., Xu, L., et al. (2016). Dioscin alleviates BDL- and DMN-induced hepatic fibrosis via Sirt1/Nrf2-mediated inhibition of p38 MAPK pathway. *Toxicol. Appl. Pharmacol.* 292, 19–29. doi: 10.1016/j.taap.2015.12.024

Guenther, M. G., Levine, S. S., Boyer, L. A., Jaenisch, R., and Young, R. A. (2007). A chromatin landmark and transcription initiation at most promoters in human cells. *Cell* 130, 77–88. doi: 10.1016/j.cell.2007.05.042

Guizzetti, M., Moore, N. H., Giordano, G., Vandemark, K. L., and Costa, L. G. (2010). Ethanol inhibits neuritogenesis induced by astrocyte muscarinic receptors. *Glia* 58, 1395–1406. doi: 10.1002/glia.21015

Gundelfinger, E. D., Frischknecht, R., Choquet, D., and Heine, M. (2010). Converting juvenile into adult plasticity: a role for the brain's extracellular matrix. *Eur. J. Neurosci.* 31, 2156–2165. doi: 10.1111/j.1460-9568.2010.07253.x

Hannon Lab, G. J. (2010). *FASTX-Toolkit*. Available at: http://hannonlab.cshl.edu/fastx_toolkit/index.html

Harper, C., and Matsumoto, I. (2005). Ethanol and brain damage. *Curr. Opin. Pharmacol.* 5, 73–78. doi: 10.1016/j.coph.2004.06.011

Hashimoto, J. G., Forquer, M. R., Tanchuck, M. A., Finn, D. A., and Wiren, K. M. (2011). Importance of genetic background for risk of relapse shown in altered prefrontal cortex gene expression during abstinence following chronic alcohol intoxication. *Neuroscience* 173, 57–75. doi: 10.1016/j.neuroscience.2010.11.006

Hashimoto, J. G., Gavin, D. P., Wiren, K. M., Crabbe, J. C., and Guizzetti, M. (2017). Prefrontal cortex expression of chromatin modifier genes in male WSP and WSR mice changes across ethanol dependence, withdrawal, and abstinence. *Alcohol* 60, 83–94. doi: 10.1016/j.alcohol.2017.01.010

Heberlein, A., Muschler, M., Wilhelm, J., Frieling, H., Lenz, B., Groschl, M., et al. (2010). BDNF and GDNF serum levels in alcohol-dependent patients during withdrawal. *Prog. Neuropsychopharmacol. Biol. Psychiatry* 34, 1060–1064. doi: 10.1016/j.pnpbp.2010.05.025

Henikoff, S., and Shilatifard, A. (2011). Histone modification: cause or cog? *Trends Genet.* 27, 389–396. doi: 10.1016/j.tig.2011.06.006

Huang, D. W., Sherman, B. T., and Lempicki, R. A. (2009). Systematic and integrative analysis of large gene lists using DAVID bioinformatics resources. *Nat. Protoc.* 4, 44–57. doi: 10.1038/nprot.2008.211

Huang, G., Chubinskaya, S., Liao, W., and Loeser, R. F. (2017). Wnt5a induces catabolic signaling and matrix metalloproteinase production in human articular chondrocytes. *Osteoarthritis Cartilage* 25, 1505–1515. doi: 10.1016/j.joca.2017.05.018

Ille, F., and Sommer, L. (2005). Wnt signaling: multiple functions in neural development. *Cell. Mol. Life Sci.* 62, 1100–1108. doi: 10.1007/s00018-005-4552-2

Kharchenko, P. V., Tolstorukov, M. Y., and Park, P. J. (2008). Design and analysis of ChIP-seq experiments for DNA-binding proteins. *Nat. Biotechnol.* 26, 1351–1359. doi: 10.1038/nbt.1508

Kosobud, A., and Crabbe, J. C. (1986). Ethanol withdrawal in mice bred to be genetically prone or resistant to ethanol withdrawal seizures. *J. Pharmacol. Exp. Ther.* 238, 170–177.

Kuang, Z., Cai, L., Zhang, X., Ji, H., Tu, B. P., and Boeke, J. D. (2014). High-temporal-resolution view of transcription and chromatin states across distinct metabolic states in budding yeast. *Nat. Struct. Mol. Biol.* 21, 854–863. doi: 10.1038/nsmb.2881

Landt, S. G., Marinov, G. K., Kundaje, A., Kheradpour, P., Pauli, F., Batzoglou, S., et al. (2012). ChIP-seq guidelines and practices of the ENCODE and modENCODE consortia. *Genome Res.* 22, 1813–1831. doi: 10.1101/gr.136184.111

Lasek, A. W. (2016). Effects of ethanol on brain extracellular matrix: implications for alcohol use disorder. *Alcohol. Clin. Exp. Res.* 40, 2030–2042. doi: 10.1111/acer.13200

Lasek, A. W., Lim, J., Kliethermes, C. L., Berger, K. H., Joslyn, G., Brush, G., et al. (2011). An evolutionary conserved role for anaplastic lymphoma kinase in behavioral responses to ethanol. *PLoS One* 6:e22636. doi: 10.1371/journal.pone.0022636

Lau, L. W., Cua, R., Keough, M. B., Haylock-Jacobs, S., and Yong, V. W. (2013). Pathophysiology of the brain extracellular matrix: a new target for remyelination. *Nat. Rev. Neurosci.* 14, 722–729. doi: 10.1038/nrn3550

Leek, J. T., Johnson, W. E., Parker, H. S., Jaffe, A. E., and Storey, J. D. (2012). The sva package for removing batch effects and other unwanted variation in high-throughput experiments. *Bioinformatics* 28, 882–883. doi: 10.1093/bioinformatics/bts034

Li, H., Brown, B., Huang, H., and Bickel, P. (2011). Measuring reproducibility of high-throughput experiments. *Ann. Appl. Stat.* 5, 1752–1779. doi: 10.1214/11-AOAS466

Li, H., and Durbin, R. (2009). Fast and accurate short read alignment with Burrows-Wheeler transform. *Bioinformatics* 25, 1754–1760. doi: 10.1093/bioinformatics/btp324

Luo, S., Shi, Q., Zha, Z., Yao, P., Lin, H., Liu, N., et al. (2013). Inactivation of Wnt/beta-catenin signaling in human adipose-derived stem cells is necessary for chondrogenic differentiation and maintenance. *Biomed. Pharmacother.* 67, 819–824. doi: 10.1016/j.biopha.2013.03.008

Mandal, C., Park, J. H., Choi, M. R., Kim, S. H., Badejo, A. C., Chai, J. C., et al. (2015a). Transcriptomic study of mouse embryonic neural stem cell differentiation under ethanol treatment. *Mol. Biol. Rep.* 42, 1233–1239. doi: 10.1007/s11033-015-3862-1

Mandal, C., Park, K. S., Jung, K. H., and Chai, Y. G. (2015b). Ethanol-related alterations in gene expression patterns in the developing murine hippocampus. *Acta Biochim. Biophys. Sin.* 47, 581–587. doi: 10.1093/abbs/gmv050

McCarthy, D. J., and Smyth, G. K. (2009). Testing significance relative to a fold-change threshold is a TREAT. *Bioinformatics* 25, 765–771. doi: 10.1093/bioinformatics/btp053

McRae, P. A., and Porter, B. E. (2012). The perineuronal net component of the extracellular matrix in plasticity and epilepsy. *Neurochem. Int.* 61, 963–972. doi: 10.1016/j.neuint.2012.08.007

Metten, P., and Crabbe, J. C. (1996). "Dependence and withdrawal," in *Pharmacological Effects of Ethanol on the Nervous System*, eds R. A. Deitrich and V. G. Erwin (Boca Ranton, FL: CRC Press), 269–290.

Moonat, S., Sakharkar, A. J., Zhang, H., Tang, L., and Pandey, S. C. (2013). Aberrant histone deacetylase2-mediated histone modifications and synaptic plasticity in the amygdala predisposes to anxiety and alcoholism. *Biol. Psychiatry* 73, 763–773. doi: 10.1016/j.biopsych.2013.01.012

Mosesson, Y., Voichek, Y., and Barkai, N. (2014). Divergence and selectivity of expression-coupled histone modifications in budding yeasts. *PLoS One* 9:e101538. doi: 10.1371/journal.pone.0101538

Muramoto, T., Muller, I., Thomas, G., Melvin, A., and Chubb, J. R. (2010). Methylation of H3K4 Is required for inheritance of active transcriptional states. *Curr. Biol.* 20, 397–406. doi: 10.1016/j.cub.2010.01.017

Nadon, N. L., Mohr, D., and Becker, K. G. (2005). National Institute on aging microarray facility–resources for gerontology research. *J. Gerontol. A Biol. Sci. Med. Sci.* 60, 413–415. doi: 10.1093/gerona/60.4.413

Olive, M. F. (2010). Pharmacotherapies for alcoholism: the old and the new. *CNS Neurol. Disord. Drug Targets* 9, 2–4. doi: 10.2174/187152710790966722

Pandey, S. C., Kyzar, E. J., and Zhang, H. (2017). Epigenetic basis of the dark side of alcohol addiction. *Neuropharmacology* 122, 74–84. doi: 10.1016/j.neuropharm.2017.02.002

Pandey, S. C., Ugale, R., Zhang, H., Tang, L., and Prakash, A. (2008). Brain chromatin remodeling: a novel mechanism of alcoholism. *J. Neurosci.* 28, 3729–3737. doi: 10.1523/JNEUROSCI.5731-07.2008

Pavri, R., Zhu, B., Li, G., Trojer, P., Mandal, S., Shilatifard, A., et al. (2006). Histone H2B monoubiquitination functions cooperatively with FACT to regulate elongation by RNA polymerase II. *Cell* 125, 703–717. doi: 10.1016/j.cell.2006.04.029

Pizzorusso, T., Medini, P., Berardi, N., Chierzi, S., Fawcett, J. W., and Maffei, L. (2002). Reactivation of ocular dominance plasticity in the adult visual cortex. *Science* 298, 1248–1251. doi: 10.1126/science.1072699

Ponomarev, I., Wang, S., Zhang, L., Harris, R. A., and Mayfield, R. D. (2012). Gene coexpression networks in human brain identify epigenetic modifications in alcohol dependence. *J. Neurosci.* 32, 1884–1897. doi: 10.1523/JNEUROSCI.3136-11.2012

Pruitt, K. D., Tatusova, T., and Maglott, D. R. (2005). NCBI Reference Sequence (RefSeq): a curated non-redundant sequence database of genomes, transcripts and proteins. *Nucleic Acids Res.* 33, D501–D504. doi: 10.1093/nar/gki025

Reynolds, P. M., Mueller, S. W., and Maclaren, R. (2015). A comparison of dexmedetomidine and placebo on the plasma concentrations of NGF, BDNF, GDNF, and epinephrine during severe alcohol withdrawal. *Alcohol* 49, 15–19. doi: 10.1016/j.alcohol.2014.11.006

Ritchie, M. E., Phipson, B., Wu, D., Hu, Y., Law, C. W., Shi, W., et al. (2015). limma powers differential expression analyses for RNA-sequencing and microarray studies. *Nucleic Acids Res.* 43:e47. doi: 10.1093/nar/gkv007

Robinson, M. D., Mccarthy, D. J., and Smyth, G. K. (2010). edgeR: a Bioconductor package for differential expression analysis of digital gene expression data. *Bioinformatics* 26, 139–140. doi: 10.1093/bioinformatics/btp616

Robison, A. J., and Nestler, E. J. (2011). Transcriptional and epigenetic mechanisms of addiction. *Nat. Rev. Neurosci.* 12, 623–637. doi: 10.1038/nrn3111

Rogers, J., Wiener, S. G., and Bloom, F. E. (1979). Long-term ethanol administration methods for rats: advantages of inhalation over intubation or liquid diets. *Behav. Neural. Biol.* 27, 466–486. doi: 10.1016/S0163-1047(79)92061-2

Sakharkar, A. J., Zhang, H., Tang, L., Shi, G., and Pandey, S. C. (2012). Histone deacetylases (HDAC)-induced histone modifications in the amygdala: a role in rapid tolerance to the anxiolytic effects of ethanol. *Alcohol. Clin. Exp. Res.* 36, 61–71. doi: 10.1111/j.1530-0277.2011.01581.x

Schubeler, D., Macalpine, D. M., Scalzo, D., Wirbelauer, C., Kooperberg, C., Van Leeuwen, F., et al. (2004). The histone modification pattern of active genes revealed through genome-wide chromatin analysis of a higher eukaryote. *Genes Dev.* 18, 1263–1271. doi: 10.1101/gad.1198204

Shannon, P., Markiel, A., Ozier, O., Baliga, N. S., Wang, J. T., Ramage, D., et al. (2003). Cytoscape: a software environment for integrated models of biomolecular interaction networks. *Genome Res.* 13, 2498–2504. doi: 10.1101/gr.1239303

Smith, M. L., Lopez, M. F., Archer, K. J., Wolen, A. R., Becker, H. C., and Miles, M. F. (2016). Time-course analysis of brain regional expression network responses to chronic intermittent ethanol and withdrawal: implications for mechanisms underlying excessive ethanol consumption. *PLoS One* 11:e0146257. doi: 10.1371/journal.pone.0146257

Stragier, E., Massart, R., Salery, M., Hamon, M., Geny, D., Martin, V., et al. (2015). Ethanol-induced epigenetic regulations at the Bdnf gene in C57BL/6J mice. *Mol. Psychiatry* 20, 405–412. doi: 10.1038/mp.2014.38

Strahl, B. D., Ohba, R., Cook, R. G., and Allis, C. D. (1999). Methylation of histone H3 at lysine 4 is highly conserved and correlates with transcriptionally active nuclei in Tetrahymena. *Proc. Natl. Acad. Sci. U.S.A.* 96, 14967–14972. doi: 10.1073/pnas.96.26.14967

Subbanna, S., Shivakumar, M., Umapathy, N. S., Saito, M., Mohan, P. S., Kumar, A., et al. (2013). G9a-mediated histone methylation regulates ethanol-induced neurodegeneration in the neonatal mouse brain. *Neurobiol. Dis.* 54, 475–485. doi: 10.1016/j.nbd.2013.01.022

Tapocik, J. D., Solomon, M., Flanigan, M., Meinhardt, M., Barbier, E., Schank, J. R., et al. (2013). Coordinated dysregulation of mRNAs and microRNAs in the rat medial prefrontal cortex following a history of alcohol dependence. *Pharmacogenomics J.* 13, 286–296. doi: 10.1038/tpj.2012.17

van der Vaart, A. D., Wolstenholme, J. T., Smith, M. L., Harris, G. M., Lopez, M. F., Wolen, A. R., et al. (2017). The allostatic impact of chronic ethanol on gene expression: a genetic analysis of chronic intermittent ethanol treatment in the BXD cohort. *Alcohol* 58, 93–106. doi: 10.1016/j.alcohol.2016.07.010

Vangipuram, S. D., and Lyman, W. D. (2012). Ethanol affects differentiation-related pathways and suppresses Wnt signaling protein expression in human neural stem cells. *Alcohol. Clin. Exp. Res.* 36, 788–797. doi: 10.1111/j.1530-0277.2011.01682.x

Wahlstrom, G. (1987). Ethanol exposure as inducer of stable voluntary ethanol drinking in the male rat. *Drug Alcohol Depend.* 20, 105–114. doi: 10.1016/0376-8716(87)90059-7

Walter, H. J., and Messing, R. O. (1999). Regulation of neuronal voltage-gated calcium channels by ethanol. *Neurochem. Int.* 35, 95–101. doi: 10.1016/S0197-0186(99)00050-9

Wang, D., and Fawcett, J. (2012). The perineuronal net and the control of CNS plasticity. *Cell Tissue Res.* 349, 147–160. doi: 10.1007/s00441-012-1375-y

Wang, X., Spandidos, A., Wang, H., and Seed, B. (2012). PrimerBank: a PCR primer database for quantitative gene expression analysis, 2012 update. *Nucleic Acids Res.* 40, D1144–D1149. doi: 10.1093/nar/gkr1013

Waszkiewicz, N., Szajda, S. D., Zalewska, A., Szulc, A., Kepka, A., Minarowska, A., et al. (2012). Alcohol abuse and glycoconjugate metabolism. *Folia Histochem. Cytobiol.* 50, 1–11. doi: 10.2478/18690

Wilhelm, C. J., Hashimoto, J. G., Roberts, M. L., Sonmez, M. K., and Wiren, K. M. (2014). Understanding the addiction cycle: a complex biology with distinct contributions of genotype vs. sex at each stage. *Neuroscience* 279, 168–186. doi: 10.1016/j.neuroscience.2014.08.041

Wiren, K. M., Hashimoto, J. G., Alele, P. E., Devaud, L. L., Price, K. L., Middaugh, L. D., et al. (2006). Impact of sex: determination of alcohol neuroadaptation and reinforcement. *Alcohol. Clin. Exp. Res.* 30, 233–242. doi: 10.1111/j.1530-0277.2006.00032.x

Wolen, A. R., Phillips, C. A., Langston, M. A., Putman, A. H., Vorster, P. J., Bruce, N. A., et al. (2012). Genetic dissection of acute ethanol responsive gene networks in prefrontal cortex: functional and mechanistic implications. *PLoS One* 7:e33575. doi: 10.1371/journal.pone.0033575

Wright, J. W., Masino, A. J., Reichert, J. R., Turner, G. D., Meighan, S. E., Meighan, P. C., et al. (2003). Ethanol-induced impairment of spatial memory and brain matrix metalloproteinases. *Brain Res.* 963, 252–261. doi: 10.1016/S0006-8993(02)04036-2

Wu, B., Crampton, S. P., and Hughes, C. C. (2007). Wnt signaling induces matrix metalloproteinase expression and regulates T cell transmigration. *Immunity* 26, 227–239. doi: 10.1016/j.immuni.2006.12.007

Yamaguchi, Y. (2000). Lecticans: organizers of the brain extracellular matrix. *Cell. Mol. Life Sci.* 57, 276–289. doi: 10.1007/PL00000690

Yamamoto, H., Kitadai, Y., Yamamoto, H., Oue, N., Ohdan, H., Yasui, W., et al. (2009). Laminin gamma2 mediates Wnt5a-induced invasion of gastric cancer cells. *Gastroenterology* 137, e241–e246. doi: 10.1053/j.gastro.2009.02.003

Ye, J., Coulouris, G., Zaretskaya, I., Cutcutache, I., Rozen, S., and Madden, T. L. (2012). Primer-BLAST: a tool to design target-specific primers for polymerase chain reaction. *BMC Bioinformatics* 13:134. doi: 10.1186/1471-2105-13-134

Zhang, X., Bhattacharyya, S., Kusumo, H., Goodlett, C. R., Tobacman, J. K., and Guizzetti, M. (2014). Arylsulfatase B modulates neurite outgrowth via astrocyte chondroitin-4-sulfate: dysregulation by ethanol. *Glia* 62, 259–271. doi: 10.1002/glia.22604

Zhang, Y., Liu, T., Meyer, C. A., Eeckhoute, J., Johnson, D. S., Bernstein, B. E., et al. (2008). Model-based analysis of ChIP-Seq (MACS). *Genome Biol.* 9:R137. doi: 10.1186/gb-2008-9-9-r137

Zhou, Z., Yuan, Q., Mash, D. C., and Goldman, D. (2011). Substance-specific and shared transcription and epigenetic changes in the human hippocampus chronically exposed to cocaine and alcohol. *Proc. Natl. Acad. Sci. U.S.A.* 108, 6626–6631. doi: 10.1073/pnas.1018514108

Conflict of Interest Statement: The authors declare that the research was conducted in the absence of any commercial or financial relationships that could be construed as a potential conflict of interest.

frontiers in Genetics

ORIGINAL RESEARCH
published: 10 September 2018
doi: 10.3389/fgene.2018.00325

Binge Ethanol Drinking Produces Sexually Divergent and Distinct Changes in Nucleus Accumbens Signaling Cascades and Pathways in Adult C57BL/6J Mice

Deborah A. Finn[1,2], Joel G. Hashimoto[1,2], Debra K. Cozzoli[1], Melinda L. Helms[1,2], Michelle A. Nipper[1,2], Moriah N. Kaufman[1], Kristine M. Wiren[1,2] and Marina Guizzetti[1,2]*

[1] Department of Behavioral Neuroscience, Oregon Health & Science University, Portland, OR, United States, [2] Research, VA Portland Health Care System, Portland, OR, United States

We previously determined that repeated binge ethanol drinking produced sex differences in the regulation of signaling downstream of Group 1 metabotropic glutamate receptors in the nucleus accumbens (NAc) of adult C57BL/6J mice. The purpose of the present study was to characterize RNA expression differences in the NAc of adult male and female C57BL/6J mice following 7 binge ethanol drinking sessions, when compared with controls consuming water. This binge drinking procedure produced high intakes (average >2.2 g/kg/30 min) and blood ethanol concentrations (average >1.3 mg/ml). Mice were euthanized at 24 h after the 7th binge session, and focused qPCR array analysis was employed on NAc tissue to quantify expression levels of 384 genes in a customized Mouse Mood Disorder array, with a focus on glutamatergic signaling (3 arrays/group). We identified significant regulation of 50 genes in male mice and 70 genes in female mice after 7 ethanol binges. Notably, 14 genes were regulated in both males and females, representing common targets to binge ethanol drinking. However, expression of 10 of these 14 genes was strongly dimorphic (e.g., opposite regulation for genes such as *Crhr2*, *Fos*, *Nos1*, and *Star*), and only 4 of the 14 genes were regulated in the same direction (*Drd5*, *Grm4*, *Ranbp9*, and *Reln*). Interestingly, the top 30 regulated genes by binge ethanol drinking for each sex differed markedly in the male and female mice, and this divergent neuroadaptive response in the NAc could result in dysregulation of distinct biological pathways between the sexes. Characterization of the expression differences with Ingenuity Pathway Analysis was used to identify Canonical Pathways, Upstream Regulators, and significant Biological Functions. Expression differences suggested that hormone signaling and immune function were altered by binge drinking in female mice, whereas neurotransmitter metabolism was a central target of binge ethanol drinking in male mice. Thus, these results indicate that the transcriptional response to repeated binge ethanol drinking was strongly influenced by sex, and they emphasize the importance of considering sex in the development of potential pharmacotherapeutic targets for the treatment of alcohol use disorder.

Keywords: alcohol, qPCR arrays, sex differences, hormone signaling, immune function, neurotransmitter metabolism, C57BL/6J mice

OPEN ACCESS

Edited by:
Kristin Hamre,
The University of Tennessee Health Science Center, United States

Reviewed by:
Richard Lowell Bell,
Indiana University, Indianapolis, United States
Richard S. Lee,
Johns Hopkins University, United States

****Correspondence:***
Deborah A. Finn
finnd@ohsu.edu

Specialty section:
This article was submitted to Behavioral and Psychiatric Genetics, a section of the journal Frontiers in Genetics

Received: *01 March 2018*
Accepted: *30 July 2018*
Published: *10 September 2018*

Citation:
Finn DA, Hashimoto JG, Cozzoli DK, Helms ML, Nipper MA, Kaufman MN, Wiren KM and Guizzetti M (2018) Binge Ethanol Drinking Produces Sexually Divergent and Distinct Changes in Nucleus Accumbens Signaling Cascades and Pathways in Adult C57BL/6J Mice. Front. Genet. 9:325. doi: 10.3389/fgene.2018.00325

INTRODUCTION

Alcohol use disorder (AUD) is a clinical problem of great significance that cost the United States $249 billion in 2010, with ¾ of the cost related to binge drinking or a pattern of drinking that brings blood alcohol concentration ≥ 80 mg/dL (or 0.8 mg/mL; NIAAA, 2004). Excessive alcohol use is the fourth leading preventable cause of death in the United States, but globally, it accounts for 5.9% of all deaths (∼3.3 million in 2012) and is the first leading risk factor for premature death and disability among people between the ages of 15 and 49 (NIAAA, 2017). Epidemiological evidence indicates that women develop alcohol-related heart disease, liver damage, and peripheral neuropathy after fewer years of heavy drinking, and that women may be more vulnerable to AUD-induced brain damage (Wiren, 2013 and references therein).

Behavioral, biochemical, and molecular pharmacological evidence indicates that *N*-methyl-D-aspartate (NMDA) receptors are one of the primary targets of ethanol. Other primary targets include γ-aminobutyric acid$_A$ (GABA$_A$), glycine, serotonin-3, and neuronal nicotinic acetylcholine receptors, as well as L-type calcium channels and G protein-activated inwardly rectifying potassium channels (reviewed in Spanagel, 2009; Cui and Koob, 2017). Concentrations as low as 1 mM produce alterations in the function of these receptors and ion channels, which initiate a cascade of intracellular events and lead to the acute behavioral effects of ethanol that range from disinhibition to sedation and hypnosis (depending on the dose). Given that practically all neurons in the brain are estimated to possess glutamatergic inputs, glutamatergic neurotransmission is in a position to regulate or influence a diverse array of neuronal processes (see Chandler, 2003; Lau and Zukin, 2007; Bell et al., 2016). A large body of evidence also implicates activity-dependent changes in the efficacy of glutamatergic neurotransmission as a major underlying event in the addicted brain (e.g., reviewed in Chandler, 2003; Tzschentke and Schmidt, 2003; Kauer and Malenka, 2007; Szumlinski et al., 2008a; Kalivas, 2009; Bell et al., 2016). Importantly, we recently found that repeated binge drinking recruited sexually divergent signaling cascades downstream of phosphoinositide 3-kinase (PI3K) in the nucleus accumbens (NAc) in C57BL/6J mice, with significant changes in males and females relatively resistant to these changes (Cozzoli et al., 2016). The functional implication of the changes was confirmed by the demonstration that intra-NAc rapamycin, which inhibits mammalian target of rapamycin (mTOR) in the PI3K signaling cascade, significantly decreased binge ethanol drinking in male but not in female mice (Cozzoli et al., 2016). Taken in conjunction with evidence that rapamycin (see Neasta et al., 2014 and references therein) and newly developed mTOR complex 1 inhibitors (Morisot et al., 2018) significantly reduce high ethanol drinking in male rodents, the results by Cozzoli et al. (2016) highlight sex differences in the influence of binge drinking on signaling cascades downstream of PI3K and presumably, metabotropic Group 1 glutamate receptors (mGluR1).

Neuroadaptive responses to binge ethanol consumption are not limited to effects on neurotransmitter systems. Microarray expression analysis in whole brain or in brain regions such as the medial prefrontal cortex (mPFC), NAc, ventral tegmental area (VTA), and amygdala have found that various models of binge drinking produced changes in expression of genes in male rodents that were involved in some of the following networks: glutamate signaling, BDNF (brain derived neurotrophic factor), synaptic vesicle fusion, synaptic transmission, apoptosis, glucocorticoid receptor (GR) signaling, anti-apoptosis, regulation of G-protein receptor signaling, transcription factors, neurogenesis, and neuroimmune-related pathways (e.g., Rodd et al., 2008; Bell et al., 2009; McBride et al., 2010; Mulligan et al., 2011; Wolstenholme et al., 2011; Agrawal et al., 2014). Binge drinking in female rodents produced changes in VTA gene expression that were associated with neuroimmune and epigenetic functions, a pro-inflammatory response, and an enhanced response to glucocorticoids and steroid hormones (McBride et al., 2013; Marballi et al., 2016), and the two top networks identified were neurological/psychological disorders and lipid/nucleic acid metabolism (Marballi et al., 2016). Changes in NAc and amygdala protein expression in female rats following binge drinking were associated with functional categories such as the cytoskeleton, cellular stress response, membrane transport, and neurotransmission (Bell et al., 2006). Although male and female rodents were never directly compared in the same study, binge-like ethanol drinking changed the expression of genes and proteins that likely alter neuronal function in several ways and that can be either adaptive or deleterious.

Chronic ethanol intoxication that results in physical dependence via continuous or intermittent ethanol vapor exposure also produces gene expression changes, with a different transcriptional response in the cortex during acute withdrawal (8 h) than after a period of abstinence (3 weeks) in male and female rodents. Studies conducted in male mice during acute withdrawal found that transcriptionally responsive genes in the PFC were involved in the Ras/MAPK (mitogen-activated protein kinase) pathway, notch signaling, and ubiquitination (Melendez et al., 2012) and that dysregulation in the expression of several chromatin remodeling genes in PFC was primarily evident during acute withdrawal rather than during a period of abstinence (Hashimoto et al., 2017). Pathways identified in cingulate cortex of male rats after a period of abstinence were involved in neurotransmission (e.g., glutamatergic, endocannabinoid, monoaminergic), signal transduction (e.g., MAPK, ERK2 or extracellular signal-related kinase 2), and synaptic plasticity (Rimondini et al., 2002). Additionally, a study designed to discover master regulator genes (i.e., key genes that drive the expression of the specific transcriptional response associated with physical dependence) during abstinence in male rats identified *Nr3c1*, the gene encoding the GR, as one of the highest master regulators in the mPFC, NAc, VTA, and central nucleus of the amygdala (Repunte-Canonigo et al., 2015). Importantly, several studies were conducted in male and female mPFC with the goal of examining sex and ethanol withdrawal severity genotype differences in gene expression profiles in mice selectively bred for high and low withdrawal. During acute withdrawal, sex rather than withdrawal genotype, correlated best with the transcriptional response in dependent mice. Females showed regulation of genes associated

with cell death/neurodegeneration, DNA/RNA binding, and inflammation/immune function whereas males showed regulation of genes associated with protein degradation, calcium ion binding pathways, inflammation/immune function, and nervous system disorders/development (Hashimoto and Wiren, 2008; Wilhelm et al., 2014). However, while NF-κB (nuclear factor kappa-light-chain-enhancer of activated B cells) signaling was identified as a significant signaling node in both males and females, the interacting proteins were completely distinct between the sexes, which was indicative of a sexually dimorphic immune response during acute withdrawal. Subsequent studies during acute withdrawal focused on glucocorticoid signaling, and bioinformatics of genes regulated in dependent mice identified activation of inflammatory signaling and cell death pathways in females, while males exhibited disease and disorder pathways that were associated with endocrine and neurological diseases (Wilhelm et al., 2015). In contrast, abstinence produced a transcriptional response that varied by withdrawal genotype rather than sex. In the low withdrawal genotype, genes associated with the biological processes thyroid hormone metabolism, glutathione metabolism, axonal guidance, and DNA damage response were identified. Classes of genes associated with acetylation and histone deacetylase were highly dimorphic between mice with a high versus (vs.) low withdrawal genotype. The top pathway identified was Death Receptor Signaling, with apoptosis as a central node, but both sexes of the withdrawal resistant genotype had increased apoptotic signaling and more up-regulated transcripts whereas the high withdrawal genotype mice had less apoptotic signaling (Hashimoto et al., 2011; Wilhelm et al., 2014). Collectively, the available data indicate that acute withdrawal following chronic intoxication or binge drinking produces sexually divergent transcriptional responses and activation of distinct networks.

Based on the above evidence for a strong dichotomy between male and female rodents in the response to ethanol during acute withdrawal, the purpose of the present study was to characterize RNA expression differences from male and female C57BL/6J mice following 7 binge ethanol sessions. Tissue was harvested from the NAc, as this brain region is a central mediator of addiction (e.g., Tzschentke and Schmidt, 2003; Kauer and Malenka, 2007; Kalivas, 2009; Koob and Volkow, 2010). Focused quantitative PCR (qPCR) array analysis was employed to quantify expression levels of 384 genes identified as important in "Mood Disorders." The results indicated that there was a largely divergent regulation of genes by binge drinking in males and females, reflecting different neuroadaptive responses in the NAc that would result in dysregulation of distinct biological pathways between the sexes.

MATERIALS AND METHODS

Subjects

Adult male and female C57BL/6J mice were purchased from Jackson Laboratories West (Sacramento, CA, United States) at 7 weeks of age. Mice were group housed and separated by sex upon arrival, acclimated to a regular 12 h light/dark cycle (lights on at 0700) in a temperature (22 ± 2°C) and humidity controlled environment, with free access to food (Labdiet 5001 rodent chow; PMI International, Richmond, IN, United States) and water. Mice were 8 weeks old at the start of the drinking study, and they were individually housed throughout the experiment. Stage of the estrous cycle was not monitored during this study, based on evidence that binge ethanol consumption was not affected by estrous cycle phase in female C57BL/6J mice and that 6 weeks of binge ethanol drinking did not affect the length or pattern of the estrous cycle (Satta et al., 2018). Results in female rats also indicate that phases of the estrous cycle did not influence ethanol drinking under binge and non-binge drinking conditions (Priddy et al., 2017). The procedures were carried out in accordance with recommendations of the National Institute of Health *Guidelines for the Care and Use of Laboratory Animals* and were compliant with Institutional Animal Care and Use Committee approved protocols. The specific protocol for these studies was approved by the Institutional Animal Care and Use Committee at the VA Portland Health Care System, where all studies were conducted. All efforts were made to minimize distress and the number of animals used.

Binge Ethanol Consumption

The Scheduled High Alcohol Consumption procedure was used to model binge drinking, based on evidence that this procedure produces high ethanol intake in male and female mice (≥2g/kg in 30 min) and blood ethanol concentrations (BECs) ≥ 1.0 mg/mL (details in Finn et al., 2005; Strong et al., 2010; Tanchuck et al., 2011; Cozzoli et al., 2016). Briefly, mild fluid restriction was used to schedule periods of fluid access so that mice would drink their daily fluid requirement on a schedule. Mice had free access to food, and animals were weighed daily. Total fluid access per day increased across time from 4 to 10 h. Every 3rd day, mice in the binge ethanol groups (binge; 9/sex) had 30 min access to a 5% v/v ethanol solution in tap water, with water provided during the remainder of the period of fluid access. This 3-day cycle of fluid access was repeated so that mice in the binge group received a total of 7 binge ethanol sessions. Retro-orbital sinus blood (20 μL) was collected immediately following the 3rd and 7th binge sessions from the binge groups and analyzed for BEC via headspace gas chromatography (Finn et al., 2007). Mice in the control group (control; 9/sex) received the same schedule of total fluid access, but consumed only water. After the final binge ethanol session, all mice were given free access to water for 24 h.

Tissue Dissection

Mice were euthanized by decapitation at 24 h after the final binge ethanol session. The brain was extracted, chilled on ice, and sectioned freehand, as described in Cozzoli et al. (2016). Briefly, the entire NAc was micropunched from the 1–2 mm coronal section containing the anterior commissure with a 16 gauge hollow needle, based on established anatomical coordinates from the mouse brain atlas (Paxinos and Franklin, 2001). Micropunches were aimed to include the following coordinates: AP: +1.45 mm from bregma, ML: ± 0.6 mm from the midsagittal suture, DV: −4.3 mm from the skull surface. All samples were placed in microcentrifuge tubes (1.5 ml), frozen

immediately in dry ice, and stored at −80°C until total RNA isolation.

RNA Isolation and Quantitative Polymerase Chain Reaction (qPCR) Array Analysis

Total RNA was isolated using RNA STAT-60 (Tel-Test, Inc.; Friendswood, TX, United States), and genomic DNA was removed with the DNA-Free RNA kit (Zymo Research; Irvine, CA, United States), using routine procedures (e.g., Hashimoto and Wiren, 2008; Hashimoto et al., 2011). First strand cDNA synthesis was carried out on the purified RNA samples (1 μg) with the RT^2 First Strand Kit (Qiagen, Valencia, CA, United States). Quantitative PCR was performed using customized neuroscience mouse qPCR arrays (Custom 384 Mouse StellARray or Mouse Mood Disorder array) by Bar Harbor BioTechnology (Trenton, ME, United States). A total of 12 qPCR arrays, 384-well PCR plates with primers targeting genes related to Mood Disorders (2.6 ng/reaction), were run by Bar Harbor BioTechnology, with three biological replicates for each sex (male, female) and treatment (binge, control). PCR plates were run on an ABI 7900 HT Real-Time instrument, and data were analyzed with SDS 2.4 software (ABI), using automatic baseline settings with a manual threshold of 0.096 across all samples. For samples with undetectable expression of any gene, a *C*t-value of 40 was assigned to that gene to allow statistical analysis. Quantitative PCR arrays have been documented to provide reliable data that do not require further confirmation, as validation studies in our laboratory have found 100% reproducibility of these data with traditional qPCR methods for testing the expression of individual genes (e.g., Wheeler et al., 2009; Wiren et al., 2010; Wilhelm et al., 2015).

Binge and control mice were chosen for the arrays, based on specific criteria. For binge mice, choices were based on the following: (1) Animals with seven binge sessions > 2 g/kg/30 min or with the greatest number of binges ≥ 2 g/kg were chosen; and (2) Mice with the most consistent BECs that exceeded binge BEC (0.80 mg/mL) were chosen. For the water control mice, choices were based on the following: (1) Consistent 30 min water intake across the 7 "binge" sessions and consistency across animals per group with group average. We also ensured that body weights were not significantly different in the control and binge animals that were chosen.

The qPCR arrays allow for the identification of changes in the expression of pre-selected gene networks associated with specific signaling cascades and pathways that are altered following repeated bouts of binge drinking. We had two rationales for using the Mouse Mood Disorder array. First, the Mouse Mood Disorder array was used by collaborators in our department to examine genes relevant to selection for high and low methamphetamine consumption, given that many of the 384 genes represented on the array are relevant to findings from other studies of addiction related processes (Wheeler et al., 2009). Second, we were able to customize the array to increase the representation of a few glutamatergic genes, including mGluR5, Homer 2, and the PI3K regulatory subunit, which are altered following various models of ethanol drinking in male rodents (e.g., Szumlinski et al., 2008b; Cozzoli et al., 2009, 2016; Obara et al., 2009). Therefore, we wanted to focus this initial examination on a subset of genes most likely to be relevant to addiction (also see Introduction for justification to increase representation of glutamate-related genes). Additionally, several advantages to the qPCR arrays exist, such as: (a) The use of qPCR arrays does not require the confirmation of gene expression differences as is required for more comprehensive arrays (e.g., Affymetrix), since qPCR is the usual confirmation procedure; and (b) We have considerable expertise in the use of qPCR arrays (e.g., Wheeler et al., 2009; Wiren et al., 2010; Wilhelm et al., 2015) and corresponding bioinformatics (Hashimoto and Wiren, 2008; Hashimoto et al., 2011, 2017; Wilhelm et al., 2014, 2015) to identify expression differences.

Quantitative Reverse-Transcriptase PCR (qRT-PCR)

Using NAc tissue from a separate group of binge and control mice, we performed real time qRT-PCR to examine the expression of additional genes not present on the array but that were implicated in downstream signaling cascades of pathways that were identified by Ingenuity Pathway Analysis (IPA) of the current qPCR array data as being affected by binge ethanol drinking (n = 4/sex/treatment). Real time qRT-PCR was performed with the iCycler IQ Real Time PCR detection system (Bio-Rad Laboratories, Inc., Hercules, CA, United States), using a one-step QuantiTect SYBR Green RT-PCR kit (Qiagen) on DNase-treated total RNA (Hashimoto et al., 2004). The qRT-PCR reactions were carried out in 25 μL with 20 ng of total RNA that was isolated from mice that were not used in the qPCR arrays. Primers were purchased pre-designed from Qiagen.

Real-time qRT-PCR efficiency was determined for each primer set by using a fivefold dilution series of total RNA, and it did not differ significantly from 100%. Specificity of the qPCR reaction was confirmed with melt curve analysis to ensure that only the expected PCR product was amplified. Relative expression of the qRT-PCR product was determined using the comparative $\Delta\Delta C$t method, after normalizing expression to total RNA measured with RiboGreen (Molecular Probes, Eugene, OR, United States; Hashimoto et al., 2004).

Statistical Analyses

Data were analyzed using R or SYSTAT (version 11, SYSTAT Software, Inc., Richmond, CA, United States). The level of significance was set at $p \leq 0.05$, and $p \leq 0.09$ was considered a trend. Results are presented as mean ± SEM.

For the drinking data, the dependent variables were BEC, volume (in mLs) of water and ethanol consumed, ethanol dose consumed (in g/kg), and body weight. Analysis of variance (ANOVA) was used to assess day, sex (male, female) and treatment (binge, control) effects or binge day and sex effects when only the ethanol data were examined. Significant interactions were followed up with *post hoc* tests. Because we were predicting sex differences, planned comparisons were conducted with or without the presence of a significant interaction.

For the qPCR array data, Bar Harbor BioTechnology identified significantly changed genes in the data set using their Global Pattern Recognition (GPR) algorithm (Akilesh et al., 2003). GPR goes through several iterations to compare the expression of each gene to every other gene in the array, establishing a global pattern where significant changes are identified and ranked. The procedure looks for the most stably expressed genes from the array across all the samples, and uses these genes to normalize the gene expression. Akilesh et al. (2003) validated that GPR provided a novel alternative to the use of relative normalization in qPCR experiments and emphasized that GPR takes advantage of biological replicates to obtain significant changes in gene expression. For comparative purposes, *p*-values from the GPR analysis were then used to calculate *q*-values to control for multiple comparisons using the "qvalue" package in R (version 2.12.0[1]). However, we used an uncorrected *p*-value to decrease the chance of excluding regulated transcripts (i.e., false negatives) as we (Hashimoto and Wiren, 2008; Hashimoto et al., 2011; Wilhelm et al., 2014) and others (e.g., see Rodd et al., 2007) have employed. All significantly regulated transcripts ($p \leq 0.05$) from either comparison (i.e., male binge vs. control, female binge vs. control) were then used to create heat maps and hierarchical clustering using the R package "gplots" (version 3.0.1) with complete linkage clustering. Bioinformatic analyses were conducted by uploading the significantly regulated genes to the IPA website[2]. Proprietary IPA software was used for the analyses, and significance was based on the relative enrichment of the regulated genes to biological function, pathway, or network using the 384 genes present in the qPCR array as the background gene-set and the Fisher's exact test. Thus, for all the pathway analyses (IPA), using the 384 genes present on the qPCR array as the background gene set controlled for the enrichment of specific gene classes (i.e., related to Mood Disorders) in our set of regulated genes.

For the qRT-PCR data, all data were calculated as fold change relative to the female controls after normalizing expression to total RNA measured with RiboGreen. Initial analyses were conducted with ANOVA to assess sex and treatment effects. When there was a significant interaction, *post hoc t*-tests were conducted to examine treatment effects in each sex.

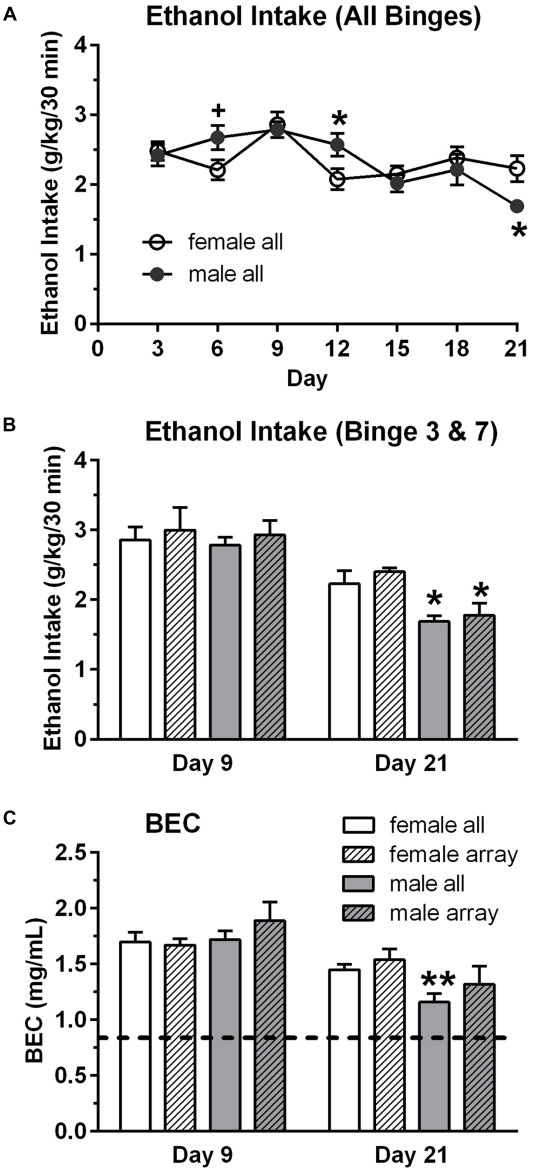

FIGURE 1 | Binge ethanol intake **(A,B)** and blood ethanol concentration (BEC, **C**) in male and female mice. Mice in the binge groups had a total of seven binge drinking sessions, with a binge session every 3rd day **(A)**. BEC was measured at the end of the 3rd (day 9) and 7th (day 21) binge sessions. Although overall binge ethanol intake, averaged across the seven sessions, did not differ in the female (2.34 g/kg) and male (2.35 g/kg) mice, ethanol intake and corresponding BECs were lower in the male vs. female mice on the final binge session (day 21, **B,C**). However, BECs greatly exceed the criteria for binge drinking on all days (0.80 mg/mL; depicted by dashed line in **C**). Shown are mean ± SEM for all mice in the binge groups (n = 9/sex), which included the mice in the subgroup that were used for the qRT-PCR analysis (n = 4/sex), and for the mice in the subgroup that were used for the qPCR arrays (n = 3/sex). $^{+}p = 0.06$, $^{*}p < 0.05$, $^{**}p < 0.01$ vs. respective female all or female array group.

RESULTS

Binge Drinking

Male and female mice had seven intermittent binge ethanol sessions (binge, 9/sex) or consumed water (control, 9/sex). Overall binge ethanol intake (g/kg/30 min) did not differ between the sexes, when collapsed across the seven binge sessions. Mean ± SEM intake was 2.34 ± 0.06 g/kg for females and 2.35 ± 0.10 g/kg for males. However, analysis of the seven binge ethanol sessions revealed that the pattern of ethanol intake across time differed in the male vs. female mice [time: $F(6,84) = 7.02$, $p < 0.001$; sex × time: $F(6,84) = 2.61$, $p < 0.05$]. Ethanol intake was significantly lower in female vs. male mice on day 12 (4th binge, $p < 0.05$, **Figure 1A**) and was significantly higher in female vs. male mice on day 21 (7th binge, $p < 0.05$, **Figures 1A,B**). The slight decrease in ethanol intake across

[1]http://github.com/jdstorey/qvalue

[2]www.ingenuity.com

binge sessions in the male mice likely reflects the increase in fluid access time across sessions, which is a finding that we have observed in some of our prior studies using this binge drinking procedure. BECs were measured after the 3rd (day 9) and 7th (day 21) binge ethanol sessions (**Figure 1C**), and they mirrored the ethanol intake data [time: $F(1,16) = 28.28$, $p < 0.001$; sex × time: $F(1,16) = 4.18$, $p = 0.058$], with *post hoc* tests confirming that BEC was significantly higher in female vs. male mice on day 21 ($p < 0.01$). A similar pattern of results was found for the subgroup of mice that were chosen for the array analysis (**Figures 1B,C**). Ethanol intake and BECs did not differ in male vs. female mice on day 9, whereas ethanol intake was significantly higher in female vs. male mice on day 21. BEC on day 21 also was higher in females vs. males, but this difference did not reach statistical significance. Importantly, the results confirm that both male and female mice in the binge groups consumed high doses of ethanol in the 30 min binge sessions and achieved BECs that exceeded the NIAAA criteria for binge drinking (0.80 mg/mL; shown as dashed line on **Figure 1C**; NIAAA, 2004).

Body weights, averaged over the 21 days of the study, were lower in female vs. male mice [$F(1,32) = 364.20$, $p < 0.001$]. Averaged body weights also were lower in the control vs. binge groups [$F(1,32) = 5.59$, $p < 0.05$], and this effect was primarily due to the significant difference in the male mice (**Table 1**). Body weights on day 1 of the study were slightly lower in the control mice when compared to the mice in the binge groups, which likely contributed to the significant difference in average body weight. However, weight gain across the 21 days of the study was similar in the control and binge groups for the male (10.1% for binge, 12.0% for control) and female (11.7% for binge, 10.1% for control) mice. Overall total fluid intake did not differ in the control vs. binge groups for the male and female mice (**Table 1**). Thus, treatment (binge vs. control) did not significantly alter body weight gain or total fluid intake in either sex.

Binge Drinking Produces Sexually Divergent Changes in Gene Expression Patterns Associated With Discrete Biological Pathways

Focused qPCR array analysis was employed to quantify expression levels of 384 genes identified as important in "Mood Disorders" (see **Supplementary Table S3** for genes in array). We found that of the 384 genes on the array, only 14 genes were regulated by binge drinking in both males and females (**Table 2**), representing common targets to binge ethanol consumption. However, only 4 genes were regulated in the same direction (*Drd5*, *Grm4*, *Ranbp9*, and *Reln*), while the expression of 10 genes was strongly dimorphic (*Crhr2*, *Dgka*, *Fos*, *Lta*, *Mc5r*, *Nos1ap*, *Nos1*, *Slc6a2*, *Star*, and *Smc4*) such that the direction of change differed between male and female mice. Additionally, we identified significant regulation by binge drinking of 70 genes in females (**Supplementary Table S1**), and the 30 most highly regulated transcripts in females are shown in **Table 3**. In male mice, a total of 50 genes were regulated significantly by binge ethanol drinking (**Supplementary Table S2**), and the 30 most highly regulated transcripts are shown in **Table 4**.

To examine further the patterns of expression differences, false color heat maps were generated for the transcripts that were regulated significantly by binge drinking, and unsupervised hierarchical cluster analysis was performed to determine the similarity of global expression patterns in the significantly regulated genes by binge ethanol drinking in male and female mice (**Figure 2**). Each column represents the combined data from 6 arrays for each sex (3 binge, 3 control) to visualize the transcriptional response at 24 h withdrawal after the 7th binge ethanol (or water) drinking session. All of the 106 significantly regulated genes were included in this analysis (14 common genes, 56 genes only in females, 36 genes only in males); these genes are depicted based on the GPR fold change for binge ethanol vs. control, with shades of color to indicate up-regulation (red) or down-regulation (blue) for a particular gene following binge ethanol drinking. Clustering analysis was used to identify groups of genes that demonstrated similar expression profiles. Genes (represented by rows in **Figure 2**) were clustered according to the similarity of their expression profile as a result of repeated binge drinking. The gene tree at the left of the image in **Figure 2** corresponds to the degree of similarity in the expression pattern for the specific genes. In general, gene clustering showed the sexually dimorphic response to repeated binge drinking experience.

To better characterize the expression differences observed following repeated binge drinking, IPA was used to identify Canonical Pathways, Upstream Regulators, and significant Biological Functions of regulated genes compared to the background 384 genes present on the qPCR array platform. In female mice, expression differences suggested that hormone signaling and immune function might be altered. Canonical Pathways that were significantly regulated included "Crosstalk between dendritic cells and natural killer cells," "MIF (macrophage migration inhibitory factor) regulation of innate immunity," "TNFR1 (tumor necrosis factor receptor 1) signaling," "TNFR2 signaling," and "MIF-mediated glucocorticoid regulation" (all $p < 0.05$). Upstream Regulator analysis identified several regulators of expression, such as: POMC (pro-opiomelanocortin), *Tac1* (encodes the protein substance P), *Notch1*, and *Vegf* (all $p < 0.005$). The two top networks included "Neurological Disease, Psychological Disorders, Behavior," and "Carbohydrate Metabolism, Lipid Metabolism, Small Molecule Biochemistry." Relationships

TABLE 1 | Body weight and total fluid intake during the Scheduled High Alcohol Consumption procedure.

Sex	Treatment	Body weight (g)	Total fluid intake (mL)
Male	Binge	21.59 ± 0.32	3.19 ± 0.11
	Control	20.69 ± 0.20*	3.24 ± 0.12
Female	Binge	16.19 ± 0.26	3.03 ± 0.12
	Control	15.81 ± 0.29	3.20 ± 0.14

*Shown are the mean ± SEM body weights and total fluid intake, averaged over the 21 days of the study, for n = 9/sex and treatment. *p < 0.05 vs. respective binge.*

TABLE 2 | Nucleus accumbens genes significantly regulated by binge ethanol drinking in both female and male mice.

Gene symbol	Gene name	Female			Male		
		Fold change	*p*-value	*q*-value	Fold change	*p*-value	*q*-value
Crhr2	Corticotropin releasing hormone receptor 2	−3.13	0.020	0.066	2.07	0.022	0.064
Dgka	Diacylglycerol kinase, alpha	11.02	0.032	0.070	−1.84	0.034	0.065
Drd5	Dopamine receptor D5	−2.07	0.034	0.070	−2.30	0.021	0.064
Fos	FBJ osteosarcoma oncogene	−3.44	0.004	0.054	1.64	0.030	0.065
Grm4	Glutamate receptor, metabotropic 4	−2.22	0.030	0.070	−2.19	0.019	0.064
Lta	Lymphotoxin A	−14.33	0.001	0.022	1.88	0.027	0.064
Mc5r	Melanocortin 5 receptor	−3.64	0.003	0.051	1.93	0.024	0.064
Nos1ap	Nitric oxide synthase 1 (neuronal) adaptor protein	−3.91	0.010	0.064	1.43	0.043	0.066
Nos1	Nitric oxide synthase 1, neuronal	2.78	0.042	0.075	−1.91	0.023	0.064
Ranbp9	RAN binding protein 9	2.30	0.036	0.070	1.59	0.047	0.066
Reln	Reelin	−1.95	0.017	0.064	−2.17	0.011	0.064
Slc6a2	Solute carrier family 6 (neurotransmitter transporter, noradrenalin), member 2	−21.58	0.019	0.064	10.49	0.000	0.016
Star	Steroidogenic acute regulatory protein	1.90	0.042	0.075	−2.18	0.018	0.064
Smc4	Structural maintenance of chromosomes 4	93.99	0.000	0.018	−2.48	0.017	0.064

A total of 14 genes in the nucleus accumbens (core and shell) were significantly regulated by 7 binge ethanol drinking sessions in male and female mice, but only 4 of the 14 genes were regulated in the same direction in the sexes. Significance is based on p-values, but q-values also are shown. Transcripts are listed in alphabetical order. Fold change of binge vs. control is shown, with negative values indicating down-regulation by binge ethanol drinking and positive values indicating up-regulation by ethanol. We note that 3 of the genes with high fold changes (Smc4 and Dgka in females, Slc6a2 in males and females) had 2 or more samples with undetected expression, indicating qualitative regulation (i.e., present in binge ethanol samples but absent in controls).

between regulated genes in these combined networks identified ERK1/2 and Akt (a serine/threonine kinase typically activated by PI3K) as central nodes. Biological Function analysis identified "Infectious Disease" ($p < 0.005$) and "Neurological Disease" ($p < 0.05$) as top targets.

A different pattern of results was found for males, where expression differences suggested that neurotransmitter metabolism was altered by repeated binge drinking. The top Canonical Pathways that were significantly regulated included "nNOS (neuronal nitric oxide synthase) signaling", "cAMP-mediated signaling," and "Folate transformations I" (all $p < 0.05$), with a trend for regulation of "Corticotropin releasing hormone (CRH) signaling" ($p = 0.09$). Several upstream regulators of gene expression were identified: indomethacin, apomorphine, Histone h3, and corticosterone (all $p < 0.0007$). The two top networks included "Behavior, Nucleic Acid Metabolism, Small Molecule Biochemistry" and "Psychological Disorders, Neurological Disease, Cell-To-Cell Signaling and Interaction." Relationships between regulated genes in these combined networks identified PKC (protein kinase C), BDNF, and NMDA as central nodes. Biological Function analysis identified "Neurological Disease" as a top target category ($p < 0.05$).

As suggested by the above pathway analysis, several neurotransmitter systems were influenced by repeated binge drinking sessions. Binge drinking produced an overall suppression in the expression of dopamine receptor genes (**Figure 4D**, bottom 4 genes; see **Supplementary Tables S1**, **S2** for significant binge vs. control gene expression changes in females and males, respectively), with similar fold decreases in expression of *Drd5* (**Table 2**, $p < 0.05$ for both sexes) and *Drd3* in males ($p < 0.07$) and females ($p < 0.05$). Binge drinking also produced a non-significant decrease in expression of *Drd2* in males and females (not shown). However, expression of *Drd1* was only decreased by binge drinking in males ($p = 0.01$), whereas *Drd4* expression was only decreased in females ($p < 0.01$). Binge ethanol drinking also significantly decreased expression of the gene encoding the dopamine transporter (*Slc6a3*) in males ($p < 0.05$) and the gene encoding the vesicular monoamine transporter 2 (*Slc18a2*) in females ($p < 0.05$). However, the gene encoding the norepinephrine transporter (*Slc6a2*) was differentially altered by binge drinking (**Table 2**), where expression was decreased in females ($p < 0.05$) and increased in males ($p < 0.001$). Overall, the functional implication of these binge ethanol-induced changes would likely be a decrease in dopamine signaling in the NAc.

Binge drinking also produced an overall increase in expression of the 4 $GABA_A$ receptor subunit genes that were on the arrays in both sexes, with significant changes for 2 of the subunit genes. Expression of *Gabra3* was increased similarly by binge drinking in females ($p < 0.05$) and males ($p = 0.051$), and

TABLE 3 | Top 30 genes significantly regulated by binge drinking in female nucleus accumbens.

Gene symbol	Gene name	Female		
		Fold change	*p*-value	*q*-value
Casp8	Caspase 8	114.71	0.001	0.021
Smc4	Structural maintenance of chromosomes 4	93.99	0.000	0.018
Alox12	Arachidonate 12-lipoxygenase	73.14	0.000	0.018
Pmch	Pro-melanin-concentrating hormone	28.46	0.001	0.022
Dgka	Diacylglycerol kinase, alpha	11.02	0.032	0.070
Prkcq	Protein kinase C, theta	9.22	0.035	0.070
Timeless	Timeless circadian clock 1	5.33	0.048	0.081
Esr1	Estrogen receptor 1 (alpha)	5.00	0.019	0.064
Dlx1	Distal-less homeobox 1	4.41	0.002	0.039
Eif2s2	Eukaryotic translation initiation factor 2, subunit 2 (beta)	4.07	0.013	0.064
Hdac1	Histone deacetylase 1	3.63	0.012	0.064
Egfr	Epidermal growth factor receptor	3.50	0.013	0.064
Pafah1b1	Platelet-activating factor acetylhydrolase, isoform 1b, subunit 1	2.99	0.015	0.064
Katnal1	Katanin p60 subunit A-like 1	2.98	0.023	0.070
Nos1	Nitric oxide synthase 1, neuronal	2.78	0.042	0.075
Fos	FBJ osteosarcoma oncogene	−3.44	0.004	0.054
Impa2	Inositol (myo)-1(or 4)-monophosphatase 2	−3.53	0.035	0.070
Drd3	Dopamine receptor D3	−3.53	0.028	0.070
Mc5r	Melanocortin 5 receptor	−3.64	0.003	0.051
Nos1ap	Nitric oxide synthase 1 (neuronal) adaptor protein	−3.91	0.010	0.064
St8sia2	ST8 alpha-N-acetyl-neuraminide alpha-2,8-sialyltransferase 2	−4.08	0.011	0.064
Nfkbib	Nuclear factor of kappa light polypeptide gene enhancer in B-cells inhibitor, beta	−4.80	0.012	0.064
Ppp1r1b	Protein phosphatase 1, regulatory (inhibitor) subunit 1B	−4.89	0.037	0.070
Il2rb	Interleukin 2 receptor, beta chain	−5.14	0.012	0.064
Il9r	Interleukin 9 receptor	−6.18	0.007	0.064
Drd4	Dopamine receptor D4	−9.72	0.006	0.064
Prf1	Perforin 1 (pore forming protein)	−11.61	0.009	0.064
Lta	Lymphotoxin A	−14.33	0.001	0.022
Fosl1	Fos-like antigen 1	−15.10	0.039	0.073
Slc6a2	Solute carrier family 6 (neurotransmitter transporter, noradrenalin), member 2	−21.58	0.019	0.064

The 15 most highly up- or down-regulated transcripts are shown from the total of 70 genes that were significantly regulated by binge ethanol drinking in females. Significance is based on p-values, but q-values also are shown. Transcripts are listed in ascending order. Fold change of binge vs. control is shown, with positive values indicating up-regulation and negative values indicating down-regulation by ethanol. Some of the genes with high fold changes (Casp8, Smc4, Alox12, Pmch, Dgka, Prkcq, Timeless, Fosl1, and Slc6a2) had 2 or more samples with undetected expression, indicating qualitative regulation (i.e., present in binge, absent in control).

the similar fold increase in *Gabra1* expression in both sexes only was significant in males ($p < 0.05$). The ethanol-induced increase in *Gabra5* expression only approached the level of a statistical trend for females ($p = 0.10$), whereas *Gabrg2* expression was not significantly altered in either females or males (not shown). Taken in conjunction with the understanding that there are many additional $GABA_A$ receptor subunits that can influence $GABA_A$ receptor-mediated inhibition, the results are suggestive of a binge ethanol-induced increase in $GABA_A$ receptor signaling.

The expression of some glutamatergic genes encoding specific metabotropic and ionotropic receptors also was influenced by binge drinking. With the exception of a similar significant decrease in expression of *Grm4* (**Table 2**), there were differential effects of binge drinking in males and females on the expression of the glutamatergic genes examined (**Figure 4D**, discussed in more detail in section "Pathways Identified by Analysis of Genes That Were Regulated by Binge Drinking in Both Males and Females").

Pathways Identified by Analysis of Genes That Were Regulated by Binge Drinking in Both Males and Females

We ran an IPA of genes that were regulated by binge drinking in both males and females and identified three canonical pathways of interest. For each pathway, we identified genes that had the potential to be significantly altered by ethanol and then used Real-Time qRT-PCR to examine the expression of those transcripts. The first pathway identified was "CRH signaling" (**Figure 3A** highlights changes in expression in males). Interestingly and as shown in **Figure 3D** (top 4 genes on table), females show inactivation of the pathway (↓ in *Crhr1* and *Crhr2*), while males show activation of the pathway (↑ in *Crh* and *Crhr2*). We

TABLE 4 | Top 30 genes significantly regulated by binge drinking in male nucleus accumbens.

Gene symbol	Gene name	Male		
		Fold change	*p*-value	*q*-value
Fasl	Fas ligand (TNF superfamily, member 6)	20.15	0.016	0.064
Chrna1	Cholinergic receptor, nicotinic, alpha polypeptide 1 (muscle)	15.31	0.019	0.064
Slc6a2	Solute carrier family 6 (neurotransmitter transporter, noradrenalin), member 2	10.49	0.000	0.016
Crh	Corticotropin releasing hormone	5.32	0.041	0.066
Ptgs2	Prostaglandin-endoperoxide synthase 2	4.66	0.009	0.064
Bdnf	Brain derived neurotrophic factor	4.26	0.008	0.064
Crhr2	Corticotropin releasing hormone receptor 2	2.07	0.022	0.064
Tuba8	Tubulin, alpha 8	1.96	0.016	0.064
Mc5r	Melanocortin 5 receptor	1.93	0.024	0.064
Cpt2	Carnitine palmitoyltransferase 2	1.91	0.025	0.064
Lta	Lymphotoxin A	1.88	0.027	0.064
Dusp6	Dual specificity phosphatase 6	1.86	0.023	0.064
Homer2	Homer homolog 2 (Drosophila)	1.83	0.027	0.064
Slc6a3	Solute carrier family 6 (neurotransmitter transporter, dopamine), member 3	1.80	0.028	0.064
Gabra1	Gamma-aminobutyric acid (GABA) A receptor, subunit alpha 1	1.67	0.045	0.066
Grm4	Glutamate receptor, metabotropic 4	−2.19	0.019	0.064
Npas2	Neuronal PAS domain protein 2	−2.20	0.011	0.064
Drd5	Dopamine receptor D5	−2.30	0.021	0.064
Rap1gap	Rap1 GTPase-activating protein	−2.37	0.033	0.065
Ccl3	Chemokine (C-C motif) ligand 3	−2.40	0.049	0.066
Smc4	Structural maintenance of chromosomes 4	−2.48	0.017	0.064
Bcr	Breakpoint cluster region	−2.52	0.030	0.065
Htr1b	5-hydroxytryptamine (serotonin) receptor 1B	−2.80	0.022	0.064
Isyna1	Myo-inositol 1-phosphate synthase A1	−2.88	0.015	0.064
Ace	Angiotensin I converting enzyme (peptidyl-dipeptidase A) 1	−3.19	0.023	0.064
Bax	BCL2-associated X protein	−3.47	0.032	0.065
Drd1	Dopamine receptor D1	−3.51	0.011	0.064
Cit	Citron	−3.96	0.010	0.064
Tfap2b	Transcription factor AP-2 beta	−15.01	0.000	0.013
S100a9	S100 calcium binding protein A9 (calgranulin B)	−24.14	0.026	0.064

The 15 most highly up- or down-regulated transcripts by binge drinking in males are shown. Significance is based on p-values, but q-values also are shown. Transcripts are listed in ascending order. Fold change of binge vs. control is shown, with positive values indicating up-regulation and negative values indicating down-regulation by ethanol. Some of the genes with high fold changes (Fasl, Chrna1, Slc6a2, and S100a9) had 2 or more samples with undetected expression, indicating qualitative regulation (i.e., present in binge, absent in control).

conducted qRT-PCR on *Gnaq* (which encodes Gαq), *Mapk1* (mitogen-activated protein kinase, which encodes Erk2) and *Mapk3* (which encodes Erk1). Expression of *Gnaq* tended to be lower in females vs. males (main effect of sex, $p < 0.07$), with a significant interaction between sex and treatment ($p < 0.05$). *Post hoc* tests showed that mRNA levels tended to be decreased by binge drinking in males ($p = 0.06$; **Figure 3B**). The result in males is consistent with the identification of PKC as a central node, suggesting that signaling downstream following binding to CRH receptors does occur via Gαq in males. In females, it is likely that signaling downstream of CRH receptors favors Gαs. For both sexes, qPCR array results indicate that binge drinking up-regulated *Gnas* (encodes Gαs, guanine nucleotide binding protein, alpha stimulating) by 1.70-fold in females ($p < 0.14$) and 1.34-fold in males ($p = 0.11$), but these differences vs. control were not statistically significant. Expression of *Mapk1* (**Figure 3C**), but not *Mapk3* (not shown), was significantly lower in females vs. males (main effect of sex, $p < 0.05$) and was significantly decreased by binge drinking in both sexes (main effect of treatment, $p < 0.01$). ERK1/2 had been identified as a central node in females, so the binge drinking-induced decrease in *Mapk1* expression in females would be consistent with the decreased expression of *Fos* following binge drinking in this sex, as it is a downstream target of ERK1/2 (**Figures 3A,D**).

The second pathway identified was "Neuropathic pain signaling" (**Figure 4A** highlights changes in expression seen in males). As shown in **Figure 4D** (top 10 genes on table), binge drinking produced a more complex change in the expression of genes in the neuropathic pain pathway, which was focused on glutamatergic and BDNF signaling. In males, binge drinking produced a significant increase in the expression of BDNF and a significant decrease in expression of AMPA receptors and mGluR4. Expression of mGluR5 tended to be decreased by binge drinking in males, while expression of Homer2 was

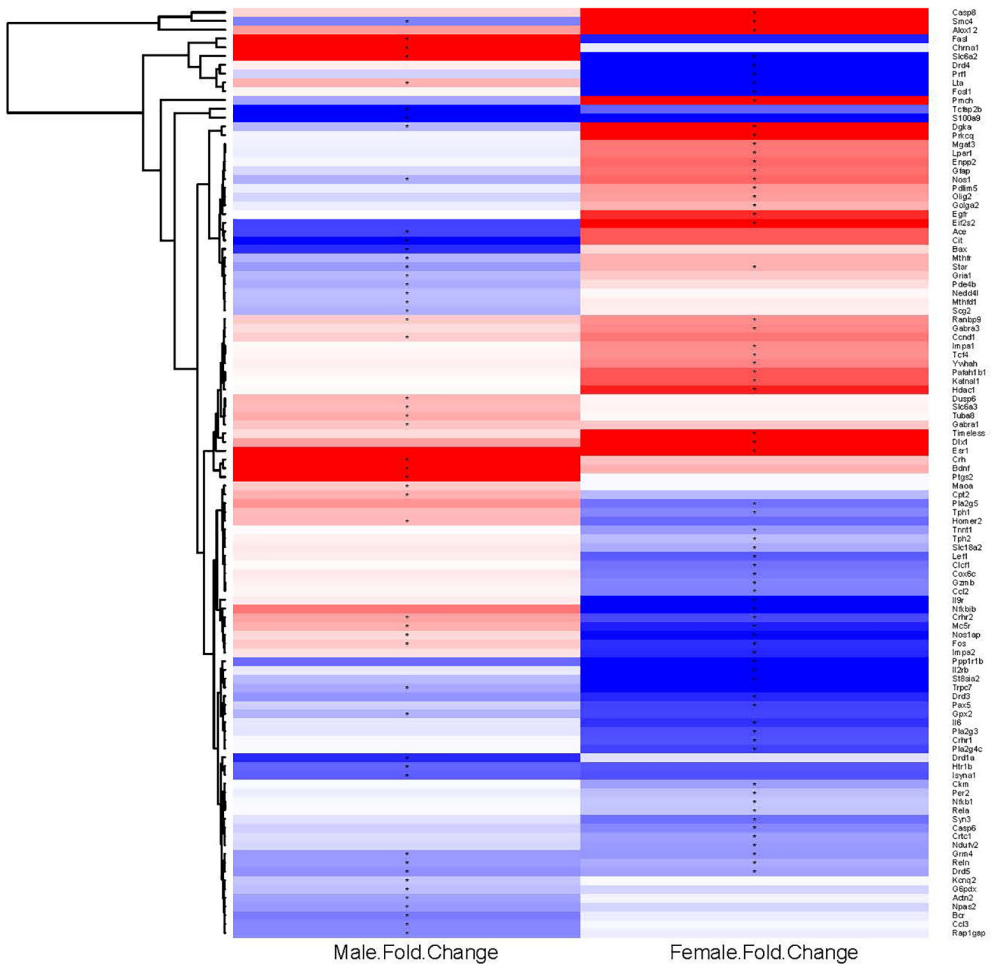

FIGURE 2 | Heat map and hierarchical cluster analysis of genes significantly regulated by repeated binge drinking in male and female mice. All significantly regulated genes (106 total) were used to generate the heat map and to perform the cluster analysis to visualize the transcriptional response at 24 h after the 7th binge ethanol drinking session. Each column represents the combined data from six arrays (three binge, three control), with the binge ethanol-induced change in expression shown for males and females in separate columns. Shades of color indicate up-regulation (red) or down-regulation (blue) for a particular gene following binge drinking. Hierarchical cluster analysis was performed on the ethanol regulated genes. Genes (represented by rows, names at the right of the image) were clustered according to the similarity of expression profile as the result of repeated binge drinking. Clustering of genes emphasizes the sexually dimorphic response to repeated binge drinking experience. *$p < 0.05$ for significantly regulated genes (binge vs. control).

significantly increased. In females, binge drinking produced a similar significant decrease in *Grm4* (**Table 2** and **Figure 4D**) but opposite effects on the remaining glutamatergic genes and BDNF. For the qRT-PCR analysis, we chose *Ntrk2* (which encodes TrkB, tropomyosin receptor kinase B), *Elk1* (which encodes the transcription factor Elk1), *Mapk1* and *Mapk3* as follow-up candidates. We also were interested in *Creb1*, but qPCR array analysis showed that the expression of this gene was not significantly altered by binge drinking in either sex (not shown). Expression of *Ntrk2* was significantly lower in females vs. males (main effect of sex, $p = 0.01$), but there was no effect of binge drinking (**Figure 4B**). However, *Elk1* expression was significantly decreased by binge drinking in both males and females (main effect of treatment, $p < 0.05$). As mentioned above, expression of *Mapk1* (**Figure 3C**) also was significantly decreased by binge drinking in males and females. At least in females, the binge drinking-induced decrease in expression of *Mapk1* (encoding for Erk2) corresponds with the decreased expression of the transcription factors *Elk1* (**Figure 4C**) and *Fos* (**Figure 4D**), which likely influence downstream gene expression mediated by these transcription factors.

The third pathway identified was "TNFR2 signaling" (**Figure 5A** highlights changes in expression seen in females). Interestingly and as shown in **Figure 5G**, the females show inactivation of the pathway (↓ in *Nfkb1*, *Nfkbib*, *Fos*, *Lta*, *Il6*, and *Rela*), while males show activation of the pathway (↑ in *Fos*, *Fasl*, and *Lta*, with a trend for ↑ in *Nfkb2* and *Nfkbib*). We conducted qRT-PCR on several genes in this signaling cascade: *Tnfrsf1a* (encodes TNFR1, which forms a heterocomplex with TNFR2; both receptors bind TNFα), *Mapk8* (encodes JNK1), *Traf2* (encodes TRAF2), *Map3k14* (encodes NIK), and 3 genes encoding subunits in the IκB kinase enzyme complex [*Chuk*

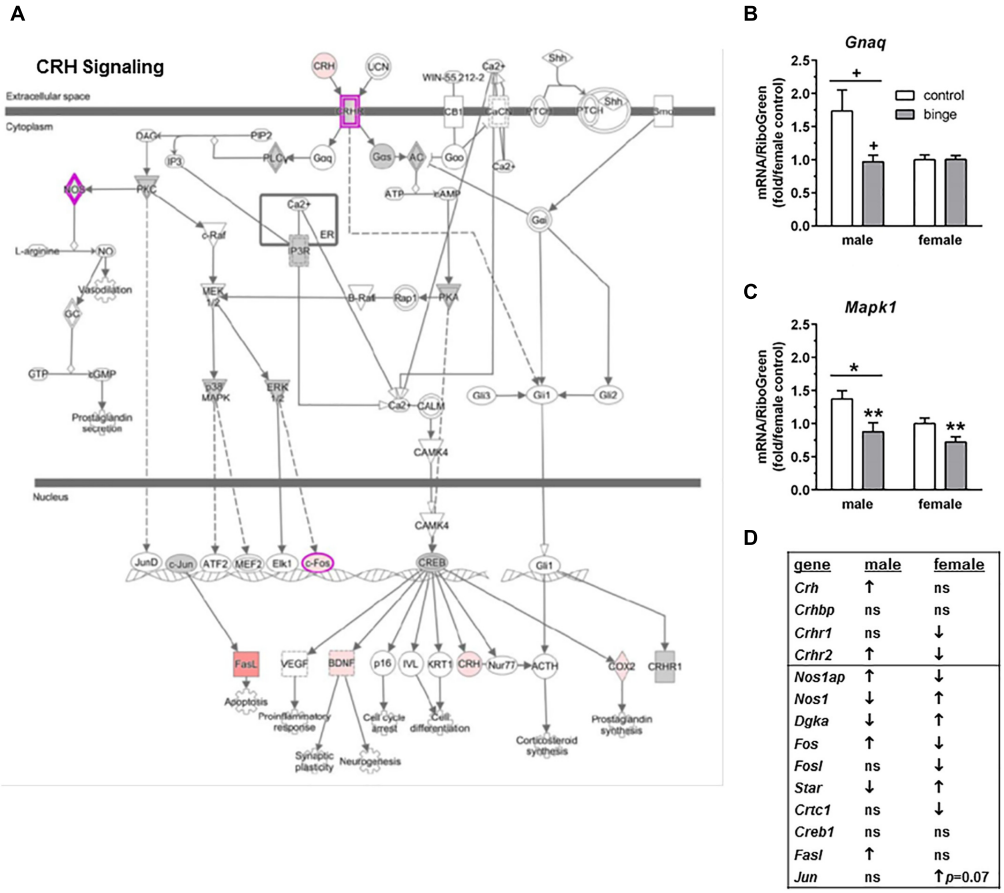

D

gene	male	female
Crh	↑	ns
Crhbp	ns	ns
Crhr1	ns	↓
Crhr2	↑	↓
Nos1ap	↑	↓
Nos1	↓	↑
Dgka	↓	↑
Fos	↑	↓
Fosl	ns	↓
Star	↓	↑
Crtc1	ns	↓
Creb1	ns	ns
Fasl	↑	ns
Jun	ns	↑ p=0.07

FIGURE 3 | Simplified corticotropin releasing hormone (CRH) signaling pathway highlights genes influenced by repeated binge drinking in male and female mice. This canonical pathway was identified by IPA as regulated by binge drinking in both males and females. **(A)** Depicts the CRH signaling pathway and highlights genes regulated by binge drinking in males (pink for up-regulation, green for down-regulation). **(B,C)** Depict qRT-PCR results and show that expression of *Gnaq* (**B** which encodes Gαq) tended to be higher in males vs. females and to be decreased by binge ethanol drinking in males. Expression of *Mapk1* (**C** which encodes Erk2) was significantly higher in males vs. females and was significantly decreased by binge drinking in both sexes. Values are the mean ± SEM for 4/sex/treatment. $^{+}p < 0.07$ vs. respective control in males or sex difference (over horizontal line); $^{*}p < 0.05$ for main effect of sex (over horizontal line), $^{**}p < 0.01$ for main effect of treatment. **(D)** Shows significant regulation by binge drinking of select genes from the qPCR array analysis that are pertinent to the CRH signaling cascade depicted in **(A)** for male and female mice (↑ for up-regulation, ↓ for down regulation; $p < 0.05$ at a minimum). For statistical trends, the p-values are provided. *Gnaq* (guanine nucleotide binding protein, alpha q polypeptide) encodes the protein Gαq. *Mapk1* (mitogen-activated protein kinase 1) encodes the protein ERK2 (extracellular signal-regulated kinase).

(encodes IKK-α or IKK1), *Ikbkb* (encodes IKK-β or IKK2), and *Ikbkg* (encodes IKK-γ or NEMO)]. We also examined *Ikbkap*, which encodes a protein (IKAP) that was initially thought to be a scaffolding protein for the IκB kinase complex. Expression of *Tnfrsf1a* was significantly lower in females vs. males (main effect of sex, $p < 0.01$), but there was no effect of binge drinking (**Figure 5B**). Expression of *Chuk* and *Ikbkb* also was not altered by binge drinking in either sex (not shown). However, *Map3k14* (**Figure 5D**) and *Ikbkap* (**Figure 5F**) expression was significantly decreased by binge drinking in both males and females (main effect of treatment, $p < 0.05$ and $p < 0.001$, respectively). Expression of *Traf2* (**Figure 5C**) and *Ikbkg* (**Figure 5E**) tended to be decreased by binge drinking in both sexes (main effect of treatment, $p < 0.09$ and $p = 0.06$, respectively). Additionally, the gene *Lta*, which encodes the protein lymphotoxin-alpha or TNF-β, was differentially altered by binge drinking (**Table 2** and **Figure 5G**), where expression was decreased in females ($p = 0.001$) and increased in males ($p < 0.05$). In general, the results in females demonstrate that binge drinking produces a fairly consistent downregulation of signaling through the tumor necrosis factor (TNF) superfamily, which likely influences activation of the transcription factor NF-κB.

DISCUSSION

The present results add to a body of evidence indicating that binge drinking and chronic ethanol intoxication leading to the development of physical dependence both produce neuroadaptive changes in neurotransmitter systems as well as numerous other cellular pathways that can alter neuronal function in a manner that can be either adaptive or deleterious

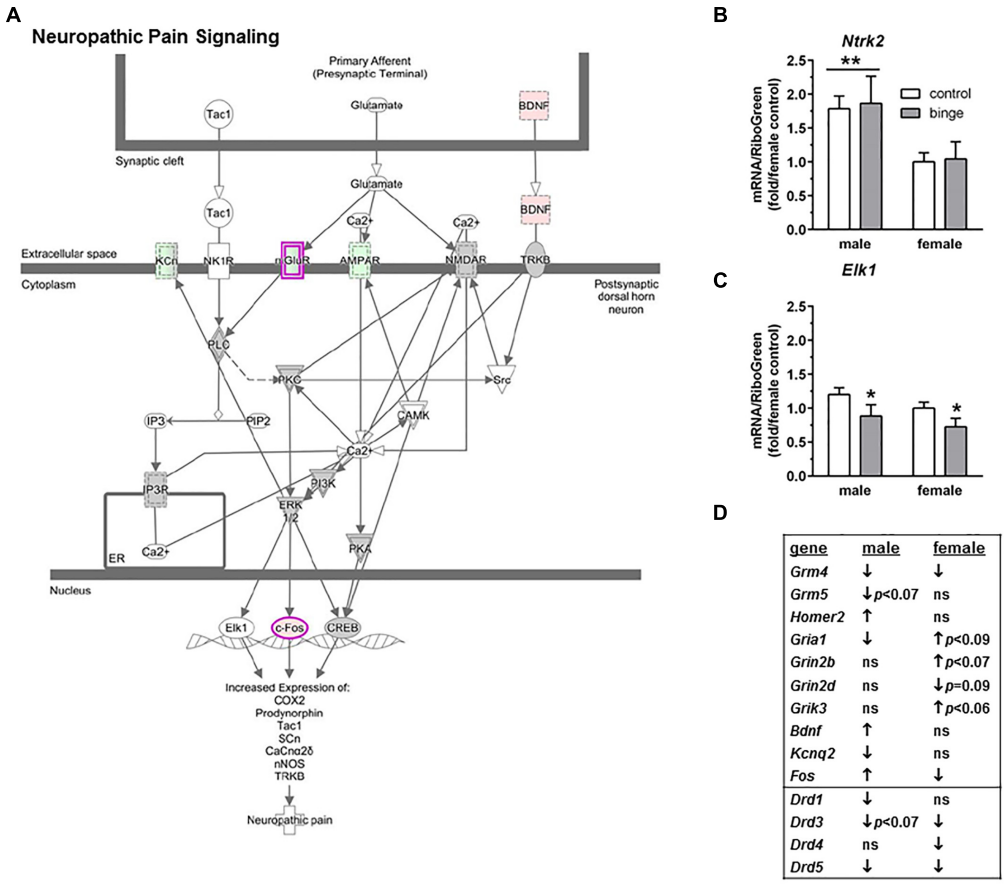

gene	male	female
Grm4	↓	↓
Grm5	↓$p<0.07$	ns
Homer2	↑	ns
Gria1	↓	↑$p<0.09$
Grin2b	ns	↑$p<0.07$
Grin2d	ns	↓$p=0.09$
Grik3	ns	↑$p<0.06$
Bdnf	↑	ns
Kcnq2	↓	ns
Fos	↑	↓
Drd1	↓	ns
Drd3	↓$p<0.07$	↓
Drd4	ns	↓
Drd5	↓	↓

FIGURE 4 | Simplified neuropathic pain signaling pathway highlights genes influenced by repeated binge drinking in male and female mice. This canonical pathway was identified by IPA as regulated by binge drinking in both males and females. **(A)** Depicts the neuropathic pain signaling pathway and highlights genes regulated by binge drinking in males (pink for up-regulation, green for down-regulation). **(B,C)** Depict qRT-PCR results and show that expression of *Ntrk2* (**B** which encodes TrkB) was significantly higher in males than in females. Expression of *Elk1* (**C** which encodes transcription factor Elk1) was significantly decreased by binge drinking in both sexes. Values are the mean ± SEM for 4/sex/treatment. $^{*}p < 0.05$ for main effect of treatment, $^{**}p = 0.01$ for main effect of sex (over horizontal line). **(D)** Shows significant regulation by binge drinking of select genes from the qPCR array analysis in male and female mice that are pertinent to the neuropathic signaling cascade depicted in **(A)** (top 10 genes) or that are pertinent to effects on other receptor systems (↑ for up-regulation, ↓ for down regulation; $p \leq 0.05$ at a minimum). For statistical trends, the *p*-values are provided. *Ntrk2* (neurotrophic tyrosine kinase, receptor, type 2) encodes the protein TrkB (tropomyosin receptor kinase B). *Elk1* (ELK1, member of ETS oncogene family) encodes the transcription factor Elk1.

(see section "Introduction"). Importantly, because we directly tested males and females following repeated binge drinking, the present results show for the first time that repeated binge drinking experience produces sexually divergent transcriptional responses and activation of distinct networks, similar to what has been reported for males and females tested during acute withdrawal following chronic intoxication (Hashimoto and Wiren, 2008; Wilhelm et al., 2014, 2015). Of the 106 genes significantly affected by binge drinking in the present study, only 4 were regulated similarly in males and females, demonstrating a profound sex difference in neuroadaptive responses in the NAc that would result in dysregulation of distinct biological pathways between the sexes. For instance, IPA identified Psychological Disorders and Neurological Disease as one of the top two networks, based on the expression differences following repeated binge drinking in male and female mice. However, the relationships between genes identified distinct molecules as significant signaling nodes, suggestive of a sexually dimorphic response that also may be related to mood disorders.

It was not surprising that neurotransmission was significantly affected by binge drinking. The current results are consistent with prior microarray studies that identified networks or biological processes related to glutamate signaling, BDNF and synaptic transmission in the NAc and central nucleus of the amygdala (Rodd et al., 2008; McBride et al., 2010) or in the PFC (Wolstenholme et al., 2011) from male rodents following binge drinking and networks related to neurotransmission in the NAc and amygdala from female rats following binge drinking (Bell et al., 2006). Neurotransmission also was one pathway identified in the cingulate cortex of dependent male rats after a period of abstinence, which included the glutamatergic and monoaminergic systems (Rimondini et al., 2002). Based on the results in dependent male rats during abstinence, in conjunction with the binge drinking-related changes in expression of

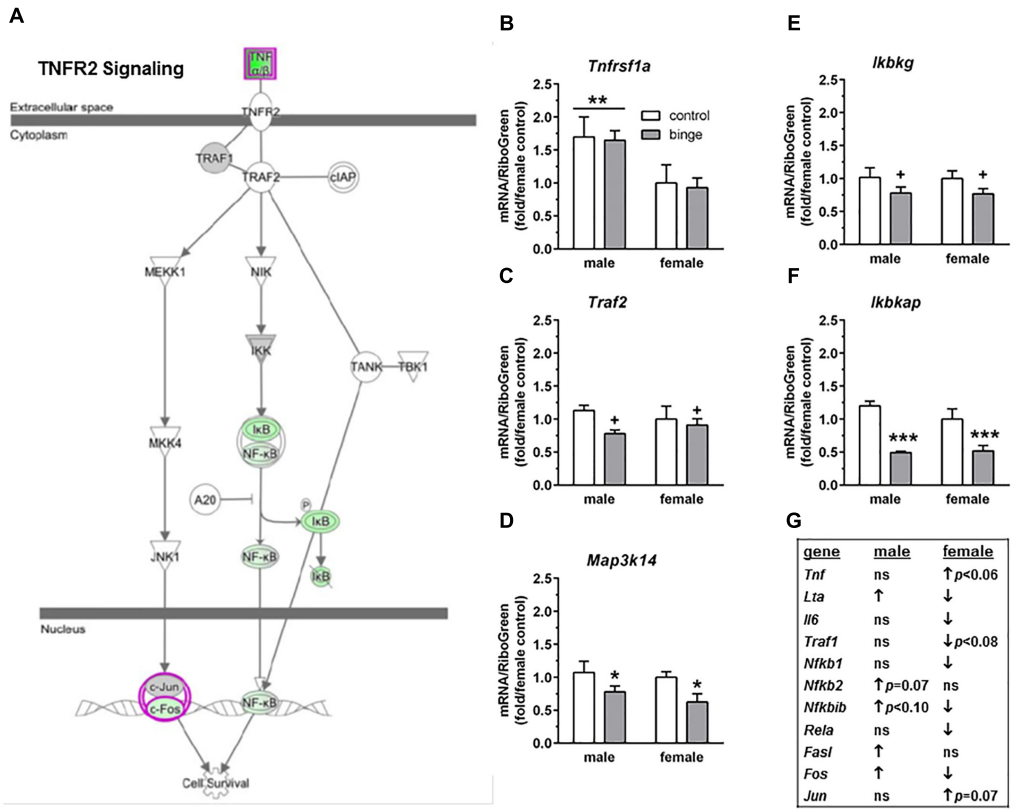

FIGURE 5 | Simplified tumor necrosis factor receptor 2 (TNFR2) signaling pathway highlights genes influenced by repeated binge drinking in male and female mice. This canonical pathway was identified by IPA as regulated by binge drinking in both males and females. **(A)** Depicts the TNFR2 signaling pathway and highlights genes regulated by binge drinking in females (pink for up-regulation, green for down-regulation). **(B–F)** Depict qRT-PCR results. Expression of *Tnfrsf1a* (**B** which encodes TNFR1 and forms a heterocomplex with TNFR2) was significantly higher in males vs. females. However, *Map3k14* (**D** encodes NIK) and *Ikbkap* (**F** encodes IKAP) expression was significantly decreased by binge drinking in both males and females, whereas expression of *Traf2* (**C** encodes TRAF2) and *Ikbkg* (**E** encodes IKK-γ) trended toward a decrease by binge drinking in both sexes. Values are the mean ± SEM for 4/sex/treatment. $^{+}p < 0.09$, $^{*}p < 0.05$, $^{***}p < 0.001$ for main effect of treatment, $^{**}p < 0.01$ for main effect of sex (over horizontal line). **(G)** Shows significant regulation by binge drinking of select genes from the qPCR array analysis in male and female mice that are pertinent to the TNFR2 signaling cascade depicted in **(A)** (↑ for up-regulation, ↓ for down regulation; $p < 0.05$ at a minimum). For statistical trends, the *p*-values are provided. *Tnfrsf1a* (tumor necrosis factor receptor superfamily, member 1a) encodes TNFR1, which is a member of the TNF receptor superfamily of proteins. *Traf2* (TNF receptor-associated factor 2) encodes TRAF2. *Map3k14* (mitogen-activated protein kinase kinase kinase 14) encodes NIK. *Ikbkg* (inhibitor of kappaB kinase gamma) encodes IKK-γ or NEMO, which is one of three subunits that forms the IκB kinase (IKK) enzyme complex. *Ikbkap* (inhibitor of kappa light polypeptide gene enhancer in B-cells, kinase complex-associated protein) encodes IKAP.

glutamatergic and dopaminergic genes in male mice in the present study, it is possible that repeated binge drinking experience produces neuroadaptive changes in glutamatergic and dopaminergic signaling that continue through the development of dependence and a period of abstinence, at least in male rodents. Consistent with this idea, 3 months of chronic ethanol intake produced a significant increase in NAc Homer2 protein levels that persisted at 2 months of abstinence in male C57BL/6J mice, and Homer2 overexpression in the NAc facilitated the effect of single or repeated ethanol injections on extracellular glutamate and dopamine levels in the NAc (Szumlinski et al., 2008b). Likewise, NAc Homer2 and mGluR5 protein levels were significantly elevated at 1 month of abstinence after 6 months of chronic ethanol drinking (Obara et al., 2009). Collectively, a large body of evidence indicates that changes in glutamate receptors, transporters, enzymes, and scaffolding proteins are critical for the development of dependence and addiction (see reviews by Szumlinski et al., 2008a; Kalivas, 2009; Bell et al., 2016).

Earlier work with the Scheduled High Alcohol Consumption model of binge drinking found that repeated bouts of binge drinking increased NAc protein levels of Homer2, NMDA receptor 2A and 2B subunits, and PI3K activation in male C57BL/6J mice, without altering protein levels of mGluR1 and mGluR5 at 24 h after the final binge session (Cozzoli et al., 2009). Recently, we replicated the lack of effect of binge drinking on NAc protein levels of mGluR1 and mGluR5, but we also observed an ethanol-induced decrease in RNA expression of *Grm1* and *Grm5* in male C57BL/6J mice, and comparable changes were not found in female C57BL/6J mice (Cozzoli et al., 2016). In the present study, binge drinking significantly increased *Homer2* expression and tended to decrease *Grm5* expression only in male mice (*Grm1* was not on the arrays), and there was a non-significant increase in *Pik3r1* expression in female (↑ 1.48-fold, $p = 0.12$) and male

(↑ 1.17-fold, $p < 0.20$) mice. As we discuss in Cozzoli et al. (2016), it is possible that some of the differences between studies were due to whether the experiments were conducted in the circadian dark vs. light phase. The majority of studies that observed a binge drinking-induced activation of PI3K at 24 h of abstinence were conducted during the circadian dark phase (Cozzoli et al., 2009, 2012; Neasta et al., 2010 – but see Neasta et al., 2011), whereas binge ethanol drinking occurred during the circadian light phase in the current and our recent studies (Cozzoli et al., 2016). In the studies by Cozzoli et al. (2016), 24 h of abstinence following repeated binge drinking significantly decreased activation of PI3K and mammalian target of rapamycin (mTOR) protein levels in NAc tissue from male but not female mice. It is interesting that intra-NAc administration of rapamycin to inhibit mTOR signaling significantly decreased binge drinking in male but not female mice (Cozzoli et al., 2016). This result suggested that rapamycin blocked a binge ethanol-induced activation of mTOR in males, because it was administered prior to the binge ethanol session, and that the ethanol-induced activation of mTOR (and presumably PI3K) in males was more transient in our studies that were conducted during the circadian light phase than what was reported in other studies that were conducted during the circadian dark phase. Regulation of circadian clock genes has been shown to influence ethanol and drug sensitivity, and ethanol also can disrupt circadian gene expression (reviewed in Parekh et al., 2015). In the present study, we did observe changes in expression of some circadian genes following binge drinking, with a significant decrease in *Per2* in females ($p < 0.05$, **Supplementary Table S1**) and trends for an opposite effect on *Clock* in females and males (females: ↑ 1.5-fold, $p < 0.10$; males: ↓ 1.5-fold, $p < 0.09$). Regardless, the results add to evidence for sex differences in the effects of binge drinking on glutamatergic signaling.

It is interesting that Akt (many times associated with PI3K) was identified as a central node in female mice following binge drinking. However, as mentioned above, we recently found that females were insensitive to the ability of intra-NAc rapamycin (inhibits mTOR, in signaling cascade downstream of PI3K and Akt) to decrease binge drinking, whereas intra-NAc rapamycin significantly decreased binge drinking in males (Cozzoli et al., 2016). The reduction in binge drinking in males is consistent with prior work (Neasta et al., 2010, 2011, 2014), so the insensitivity of females suggests that an alternate signaling pathway that is independent of PI3K and that links Group 1 mGluRs to transcriptional changes in the nucleus (i.e., protein kinase A, calcium calmodulin dependent protein kinase, or MAPK; see Wang and Zhuo, 2012) is influenced by binge drinking in females. One possible mechanism would be via the ability of membrane estrogen receptors (mER) to stimulate mGluRs, as coupling of mERα to mGluRs can initiate independent signal transduction pathways (see review by Meitzen and Mermelstein, 2011). Related to this point, the present study found that binge drinking produced a fivefold upregulation in *Esr1* (which encodes ERα) only in female mice ($p < 0.05$, **Table 3**), and evidence indicates that ERα also can localize to the plasma membrane and initiate signal transduction through PI3K (reviewed in Levin, 2009). So, it is not known whether the identification of Akt (and presumably the Akt-PI3K pathway) as a central node in females following binge drinking is related to signaling downstream of mERα or downstream from the coupling of mERα to mGluRs.

Characterization of the expression differences following binge drinking also identified hormone signaling in female mice, with a trend for regulation of CRH signaling in male mice. In fact, "CRH signaling" was identified as a canonical pathway of interest from the analysis of genes that were regulated by binge drinking in both males and females (**Figure 3**). Importantly, the effects of binge drinking on CRH signaling were divergent for all the genes listed in **Figure 3D**. An examination of the genes responsible for the initiation of CRH signaling indicate that binge drinking reduces activity of the pathway in females (↓ *Crhr1* and *Crhr2*), while it increased activity of the pathway in males (↑ *Crh* and *Crhr2*). The decreased activity of the CRH pathway in females is interesting, given evidence for sex differences in the coupling of CRHR1 with the Gs and β-arrestin 2 proteins that render females more responsive to acute stress and less able to adapt to chronic stress as a result of compromised CRHR1 internalization (Valentino et al., 2013a,b). Consistent with this, we found that 1 month of continuous ethanol drinking with intermittent traumatic stress exposure upregulated protein levels of CRHR1 in the hippocampus and protein levels of GR in the hippocampus and PFC of female but not male C57BL/6J mice (Finn et al., 2018). Taken in conjunction with the present results, it is possible that binge drinking alone produces an opposite effect on CRH signaling than the combination of stress and ethanol consumption.

The transcriptional response to repeated binge drinking identified "MIF-mediated glucocorticoid regulation" in the NAc of females in the present study, despite the divergent and non-significant binge drinking-related changes in expression of the gene encoding GR (*Nr3c1*; females: ↓ 1.1-fold, $p = 0.19$; males: ↑ 1.2-fold, $p < 0.19$) and the gene encoding the chaperone heat shock protein 90 (*Hsp90b1*; females: ↑ 2-fold, $p < 0.08$; males: ↓ 1.3-fold, $p = 0.18$). Similarly, the identification of GR signaling in the NAc and central nucleus of the amygdala of male rats (McBride et al., 2010) and an enhanced response to glucocorticoids in the VTA of female rats (McBride et al., 2013) following chronic binge drinking experience (8 weeks for male rats; 10 weeks for female rats) was based on significant binge ethanol-induced regulation of the expression of genes that did not include GR. It is well documented that glucocorticoids can act via a nuclear GR to regulate many transcriptional pathways, including homeostasis, metabolism, and inflammation (reviewed in Biddie et al., 2012). But, while glucocorticoids can have anti-inflammatory and immunosuppressive properties, long term and/or high dose glucocorticoid administration can lead to symptoms of depression and decreased immunological function. Relevant to the pathway identified in females in the present study, MIF is able to directly regulate the immunosuppressive action of glucocorticoids (reviewed in Flaster et al., 2007). MIF can be produced at all levels of the hypothalamic-pituitary-adrenal axis, and plasma MIF levels fluctuate in a circadian rhythm relative to cortisol. Early studies found that MIF counteracted the glucocorticoid-induced suppression of inflammatory cytokine secretion in activated macrophages (e.g.,

TNF, IL-1, IL-6, IL-8) and completely blocked the protective effect of the synthetic glucocorticoid dexamethasone in a model of lethal, endotoxic shock induced by lipopolysaccharide (Calandra et al., 1995), providing evidence that the regulatory effect of MIF on glucocorticoid immunosuppression occurs *in vivo*. Additionally, cross-talk between GR and NF-κB occurs via a physical interaction that produces a dose-dependent and mutual antagonism effect mediated by the p65 (RelA, encoded by *Rela*) subunit of NF-κB (McKay and Cidlowski, 1998). Glucocorticoids also inhibit NF-κB activation, in part by increasing the expression of the IκB complex that maintains NF-κB in an inactive state until IκB dissociates from NF-κB following its phosphorylation (Flaster et al., 2007; Lang et al., 2015; simplified NF-κB and IκB interaction depicted in **Figure 5A**). And, one effect of MIF is to prevent glucocorticoids from increasing the expression of IκB, which would offset the glucocorticoid-mediated inhibition of NF-κB (Flaster et al., 2007; Lang et al., 2015). Since the immunosuppressive and anti-inflammatory effects of glucocorticoids are thought to depend on the inhibition of NF-κB, which is a transcription factor that plays a role in immune signaling and cell survival (Li and Verma, 2002), counteracting this effect with MIF could result in sustained inflammatory signaling in females with binge drinking experience.

Acute withdrawal following chronic intoxication affected pathways related to inflammatory activation and apoptotic/cell death signaling in PFC from females vs. males (Hashimoto and Wiren, 2008; Wilhelm et al., 2014, 2015). Acute withdrawal from repeated binge drinking also affected several pathways related to immune function only in female NAc in the present study ("MIF regulation of innate immunity," "TNFR1 signaling," and "TNFR2 signaling"). And, "TNFR2 signaling" was identified as a canonical pathway of interest from the analysis of genes that were regulated by binge drinking in the NAc from both males and females (**Figure 5**). Notably, binge drinking produced a significant and opposite change in the expression of *Lta* (encodes TNF-β or lymphotoxin-α), with a decrease in females and increase in males (**Table 2** and **Figure 5G**), and this protein also is involved in cell survival, proliferation, differentiation, apoptosis, and immune regulation. So, the sex difference in significant expression change in *Lta* by binge drinking (↓ in females, ↑ in males, **Table 2** and **Figure 5G**) would be predicted to have opposite effects on cell survival and immune responses. In addition, binge drinking significantly decreased expression of *Il6* only in females; an ethanol-induced reduction in levels of these two cytokines in females would be consistent with a decrease in the initiation of signaling at TNFR1 (see Figure 2 in Mayfield et al., 2013) and TNFR2 (**Figure 5A**). Overall, the results in females demonstrate that binge drinking produced a fairly consistent decrease in expression of genes in the signaling cascade through the TNF superfamily, with the exception of a trend for an increase in expression of *Tnf* (encodes TNF-α). These binge ethanol-induced changes in females, including the downregulation of the RelA subunit of NF-κB, likely produce a decrease in the activation of NF-κB. A more complex pattern of changes was identified in males following binge drinking, so the influence on NF-κB activation in males is unclear. Regardless, the results in females in the present study would be consistent with a decrease in cell survival, and an increase in apoptosis and inflammation via a decrease in the activation of the NF-κB. It is interesting that acute withdrawal from chronic intoxication also identified NF-κB as a central node in both male and female networks, but the interacting gene sets were completely distinct between the sexes (Wilhelm et al., 2014). An examination of the genes regulated by chronic intoxication in these pathways revealed that several of the genes in females were indicative of a proinflammatory response, while the genes in males were suggestive of overall immunosuppression (Wilhelm et al., 2014). Collectively, binge drinking experience and chronic intoxication leading to the development of physical dependence both produced sexually divergent changes in inflammatory signaling in the NAc and PFC from mice.

CONCLUSION

The repeated binge drinking sessions produced sexually divergent transcriptional responses and activation of distinct networks. These results add to a body of evidence indicating that binge drinking and chronic ethanol intoxication both produce neuroadaptive changes in neurotransmitter systems and in many cellular pathways that likely alter neuronal function in a manner that can be either adaptive or deleterious. The opposite effects of binge drinking on immune function in the present study, with changes in females consistent with a decrease in cell survival and an increase in inflammation and apoptosis, have important implications, given the evidence for a role of neuroimmune signaling in the acute and chronic effects of ethanol, including neurodegeneration (reviewed in Mayfield et al., 2013; Crews et al., 2015). Related to this point, chronic intoxication activated inflammatory signaling and cell death pathways in female but not male mice, and confirmation studies showed that ethanol dependent females exhibited significant neuronal degeneration in cortical regions, whereas cell death in males was significantly reduced (Hashimoto and Wiren, 2008; Wilhelm et al., 2015). Finally, a broader implication of the current findings is pertinent to sex differences in the immune system and the relationship to mood disorders (reviewed in Rainville and Hodes, 2018). Taken in conjunction with sex differences in mood and anxiety disorders (e.g., Altemus et al., 2014), future studies examining potential immune or stress-related mechanisms that may contribute to stress and ethanol susceptibility and associated mood disorders will be important.

One limitation of the present investigation is that we did not conduct confirmation studies to identify protein changes, neuronal degeneration, or behavioral changes that could possibly account for the sex-specific gene expression profiles that we observed. However, we did examine the expression of additional select genes that were not present on the arrays but that were implicated in the downstream signaling cascades of the IPA-identified pathways to strengthen conclusions about the select pathways that were altered by binge drinking. Future studies will determine whether the current gene expression changes correspond to behavioral and/or physiological differences.

Importantly, an increased understanding of sexually dimorphic molecular pathways influenced by binge drinking and chronic intoxication leading to dependence may identify novel treatment options for males and females. The current study is contributing data sets that can be used to generate sex-specific bioinformatics tools, which have the potential to enormously accelerate the discovery of sex-specific changes associated with AUD. Finally, we recently reported that binge drinking produced sex differences in the regulation of PI3K signaling in the NAc and in the ability of intra-NAc rapamycin to decrease binge drinking, with females resistant to these molecular changes (Cozzoli et al., 2016). The functional implication of the report by Cozzoli et al. (2016) emphasizes that targeting a pathway that is unaffected by binge drinking in females will not be an effective pharmacotherapeutic strategy. Collectively, the fundamental sex differences identified in the present and prior work provide evidence for distinct pathways that could be targeted therapeutically for the treatment of AUD in males and females.

DATA AVAILABILITY

The raw data supporting the conclusions of this manuscript will be made available by the authors, without undue reservation, to any qualified researcher.

AUTHOR CONTRIBUTIONS

DF and KW contributed conception and study design. DF, DC, MN, and MK conducted the drinking study. DC dissected accumbens tissue. JH isolated RNA and prepared samples for qPCR array analysis. DF conducted preliminary analysis of drinking data and identified animals for the qPCR analysis. DF, MN, and MK participated in final analysis of drinking data. MH conducted follow-up qRT-PCR analysis, with assistance from JH. JH and KW performed Pathway Analysis. JH, KW, and MG assisted in the interpretation of the array and pathway analyses. DF wrote the first draft of the manuscript, but JH and KW wrote sections of the "Materials and Methods and Results." All authors contributed to the final version of the manuscript, read, and approved the final version.

FUNDING

This study was supported by VA Merit grants (BX001070 and BX002966 to DF) from the United States Department of Veterans Affairs and by resources and facilities at the VA Portland Health Care System (DF, KW, and MG). RO1 AA021468 (KW and MG) from the National Institute on Alcohol Abuse and Alcoholism provided additional support. We thank Mr. Chris Snelling for the assessment of blood ethanol concentration.

SUPPLEMENTARY MATERIAL

The Supplementary Material for this article can be found online at: https://www.frontiersin.org/articles/10.3389/fgene.2018.00325/full#supplementary-material

REFERENCES

Agrawal, R. G., Owen, J. A., Levin, P. S., Hewetson, A., Berman, A. E., Franklin, S. R., et al. (2014). Bioinformatics analyses reveal age-specific neuroimmune modulation as a target for treatment of high ethanol drinking. *Alcohol. Clin. Exp. Res.* 38, 428–437. doi: 10.1111/acer.12288

Akilesh, S., Shaffer, D. J., and Roopenian, D. (2003). Customized molecular phenotyping by quantitative gene expression and pattern recognition analysis. *Genome Res.* 13, 1719–1727. doi: 10.1101/gr.533003

Altemus, M., Sarvaiya, N., and Epperson, C. N. (2014). Sex differences in anxiety and depression clinical perspectives. *Front. Neuroendocrinol.* 35:320–330. doi: 10.1016/j.yfrne.2014.05.004

Bell, R. L., Hauser, S. R., McClintick, J., Rahman, S., Edenberg, H. J., Szumlinski, K. K., et al. (2016). Ethanol-associated changes in glutamate reward neurocircuitry: A minireview of clinical and preclinical genetic findings. *Prog. Mol. Biol. Transl. Sci.* 137, 41–85. doi: 10.1016/bs.pmbts.2015.10.018

Bell, R. L., Kimpel, M. W., McClintick, J. N., Strother, W. N., Carr, L. G., Liang, T., et al. (2009). Gene expression changes in the nucleus accumbens of alcohol-preferring rats following chronic ethanol consumption. *Pharmacol. Biochem. Behav.* 94, 131–147. doi: 10.1016/j.pbb.2009.07.019

Bell, R. L., Kimpel, M. W., Rodd, Z. A., Strother, W. N., Bai, F., Peper, C. L., et al. (2006). Protein expression changes in the nucleus accumbens and amygdala of inbred alcohol-preferring rats given either continuous or scheduled access to ethanol. *Alcohol* 40, 3–17. doi: 10.1016/j.alcohol.2006.10.001

Biddie, S. C., Conway-Campbell, B. L., and Lightman, S. L. (2012). Dynamic regulation of glucocorticoid signalling in health and disease. *Rheumatology* 51, 403–412. doi: 10.1093/rheumatology/ker215

Calandra, T., Bernhagen, J., Metz, C., Spiegel, L. A., Bacher, M., Donnelly, T., et al. (1995). MIF as a glucocorticoid-induced modulator of cytokine production. *Nature* 377, 68–71. doi: 10.1038/377068a0

Chandler, L. J. (2003). Ethanol and brain plasticity: receptors and molecular networks of the postsynaptic density as targets of ethanol. *Pharmacol. Ther.* 99, 311–326. doi: 10.1016/S0163-7258(03)00096-2

Cozzoli, D. K., Courson, J., Caruana, A. L., Miller, B. W., Greentree, D. I., Thompson, A. B., et al. (2012). Nucleus accumbens mGluR5-associated signaling regulates binge alcohol drinking under drinking-in-the-dark procedures. *Alcohol. Clin. Exp. Res.* 36, 435–444. doi: 10.1111/j.1530-0277.2012.01776.x

Cozzoli, D. K., Goulding, S. P., Zhang, P. W., Xiao, B., Hu, J.-H., Ary, A. W., et al. (2009). Binge drinking upregulates accumbens mGluR5-Homer2-PI3K signaling: functional implications for alcoholism. *J. Neurosci.* 29, 8655–8668. doi: 10.1523/JNEUROSCI.5900-08.2009

Cozzoli, D. K., Kaufman, M. N., Nipper, M. A., Hashimoto, J. G., Wiren, K. M., and Finn, D. A. (2016). Functional regulation of PI3K-associated signaling in the accumbens by binge alcohol drinking in male but not female mice. *Neuropharmacology* 105, 164–174. doi: 10.1016/j.neuropharm.2016.01.010

Crews, F. T., Sarkar, D. K., Qin, L., Zou, J., Boyadjieva, N., and Vetreno, R. P. (2015). Neuroimmune function and the consequences of alcohol exposure. *Alcohol. Res.* 37, 344–351.

Cui, C., and Koob, G. F. (2017). Titrating tipsy targets: The neurobiology of low-dose alcohol. *Trends Pharmacol. Sci.* 38, 556–568. doi: 10.1016/j.tips.2017.03.002

Finn, D. A., Belknap, J. K., Cronise, K., Yoneyama, N., Murillo, A., and Crabbe, J. C. (2005). A procedure to produce high alcohol intake in mice. *Psychopharmacology* 178, 471–480. doi: 10.1007/s00213-004-2039-8

Finn, D. A., Helms, M. L., Nipper, M. A., Cohen, A., Jensen, J. J., and Devaud, L. L. (2018). Sex differences in the synergistic effect of prior binge drinking and traumatic stress on subsequent ethanol intake and neurochemical responses in adult C57BL/6J mice. *Alcohol* 71, 33–45. doi: 10.1016/j.alcohol.2018.02.004

Finn, D. A., Snelling, C., Fretwell, A. M., Tanchuck, M. A., Underwood, L., Cole, M., et al. (2007). Increased drinking during withdrawal from intermittent ethanol exposure is blocked by the CRF receptor antagonist D-Phe-CRF(12-41). *Alcohol. Clin. Exp. Res.* 31, 939–949. doi: 10.1111/j.1530-0277.2007.00379.x

Flaster, H., Bernhagen, J., Calandra, T., and Bucala, R. (2007). The macrophage migration inhibitory factor-glucocorticoid dyad: regulation of inflammation and immunity. *Mol. Endocrinol.* 21, 1267–1280. doi: 10.1210/me.2007-0065

Hashimoto, J. G., Beadles-Bohling, A. S., and Wiren, K. M. (2004). Comparison of RiboGreen and 18S rRNA quantitation for normalizing real-time RT-PCR expression analysis. *Biotechniques* 36, 58–60. doi: 10.2144/04361BM06

Hashimoto, J. G., Forquer, M. R., Tanchuck, M. A., Finn, D. A., and Wiren, K. M. (2011). Importance of genetic background for risk of relapse shown in altered prefrontal cortex gene expression during abstinence following chronic alcohol intoxication. *Neuroscience* 173, 57–75. doi: 10.1016/j.neuroscience.2010.11.006

Hashimoto, J. G., Gavin, D. P., Wiren, K. M., Crabbe, J. C., and Guizzetti, M. (2017). Prefrontal cortex expression of chromatin modifier genes in male WSP and WSR mice changes across ethanol dependence, withdrawal, and abstinence. *Alcohol* 60, 83–94. doi: 10.1016/j.alcohol.2017.01.010

Hashimoto, J. G., and Wiren, K. M. (2008). Neurotoxic consequences of chronic alcohol withdrawal: expression profiling reveals importance of gender over withdrawal severity. *Neuropsychopharmacology* 33, 1084–1096. doi: 10.1038/sj.npp.1301494

Kalivas, P. W. (2009). The glutamate hypothesis of addiction. *Nat. Rev. Neurosci.* 10, 561–572. doi: 10.1038/nrn2515

Kauer, J. A., and Malenka, R. C. (2007). Synaptic plasticity and addiction. *Nat. Rev. Neurosci.* 8, 844–858. doi: 10.1038/nrn2234

Koob, G. F., and Volkow, N. D. (2010). Neurocircuitry of addiction. *Neuropsychopharmacology* 35, 217–238. doi: 10.1038/npp.2009.110

Lang, T., Foote, A., Lee, J. P. W., Morand, E. F., and Harris, J. (2015). MIF: Implications in the pathoetiology of systemic lupus erythematosus. *Front. Immunol.* 6:577. doi: 10.3389/fimmu.2015.00577

Lau, C. G., and Zukin, R. S. (2007). NMDA receptor trafficking in synaptic plasticity and neuropsychiatric disorders. *Nat. Rev. Neurosci.* 8, 413–426. doi: 10.1038/nrn2153

Levin, E. R. (2009). Plasma membrane estrogen receptors. *Trends Endocrinol. Metab.* 20, 477–482. doi: 10.1016/j.tem.2009.06.009

Li, Q., and Verma, I. M. (2002). NF-κB regulation in the immune system. *Nat. Rev. Immunol.* 2, 725–734. doi: 10.1038/nri910

Marballi, K., Genabai, N. K., Blednov, Y. A., Harris, R. A., and Ponomarev, I. (2016). Alcohol consumption induces global gene expression changes in VTA dopaminergic neurons. *Genes Brain Behav.* 15, 318–326. doi: 10.1111/gbb.12266

Mayfield, J., Ferguson, L., and Harris, R. A. (2013). Neuroimmune signaling: a key component of alcohol abuse. *Curr. Opin. Neurobiol.* 23, 513–520. doi: 10.1016/j.conb.2013.01.024

McBride, W. J., Kimpel, M. W., McClintick, J. N., Ding, Z.-M., Hauser, S. R., Edenberg, H. J., et al. (2013). Changes in gene expression within the ventral tegmental area following repeated excessive binge-like alcohol drinking by alcohol-preferring (P) rats. *Alcohol* 47, 367–380. doi: 10.1016/j.alcohol.2013.04.002

McBride, W. J., Kimpel, M. W., Schultz, J. A., McClintick, J. N., Edenberg, H. J., and Bell, R. L. (2010). Changes in gene expression in regions of the extended amygdala of alcohol-preferring rats after binge-like alcohol drinking. *Alcohol* 44, 171–183. doi: 10.1016/j.alcohol.2009.12.001

McKay, L. I., and Cidlowski, J. A. (1998). Cross-talk between nuclear factor-κB and the steroid hormone receptors: mechanisms of mutual antagonism. *Mol. Endocrinol.* 12, 45–56. doi: 10.1210/mend.12.1.0044

Meitzen, J., and Mermelstein, P. G. (2011). Estrogen receptors stimulate brain region specific metabotropic glutamate receptors to rapidly initiate signal transduction pathways. *J. Chem. Neuroanat.* 42, 236–241. doi: 10.1016/j.jchemneu.2011.02.002

Melendez, R. I., McGinty, J. F., Kalivas, P. W., and Becker, H. C. (2012). Brain region-specific gene expression changes after chronic intermittent ethanol exposure and early withdrawal in C57BL/6J mice. *Addict. Biol.* 17, 351–364. doi: 10.1111/j.1369-1600.2011.00357.x

Morisot, N., Novotny, C. J., Shokat, K. M., and Ron, D. (2018). A new generation of mTORC1 inhibitor attenuates alcohol intake and reward in mice. *Addict. Biol.* 23, 713–722. doi: 10.1111/adb.12528

Mulligan, M. K., Rhodes, J. S., Crabbe, J. C., Mayfield, R. D., Harris, R. A., and Ponomarev, I. (2011). Molecular profiles of drinking alcohol to intoxication in C57BL/6J mice. *Alcohol. Clin. Exp. Res.* 35, 659–670. doi: 10.1111/j.1530-0277.2010.01384.x

Neasta, J., Barak, S., Hamida, S. B., and Ron, D. (2014). mTOR complex 1: a key player in neuroadaptation induced by drugs of abuse. *J. Neurochem.* 130, 172–184. doi: 10.1111/jnc.12725

Neasta, J., Ben Hamida, S., Yowell, Q., Carnicella, S., and Ron, D. (2010). Role for mammalian target of rapamycin complex 1 signaling in neuroadaptations underlying alcohol-related disorders. *Proc. Natl. Acad. Sci. U.S.A.* 107, 20093–20098. doi: 10.1073/pnas.1005554107

Neasta, J., Ben Hamida, S., Yowell, Q., Carnicella, S., and Ron, D. (2011). AKT signaling pathway in the nucleus accumbens mediates excessive alcohol drinking behaviors. *Biol. Psychiatry* 70, 575–582. doi: 10.1016/j.biopsych.2011.03.019

NIAAA (2004). *NIAAA Council Approves Definition of Binge Drinking. NIAAA Newsletter*. Available at: https://pubs.niaaa.nih.gov/publications/Newsletter/winter2004/Newsletter_Number3.pdf

NIAAA (2017). *Alcohol Facts and Statistics*. Available at: https://pubs.niaaa.nih.gov/publications/AlcoholFacts&Stats/AlcoholFacts&Stats.pdf

Obara, I., Bell, R. L., Goulding, S. P., Reyes, C. M., Larson, L. A., Ary, A. W., et al. (2009). Differential effects of chronic ethanol consumption and withdrawal on Homer/glutamate receptor expression in subregions of the accumbens and amygdala of P rats. *Alcohol. Clin. Exp. Res.* 33, 1924–1934. doi: 10.1111/j.1530-0277.2009.01030.x

Parekh, P. K., Ozburn, A. R., and McClung, C. A. (2015). Circadian clock genes: effects on dopamine, reward and addiction. *Alcohol* 49, 341–349. doi: 10.1016/j.alcohol.2014.09.034

Paxinos, G., and Franklin, K. (2001). *The Mouse Brain in Stereotaxic Coordinates,* 2nd Edn. San Diego, CA: Academic Press.

Priddy, B. M., Carmack, S. A., Thomas, L. C., and Vendruscolo, J. C. M. (2017). Sex, strain, and estrous cycle influences on alcohol drinking in rats. *Pharmacol. Biochem. Behav.* 152, 61–67. doi: 10.1016/j.pbb.2016.08.001

Rainville, J. R., and Hodes, G. E. (2018). Inflaming sex differences in mood disorders. *Neuropsychopharmacology*. doi: 10.1038/s41386-018-0124-7 [Epub ahead of print].

Repunte-Canonigo, V., Shin, W., Vendruscolo, L. F., Lefebvre, C., van der Stap, L., Kawamura, T., et al. (2015). Identifying candidate drivers of alcohol dependence-induced excessive drinking by assembly and interrogation of brain-specific regulatory networks. *Gen. Biol.* 16:68. doi: 10.1186/s13059-015-0593-5

Rimondini, R., Arlinde, C., Sommer, W., and Heilig, M. (2002). Long-lasting increase in voluntary ethanol consumption and transcriptional regulation in the rat brain after intermittent exposure to alcohol. *FASEB J.* 16, 27–35. doi: 10.1096/fj.01-0593com

Rodd, Z. A., Bertsch, B. A., Strother, W. N., Le-Niculescu, H., Balaram, Y., Hayden, E., et al. (2007). Candidate genes, pathways and mechanisms for alcoholism: an expanded convergent functional genomics approach. *Pharmacogen. J.* 7, 222–256. doi: 10.1038/sj.tpj.6500420

Rodd, Z. A., Kimpel, M. W., Edenberg, H. J., Bell, R. L., Strother, W. N., McClintick, J. N., et al. (2008). Differential gene expression in the nucleus accumbens with ethanol self-administration in inbred alcohol-preferring rats. *Pharmacol. Biochem. Behav.* 89, 481–498. doi: 10.1016/j.pbb.2008.01.023

Satta, R., Hilderbrand, E. R., and Lasek, A. W. (2018). Ovarian hormones contribute to high levels of binge-like drinking by female mice. *Alcohol. Clin. Exp. Res.* 42, 286–294. doi: 10.1111/acer.13571

Spanagel, R. (2009). Alcoholism: a systems approach from molecular physiology to addictive behavior. *Physiol. Rev.* 89, 649–705. doi: 10.1152/physrev.00013.2008

Strong, M. N., Yoneyama, N., Fretwell, A. M., Snelling, C., Tanchuck, M. A., and Finn, D. A. (2010). "Binge" drinking experience in adolescent mice shows sex

differences and elevated ethanol intake in adulthood. *Horm. Behav.* 58, 82–90. doi: 10.1016/j.yhbeh.2009.10.008

Szumlinski, K. K., Ary, A. W., and Lominac, K. D. (2008a). Homers regulate drug-induced neuroplasticity: implications for addiction. *Biochem. Pharmacol.* 75, 112–133.

Szumlinski, K. K., Ary, A. W., Lominac, K. D., Klugmann, M., and Kippin, T. E. (2008b). Accumbens Homer2 overexpression facilitates alcohol-induced neuroplasticity in C57BL/6J mice. *Neuropsychopharmacology* 33, 1365–1378.

Tanchuck, M. A., Yoneyama, N., Ford, M. M., Fretwell, A. M., and Finn, D. A. (2011). Assessment of GABA-B, metabotropic glutamate and opioid receptor involvement in an animal model of binge drinking. *Alcohol* 45, 33–44. doi: 10.1016/j.alcohol.2010.07.009

Tzschentke, T. M., and Schmidt, W. J. (2003). Glutamatergic mechanisms in addiction. *Mol. Psychiatry* 8, 373–382. doi: 10.1038/sj.mp.4001269

Valentino, R. J., Bangasser, D., and Van Bockstaele, E. J. (2013a). Sex-biased stress signaling: the corticotropin-releasing factor receptor as a model. *Mol. Pharmacol.* 83, 737–745. doi: 10.1124/mol.112.083550

Valentino, R. J., Van Bockstaele, E., and Bangasser, D. (2013b). Sex-specific cell signaling: the corticotropin-releasing factor receptor model. *Trends Pharmacol. Sci.* 34, 437–444. doi: 10.1016/j.tips.2013.06.004

Wang, H., and Zhuo, M. (2012). Group 1 metabotropic glutamate receptor-mediated gene transcription and implications for synaptic plasticity and diseases. *Front. Pharmacol.* 3:189. doi: 10.3389/fphar.2012.00189

Wheeler, J. M., Reed, C., Burkhart-Kasch, S., Li, N., Cunningham, C. L., Janowsky, A., et al. (2009). Genetically correlated effects of selective breeding for high and low methamphetamine consumption. *Genes Brain Behav.* 8, 758–771. doi: 10.1111/j.1601-183X.2009.00522.x

Wilhelm, C. J., Hashimoto, J. G., Roberts, M. L., Bloom, S. H., Beard, D. K., and Wiren, K. M. (2015). Females uniquely vulnerable to alcohol-induced neurotoxicity show altered glucocorticoid signaling. *Brain Res.* 1601, 102–116. doi: 10.1016/j.brainres.2015.01.002

Wilhelm, C. J., Hashimoto, J. G., Roberts, M. L., Sonmez, M. K., and Wiren, K. M. (2014). Understanding the addiction cycle: a complex biology with distinct contributions of genotype vs. sex at each stage. *Neuroscience* 279, 168–186. doi: 10.1016/j.neuroscience.2014.08.041

Wiren, K. M. (2013). Males and females are just different: sexually dimorphic responses to chronic ethanol exposure in hippocampal slice cultures. *Neurosci. Lett.* 550, 1–5. doi: 10.1016/j.neulet.2013.06.030

Wiren, K. M., Semirale, A. A., Hashimoto, J. G., and Zhang, X. W. (2010). Signaling pathways implicated in androgen regulation of endocortical bone. *Bone* 46, 710–723. doi: 10.1016/j.bone.2009.10.039

Wolstenholme, J. T., Warner, J. A., Capparuccini, M. I., Archer, K. J., Shelton, K. L., and Miles, M. F. (2011). Genomic analysis of individual differences in ethanol drinking: Evidence for non-genetic factors in C57BL/6J mice. *PLoS One* 6:6. doi: 10.1371/journal.pone.0021100

Conflict of Interest Statement: The authors declare that the research was conducted in the absence of any commercial or financial relationships that could be construed as a potential conflict of interest.

frontiers in Genetics

ORIGINAL RESEARCH
published: 24 September 2018
doi: 10.3389/fgene.2018.00402

Ethanol-Induced Behavioral Sensitization Alters the Synaptic Transcriptome and Exon Utilization in DBA/2J Mice

Megan A. O'Brien[1†], Rory M. Weston[1†], Nihar U. Sheth[2], Steven Bradley[2], John Bigbee[3], Ashutosh Pandey[4], Robert W. Williams[4], Jennifer T. Wolstenholme[1,2] and Michael F. Miles[1,2,5]*

[1] Department of Pharmacology and Toxicology, Virginia Commonwealth University, Richmond, VA, United States, [2] VCU Alcohol Research Center, Virginia Commonwealth University, Richmond, VA, United States, [3] Department of Anatomy and Neurobiology, Virginia Commonwealth University, Richmond, VA, United States, [4] Department of Genetics, Genomics and Informatics, The University of Tennessee Health Science Center, Memphis, TN, United States, [5] Department of Neurology, Virginia Commonwealth University, Richmond, VA, United States

OPEN ACCESS

Edited by:
Kristin Hamre,
The University of Tennessee Health Science Center, United States

Reviewed by:
Owen Murray Rennert,
Eunice Kennedy Shriver National Institute of Child Health and Human Development (NICHD), United States
Minati Singh,
The University of Iowa, United States

***Correspondence:**
Michael F. Miles
Michael.Miles@vcuhealth.org

[†] These authors have contributed equally to this work

Specialty section:
This article was submitted to Behavioral and Psychiatric Genetics, a section of the journal Frontiers in Genetics

Received: 06 July 2018
Accepted: 03 September 2018
Published: 24 September 2018

Citation:
O'Brien MA, Weston RM, Sheth NU, Bradley S, Bigbee J, Pandey A, Williams RW, Wolstenholme JT and Miles MF (2018) Ethanol-Induced Behavioral Sensitization Alters the Synaptic Transcriptome and Exon Utilization in DBA/2J Mice. Front. Genet. 9:402. doi: 10.3389/fgene.2018.00402

Alcoholism is a complex behavioral disorder characterized by loss of control in limiting intake, and progressive compulsion to seek and consume ethanol. Prior studies have suggested that the characteristic behaviors associated with escalation of drug use are caused, at least in part, by ethanol-evoked changes in gene expression affecting synaptic plasticity. Implicit in this hypothesis is a dependence on new protein synthesis and remodeling at the synapse. It is well established that mRNA can be transported to distal dendritic processes, where it can undergo localized translation. It is unknown whether such modulation of the synaptic transcriptome might contribute to ethanol-induced synaptic plasticity. Using ethanol-induced behavioral sensitization as a model of neuroplasticity, we investigated whether repeated exposure to ethanol altered the synaptic transcriptome, contributing to mechanisms underlying subsequent increases in ethanol-evoked locomotor activity. RNAseq profiling of DBA/2J mice subjected to acute ethanol or ethanol-induced behavioral sensitization was performed on frontal pole synaptoneurosomes to enrich for synaptic mRNA. Genomic profiling showed distinct functional classes of mRNA enriched in the synaptic vs. cytosolic fractions, consistent with their role in synaptic function. Ethanol sensitization regulated more than twice the number of synaptic localized genes compared to acute ethanol exposure. Synaptic biological processes selectively perturbed by ethanol sensitization included protein folding and modification as well as and mitochondrial respiratory function, suggesting repeated ethanol exposure alters synaptic energy production and the processing of newly translated proteins. Additionally, marked differential exon usage followed ethanol sensitization in both synaptic and non-synaptic cellular fractions, with little to no perturbation following acute ethanol exposure. Altered synaptic exon usage following ethanol sensitization strongly affected genes related to RNA processing and stability, translational regulation, and synaptic function. These genes were also enriched for

targets of the FMRP RNA-binding protein and contained consensus sequence motifs related to other known RNA binding proteins, suggesting that ethanol sensitization altered selective mRNA trafficking mechanisms. This study provides a foundation for investigating the role of ethanol in modifying the synaptic transcriptome and inducing changes in synaptic plasticity.

Keywords: synaptic, mRNA trafficking, RNAseq, exon utilization, ethanol, sensitization

INTRODUCTION

Alcoholism is a chronic disease characterized by compulsive drug-seeking undeterred by negative consequences, as well as cravings and potential for relapse that persist despite years of abstinence. The endurance of these pernicious behaviors supports the theory that addiction arises from progressive and lasting cellular and molecular adaptations in response to repeated ethanol exposure (Nestler et al., 1993; Nestler, 2001). A more complete comprehension of neuronal plasticity that underlies the transition to compulsive drug use could lead to novel therapeutic strategies for alcohol use disorders.

The morphological specialization of neurons, where synapses appear to be regulated in an individual manner, advocates the need for local mechanisms controlling synaptic function. Local synaptic protein synthesis is supported by the finding of synthesis machinery at post-synaptic sites, including ribosomes, tRNA, translation factors, endoplasmic reticulum, and Golgi apparatus (Steward and Levy, 1982; Steward and Reeves, 1988). Furthermore, through *in situ* hybridization (Lyford et al., 1995; Poon et al., 2006) and studies characterizing synapse-enriched subcellular fractions (Chicurel et al., 1993; Rao and Steward, 1993; Poon et al., 2006; Matsumoto et al., 2007) and microdissected neuropil (Cajigas et al., 2012), a number of mRNA species have been identified at synapses. mRNA transport has been shown to occur in an activity dependent manner. For instance, mRNA of the immediate early gene, *Arc*, as well as *GluR1* and *GluR2* transcripts have been shown to be localized to dendrites following NMDA and metabotropic glutamate receptor activation, respectively (Steward and Worley, 2001; Grooms et al., 2006). Also, depolarization extends transport of mRNA for BDNF and its receptor, TrkB, to the distal processes in neuronal cell culture (Tongiorgi et al., 1997). Studies using protein synthesis inhibitors have shown that protein synthesis is required for behavioral and synaptic plasticity, assumedly for establishing enduring modifications (Kang and Schuman, 1996; Steward and Schuman, 2001). Thus, targeting of specific RNAs to dendrites may be an efficient way of rapidly localizing proteins involved in synaptic function. Alterations in dendritic mRNA transport, stability, or translation could thus modulate synaptic plasticity (Steward and Banker, 1992; Chicurel et al., 1993).

Previous research from our laboratory that examined ethanol regulation of gene expression across a variety of mouse strains has found significant enrichment of genes involved with synaptic functioning and plasticity, reproducibly among several brain regions (Kerns et al., 2005; Wolen et al., 2012). There is also evidence to support that adaptive responses underlying ethanol tolerance and dependence are synaptic in nature, in part involving changes in glutamate neurotransmission (Tsai and Coyle, 1998). Ethanol administration has been shown to induce structural synaptic plasticity as well. Alcohol-preferring rats exposed to 14 weeks of continuous access or subjected to repeated deprivations of ethanol exhibited decreased density and increased size of spines in a subpopulation of neurons in the nucleus accumbens (Zhou et al., 2007). Cortical neurons exposed to chronic intermittent ethanol administration had significant increases in NMDA receptor surface expression (Qiang et al., 2007) and hippocampal cultures receiving prolonged ethanol exposures exhibited increased co-localization of PSD95 and f-actin (Carpenter-Hyland and Chandler, 2006) leading to enlargement of spine heads. Together these data suggest that dendritic spines may be an important target for the adaptive actions of ethanol. Therefore, we investigated whether ethanol evoked changes to the synaptic transcriptome in a well-characterized model of behavioral plasticity, ethanol locomotor sensitization.

It has been proposed that behavioral sensitization is a process that occurs following repeated drug exposure as the result of neuroadaptations in brain reward systems that contribute to such phenomenon as drug craving and relapse in alcoholics (Piazza et al., 1990; Robinson and Berridge, 1993). Intermittent administration of many drugs of abuse, including ethanol, propagates the development of long-lasting sensitized responses to their stimulant effects, often measured as augmented locomotor activation in rodent models (Shuster et al., 1975; Hirabayashi and Alam, 1981; Masur et al., 1986). Behavioral sensitization has been associated with neurochemical and molecular adaptions that effect neurotransmission (Kalivas and Stewart, 1991; White and Kalivas, 1998; Vanderschuren and Kalivas, 2000). There is also evidence that brain regions mediating reinforcement and reward undergo neuroadaptations with cocaine or amphetamine sensitization causing increased incentive salience and self-administration of the drug (Horger et al., 1990; Piazza et al., 1990). Increased voluntary consumption of ethanol has also been observed following intermittent repeated exposure (Lessov et al., 2001; Camarini and Hodge, 2004).

We therefore hypothesize that ethanol-induced sensitization may result, at least in part, from alterations in the synaptic transcriptome, contributing to synaptic remodeling and plasticity. Here we utilize synaptoneurosomes (Williams et al., 2009) prepared from ethanol sensitized DBA2/J mice to enrich for synaptic mRNAs for the purpose of RNAseq analysis. Our expression profiling reveals that repeated ethanol exposure elicits distinctive changes to the complement of mRNA present at the

synapse. Furthermore, our detailed analysis identifies, for the first time, that ethanol behavioral sensitization produces a striking alteration in exon utilization in the synaptic compartment. This analysis of the synaptic transcriptome in response to ethanol sensitization increases our understanding of mechanisms underlying ethanol-induced synaptic plasticity and highlights the complexity of genomic regulation at the subcellular level.

MATERIALS AND METHODS

Ethics Statement

All procedures were approved by Virginia Commonwealth University Institutional Animal Care and Use Committee under protocol AM10332 and followed the NIH Guide for the Care and Use of Laboratory Animals (NIH Publications No. 80-23, 1996).

Animals

Male DBA/2J (D2) mice were purchased from Jackson Laboratories (Bar Harbor, ME) at 8–9 weeks of age. Animals were housed four per cage and had *ad libitum* access to standard rodent chow (#7912, Harlan Teklad, Madison, WI, United States) and water in a 12-h light/dark cycle (6 am on, 6 pm off). Mice were housed with Teklad corn cob bedding (#7092, Harlan Teklad, Madison, WI, United States) and cages were changed weekly. Subjects were allowed to habituate to the animal facility for 1 week prior to starting behavioral experiments. Behavioral assays were performed during the light cycle between the hours of 8 am and 2 pm.

Ethanol-Induced Behavioral Sensitization and Tissue Collection

Ethanol (EtOH) behavioral sensitization was induced as previously described (Costin et al., 2013a,b). Briefly, mice were divided into three treatment groups (n = 16 each): saline–saline (SS), saline–EtOH (SE), and EtOH–EtOH (EE). Mice were acclimated to the behavioral room for 1 hour prior to the start of the experiment on testing days. All locomotor activity was measured immediately following i.p. injection with either saline or ethanol during 10-min sessions in sound-attenuating locomotor chambers (Med Associates, model ENV-515, St. Albans, VT, United States). The system is interfaced with Med Associates software that assesses activity using a set of 16 infrared beam sensors along the X–Y plane. Animals received 2 days of saline injections and placement in the testing apparatus for habituation to the experimental procedure. On test day 3, acute locomotor responses to i.p. saline (SS, SE) or 2.0 g/kg ethanol (EE) were measured. On conditioning days 4–13, animals received daily i.p. injections in their home cages of either saline (SS, SE) or 2.5 g/kg ethanol (EE). On the final testing day 14, the SS group received saline and the SE and EE groups received 2.0 g/kg ethanol and all groups were subsequently monitored in activity chambers for 10 min. On day 14 of the behavioral sensitization paradigm, mice were sacrificed by cervical dislocation 4 h following i.p. injection. Immediately afterward, brains were removed and chilled for one minute in ice-cold 1x phosphate buffered saline. The frontal pole was dissected by making a cut rostral of the optic chiasm and then removing the olfactory bulbs. Excised tissue was stored in a tube on ice for less than 8 min before processing for synaptoneurosome isolation.

Synaptoneurosome Preparation

The protocol for preparation of synaptoneurosomes was adapted from Williams et al. (2009). Fresh tissue from four animals was pooled (approximately 0.45 g) and manually homogenized utilizing a 15 mL Potter-Elvehjem Safe-Grind® tissue grinder (#358009, Wheaton, Millville, NJ, United States) and diluted 1:10 in synaptoneurosome homogenization buffer. The buffer consisted of 0.35 M nuclease free sucrose (CAS #57-50-1, Acros Organics, NJ), 10 mM HEPES (#15630-056, Life Technologies, Carlsbad, CA, United States), and 1 mM EDTA (#AM9260G, Ambion, Carlsbad, CA, United States), which was brought to a pH of 7.4 and filter sterilized. Immediately before use, 0.25 mM DTT (CAS #3483-12-3, Fisher Scientific, Waltham, MA, United States), 30 U/mL RNase Out (#10777-019, Invitrogen, Carlsbad, CA, United States), and protease inhibitor cocktail containing AEBSF, aprotinin, bestatin, E64, leupeptin, and pepstatin A (#1862209, Halt, Thermo Scientific, Rockford, IL, United States) were added to buffer. Centrifugation of whole homogenate (WH) at 500 × g for 10 min at 4°C removed nuclei and cellular debris, yielding pellet, P1 and supernatant, S1. The S1 fraction was passed through a series of nylon filters with successively decreasing pore sizes of 70, 35, and 10 μm (#03-70, #03-35, #03-10, SEFAR, Buffalo, NY). The filtrate was then diluted with 3 volumes of homogenization buffer and centrifuged at 2000 × g for 15 min at 4°C to yield the synaptoneurosome enriched pellet, P2, and a cellular supernatant fraction, S2. Fractions were frozen on dry ice and then stored at −80°C until further processing. Aliquots from each fraction of a synaptoneurosomal preparation were examined for the presence of contaminating nuclei using 4′,6-diamidino-2-phenylindole (DAPI) staining. Representative fields at 20x magnification were assessed for nuclear content.

Transmission Electron Microscopy (TEM)

Morphological integrity of synaptoneurosomes was confirmed by transmission electron microscopy (TEM). The P2 fraction was washed in PBS and centrifuged at 2000 × g for 8 min. The supernatant was decanted and pellet was fixed with 2% glutaraldehyde in 0.1 M sodium cacodylate buffer at room temperature. After initial fixation, the sample was rinsed in 0.1 M cacodylate buffer for 5–10 min and then post-fixed in 1% osmium tetroxide in 0.1 M cacodylate buffer for 1 h, followed by another 5–10 min rinse in 0.1 M cacodylate buffer. Preparation continued with a serial dehydration with ethanol: 50, 70, 80, and 95% – for 5–10 min each, followed by 100% ethanol for 10–15 min (3x), and incubation in propylene oxide for 10–15 min (3x). The sample was then infiltrated with a 50/50 mix of propylene oxide and PolyBed 812 resin (Polysciences, Inc., Warrington, PA, United States) overnight, which was then replaced with pure resin once again overnight. The sample was embedded in a mold, placed in a 60°C oven overnight, and then sectioned with a Leica EM UC6i Ultramicrome (Leica Microsystems, Wetzlar,

Germany), stained with 5% Uranyl acetate and Reynold's Lead Citrate, and examined on JEOL JEM-1230 transmission electron microscope (JEOL USA, Inc., Peabody, MA, United States). Images of various magnifications (2000x–10,000x) were captured with the Gatan Ultrascan 4000 digital camera (Gatan, Inc., Pleasanton, CA, United States).

Immunoblotting

Pellets (P1 and P2) and liquid aliquots (WH, S1, and S2) from synaptoneurosomal preparations were used to perform semi-quantitative immunoblotting. Pellets were triturated with NuPAGE LDS (#NP0008, Life Technologies, Carlsbad, CA, United States) diluted to 1x and containing protease inhibitor cocktail (#1862209, Halt, Thermo Scientific, Rockford, IL, United States), while liquid aliquots were lysed directly with 4x LDS with added proteinase inhibitor. Samples were sonicated on ice water until no longer viscous. Protein concentrations were determined using the bicinchoninic acid assay (#23227, Thermo Scientific, Rockford, IL, United States) and absorbance at 562 nm. Sample concentrations were balanced using 1x LDS, 10x NuPAGE reducing agent (#NP0004, Life Technologies, Carlsbad, CA, United States) and boiled for 10 min. For each synaptoneurosome fraction, 10 μg of protein was loaded per lane on a 10% or a 4–12% NuPAGE bis-tris gel (#NP0303BOX, #NP0322BOX, Life Technologies, Carlsbad, CA, United States). Electrophoresis was performed at 150 V followed by transfer to 0.45 μm nitrocellulose membrane for 1.5 h at 30 V on ice. Membranes were incubated with Ponceau S for 10 min, and densitometric analysis of staining was performed using ImageJ processing and analysis software (National Institutes of Health). Prior to primary antibody incubation, the membranes were blocked with 5% non-fat dried milk in 1x TBST for 45 min. Primary and secondary antibody catalog numbers, dilutions, and incubation times are provided in **Supplementary Table S1**. Immunoblots were visualized on GeneMate Blue Autoradiography film (BioExpress, Kaysville, UT, United States) using the Amersham ECL Western Blotting Detection Reagent (#RPN2106, GE Healthcare Life Sciences, Pittsburgh, PA, United States) and quantified using ImageJ. All detected proteins were normalized to the total protein loaded per well as measured by Ponceau S staining. Statistical analysis of immunoblot data was performed by one-way ANOVA across synaptoneurosome fractions followed by Tukey's *post hoc* analysis.

Quantitative Reverse Transcriptase PCR (qRT-PCR)

Synaptoneurosomal fractions, S2 and P2, prepared from mice subjected to the sensitization protocol were assessed for enrichment of known dendritically-trafficked and somatically-restricted transcripts using qRT-PCR. Total RNA was isolated the using guanidine/phenol/chloroform method (#Cs-502, Stat-60, Tel-Test Inc., Friendswood, TX, United States) and a Tekmar homogenizer as per the STAT-60 protocol. RNA concentration was determined by measuring absorbance at 260 nm and RNA quality was assessed by electrophoresis on an Experion Analyzer (Bio-Rad, Hercules, CA, United States) and 260/280 absorbance ratios. All RNA samples had RNA quality indices (RQI) $\geq$ 7.6 and 260/280 ratios were between 1.97 and 2.06. cDNA was generated from 995 ng of total DNase-treated RNA and 5 ng of luciferase mRNA (#L4561, Promega, Madison, WI, United States) using Deoxyribonuclease I (#18068-015, Invitrogen, Carlsbad, CA, United States) and the iScript cDNA kit (#170-8891, Bio-Rad, Hercules, CA, United States) according to manufacturer's instructions. qRT-PCR was performed using the iCycler iQ system (Bio-Rad, Hercules, CA, United States) according to manufacturer's instructions for iQ SYBR Green Supermix (#170-8880, Bio-Rad, Hercules, CA, United States). Primer sequences, annealing temperatures, amplicon sizes, and cDNA dilutions used for each gene are listed in **Supplementary Table S1**. Relative expression was calculated by comparing Ct values to a standard curve produced from S2 fraction cDNA (diluted 1:5, 1:25, 1:125, 1:625). Expression values were normalized to the exogenous internal reference mRNA, luciferase, to control for losses and inefficacies of downstream processing (Johnson et al., 2005). Statistical analysis of qRT-PCR data was performed using a Student's *t*-test between the two fractions.

RNAseq Library Preparation and Sequencing

RNAseq data have been deposited with the Gene Expression Omnibus resource (GSE73018). Total RNA isolated for qRT-PCR was also used for gene expression profiling using RNAseq performed by the VCU Genomics Core Laboratory. To avoid non-biological experimental variation that arises from sample batch structure, supervised randomization of samples prior to each processing stage (RNA extraction, library amplification, and lane assignment) was performed. A total of four biological replicates, each representing a pool from four animals, were obtained for each treatment group/fraction (**Figure 1**; SSS, SES, EES, SSP, SEP, EEP). Preparation of cDNA libraries was conducted following standard protocols using TruSeq RNA Sample Preparation Kit (#RS-122-2001, Illumina, San Diego, CA, United States). Briefly, mRNA was isolated from total RNA using poly-T oligo-attached magnetic beads and then fragmented in the presence of divalent cations at 94°C. Fragmented RNA was converted into double stranded cDNA followed by ligation of Illumina specific adaptors. Adaptor ligated DNA was amplified with 15 cycles of PCR and purified using QIAquick PCR Purification Kit (#28104, Qiagen, Venlo, Netherlands). Library insert size was determined using an Agilent Bioanalyzer. Library quantification was performed by qRT-PCR assay using KAPA Library Quant Kit (#KK4835, KAPA, Wilmington, MA, United States). RNAseq libraries were analyzed using Illumina TruSeq Cluster V3 flow cells and TruSeq SBS Kit V3 (#FC-401-3001, Illumina, San Diego, CA, United States), with six libraries of different indices pooled together in equal amounts loaded on to a single lane at a concentration of 13 pM and sequenced (2 $\times$ 100 paired end reads) on an Illumina HiSeq 2000. Sample EE6_P2 was removed from subsequent analyses due to over-amplification artifacts.

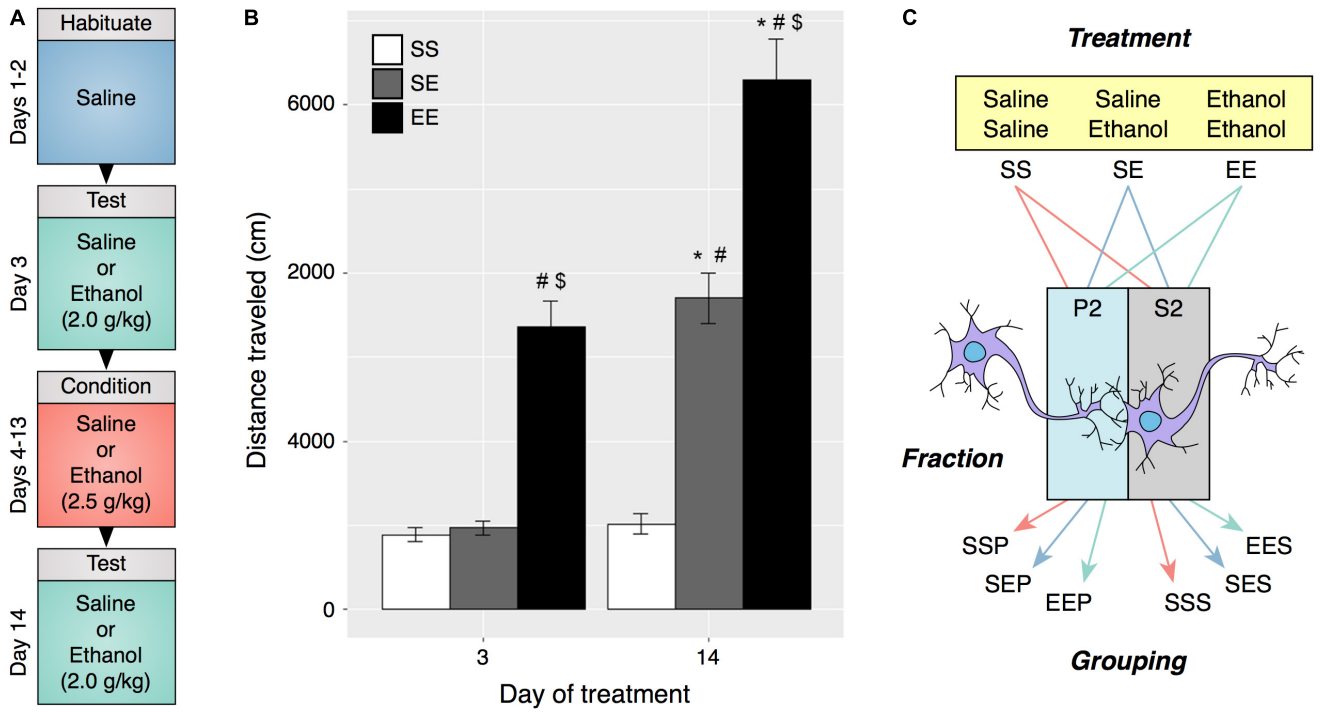

FIGURE 1 | Ethanol behavioral sensitization in male DBA2/J mice. **(A)** Experimental protocol and timeline for induction of behavioral sensitization. **(B)** Repeated ethanol exposure induced behavioral sensitization as measured by locomotor activity on day 14 (EE) as compared to acute ethanol administered on day 3 (EE) and day 14 (SE). **(C)** Experimental groupings used for RNA sequencing and bioinformatic analysis were derived from ethanol treatment type and specific cellular fraction. (#$p < 0.001$ compared to SS within same day, \$$p < 0.001$ compared to SE within same day, *$p < 0.001$ compared to same treatment on day 3, repeated measures two-way ANOVA with Tukey's *post hoc* analysis).

A summary of RNAseq metrics can be found in **Supplementary Table S2**.

RNAseq Alignment

FASTQ formatted sequence files were aligned using TopHat2 v2.0.8 (Kim et al., 2013) with GRCm38/mm10 reference genome and annotations obtained from the UCSC genome table browser[1] (Karolchik, 2004). The C57BL/6 (B6) reference genome (mm10) was edited to include DBA2/J (D2) single nucleotide polymorphisms (Wang et al., 2016). Aligned BAM files produced by TopHat2 were validated for mapping quality with Samtools v0.1.9 (Li et al., 2009) and for completeness using BamUtil v1.0.13[2]. BAM files were converted to sorted SAM files for downstream feature count-based analysis with Samtools.

Differential Gene Expression Analysis

Raw read counts were produced from each SAM file using the python package HTSeq v0.6.1 (Anders et al., 2012) script *htseq-count* with the read overlap handler set to *union*. Resulting raw count files were analyzed for differential gene expression (DGE) between ethanol sensitized (EE) or acutely exposed (SE) animals and ethanol naïve (SS) animals within either the synaptic P2 fractions or the cellular supernatant S2 fractions using the R[3] package edgeR v3.10.2 (Robinson et al., 2010) with a negative binomial generalized log-linear model approach (Mccarthy et al., 2012). Lowly expressed genes were filtered out if not present in at least three libraries with counts per million of 3.4 or greater, corresponding with approximately five total counts in the smallest library. Genes meeting a false discovery rate (FDR) cutoff of 0.10 were considered significantly altered and used in downstream bioinformatic analysis.

Differential Exon Usage Analysis

A GFF annotation file containing collapsed exon counting bins was prepared from the UCSC GRCm38/mm10 GTF file using the DEXSeq v1.16.10 (Anders et al., 2012) Python script *dexseq_prepare_annotation.py* with gene aggregation disabled. The number of reads overlapping each exon bin was then counted using the DEXSeq Python script *dexseq_count.py*, the GFF file, and each sample's SAM file. Differential exon usage (DEU) analysis was then carried out for the same contrasts studied in our DGE analysis using the DEXSeq R package standard analysis workflow. Ensembl transcript IDs produced in the DEXSeq results files were translated to gene symbols using the R package BiomaRt v2.32.0 (Durinck et al., 2009). Genes with transcripts possessing at least one differentially utilized exon bin with an

[1]https://genome.ucsc.edu/cgi-bin/hgTables

[2]http://genome.sph.umich.edu/wiki/BamUtil

[3]https://www.r-project.org

adjusted p-value ($p$adj) less than 0.01 were considered to be significantly altered and were used in downstream bioinformatic analysis.

Bioinformatic Analysis

Functional enrichment analyses for DGE and DEU results were performed using ToppFun, available as part of the ToppGene suite of web-based applications[4] (Chen et al., 2009). Mouse gene symbols were submitted and analyzed for over-representation of genes that belong to Gene Ontology categories (molecular function, biological processes, and cellular component), mouse phenotypes, and biological pathway databases including KEGG and Reactome. Only categories with p-values less than 0.01 and possessing between 3 and 1000 total genes were considered. The webtool REVIGO (Supek et al., 2011) was used for data reduction by semantic similarity, and visualization of GO terms lists resulting from this analysis.

RNA Binding Protein Enrichment Analysis

Genes possessing DEU between EEP and SSP groups ($p$adj < 0.01) were intersected with the genes possessing basal DEU between SSP and SSS groups ($p$adj < 0.01) in order to produce a list of genes with synapse-specific DEU that was also regulated by ethanol sensitization. The same was done to produce a synaptic sensitization-induced DGE gene list using FDR cutoffs of 0.1. These two lists of genes were then intersected with gene list obtained from two public databases of known and predicted RNA binding proteins (RBPs): RBPDB (Cook et al., 2011) and ATtRACT (Giudice et al., 2016). The synaptic ethanol-sensitive DEU gene list was also intersected with a list of mRNA targets of the RBP fragile X mental retardation protein (FMRP), which was obtained from **Supplementary Table S2a** of Darnell et al. (2011). For RNABP and FMRP enrichment analyses, the R package GeneOverlap (version 1.16.0[5]) was used to calculate odds ratios for relative enrichment of synaptic ethanol sensitive DEU genes and Fisher's exact tests to calculate enrichment p-values.

Sequence Motif Analysis

Chromosomal coordinates for the differentially utilized exon bins from the synaptic sensitization-induced DEU gene lists used in the RNABP analysis were provided to BEDTools v2.26.0 (Quinlan and Hall, 2010) in order to obtain their respective nucleotide sequences. Sequences for the 475 exon bins (**Supplementary Table S12**) containing a minimum of eight base pairs were then supplied to the web-based motif discovery tool MEME (Bailey et al., 2009) to search for known or novel motifs common between them. Any motifs identified that met an E-value cutoff of 0.05 were aligned to the CISBP-RNA database of RNABP motifs and specificities using the MEME Suite tool Tomtom (Gupta et al., 2007). Database motif alignments were considered significant if the alignment score had an E-value ≤ 0.05.

[4] toppgene.cchmc.org

[5] http://shenlab-sinai.github.io/shenlab-sinai/

RESULTS

Synaptoneurosome Fractions Are Enriched in mRNA Coding Synaptic Components

DBA/2J (D2) mice were chosen for these studies due to their characteristic sensitivity to ethanol psychomotor stimulation and development of sensitization (Phillips et al., 1994). Distance traveled on test days 3 and 14 was compared and a significant increase in activity on day 14 was interpreted as an induction of ethanol sensitization (**Figures 1A,B**). Daily i.p. injections of 2.5 g/kg ethanol elicited an augmented locomotor response to 2.0 g/kg ethanol on day 14 as compared to day 3 (two-way repeated measures ANOVA, $F_{\text{Treatment}}[2,45] = 96.76$, $p < 0.001$, $F_{\text{Day}}[1.45] = 77.47$, $p < 0.001$, $F_{\text{Interaction}}[2,45] = 16.89$, $p < 0.001$, $n = 16$). Frontal pole brain tissue obtained from mice in this experiment was utilized in preparation of synaptoneurosome enriched samples.

The synaptoneurosomal fractionation protocol (**Supplementary Figure S1A**) was validated in preliminary studies by TEM (**Figure 2A**). As suggested previously (Williams et al., 2009), the intact pre- and post-synaptic terminals, identified by TEM, provide for selective extraction of synaptic mRNAs. Absence of intact nuclei throughout synaptoneurosomal fractions was verified by DAPI staining (**Supplementary Figure S1B**), while immunoblotting for subcellular protein markers was used to ascertain purity of the preparation (**Supplementary Figure S1C**). Together these data indicate that P2 fractions contain synaptic elements enriched for the synaptic protein markers, synaptotagmin and PSD-95 (one-way ANOVA, $F_{\text{SYT}}[4,10] = 9.83$, $p = 0.0017$, $F_{\text{PSD95}}[4,10] = 11.09$, $p = 0.0011$, $n = 3$), and are devoid of appreciable nuclear contamination (one-way ANOVA, $F_{\text{H4}}[4,10] = 125.3$, $p < 0.0001$, $n = 3$),

To ensure enrichment in experimental tissues, total RNA isolated from S2 and P2 fractions of mice subjected to the ethanol behavioral sensitization paradigm was evaluated by qRT-PCR (**Figure 2B**). P2 fractions had higher relative expression levels of known synaptically targeted transcripts, *CamK2a* and *Arc* (Burgin et al., 1990; Link et al., 1995; Lyford et al., 1995), while transcripts known to be somatically restricted, *Gapdh* and *Snrpn* (Litman et al., 1994; Poon et al., 2006), were more abundant in the S2 fraction (Student's paired t-test, $t_{\text{CamK2a}}[7] = 6.941$, $p = 0.0002$, $t_{\text{Arc}}[7] = 2.646$, $p = 0.0331$, $t_{\text{Gapdh}}[7] = 4.181$, $p = 0.0041$, $t_{\text{Snrpn}}[7] = 8.439$, $p < 0.0001$, $n = 8$).

RNAseq was used to evaluate global gene expression in the S2 and P2 fractions (**Supplementary Table S3**). DGE analysis (**Supplementary Tables S4**, **S5**) demonstrated widespread and highly significant differences in P2 vs. S2 samples at the gene level in saline control samples (SSP_SSS), with 1829 genes differentially expressed at an FDR ≤ 0.1 and $\log_2$ fold-change ≥ 1 or ≤ -1. Of these, 1408 were found to be enriched (>twofold increased expression) in the P2 fraction (**Supplementary Table S5**) and 421 enriched in the S2 fraction (**Supplementary Table S5**). Of note, our RNAseq data faithfully replicated the qRT-PCR results of **Figure 2B**, even though derived

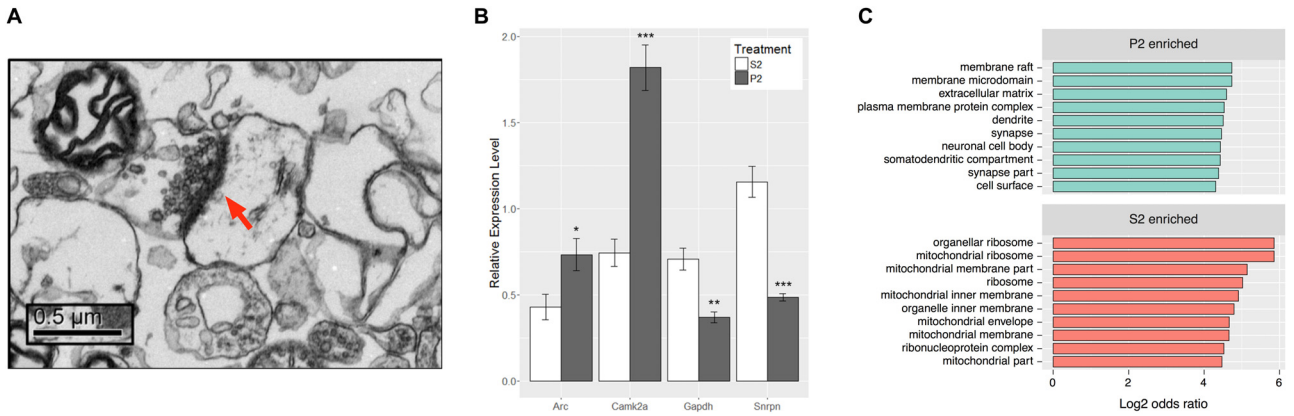

FIGURE 2 | Synaptoneurosome preparation produces distinct RNA populations between P2 and S2 fractions. **(A)** Representative electron micrograph from P2 fraction observed at 10,000x magnification. Post-synaptic density is labeled by red arrow and presynaptic elements with synaptic vesicles can be observed immediately adjacent. **(B)** RNA isolated from S2 and P2 fractions of behaviorally sensitized mice was assayed for transcripts of known subcellular localization to ensure enrichment of synaptic RNAs. *Camk2a* and *Arc* are transcripts known to be synaptically targeted, while *Gapdh* and *Snrpn* are somatically restricted. Paired Student's *t*-test between fraction for each gene, *Camk2a* ($t[7] = 6.941$, $^{***}p = 0.0002$), *Arc* ($t[7] = 2.646$, $^{*}p = 0.0331$), *Gapdh* ($t[7] = 4.181$, $^{**}p = 0.0041$), *Snrpn* ($t[7] = 8.439$, $^{****}p < 0.0001$), $n = 8$. **(C)** Top 10 Gene Ontology Cellular Compartment categories according to *p*-value as derived from functional enrichment analysis of the untreated P2 enriched gene list (SSP vs. SSS), sorted by $\log_2$ of the categories' odds ratio.

from a totally separate experiment and synaptoneurosome preparation (**Supplementary Table S6**). This supports the rigor of our RNAseq studies. Functional enrichment analysis of the P2 enriched gene list revealed significant over-representation of cellular categories related to the structure of the synapse (**Figure 2C**) and molecular or biological categories relating to calcium ion binding, cell adhesion, and growth factor binding among others relevant to the synapse (**Supplementary Table S5**). In contrast, the S2 fraction showed cellular category enrichment relating to protein synthesis and mitochondria (**Supplementary Table S5**). These results establish that, in contrast to the cellular supernatant S2 fraction, the P2 synaptoneurosome fraction was enriched for mRNA relevant to synaptic function.

Sensitizing Ethanol Treatment Alters the Synaptic Transcriptome

To focus our attention on functional reorganization of the synapse occurring with acute ethanol or ethanol sensitization, we identified treatment-responsive DGE within cellular fractions through gene-level analyses in edgR. For these analyses, we used only an FDR cutoff ($\leq$0.1) without further filtering for fold-change. **Figure 3A** and **Supplementary Table S7** show that more than twice as many genes responded to ethanol sensitization (EEP vs. SSP; $n = 776$) as to acute ethanol (SEP vs. SSP; $n = 375$) in the P2 fraction. The S2 fraction (**Figure 3B** and **Supplementary Table S8**) showed an even larger divergence between acute and repeated ethanol exposures with 686 genes regulated by sensitization (EES vs. SSS) and 126 responding to acute ethanol (SES vs. SSS).

Functional over-representation analysis of these DGE groups showed striking divergence between responses to acute vs. sensitizing ethanol treatments within both the P2 and S2 compartments. REVIGO semantic similarity analysis was used to group similar Gene Ontology Biological Process categories and thus reduce the complexity of the functional group analysis. **Figure 3D** demonstrates functional clusters relating to post-synaptic membrane potential, post-translational protein modification, protein folding, and molecular chaperones and mitochondrial respiratory function in the EEP vs. SSP comparison. In contrast, none of these clusters are present in the SEP vs. SSP analysis of acute ethanol responses (**Figure 3D**), which did show categories related to actin filament function and small GTPase signal transduction (**Figure 3C**). Similarly, the EES vs. SSS and SES vs. SSS comparisons showed functional dissimilarity with each other and the P2 comparisons for the most part (**Figures 3E,F**) except for the occurrence of clusters relating to molecular chaperone function in the EES vs. SSS comparison, similar to that seen in the P2 sensitization response (**Figure 3D**). Complete details of all functional over-representation studies for these group comparisons are contained in **Supplementary Tables S6**, **S7**. Overall, this gene level functional analysis suggests that ethanol sensitization produces a striking synaptic transcriptome response with changes in expression groups affecting energy production, protein trafficking/folding, and post-synaptic membrane currents.

Ethanol Sensitization Is Accompanied by Differential Splicing Events

Since differential splicing and transcript utilization are prominent in the nervous system, we performed an exon-level analysis of treatment effects within the P2 and S2 compartments using DEXSeq. We used a more stringent statistical threshold (adjusted *p*-value $\leq$ 0.01) to defined DEU due to the nearly 30-fold greater number of exons detected ($n = 356{,}131$; **Supplementary Table S9**) compared to the number of genes detected with edgR ($n = 11{,}764$; **Supplementary Table S3**). DEXSeq analysis

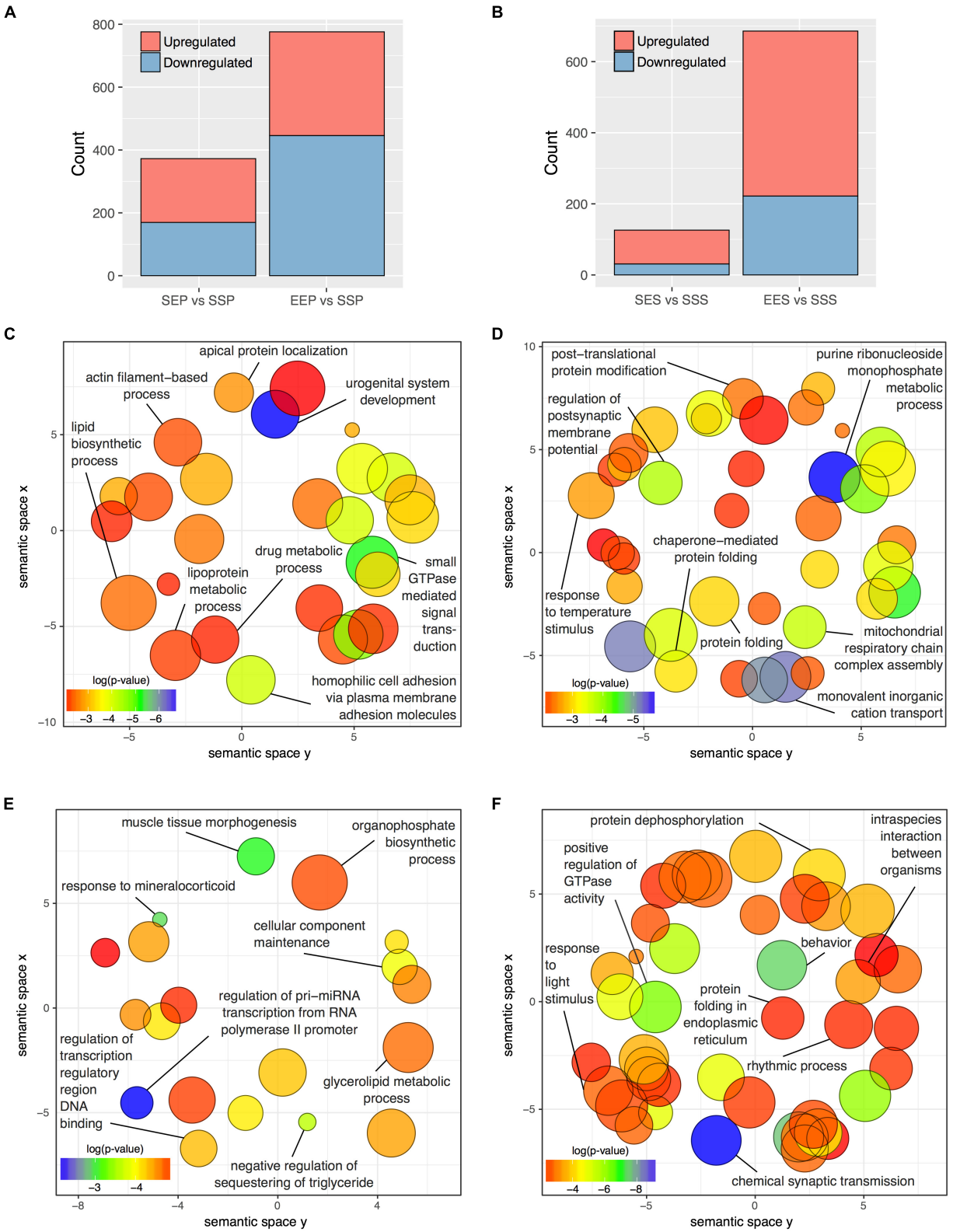

FIGURE 3 | DGE in P2 and S2 fractions following acute ethanol exposure or sensitization. The number of genes found to be significantly altered (FDR < 0.1) by sensitization and acute exposure to ethanol treatments in the **(A)** P2 fraction and **(B)** S2 fractions. Scatterplots of representative Gene Ontology Biological Process categories derived from functional enrichment analysis of genes regulated by acute ethanol **(C,E)** or ethanol sensitization **(D,F)** in the P2 fraction **(C,D)** and S2 fraction **(E,F)**. Scatterplots depict semantic similarity on axes, dispensability by size, and $\log_{10}$ *p*-value as color.

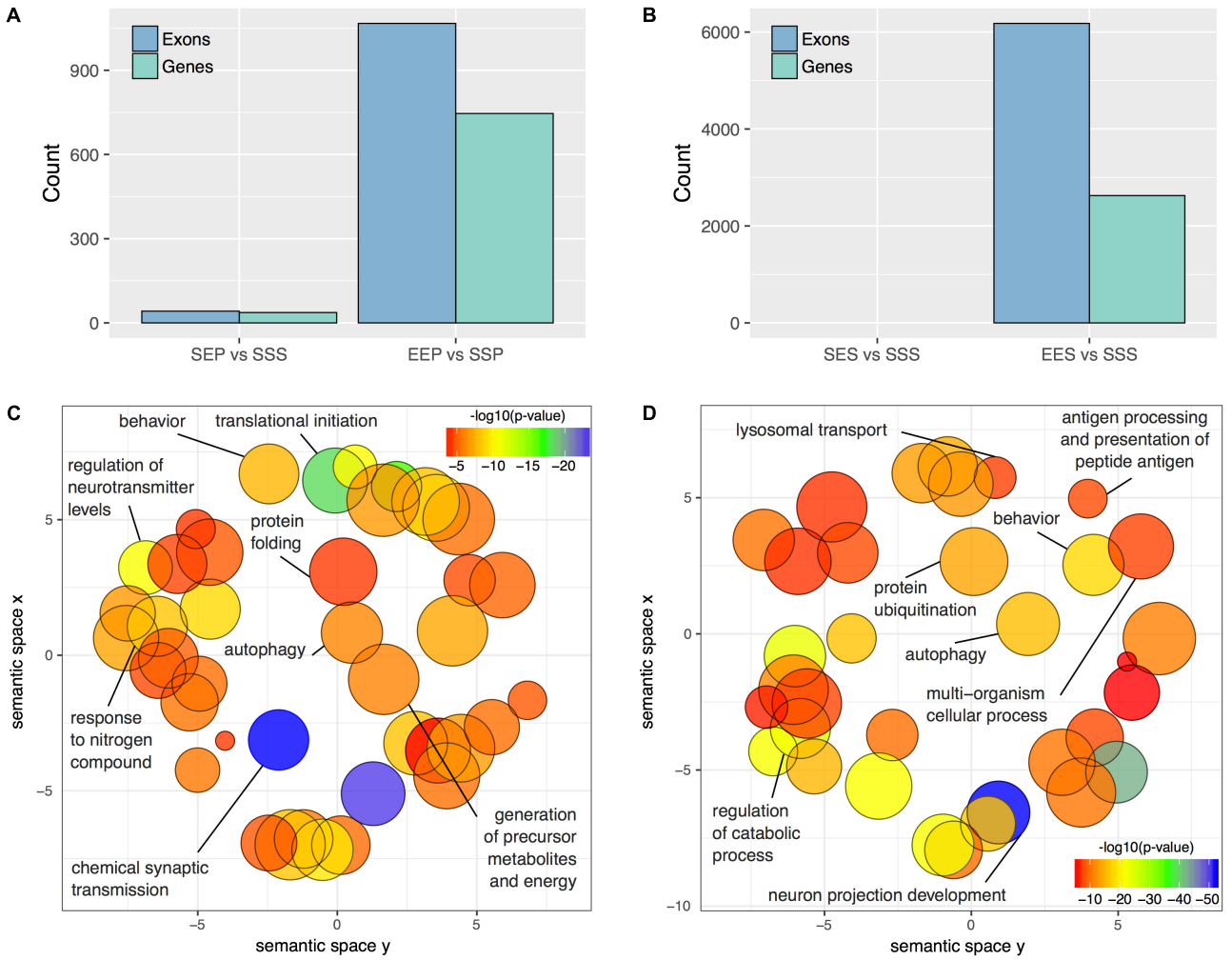

FIGURE 4 | DEU in P2 and S2 fractions following acute ethanol exposure or sensitization. The number of differentially utilized exons (*padj* < 0.01) and unique genes possessing a minimum of one differentially utilized exon observed in the P2 **(A)** and S2 **(B)** fractions following acute ethanol exposure or sensitization. Gene Ontology reduction plots depicting clustering of top biological processes associated with ethanol sensitization and acute exposure induced DEU are displayed for the P2 **(C)** and S2 **(D)** fractions.

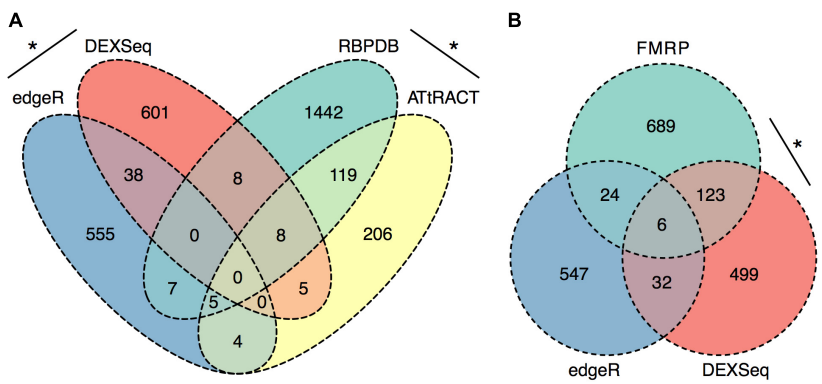

FIGURE 5 | Synapse-Specific DEU is enriched in RNABP targets. Ethanol sensitization altered synaptic exon usage for targets of RNA binding proteins. Ethanol sensitization did not enrich gene expression or differential exon usage **(A)** of RNA binding proteins at synapses. Synaptic DEU but not DGE were enriched for targets of FMRP following ethanol sensitization **(B)** (*$p < 0.05$, Fisher's exact test).

revealed widespread alternative splicing events in the frontal pole S2 and P2 of ethanol sensitized mice. 1067 exons were differentially utilized in the P2 fraction following ethanol sensitization (EEP vs. SSP), representing 746 unique genes (**Figure 4A** and **Supplementary Table S10**). In contrast, only 42 exons representing 36 genes were differentially utilized in the acute ethanol exposure group (SEP vs. SSP; **Figure 4A** and **Supplementary Table S10**). In the somatic fractions of sensitized mice, 6179 exons representing 2627 genes were differentially utilized (EES vs. SSS), whereas no exons passed our statistical threshold in the acute ethanol exposure group (**Figure 4B** and **Supplementary Table S11**).

Functional enrichment analysis of P2 genes affected by ethanol sensitization-induced DEU revealed perturbed Gene Ontology Biological Processes ($p < 0.01$) relevant to translation regulation, mRNA processing, protein stability, and synaptic function (**Figure 4C** and **Supplementary Table S10**). In contrast, Gene Ontology Biological Processes affected by sensitization ($p < 0.01$) in the S2 fraction were primarily involved in catabolism, autophagy, and regulation of cellular morphology (**Figure 4D** and **Supplementary Table S11**). Over-representation analysis was not performed for the acute ethanol exposure groups due to the low level of affected exons.

RNA Binding Protein Targets Are Enriched in P2 Exons Regulated by Ethanol Sensitization

To further evaluate the RNA processing and translation-related functional categories present in the ethanol sensitization-dependent P2 DEU functional enrichment analysis, the significant P2 DEU and DGE gene lists were analyzed for enrichment in RBPs using two publicly available databases, RBPDB and ATtRACT. To focus more conservatively on synaptic mRNA regulated by ethanol sensitization, we used the intersection of EEP vs. SSP and SSP vs. SSS gene or exon datasets for these analyses. The DGE (**Supplementary Table S4**) and DEU (**Supplementary Table S12**) gene lists showed a modest but significant overlap with each other (OR = 2.3, $p = 1 \times 10^{-5}$) as did the databases of RBPDB and ATtRACT (OR = 8.8, $p = 9.6 \times 10^{-63}$; **Figure 5A**). However, the DGE list was not enriched for RNABPs from RBPDB (OR = 0.3, $p = 1$) or ATtRACT (OR = 1, $p = 0.59$) nor was the DEU list enriched for RNABPs from RBPDB (OR = 0.3, $p = 1$) or ATtRACT (OR = 1.3, $p = 0.22$; **Figure 5A**).

The same sensitization-induced synaptic DGE and DEU gene lists were then evaluated for enrichment of RNA targets of a synaptically ubiquitous RNABP, FMRP. FMRP has previously been identified as being involved in ethanol regulation of $GABA_B$ receptor membrane abundance (Wolfe et al., 2016). The DGE gene list was not found to be enriched in FMRP targets (OR = 1.4, $p = 0.07$) whereas the DEU gene list showed marked over-representation for FMRP targets (OR = 7.2, $p = 1.1 \times 10^{-56}$; **Figure 5B**).

Due to the lack of enrichment of RNABPs but over-representation of RNABP targets in the sensitization-induced synaptic DEU gene list, the possibility for novel or known sequence motifs governing RNABP target preference was investigated within the differentially utilized exon bins. Exon bin sequences were supplied to the web-based motif discovery tool MEME and five novel sequence motifs were detected within the exon list having E-values ≤ 0.05 (**Table 1** and **Supplementary Table S13**). Of these, four were also found to have high sequence alignment with known RNABP sequence preferences ($E \leq 0.05$) from the CISRNA-BP database. These findings suggest that a discreet set of RNABPs may regulate synaptic trafficking of ethanol sensitization-responsive transcripts.

DISCUSSION

The studies contained here provided the first genomic analysis of acute ethanol and ethanol sensitization regulation of the synaptic transcriptome. Using a well-characterized synaptoneurosomal preparation, we validated enrichment of synapse-related mRNA. RNAseq analysis showed that both acute ethanol and ethanol sensitization, a model of behavioral plasticity, produced unique changes in the synaptic transcriptome. In particular, ethanol sensitization produced increased synaptic expression of genes that function in protein synthesis and folding and dendritic structure, among others. We also demonstrated, using an exon-level analysis, a striking preponderance of differential exon utilization occurring following ethanol sensitization. The genes showing DEU with ethanol sensitization were over-represented for targets of specific RBPs, including FMRP. Thus, ethanol sensitization has a major impact on the synaptic transcriptome in both regulation of gene expression and transcript composition. The genes identified here as regulated by ethanol sensitization in the synaptic transcriptome may provide unique understanding of the mechanisms underlying synaptic plasticity contributing to behavioral changes occurring with chronic ethanol exposure.

Neurons are highly specialized polarized cells, whose dendritic and axonal arborizations contain thousands of synapses that function and change individually in response to stimulation (Steward and Levy, 1982; Steward et al., 1998; Wallace et al., 1998). It has been proposed that activity-dependent synaptic plasticity requires the transport and translation of specific mRNA species, creating a unique complement of proteins that are able to function in response to a specific stimulus (Bramham and Wells, 2007). Comparing the somatic and synaptic transcriptomes in response to acute or sensitizing treatments of ethanol, we were able to detect compartmentalized differences in ethanol regulation of gene expression. Through our initial characterization studies, we are confident in our assessment that the differences observed when analyzing the P2 and S2 fractions are a survey of ethanol's effect on gene expression in distinct subcellular locations. The exact means by which ethanol is exerting its regulation of the synaptic transcriptome has yet to be determined. Conceivably, ethanol could be affecting synaptic transcript abundances through overall modulation of gene expression that could have a global effect on mRNA levels within the cell, and ultimately, through the mere altered availability of transcript, results in changes at the synapse. Our data indicate that this is not an adequate explanation, as we were

TABLE 1 | Sequence motif discovery in P2 ethanol sensitization-regulated exons.

Motif	Logo	*E*-value	Similar motifs
1	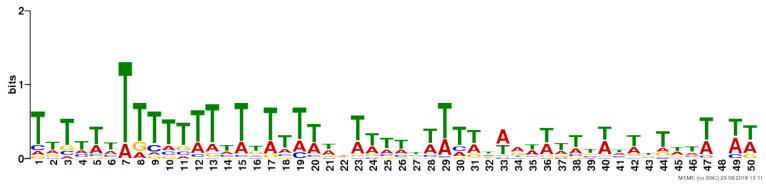	1×10^{-170}	Gm10110
2	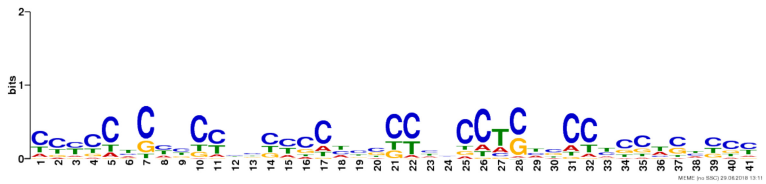	3.6×10^{-93}	Srsf4
3	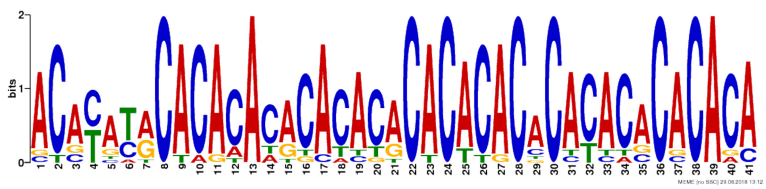	3.8×10^{-13}	Celf3 Celf4 Hnrpll Rbm38
4	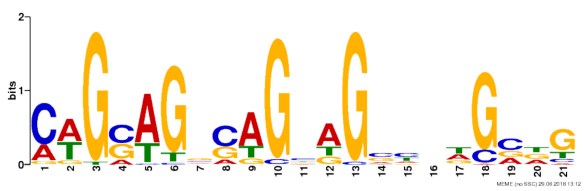	1.2×10^{-8}	None known
5	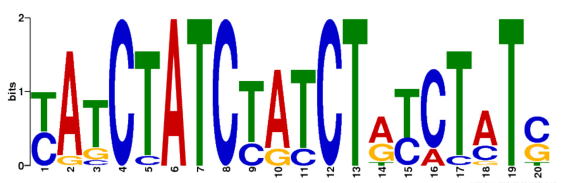	2.5×10^{-8}	Hnrpdl

able to detect distinct gene sets representing different biological function categories in the P2 and S2 fractions. Furthermore, there was a striking lack of overlap between functional categories regulated by acute vs. sensitizing ethanol treatments, despite both assays being done at the same time frame post-ethanol exposure. This is clear evidence of reorganization of the synaptic transcriptome with chronic ethanol exposure.

The trafficking and localization of transcripts to the synapse offers another possible means of regulatory control. Synaptic tagging is a process whereby synaptic activation induces a transient synapse-specific change that allows the synapse to capture mRNA or proteins required for long-term plasticity, which has explicitly been studied for its role in long-term potentiation (Frey and Morris, 1997). The exact physical nature of the synaptic tag has not been absolutely defined, but candidate molecular tags that have been proposed include post-translation modifications to existing synaptic proteins, alterations to protein conformational states, initiation of localized translation or proteolysis, and reorganization of the local cytoskeleton (Martin and Kosik, 2002; Kelleher et al., 2004; Doyle and Kiebler, 2011). All of these mechanisms have the potential of being initiated by signaling events that result from membrane receptor activation. For instance, one pharmacological effect of ethanol is the release of dopamine in the nucleus accumbens, which when acting at D1-like receptors increases activity of adenylyl cyclase, thereby increasing cAMP levels and PKA activity. It has been shown that PKA activation is required for the formation of the synaptic tag (Casadio et al., 1999; Barco et al., 2002). The premise that signaling cascades downstream of ethanol could alter the ability of activated synapses to capture dendritically targeted mRNA requires examination.

Regardless of the exact mechanisms for synaptic localization of mRNA, our data here clearly suggest that differential activation or expression of RBPs by ethanol sensitization may be a major mechanism for restructuring the synaptic transcriptome to produce enhanced locomotor activation following repeated ethanol exposure. Our motif binding overrepresentation analysis of DEU results adds supportive evidence for ethanol sensitization utilizing specific mRNA binding proteins for modulating the synaptic transcriptome by identifying five novel consensus

sequences with high similarity to known or predicted RNABP targets. Furthermore, this mechanism is strongly supported by our finding that genes with ethanol sensitization-induced DEU in the synaptic fraction are strongly over-represented for targets of the mRNA binding protein FMRP. FMRP is a known RNA-binding protein involved in mRNA transport and regulation of synaptic protein translation, as well as dendritic spine development (Darnell et al., 2011; Cruz-Martin et al., 2012; Michaelsen-Preusse et al., 2018). Prior studies on ethanol and FMRP have shown that the protein can regulate an acute ethanol-induced alteration in GABA type B receptor (GABABR) dendritic expression (Wolfe et al., 2016). Spencer et al. (2016) also showed that chronic ethanol exposure altered expression of NMDA, Kv4.2, and KChIP3 in hippocampus in an FMRP-dependent fashion, possibly by altering phosphorylation of FMRP and its translational inhibitory properties. Our studies here greatly extend this connection between ethanol, FMRP, and synaptic plasticity. **Figure 5** demonstrates that 20% (129/660; $p = 1.1 \times 10^{-56}$) of the genes showing ethanol sensitization-induced DEU and enriched in the P2 fraction also overlapped with presumed FMRP target mRNA. This utilization of FMRP targeting by ethanol sensitization clearly implicates this subset of genes in mechanisms of ethanol-induced synaptic plasticity and may have implications for overlap of AUD with other neurological disorders.

Another major finding in these studies is that repeated dosing of ethanol to produce sensitization in D2 males induces substantially more DGE than acute ethanol in both the P2 and S2 fractions. Strikingly, DEU was almost exclusively seen in the ethanol sensitized mice. The bioinformatics analysis of our P2 candidate gene list indicated that transcripts altered in response to repeated ethanol are significantly enriched for biological functions associated with post-synaptic membrane potential, posttranslational protein modifications, protein folding and molecular chaperones, and mitochondrial function. Previously, our laboratory has shown that ethanol regulates transcription and mRNA abundance of molecular chaperones *in vitro* and *in vivo* (Miles et al., 1991, 1994; Kerns et al., 2005). The present study extends these findings by providing evidence that this regulation may be localized or at least occurring at the synapse. Acute ethanol induced significantly fewer expression changes that represented distinct biological categories including actin filament and small GTPase signal transduction. The robust expression response to ethanol sensitization is striking in that some of our prior studies have documented actual habituation of some expression responses (*Sgk1*) to acute ethanol following ethanol sensitization induction (Costin et al., 2013a).

The large expression responses to both acute ethanol and ethanol sensitization with gene-level analysis of our RNAseq data was in striking contrast to our finding that ethanol sensitization alone led to robust alterations of exon usage in both the synaptoneurosome and somatic fractions. Very few exons were differentially utilized following acute ethanol. However, the categories of genes altered by ethanol sensitization either at the gene level or exon utilization show functional overlap with biological processes of RNA translation, RNA processing, and cellular energetics. This functional over-representation is consistent with altered demands on synaptic activity and synaptic protein synthesis with sensitization. However, the striking predominance of exon utilization regulation by sensitization suggests that a form of transcriptional plasticity accompanying the synaptic and behavioral plasticity seen with repeated ethanol exposure. The mechanism(s) for such differential exon utilization may be linked to the need for trafficking mRNA to the synapse. Such a response is suggested by our finding that sensitization-responsive DEU genes were over-represented for FMRP target mRNA, but that at the gene level, sensitization did not evoke an over-representation of FMRP targets in the synaptic transcriptome (data not shown). The mechanism whereby sensitization might alter promoter utilization, splicing or mRNA stability in producing such a robust DEU response at the synapse remains to be determined.

In *a prior* study, Most et al. (2015) reported microarray analysis of expression changes in a synaptoneurosome preparation from amygdala in C57BL/6J mice following prolonged ethanol oral consumption. That study also identified changes relating to protein synthesis in the ethanol-regulated synaptic mRNA. However, there was no clear connection to a form of plasticity in their studies, although progressive ethanol consumption is thought to involve synaptic plasticity. Furthermore, those studies did not involve an exon-level analysis so direct comparison to our results here is not possible. Regardless, Most et al. (2015) did find a much more vigorous ethanol-responsive gene expression regulation in the synaptoneurosome as compared to a total cellular lysate. Their studies thus complement our findings on the dramatic response to ethanol at the level of the synaptic transcriptome. Together, our studies emphasize the importance of analyzing ethanol transcriptional responses at a more precise cellular and subcellular level so as to more clearly identify biological mechanisms and consequences. A minor drawback to both our current studies and those of Most et al. (2015) is the lack of validation of RNAseq results by additional techniques such as RT-PCR or western blot analysis, or preferably, by cellular resolution techniques such as *in situ* hybridization or immunohistochemistry. Such studies were not a major goal of the current report, where we have focused on network- or pathway-level finding rather that single genes. We did provide at least a partial cross validation of our molecular findings in our studies on select candidate genes shown in **Figure 2B** and **Supplementary Table S6**. However, future detailed cellular validation studies are clearly needed.

Using expression analysis, our study is the first to characterize regulation of the synaptic transcriptome by ethanol (or any exogenous drug) in an *in vivo* model of synaptic plasticity. With repeated intermittent exposure to ethanol that resulted in a sensitized response, we observed changes to the complement of mRNA present at the synapse and alterations in the exonic composition of synaptic mRNA that we hypothesize contribute to the development of the behavioral phenotype in D2 mice. The individual genes and functional groups (e.g., molecular

chaperones) identified in these studies provide important new information regarding the mechanisms of ethanol-induced synaptic plasticity. Perhaps most importantly, however, our studies have identified that ethanol sensitization uniquely regulates exon utilization at the synapse in a manner that implicates specific RBP targeting, such as by FMRP. Functional analyses will be required to further validate these results with the ultimate goal of disrupting synaptic targeting of specific transcripts or groups of transcripts in order to causally relate this mechanism to synaptic plasticity and modulation of ethanol behaviors.

AUTHOR CONTRIBUTIONS

MO'B and MM conceived and designed the study. MO'B conducted primary behavioral studies, synaptoneurosome optimization and isolation, and initial molecular studies. RMW conducted primary RNAseq analysis including detailed exon-level studies and motif analysis. NS and SB performed initial low-level analysis of RNAseq data. JB assisted with electron microscopy studies. AP and RWW provided DBA/2J genomic sequence data to identify SNP modifications to C57BL6/J genome for RNAseq alignments. MO'B, RMW, and MM conducted bioinformatics analyses and prepared primary versions of the manuscript. JW assisted on manuscript design, editing, and interpretation of results. MM provided resources for conducting experiments.

FUNDING

Funding was provided by NIAAA grants U01AA016667, P50AA022537, and R01AA020634 to MM, F31AA021035 to MO'B, F30 AA026497 to RMW, and U01AA013499 to RWW.

ACKNOWLEDGMENTS

We would like to thank Dr. Myrna Serrano for cDNA library preparation and running the RNAseq studies, Dr. Sean Farris for assistance during the pilot stages of this project, and members of the Miles laboratory for helpful discussion.

Motifs are ranked by *E*-value and nucleotide letter sizes in logos are proportionate to relative frequency within motif sequence. Four of the novel motifs have high sequence similarity with known or predicted RBP target sequence preferences (*E*-value ≤ 0.05).

SUPPLEMENTARY MATERIAL

The Supplementary Material for this article can be found online at: https://www.frontiersin.org/articles/10.3389/fgene.2018.00402/full#supplementary-material

FIGURE S1 | Characterization of the synaptoneurosome preparation. **(A)** Schematic depicting synaptoneurosome preparation. Whole homogenate (WH) processed from pooled frontal pole tissue of four mice was used in the centrifugation/filtration scheme depicted here. The initial pellet (P1) contained cellular debris and nuclei. The supernatant from the initial centrifugation (S1) was filtered and subjected to a second centrifugation. The pellet, P2, was enriched for synaptic elements and dendritically targeted RNA as compared to the supernatant, S2, which contained the remainder of the somatodendritic RNA. **(B)** DAPI staining of synaptoneurosome fractions at 20x magnification indicting that most, if not all the nuclei were removed during the initial centrifugation step to produce the P1 pellet. **(C)** Quantification of immunoblots probing subcellular protein markers across synaptoneurosome fractions (H4 = nuclear; LDH = cytosolic; PSD95 = post-synaptic; SYT = presynaptic).

TABLE S1 | (a) Antibody specifications. **(b)** qRT-PCR primer specifications.

TABLE S2 | RNA-Seq metrics.

TABLE S3 | EdgeR CPM data (gene level).

TABLE S4 | EdgeR differential expression results (unfiltered data).

TABLE S5 | P2 enriched and S2 enriched genes and ToppGene analysis.

TABLE S6 | RNAseq results for control genes.

TABLE S7 | EEP_SSP or SEP_SSP regulated genes (RNA-Seq, edgeR, FDR = 0.1), ToppFun functional enrichment analysis summary.

TABLE S8 | EES_SSS or SES_SSS regulated genes (RNA-Seq, edgeR, FDR = 0.1), ToppFun functional enrichment analysis summary.

TABLE S9 | DEXSeq differential exon usage results (unfiltered data).

TABLE S10 | EEP_SSP or SEP_SSP regulated exon genes (RNA-Seq, DEXSeq, *p*adj < 0.01), ToppFun functional enrichment analysis summary.

TABLE S11 | EES_SSS or SES_SSS regulated exon genes (RNA-Seq, DEXSeq, *p*adj < 0.01), ToppFun functional enrichment analysis summary.

TABLE S12 | Synapse-specific differential exon usage.

TABLE S13 | MEME motif count matrices.

REFERENCES

Anders, S., Reyes, A., and Huber, W. (2012). Detecting differential usage of exons from RNA-seq data. *Genome Res.* 22, 2008–2017. doi: 10.1101/gr.133744.111

Bailey, T. L., Boden, M., Buske, F. A., Frith, M., Grant, C. E., Clementi, L., et al. (2009). MEME Suite: tools for motif discovery and searching. *Nucleic Acids Res.* 37, W202–W208. doi: 10.1093/nar/gkp335

Barco, A., Alarcon, J. M., and Kandel, E. R. (2002). Expression of constitutively active CREB protein facilitates the late phase of long-term potentiation by enhancing synaptic capture. *Cell* 108, 689–703. doi: 10.1016/S0092-8674(02)00657-8

Bramham, C. R., and Wells, D. G. (2007). Dendritic mRNA: transport, translation and function. *Nat. Rev. Neurosci.* 8, 776–789. doi: 10.1038/nrn2150

Burgin, K. E., Waxham, M. N., Rickling, S., Westgate, S. A., Mobley, W. C., and Kelly, P. T. (1990). In situ hybridization histochemistry of Ca2+/calmodulin-dependent protein kinase in developing rat brain. *J. Neurosci.* 10, 1788–1798. doi: 10.1523/JNEUROSCI.10-06-01788.1990

Cajigas, I. J., Tushev, G., Will, T. J., Tom Dieck, S., Fuerst, N., and Schuman, E. M. (2012). The local transcriptome in the synaptic neuropil revealed by deep sequencing and high-resolution imaging. *Neuron* 74, 453–466. doi: 10.1016/j.neuron.2012.02.036

Camarini, R., and Hodge, C. W. (2004). Ethanol preexposure increases ethanol self-administration in C57BL/6J and DBA/2J mice. *Pharmacol. Biochem. Behav.* 79, 623–632. doi: 10.1016/j.pbb.2004.09.012

Carpenter-Hyland, E. P., and Chandler, L. J. (2006). Homeostatic plasticity during alcohol exposure promotes enlargement of dendritic spines. *Eur. J. Neurosci.* 24, 3496–3506. doi: 10.1111/j.1460-9568.2006.05247.x

Casadio, A., Martin, K. C., Giustetto, M., Zhu, H., Chen, M., Bartsch, D., et al. (1999). A transient, neuron-wide form of CREB-mediated long-term facilitation can be stabilized at specific synapses by local protein synthesis. *Cell* 99, 221–237. doi: 10.1016/S0092-8674(00)81653-0

Chen, J., Bardes, E. E., Aronow, B. J., and Jegga, A. G. (2009). ToppGene Suite for gene list enrichment analysis and candidate gene prioritization. *Nucleic Acids Res.* 37, W305–W311. doi: 10.1093/nar/gkp427

Chicurel, M. E., Terrian, D. M., and Potter, H. (1993). mRNA at the synapse: analysis of a synaptosomal preparation enriched in hippocampal dendritic spines. *J. Neurosci.* 13, 4054–4063. doi: 10.1523/JNEUROSCI.13-09-04054.1993

Cook, K. B., Kazan, H., Zuberi, K., Morris, Q., and Hughes, T. R. (2011). RBPDB: a database of RNA-binding specificities. *Nucleic Acids Res.* 39, D301–D308. doi: 10.1093/nar/gkq1069

Costin, B. N., Dever, S. M., and Miles, M. F. (2013a). Ethanol regulation of serum glucocorticoid kinase 1 expression in DBA2/J mouse prefrontal cortex. *PLoS One* 8:e72979. doi: 10.1371/journal.pone.0072979

Costin, B. N., Wolen, A. R., Fitting, S., Shelton, K. L., and Miles, M. F. (2013b). Role of adrenal glucocorticoid signaling in prefrontal cortex gene expression and acute behavioral responses to ethanol. *Alcohol Clin. Exp. Res.* 37, 57–66. doi: 10.1111/j.1530-0277.2012.01841.x

Cruz-Martin, A., Crespo, M., and Portera-Cailliau, C. (2012). Glutamate induces the elongation of early dendritic protrusions via mGluRs in wild type mice, but not in fragile X mice. *PLoS One* 7:e32446. doi: 10.1371/journal.pone.0032446

Darnell, J. C., Van Driesche, S. J., Zhang, C., Hung, K. Y., Mele, A., Fraser, C. E., et al. (2011). FMRP stalls ribosomal translocation on mRNAs linked to synaptic function and autism. *Cell* 146, 247–261. doi: 10.1016/j.cell.2011.06.013

Doyle, M., and Kiebler, M. A. (2011). Mechanisms of dendritic mRNA transport and its role in synaptic tagging. *EMBO J.* 30, 3540–3552. doi: 10.1038/emboj.2011.278

Durinck, S., Spellman, P. T., Birney, E., and Huber, W. (2009). Mapping identifiers for the integration of genomic datasets with the R/ Bioconductor package biomaRt. *Nat. Protoc.* 4, 1184–1191. doi: 10.1038/nprot.2009.97

Frey, U., and Morris, R. G. (1997). Synaptic tagging and long-term potentiation. *Nature* 385, 533–536. doi: 10.1038/385533a0

Giudice, G., Sánchez-Cabo, F., Torroja, C., and Lara-Pezzi, E. (2016). ATtRACT-a database of RNA-binding proteins and associated motifs. *Database* 2016:baw035. doi: 10.1093/database/baw035

Grooms, S. Y., Noh, K. M., Regis, R., Bassell, G. J., Bryan, M. K., Carroll, R. C., et al. (2006). Activity bidirectionally regulates AMPA receptor mRNA abundance in dendrites of hippocampal neurons. *J. Neurosci.* 26, 8339–8351. doi: 10.1523/JNEUROSCI.0472-06.2006

Gupta, S., Stamatoyannopoulos, J. A., Bailey, T. L., and Noble, W. S. (2007). Quantifying similarity between motifs. *Genome Biol.* 8:R24. doi: 10.1186/gb-2007-8-2-r24

Hirabayashi, M., and Alam, M. R. (1981). Enhancing effect of methamphetamine on ambulatory activity produced by repeated administration in mice. *Pharmacol. Biochem. Behav.* 15, 925–932. doi: 10.1016/0091-3057(81)90056-3

Horger, B. A., Shelton, K., and Schenk, S. (1990). Preexposure sensitizes rats to the rewarding effects of cocaine. *Pharmacol. Biochem. Behav.* 37, 707–711. doi: 10.1016/0091-3057(90)90552-S

Johnson, D. R., Lee, P. K., Holmes, V. F., and Alvarez-Cohen, L. (2005). An internal reference technique for accurately quantifying specific mRNAs by real-time PCR with application to the tceA reductive dehalogenase gene. *Appl. Environ. Microbiol.* 71, 3866–3871. doi: 10.1128/AEM.71.7.3866-3871.2005

Kalivas, P. W., and Stewart, J. (1991). Dopamine transmission in the initiation and expression of drug- and stress-induced sensitization of motor activity. *Brain Res. Brain Res. Rev.* 16, 223–244. doi: 10.1016/0165-0173(91)90007-U

Kang, H., and Schuman, E. M. (1996). A requirement for local protein synthesis in neurotrophin-induced hippocampal synaptic plasticity. *Science* 273, 1402–1406. doi: 10.1126/science.273.5280.1402

Karolchik, D. (2004). The UCSC Table Browser data retrieval tool. *Nucleic Acids Res.* 32, 493D–496D. doi: 10.1093/nar/gkh103

Kelleher, R. J. III, Govindarajan, A., and Tonegawa, S. (2004). Translational regulatory mechanisms in persistent forms of synaptic plasticity. *Neuron* 44, 59–73. doi: 10.1016/j.neuron.2004.09.013

Kerns, R. T., Ravindranathan, A., Hassan, S., Cage, M. P., York, T., Sikela, J. M., et al. (2005). Ethanol-responsive brain region expression networks: implications for behavioral responses to acute ethanol in DBA/2J versus C57BL/6J mice. *J. Neurosci.* 25, 2255–2266. doi: 10.1523/JNEUROSCI.4372-04.2005

Kim, D., Pertea, G., Trapnell, C., Pimentel, H., Kelley, R., and Salzberg, S. L. (2013). TopHat2: accurate alignment of transcriptomes in the presence of insertions, deletions and gene fusions. *Genome Biol.* 14:R36. doi: 10.1186/gb-2013-14-4-r36

Lessov, C. N., Palmer, A. A., Quick, E. A., and Phillips, T. J. (2001). Voluntary ethanol drinking in C57BL/6J and DBA/2J mice before and after sensitization to the locomotor stimulant effects of ethanol. *Psychopharmacology* 155, 91–99. doi: 10.1007/s002130100699

Li, H., Handsaker, B., Wysoker, A., Fennell, T., Ruan, J., Homer, N., et al. (2009). The Sequence Alignment / Map format and SAMtools. *Bioinformatics* 25, 2078–2079. doi: 10.1093/bioinformatics/btp352

Link, W., Konietzko, U., Kauselmann, G., Krug, M., Schwanke, B., Frey, U., et al. (1995). Somatodendritic expression of an immediate early gene is regulated by synaptic activity. *Proc. Natl. Acad. Sci. U.S.A.* 92, 5734–5738. doi: 10.1073/pnas.92.12.5734

Litman, P., Barg, J., and Ginzburg, I. (1994). Microtubules are involved in the localization of tau mRNA in primary neuronal cell cultures. *Neuron* 13, 1463–1474. doi: 10.1016/0896-6273(94)90432-4

Lyford, G. L., Yamagata, K., Kaufmann, W. E., Barnes, C. A., Sanders, L. K., Copeland, N. G., et al. (1995). Arc, a growth factor and activity-regulated gene, encodes a novel cytoskeleton-associated protein that is enriched in neuronal dendrites. *Neuron* 14, 433–445. doi: 10.1016/0896-6273(95)90299-6

Martin, K. C., and Kosik, K. S. (2002). Synaptic tagging – who's it? *Nat. Rev. Neurosci.* 3, 813–820. doi: 10.1038/nrn942

Masur, J., Oliveira, De Souza, M. L., and Zwicker, A. P. (1986). The excitatory effect of ethanol: absence in rats, no tolerance and increased sensitivity in mice. *Pharmacol. Biochem. Behav.* 24, 1225–1228. doi: 10.1016/0091-3057(86)90175-9

Matsumoto, M., Setou, M., and Inokuchi, K. (2007). Transcriptome analysis reveals the population of dendritic RNAs and their redistribution by neural activity. *Neurosci. Res.* 57, 411–423. doi: 10.1016/j.neures.2006.11.015

Mccarthy, D. J., Chen, Y., and Smyth, G. K. (2012). Differential expression analysis of multifactor RNA-Seq experiments with respect to biological variation. *Nucleic Acids Res.* 40, 4288–4297. doi: 10.1093/nar/gks042

Michaelsen-Preusse, K., Feuge, J., and Korte, M. (2018). Imbalance of synaptic actin dynamics as a key to fragile X syndrome. *J. Physiol.* 596, 2773–2782. doi: 10.1113/JP275571

Miles, M. F., Diaz, J. E., and Deguzman, V. S. (1991). Mechanisms of neuronal adaptation to ethanol. Ethanol induces Hsc70 gene transcription in NG108-15 neuroblastoma x glioma cells. *J. Biol. Chem.* 266, 2409–2414.

Miles, M. F., Wilke, N., Elliot, M., Tanner, W., and Shah, S. (1994). Ethanol-responsive genes in neural cells include the 78-kilodalton glucose-regulated protein (GRP78) and 94-kilodalton glucose-regulated protein (GRP94) molecular chaperones. *Mol. Pharmacol.* 46, 873–879.

Most, D., Ferguson, L., Blednov, Y., Mayfield, R. D., and Harris, R. A. (2015). The synaptoneurosome transcriptome: a model for profiling the emolecular effects of alcohol. *Pharmacogenom. J.* 15, 177–188. doi: 10.1038/tpj.2014.43

Nestler, E. J. (2001). Molecular neurobiology of addiction. *Am. J. Addict.* 10, 201–217. doi: 10.1080/105504901750532094

Nestler, E. J., Hope, B. T., and Widnell, K. L. (1993). Drug addiction: a model for the molecular basis of neural plasticity. *Neuron* 11, 995–1006. doi: 10.1016/0896-6273(93)90213-B

Phillips, T. J., Dickinson, S., and Burkhart-Kasch, S. (1994). Behavioral sensitization to drug stimulant effects in C57BL/6J and DBA/2J inbred mice. *Behav. Neurosci.* 108, 789–803. doi: 10.1037/0735-7044.108.4.789

Piazza, P. V., Deminiere, J. M., Le Moal, M., and Simon, H. (1990). Stress- and pharmacologically-induced behavioral sensitization increases vulnerability to acquisition of amphetamine self-administration. *Brain Res.* 514, 22–26. doi: 10.1016/0006-8993(90)90431-A

Poon, M. M., Choi, S. H., Jamieson, C. A., Geschwind, D. H., and Martin, K. C. (2006). Identification of process-localized mRNAs from cultured rodent hippocampal neurons. *J. Neurosci.* 26, 13390–13399. doi: 10.1523/JNEUROSCI.3432-06.2006

Qiang, M., Denny, A. D., and Ticku, M. K. (2007). Chronic intermittent ethanol treatment selectively alters N-methyl-D-aspartate receptor subunit surface expression in cultured cortical neurons. *Mol. Pharmacol.* 72, 95–102. doi: 10.1124/mol.106.033043

Quinlan, A. R., and Hall, I. M. (2010). BEDTools: a flexible suite of utilities for comparing genomic features. *Bioinformatics* 26, 841–842. doi: 10.1093/bioinformatics/btq033

Rao, A., and Steward, O. (1993). Evaluation of RNAs present in synaptodendrosomes: dendritic, glial, and neuronal cell body contribution. *J. Neurochem.* 61, 835–844. doi: 10.1111/j.1471-4159.1993.tb03594.x

Robinson, M. D., Mccarthy, D. J., and Smyth, G. K. (2010). edgeR: a Bioconductor package for differential expression analysis of digital gene expression data. *Bioinformatics* 26, 139–140. doi: 10.1093/bioinformatics/btp616

Robinson, T. E., and Berridge, K. C. (1993). The neural basis of drug craving: an incentive-sensitization theory of addiction. *Brain Res. Brain Res. Rev.* 18, 247–291. doi: 10.1016/0165-0173(93)90013-P

Shuster, L., Webster, G. W., and Yu, G. (1975). Increased running response to morphine in morphine-pretreated mice. *J. Pharmacol. Exp. Ther.* 192, 64–67.

Spencer, K. B., Mulholland, P. J., and Chandler, L. J. (2016). FMRP Mediates Chronic Ethanol-Induced Changes in NMDA, Kv4.2, and KChIP3 Expression in the Hippocampus. *Alcohol Clin. Exp. Res.* 40, 1251–1261. doi: 10.1111/acer.13060

Steward, O., and Banker, G. A. (1992). Getting the message from the gene to the synapse: sorting and intracellular transport of RNA in neurons. *Trends Neurosci.* 15, 180–186. doi: 10.1016/0166-2236(92)90170-D

Steward, O., and Levy, W. B. (1982). Preferential localization of polyribosomes under the base of dendritic spines in granule cells of the dentate gyrus. *J. Neurosci.* 2, 284–291. doi: 10.1523/JNEUROSCI.02-03-00284.1982

Steward, O., and Reeves, T. M. (1988). Protein-synthetic machinery beneath postsynaptic sites on CNS neurons: association between polyribosomes and other organelles at the synaptic site. *J. Neurosci.* 8, 176–184. doi: 10.1523/JNEUROSCI.08-01-00176.1988

Steward, O., and Schuman, E. M. (2001). Protein synthesis at synaptic sites on dendrites. *Annu. Rev. Neurosci.* 24, 299–325. doi: 10.1146/annurev.neuro.24.1.299

Steward, O., Wallace, C. S., Lyford, G. L., and Worley, P. F. (1998). Synaptic activation causes the mRNA for the IEG Arc to localize selectively near activated postsynaptic sites on dendrites. *Neuron* 21, 741–751. doi: 10.1016/S0896-6273(00)80591-7

Steward, O., and Worley, P. F. (2001). Selective targeting of newly synthesized Arc mRNA to active synapses requires NMDA receptor activation. *Neuron* 30, 227–240. doi: 10.1016/S0896-6273(01)00275-6

Supek, F., Bošnjak, M., Škunca, N., and Šmuc, T. (2011). Revigo summarizes and visualizes long lists of gene ontology terms. *PLoS One* 6:e21800. doi: 10.1371/journal.pone.0021800

Tongiorgi, E., Righi, M., and Cattaneo, A. (1997). Activity-dependent dendritic targeting of BDNF and TrkB mRNAs in hippocampal neurons. *J. Neurosci.* 17, 9492–9505. doi: 10.1523/JNEUROSCI.17-24-09492.1997

Tsai, G., and Coyle, J. T. (1998). The role of glutamatergic neurotransmission in the pathophysiology of alcoholism. *Annu. Rev. Med.* 49, 173–184. doi: 10.1146/annurev.med.49.1.173

Vanderschuren, L. J., and Kalivas, P. W. (2000). Alterations in dopaminergic and glutamatergic transmission in the induction and expression of behavioral sensitization: a critical review of preclinical studies. *Psychopharmacology* 151, 99–120. doi: 10.1007/s002130000493

Wallace, C. S., Lyford, G. L., Worley, P. F., and Steward, O. (1998). Differential intracellular sorting of immediate early gene mRNAs depends on signals in the mRNA sequence. *J. Neurosci.* 18, 26–35. doi: 10.1523/JNEUROSCI.18-01-00026.1998

Wang, X., Pandey, A. K., Mulligan, M. K., Williams, E. G., Mozhui, K., Li, Z., et al. (2016). Joint mouse-human phenome-wide association to test gene function and disease risk. *Nat. Commun.* 7:10464. doi: 10.1038/ncomms10464

White, F. J., and Kalivas, P. W. (1998). Neuroadaptations involved in amphetamine and cocaine addiction. *Drug Alcohol Depend.* 51, 141–153. doi: 10.1016/S0376-8716(98)00072-6

Williams, C., Mehrian Shai, R., Wu, Y., Hsu, Y. H., Sitzer, T., Spann, B., et al. (2009). Transcriptome analysis of synaptoneurosomes identifies neuroplasticity genes overexpressed in incipient Alzheimer's disease. *PLoS One* 4:e4936. doi: 10.1371/journal.pone.0004936

Wolen, A. R., Phillips, C. A., Langston, M. A., Putman, A. H., Vorster, P. J., Bruce, N. A., et al. (2012). Genetic dissection of acute ethanol responsive gene networks in prefrontal cortex: functional and mechanistic implications. *PLoS One* 7:e33575. doi: 10.1371/journal.pone.0033575

Wolfe, S. A., Workman, E. R., Heaney, C. F., Niere, F., Namjoshi, S., Cacheaux, L. P., et al. (2016). FMRP regulates an ethanol-dependent shift in GABABR function and expression with rapid antidepressant properties. *Nat. Commun.* 7:12867. doi: 10.1038/ncomms12867

Zhou, F. C., Anthony, B., Dunn, K. W., Lindquist, W. B., Xu, Z. C., and Deng, P. (2007). Chronic alcohol drinking alters neuronal dendritic spines in the brain reward center nucleus accumbens. *Brain Res.* 1134, 148–161. doi: 10.1016/j.brainres.2006.11.046

Conflict of Interest Statement: The authors declare that the research was conducted in the absence of any commercial or financial relationships that could be construed as a potential conflict of interest.

The handling Editor declared a shared affiliation, though no other collaboration, with the authors AP and RWW at the time of review.

frontiers in Genetics

ORIGINAL RESEARCH
published: 25 September 2018
doi: 10.3389/fgene.2018.00370

Genetic Contribution to Initial and Progressive Alcohol Intake Among Recombinant Inbred Strains of Mice

Megan K. Mulligan[1], Wenyuan Zhao[1], Morgan Dickerson[1], Danny Arends[2], Pjotr Prins[3], Sonia A. Cavigelli[4], Elena Terenina[5], Pierre Mormede[5], Lu Lu[1] and Byron C. Jones[1]**

[1] Department of Genetics, Genomics, and Informatics, The University of Tennessee Health Science Center, Memphis, TN, United States, [2] Albrecht Daniel Thaer-Institut für Agrar- und Gartenbauwissenschaften, Humboldt-Universität zu Berlin, Berlin, Germany, [3] Biomedical Genetics, University Medical Center Utrecht, Utrecht, Netherlands, [4] Department of BioBehavioral Health, The Pennsylvania State University, University Park, PA, United States, [5] GenPhySE, INRA, ENVT, Université de Toulouse, Castanet-Tolosan, France

We profiled individual differences in alcohol consumption upon initial exposure and during 5 weeks of voluntary alcohol intake in female mice from 39 BXD recombinant inbred strains and parents using the drinking in the dark (DID) method. In this paradigm, a single bottle of 20% (v/v) alcohol was presented as the sole liquid source for 2 or 4 h starting 3 h into the dark cycle. For 3 consecutive days mice had access to alcohol for 2 h followed by a 4th day of 4 h access and 3 intervening days where alcohol was not offered. We followed this regime for 5 weeks. For most strains, 2 or 4 h alcohol intake increased over the 5-week period, with some strains demonstrating greatly increased intake. There was considerable and heritable genetic variation in alcohol consumption upon initial early and sustained weekly exposure. Two different mapping algorithms were used to identify QTLs associated with alcohol intake and only QTLs detected by both methods were considered further. Multiple suggestive QTLs for alcohol intake on chromosomes (Chrs) 2, 6, and 12 were identified for the first 4 h exposure. Suggestive QTLs for sustained intake during later weeks were identified on Chrs 4 and 8. Thirty high priority candidate genes, including *Entpd2*, *Per3*, and *Fto* were nominated for early and sustained alcohol intake QTLs. In addition, a suggestive QTL on Chr 15 was detected for change in 2 h alcohol intake over the duration of the study and *Adcy8* was identified as a strong candidate gene. Bioinformatic analyses revealed that early and sustained alcohol intake is likely driven by genes and pathways involved in signaling, and/or immune and metabolic function, while a combination of epigenetic factors related to alcohol experience and genetic factors likely drives progressive alcohol intake.

Keywords: BXD, DID, QTL, alcoholism, alcohol intake, genetic variation, B6, D2

OPEN ACCESS

Edited by:
Feng C. Zhou,
Indiana University Bloomington, United States

Reviewed by:
Mark Z. Kos,
University of Texas Rio Grande Valley Edinburg, United States
Steven Hicks,
Penn State Hershey Children's Hospital, United States

****Correspondence:***
Megan K. Mulligan
mkmulligan@uthsc.edu;
mmulliga@uthsc.edu
Byron C. Jones
bjone129@uthsc.edu

Specialty section:
This article was submitted to Behavioral and Psychiatric Genetics, a section of the journal Frontiers in Genetics

Received: *25 May 2018*
Accepted: *22 August 2018*
Published: *25 September 2018*

Citation:
Mulligan MK, Zhao W, Dickerson M, Arends D, Prins P, Cavigelli SA, Terenina E, Mormede P, Lu L and Jones BC (2018) Genetic Contribution to Initial and Progressive Alcohol Intake Among Recombinant Inbred Strains of Mice. Front. Genet. 9:370. doi: 10.3389/fgene.2018.00370

INTRODUCTION

According to Cloninger (1987) and Babor et al. (1992) there are multiple types of alcohol use disorders and likely different genetic contributions to each type. For each, though there is an initiating event, usually voluntary consumption and subsequent developments from avoidance to steady-state or ever increasing consumption and associated problems.

Genetic populations of animals have been used to model individual differences in the propensity to consume alcohol. One murine population that has contributed greatly to

alcohol and addiction research is the BXD recombinant inbred family derived from C57BL/6J (B6) and DBA/2J (D2) inbred strains. Mice from these parental strains were crossbred to produce an F_1 generation and then this generation was interbred for several generations to produce genetically segregating stocks. Next, families were selected for inbreeding to fix the alleles. The approach is described in more detail by Peirce et al. (2004). The result is a large number of inbred strains in which the alleles from B6 and D2 were recombined and redistributed. The BXD strains are segregating over five million variants that distinguish the parental B6 and D2 strains and all of the strains have been densely genotyped. Over 10 brain regions have been subjected to microarray analysis of gene expression and there is a freely available database[1] consisting of more than 5,000 phenotypes contributed by many laboratories. This includes over 15 alcohol-related data sets in which the BXD family has been used to measure alcohol acceptance, consumption and preference (Phillips et al., 1994; Rodriguez et al., 1994; Gill et al., 1996; Fernandez et al., 1999); metabolism (Browman and Crabbe, 2000; Grisel et al., 2002; Philip et al., 2010); hypothermia, withdrawal, tolerance, and sensitivity (Belknap et al., 1993; Roberts et al., 1995; Crabbe et al., 1996; Phillips et al., 1996; Buck et al., 1997; Crabbe, 1998; Browman and Crabbe, 2000; Philip et al., 2010); locomotor response (Phillips et al., 1995; Browman and Crabbe, 2000; Philip et al., 2010); ethanol induced conditioned taste aversion (Risinger and Cunningham, 1998); and ethanol conditioned place preference (Cunningham, 1995). This family also contributed to the most detailed meta-analysis of genes that contribute to the predisposition for high alcohol consumption (Mulligan et al., 2006).

The research that we present here is a continuation of these studies in which we report on initial early intake and sustained alcohol consumption over a 5-week period in 39 BXD strains using the "drinking in the dark" (DID) protocol described by Rhodes et al. (2005). This protocol is used to elicit high alcohol consumption over a short time span and has been used to model binge-like alcohol consumption. There was considerable genetic variation among inbred strains of mice in alcohol intake using the DID paradigm (Rhodes et al., 2007; Crabbe et al., 2014). However, the DID procedure has typically been used to measure intake during a single week and has never been used to measure alcohol intake over multiple weeks in a recombinant inbred population. Here, we leverage the BXD family and accompanying legacy molecular, alcohol-trait, and other existing phenotypes to provide a systems genetics analysis of the factors driving alcohol consumption in the BXD family.

MATERIALS AND METHODS

Animals

The subjects were female mice from 39 BXD recombinant inbred mouse strains and the two parental strains for the BXDs, B6 and D2 (within strain replicates ranged from 1 to 16, **Supplementary Table S1**). The animals were 60–80 days old at the start of the study. The mice were individually housed and fed a standard laboratory diet (Harlan Teklad 7912) with food and water available *ad libitum* except during exposure to alcohol (see below). The light cycle was 23:00 h lights on and 11:00 h lights off. This light cycle facilitated alcohol administration and measurement of alcohol intake. Mice were weighed weekly, and all procedures included here were approved by the UTHSC Institutional Animal Care and Use Committee.

Drinking in the Dark

Alcohol consumption was evaluated using the DID method (Rhodes et al., 2005). The protocol calls for 4 consecutive days of testing. Each day, starting on a Tuesday 3 h after lights were turned off, the water bottles were removed from the cages and replaced with 15 ml centrifuge tubes filled with 20% (v/v) ethanol from 95% USP ethanol. On days 1–3 (Tuesday through Thursday) the length of exposure was 2 h and on the 4th day (Friday) the exposure was 4 h. No alcohol was offered in the intervening period (Saturday through Monday). This protocol was repeated weekly for 5 weeks. Tubes were weighed immediately before and after the exposure period. Volume consumed was converted to g/kg body weight of ethanol. Subsequent weekly 2 or 4 h measurements were averaged by strain and used as the dependent variable for data analysis and QTL mapping. The data were deposited in Gene Network (GN)[1] and are available as traits 20010 through 20014 and 20077 through 20082 in the BXD Published Phenotypes database.

Data Analysis

Statistical evaluation of daily alcohol intake was performed by ANOVA testing in R using the ***lm*** function for a 1 between-subjects variable (strain). Heritability at each time point was estimated from the ANOVA results by ss_{strain}/ss_{total} (where ss = sum of squares, Belknap, 1998). Average weekly 2 h or 4 h intake was used to compute slopes and intercepts for each strain over the 5-week observation period.

Genetic correlational analyses among the DID phenotypes, between the DID phenotypes and BXD legacy phenotype data, and traditional quantitative trait loci (QTL) analysis were performed using a combination of R and GN software (Sloan et al., 2016)[1]. Traditional interval mapping in GN was performed using a simple regression method (Haley–Knott or HK) to compute QTL probability given strain genotypes and alcohol intake averaged by strain (Chesler et al., 2005; Mulligan et al., 2017). For traditional interval mapping, genome-wide suggestive (adjusted $p < 0.63$) and significant (adjusted $p < 0.05$) thresholds were determined based on 1,000 permutations of the trait data for each phenotype (GN default). The suggestive threshold is very permissive (see GN glossary of terms and features at www.genenetwork.org/glossary.html for more details) but strikes a balance between detection of false positives and highlighting loci that might be worth further investigation.

QTL analysis using genome-wide efficient mixed model association (GEMMA; Zhou and Stephens, 2012) was performed as a secondary method to traditional HK mapping in GN version 2 to assess the effect of population structure (kinship) between individuals. Full GEMMA Linear Mixed Model (LMM)

[1] www.GeneNetwork.org

support with the optional leave one chromosome out (LOCO) method was recently added to GN. GEMMA software is a computationally efficient LMM method for QTL mapping while explicitly accounting for genetic non-independence within each sample (Zhou and Stephens, 2012). Even for small sample sizes, after running Haley-Knott QTL mapping, GEMMA potentially allows for explorative fine-tuning of results at the SNP level. At each time point, and for each of 7,320 SNPs and phenotypes, we fitted the LMM using a kinship matrix K computed over the SNP genotypes. We also estimated significance thresholds with GEMMA using a permutation approach computing results 1,000 times while shuffling the phenotypes but keeping the genotypes and K the same (Churchill and Doerge, 1994). From every permutation we stored the highest Wald-test p-value in an ordered set and set the significance threshold at the 95th percentile and the suggestive threshold at the 67th percentile. For our data set, the average GEMMA significance threshold was LOD 4.1 and the average suggestive threshold was at LOD 3.3.

GEMMA was included as a mapping method for two main reasons. The first reason is that additional power can be gained when using mixed-model association methods. The increase in power results both from accounting for phenotypic covariance due to genetic similarity and by conditioning on associated markers as opposed to a single candidate locus (Yang et al., 2014). The second reason is that the impact of background structure on QTL detection has not been rigorously evaluated in BXD data sets. Thus, GEMMA can be applied in addition to traditional HK mapping to minimize detection of false positive QTLs resulting from kinship. QTLs identified by both approaches are unlikely to result from genetic similarity. Using both approaches has advantages over using a single mapping model because genetic relatedness is not addressed by the HK model and our data set is small (e.g., underpowered) for GEMMA.

For both HK and GEMMA QTL mapping methods, a 1.5 LOD drop from the top marker was used to define QTL confidence interval regions. Loci detected using traditional HK mapping (suggestive threshold or above) that were also detected using the secondary GEMMA method (LOD > 3) were considered for further analysis.

Enrichment analysis was performed using tools available at Enrichr (Kuleshov et al., 2016). Default settings were used for Enrichr.

B6 and D2 polymorphic genes with SNPs and/or small insertions/deletions (InDels) were identified using tools available at the Sanger Institute Mouse Genomes Project[2] (Keane et al., 2011). The Sanger website provides annotations for variants and, for our analysis, a SNP or InDel was considered to be of potentially high impact if it was annotated as a "coding sequence variant," "feature elongation," "feature truncation," "incomplete terminal codon variant," "initiator codon variant," "mature miRNA variant," "missense variant," "NMD transcript variant," "regulatory region ablation," "regulatory region amplification," "regulatory region variant," "splice acceptor variant," "splice donor variant," "splice region variant," "stop gained," "stop lost," "TF binding site variant," "TFBS ablation," "TFBS amplification," "transcript ablation," or "transcript amplification."

A large BXD database of hippocampal gene expression profiles generated from 67 naïve BXD strains [Hippocampus Consortium M430v2 (Jun 06); GN110; (Overall et al., 2009)] was used to prioritize candidate genes based on correlation with DID week 1 and 4 h phenotype data and cis expression QTL (eQTL) mapping.

For all candidate genes, literature associations between the term "alcohol" and each candidate gene were mined using the Chilibot[3] website (Chen and Sharp, 2004).

RESULTS

Initial Alcohol Consumption Is Variable and Heritable in the BXD Panel and Increases Over Time

Intake of 20% alcohol for 2 or 4 h during the first and 5th week was variable in female B6, D2, and 39 BXD strains (**Figure 1**). Alcohol intake during the first 2 h exposure ranged from 1 to 3.55 g/kg compared to the last 2 h (week 5 day 3 or W5D3) exposure, which ranged from 1.67 to 5.01 g/kg. On the first 4 h exposure, alcohol intake ranged from 2.42 to 6.33 g/kg compared to intake on the last exposure, which ranged from 2.77 to 7.41 g/kg. ANOVA revealed a significant strain effect (all $p < 0.0001$) on intake for each time point with associated heritability estimates of 0.3 or greater, except for the first exposure on week 1 day 1 (W1D1) and W4D4 (**Table 1**). As expected, heritability on the first exposure to alcohol is lower than on subsequent exposure. Also as expected, heritability of 2 h weekly intake averaged for each strain over 3 days is much higher than strain-averaged 4 h intake resulting from a single measurement.

Average 2 or 4 h intake across all strains and the overall distribution of intake changed between week 1 and later weeks reflecting changes in drinking patterns that resulted from increased consumption over time (**Figure 1**). For 2 h intake, week was significantly associated ($p < 0.0001$; $R^2 = 0.039$) with a 0.14 g/kg increase in alcohol intake per week (∼0.6 g/kg average increase in intake between weeks 1 and 5). For 4 h intake, week was significantly associated ($p < 0.0001$; $R^2 = 0.025$) with a 0.2 g/kg increase in alcohol intake per week (∼0.8 g/kg average increase in intake between weeks 1 and 5). Pairwise correlations between initial daily, 2 h weekly average, and 4 h weekly alcohol intake tended to be higher between adjacent weeks and degrade as the interval between each week increases (**Supplementary Figure S1**).

Genetic Differences in Alcohol Intake Over Time

Most strains demonstrated a gradual increase in alcohol intake over time (**Table 2**) during 2 or 4 h exposure. Strains with significantly increased 2 h intake over the 5-week period included BXD 40, 24, 49, 34, 50, 77, and 83. Of these strains, BXD 34, 50, 77, and 83 also demonstrated significantly elevated 4 h intake. Of

[2]http://www.sanger.ac.uk/sanger/Mouse_SnpViewer/

[3]www.chilibot.net

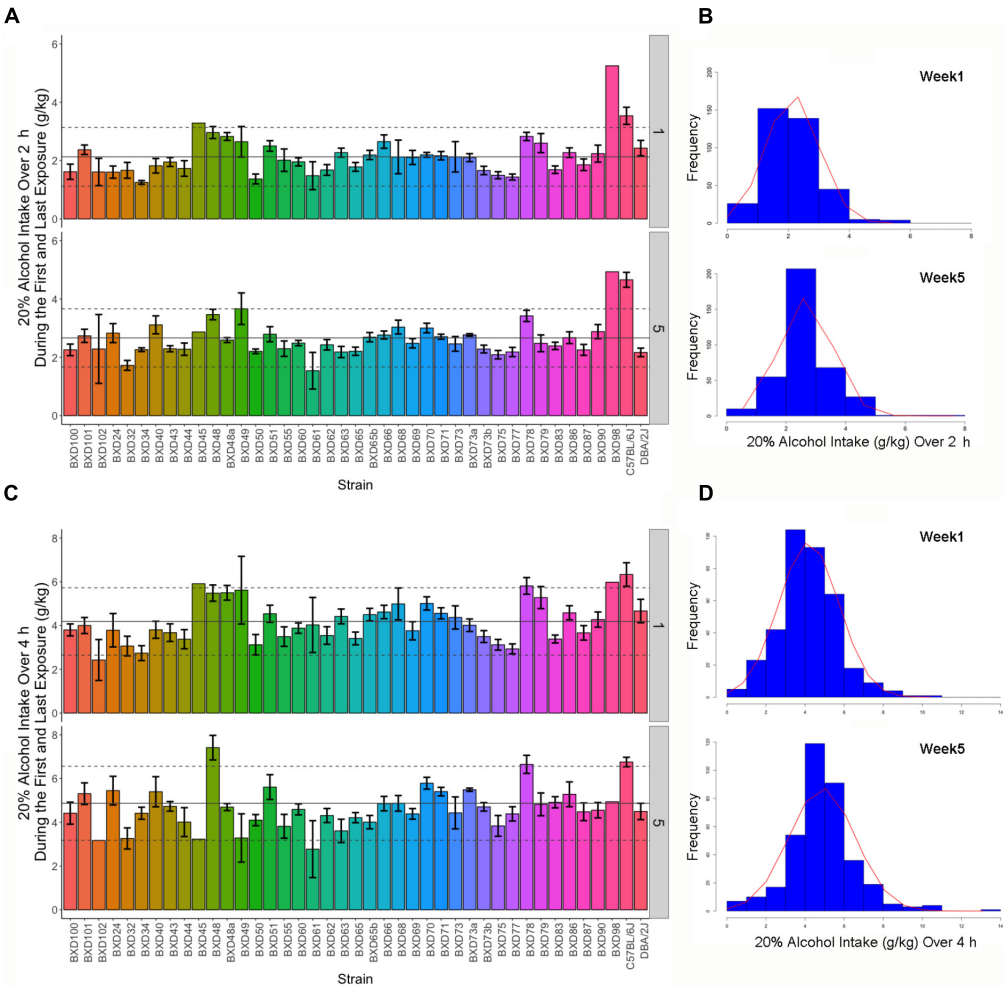

FIGURE 1 | Strain distribution of 2 or 4 h alcohol intake over 5 weeks. **(A)** Alcohol intake of 20% (v/v) over a 2 h access period is shown in g/kg on the Y-axis by week and the X-axis lists the BXD strain numbers with B6 and D2 parental strains shown to the far right (bar graph, each color represents an inbred strain). Population mean and standard deviation are shown for each week by the solid and dashed horizontal line, respectively. Weekly 2 h intake was variable among BXD strains and increased over time. **(B)** Distribution (histogram) reflects week-averaged intake from individual B6, D2, and 39 BXD strains recorded over three consecutive days of 2 h exposure. The distribution of alcohol intake changed between weeks 1 and 5 indicating increased alcohol intake. **(C)** Alcohol intake of 20% (v/v) over a 4 h access period is shown in g/kg on the Y-axis by week and the X-axis lists the BXD strain numbers with B6 and D2 parental strains shown to the far right (bar graph). Alcohol intake of 20% alcohol during the 4 h access period (bar graph) was variable among BXD strains and increased over time. **(D)** Distribution (histogram) reflects intake from B6, D2, and 39 BXD strains recorded over a single 4 h exposure. The distribution of alcohol intake changed between weeks 1 and 5 indicating increased alcohol intake. For the 2 and 4 h exposure, alcohol intake varied by strain both within and across weeks. For both exposures, mean intake increased between weeks 1 and 5.

TABLE 1 | Anova results table.

	2 h access						4 h access				
Strain Effect	**W1D1**	**W1avg**	**W2avg**	**W3avg**	**W4avg**	**W5avg**	**W1D4**	**W2D4**	**W3D4**	**W4D4**	**W5D4**
R-value	1.20E-09	<2.20E-16	<2.20E-16	<2.20E-16	<2.20E-16	<2.20E-16	1.22E-11	1.69E-13	2.89E-15	3.80E-08	2.06E-12
F-value	3.36	5.19	4.91	7.89	5.48	6.69	3.79	4.19	4.6	3.0	3.962
Df	39	40	40	40	40	40	40	40	40	40	40
h2	0.29	0.39	0.37	0.49	0.40	0.45	0.32	0.34	0.36	0.27	0.33

note, some strains with high genetic similarity (∼80%, denoted by letters following strain name), such as BXD48 and BXD48a, showed highly divergent intake patterns over time with BXD48 showing significantly increased intake and BXD48a displaying stable or slightly decreased intake over time. The parental B6 strain demonstrated increased 2 h intake over the 5-week period

TABLE 2 | Change in 2 and 4 h alcohol intake over 5-week.

	2 h			4 h		
Strain	**Slope**	**Intercept**	**SE**	**Slope**	**Intercept**	**SE**
BXD40	***0.329***	1.54	0.07	0.541	3.05	0.54
BXD24	***0.297***	1.51	0.07	0.545	3.20	0.55
C57BL/6J	0.278	3.20	0.11	−0.077	6.60	−0.08
BXD49	***0.246***	2.48	0.03	−0.455	6.01	−0.46
BXD34	***0.238***	1.16	0.04	***0.408***	2.46	0.41
BXD68	0.218	2.09	0.07	−0.002	4.96	0.00
BXD50	***0.211***	1.18	0.01	***0.232***	2.83	0.23
BXD77	***0.199***	1.22	0.02	***0.374***	2.47	0.37
BXD83	***0.197***	1.50	0.03	***0.408***	3.02	0.41
BXD62	***0.183***	1.57	0.03	0.153	3.59	0.15
BXD90	***0.169***	1.93	0.03	0.188	4.05	0.19
BXD73a	***0.168***	1.95	0.01	***0.362***	3.80	0.36
BXD75	***0.166***	1.21	0.04	0.198	2.62	0.20
BXD100	***0.161***	1.57	0.04	0.139	3.54	0.14
BXD70	0.160	2.23	0.06	0.132	4.88	0.13
BXD98	0.150	4.28	0.30	−0.318	6.87	−0.32
BXD73b	***0.146***	1.58	0.01	***0.319***	3.04	0.32
BXD78	***0.146***	2.61	0.03	***0.195***	5.72	0.19
BXD71	***0.144***	1.91	0.03	0.272	4.37	0.27
BXD60	***0.134***	1.75	0.02	***0.150***	3.81	0.15
BXD65b	***0.134***	1.96	0.04	−0.109	4.42	−0.11
BXD48	***0.134***	2.76	0.02	***0.542***	5.02	0.54
BXD44	0.127	1.74	0.06	0.296	2.91	0.30
BXD101	0.125	2.19	0.06	0.355	3.85	0.35
BXD87	0.120	1.58	0.04	***0.219***	3.23	0.22
BXD73	0.118	1.94	0.04	0.060	4.28	0.06
BXD65	***0.116***	1.73	0.03	0.232	3.36	0.23
BXD61	0.109	1.21	0.08	−0.372	3.90	−0.37
BXD43	***0.107***	1.83	0.03	***0.288***	3.39	0.29
BXD102	0.103	1.14	0.19	0.183	1.84	0.18
BXD86	***0.103***	2.09	0.03	0.218	4.13	0.22
BXD69	***0.101***	2.03	0.03	0.197	3.58	0.20
BXD55	0.088	1.79	0.04	0.122	3.17	0.12
BXD51	0.080	2.36	0.03	0.379	4.08	0.38
BXD66	0.047	2.47	0.03	0.085	4.33	0.09
BXD32	0.018	1.61	0.01	0.075	2.73	0.07
BXD4S	0.007	2.56	0.21	−0.356	5.57	−0.36
BXD79	−0.017	2.61	0.03	−0.080	5.25	−0.08
BXD63	−0.026	2.25	0.05	−0.125	4.52	−0.13
DBA/2J	−0.041	2.17	0.09	−0.040	4.32	−0.04
BXD48a	−0.046	2.89	0.05	−0.264	5.72	−0.26

Slope (g/kg per week) and associated y-intercept (g/kg) and standard error (SE) are shown for the 2 or 4 h exposure period by strain. Slopes sorted by 2 h exposure period. All slopes calculated from strain-averaged intake (4 h g/kg) or average weekly intake by strain (2 h g/kg). Bold italic slope values indicate significant ($p < 0.05$) effect of week on g/kg alcohol intake after linear regression. Intake is variable but generally increases over time for both the 2 and 4 h exposures in the BXD strains. However, slope at 2 h is not always identical to slope at 4 h and both traits are modestly correlated (r = 0.41). Parental strains are highlighted.

and slightly decreased 4 h intake in contrast to the D2 strain, which showed relatively stable or slightly decreased intake for both the 2 and 4 h intake period. However, these changes in the parental strains were not statistically significant. Although modestly correlated ($r = 0.41$), change in 2 and 4 h intake over 5 weeks was not identical within strain. We observed a strong, negative correlation (−0.62) between slope (alcohol intake over time) and the y-intercept (baseline intake) for 4 h intake. As demonstrated in **Table 2**, strains with high initial intake tended to evince more stable or slightly decreased drinking over time. This negative relationship was present, albeit much weaker, for the 2 h time point ($r = -0.25$).

Identification of QTLs for Alcohol Intake

We first assessed whether there were QTLs associated with the heritable variation in initial (week 1) or sustained weekly alcohol intake using two different mapping methods (traditional HK and GEMMA to correct for kinship). As expected, based on the inclusion of 39 strains, no significant QTLs were detected following multiple test correction (**Supplementary Table S2**). Using a suggestive threshold, seven QTLs were identified for HK and GEMMA (**Table 3**). QTLs detected by both methods are expected to be more robust than QTLs detected by HK alone, because these QTLs do not arise as a result of genetic relatedness. We prioritized the overlapping QTLs detected by both methods for further analysis. In all seven cases, inheritance of the B6 parental allele was associated with higher 2 or 4 h alcohol intake. QTLs on Chrs 2, 6, and 12 were only identified for 4 h intake on week 1. In contrast, overlapping QTLs on Chr 4 were only identified for 2 h intake on weeks 2 and 3, and the QTL on Chr 8 was identified for 4 h intake on week 3 and 2 h intake on week 5.

Next, we identified QTLs for progressive alcohol intake using slope analysis of 2 or 4 h intake over 5-weeks. No significant or suggestive QTLs were identified for progressive 4 h intake. However, a suggestive QTL on Chr 15 was identified for progressive 2 h alcohol intake using both HK and GEMMA mapping methods (**Table 3**). In contrast to the other seven QTLs, the 2 h progressive intake QTL was associated with higher intake and inheritance of the D2 parental allele.

Identification of Candidate Genes Driving Initial Alcohol Intake

The majority of suggestive overlap QTLs detected were associated with variation in initial 4 h alcohol intake on week 1 (W1.4 h, **Table 3**). Thus we prioritized these QTLs on Chrs 2 (9–30.4 Mb), 6 (89–93.6 Mb), and 12 (9.8–15.8 Mb) for identification of candidate genes driving variation in initial early alcohol intake. Hereafter, all QTLs are referred to by their QTL (Q) Chr number. The number of candidate genes located within each confidence interval varies [Q2 = 325, Q6 = 54, Q12 = 25; based on mouse assembly GRCm38/mm10 and UCSC RefSeq (refGene) Table Browser annotations, **Supplementary Table S3**]. Using genome sequence data generated for the parental strains we identified all genes (excluding gene models, predicted genes, non-coding and pseudo-genes) within each interval that were polymorphic and overlapped by higher impact sequence variants (see Methods). This reduced the number of candidate genes within each interval to Q2 = 60, Q6 = 13, and Q12 = 4 (**Supplemental Table S4**). These genes were further prioritized using naïve hippocampal

TABLE 3 | Suggestive QTL detected by multiple mapping methods.

Time	Method	Chr	Locus	Mb	Additive Effect	LOD	CIMb (left)	CIMb (right)
W1.4 h	*HK*	*2*	*rs13476358*	*16.306*	*–0.459*	*2.43*	*9.336*	*42.674*
W1.4 h	*GEMMA*	*2*	*Affy_PC2_15*	*15.000*	–	*3.07*	*9.000*	*30.441*
W2.2 h	*HK*	*4*	*rs32939068*	*153.934*	*–0.247*	*2.46*	*151.094*	*156.101*
W2.2 h	*GEMMA*	*4*	*rs32939068*	*153.934*	–	*3.44*	*153.372*	*155.226*
W3.2 h	*HK*	*4*	*rs32939068*	*153.934*	*–0.303*	*2.81*	*151.094*	*156.101*
W3.2 h	*GEMMA*	*4*	*rs32939068*	*153.934*	–	*4.08*	*153.372*	*155.493*
W1.4 h	*HK*	*6*	*rs30422489*	*91.707*	*–0.508*	*3.08*	*89.011*	*93.600*
W1.4 h	*GEMMA*	*6*	*rs30422489*	*91.707*	–	*3.23*	*89.011*	*93.600*
W3.4 h	*HK*	*8*	*rs49907965*	*89.094*	*–0.573*	*2.67*	*80.460*	*95.747*
W3.4 h	*GEMMA*	*8*	*rs49907965*	*89.094*	–	*3.16*	*86.380*	*95.747*
W5.2 h	*HK*	*8*	*rs49907965*	*89.094*	*–0.325*	*2.77*	*82.870*	*95.736*
W5.2 h	*GEMMA*	*8*	*rs49907965*	*89.094*	–	*3.23*	*82.870*	*95.747*
W1.4 h	*HK*	*12*	*rs3717933*	*11.076*	*–0.488*	*2.76*	*9.864*	*15.820*
W1.4 h	*GEMMA*	*12*	*rs49972008*	*12.603*	–	*3.07*	*7.991*	*26.035*
Slope. 2 h	*HK*	*15*	*rs31691968*	*63.392*	*0.045*	*3.19*	*58.000*	*67.990*
Slope. 2 h	*GEMMA*	*15*	*rs31691968*	*63.392*	–	*3.69*	*58.000*	*67.990*

QTLs were mapped for each week (W) of 2 or 4 h alcohol intake or for progressive 2 or 4 h alcohol intake based on slope analysis over five weeks of the DID paradigm. Additive effect, based on HK, mapping, is the contribution of parental alleles to mean trait expression. Negative additive values are associated with higher expression of the B6 allele. CI indicates the 1.5 LOD drop confidence interval. Text color indicates whether higher intake is driven by the inheritance of the B6 (blue) or D2 (red) parental allele at the locus. All QTL were detected at the suggestive threshold.

expression data generated for the BXD family (**Table 4** and **Supplemental Table S5**). For Q2, *Arhgap21, Gpr158, Mrpl41, Myo3a, Entpd4, Lhx3, Rapgef1,* and *Nup188* were all significantly correlated with alcohol intake during the first 4 h exposure in week 1, and the expression of each candidate was also regulated by local sequence variants (cis eQTL). Top candidates for Q6 included *Adamts9* and *Fgd5*. For Q12, *Nt5c1b* was the only candidate that contained putative high impact variants and whose expression covaried with 4 h alcohol intake on week 1. Products of all candidate genes in Q2, Q6, and Q12 played a role in signal transduction, metabolism, development, or endothelial cell response.

Identification of Candidate Genes Driving Variation in Sustained Weekly Alcohol Intake

The same strategy used to identify candidates driving variation in initial consumption was used to identify candidates on Q4 (151–155 Mb) and Q8 (86.4–95.7 Mb) associated with variation in 2 h intake on weeks 2 and 3, and variation in 4 h intake on week 3 and 2 h intake on week 5, respectively. The number of candidates within each interval was 51 for Q4 and 93 for Q8 (**Supplementary Table S3**). The number of candidate genes overlapping higher impact variants within each locus was 36 for Q8 and 16 for Q4 (**Supplementary Table S4**). For the Q4 interval, the highest priority candidates based on genetic cis-regulation and co-variation analysis using hippocampal expression data were *Per3* and *Prdm16* (**Table 4** and **Supplementary Table S5**). Top candidates for the Q8 interval included *Cyld, Aktip, Fto, Crnde, Mmp2, and Kifc3*. All of these high priority candidate genes were involved in circadian signaling, metabolism, or immune response.

Identification of Candidate Genes and Pathways Driving Variation in Progressive Alcohol Intake

Variation in progressive 2 h alcohol intake was associated with a suggestive QTL on Q15 (58–68 Mb) that contained 54 candidate genes (**Supplementary Table S3**). Only four of these genes (*Adcy8, Tg, Ndrg1*, and *Wisp*) were overlapped by variants of predicted higher impact (**Supplementary Table S4**). None of these candidates were modulated by cis eQTLS in naïve BXD hippocampus or correlated with the slope for 2 h alcohol intake over 5 weeks (**Supplemental Table S5**).

Trait Covariation With Initial Alcohol Intake

Trait data have been collected for the BXDs since the generation of the first BXD cohort in the late 1970's and much of this data is available in the BXD Published Phenotypes database available on GN. We queried this database to retrieve traits that were significantly correlated with W1.4 h, a heritable and QTL modulated trait associated with alcohol intake at early exposure. Forty-one traits were significantly correlated ($p < 0.005$) with the

TABLE 4 | Prioritized QTL candidate genes.

Symbol	Description	Gene Wiki	QTL	HIP:Mean Expr	HIP:cis eQTL	HIP:Trait Correlation
Dnajc1	DnaJ (Hsp40) homolog. subfamily C, member 1	GRP78 partner in ER; translation, beneficial effects in ER stress induced metabolic dysfunction	Q2: Initial	8.74	Sug	–
Armc3	armadillo repeat containing 3	?	Q2: Initial	**5.64**	Sig	–
Arhgap21	Rho GTPase activating protein 21	Signaling	Q2: Initial	11.76	Sig	Sig
Gpr158	G protein-coupled receptor 158	Regulator of RGS complexes and Rgs7 signaling in brain; human variants may influence energy expenditue and metabolism	Q2: Initial	6.51	Sig	Sig
Myo3a	Myosin IIIA	Acin based motor protein with kinase activity	Q2: Initial	6.35	–	Sig
Mrpl41	Mitochondrial ribosomal protein L41	Regulation of cell death	Q2: Initial	10.29	Sig	Sig
Uap1l1	UDP-N-acetylglucosamine pyrophorylase 1 like 1	?	Q2: Initial	9.01	Sig	–
Entpd2	Ectonucleoside triphosphate diphosphohydrolase 2	Metabolism	Q2: Initial	9.72	Sig	Sig
Ptgds	Prostaglandin D2 synthase	Glucose and insulin metabolism; regulated by estradiol; inflammatory response	Q2: Initial	13.90	Sig	–
C8g	Complement component 8, gamma subunit	Immune function	Q2: Initial	7.13	Sig	–
Kcnt1	Potassium channel, subfamily T, member 1 (slack, low threshold slowly adapting)	Localized to the postsynaptic density; involved in learning and memory and initial response to novel situations and environments	Q2: Initial	8.98	Sig	–
Lhx3	LIM homeobox protein 3	Trancription factor activity, nervous system development	Q2: Initial	6.23	–	Sig
Egfl7	EGF-like domain 7	Development	Q2: Initial	7.81	Sug	–
Rapgef1	Rap guanine nucleotide exchange factor (GEF) 1	Signaling; GABAergic neuronal development	Q2: Initial	7.41	Sug	Sig
Nup188	Nucleoporin 188	Development	Q2: Initial	8.50	–	Sig
Plxna1	plexin A1	Development; signaling	Q6: Initial	9.77	Sig	–
Fgd5	FYVE, RhoGEF and PH domain containing 5	Endothelial specific gene	Q6: Initial	8.00	–	Sig
Adamts9	A disintegrin-like and metalloprotease (reprolysin type} with thrombospondin type 1 motif, 9	Endothelial and vascular response	Q6: Initial	9.38	Sug	Siq
Nt5c1b	5′-nucleotidase, cytosolic 1B	Metabolism	Q12: Initial	7.18	Sug	Sig
Per3	Period 3	Circadian signaling	Q4: Sustained	7.11	Sig	Sig
Prdm16	PR domain containing 16	Metabolism; brown versus white fat differentiation	Q4: Sustained	6.52	Sig	Sig
Tnfrsf14	Tumor necrosis factor receptor superfamily, member 14 (herpesvirus entry mediator)	Inflammation and immune response	Q4: Sustained	**5.20**	Sig	–
Cyld	Cylindromatosis (turban tumor syndrome}	Immune; regulator of NF-kappaB signaling	Q8: Sustained	10.41	Sig	Sig
Chd9	Chromodomain helicase DNA binding protein 9	Expressed in osteoprogenitors	Q8: Sustained	9.55	Sig	–
Aktip	AKT interacting protein	Ft1 protein; telomere maintenance; development	Q8: Sustained	7.49	Sig	Sig

(Continued)

TABLE 4 | Continued

Symbol	Description	Gene Wiki	QTL	HIP:Mean Expr	HIP:cis eQTL	HIP:Trait Correlation
Fto	Fat mass and obesity associated (alpha-ketoglutarate-dependent dioxygenase FTO)	Metabolism; energy homeostasis; regulator of adipogenesis	Q8: Sustained	6.94	Sig	Sig
Crnde	Colorectal neoplasia differentially expressed (non-protein coding}	Metabolism; control of glucose and lipid metabolism	Q8: Sustained	6.63	Sig	Sig
Mmp2	Matrix metaloproteinase 2	Immune system; inflammatory response	Q8: Sustained	6.66	Sig	Sig
Coq9	Coenzyme QB	Metabolism: deficiency impacts mitochondrial function	Q8: Sustained	10.49	Sig	Sig
Kifc3	Kinesin family member C3	Peroxisomal transport	Q8: Sustained	10.01	Sig	Sig

High priority candidate genes selected based on regulation of expression by local sequence variants (cis eQTL) and co-expression with DID intake traits (Slope2 hWeek, 2 h.W3avg, 2 h.W5avg, and W1.4 h). See ***Supplementary Table S5*** *for full results. Gene expression signatures for each gene generated on the Affymetrix M430 platform for BXD hippocampus (HIP, naïve to treatment). Genes in bold have hippocampal gene expression that is significantly regulated by a cis eQTL (Sig) and significantly ($p < 0.05$) coexpressed (Sig; based on Pearson's r-value) with DID alcohol intake traits. Bold text in the HIP:MeanExpr column used to indicate genes with very low expression in hippocampus. In the hippocampal data set mean expression is 8 ± 2 log_2 units. Function summarized using GN Gene Wiki tool.*

first 4 h alcohol intake trait. Representative scatterplots are shown in **Figure 2**. Correlated traits were subdivided into six categories: behavior; blood and brain chemistry, and hematology; drug response (morphine and alcohol); immune function; metabolism, and microbiome (**Supplementary Table S6**).

DISCUSSION

Here, we report large variability in 2 and 4 h alcohol consumption in B6, D2, and 39 BXD strains using a DID protocol over a 5-week time period. BXD strains demonstrated high, low, or intermediate alcohol intake relative to parental strains (**Figure 1**). Regression analysis revealed that, in general, alcohol intake increased from weeks 1 to 5 regardless of session duration. Although it is important to note that some strains demonstrated greatly increased intake while others remained relatively stable or decreased slightly over the 5-week period. Our study both replicated previous findings on DID alcohol intake and generated novel insight into progressive drinking. In contrast to our study, most of the previous DID studies in male and female inbred strains focused primarily on the first few weeks of DID. These studies reported higher intake in B6 compared to D2, and that alcohol consumption "stabilized" by the second day of access (Rhodes et al., 2005). When these studies were extended for 12 consecutive days in male B6 mice, intake levels were reported to be constant (Rhodes et al., 2005). We also reported stabilization of alcohol intake early in week 1 in that heritability was reduced at first exposure compared to subsequent exposures. This was a result of greater within strain variation upon first experience with alcohol. Accordingly, we also observed much higher intake of 20% alcohol at 2 and 4 h in the B6 parental strain relative to D2. By lengthening the DID protocol to 5 weeks, our work extends the findings of previous studies and we reported increased consumption and, at least for 2 h intake, higher heritability (less within strain variation) during later weeks (3, 4, and 5). Similar increases in intake have been reported for B6 males over a 14-day DID access period (Linsenbardt and Boehm, 2014). Taken together, these results provide evidence that extended access DID protocols of 2 weeks or longer result in increased alcohol intake in B6J. For the first time, we report that this trend of enhanced consumption during extended DID is also apparent in the BXD family of strains. Patterns of initial weekly and progressive intake during 2 or 4 h sessions over 5 weeks varied between B6, D2, and the BXD strains. This variability was heritable and we were able to identify several suggestive loci for variation in initial intake during week 1, and variation in sustained and progressive intake.

The DID paradigm typically employs both a 2 h and a longer 4 h access period. In our study, some strains displayed marked differences in alcohol intake between access periods and identified QTLs were not always consistently detected for both periods. There are several explanations for the lack of complete congruency between the 2 and 4 h measures. First, the 2 h time point is a repeated measure and is thus a much more stable measure of weekly progressive intake. In addition, the extended 4 h access time period probably reflects a larger behavioral repertoire related to differences in learning and consummatory behavior. For example, male B6 mice allowed to drink alcohol in a modified DID paradigm in which they were given a 2 h access period over 14 consecutive days not only increased their intake over sessions, but also learned to "front load" their intake, and consumed the majority of their alcohol on the last session within the first few minutes of the 2 h access period (Linsenbardt and Boehm, 2014). In our study using female mice, we observed increased intake over the 5-week period in B6 females for the 2 h time point (**Table 2**), but the same trend was not observed for the 4 h time point. However, several strains, such as BXD 40, 29, and 34, showed increased intake over 5 weeks for both the 2 and 4 h sessions. It is unknown whether B6 females display front loading, but differences in this behavior, or a ceiling effect on intake in the 4 h access period, may be an additional source of variation that contributes to differences between the 2 and 4 h access period between and within strain in our study. For genetic mapping, the 2 h trait has higher heritability and is more amenable to mapping.

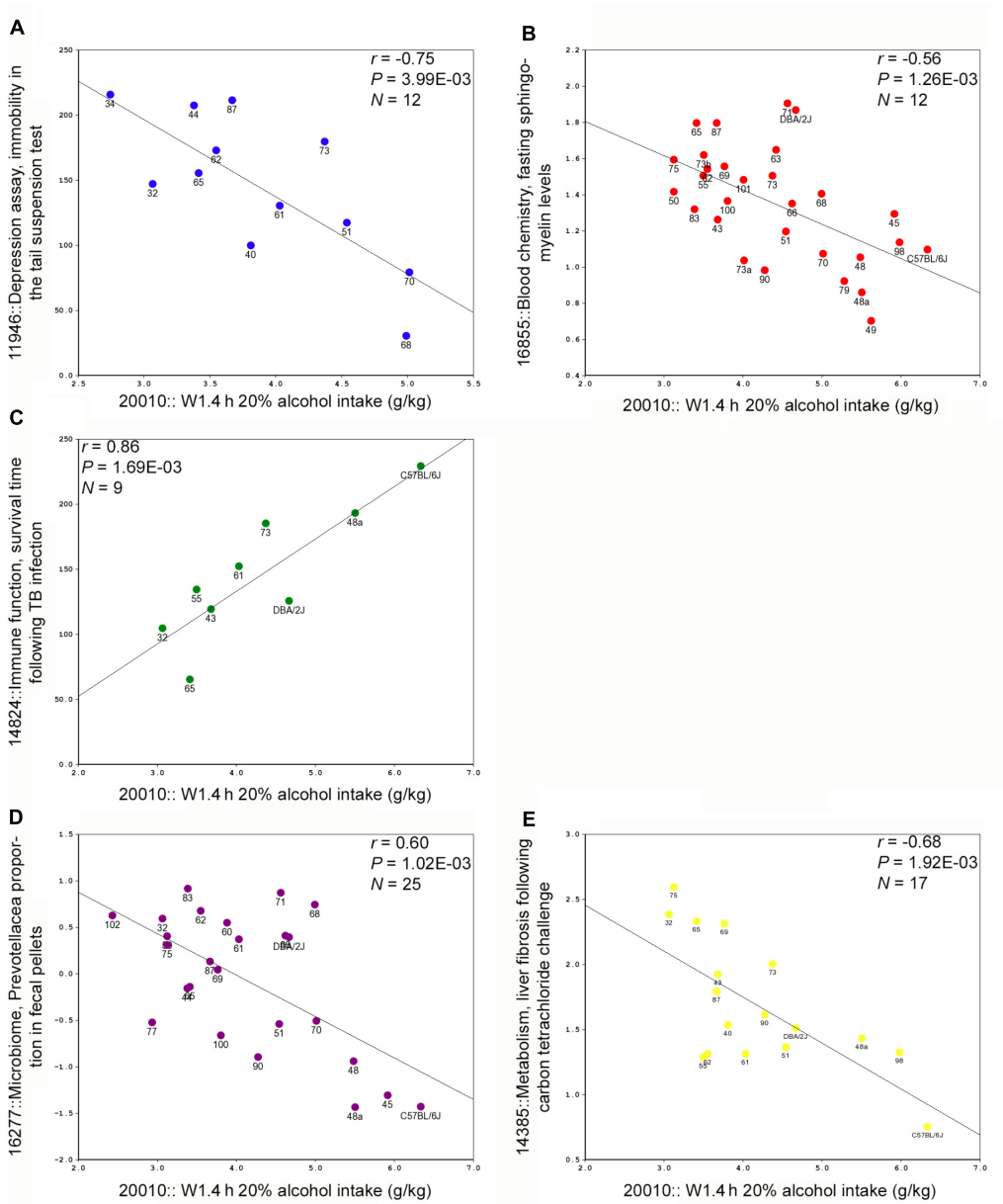

FIGURE 2 | Representative scatterplots representing correlations between BXD legacy trait data and alcohol intake during the first 4 h exposure on week 1. **(A)** A measure of depression (immobility in the tail suspension test) is negatively correlated with alcohol intake. **(B)** Fasting sphingomyelin levels are also negatively correlated with intake. **(C)** A measure of immune function, infection survival time is positively correlated with intake. **(D)** Measures of one member of the gut microbime are negatively correlated with intake. **(E)** A metabolic/immune trait, liver injury following insult, is negatively correlated with intake.

However, it is also possible that different genetic factors control each trait. Temporal dissection of intake over the 2 and 4 h access period for strains with similar and dissimilar 2 and 4 h intake would be needed to reconcile some of these differences.

Our study included 39 BXDs strains with a variable number of replicates within strain (1–16). Traditional QTL mapping incorporates the mean of the dependent measure for each BXD strain. Power to detect QTLs is derived largely from the number of strains (Belknap, 1998; Andreux et al., 2012). However, the traditional mapping method used for BXD data does not account for population structure and may result in false positives. To account for this, we mapped QTLs using both a simple regression method (HK) in GN that does not account for kinship, and another mapping algorithm (GEMMA) available in GN, version 2, that does. Even though GEMMA is not typically used for smaller data sets, several QTLs were replicated using both methods, albeit at a suggestive level. Both methods used the same marker panel and dependent variables for alcohol intake. QTLs detected by both methods are expected to be more robust against identification of false positives due to genetic relatedness

compared to using either model alone (see methods). With 39 strains and a variable number of replicates within strain, our study was only powered to detect QTLs of large effect. As expected, we did not identify any significant loci. However, using both mapping methods we identified: suggestive QTLs associated with variation in alcohol intake during early exposure (W1.4 h) on Chr 2, 6, and 12, and suggestive QTLs associated with variation in sustained intake during later weeks on Chrs 4 and 8. We were also able to identify a QTL on Chr 15 associated with progressive alcohol intake. To assess whether these QTLs are likely to reach significance if more strains are added we winsorized (transformation of the data by limiting extreme values) the existing 39 strain data to better fit assumptions of normality assumed when using HK and GEMMA mapping methods. Winsorizing the data resulted in higher LOD scores for all QTLs for both mapping methods. This suggests that, assuming a normal trait distribution in the BXD population, testing a larger number of BXD strains will result in significant LOD scores. Thus, the provisional QTLs identified in our study are worth investigating further and may contain genes that drive higher or lower initial or sustained alcohol consumption. As such, we used multiple lines of evidence based on overlapping gene variants and gene expression to nominate candidate genes for suggestive QTLs identified in this study. An important caveat of this approach is that mutations that impact protein function without modulating gene expression will be missed. However, this is a powerful and integrative approach that nominates the best candidates based on all available data. Candidates associated with genetic predisposition for high or low intake during the 1st week of exposure to alcohol included *Arhgap21, Gpr158, Mrpl41, Myo3a, Entpd2, Lhx3*, *Rapgef1*, and *Nup188* (Q2); *Adamts9* and *Fgd5* (Q6); and *Nt5c1b* (Q12). All candidates were overlapped by variants that may impact gene regulation or function, and their expression in hippocampus was cis-modulated and correlated with 4 h intake during week 1. Therefore, pre-existing patterns of expression in these genes due to the presence of functional gene variants could alter initial alcohol intake behavior. Only one of these genes, Entpd2, had been directly implicated in alcohol-related responses in animal model systems (Rico et al., 2008). Rico and colleagues found that acute alcohol exposure led to alterations in brain nucleotide (specifically, ATP hydrolysis) metabolism *in vivo* and a reduction in the mRNA level of the zebrafish homolog of ENTPD2 (NTPDase2). Although not directly associated with alcohol related traits in human or animal model systems, *Nt5c1b* was also involved in nucleotide metabolism (specifically, adenosine formation following ATP hydrolysis; Sala-Newby and Newby, 2001). Other candidates were involved in intracellular signaling pathways (*Arhgap21, Gpr158, Rapgef1*, *Adamts9*, *Fgd5, Mrpl41, Nt5c1b*) that mediated diverse biological processes related to metabolism, G-protein coupled receptor signaling, and endothelial response (**Table 4**). Taken together, these results suggest that alterations in ATP metabolism and other signaling pathways could drive variation in initial alcohol intake in the DID paradigm.

Using a similar approach we also identified *Per3* and *Prdm16* (Q4) and *Cyld, Aktip, Fto, Crnde, Mmp2, and Kifc3* (Q8) as high priority candidate genes for variation (higher or lower) in sustained intake during later weeks. Variation in 2 h intake on weeks 2 and 3 was associated with Q4, and variation in 4 h intake on week 3 and 2 h intake on week 5 was associated with Q8. Importantly, the Q4 and Q8 intervals were detected at multiple time points over the course of the 5-week DID study. These concordant and reproducible QTLs are less likely to represent false positives. Candidates for the Q4 and Q8 interval play key roles in circadian signaling (*Per3*), metabolic (*Prdm16*, *Fto*, *Crnde*), and immune response (*Mmp2*, *Cyld*). Alterations in metabolism (e.g., mitochondrial dysfunction, insulin/glucose dysregulation), circadian cycle, sleep disruptions, and inflammation have long been associated with chronic alcohol use, abuse, and alcoholism. In particular, several of these genes, *Per3* (Q4) and *Fto*, and *Mmp2*(Q8) have all been previously associated with ethanol response. In human populations, PER3 variants were associated with insomnia severity in alcohol-dependent patients (Brower et al., 2012). In the BXD panel, a promoter mutation in *Per3* was associated with expression variation in naïve animals (cis-modulation) as well as variation in alcohol-related traits and expression changes following stress and alcohol exposure (Wang et al., 2012). Altered circadian expression of *Per3* was also associated with administration of a liquid alcohol diet in rats (Chen et al., 2004). Another strong candidate for sustained intake was *Fto*, a gene regulating fat mass, located on Chr 8 and associated with variation in intake during week 5. *Fto* variants were associated with frequency of alcohol consumption (Sobczyk-Kopciol et al., 2011; Young et al., 2016) and alcohol dependence (Wang et al., 2013) in human populations. *Mmp2*, also located on Chr 8, is known to be regulated by alcohol exposure in numerous human and animal systems and in many different cell and tissue types (Partridge et al., 1999; Burnham et al., 2007; Fiotti et al., 2008; Peng et al., 2013), however, a role for this gene in regulating alcohol intake is unclear. Here we report *Per3* and *Fto* as a strong candidate genes located on Chr 4 and Chr 8, respectively, that may underly variation in sustained alcohol intake during DID in the BXD family. Both were associated with alcohol-related traits in human and rodent model systems, and their expression was correlated with 2 h intake during week 3 (negative correlation, *Per3*) or week 5 (positive correlation, *Fto*) of DID. In addition, *Per3* contains functional polymorphic regulatory variants known to impact expression in the BXD panel and *Fto* is a cis-modulated gene containing multiple missense variants between B6 and D2.

By extending the DID paradigm to a longer 5-week period we were also able to identify a suggestive QTL on Chr 15 for variation (higher or lower) in progressive alcohol intake. None of the genes located within the QTL confidence interval was cis-modulated in BXD hippocampus. This was an expected negative result based on the use of an expression data set generated from naïve animals. However, there were only a handful of genes (*Adcy8*, *Tg, Ndgr1*, and *Wisp*) within this interval that contained variants likely to impact gene regulation or function. Of these, only *Adcy8* was previously associated with alcohol-related traits (Procopio et al., 2013). Procopio and colleagues reported that a haplotype within the coding region of ADCY8 was associated with alcohol dependence co-occurring with depression in females. Given that progressive alcohol intake likely reflects changing alcohol consumption over time, it is

reasonable to expect that the underlying gene variants may interact with alcohol exposure to produce variation in intake over time. Of interest, genes located within the Q15 interval were significantly enriched (adjusted $p < 0.05$) for HDAC2 and PPARD binding based on consensus genome-wide ChIP-X data from ENCODE and integrated ChIP Enrichment Analysis (ChEA). None of the other QTL intervals (Q2, Q4, Q6, Q8, or Q12) were enriched for transcription factor binding or histone modifications based on Enrichr analysis, suggesting that gene variants in the Q15 region may exert their effect through alcohol experience dependent epigenetic modulation.

This is the first work of its kind to elucidate genetic influence on ethanol consumption at first opportunity and repeated opportunities over several weeks in a large genetic reference population of mice. As in other studies, the DID paradigm has been applied successfully to reveal genetic influences on alcohol consumption and the impact of alcohol intake on brain gene transcription (Rhodes et al., 2005, 2007; Mulligan et al., 2011; Thiele and Navarro, 2014; Thiele et al., 2014). The DID paradigm allows the animal to achieve significant blood ethanol concentrations, i.e., binge drinking. Indeed, we found that some strains consume large amounts of alcohol and that most of the strains studied increased their consumption by more than 0.5 g/kg. However, a caveat of our study is that we did not measure blood alcohol concentrations (BACs) weekly. We did not attempt to obtain BACs because of the added stressor of blood collection. However, this precludes an analysis of metabolic effects that may have contributed to changes in alcohol intake among strains.

One of the great advantages of a systems approach in the BXD panel is the ability to find associations between a trait of interest and other phenotypes generated in-house, and by others, in the extensive BXD trait database available at GN. Not only were we able to nominate candidate genes for suggestive QTL related to initial, sustained, and progressive alcohol intake, but we were also able to leverage 1000s of legacy trait records available for the BXD strains to associate variation in initial alcohol consumption with variation in metabolic, metagenomic, immune, and behavioral traits in the BXDs (**Supplementary Table S4**). Some of these associations were expected (e.g., correlations with depression- and anxiety-related traits and alcohol intake; and covariation with morphine and other alcohol response traits), while others were novel and may uncover new areas of interest. For example, and perhaps most surprising, a negative correlation between components of the gut microbiome and initial 4 h alcohol intake (**Figure 2D**). Of interest, Prevotellaceae was found to be enriched in fecal samples from alcohol cirrhosis patients relative to control samples (Chen et al., 2011). Oral levels of Lactobacillales and Prevotellaceae were also altered following alcohol intake in humans (Fan et al., 2018). Taken together these novel findings could indicate the presence of latent relationships between alcohol-related diseases and members of the microbial community. This opens the research area to what these associations mean in the general physiology and behavior of mice and other species, by hypothesis generation. In conclusion, we have shown here that there is a large genetic component to both initial, sustained, and progressive consumption of alcohol in the DID paradigm among the BXD family of mice. Moreover, through forward genetic mapping and systems biology, we have identified candidate genes and pathways likely to mediate high alcohol intake.

AUTHOR CONTRIBUTIONS

MKM, MD, and BCJ wrote the manuscript. MKM, DA, PP, WZ, and BCJ analyzed the data. LL, BCJ, WZ, MKM, ET, SAC, and PM designed and implemented the study.

ACKNOWLEDGMENTS

We would like to acknowledge Dr. Rob Williams for his intellectual support, contribution of BXD strains, and for GN development. We also acknowledge Arthur Centeno for his assistance with data integration into GN. Partial support for this study was provided by USPHS (NIH) Grants U01AA014425 and R01AA021951.

SUPPLEMENTARY MATERIAL

The Supplementary Material for this article can be found online at: https://www.frontiersin.org/articles/10.3389/fgene.2018.00370/full#supplementary-material

FIGURE S1 | Bivariate correlations of alcohol intake at initial exposure and across 2 or 4 h weekly intake. Correlations based on weekly (W) and daily (D) intake (g/kg) for individuals from B6, D2, and 39 BXD strains. Data averaged by strain for the first day of 2 h alcohol exposure (2 h:W1D1) and for each 4 h exposure. Data averaged by strain and week for subsequent 2 h exposures. All correlations were positive. Intake at first exposure for 2 h on W1D1 is highly correlated with subsequent average 2 and 4 h weekly intake. Correlations are higher between adjacent weeks and generally decay slightly over time. Compared to correlations between 4 h intake on the first and last exposure, correlations between intake at first (W1D1 or W1avg) and last exposure are higher for 2 h intake.

TABLE S1 | Strain and replicate summary.

TABLE S2 | QTL comparison table.

TABLE S3 | Candidate genes located within QTL confidence intervals.

TABLE S4 | Candidate genes within QTL confidence intervals overlapped by higher impact sequence variants.

TABLE S5 | Full list of high priority candidate genes and evidence for selection.

TABLE S6 | BXD trait correlations.

REFERENCES

Andreux, P. A., Williams, E. G., Koutnikova, H., Houtkooper, R. H., Champy, M. F., Henry, H., et al. (2012). Systems genetics of metabolism: the use of the BXD murine reference panel for multiscalar integration of traits. *Cell* 150, 1287–1299. doi: 10.1016/j.cell.2012.08.012

Babor, T. F., Dolinsky, Z. S., Meyer, R. E., Hesselbrock, M., Hofmann, M., and Tennen, H. (1992). Types of alcoholics: concurrent and predictive validity of

some common classification schemes. *Br. J. Addict.* 87, 1415–1431. doi: 10.1111/j.1360-0443.1992.tb01921.x

Belknap, J. K. (1998). Effect of within-strain sample size on QTL detection and mapping using recombinant inbred mouse strains. *Behav. Genet.* 28, 29–38. doi: 10.1023/A:1021404714631

Belknap, J. K., Metten, P., Helms, M. L., O'Toole, L. A., Angeli-Gade, S., Crabbe, J. C., et al. (1993). Quantitative trait loci (QTL) applications to substances of abuse: physical dependence studies with nitrous oxide and ethanol in BXD mice. *Behav. Genet.* 23, 213–222. doi: 10.1007/BF01067426

Brower, K. J., Wojnar, M., Sliwerska, E., Armitage, R., and Burmeister, M. (2012). PER3 polymorphism and insomnia severity in alcohol dependence. *Sleep* 35, 571–577. doi: 10.5665/sleep.1748

Browman, K. E., and Crabbe, J. C. (2000). Quantitative trait loci affecting ethanol sensitivity in BXD recombinant inbred mice. *Alcohol. Clin. Exp. Res.* 24, 17–23. doi: 10.1111/j.1530-0277.2000.tb04547.x

Buck, K. J., Metten, P., Belknap, J. K., and Crabbe, J. C. (1997). Quantitative trait loci involved in genetic predisposition to acute alcohol withdrawal in mice. *J. Neurosci.* 17, 3946–3955. doi: 10.1523/JNEUROSCI.17-10-03946.1997

Burnham, E. L., Moss, M., Ritzenthaler, J. D., and Roman, J. (2007). Increased fibronectin expression in lung in the setting of chronic alcohol abuse. *Alcohol. Clin. Exp. Res.* 31, 675–683. doi: 10.1111/j.1530-0277.2007.00352.x

Chen, C. P., Kuhn, P., Advis, J. P., and Sarkar, D. K. (2004). Chronic ethanol consumption impairs the circadian rhythm of pro-opiomelanocortin and period genes mRNA expression in the hypothalamus of the male rat. *J. Neurochem.* 88, 1547–1554. doi: 10.1046/j.1471-4159.2003.02300.x

Chen, H., and Sharp, B. M. (2004). Content-rich biological network constructed by mining PubMed abstracts. *BMC Bioinformatics* 5:147. doi: 10.1186/1471-2105-5-147

Chen, Y., Yang, F., Lu, H., Wang, B., Chen, Y., Lei, D., et al. (2011). Characterization of fecal microbial communities in patients with liver cirrhosis. *Hepatology* 54, 562–572. doi: 10.1002/hep.24423

Chesler, E. J., Lu, L., Shou, S., Qu, Y., Gu, J., Wang, J., et al. (2005). Complex trait analysis of gene expression uncovers polygenic and pleiotropic networks that modulate nervous system function. *Nat. Genet.* 37, 233–242. doi: 10.1038/ng1518

Churchill, G. A., and Doerge, R. W. (1994). Empirical threshold values for quantitative trait mapping. *Genetics* 138, 963–971.

Cloninger, C. R. (1987). Neurogenetic adaptive mechanisms in alcoholism. *Science* 236, 410–416. doi: 10.1126/science.2882604

Crabbe, J. C. (1998). Provisional mapping of quantitative trait loci for chronic ethanol withdrawal severity in BXD recombinant inbred mice. *J. Pharmacol. Exp. Ther.* 286, 263–271.

Crabbe, J. C., Metten, P., Belknap, J. K., Spence, S. E., Cameron, A. J., Schlumbohm, J. P., et al. (2014). Progress in a replicated selection for elevated blood ethanol concentrations in HDID mice. *Genes Brain Behav.* 13, 236–246. doi: 10.1111/gbb.12105

Crabbe, J. C., Phillips, T. J., Gallaher, E. J., Crawshaw, L. I., and Mitchell, S. R. (1996). Common genetic determinants of the ataxic and hypothermic effects of ethanol in BXD/Ty recombinant inbred mice: genetic correlations and quantitative trait loci. *J. Pharmacol. Exp. Ther.* 277, 624–632.

Cunningham, C. L. (1995). Localization of genes influencing ethanol-induced conditioned place preference and locomotor activity in BXD recombinant inbred mice. *Psychopharmacology* 120, 28–41. doi: 10.1007/BF02246142

Fan, X., Peters, B. A., Jacobs, E. J., Gapstur, S. M., Purdue, M. P., Freedman, N. D., et al. (2018). Drinking alcohol is associated with variation in the human oral microbiome in a large study of American adults. *Microbiome* 6:59. doi: 10.1186/s40168-018-0448-x

Fernandez, J. R., Vogler, G. P., Tarantino, L. M., Vignetti, S., Plomin, R., and McClearn, G. E. (1999). Sex-exclusive quantitative trait loci influences in alcohol-related phenotypes. *Am. J. Med. Genet.* 88, 647–652. doi: 10.1002/(SICI)1096-8628(19991215)88:6<647::AID-AJMG13>3.0.CO;2-6

Fiotti, N., Tubaro, F., Altamura, N., Grassi, G., Moretti, M., Dapas, B., et al. (2008). Alcohol reduces MMP-2 in humans and isolated smooth muscle cells. *Alcohol* 42, 389–395. doi: 10.1016/j.alcohol.2008.02.001

Gill, K., Liu, Y., and Deitrich, R. A. (1996). Voluntary alcohol consumption in BXD recombinant inbred mice: relationship to alcohol metabolism. *Alcohol. Clin. Exp. Res.* 20, 185–190. doi: 10.1111/j.1530-0277.1996.tb01063.x

Grisel, J. E., Metten, P., Wenger, C. D., Merrill, C. M., and Crabbe, J. C. (2002). Mapping of quantitative trait loci underlying ethanol metabolism in BXD recombinant inbred mouse strains. *Alcohol. Clin. Exp. Res.* 26, 610–616. doi: 10.1111/j.1530-0277.2002.tb02582.x

Keane, T. M., Goodstadt, L., Danecek, P., White, M. A., Wong, K., Yalcin, B., et al. (2011). Mouse genomic variation and its effect on phenotypes and gene regulation. *Nature* 477, 289–294. doi: 10.1038/nature10413

Kuleshov, M. V., Jones, M. R., Rouillard, A. D., Fernandez, N. F., Duan, Q., Wang, Z., et al. (2016). Enrichr: a comprehensive gene set enrichment analysis web server 2016 update. *Nucleic Acids Res.* 44, W90–W97. doi: 10.1093/nar/gkw377

Linsenbardt, D. N., and Boehm, S. L. II (2014). Alterations in the rate of binge ethanol consumption: implications for preclinical studies in mice. *Addict. Biol.* 19, 812–825. doi: 10.1111/adb.12052

Mulligan, M. K., Mozhui, K., Prins, P., and Williams, R. W. (2017). GeneNetwork: a toolbox for systems genetics. *Methods Mol. Biol.* 1488, 75–120. doi: 10.1007/978-1-4939-6427-7_4

Mulligan, M. K., Ponomarev, I., Hitzemann, R. J., Belknap, J. K., Tabakoff, B., Harris, R. A., et al. (2006). Toward understanding the genetics of alcohol drinking through transcriptome meta-analysis. *Proc. Natl. Acad. Sci. U.S.A.* 103, 6368–6373. doi: 10.1073/pnas.0510188103

Mulligan, M. K., Rhodes, J. S., Crabbe, J. C., Mayfield, R. D., Harris, R. A., and Ponomarev, I. (2011). Molecular profiles of drinking alcohol to intoxication in C57BL/6J mice. *Alcohol. Clin. Exp. Res.* 35, 659–670. doi: 10.1111/j.1530-0277.2010.01384.x

Overall, R. W., Kempermann, G., Peirce, J., Lu, L., Goldowitz, D., Gage, F. H., et al. (2009). Genetics of the hippocampal transcriptome in mouse: a systematic survey and online neurogenomics resource. *Front. Neurosci.* 3:55. doi: 10.3389/neuro.15.003.2009

Partridge, C. R., Sampson, H. W., and Forough, R. (1999). Long-term alcohol consumption increases matrix metalloproteinase-2 activity in rat aorta. *Life Sci.* 65, 1395–1402. doi: 10.1016/S0024-3205(99)00381-1

Peirce, J. L., Lu, L., Gu, J., Silver, L. M., and Williams, R. W. (2004). A new set of BXD recombinant inbred lines from advanced intercross populations in mice. *BMC Genet.* 5:7. doi: 10.1186/1471-2156-5-7

Peng, C., Li, W. A., Fu, P., Chakraborty, T., Hussain, M., Guthikonda, M., et al. (2013). At low doses ethanol maintains blood-brain barrier (BBB) integrity after hypoxia and reoxygenation: a brain slice study. *Neurol. Res.* 35, 790–797. doi: 10.1179/1743132813Y.0000000198

Philip, V. M., Duvvuru, S., Gomero, B., Ansah, T. A., Blaha, C. D., Cook, M. N., et al. (2010). High-throughput behavioral phenotyping in the expanded panel of BXD recombinant inbred strains. *Genes Brain Behav.* 9, 129–159. doi: 10.1111/j.1601-183X.2009.00540.x

Phillips, T. J., Crabbe, J. C., Metten, P., and Belknap, J. K. (1994). Localization of genes affecting alcohol drinking in mice. *Alcohol. Clin. Exp. Res.* 18, 931–941. doi: 10.1111/j.1530-0277.1994.tb00062.x

Phillips, T. J., Huson, M., Gwiazdon, C., Burkhart-Kasch, S., and Shen, E. H. (1995). Effects of acute and repeated ethanol exposures on the locomotor activity of BXD recombinant inbred mice. *Alcohol. Clin. Exp. Res.* 19, 269–278. doi: 10.1111/j.1530-0277.1995.tb01502.x

Phillips, T. J., Lessov, C. N., Harland, R. D., and Mitchell, S. R. (1996). Evaluation of potential genetic associations between ethanol tolerance and sensitization in BXD/Ty recombinant inbred mice. *J. Pharmacol. Exp. Ther.* 277, 613–623.

Procopio, D. O., Saba, L. M., Walter, H., Lesch, O., Skala, K., Schlaff, G., et al. (2013). Genetic markers of comorbid depression and alcoholism in women. *Alcohol. Clin. Exp. Res.* 37, 896–904. doi: 10.1111/acer.12060

Rhodes, J. S., Best, K., Belknap, J. K., Finn, D. A., and Crabbe, J. C. (2005). Evaluation of a simple model of ethanol drinking to intoxication in C57BL/6J mice. *Physiol. Behav.* 84, 53–63. doi: 10.1016/j.physbeh.2004.10.007

Rhodes, J. S., Ford, M. M., Yu, C. H., Brown, L. L., Finn, D. A., Garland, T., et al. (2007). Mouse inbred strain differences in ethanol drinking to intoxication. *Genes Brain Behav.* 6, 1–18. doi: 10.1111/j.1601-183X.2006.00210.x

Rico, E. P., Rosemberg, D. B., Senger, M. R., de Bem Arizi, M., Dias, R. D., Souto, A. A., et al. (2008). Ethanol and acetaldehyde alter NTPDase and 5′-nucleotidase from zebrafish brain membranes. *Neurochem. Int.* 52, 290–296. doi: 10.1016/j.neuint.2007.06.034

Risinger, F. O., and Cunningham, C. L. (1998). Ethanol-induced conditioned taste aversion in BXD recombinant inbred mice. *Alcohol. Clin. Exp. Res.* 22, 1234–1244. doi: 10.1111/j.1530-0277.1998.tb03904.x

Roberts, A. J., Phillips, T. J., Belknap, J. K., Finn, D. A., and Keith, L. D. (1995). Genetic analysis of the corticosterone response to ethanol in BXD recombinant inbred mice. *Behav. Neurosci.* 109, 1199–1208. doi: 10.1037/0735-7044.109.6.1199

Rodriguez, L. A., Plomin, R., Blizard, D. A., Jones, B. C., and McClearn, G. E. (1994). Alcohol acceptance, preference, and sensitivity in mice. I. Quantitative genetic analysis using BXD recombinant inbred strains. *Alcohol. Clin. Exp. Res.* 18, 1416–1422. doi: 10.1111/j.1530-0277.1994.tb01444.x

Sala-Newby, G. B., and Newby, A. C. (2001). Cloning of a mouse cytosolic 5′-nucleotidase-I identifies a new gene related to human autoimmune infertility-related protein. *Biochim. Biophys. Acta* 1521, 12–18. doi: 10.1016/S0167-4781(01)00278-0

Sloan, Z., Arends, D., Broman, K. W., Centeno, A., Furlotte, N. A., Nijveen, H., et al. (2016). GeneNetwork: framework for web-based genetics. *J. Open Source Softw.* 1:25. doi: 10.21105/joss.00025

Sobczyk-Kopciol, A., Broda, G., Wojnar, M., Kurjata, P., Jakubczyk, A., Klimkiewicz, A., et al. (2011). Inverse association of the obesity predisposing FTO rs9939609 genotype with alcohol consumption and risk for alcohol dependence. *Addiction* 106, 739–748. doi: 10.1111/j.1360-0443.2010.03248.x

Thiele, T. E., Crabbe, J. C., and Boehm, S. L. II (2014). "Drinking in the Dark" (DID): a simple mouse model of binge-like alcohol intake. *Curr. Protoc. Neurosci.* 68, 9.49.1–9.49.12. doi: 10.1002/0471142301.ns0949s68

Thiele, T. E., and Navarro, M. (2014). "Drinking in the dark" (DID) procedures: a model of binge-like ethanol drinking in non-dependent mice. *Alcohol* 48, 235–241. doi: 10.1016/j.alcohol.2013.08.005

Wang, L., Liu, X., Luo, X., Zeng, M., Zuo, L., and Wang, K. S. (2013). Genetic variants in the fat mass- and obesity-associated (FTO) gene are associated with alcohol dependence. *J. Mol. Neurosci.* 51, 416–424. doi: 10.1007/s12031-013-0044-2

Wang, X., Mozhui, K., Li, Z., Mulligan, M. K., Ingels, J. F., Zhou, X., et al. (2012). A promoter polymorphism in the Per3 gene is associated with alcohol and stress response. *Transl. Psychiatry* 2:e73. doi: 10.1038/tp.2011.71

Yang, J., Zaitlen, N. A., Goddard, M. E., Visscher, P. M., and Price, A. L. (2014). Advantages and pitfalls in the application of mixed-model association methods. *Nat. Genet.* 46, 100–106. doi: 10.1038/ng.2876

Young, A. I., Wauthier, F., and Donnelly, P. (2016). Multiple novel gene-by-environment interactions modify the effect of FTO variants on body mass index. *Nat. Commun.* 7:12724. doi: 10.1038/ncomms12724

Zhou, X., and Stephens, M. (2012). Genome-wide efficient mixed-model analysis for association studies. *Nat. Genet.* 44, 821–824. doi: 10.1038/ng.2310

Conflict of Interest Statement: The authors declare that the research was conducted in the absence of any commercial or financial relationships that could be construed as a potential conflict of interest.

frontiers in Genetics

ORIGINAL RESEARCH
published: 27 November 2018
doi: 10.3389/fgene.2018.00566

Genetic Model to Study the Co-Morbid Phenotypes of Increased Alcohol Intake and Prior Stress-Induced Enhanced Fear Memory

Patrick Henry Lim[1†], Guang Shi[2†], Tengfei Wang[3], Sophia T. Jenz[1], Megan K. Mulligan[4], Eva E. Redei[1] and Hao Chen[3]**

[1] Department of Psychiatry and Behavioral Science, Feinberg School of Medicine, Northwestern University, Chicago, IL, United States, [2] Liaoning Provincial People's Hospital, Liaoning Sheng, China, [3] Department of Pharmacology, University of Tennessee Health Science Center, Memphis, TN, United States, [4] Department of Genetics Genomics and Informatics, University of Tennessee Health Science Center, Memphis, TN, United States

OPEN ACCESS

Edited by:
Frank Middleton,
Upstate Medical University,
United States

Reviewed by:
Richard Lowell Bell,
Indiana University, Indianapolis,
United States
Robert Philibert,
University of Iowa, United States

***Correspondence:**
Eva E. Redei
e-redei@northwestern.edu
Hao Chen
hchen@uthsc.edu

[†]Co-first authors

Specialty section:
This article was submitted to Behavioral and Psychiatric Genetics, a section of the journal Frontiers in Genetics

Received: 23 April 2018
Accepted: 06 November 2018
Published: 27 November 2018

Citation:
Lim PH, Shi G, Wang T, Jenz ST, Mulligan MK, Redei EE and Chen H (2018) Genetic Model to Study the Co-Morbid Phenotypes of Increased Alcohol Intake and Prior Stress-Induced Enhanced Fear Memory. Front. Genet. 9:566. doi: 10.3389/fgene.2018.00566

Posttraumatic Stress Disorder (PTSD) is a complex illness, frequently co-morbid with depression, caused by both genetics, and the environment. Alcohol Use Disorder (AUD), which also co-occurs with depression, is often co-morbid with PTSD. To date, very few genes have been identified for PTSD and even less for PTSD comorbidity with AUD, likely because of the phenotypic heterogeneity seen in humans, combined with each gene playing a relatively small role in disease predisposition. In the current study, we investigated whether a genetic model of depression-like behavior, further developed from the depression model Wistar Kyoto (WKY) rat, is a suitable vehicle to uncover the genetics of co-morbidity between PTSD and AUD. The by-now inbred WKY More Immobile (WMI) and the WKY Less Immobile (WLI) rats were generated from the WKY via bidirectional selective breeding using the forced swim test, a measure of despair-like behavior, as the functional selector. The colonies of the WMIs that show despair-like behavior and the control strain showing less or no despair-like behavior, the WLI, are maintained with strict inbreeding over 40 generations to date. WMIs of both sexes intrinsically self-administer more alcohol than WLIs. Alcohol self-administration is increased in the WMIs without sucrose fading, water deprivation or any prior stress, mimicking the increased voluntary alcohol-consumption of subjects with AUD. Prior Stress-Enhanced Fear Learning (SEFL) is a model of PTSD. WMI males, but not females, show increased SEFL after acute restraint stress in the context-dependent fear conditioning paradigm, a sexually dimorphic pattern similar to human data. Plasma corticosterone differences between stressed and not-stressed WLI and WMI male and female animals immediately prior to fear conditioning predict SEFL results. These data demonstrate that the WMI male and its genetically close, but behaviorally divergent control the WLI male, would be suitable for investigating the underlying genetic basis of comorbidity between SEFL and alcohol self-administration.

Keywords: alcohol self-administration, genetic model of depression, contextual fear conditioning, corticosterone, glucocorticoid receptor, alcohol use disorder, post traumatic stress disorder, inbred rat strains

INTRODUCTION

Comorbid posttraumatic stress disorder (PTSD) and alcohol use disorder (AUD) is a prevalent and devastating disorder. While exposure to a traumatic event is required for diagnosis, not all subjects who experience a traumatic event develop PTSD. PTSD has an overall lifetime prevalence rate of 7–8% and is the fifth most common major psychiatric disorder in the United States (Keane et al., 2006). PTSD has a high comorbidity with major depression (50–84%; Spinhoven et al., 2014; Flory and Yehuda, 2015) and other anxiety disorders (49%; Smith et al., 2016). AUD occurs in 30% of PTSD subjects and up to 54% in veterans (Smith et al., 2016). The cause of these high comorbidities might be that the preexistence of these disorders increases susceptibility to traumatic events (Breslau, 2009) or that all these disorders are the consequences of the traumatic exposure (Pietrzak et al., 2011). However, the odds of having PTSD are 30% greater for those with a lifetime AUD (Grant et al., 2015, 2016). Individual differences in heritable factors affect the risk to develop PTSD. Twin studies show that the heritability of PTSD alone is between 30–46% (Stein et al., 2002; Wolf et al., 2014). Nevertheless, genome-wide association studies have had limited success identifying these factors (Duncan et al., 2018; Polimanti et al., 2018), which is not surprising given the heterogeneity of the symptoms and comorbidities. Individual variations in comorbidity, namely that some PTSD patients do, while others do not have AUD, supports the hypothesis of overlapping genetic vulnerability to PTSD and AUD in some patients (McLeod et al., 2001; Frías and Palma, 2015). Critically, there is a paucity of data on the genetic vulnerabilities that cause the PTSD-AUD comorbidity. Novel animal models may lead to the identification of genetic vulnerabilities to this comorbidity and potentially to effective treatments for this refractory condition. Comorbidity with a disorder or illness is commonly defined as a condition existing simultaneously with and usually independently of another medical condition. The ideal animal model of comorbidity thus would show intrinsic characteristics modeling both conditions. One of the goals of this study is to establish a rat model of comorbidity between PTSD and AUD.

Valid animal models could help identify the genetic components of PTSD vulnerability. Among the many proposed rodent models, consensus as to what constitutes a PTSD-like model is just starting to emerge. PTSD has been related to exaggerated implicit fear memory, resulting from associative fear conditioning and non-associative sensitization processes (e.g., Foa et al., 1992; Charney et al., 1993). Most models have in common the study of emotional memories according to a Pavlovian learning paradigm. This associative learning process consists of the pairing of a neutral conditioned stimulus, such as a place or context, with an aversive unconditioned stimulus (e.g., shock) eliciting a conditioned fear response. Prior stress enhances fear conditioning in male rodents with long-term consequences (Blouin et al., 2016). This model represents an environmental enhancement (by prior stress) of fear memory, which closely reproduces many core symptoms of PTSD, including enhanced fear learning, generalized anxiety and impaired extinction (Rau et al., 2005).

Pavlovian fear conditioning also mimics the traumatic event-induced symptoms of intense and recurrent fear, characteristic of patients with PTSD (Zovkic and Sweatt, 2013). The advantages of fear conditioning as a model of PTSD include: (1) stress-induced exaggeration of fear conditioning, induced by exposing rodents to trauma prior to fear conditioning, models the environment-induced predisposition to PTSD; (2) rodent strains that vary in stress-induced exaggeration of fear memory can be used to dissect genetic predisposition to PTSD; (3) brain regions involved in the regulation of fear conditioning have also been implicated in the psychopathology of PTSD (Bremner, 2007; Hall et al., 2012; Zoladz and Diamond, 2013), and (4) the measurement of fear memory is automated and highly reproducible.

Stress-enhanced fear learning (SEFL) is an animal model of PTSD that encompasses both stress-sensitizing effects and conditioned fear memory components of the PTSD pathology (Rau et al., 2005; Blouin et al., 2016). Stress-induced release of peripheral corticosterone (CORT) has been suggested to be necessary for SEFL induction, and these changes are mediated by glucocorticoid (Nr3c1) and mineralcorticoid (Nr3c2) receptors (Donley et al., 2005; Rodrigues et al., 2009; Perusini et al., 2016). If prior stress exaggerates fear memory in one strain of animals, but not in another, it may present a model of PTSD that mirrors the variability in susceptibility to PTSD in humans (Skelton et al., 2012). Through a genetic animal model of depression, we aim to investigate the comorbid relationship between increased alcohol intake, acute stress-induced changes in fear memory and possible sex differences in these measures.

The genetic rat model of depression was developed from the near-inbred Wistar Kyoto (WKY) rat strain, an established model of major depression with co-morbid anxiety (Pare and Redei, 1993a,b; Pare, 1994; Solberg et al., 2001, 2004; Baum et al., 2006) and hormonal and sleep characteristics similar to those of depressed humans. Two inbred strains were generated from the WKYs by selective breeding based on immobility behavior in the forced swim test, resulting in two nearly isogenic inbred strains of their 38–41th generation at the time of this study. These are the WKY More Immobile (depressed WMI) showing despair-like behavior and its genetically similar, but behaviorally different control strain, the Wistar Kyoto Less Immobile (WLI). The WMI rats consistently display depression-like behavior in the forced swim test compared to their genetically very close less immobile (WLI) control strain (Will et al., 2003; Andrus et al., 2012; Mehta et al., 2013).

We hypothesized that WMIs would likely display increased fear memory sensitized by a prior acute stress, as 50–84% of PTSD patients have been diagnosed with major depression as well. We further hypothesized that WMI would likely consume more alcohol than the WLI controls based on clinical reports that the odds of having PTSD are 30% greater for those with AUD and major depression is also co-morbid with AUD. To test these hypotheses and the possibility that WMIs could serve as genetic model for the comorbidity of PTSD and AUD, we exposed adult male and female WMIs and WLIs to SEFL and another set of animals to an operant alcohol drinking paradigm.

MATERIALS AND METHODS

Experimental Design and Statistical Analysis

Different cohorts of animals were used in the three different sets of experiments. In the first set of experiments, 6 to 7-month-old WLI and WMI males and females were either exposed to acute restraint stress (ARS) or received no stress (NRS). Forty-eight hours later they were exposed to contextual fear conditioning (CFC). In the second set of experiments, age matched male and female rats were exposed to ARS or NRS and then sacrificed 48 h later without CFC test to measure brain gene expression and plasma corticosterone levels. The third set of WLI and WMI male and female animals received alcohol via a self-administration protocol. Sample numbers are indicated in the figure legends.

Activity and fear memory in the CFC, and plasma corticosterone levels were analyzed first by three-way ANOVA (strain, sex, and stress), followed by separate two-way ANOVAs for males and females to identify strain and stress effects, specifically. Bonferroni corrections for *post-hoc* comparisons were used to identify differences between groups. ANOVA results are described in the results section, while *post-hoc* comparisons are indicated on the figures and in the figure legends. Significance was considered $p < 0.05$. Effect size (Cohen's d; Cohen, 1988) was calculated using the 'effsize' package of the R language. Statistical analyses were carried out by GraphPad Prism 7 (La Jolla, CA, United States) and Systat softwares.

Animals and Behavioral Tests

The animal colonies are maintained at Northwestern University, Feinberg School of Medicine and at the University of Tennessee Health Science Center. The Institutional Animal Care and Use Committee of Northwestern University and the University of Tennessee Health Science Center approved all animal procedures. The guidelines described in the Public Health Service Policy on Humane Care and Use of Laboratory Animals are followed. Animals were housed in a temperature and humidity-controlled environment. Male and female WMIs and WLIs were employed at 6 to 7-months-of-age.

Acute Restraint Stress

The rats were placed into flexible plastic bags with an opening for their mouth and nose. The animals could not turn around in this apparatus nor move the plastic bags. The restraint was conducted between 1200–1600 h. After 2 h, the rats were placed back into their home-cages and 48 h later, one cohort was sacrificed by fast decapitation to obtain blood and brain tissue and another cohort was tested in contextual fear conditioning.

Contextual Fear Conditioning

Rats were placed into an automated fear conditioning apparatus of Technical & Scientific Equipment (TSE, Bad Homburg, Germany) for 3 min of habituation, followed by three mild shocks (0.8 mA, 1 s per min) over 3 min. Between animals, the chamber was cleaned using 75% ethanol to eliminate behavioral changes caused by odor. Twenty-four hours later, the rats were placed in the same chamber for 3 min without any shocks and examined for contextual fear memory as measured by freezing duration and total locomotion (distance traveled) through the use of an infrared beam system (detection rate 10 Hz). Any rats that did not respond to the initial shock were excluded from the study.

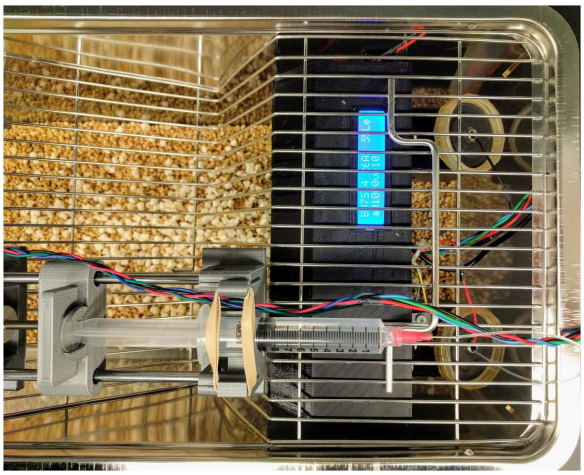

FIGURE 1 | Operant licking device for oral alcohol self-administration. The device has a lick sensor that records licking events from both the active and inactive spouts. Licking on the active spout meeting a variable ratio schedule triggers the syringe pump to push one drop (60 μl) of alcohol to the tip of the spout. A visual cue (an LED) is turned on for 1 s with each reward. Licking on the inactive spout has no programed consequence.

Operant Alcohol Self-Administration

Oral alcohol self-administration using licking as the operant response was carried out in an open source device we described previously (Longley et al., 2017). **Figure 1** shows the device employed for alcohol self-administration. It is constructed from a 3D printed frame and contained a single-board computer that monitors two licking spouts. When the number of licks on the active spout met variable ratio 10 reinforcement criteria, the computer advanced a syringe pump and pushes one drop (60 μl) of 6.5% alcohol to the tip of the spout. A visual cue (an LED) was turned on for 1 s with each reward. Licking events were recorded on the inactive spout, or on the active spout within the 20 s timeout period after the reward was delivered but no consequence are programmed for these events. Rats were tested individually during the light off phase of the diurnal cycle without prior operant training, water deprivation or sucrose training. A total of 10 daily 1 h sessions were conducted.

Plasma Corticosterone (CORT) ELISA

Trunk blood samples were collected into EDTA-coated tubes on ice. The samples were centrifuged at 3500 rpm for 10 min. Plasma was stored at −80°C for later analysis. Plasma corticosterone levels were measured by immunoassay using a commercially available competitive ELISA kit (Corticosterone Competitive ELISA kit, ThermoFisher, United States).

Measurement of Hippocampal Glucocorticoid and Mineralocorticoid Receptor mRNA Levels

Rat brains were rapidly dissected on ice using Paxinos coordinates (Paxinos and Watson, 2013) for the whole hippocampus (AP−2.12 to −6.0, ML 0 to 5.0, DV 5.4 to 7.6). Tissues were collected into RNAlater reagent (Ambion, Austin, TX, United States) and stored at −80°C.

RNA extraction using the Direct-zol RNA Miniprep kit (Zymo Research, Irvine, CA, United States) and quantitative PCR (qPCR) using the QuantStudio 7 Flex Real-Time PCR System (Thermo Fisher Scientific, Waltham, MA, United States) were performed as described previously (Tunc-Ozcan et al., 2017). Target gene expression (*Nr3c1* and *Nr3c2*) was normalized to *Gapdh* as the housekeeping gene and a general calibrator using the $2^{-\Delta\Delta Ct}$ method. Primer sequences are listed in **Supplementary Table 1**.

RESULTS

Stress Enhanced Fear Learning

Habituation to Test Environment

During the fear learning phase of CFC (Day 1), the activity of the rats and the responsiveness to the foot-shocks were measured by the distance traveled prior to the shock. In general, males were more active than females [sex, $F(1,117) = 11.15$, $p < 0.001$] (**Figures 2A,B**). Although there were no strain differences in distance traveled during habituation, WLI males and WMI females were in general more active than the sex-matched opposite strain [strain × sex, $F(1,117) = 5.16$, $p < 0.05$]. Exposure to acute restraint stress 48 h prior to the CFC test significantly increased travel distance during the habituation period [stress, $F(1,117) = 6.24$, $p = 0.01$], specifically in females but not in males [stress × sex, $F(1,117) = 8.26$, $p < 0.01$].

Fear Memory

When exposed to the CFC chamber a second time without the shock, both males and females showed a significant difference in activity after stress [stress: $F(1,129) = 7.55$, $p < 0.01$]. There was a significant strain-by-sex-by-stress interaction for activity [$F(1,129) = 7.23$, $p < 0.01$). Previously stressed ARS WLI females showed attenuated activity compared to non-stressed NRS WLI females (**Figure 2C**). The opposite pattern was observed in males where ARS WMI males demonstrated attenuated activity compared to NRS WMI males (**Figure 2D**). No attenuation in activity was observed for ARS WMI females or ARS WLI males relative to their respective NRS controls.

The inverse, but also significant, change was seen in freeze duration between the NRS and ARS males and females [stress: $F(1,129) = 8.79$, $p < 0.01$]. Freeze duration after stress were significantly and sex-dependently different between WLIs and WMIs. Increased freeze duration relative to NRS control rats was seen for ARS WLI females, but not in ARS WMI females (**Figure 2E**). Similarly, ARS WMI males showed increased freeze duration, an indication of enhanced fear memory, compared to NRS WMI males [**Figure 2F**, strain × sex, $F(1,129) = 8.51$, $p < 0.01$; strain × sex × stress, $F(1,129) = 13.69$, $p < 0.001$].

Plasma Corticosterone (CORT) and Hippocampal Glucocorticoid (Nr3c1) and Mineralocorticoid (Nr3c2) Receptor mRNA Levels 48 h Post-Acute Restraint Stress

Plasma CORT levels were measured in both the NRS and ARS groups at 48 h after the ARS group received restraint stress. CORT levels differed by strain and sex. Specifically in females, baseline (NRS) CORT levels were significantly higher in the WMIs compared to the WLIs, while the opposite was true in males [strain × sex, $F(1,32) = 12.31$; $p < 0.01$; **Figures 3A,B**]. Plasma CORT levels after stress were generally higher than in the NRS group [stress, $F(1,32) = 11.30$; $p < 0.01$], but they significantly and sex-dependently differed between WLIs and WMIs [strain × sex × stress, $F(1,32) = 10.54$, $p < 0.01$]. ARS significantly increased CORT levels in WLI females but did not result in a further increase in CORT levels in WMI females (**Figure 3A**). In direct contrast to the results in females, ARS significantly increased CORT levels of the WMI males only, with no further increase in CORT levels in WLI males (**Figure 3B**).

Hippocampal *Nr3c1* transcript levels, measured in the same animals as plasma CORT, did not show overall significant sex or strain differences although the trend ($p < 0.1$) was there for both variables [strain, $F(1,31) = 3.46$; $p = 0.072$; sex, $F(1,31) = 3.94$; $p = 0.056$; **Figures 3C,D**). However, there were significant strain-by-sex interactions [strain × sex, $F(1,31) = 18.60$; $p < 0.001$]. In females, *Nr3c1* mRNA levels were significantly higher in the WLI hippocampus, while in males, expression was greater in the WMI hippocampus without prior restraint stress compared to the other strain. However, in contrast to the ARS-induced changes in plasma CORT, acute restraint stress increased hippocampal *Nr3c1* expression in the WMI female, but decreased it in the WMI male hippocampus [stress, $F(1,31) = 4.30$; $p < 0.05$; strain × stress, $F(1,11) = 4.85$; $p < 0.05$; sex × stress, $F(1,31) = 9.97$, $p < 0.01$; strain × sex × stress, $F(1,31) = 27.71$, $p < 0.001$].

Hippocampal *Nr3c2* expression was in general higher in females than in males [sex, $F(1,42) = 7.29$, $p = 0.01$; **Figures 3E,F**]. The prior stress-induced changes were small and strain dependent [strain × stress, $F(1,42) = 6.76$, $p = 0.013$].

The overall association between plasma CORT levels and hippocampal *Nr3c1* expression is shown on **Figure 4**. In males, linear regression identified a significant negative association between plasma CORT and hippocampal *Nr3c1* transcript levels [$F(1,16) = 4.78$, $p < 0.05$]. No association was detected for females.

Operant Oral Alcohol Self-Administration

The number of licks on the active spout by the WMI rats were greater than those of the WLI rats throughout the 10 daily test sessions (**Figure 5A**). Repeated measures ANOVA found a significant strain effect [$F(1,30) = 9.01$, $p = 0.005$]. The differences in licks on the inactive spouts were not significantly different

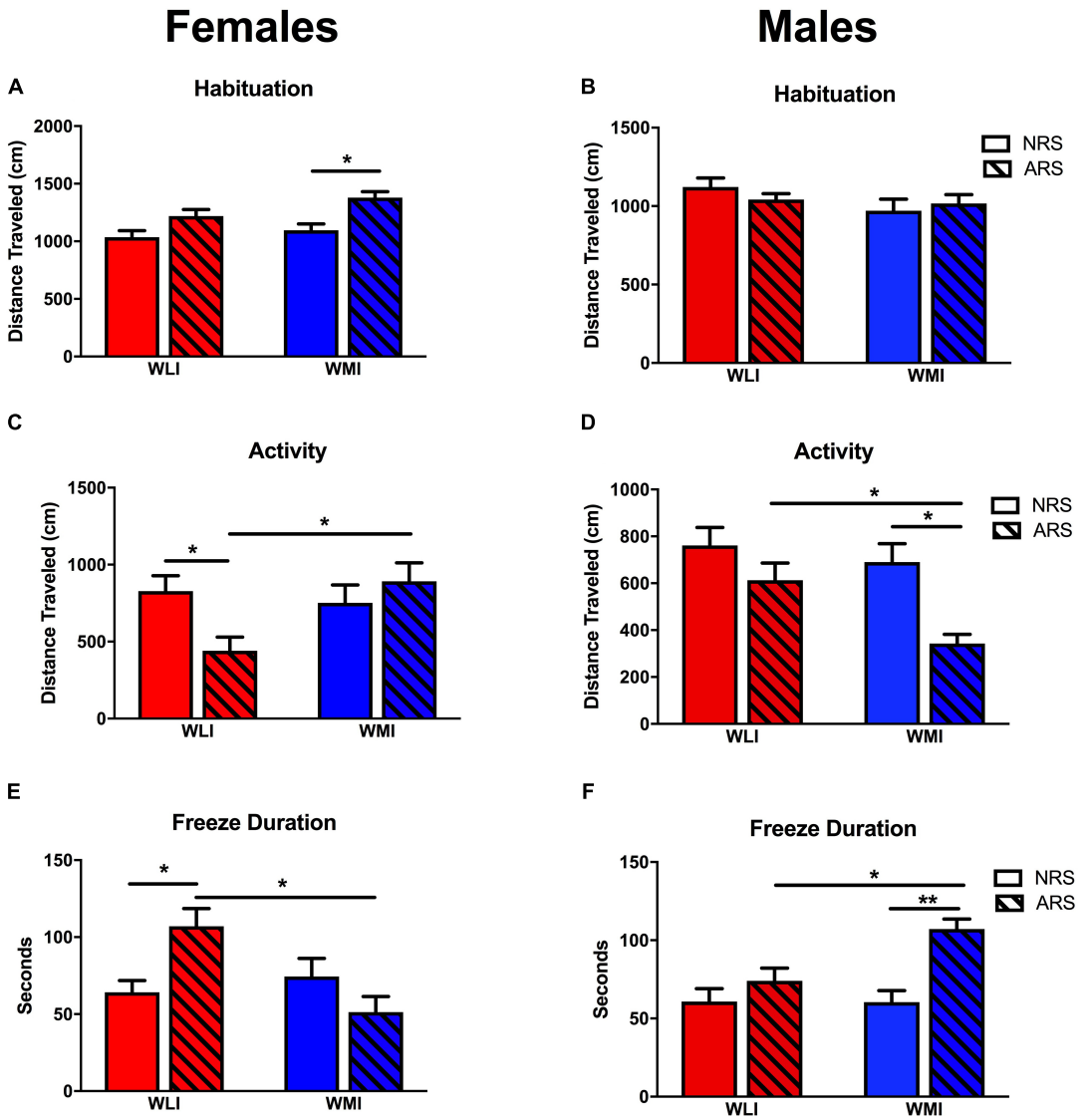

FIGURE 2 | Fear Memory in CFC. Pre-CFC activity, measured by distance traveled in females **(A)** and males **(B)**. Distance traveled prior to the conditioning stimulus did not differ significantly between strains or acute stress (ARS) and no-stress (NRS) conditions except for WMI females, which showed increased activity after acute restraint stress. Distance traveled on the second day of the contextual fear conditioning did not differ between NRS WLI and WMI females **(C)** or NRS males **(D)**. However, WLI females and WMI males showed significantly decreased distance traveled after ARS. Showing the inverse relationship, WLI females and WMI males showed significantly increased freeze duration after ARS, with no differences in fear duration between the strains in the NRS condition **(E**,**F)**. Values are shown as mean ± SEM; $*p < 0.05$, $**p < 0.01$, *post-hoc* following ANOVA. WLI NRS male $n = 26$; NRS female $n = 23$; AS male $n = 17$, AS female $n = 13$; WMI NRS male $n = 15$, NRS female $n = 18$, AS male $n = 15$, AS female $n = 10$.

between the strains [$F(1,30) = 0.007$, $p > 0.05$]. WLIs licked 134.5 ± 29.1 times on the active spout and 76.9 ± 13.1 times on the inactive spout during the first session. WMIs licked 208.5 ± 49.9 times on the active spout and 63.9 ± 7.1 times on the inactive spouts during the first session. The number of licks on the active spout increased significantly across the test sessions [$F(9,143) = 6.9$, $p = 2.68 \times 10^{-8}$) in both strains. By session 10, WLI licked 446.0 ± 67.8 times on the active spout and 78.8 ± 16.8 times on the inactive spout. The number of licks on the active spouts were significantly greater than those on the inactive spouts [$F(1,11) = 89.4$, $p = 1.29 \times 10^{-6}$) in both strains. Increases in the number of active licks across the test sessions was statistically highly significant [$F(1,19) = 133.5$, $p = 4.9 \times 10^{-10}$). For the WMIs, the number of licks increased to 558.9 ± 71.4 on the active spout but declined to 50.8 ± 6.2 on the inactive spout in session 10 (**Figure 5A**).

Alcohol intake (mg/kg bodyweight; **Figure 5B**) did not change significantly across the sessions in the WLI strain [$F(9,123) = 1.35$, $p > 0.05$] but increased significantly in the WMI strain [$F(9,175) = 2.86$, $p < 0.01$]. The amount of alcohol consumed was independent of sex for both strains [$F(1,6) = 5.16$, $p > 0.05$ for WLI and $F(1,15) = 1.18$, $p > 0.05$ for WMI]. When

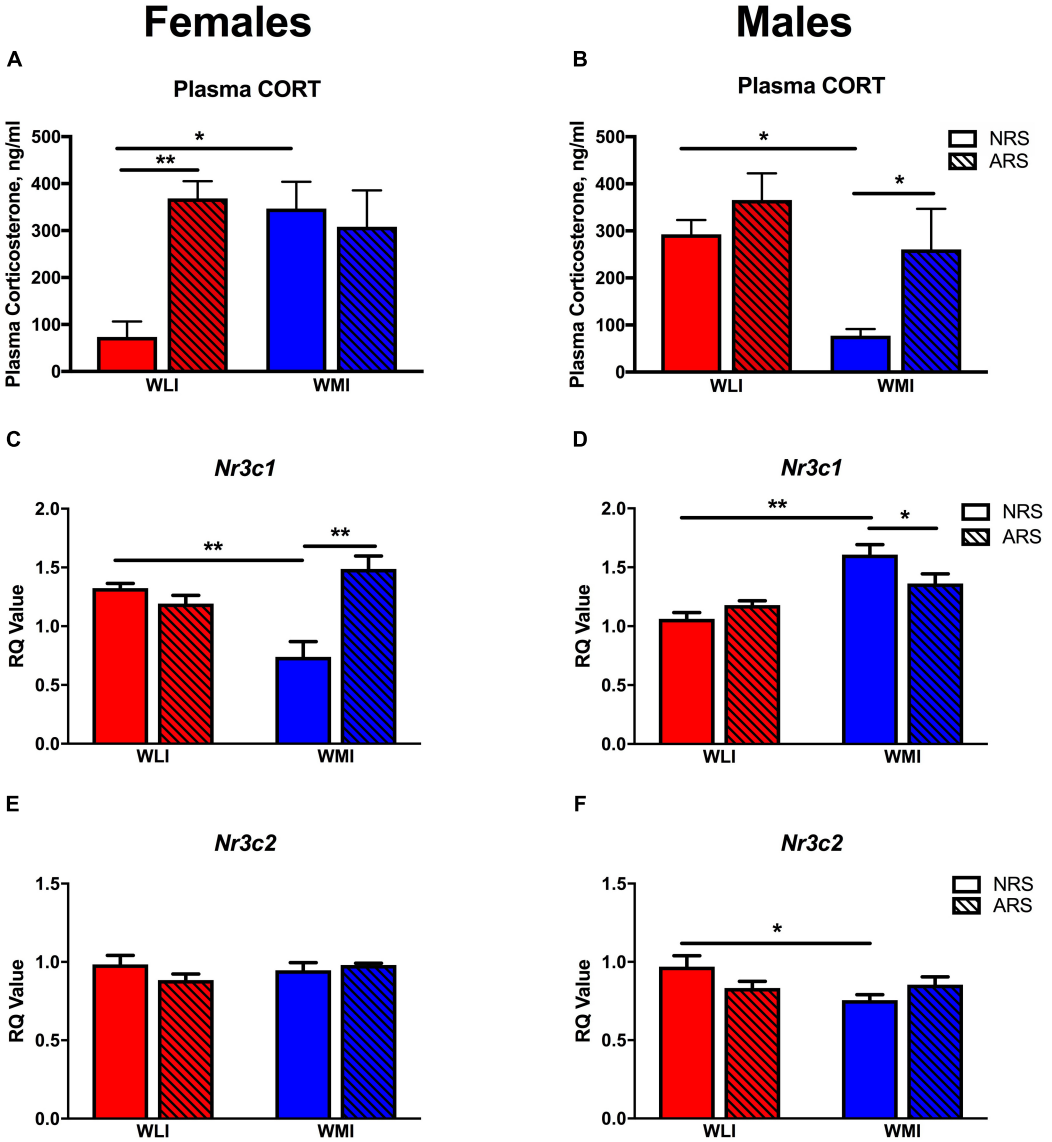

FIGURE 3 | Plasma corticosterone and hippocampal glucocorticoid and mineralcorticoid receptor expression. CORT levels were significantly higher in NRS WMI females **(A)** and NRS WLI males **(B)** compared to the other strain. Acute restraint stress resulted significantly higher CORT levels in the WLI females and WMI males compared to their NRS counterparts **(A**,**B)**, respectively. Hippocampal *Nr3c1* transcript levels showed the opposite pattern to that of plasma CORT. *Nr3c1* expression is decreased in the NRS WMI female **(C)** and in the NRS WLI male **(D)** compared to the other strain in the NRS condition. Acute stress increased *Nr3c1* expression in the WMI female but decreased it in the male hippocampus **(C**,**D)**, respectively. Hippocampal *Nr3c2* transcript levels showed no significant differences in females **(E)**, but decreased expression in NRS WMI compared to NRS WLI **(F)**. Plasma CORT levels, were measured by ELISA, in samples collected 48 h after the restrain stress or no stress applied. Transcript levels were measured in the hippocampus collected at the same time. The RT-PCR used GAPDH as the housekeeping gene and a general calibrator. Relative quantification (RQ) employed the $2^{-\Delta\Delta Ct}$ method. Values are shown as mean ± SEM; $*p < 0.05$; $**p < 0.01$. NRS, no stress; ARS, acute restraint stress; CORT, corticosterone; *Nr3c1*, glucocorticoid receptor; *Nr3c2*, mineralcorticoid receptor. WLI NRS male n = 5(CORT), 4(*Nr3c1*), 6(*Nr3c2*); NRS female n = 6(CORT), 5(*Nr3c1*), 8(*Nr3c2*); ARS male n = 4(CORT), 5(*Nr3c1*), 5(*Nr3c2*); ARS female n = 6(CORT), 6(*Nr3c1*), 6(*Nr3c2*); WMI NRS male n = 5(CORT), 4(*Nr3c1*), 6(*Nr3c2*); NRS female n = 4(CORT), 4(*Nr3c1*), 8(*Nr3c2*); ARS male n = 4(CORT), 5(*Nr3c1*), 5(*Nr3c2*); ARS female n = 6(CORT), 6(*Nr3c1*), 6(*Nr3c2*).

the two strains were compared, alcohol intake in the WMI was significantly greater than that of the WLI [$F(1,21) = 7.6, p < 0.01$].

Heritability

Heritability can be estimated from inbred strain trait data and used to determine the feasibility of genetic mapping. Heritabilities of 0.2 or higher demonstrate that genetic factors are a major contributor to phenotypic variation. Broad sense heritability or $H2$ (Hegmann and Possidente, 1981; Falconer and Mackay, 1996) was estimated from ANOVA for SEFL and alcohol intake by dividing the variance component among strains [AS_{com}, calculated as the mean square between strain subtracted

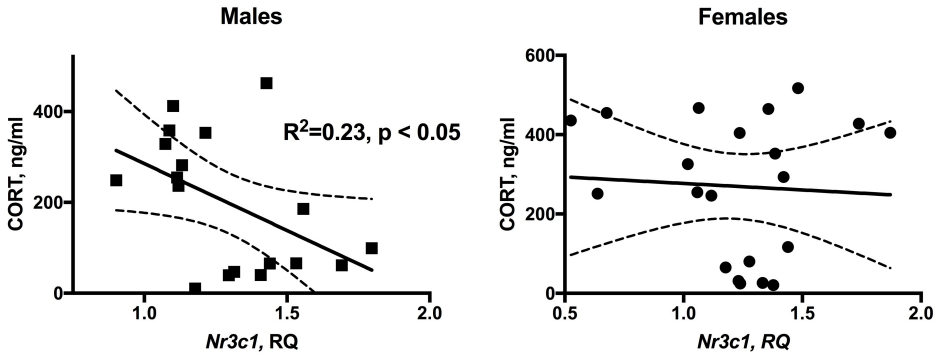

FIGURE 4 | Significant inverse relationship between plasma CORT levels and hippocampal *Nr3c1* expression in male WLI and WMI rats. There is no relationship in females. NRS and ARS data were combined. n = 18 (males) and n = 20 (females).

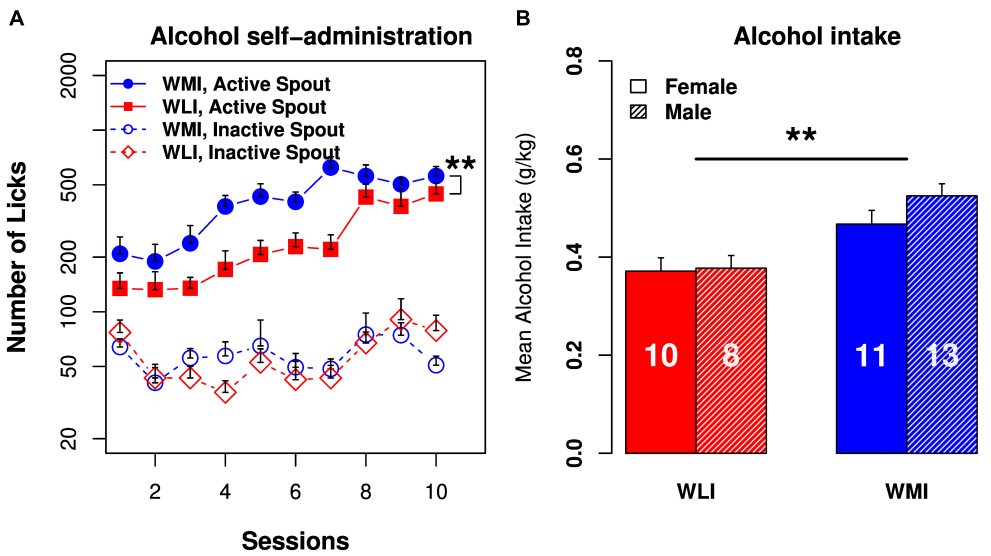

FIGURE 5 | Operant licking alcohol self-administration in WLI and WMI rats. **(A)** Both WMI and WLI rats licked more on the active spouts that delivered EtOH (6.5%) than on the inactive spouts. WMI licked significantly more than the WLI on the active spouts. The number of licks on the inactive spouts were not significantly different between strains. **(B)** Average alcohol intake per session was significantly greater in the WMI than in the WLI strain of animals. There was no sex difference in alcohol intake. Sample sizes are shown in the bar. $^{**}p < 0.01$.

by the variance component within strains (WS_{com}, mean square within strain)] by the total variance component (AS_{com} + WS_{com}). Heritability of the SEFL was estimated at 0.74 and 0.70 for females and males, respectively. The effect size (Cohen's D) for SEFL is 1.53 and 1.13 for females and males, respectively. Both are large effects. Heritability for alcohol self-administration was 0.45 with no sex difference. The corresponding effect size is 0.76 (medium size). These heritability estimates indicate that a significant proportion of variation in these phenotypes is due to genetic factors.

DISCUSSION

To our knowledge, this is the first study showing both *intrinsically* higher alcohol consumption and SEFL in an animal model. The major findings of the study include moderately high heritability and sex and strain differences in SEFL and high heritability and sex-independent strain differences in alcohol consumption. We demonstrated increased alcohol consumption of the WMI strain, developed as a genetic model of depression-like behavior, compared to its genetically close control WLI strain. We also confirmed previously observed sex differences in SEFL behavior, namely that male WMI demonstrate SEFL behavior (decreased activity and increased fear memory), while female WMI do not. Even more intriguing is that the control WLI strain displayed an inverse effect, with the WLI females exhibiting SEFL, while male WLIs did not. These behavioral differences in stress response coincide with the sexually dimorphic hormonal response to stress between the WLIs and WMIs; differences in NRS and ARS plasma CORT levels paralleled the presence of SEFL in contextual fear conditioning with higher CORT

levels associated with ARS in female WLI and male WMI only.

Alcohol self-administration was conducted without sucrose fading or water deprivation. Both of these strategies could affect the motivation to obtain alcohol that may or may not be relevant to increased alcohol intake. In the present study, the voluntary alcohol consumption of WMIs was significantly greater compared to those of WLIs, with strain having a medium effect size on alcohol drinking. This finding indicates a genetic predisposition, similarly to those occurring in many subjects with AUD (Foulds et al., 2015). Although the amount of alcohol consumed by these strains in the 1 h test period is only ∼0.5 g/kg body weight, it is similar to consuming two standard alcoholic drinks by a 70 kg human. Future experiments will seek to increase alcohol consumption by extending the length of the alcohol sessions and/or force withdrawal periods between sessions, which has been shown to better model human alcohol drinking (Smutek et al., 2014) The parental WKY strain of both the WMI and the WLI has been accepted as an animal model of depression (Pare and Redei, 1993a; Dugovic et al., 2000; Jeannotte et al., 2009; Tizabi et al., 2012). The WKY strain is also reported to consume more alcohol than the Sprague-Dawley strain (Pare et al., 1999) or the Wistar strain (Jiao et al., 2006; Yaroslavsky and Tejani-Butt, 2010). Others have reported that WKYs consume low levels of alcohol (Li and Lumeng, 1984; Khanna et al., 1990) compared to other strains, albeit in a sex-specific manner. These latter studies employ two different WKY strains, both of which are different from our parental WKY strain and from those used in the studies showing elevated alcohol consumption compared to other strains. This is a significant issue as we and others have reported genetic and phenotypic sub-strain differences according to suppliers of the WKY strain of animals (Kurtz and Morris, 1987; Kurtz et al., 1989; Matsumoto et al., 1991; Deschepper et al., 1997; Pare and Kluczynski, 1997; Okuda et al., 2002; Will et al., 2003; Zhang-James et al., 2013).

Strain and sex-dependent SEFL results presented in this study both confirmed and extended previous findings. This model was developed originally as an animal model of acute stress that parallels many symptoms of PTSD (Perusini et al., 2016). The SEFL paradigm developed by Fanselow and colleagues (Rau et al., 2005), employs a series of 15 shocks, which leads to subsequently exaggerated contextual fear. We have generated the same SEFL using a single 2 h acute restraint stress 48 h prior to the commencement of the contextual fear conditioning, similarly to previous studies (Cordero et al., 2003; Rodriguez Manzanares et al., 2005; Blouin et al., 2016). The similarity between the present and previous studies is the profound sex difference, namely that WMI males show SEFL, an indicator of enhanced fear memory, while WMI females do not. However, a surprising finding is the opposite effect in WLI females, where WLI females show SEFL, while WLI males do not.

We assessed the possibility that these differences are related to the basic anxiety-like behavior in these strains. The paternal WKY strain shows anxiety-like behavior in multiple behavioral paradigms (Pare and Redei, 1993a,b; Pare, 1994; Tizabi et al., 2010). Although the selective breeding of WKYs into the WLI and WMI strains was based on depression-like behavior in the forced swim test, the segregation of the depression- and anxiety-like behaviors of the male WMIs/WLIs occurred progressively throughout the generations (Mehta et al., 2013). Thus, male WMIs show lower levels of anxiety than WLIs, while both WLI and WMI females show equal level of anxiety-like behavior. If the higher trait anxiety is the cause of these paradoxical SEFL responses, then WLI males and both WLI and WMI females should show greater fear memory than that of WMI male. Because that is not the case, it is unlikely that the differences in SEFL are a result of differences in trait anxiety.

However, the stress-state of these animals differed significantly, as measured by plasma CORT levels at the time when contextual fear learning would be initiated. The mechanism of the unexpected findings; elevated CORT levels in the unstressed WMI females and WLI males and persistent plasma CORT elevations in the WLI females and WMI males 48 h after an acute restraint stress will need to be explored in the future. The high unstressed CORT levels of WMI females are not likely related to the depression-like behavior in these strains, as we have shown previously that the depression-like behavior of the parental WKY strain and CORT regulation are independent traits (Solberg et al., 2003), and the WLI male also show these high CORT levels. Sensitization of the hypothalamic-pituitary- by prior exposure to a single immobilization session has been shown to lasts for around 1 week (Belda et al., 2008, 2012, 2015). Whether the removal from the home cage and euthanasia is the cause, or whether the time between the removal from home cage and the collection of blood samples is sufficient time to show this presumed sensitization will need to be determined. The lack of change by ARS in plasma CORT levels of WLI males and WMI females might be related to their already high unstimulated levels of plasma CORT. Acute stress could possibly increase CORT levels in these animals as well in the usual stress response time frame such as 20–40 min after the onset of acute stress.

The surprising parallel between the plasma CORT level differences between non-stressed and stressed males and females and their SEFL measures suggest that a differential stress regulation drives the strain-, and sex-specificity of SEFL. In contextual fear conditioning, the presence of CORT is needed prior to conditioning to support the consolidation of a long-term representation of the context (Pugh et al., 1997). Administration of CORT is known to enhance fear conditioning in rats (Cordero et al., 2003; Thompson et al., 2004; Perusini et al., 2016). Inversely, blocking CORT synthesis prior to stress, but not any time after that, attenuates SEFL (Perusini et al., 2016). In that study it is concluded that CORT is necessary, but not sufficient to SEFL. In the present study, we observed large differences in the non-stressed CORT levels between the strains, but there were no differences in the stressed CORT levels 48 h post-stress. Thus, persistent elevation of plasma CORT levels without stress are not sufficient to elicit enhanced fear responses, but rather the elevation of levels from normally low basal CORT levels in response to stress are necessary. It is important to note, that patients with PTSD are often show lower cortisol levels compared with individuals without PTSD (Mason et al., 1986; Yehuda, 1997, 2001). Lower basal CORT levels in the WMI males and WLI females may be the necessary and sufficient criteria for showing

SEFL. This is an intriguing possibility that needs to be explored further.

The inverse relationship between plasma CORT and hippocampal glucocorticoid receptor expression is further evidence of the sex-specific differential regulation of the stress response in these strains. The linear regression between plasma CORT levels and hippocampal *Nr3c1* expression clearly shows that males have a significant association between these parameters, while females do not. While female rats are known to have higher basal CORT levels and enhanced CORT responses to stress compared to males, their glucocorticoid-regulated other functions are not enhanced (Hulshof et al., 2012). This implies a reduced efficacy of the CORT in females, including that of regulation of *Nr3c1* expression. As glucocorticoid receptor expression is subject to ligand mediated negative autoregulation, the higher *Nr3c1* expression in the WMI males without stress does suggest downregulation of the hypothalamic-pituitary adrenal axis activity in these animals. Since the WMI males are also the ones showing enhanced fear memory similar to those of subjects with PTSD, the lower basal (no-stress) CORT levels in these animals is in striking agreement with those reported for PTSD patients (Yehuda, 2001). Comparing our findings with that of human PTSD, albeit difficult, resulted in surprising parallels. High GR expression, although not in the hippocampus, but in peripheral blood, predicted high levels of PTSD symptoms in military personnel prior to deployment (van Zuiden et al., 2012; Girgenti and Duman, 2018; Daskalakis et al., 2018). Thus, the high GR expression of WMI males compared to WLI males without prior stress correctly predicts their SEFL, just as the opposite strain differences in GR expression predict it in females.

In the present study no plasma CORT levels were measured after the alcohol intake experiment. Although it has been suggested that individual variation in alcohol intake may not be related to endogenous CORT levels (Fahlke et al., 1994), whether that is true in the case of the WLI and WMI strains will need to be determined in the future. Measuring alcohol consumption after SEFL or conducting the SEFL after alcohol dependence could also answer important questions about this animal model in the future.

In conclusion, the male WMI is a unique, genetic model of comorbidity of PTSD- and AUD-like traits as it differs in these phenotypes from its nearly isogenic WLI control strain. This rodent model provides a unique opportunity to disentangle these comorbid phenotypes and dissect the influences of genetic and sex-specific factors, as the WMI strain likely harbor genetic variation(s) predisposing them to both higher alcohol intake and increased susceptibility to exaggerated fear learning following stress exposure.

AUTHOR CONTRIBUTIONS

HC, MM, and ER designed the study. PL, GS, TW, STJ, and HC carried out the experimental work. PL, GS, ER, and HC analyzed the data. PL, MM, ER, and HC drafted the manuscript. All authors approved the final manuscript.

FUNDING

This work was supported by the Davee Foundation (ER), NIH P50DA037844 (HC), NIH R01AA023774 (MM) and NIH R01ES022614 (MM).

SUPPLEMENTARY MATERIAL

The Supplementary Material for this article can be found online at: https://www.frontiersin.org/articles/10.3389/fgene.2018.00566/full#supplementary-material

REFERENCES

Andrus, B. M., Blizinsky, K., Vedell, P. T., Dennis, K., Shukla, P. K., Schaffer, D. J., et al. (2012). Gene expression patterns in the hippocampus and amygdala of endogenous depression and chronic stress models. *Mol. Psychiatry* 17, 49–61. doi: 10.1038/mp.2010.119

Baum, A. E., Solberg, L. C., Churchill, G. A., Ahmadiyeh, N., Takahashi, J. S., and Redei, E. E. (2006). Test- and behavior-specific genetic factors affect WKY hypoactivity in tests of emotionality. *Behav. Brain Res.* 169, 220–230. doi: 10.1016/j.bbr.2006.01.007

Belda, X., Daviu, N., Nadal, R., and Armario, A. (2012). Acute stress-induced sensitization of the pituitary-adrenal response to heterotypic stressors: independence of glucocorticoid release and activation of CRH1 receptors. *Horm. Behav.* 62, 515–524. doi: 10.1016/j.yhbeh.2012.08.013

Belda, X., Fuentes, S., Daviu, N., Nadal, R., and Armario, A. (2015). Stress-induced sensitization: the hypothalamic-pituitary-adrenal axis and beyond. *Stress* 18, 269–279. doi: 10.3109/10253890.2015.1067678

Belda, X., Fuentes, S., Nadal, R., and Armario, A. (2008). A single exposure to immobilization causes long-lasting pituitary-adrenal and behavioral sensitization to mild stressors. *Horm. Behav.* 54, 654–661. doi: 10.1016/j.yhbeh.2008.07.003

Blouin, A. M., Sillivan, S. E., Joseph, N. F., and Miller, C. A. (2016). The potential of epigenetics in stress-enhanced fear learning models of PTSD. *Learn. Mem.* 23, 576–586. doi: 10.1101/lm.040485.115

Bremner, J. D. (2007). Neuroimaging in posttraumatic stress disorder and other stress-related disorders. *Neuroimaging Clin. N. Am.* 17, 523–538. doi: 10.1016/j.nic.2007.07.003

Breslau, N. (2009). The epidemiology of trauma, PTSD, and other posttrauma disorders. *Trauma Violence Abuse* 10, 198–210. doi: 10.1177/1524838009334448

Charney, D. S., Deutch, A. Y., Krystal, J. H., Southwick, S. M., and Davis, M. (1993). Psychobiologic mechanisms of posttraumatic stress disorder. *Arch. Gen. Psychiatry* 50, 294–305. doi: 10.1001/archpsyc.1993.01820160064008

Cohen, J. (1988). *Statistical Power Analysis for the Behavioral Sciences*, 2nd Edn. New York, NY: Academic Press.

Cordero, M. I., Venero, C., Kruyt, N. D., and Sandi, C. (2003). Prior exposure to a single stress session facilitates subsequent contextual fear conditioning in rats. Evidence for a role of corticosterone. *Horm. Behav.* 44, 338–345. doi: 10.1016/S0018-506X(03)00160-0

Daskalakis, N. P., Provost, A. C., Hunter, R. G., and Guffanti, G. (2018). Noncoding RNAs: Stress, Glucocorticoids, and Posttraumatic Stress Disorder. *Biol. Psychiatry* 83, 849–865. doi: 10.1016/j.biopsych.2018.01.009

Deschepper, C. F., Prescott, G., Hendley, E. D., and Reudelhuber, T. L. (1997). Genetic characterization of novel strains of rats derived from crosses between

Wistar-Kyoto and spontaneously hypertensive rats, and comparisons with their parental strains. *Lab. Anim. Sci.* 47, 638–646.

Donley, M. P., Schulkin, J., and Rosen, J. B. (2005). Glucocorticoid receptor antagonism in the basolateral amygdala and ventral hippocampus interferes with long-term memory of contextual fear. *Behav. Brain Res.* 164, 197–205. doi: 10.1016/j.bbr.2005.06.020

Dugovic, C., Solberg, L. C., Redei, E., Van Reeth, O., and Turek, F. W. (2000). Sleep in the Wistar-Kyoto rat, a putative genetic animal model for depression. *Neuroreport* 11, 627–631. doi: 10.1097/00001756-200002280-00038

Duncan, L. E., Ratanatharathorn, A., Aiello, A. E., Almli, L. M., Amstadter, A. B., Ashley-Koch, A. E., et al. (2018). Largest GWAS of PTSD (N = 20 070) yields genetic overlap with schizophrenia and sex differences in heritability. *Mol. Psychiatry* 23, 666–673. doi: 10.1038/mp.2017.77

Fahlke, C., Engel, J. A., Peter Eriksson, C. J., Hård, E., and Söderpalm, B. (1994). Involvement of corticosterone in the modulation of ethanol consumption in the rat. *Alcohol* 11, 195–202. doi: 10.1016/0741-8329(94)90031-0

Falconer, D. S., and Mackay, T. F. C. (1996). *Introduction to Quantitative Genetics*, 4th Edn. Harlow: Addison Wesley Longman, 160–183.

Flory, J. D., and Yehuda, R. (2015). Comorbidity between post-traumatic stress disorder and major depressive disorder: alternative explanations and treatment considerations. *Dialogues Clin. Neurosci.* 17, 141–150.

Foa, E. B., Zinbarg, R., and Rothbaum, B. O. (1992). Uncontrollability and unpredictability in post-traumatic stress disorder: an animal model. *Psychol. Bull.* 112, 218–238. doi: 10.1037/0033-2909.112.2.218

Foulds, J. A., Adamson, S. J., Boden, J. M., Williman, J. A., and Mulder, R. T. (2015). Depression in patients with alcohol use disorders: systematic review and meta-analysis of outcomes for independent and substance-induced disorders. *J. Affect. Disord.* 185, 47–59. doi: 10.1016/j.jad.2015.06.024

Frías, Á, and Palma, C. (2015). Comorbidity between post-traumatic stress disorder and borderline personality disorder: a review. *Psychopathology* 48, 1–10. doi: 10.1159/000363145

Girgenti, M. J., and Duman, R. S. (2018). Transcriptome alterations in posttraumatic stress disorder. *Biol. Psychiatry* 83, 840–848. doi: 10.1016/j.biopsych.2017.09.023

Grant, B. F., Goldstein, R. B., Smith, S. M., Jung, J., Zhang, H., Chou, S. P., et al. (2015). The Alcohol Use Disorder and Associated Disabilities Interview Schedule-5 (AUDADIS-5): reliability of substance use and psychiatric disorder modules in a general population sample. *Drug Alcohol Depend.* 148, 27–33. doi: 10.1016/j.drugalcdep.2014.11.026

Grant, B. F., Saha, T. D., Ruan, W. J., Goldstein, R. B., Chou, S. P., Jung, J., et al. (2016). Epidemiology of DSM-5 drug use disorder: results from the national epidemiologic survey on alcohol and related conditions-III. *JAMA Psychiatry* 73, 39–47. doi: 10.1001/jamapsychiatry.2015.2132

Hall, T., Galletly, C., Clark, C. R., Veltmeyer, M., Metzger, L. J., Gilbertson, M. W., et al. (2012). The relationship between Hippocampal asymmetry and working memory processing in combat-related PTSD - a monozygotic twin study. *Biol. Mood Anxiety Disord.* 2:21. doi: 10.1186/2045-5380-2-21

Hegmann, J. P., and Possidente, B. (1981). Estimating genetic correlations from inbred strains. *Behav. Genet* 11, 103–114. doi: 10.1007/BF01065621

Hulshof, H. J., Novati, A., Luiten, P. G. M., den Boer, J. A., and Meerlo, P. (2012). Despite higher glucocorticoid levels and stress responses in female rats, both sexes exhibit similar stress-induced changes in hippocampal neurogenesis. *Behav. Brain Res.* 234, 357–364. doi: 10.1016/j.bbr.2012.07.011

Jeannotte, A. M., McCarthy, J. G., Redei, E. E., and Sidhu, A. (2009). Desipramine modulation of alpha-, gamma-synuclein, and the norepinephrine transporter in an animal model of depression. *Neuropsychopharmacology* 34, 987–998. doi: 10.1038/npp.2008.146

Jiao, X., Pare, W. P., and Tejani-Butt, S. M. (2006). Alcohol consumption alters dopamine transporter sites in Wistar-Kyoto rat brain. *Brain Res.* 107, 175–182. doi: 10.1016/j.brainres.2005.12.009

Keane, T. M., Marshall, A. D., and Taft, C. T. (2006). Posttraumatic stress disorder: etiology, epidemiology, and treatment outcome. *Annu. Rev. Clin. Psychol.* 2, 161–197. doi: 10.1146/annurev.clinpsy.2.022305.095305

Khanna, J. M., Kalant, H., Chau, A. K., and Sharma, H. (1990). Initial sensitivity, acute tolerance and alcohol consumption in four inbred strains of rats. *Psychopharmacology* 101, 390–395. doi: 10.1007/BF02244059

Kurtz, T. W., Montano, M., Chan, L., and Kabra, P. (1989). Molecular evidence of genetic heterogeneity in Wistar-Kyoto rats: implications for research with the spontaneously hypertensive rat. *Hypertension* 13, 188–192. doi: 10.1161/01.HYP.13.2.188

Kurtz, T. W., and Morris, R. C Jr (1987). Biological variability in Wistar-Kyoto rats. Implications for research with the spontaneously hypertensive rat. *Hypertension* 10, 127–131. doi: 10.1161/01.HYP.10.1.127

Li, T. K., and Lumeng, L. (1984). Alcohol preference and voluntary alcohol intakes of inbred rat strains and the National Institutes of Health heterogeneous stock of rats. *Alcohol. Clin. Exp. Res.* 8, 485–486. doi: 10.1111/j.1530-0277.1984.tb05708.x

Longley, M., Willis, E. L., Tay, C. X., and Chen, H. (2017). An open source device for operant licking in rats. *PeerJ* 5:e2981. doi: 10.7717/peerj.2981

Mason, J. W., Giller, E. L., Kosten, T. R., Ostroff, R. B., and Podd, L. (1986). Urinary free-cortisol levels in posttraumatic stress disorder patients. *J. Nerv. Ment. Dis.* 174, 145–149. doi: 10.1097/00005053-198603000-00003

Matsumoto, K., Yamada, T., Natori, T., Ikeda, K., Yamada, J., and Yamori, Y. (1991). Genetic variability in SHR (SHRSR), SHRSP and WKY strains. *Clin. Exp. Hypertens. A* 13, 925–938. doi: 10.3109/10641969109042098

McLeod, D. S., Koenen, K. C., Meyer, J. M., Lyons, M. J., Eisen, S., True, W., et al. (2001). Genetic and environmental influences on the relationship among combat exposure, posttraumatic stress disorder symptoms, and alcohol use. *J. Trauma. Stress* 14, 259–275. doi: 10.1023/A:1011157800050

Mehta, N. S., Wang, L., and Redei, E. E. (2013). Sex differences in depressive, anxious behaviors and hippocampal transcript levels in a genetic rat model. *Genes Brain Behav.* 12, 695–704. doi: 10.1111/gbb.12063

Okuda, T., Sumiya, T., Iwai, N., and Miyata, T. (2002). Difference of gene expression profiles in spontaneous hypertensive rats and Wistar-Kyoto rats from two sources. *Biochem. Biophys. Res. Commun.* 296, 537–543. doi: 10.1016/S0006-291X(02)00902-6

Pare, A. M., Pare, W. P., and Kluczynski, J. (1999). Negative affect and voluntary alcohol consumption in Wistar-Kyoto (WKY) and Sprague-Dawley rats. *Physiol. Behav.* 67, 219–225. doi: 10.1016/S0031-9384(99)00054-2

Pare, W. P. (1994). Open field, learned helplessness, conditioned defensive burying, and forced-swim tests in WKY rats. *Physiol. Behav.* 55, 433–439. doi: 10.1016/0031-9384(94)90097-3

Pare, W. P., and Kluczynski, J. (1997). Differences in the stress response of Wistar-Kyoto (WKY) rats from different vendors. *Physiol. Behav.* 62, 643–648. doi: 10.1016/S0031-9384(97)00191-1

Pare, W. P., and Redei, E. (1993a). Depressive behavior and stress ulcer in Wistar Kyoto rats. *J. Physiol. Paris* 87, 229–238. doi: 10.1016/0928-4257(93)90010-Q

Pare, W. P., and Redei, E. (1993b). Sex differences and stress response of WKY rats. *Physiol. Behav.* 54, 1179–1185. doi: 10.1016/0031-9384(93)90345-G

Paxinos, G., and Watson, C. (2013). *The Rat Brain in Stereotaxic Coordinates*, 7thEdition Edn. Amsterdam: Elsevier.

Perusini, J. N., Meyer, E. M., Long, V. A., Rau, V., Nocera, N., Avershal, J., et al. (2016). Induction and expression of fear sensitization caused by acute traumatic stress. *Neuropsychopharmacology* 41, 45–57. doi: 10.1038/npp.2015.224

Pietrzak, R. H., Goldstein, R. B., Southwick, S. M., and Grant, B. F. (2011). Prevalence and Axis I comorbidity of full and partial posttraumatic stress disorder in the United States: results from wave 2 of the national epidemiologic survey on alcohol and related conditions. *J. Anxiety Disord.* 25, 456–465. doi: 10.1016/j.janxdis.2010.11.010

Polimanti, R., Kaufman, J., Zhao, H., Kranzler, H. R., Ursano, R. J., Kessler, R. C., et al. (2018). A genome-wide gene-by-trauma interaction study of alcohol misuse in two independent cohorts identifies PRKG1 as a risk locus. *Mol. Psychiatry* 23, 154–160. doi: 10.1038/mp.2017.24

Pugh, C. R., Tremblay, D., Fleshner, M., and Rudy, J. W. (1997). A selective role for corticosterone in contextual-fear conditioning. *Behav. Neurosci.* 111, 503–511. doi: 10.1037/0735-7044.111.3.503

Rau, V., DeCola, J. P., and Fanselow, M. S. (2005). Stress-induced enhancement of fear learning: an animal model of posttraumatic stress disorder. *Neurosci. Biobehav. Rev.* 29, 1207–1223. doi: 10.1016/j.neubiorev.2005.04.010

Rodrigues, S. M., LeDoux, J. E., and Sapolsky, R. M. (2009). The influence of stress hormones on fear circuitry. *Annu. Rev. Neurosci.* 32, 289–313. doi: 10.1146/annurev.neuro.051508.135620

Rodriguez Manzanares, P. A., Isoardi, N. A., Carrer, H. F., and Molina, V. A. (2005). Previous stress facilitates fear memory, attenuates GABAergic inhibition, and

increases synaptic plasticity in the rat basolateral amygdala. *J. Neurosci.* 25, 8725–8734. doi: 10.1523/JNEUROSCI.2260-05.2005

Skelton, K., Ressler, K. J., Norrholm, S. D., Jovanovic, T., and Bradley-Davino, B. (2012). PTSD and gene variants: new pathways and new thinking. *Neuropharmacology* 62, 628–637. doi: 10.1016/j.neuropharm.2011.02.013

Smith, S. M., Goldstein, R. B., and Grant, B. F. (2016). The association between post-traumatic stress disorder and lifetime DSM-5 psychiatric disorders among veterans: data from the National Epidemiologic Survey on Alcohol and Related Conditions-III (NESARC-III). *J. Psychiatr. Res.* 82, 16–22. doi: 10.1016/j.jpsychires.2016.06.022

Smutek, M., Turbasa, M., Sikora, M., Piechota, M., Zajdel, J., Przewlocki, R., et al. (2014). A model of alcohol drinking under an intermittent access schedule using group-housed mice. *PLoS One* 9:e968787. doi: 10.1371/journal.pone.0096787

Solberg, L. C., Ahmadiyeh, N., Baum, A. E., Vitaterna, M. H., Takahashi, J. S., Turek, F. W., et al. (2003). Depressive-like behavior and stress reactivity are independent traits in a Wistar Kyoto × Fisher 344 cross. *Mol. Psychiatry* 8, 423–433. doi: 10.1038/sj.mp.4001255

Solberg, L. C., Baum, A. E., Ahmadiyeh, N., Shimomura, K., Li, R., Turek, F. W., et al. (2004). Sex- and lineage-specific inheritance of depression-like behavior in the rat. *Mamm. Genome* 15, 648–662. doi: 10.1007/s00335-004-2326-z

Solberg, L. C., Olson, S. L., Turek, F. W., and Redei, E. (2001). Altered hormone levels and circadian rhythm of activity in the WKY rat, a putative animal model of depression. *Am. J. Physiol. Regul. Integr. Comp. Physiol.* 281, R786–R794. doi: 10.1152/ajpregu.2001.281.3.R786

Spinhoven, P., Penninx, B. W., van Hemert, A. M., de Rooij, M., and Elzinga, B. M. (2014). Comorbidity of PTSD in anxiety and depressive disorders: prevalence and shared risk factors. *Child Abuse Negl.* 38, 1320–1330. doi: 10.1016/j.chiabu.2014.01.017

Stein, M. B., Jang, K. L., Taylor, S., Vernon, P. A., and Livesley, W. J. (2002). Genetic and environmental influences on trauma exposure and posttraumatic stress disorder symptoms: a twin study. *Am. J. Psychiatry* 159, 1675–1681. doi: 10.1176/appi.ajp.159.10.1675

Thompson, B. L., Erickson, K., Schulkin, J., and Rosen, J. B. (2004). Corticosterone facilitates retention of contextually conditioned fear and increases CRH mRNA expression in the amygdala. *Behav. Brain Res.* 149, 209–215. doi: 10.1016/S0166-4328(03)00216-X

Tizabi, Y., Bhatti, B. H., Manaye, K. F., Das, J. R., and Akinfiresoye, L. (2012). Antidepressant-like effects of low ketamine dose is associated with increased hippocampal AMPA/NMDA receptor density ratio in female Wistar-Kyoto rats. *Neuroscience* 213, 72–80. doi: 10.1016/j.neuroscience.2012.03.052

Tizabi, Y., Hauser, S. R., Tyler, K. Y., Getachew, B., Madani, R., Sharma, Y., et al. (2010). Effects of nicotine on depressive-like behavior and hippocampal volume of female WKY rats. *Prog. Neuropsychopharmacol. Biol. Psychiatry* 34, 62–69. doi: 10.1016/j.pnpbp.2009.09.024

Tunc-Ozcan, E., Wert, S. L., Lim, P. H., Ferreira, A., and Redei, E. E. (2017). Hippocampus-dependent memory and allele-specific gene expression in adult offspring of alcohol-consuming dams after neonatal treatment with thyroxin or metformin. *Mol. Psychiatry* 23, 1643–1651. doi: 10.1038/mp.2017.129

van Zuiden, M., Heijnen, C. J., Maas, M., Amarouchi, K., Vermetten, E., Geuze, E., et al. (2012). Glucocorticoid sensitivity of leukocytes predicts PTSD, depressive and fatigue symptoms after military deployment: A prospective study. *Psychoneuroendocrinology* 37, 1822–1836. doi: 10.1016/j.psyneuen.2012.03.018

Will, C. C., Aird, F., and Redei, E. E. (2003). Selectively bred Wistar-Kyoto rats: an animal model of depression and hyper-responsiveness to antidepressants. *Mol. Psychiatry* 8, 925–932. doi: 10.1038/sj.mp.4001345

Wolf, E. J., Mitchell, K. S., Koenen, K. C., and Miller, M. W. (2014). Combat exposure severity as a moderator of genetic and environmental liability to post-traumatic stress disorder. *Psychol. Med.* 44, 1499–1509. doi: 10.1017/S0033291713002286

Yaroslavsky, I., and Tejani-Butt, S. M. (2010). Voluntary alcohol consumption alters stress-induced changes in dopamine-2 receptor binding in Wistar-Kyoto rat brain. *Pharmacol. Biochem. Behav.* 94, 471–476. doi: 10.1016/j.pbb.2009.10.010

Yehuda, R. (1997). Sensitization of the hypothalamic-pituitary-adrenal axis in posttraumatic stress disorder. *Ann. N. Y. Acad. Sci.* 821, 57–75. doi: 10.1111/j.1749-6632.1997.tb48269.x

Yehuda, R. (2001). Biology of posttraumatic stress disorder. *J. Clin. Psychiatry* 62(Suppl. 17), 41–46.

Zhang-James, Y., Middleton, F. A., and Faraone, S. V. (2013). Genetic architecture of Wistar-Kyoto rat and spontaneously hypertensive rat substrains from different sources. *Physiol. Genomics* 45, 528–538. doi: 10.1152/physiolgenomics.00002.2013

Zoladz, P. R., and Diamond, D. M. (2013). Current status on behavioral and biological markers of PTSD: a search for clarity in a conflicting literature. *Neurosci. Biobehav. Rev.* 37, 860–895. doi: 10.1016/j.neubiorev.2013.03.024

Zovkic, I. B., and Sweatt, J. D. (2013). Epigenetic mechanisms in learned fear: implications for PTSD. *Neuropsychopharmacology* 38, 77–93. doi: 10.1038/npp.2012.79

Conflict of Interest Statement: The authors declare that the research was conducted in the absence of any commercial or financial relationships that could be construed as a potential conflict of interest.

frontiers in Genetics

ORIGINAL RESEARCH
published: 29 November 2018
doi: 10.3389/fgene.2018.00567

Sex and β-Endorphin Influence the Effects of Ethanol on Limbic *Gabra2* Expression in a Mouse Binge Drinking Model

*Erin M. Rhinehart[1], Todd B. Nentwig[2], Diane E. Wilson[1], Kiarah T. Leonard[2], Bernie N. Chaney[2] and Judith E. Grisel[2]**

[1] Department of Biology, Susquehanna University, Selinsgrove, PA, United States, [2] Department of Psychology, Neuroscience Program, Bucknell University, Lewisburg, PA, United States

Binge drinking is a widespread problem linked to increased risk for alcohol-related complications, including development of alcohol use disorders. In the last decade, binge drinking has increased significantly, specifically in women. Clinically, sexually dimorphic effects of alcohol are well-characterized, however, the underlying mechanisms for these dimorphisms in the physiological and behavioral effects of alcohol are poorly understood. Among its many effects, alcohol consumption reduces anxiety via the inhibitory neurotransmitter GABA, most likely acting upon receptors containing the α-2 subunit (*Gabra2*). Previous research from our laboratory indicates that female mice lacking the endogenous opioid peptide β-endorphin (βE) have an overactive stress axis and enhanced anxiety-like phenotype, coupled with increased binge-like alcohol consumption. Because βE works via GABA signaling to reduce anxiety, we sought to determine whether sexually dimorphic binge drinking behavior in βE deficient mice is coupled with differences in CNS *Gabra2* expression. To test this hypothesis, we used βE knock-out mice in a "drinking in the dark" model where adult male and female C57BL/6J controls (βE +/+) and βE deficient (βE −/−; B6.129S2-Pomc^{tm1Low}/J) mice were provided with one bottle of 20% ethanol (EtOH) and one of water (EtOH drinkers) or two bottles of water (water drinkers) 3 h into the dark cycle for four consecutive days. Following a binge test on day 4, limbic tissue was collected and frozen for subsequent qRT-PCR analysis of *Gabra2* mRNA expression. Water-drinking βE +/+ females expressed more *Gabra2* in central nucleus of the amygdala and the bed nucleus of the stria terminalis than males, but this sex difference was absent in the βE −/− mice. Genotype alone had no effect on alcohol consumption or drug-induced increase in *Gabra2* expression. In contrast, βE expression had bi-directional effects in females: in wildtypes, *Gabra2* mRNA was reduced by binge EtOH consumption, while EtOH increased expression in βE −/− females to levels commensurate with drug-naïve βE +/+ females. These results support the contention that βE plays a role in sexually dimorphic binge-like EtOH consumption, perhaps through differential expression of $GABA_A$ α2 subunits in limbic structures known to play key roles in the regulation of stress and anxiety.

Keywords: alcohol, BNST, CeA, $GABA_A$, sex differences, stress, POMC

OPEN ACCESS

Edited by:
Kristin Hamre, The University of Tennessee Health Science Center (UTHSC), United States

Reviewed by:
Richard S. Lee, Johns Hopkins University, United States
Dai N. Stephens, University of Sussex, United Kingdom

***Correspondence:**
Judith E. Grisel
j.grisel@bucknell.edu

Specialty section:
This article was submitted to Behavioral and Psychiatric Genetics, a section of the journal Frontiers in Genetics

Received: *25 May 2018*
Accepted: *06 November 2018*
Published: *29 November 2018*

Citation:
Rhinehart EM, Nentwig TB, Wilson DE, Leonard KT, Chaney BN and Grisel JE (2018) Sex and β-Endorphin Influence the Effects of Ethanol on Limbic Gabra2 Expression in a Mouse Binge Drinking Model. Front. Genet. 9:567. doi: 10.3389/fgene.2018.00567

INTRODUCTION

At least 10 million Americans have an alcohol use disorder (AUD), making alcohol one of the most abused drugs in the United States (Substance Abuse and Mental Health Services, 2018). According to epidemiological data, more men than women have AUDs; however, the gap between the rates of AUD in men and women is rapidly closing (Keyes et al., 2011; Gowing et al., 2015; Grant et al., 2017; Substance Abuse and Mental Health Services, 2018). In fact, male and female teenagers, aged 12–17, have equivalent alcohol usage rates (Gowing et al., 2015; Becker et al., 2017; Grant et al., 2017; Substance Abuse and Mental Health Services, 2018), with females exhibiting a disconcertingly rapid increase in binge drinking behavior (Jennison, 2004; Dwyer-Lindgren et al., 2015; Gowing et al., 2015; Becker et al., 2017; Grant et al., 2017; Substance Abuse and Mental Health Services, 2018). AUDs have complex etiologies with a strong genetic component (Gelernter and Kranzler, 2009). The changing sociocultural landscape has undoubtedly contributed to the escalating incidence of AUD in females (for example: da Mata Ribeiro et al., 2014; Glantz et al., 2014), but females who begin drinking alcohol may have greater vulnerability to AUD due to a variety of biological factors, such as sexually dimorphic gene expression in the brain (for review see: Becker et al., 2017). While historically fewer females than males experiment with drugs and alcohol, when females do imbibe they progress to addiction more often and more quickly than males (Piazza et al., 1989; Keyes et al., 2010; Valentino and Bangasser, 2016; Becker et al., 2017). This sexually dimorphic "telescoping" phenomenon, frequently observed in women is likely to be at least partly rooted in biological factors (Marinelli et al., 2003; Svikis et al., 2006; Rajasingh et al., 2007; Satta et al., 2018). In accordance, greater voluntary alcohol intake in females has been reported in multiple species (Forger and Morin, 1982; Morin and Forger, 1982; Li and Lumeng, 1984; Tambour et al., 2008) supporting the notion that females may possess greater vulnerability to alcohol addiction (Lynch, 2006).

There are a wide variety of potential explanations for sex differences in AUD vulnerability. For example, sexual dimorphisms in stress reactivity and stress-related disorders (Breslau et al., 1998; Bangasser et al., 2010; Hartwell and Ray, 2013; Bangasser and Valentino, 2014; Bandelow and Michaelis, 2015) could be partly responsible (Lynch, 2006). A preponderance of evidence indicates that stress-related psychiatric disorders, such as anxiety and post-traumatic stress disorder, occur more frequently in women than men (Breslau et al., 1998; Bangasser et al., 2010; Hartwell and Ray, 2013; Bangasser and Valentino, 2014; Bandelow and Michaelis, 2015). Sexual dimorphisms in the incidence of stress-related disorders are partly related to gender differences in psychological affect, social role identification and other sociocultural factors, but a significant sex disparity remains even after the contribution of these variables has been removed (Kendler et al., 1995a,b; Breslau et al., 1998; Tolin and Foa, 2006). In addition, AUD is frequently comorbid with anxiety disorders (Cullen et al., 2013; Gilpin and Weiner, 2017), providing additional evidence of a connection between AUD and stress-related disorders. In humans and other species, stress increases vulnerability to addiction, and it is an intrinsic driver of alcohol use and relapse (McGonigle et al., 2016; Clay et al., 2018; Milivojevic and Sinha, 2018). In addition, the anxiolytic properties of alcohol make it viable as a potential stress-coping strategy (Watt et al., 2014; Bos et al., 2016; McGonigle et al., 2016; Gorka and Shankman, 2017). Interestingly, females are more likely to drink alcohol to alleviate a negative emotional state, like that induced by chronic stress (Adams et al., 1991; Erol and Karpyak, 2015; Karpyak et al., 2016), and females are more susceptible to stress-induced drinking behaviors (Gorka et al., 2012; McGonigle et al., 2016). Therefore, it is critical to understand the influence of stress-reactivity on the mechanisms underlying sex differences in addiction, especially as the incidence of stress-related disorders continues to increase (Grucza et al., 2008; Thorisdottir et al., 2017).

When functioning properly, behavioral and physiological stress responses are adaptive. An adaptive stress response is limited in duration and followed by the restoration of homeostasis. Acute stress activates the hypothalamic-pituitary-adrenal (HPA) axis, stimulating corticotropin-releasing hormone (CRH) secretion from the paraventricular nucleus (PVN) of the hypothalamus and a subsequent increase in the precursor protein, proopiomelanocortin (POMC). POMC is then proteolytically cleaved into several signaling peptides, including the endogenous opioid peptide, β-endorphin (βE), an opioid agonist with high affinity for μ- and δ-opioid receptors. βE provides negative feedback to limit the duration of HPA axis activation, and it acts within the amygdala (AMY) to regulate behavioral responses to stressful stimuli and restore homeostasis (Charmandari et al., 2005). Genetic conditions that result in a reduction or elimination of βE signaling lead to an overactive HPA axis and an inability to exhibit adaptive coping responses to stress (Grisel et al., 2008; Barfield et al., 2010; McGonigle et al., 2016; Nentwig et al., 2018). In general, there is an inverse relationship between βE and anxiety-like behavior in mice (Grisel et al., 2008; Barfield et al., 2010; Nentwig et al., 2018), and lack of βE induces hyperactivity of the HPA axis (McGonigle et al., 2016; Nentwig et al., 2018). Therefore, genetic variability in the βE system may underlie stress-related disease vulnerability, which would impact the risk of AUD.

Because alcohol is frequently used for anxiolytic purposes, innate hyper-reactivity to stress increases addiction vulnerability (Sinha, 2001; Stephens and Wand, 2012; Blaine and Sinha, 2017). The anxiolytic effects of alcohol are mediated by the inhibitory neurotransmitter, gamma-amino butyric acid (GABA) (Engin et al., 2012; Lindemeyer et al., 2017). Alcohol potentiates GABA signaling at the $GABA_A$ receptor ($GABA_AR$) in limbic regions of the brain such as the ventral tegmental area (VTA), nucleus accumbens (NAc), central nucleus of the amygdala (CeA), and bed nucleus of the stria terminalis (BNST) (Suzdak et al., 1986; Hyytia and Koob, 1995; Xiao and Ye, 2008; Guan and Ye, 2010; Melon and Boehm, 2011). The $GABA_AR$ is a heterogeneous pentameric, transmembrane chloride ion channel, and the subunit composition of this receptor determines the pharmacological properties of the receptor (Barnard et al., 1998; Hevers and Luddens, 1998; Boehm et al., 2004; Olsen and Sieghart, 2009). The gene for the α2 ($GABA_Aα2$) subunit of

the $GABA_AR$ is highly connected with vulnerability to addiction in humans (Haughey et al., 2008; Enoch et al., 2009; Bierut et al., 2010; Enoch et al., 2012). The $GABA_A\alpha2$ gene (*Gabra2*) is expressed in the AMY, NAc, VTA, BNST, cortex, thalamus, and hypothalamus (Herbison and Fenelon, 1995; Schwarzer et al., 2001; Boehm et al., 2004; Dixon et al., 2010), with 15–20% of all GABAAR in the brain containing the GABAAα2 subunit (Pirker et al., 2000; Engin et al., 2012). Mice with a mutation in the Gabra2 gene have heightened baseline levels of anxiety (Dixon et al., 2008; Vollenweider Smith et al., 2011; Engin et al., 2012). Moreover, single nucleotide polymorphisms (SNPs) in the Gabra2 gene are robustly related to increased risk for AUDs (Edenberg et al., 2004; Enoch et al., 2006, 2012; Haughey et al., 2008; Bierut et al., 2010; Engin et al., 2012; Ittiwut et al., 2012; Uhart et al., 2013; Kuperman et al., 2017). Therefore, α2-containing $GABA_AR$s represent a potential link between sexually dimorphic stress-related disorders and AUD vulnerability.

A variety of previous studies have used animal models to attempt to elucidate the mechanisms underlying sex differences in EtOH-related behavior to shed light on the increasing female incidence of AUD. Data from rodent studies support the notion that females exposed to alcohol will imbibe more than males and become dependent more quickly than males (Li and Lumeng, 1984; Adams et al., 1991). Previous data from our laboratory indicate that βE is integral in the sexually dimorphic connection between stress and EtOH consumption (Barfield et al., 2010; McGonigle et al., 2016; Nentwig et al., 2018). For example, βE deficient mice have enhanced stress reactivity and anxiety-like behaviors as well as a decreased ability to behaviorally manage stress (Grisel et al., 2008; Barfield et al., 2010; McGonigle et al., 2016; Nentwig et al., 2018). These phenotypic differences are accompanied by greater CRH expression in the hypothalamus, AMY and BNST, which is correlated with increased serum cortisol and hypertrophied adrenal glands (McGonigle et al., 2016). Previous studies have also shown that stressed female βE deficient animals exhibit greater alcohol consumption (McGonigle et al., 2016), possibly in an effort to normalize HPA axis hyperactivity. Using the drinking in the dark (DID) paradigm, our laboratory also has also shown that female mice deficient for βE can use binge drinking behavior to normalize cortisol levels and decrease CRH expression in the BNST and CeA (Nentwig et al., 2018). These data provide support for the interaction of sex, βE and the stress axis in the behavioral regulation of EtOH consumption. The underlying molecular substrates of this interaction are currently unknown. Given the connection between AUD, stress, and the *Gabra2* gene outlined above, we tested the hypothesis that βE deficiency correlates with sexually dimorphic differences in *Gabra2* gene expression in the limbic system.

MATERIALS AND METHODS

Animals

Adult male and female C57BL/6J (βE +/+) and B6.129S2-$Pomc^{tm1Low}$/J (βE −/−) mice were either bred in-house and weaned at 21 days from stock obtained from Jackson Laboratories (Bar Harbor, ME, United States) or purchased as adults from Jackson Laboratories in which case they were acclimated at least 10 days prior to the onset of any experimental procedures. The βE −/− mice were developed in the laboratory of Malcolm Low and are fully backcrossed onto a C57BL/6J background. Transgenic mice harbor a truncated *Pomc* transgene that prevents synthesis of βE, although other POMC protein products remain unchanged, such that homozygotes cannot synthesize βE and heterozygotes produce ∼50% of wildtype levels (Rubinstein et al., 1996). βE −/− males have been shown to exhibit an overweight phenotype that increases with age, although we observed no differences in weight across genotypes of either sex in the present study. Mice were group-housed by sex and genotype before the start of the experiment, and individually during the experiment, in Plexiglas® cages with corncob bedding and *ad libitum* access to chow and water. The animal colony and experimental room were maintained at ∼21°C with a 12-h/12-h reverse light/dark cycle (lights off at 0930). We assessed mRNA expression from brains harvested in animals used in a previous study (Nentwig et al., 2018) and evaluated a separate group of naïve subjects in the DID protocol. Procedures were in accordance with the National Institute of Health guidelines and approved by the Bucknell University Institutional Animal Care and Use Committee.

Drinking in the Dark (DID) Procedures

A 2-bottle, 4-day DID procedure was performed as described previously (Nentwig et al., 2018) with water continuously available in one bottle for all mice. Mice were acclimated to individual housing for at least 7 days prior to the 4-day DID testing. On days 1–3 of DID testing, for 2 h beginning 3 h into the dark cycle, mice had access to two 25 mL graduated cylinders containing either 20% EtOH in tap water (v/v) or tap water alone (EtOH drinkers), while control groups received tap water in both bottles (water drinkers). On day 4, access to EtOH or the additional water tube was extended to a 4 h binge test session. Fluid intake levels were measured by a trained observer blind to experimental condition by reading gradations on bottles with accuracy to the nearest 0.1 mL.

Brain Punch Protocol and qRT-PCR

Immediately following the 4 h binge test on day 4, subjects were individually transported to an adjacent room, anesthetized using isoflurane, and rapidly decapitated. Brains were removed, frozen on dry ice, and stored at −80°C for gene expression using qRT-PCR. Frozen tissue was sliced on a Thermo Fisher HM 550 cryostat (Thermo Fisher Scientific, Waltham, MA, United States) and bilateral 1.5 mm cylindrical punches were taken of the NAc (+1.94 to +0.86 mm, with respect to bregma), BNST (+0.62 to −0.22 mm), and CeA (−0.82 to −1.82 mm) and immediately submerged in QIAzol lysis buffer (Qiagen GmbH, Hilden, Germany). Each sample tube containing one brain region from one mouse was homogenized immediately after sectioning. Total RNA was extracted using the Qiagen RNeasy Lipid Tissue Minikit (Qiagen GmbH, Hilden, Germany) according to manufacturer's instructions. Concentration and purity of eluted RNA was verified using the NanoDrop Lite UV spectrophotometer (Thermo Fisher Scientific, Waltham, MA,

United States) and 500 ng of total RNA was reverse-transcribed using the iScript™ cDNA Synthesis Kit (BioRad, Hercules, CA, United States) also according to manufacturer's instructions. qRT-PCR was performed using FastStart Essential DNA Probes Master Mix (Roche Diagnostics, Indianapolis, IN, United States) according to manufacturer's instructions. PrimeTime® XL qRT-PCR Assays designed by IDT (Integrated DNA Technologies, Coralville, IA, United States) were performed in duplicate on a LightCycler 96 (Roche Diagnostics, Indianapolis, IN, United States). All assays had similar optimum PCR efficiencies. For all qRT-PCR experiments, GAPDH gene expression was used as the reference gene and relative changes in gene expression were illustrated using the $2^{-\Delta\Delta CT}$ method (Schmittgen and Livak, 2008).

Statistical Analysis

EtOH consumption and preference were calculated daily. From these we determined the average intake per 2 h period, the average preference across the 4-day procedure and the intake during the 4 h binge test. Two-way ANOVAs with genotype and treatment (EtOH drinkers vs. water drinkers) as factors were used to analyze EtOH consumption and preference as well as *Gabra2* mRNA expression in the NAc, BNST, VTA, and CeA. Statistical analyses for the mRNA expression were conducted on raw data before transformation using the $2^{-\Delta\Delta CT}$ method. Bonferroni *post hoc* tests were used to correct for multiple comparisons following significant main effects and interactions. Degrees of freedom may differ between groups/brain regions due to unquantifiable tissue. Drinking data were analyzed using SPSS 24.0 software while GraphPad Prism 7.0 was used to assess differences in gene expression between groups. Data are presented as mean ± SEM. Effects were considered statistically significant at $p \leq 0.05$.

RESULTS

Female Mice Lacking βE Exhibit Enhanced Proclivity for Binge-Like Alcohol Consumption

Replicating previous results (Nentwig et al., 2018), we found that the absence of βE resulted in sex differences in drinking behavior. **Figure 1A** shows the average 2 h intake across all 4 days of the DID procedure in each group. There was a main effect of sex [$F_{(1,28)} = 6.73$, $p < 0.05$] but not genotype [$F_{(1,28)} = 0.041$, $p > 0.05$]. There was a significant interaction between sex and genotype reflecting the fact that female βE −/− mice consumed more than other groups [$F_{(1,28)} = 4.736$, $p < 0.05$]. There were neither sex nor strain differences in preference for EtOH [$F_{(1,28)} = 0.001$ and 1.087, respectively, both $p > 0.05$], however, there was a significant interaction between sex and genotype for EtOH preference [$F_{(1,28)} = 4.772$, $p < 0.05$] (**Figure 1B**). Finally, during the 4 h binge test (**Figure 1C**), there was a main effect of sex [$F_{(1,28)} = 7.426$, $p < 0.05$], but not genotype [$F_{(1,28)} = 0.013$, $p > 0.05$], and again a significant interaction between sex and genotype [$F_{(1,28)} = 8.983$, $p < 0.05$]. To follow up on the significant interaction suggesting that for females absent βE increased alcohol preference and consumption while the opposite was true for males (deficiency decreased drinking) simple effects of genotype were evaluated within each sex. After Bonferroni correction (i.e., alpha set at 0.025) none of these comparisons reached significance, indicating that the interactive effects of genotype and sex support a moderate bi-directional influence of βE on behavior (*p*'s for females: 0.186, 0.053, and 0.082 for average g/kg, average preference, and binge consumption; and for males the analogous values were 0.078, 0.390, and 0.029).

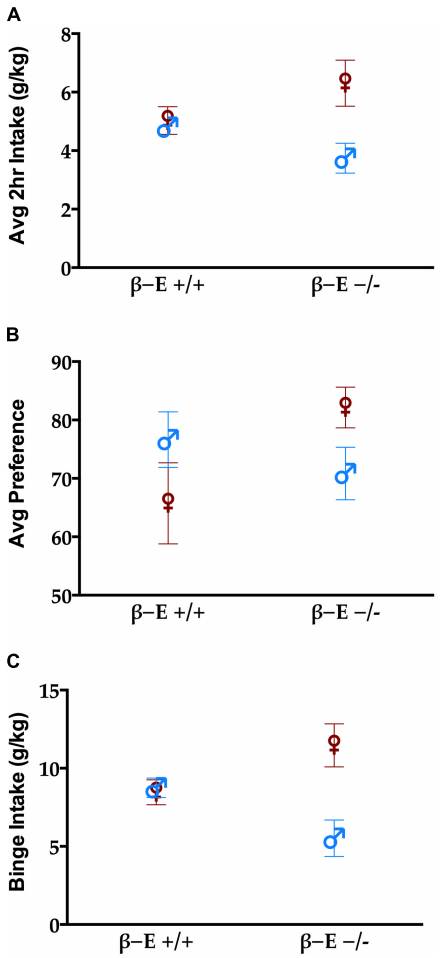

FIGURE 1 | βE masks sex differences in binge-like EtOH consumption. **(A)** Average 2 h intake across 4 day drinking in the dark (DID). **(B)** Preference for EtOH solution during the 4 h binge test. **(C)** Consumption of EtOH during the 4 h binge test on day 4 of the DID procedure. A two-way ANOVA revealed a main effect of sex (female mice > male mice) and a sex by genotype interaction. Post hoc analyses indicated that the βE –/– female mice consumed more EtOH than βE –/– male and βE +/+ female mice. Data are presented as means ± SEM.

In Female Mice, the Effects of EtOH on *Gabra2* Gene Expression Depend Upon βE

To determine if differential expression of the *Gabra2* gene is involved in the mechanism underlying the sexually dimorphic

effects of βE expression on binge-like EtOH consumption, we used qRT-PCR to analyze *Gabra2* gene expression in the BNST, CeA, NAc, and VTA of male and female βE +/+ and βE −/− mice. Two-way ANOVAs on *Gabra2* expression were performed for each brain region and they all yielded significant genotype by treatment interactions [BNST: [$F_{(1,20)}$ = 30.637, $p < 0.001$], CeA: [$F_{(1,25)}$ = 9.963, $p = 0.004$], NAc: [$F_{(1,22)}$ = 11.931, $p = 0.002$], VTA: [$F_{(1,21)}$ = 17.936, $p < 0.001$]], but no main effects of genotype [BNST: [$F_{(1,20)}$ = 0.429, $p = 0.520$], CeA: [$F_{(1,25)}$ = 1.539, $p = 0.226$], NAc: [$F_{(1,22)}$ = 3.079, $p = 0.093$], VTA: [$F_{(1,21)}$ = 0.015, $p = 0.905$]] or treatment [BNST: [$F_{(1,20)}$ = 2.700, $p = 0.116$], CeA: [$F_{(1,25)}$ = 0.891, $p = 0.354$], NAc: [$F_{(1,22)}$ = 0.017, $p = 0.898$], VTA: [$F_{(1,21)}$ = 0.196, $p = 0.663$]]. *Post hoc* analysis following the BNST genotype by treatment interaction indicated that, under basal conditions (water drinkers), βE −/− females have lower *Gabra2* expression, relative to βE +/+ females ($p < 0.05$). Further, EtOH consumption reduced *Gabra2* expression in βE +/+ females ($p < 0.05$), but increased expression in βE −/−females ($p < 0.05$), such that βE −/− females exhibited higher *Gabra2* expression than βE +/+ females who engage in binge-like EtOH consumption ($p < 0.05$; **Figure 2A**). *Post hoc* analysis following the CeA genotype by treatment interaction indicated that, under basal conditions, βE −/− females have lower *Gabra2* expression, relative to βE +/+ females ($p < 0.05$). Similar to the BNST, EtOH also reduced *Gabra2* expression in the CeA of βE +/+ females ($p < 0.05$; **Figure 2B**). *Post hoc* analysis following the NAc genotype by treatment interaction indicated that, under basal conditions, βE −/− females have lower *Gabra2* expression, relative to βE +/+ females ($p < 0.05$; **Figure 2C**). *Post hoc* analysis following the VTA genotype by treatment interaction indicated that, under basal conditions, βE −/− females have lower *Gabra2* expression, relative to βE +/+ females ($p < 0.05$). Following EtOH consumption, βE +/+ females exhibited lower *Gabra2* expression than EtOH-consuming βE −/− females ($p < 0.05$) due to an EtOH-induced reduction in *Gabra2* in βE +/+ females ($p < 0.05$; **Figure 2D**).

βE Expression Has No Effect on *Gabra2* Gene Expression in Limbic Brain Areas of Male Mice

A two-way ANOVA on *Gabra2* expression in the BNST of male mice revealed a significant genotype by treatment interaction [$F_{(1,27)}$ = 4.693, $p = 0.039$], but no significant main effects of genotype [$F_{(1,27)}$ = 0.093, $p = 0.763$] or treatment [$F_{(1,27)}$ = 1.753, $p = 0.197$]. *Post hoc* analysis following the genotype by treatment interaction did not indicate any significant group differences (p's > 0.05; **Figure 3A**). A two-way ANOVA on *Gabra2* expression in the CeA revealed a genotype by treatment interaction [$F_{(1,26)}$ = 5.464, $p = 0.027$] and a main effect of treatment [$F_{(1,26)}$ = 5.903, $p = 0.022$], but no main effect of genotype [$F_{(1,26)}$ = 0.009, $p = 0.927$]. *Post hoc* analysis following the genotype by treatment interaction indicated that βE −/− males exhibited increased *Gabra2* expression following EtOH consumption, relative to basal conditions ($p < 0.05$; **Figure 3B**). A two-way ANOVA on *Gabra2* expression in the NAc revealed no significant main effect of genotype [$F_{(1,26)}$ = 0.047, $p = 0.830$] or treatment [$F_{(1,26)}$ = 0.3.271, $p = 0.082$], and no significant genotype by treatment interaction [$F_{(1,26)}$ = 2.372, $p = 0.136$; **Figure 3C**]. A two-way ANOVA on *Gabra2* expression in the VTA revealed a genotype by treatment interaction [$F_{(1,26)}$ = 4.798, $p = 0.038$], but no main effects of genotype [$F_{(1,26)}$ = 0.687, $p = 0.415$] or treatment [$F_{(1,26)}$ = 1.666, $p = 0.208$]. *Post hoc* analysis following the genotype by treatment interaction did not indicate any significant differences between groups (p's > 0.05; **Figure 3D**).

DISCUSSION

This study supports the finding that genetic differences in βE expression affect binge-like EtOH consumption in a sex dependent manner (Nentwig et al., 2018), and further suggests that these effects involve modifications to GABAergic signaling in the limbic system. In female wildtype C57BL/6J mice, EtOH intake reduced *Gabra2* expression in multiple areas of the brain. In contrast, both wildtype and βE −/− males tended to increase expression of *Gabra2* mRNA after EtOH drinking. This finding is congruent with other studies using only males, which show that acute EtOH treatment increases *Gabra2* expression (Lindemeyer et al., 2017), while chronic alcohol exposure downregulates expression (Enoch et al., 2012; Jin et al., 2014; Forstera et al., 2016). Though we did not observe sex differences in EtOH intake in wildtypes animals as prior studies have reported (Tambour et al., 2008) this may be attributable to the number of drinking days used in various versions of the DID model. Sex differences in EtOH intake in the DID model are not always observed (Kaur et al., 2012; Nentwig et al., 2018) and appear more likely to emerge after several days to weeks of EtOH drinking, unlike the 4-day version used in the present study (Rhodes et al., 2005). Thus, the reductions in *Gabra2* expression in wildtype females may represent an adaptation that contributes to sex differences in binge EtOH intake as drinking progresses. Unlike wildtype counterparts, female βE −/− mice increased limbic expression of *Gabra2* mRNA following binge-like alcohol consumption. These mice also voluntarily consumed the most alcohol suggesting that the mechanisms responsible for sex differences in AUD development may involve βE interacting with $GABA_A$ receptors in a sex-dependent manner.

The CeA is well-known for its role in chronic stress responses. It is responsible for converting emotionally relevant stimuli into behavioral and physiological responses, and it is highly interconnected with the NAc, BNST, and VTA (Gilpin et al., 2015). Previous studies have shown that EtOH increases GABA input onto the CeA which can disinhibit the BNST and VTA to reduce anxiety and stimulate reward, respectively (Leriche et al., 2008; Harrison et al., 2017). Interestingly, many studies examining the effects of alcohol on the CeA have been done exclusively in males. For example, in males, EtOH affects the activity of the CeA but not the BNST and *Gabra2* expression in the CeA is reduced in high anxiety or alcoholic subjects (Thiele et al., 1997; Jin et al., 2014; Skorzewska Lehner et al., 2015). Male rats innately have more GABAergic cells in the CeA compared

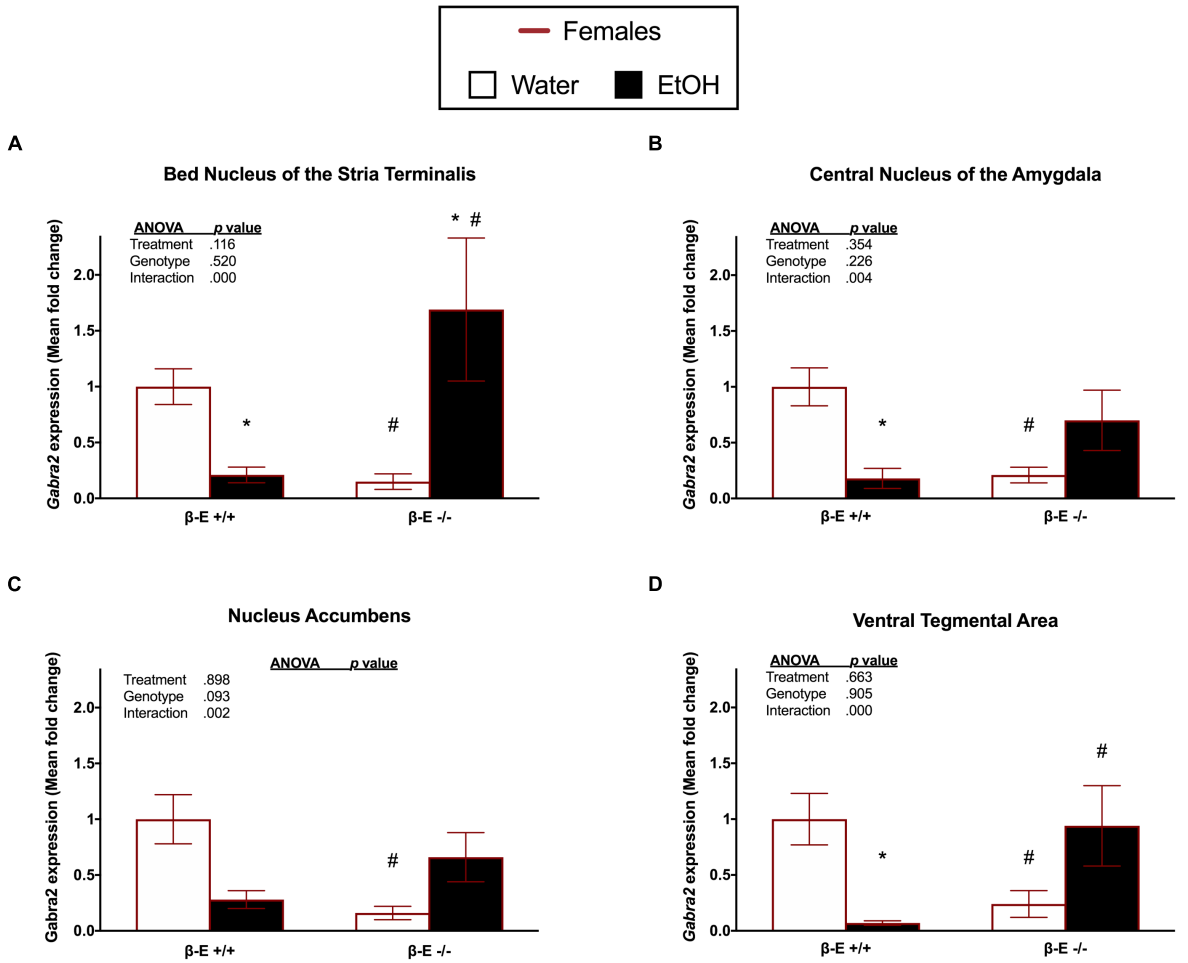

FIGURE 2 | Effects of ethanol on *Gabra2* gene expression in stress- and reward-related brain regions of βE +/+ and βE –/– female mice. *Gabra2* mRNA expression following binge-like consumption of either EtOH and water or water only in the DID paradigm. Two-way ANOVAs were used to examine the main and interaction effects of genotype (βE +/+, βE –/–) and treatment (EtOH drinker, water drinkers) in each brain region, results of which are depicted within each graph. **(A)** In the BNST, *post hoc* analysis indicated that, under basal conditions (water drinkers), βE –/– females have less *Gabra2* expression, relative to βE +/+ females. Further, EtOH consumption reduced *Gabra2* expression in βE +/+ females, but increased expression in βE –/– females, such that βE –/– females exhibited higher *Gabra2* expression than βE +/+ females who engaged in binge-like EtOH consumption. **(B)** In the CeA, *post hoc* analysis indicated that, under basal conditions, βE –/– females have lower *Gabra2* expression, relative to βE +/+ females. Similar to the BNST, EtOH also reduced *Gabra2* expression in the CeA of βE +/+ females. **(C)** In the NAc, *post hoc* analysis indicated that, under basal conditions, βE –/– females have lower *Gabra2* expression, relative to βE +/+ females. **(D)** In the VTA, *post hoc* analysis indicated that, under basal conditions, βE –/– females have lower *Gabra2* expression, relative to βE +/+ females. Following EtOH consumption, βE +/+ females exhibited lower *Gabra2* expression than EtOH-drinking βE –/– females due to an EtOH-induced reduction in *Gabra2* in βE +/+ females. $^{*}p < 0.05$ compared with the water drinkers within the same genotype and $^{\#}p < 0.05$ compared with the βE +/+ genotype group that received the same treatment. Data are presented as means ± SEM; Bonferroni correction for multiple comparisons.

to females (Ravenelle et al., 2014). More recently, studies have begun to include both males and females, and these seem to indicate that the effects of EtOH on the CeA in males is greater than in females (Logrip et al., 2017). The results of the present study further support the notion that the effects of alcohol on the CeA are different for males and females. More specifically, the greater effect of EtOH on CeA *Gabra2* expression in males is unmasked by the deficiency of βE expression, with EtOH consumption causing significant increases in *Gabra2* expression only in βE −/− males.

In females, EtOH affected *Gabra2* mRNA expression most dramatically in the BNST, an effect that was entirely dependent upon βE: the drug decreased *Gabra2* expression in wildtypes and while increasing it in βE −/− females. The BNST is an integral structure for the modulation of both the reward and stress neural circuitry. Most of the neurons in the BNST are GABAergic and activation of the BNST is generally anxiogenic (Ch'ng et al., 2018). Alcohol decreases the excitability of the BNST, which is crucial to the anxiolytic properties of EtOH (Leriche et al., 2008; Sharko et al., 2016). One of the ways that EtOH may be acting to reduce anxiety could be through increased expression of *Gabra2*. Stress and treatment with the stress neuropeptide, CRH, significantly increase the activity of the BNST neurons in females but not males (Sterrenburg et al., 2012; Babb et al., 2013;

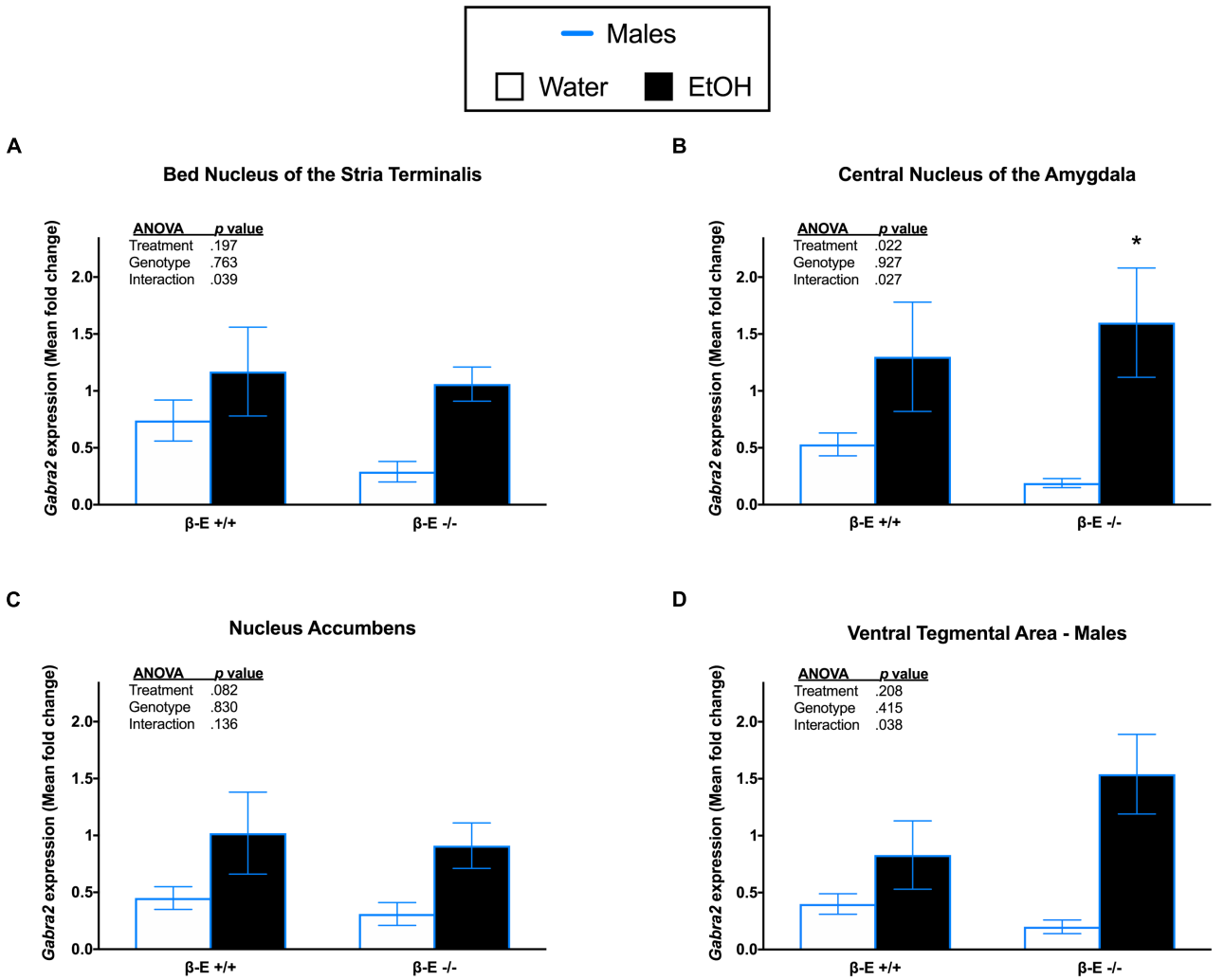

FIGURE 3 | Effects of ethanol on *Gabra2* gene expression in stress- and reward-related brains regions of βE +/+ and βE –/– male mice. *Gabra2* mRNA expression following binge-like consumption of either EtOH and water or water only in the DID paradigm. Two-way ANOVAs were used to examine the main and interaction effects of genotype (βE +/+, βE –/–) and treatment (EtOH drinker, water drinkers) in each brain region, results of which are depicted within each graph. **(A)** In the BNST, there was a significant interaction, but *post hoc* analysis did not reveal any significant differences between groups. **(B)** In the CeA, *post hoc* analysis indicated that binge-like EtOH consumption increased *Gabra2* expression in βE –/– males. **(C)** In the NAc, there was a significant interaction, but *post hoc* analysis revealed no significant differences between groups. **(D)** Similar to the NAc, in the VTA there was a significant interaction, but *post hoc* analysis revealed no significant differences between groups. $^*p < 0.05$ compared with the water group within the same genotype. Data are presented as means ± SEM; Bonferroni correction for multiple comparisons.

Salvatore et al., 2018). In addition, females innately have more CRH neurons in the BNST compared with males (Funabashi et al., 2004). The results of the present study provide additional support for the BNST as a critical mediator of the effects of EtOH in females, suggesting that the BNST is a critical node for the interaction of βE and sex in modulating the effects of EtOH on GABAergic signaling.

Data from a wide array of sources have suggested that females are inherently more vulnerable to stress-related disorders (Bale, 2009; Valentino and Bangasser, 2016). We previously showed that female βE −/− mice exhibit enhanced stress-sensitivity with hyperactivity of the HPA axis that can be ameliorated via binge-like EtOH consumption (Nentwig et al., 2018). While changes in mRNA expression do not necessarily translate to differences in functional receptor expression, in the present study stress-sensitive naive female βE −/− mice expressed significantly less *Gabra2* mRNA than βE +/+ mice in all of the brain regions examined. Similarly, data from both rats and mice demonstrated an association between lower baseline *Gabra2* expression and a high anxiety phenotype (Raud et al., 2009; Skorzewska Lehner et al., 2015). In addition, $GABA_AR$ agonist drugs like diazepam that reduce anxiety increase central *Gabra2* mRNA expression (Skorzewska Lehner et al., 2015). We see a similar effect here where EtOH intake, which has previously been shown to reduce the activity of the stress axis (Nentwig et al., 2018), increases *Gabra2* expression in female βE −/− mice. Therefore, our

data and that of others supports a site-specific, sex-dependent inverse relationship between *Gabra2* expression and chronic upregulation of the HPA axis.

CONCLUSION

Few preclinical studies have specifically examined the underlying mechanisms responsible for binge EtOH intake in females. The data presented here shed light on sexually dimorphic effects of voluntary drinking on GABAergic signaling that depend on βE expression. Along with previous studies, our results suggest an inverse correlation between *Gabra2* expression and anxiety, with subjects that have a lower baseline of *Gabra2* expression exhibiting an overly anxious phenotype and with *Gabra2* expression increases associated with significant anxiolytic responses. These data and others illustrate sex differences in central circuits mediating stress and reward that are responsible for the effects of EtOH on the brain, and perhaps provide a potential explanation for the increased proclivity of females to consume excessive quantities of EtOH, especially in the absence of βE.

AUTHOR CONTRIBUTIONS

ER, TN, and JG designed the study, performed the data analysis, and wrote the manuscript. TN, KL, and BC performed the behavioral data acquisition, and TN with the assistance of DW performed the qRT-PCR analysis.

FUNDING

This work was supported by the National Institute on Alcohol Abuse and Alcoholism, Grant AA022506.

REFERENCES

Adams, N., Shihabi, Z. K., and Blizard, D. A. (1991). Ethanol preference in the harrington derivation of the maudsley reactive and non-reactive strains. *Alcohol Clin. Exp. Res.* 15, 170–174. doi: 10.1111/j.1530-0277.1991.tb01849.x

Babb, J. A., Masini, C. V., Day, H. E., and Campeau, S. (2013). Sex differences in activated corticotropin-releasing factor neurons within stress-related neurocircuitry and hypothalamic-pituitary-adrenocortical axis hormones following restraint in rats. *Neuroscience* 234, 40–52. doi: 10.1016/j.neuroscience.2012.12.051

Bale, T. L. (2009). Neuroendocrine and immune influences on the CNS: it's a matter of sex. *Neuron* 64, 13–16. doi: 10.1016/j.neuron.2009.09.036

Bandelow, B., and Michaelis, S. (2015). Epidemiology of anxiety disorders in the 21st century. *Dial. Clin. Neurosci.* 17, 327–335.

Bangasser, D. A., Curtis, A., Reyes, B. A., Bethea, T. T., Parastatidis, I., Ischiropoulos, H., et al. (2010). Sex differences in corticotropin-releasing factor receptor signaling and trafficking: potential role in female vulnerability to stress-related psychopathology. *Mol. Psychiatry* 15 877–904. doi: 10.1038/mp.2010.66

Bangasser, D. A., and Valentino, R. J. (2014). Sex differences in stress-related psychiatric disorders: neurobiological perspectives. *Front. Neuroendocrinol.* 35, 303–319. doi: 10.1016/j.yfrne.2014.03.008

Barfield, E. T., Barry, S. M., Hodgin, H. B., Thompson, B. M., Allen, S. S., and Grisel, J. E. (2010). Beta-endorphin mediates behavioral despair and the effect of ethanol on the tail suspension test in mice. *Alcohol Clin. Exp. Res.* 34, 1066–1072. doi: 10.1111/j.1530-0277.2010.01182.x

Barnard, E. A., Skolnick, P., Olsen, R. W., Mohler, H., Sieghart, W., Biggio, G., et al. (1998). International union of pharmacology. XV. Subtypes of gamma-aminobutyric acidA receptors: classification on the basis of subunit structure and receptor function. *Pharmacol. Rev.* 50, 291–313.

Becker, J. B., McClellan, M. L., and Reed, B. G. (2017). Sex differences, gender and addiction. *J. Neurosci. Res.* 95, 136–147. doi: 10.1002/jnr.23963

Bierut, L. J., Agrawal, A., Bucholz, K. K., Doheny, K. F., Laurie, C., Pugh, E., et al. (2010). A genome-wide association study of alcohol dependence. *Proc. Natl. Acad. Sci. U.S.A.* 107, 5082–5087. doi: 10.1073/pnas.0911109107

Blaine, S. K., and Sinha, R. (2017). Alcohol, stress, and glucocorticoids: from risk to dependence and relapse in alcohol use disorders. *Neuropharmacoloy* 122, 136–147. doi: 10.1016/j.neuropharm.2017.01.037

Boehm, S. L., Ponomarev, I., Jennings, A. W., Whiting, P. J., Rosahl, T. W., Garrett, E. M., et al. (2004). gamma-aminobutyric acid A receptor subunit mutant mice: new perspectives on alcohol actions. *Biochem. Pharmacol.* 68, 1581–1602. doi: 10.1016/j.bcp.2004.07.023

Bos, H., van, B. G., and Sandfort, T. (2016). Drinking motives. alcohol use, and sexual attraction in youth. *J. Sex Res.* 53, 309–312. doi: 10.1080/00224499.2015.1020355

Breslau, N., Kessler, R. C., Chilcoat, H. D., Schultz, L. R., Davis, G. C., and Andreski, P. (1998). Trauma and posttraumatic stress disorder in the community: the 1996 Detroit Area Survey of Trauma. *Arch. Gen. Psychiatry* 55, 626–632. doi: 10.1001/archpsyc.55.7.626

Charmandari, E., Tsigos, C., and Chrousos, G. (2005). Endocrinology of the stress response. *Annu. Rev. Physiol.* 67, 259–284. doi: 10.1146/annurev.physiol.67.040403.120816

Ch'ng, S., Fu, J., Brown, R. M., McDougall, S. J., and Lawrence, A. J. (2018). The intersection of stress and reward: BNST modulation of aversive and appetitive states. *Prog. Neuropsychopharmacol. Biol. Psychiatry* 87, 108–125. doi: 10.1016/j.pnpbp.2018.01.005

Clay, J. M., Adams, C., Archer, P., English, M., Hyde, A., Stafford, L. D., et al. (2018). Psychosocial stress increases craving for alcohol in social drinkers: effects of risk-taking. *Drug Alcohol. Depend.* 185, 192–197. doi: 10.1016/j.drugalcdep.2017.12.021

Cullen, B. A., La Flair, L. N., Storr, C. L., Green, K. M., Alvanzo, A. A., Mojtabai, R., et al. (2013). Association of comorbid generalized anxiety disorder and alcohol use disorder symptoms with health-related quality of life: results from the National Epidemiological Survey on Alcohol and Related Conditions. *J. Addict. Med.* 7, 394–400. doi: 10.1097/ADM.0b013e31829faa1c

da Mata Ribeiro, G. B., Nascimento, L. C., Silva, M. A., de Campos, E. A., and Pillon, S. C. (2014). The context of alcohol consumption among adolescents and their families. *Int. J. Adolesc. Med. Health* 26, 393–402.

Dixon, C. I., Morris, H. V., Breen, G., Desrivieres, S., Jugurnauth, S., Steiner, R. C., et al. (2010). Cocaine effects on mouse incentive-learning and human addiction are linked to alpha2 subunit-containing GABAA receptors. *Proc. Natl. Acad. Sci. U.S.A.* 107, 2289–2294. doi: 10.1073/pnas.0910117107

Dixon, C. I., Rosahl, T. W., and Stephens, D. N. (2008). Targeted deletion of the GABRA2 gene encoding alpha2-subunits of GABA(A) receptors facilitates performance of a conditioned emotional response, and abolishes anxiolytic effects of benzodiazepines and barbiturates. *Pharmacol. Biochem. Behav.* 90, 1–8. doi: 10.1016/j.pbb.2008.01.015

Dwyer-Lindgren, L., Flaxman, A. D., Ng, M., Hansen, G. M., Murray, C. J., and Mokdad, A. H. (2015). Drinking patterns in US counties from 2002 to 2012. *Am. J. Public Health* 105, 1120–1127. doi: 10.2105/AJPH.2014.302313

Edenberg, H. J., Dick, D. M., Xuei, X., Tian, H., Almasy, L., Bauer, L. O., et al. (2004). Variations in GABRA2, encoding the alpha 2 subunit of the GABA(A) receptor, are associated with alcohol dependence and with brain oscillations. *Am. J. Hum. Genet.* 74, 705–714. doi: 10.1086/383283

Engin, E., Liu, J., and Rudolph, U. (2012). alpha2-containing GABA(A) receptors: a target for the development of novel treatment strategies for CNS disorders. *Pharmacol. Ther.* 136, 142–152. doi: 10.1016/j.pharmthera.2012.08.006

Enoch, M. A., Hodgkinson, C. A., Yuan, Q., Albaugh, B., Virkkunen, M., and Goldman, D. (2009). GABRG1 and GABRA2 as independent predictors for

alcoholism in two populations. *Neuropsychopharmacology* 34, 1245–1254. doi: 10.1038/npp.2008.171

Enoch, M. A., Schwartz, L., Albaugh, B., Virkkunen, M., and Goldman, D. (2006). Dimensional anxiety mediates linkage of GABRA2 haplotypes with alcoholism. *Am. J. Med. Genet. B Neuropsychiatr. Genet.* 141B, 599–607. doi: 10.1002/ajmg.b.30336

Enoch, M. A., Zhou, Z., Kimura, M., Mash, D. C., Yuan, Q., and Goldman, D. (2012). GABAergic gene expression in postmortem hippocampus from alcoholics and cocaine addicts; corresponding findings in alcohol-naive P and NP rats. *PLoS. One* 7:e29369. doi: 10.1371/journal.pone.0029369

Erol, A., and Karpyak, V. M. (2015). Sex and gender-related differences in alcohol use and its consequences: contemporary knowledge and future research considerations. *Drug Alcohol. Depend.* 156, 1–13. doi: 10.1016/j.drugalcdep.2015.08.023

Forger, N. G., and Morin, L. P. (1982). Reproductive state modulates ethanol intake in rats: effects of ovariectomy, ethanol concentration, estrous cycle and pregnancy. *Pharmacol. Biochem. Behav.* 17, 323–331. doi: 10.1016/0091-3057(82)90087-9

Forstera, B., Castro, P. A., Moraga-Cid, G., and Aguayo, L. G. (2016). Potentiation of gamma aminobutyric acid receptors (GABAAR) by ethanol: how are inhibitory receptors affected? *Front. Cell. Neurosci.* 10:114. doi: 10.3389/fncel.2016.00114

Funabashi, T., Kawaguchi, M., Furuta, M., Fukushima, A., and Kimura, F. (2004). Exposure to bisphenol A during gestation and lactation causes loss of sex difference in corticotropin-releasing hormone-immunoreactive neurons in the bed nucleus of the stria terminalis of rats. *Psychoneuroendocrinology* 29, 475–485. doi: 10.1016/S0306-4530(03)00055-6

Gelernter, J., and Kranzler, H. R. (2009). Genetics of alcohol dependence. *Hum. Genet.* 126, 91–99. doi: 10.1007/s00439-009-0701-2

Gilpin, N. W., Herman, M. A., and Roberto, M. (2015). The central amygdala as an integrative hub for anxiety and alcohol use disorders. *Biol. Psychiatry* 77, 859–869. doi: 10.1016/j.biopsych.2014.09.008

Gilpin, N. W., and Weiner, J. L. (2017). Neurobiology of comorbid post-traumatic stress disorder and alcohol-use disorder. *Genes Brain Behav.* 16, 15–43. doi: 10.1111/gbb.12349

Glantz, M. D., Medina-Mora, M. E., Petukhova, M., Andrade, L. H., Anthony, J. C., and de Girolamo, G. (2014). Alcohol abuse in developed and developing countries in the World Mental Health surveys: socially defined consequences or psychiatric disorder? *Am. J. Addict.* 23, 145–155. doi: 10.1111/j.1521-0391.2013.12082.x

Gorka, S. M., Ali, B., and Daughters, S. B. (2012). The role of distress tolerance in the relationship between depressive symptoms and problematic alcohol use. *Psychol. Addict. Behav.* 26, 621–626. doi: 10.1037/a0026386

Gorka, S. M., and Shankman, S. A. (2017). Preliminary evidence that reactivity to uncertain threat is an endophenotype for alcohol use disorder. *Drug Alcohol. Depend.* 180, 265–271. doi: 10.1016/j.drugalcdep.2017.08.023

Gowing, L. R., Ali, R. L., Allsop, S., Marsden, J., Turf, E. E., West, R., et al. (2015). Global statistics on addictive behaviours: 2014 status report. *Addiction* 110, 904–919. doi: 10.1111/add.12899

Grant, B. F., Chou, S. P., Saha, T. D., Pickering, R. P., Kerridge, B. T., Ruan, W. J., Huang, B., Jung, J., Zhang, H., Fan, A., and Hasin, D. S. (2017). Prevalence of 12-month alcohol use, high-risk drinking, and DSM-IV alcohol use disorder in the United States, 2001-2002 to 2012-2013: results from the national epidemiologic survey on alcohol and related conditions. *JAMA Psychiatry* 74, 911–923. doi: 10.1001/jamapsychiatry.2017.2161

Grisel, J. E., Bartels, J. L., Allen, S. A., and Turgeon, V. L. (2008). Influence of beta-Endorphin on anxious behavior in mice: interaction with EtOH. *Psychopharmacology (Berl)* 200, 105–115. doi: 10.1007/s00213-008-1161-4

Grucza, R. A., Norberg, K., Bucholz, K. K., and Bierut, L. J. (2008). Correspondence between secular changes in alcohol dependence and age of drinking onset among women in the United States. *Alcohol. Clin. Exp. Res.* 32, 1493–1501. doi: 10.1111/j.1530-0277.2008.00719.x

Guan, Y. Z., and Ye, J. H. (2010). Ethanol blocks long-term potentiation of GABAergic synapses in the ventral tegmental area involving mu-opioid receptors. *Neuropsychopharmacology* 35, 1841–1849. doi: 10.1038/npp.2010.51

Harrison, N. L., Skelly, M. J., Grosserode, E. K., Lowes, D. C., Zeric, T., Phister, S., et al. (2017). Effects of acute alcohol on excitability in the CNS. *Neuropharmacoloy* 122, 36–45. doi: 10.1016/j.neuropharm.2017.04.007

Hartwell, E. E., and Ray, L. A. (2013). Sex moderates stress reactivity in heavy drinkers. *Addict. Behav.* 38, 2643–2646. doi: 10.1016/j.addbeh.2013.06.016

Haughey, H. M., Ray, L. A., Finan, P., Villanueva, R., Niculescu, M., and Hutchison, K. E. (2008). Human gamma-aminobutyric acid A receptor alpha2 gene moderates the acute effects of alcohol and brain mRNA expression. *Genes Brain Behav.* 7, 447–454. doi: 10.1111/j.1601-183X.2007.00369.x

Herbison, A. E., and Fenelon, V. S. (1995). Estrogen regulation of GABAA receptor subunit mRNA expression in preoptic area and bed nucleus of the stria terminalis of female rat brain. *J. Neurosci.* 15, 2328–2337. doi: 10.1523/JNEUROSCI.15-03-02328.1995

Hevers, W., and Luddens, H. (1998). The diversity of GABAA receptors. Pharmacological and electrophysiological properties of GABAA channel subtypes. *Mol. Neurobiol.* 18, 35–86. doi: 10.1007/BF02741459

Hyytia, P., and Koob, G. F. (1995). GABAA receptor antagonism in the extended amygdala decreases ethanol self-administration in rats. *Eur. J. Pharmacol.* 283, 151–159. doi: 10.1016/0014-2999(95)00314-B

Ittiwut, C., Yang, B. Z., Kranzler, H. R., Anton, R. F., Hirunsatit, R., Weiss, R. D., et al. (2012). GABRG1 and GABRA2 variation associated with alcohol dependence in African Americans. *Alcohol. Clin. Exp. Res.* 36, 588–593. doi: 10.1111/j.1530-0277.2011.01637.x

Jennison, K. M. (2004). The short-term effects and unintended long-term consequences of binge drinking in college: a 10-year follow-up study. *Am. J. Drug Alcohol Abuse* 30, 659–684. doi: 10.1081/ADA-200032331

Jin, Z., Bhandage, A. K., Bazov, I., Kononenko, O., Bakalkin, G., Korpi, E. R., et al. (2014). Expression of specific ionotropic glutamate and GABA-A receptor subunits is decreased in central amygdala of alcoholics. *Front. Cell. Neurosci.* 8:288. doi: 10.3389/fncel.2014.00288

Karpyak, V. M., Biernacka, J. M., Geske, J. R., Abulseoud, O. A., Brunner, M. D., Chauhan, M., et al. (2016). Gender-specific effects of comorbid depression and anxiety on the propensity to drink in negative emotional states. *Addiction* 111, 1366–1375. doi: 10.1111/add.13386

Kaur, S., Li, J., Stenzel-Poore, M. P., and Ryabinin, A. E. (2012). Corticotropin-releasing factor acting on corticotropin-releasing factor receptor type 1 is critical for binge alcohol drinking in mice. *Alcohol. Clin. Exp. Res.* 36, 369–376. doi: 10.1111/j.1530-0277.2011.01610.x

Kendler, K. S., Kessler, R. C., Walters, E. E., MacLean, C., Neale, M. C., Heath, A. C., et al. (1995a). Stressful life events, genetic liability, and onset of an episode of major depression in women. *Am. J. Psychiatry* 152, 833–842. doi: 10.1176/ajp.152.6.833

Kendler, K. S., Walters, E. E., Neale, M. C., Kessler, R. C., Heath, A. C., and Eaves, L. J. (1995b). The structure of the genetic and environmental risk factors for six major psychiatric disorders in women. Phobia, generalized anxiety disorder, panic disorder, bulimia, major depression, and alcoholism. *Arch. Gen. Psychiatry* 52, 374–383. doi: 10.1001/archpsyc.1995.03950170048007

Keyes, K. M., Li, G., and Hasin, D. S. (2011). Birth cohort effects and gender differences in alcohol epidemiology: a review and synthesis. *Alcohol Clin. Exp. Res.* 35, 2101–2112. doi: 10.1111/j.1530-0277.2011.01562.x

Keyes, K. M., Martins, S. S., Blanco, C., and Hasin, D. S. (2010). Telescoping and gender differences in alcohol dependence: new evidence from two national surveys. *Am. J. Psychiatry* 167, 969–976. doi: 10.1176/appi.ajp.2009.09081161

Kuperman, S., Chan, G., Kramer, J., Wetherill, L., Acion, L., Edenberg, H. J., et al. (2017). A GABRA2 polymorphism improves a model for prediction of drinking initiation. *Alcohol* 63, 1–8. doi: 10.1016/j.alcohol.2017.03.003

Leriche, M., Mendez, M., Zimmer, L., and Berod, A. (2008). Acute ethanol induces Fos in GABAergic and non-GABAergic forebrain neurons: a double-labeling study in the medial prefrontal cortex and extended amygdala. *Neuroscience* 153, 259–267. doi: 10.1016/j.neuroscience.2008.01.069

Li, T. K., and Lumeng, L. (1984). Alcohol preference and voluntary alcohol intakes of inbred rat strains and the National Institutes of Health heterogeneous stock of rats. *Alcohol Clin. Exp. Res.* 8, 485–486. doi: 10.1111/j.1530-0277.1984.tb05708.x

Lindemeyer, A. K., Shen, Y., Yazdani, F., Shao, X. M., Spigelman, I., Davies, D. L., et al. (2017). alpha2 subunit-containing GABAA receptor subtypes are upregulated and contribute to alcohol-induced functional plasticity in the rat hippocampus. *Mol. Pharmacol.* 92, 101–112. doi: 10.1124/mol.116.107797

Logrip, M. L., Oleata, C., and Roberto, M. (2017). Sex differences in responses of the basolateral-central amygdala circuit to alcohol, corticosterone and their interaction. *Neuropharmacology* 114, 123–134. doi: 10.1016/j.neuropharm.2016.11.021

Lynch, W. J. (2006). Sex differences in vulnerability to drug self-administration. *Exp. Clin. Psychopharmacol.* 14, 34–41. doi: 10.1037/1064-1297.14.1.34

Marinelli, P. W., Quirion, R., and Gianoulakis, C. (2003). Estradiol valerate and alcohol intake: a comparison between Wistar and Lewis rats and the putative role of endorphins. *Behav. Brain Res.* 139, 59–67. doi: 10.1016/S0166-4328(02)00057-8

McGonigle, C. E., Nentwig, T. B., Wilson, D. E., Rhinehart, E. M., and Grisel, J. E. (2016). beta-endorphin regulates alcohol consumption induced by exercise restriction in female mice. *Alcohol* 53, 51–60. doi: 10.1016/j.alcohol.2016.04.003

Melon, L. C., and Boehm, S. L. (2011). GABAA receptors in the posterior, but not anterior, ventral tegmental area mediate Ro15-4513-induced attenuation of binge-like ethanol consumption in C57BL/6J female mice. *Behav. Brain Res.* 220, 230–237. doi: 10.1016/j.bbr.2011.02.014

Milivojevic, V., and Sinha, R. (2018). Central and peripheral biomarkers of stress response for addiction risk and relapse vulnerability. *Trends Mol. Med.* 24, 173–186. doi: 10.1016/j.molmed.2017.12.010

Morin, L. P., and Forger, N. G. (1982). Endocrine control of ethanol intake by rats or hamsters: relative contributions of the ovaries, adrenals and steroids. *Pharmacol. Biochem. Behav.* 17, 529–537. doi: 10.1016/0091-3057(82)90315-X

Nentwig, T. B., Wilson, D. E., Rhinehart, E. M., and Grisel, J. E. (2018). Sex differences in binge-like EtOH drinking, corticotropin-releasing hormone and corticosterone: effects of beta-endorphin. *Addict. Biol.* [Epub ahead of print]. doi: 10.1111/adb.12610

Olsen, R. W., and Sieghart, W. (2009). GABA A receptors: subtypes provide diversity of function and pharmacology. *Neuropharmacoloy* 56, 141–148. doi: 10.1016/j.neuropharm.2008.07.045

Piazza, N. J., Vrbka, J. L., and Yeager, R. D. (1989). Telescoping of alcoholism in women alcoholics. *Int. J. Addict.* 24, 19–28. doi: 10.3109/10826088909047272

Pirker, S., Schwarzer, C., Wieselthaler, A., Sieghart, W., and Sperk, G. (2000). GABA(A) receptors: immunocytochemical distribution of 13 subunits in the adult rat brain. *Neuroscience* 101, 815–850. doi: 10.1016/S0306-4522(00)00442-5

Rajasingh, J., Bord, E., Qin, G., Ii, M., Silver, M., Hamada, H., et al. (2007). Enhanced voluntary alcohol consumption after estrogen supplementation negates estrogen-mediated vascular repair in ovariectomized mice. *Endocrinology* 148, 3618–3624. doi: 10.1210/en.2006-1357

Raud, S., Sutt, S., Luuk, H., Plaas, M., Innos, J., Koks, S., et al. (2009). Relation between increased anxiety and reduced expression of alpha1 and alpha2 subunits of GABA(A) receptors in Wfs1-deficient mice. *Neurosci. Lett.* 460, 138–142. doi: 10.1016/j.neulet.2009.05.054

Ravenelle, R., Neugebauer, N. M., Niedzielak, T., and Donaldson, S. T. (2014). Sex differences in diazepam effects and parvalbumin-positive GABA neurons in trait anxiety long evans rats. *Behav. Brain Res.* 270, 68–74. doi: 10.1016/j.bbr.2014.04.048

Rhodes, J. S., Best, K., Belknap, J. K., Finn, D. A., and Crabbe, J. C. (2005). Evaluation of a simple model of ethanol drinking to intoxication in C57BL/6J mice. *Physiol. Behav.* 84, 53–63. doi: 10.1016/j.physbeh.2004.10.007

Rubinstein, M., Mogil, J. S., Japon, M., Chan, E. C., Allen, R. G., and Low, M. J. (1996). Absence of opioid stress-induced analgesia in mice lacking beta-endorphin by site-directed mutagenesis. *Proc. Natl. Acad. Sci. U.S.A.* 93, 3995–4000. doi: 10.1073/pnas.93.9.3995

Salvatore, M., Wiersielis, K. R., Luz, S., Waxler, D. E., Bhatnagar, S., and Bangasser, D. A. (2018). Sex differences in circuits activated by corticotropin releasing factor in rats. *Horm. Behav.* 97, 145–153. doi: 10.1016/j.yhbeh.2017.10.004

Satta, R., Hilderbrand, E. R., and Lasek, A. W. (2018). Ovarian hormones contribute to high levels of binge-like drinking by female mice. *Alcohol Clin. Exp. Res.* 42, 286–294. doi: 10.1111/acer.13571

Schmittgen, T. D., and Livak, K. J. (2008). Analyzing real-time PCR data by the comparative C(T) method. *Nat. Protoc.* 3, 1101–1108. doi: 10.1038/nprot.2008.73

Schwarzer, C., Berresheim, U., Pirker, S., Wieselthaler, A., Fuchs, K., Sieghart, W., et al. (2001). Distribution of the major gamma-aminobutyric acid(A) receptor subunits in the basal ganglia and associated limbic brain areas of the adult rat. *J. Comp Neurol.* 433, 526–549. doi: 10.1002/cne.1158

Sharko, A. C., Kaigler, K. F., Fadel, J. R., and Wilson, M. A. (2016). Ethanol-induced anxiolysis and neuronal activation in the amygdala and bed nucleus of the stria terminalis. *Alcohol* 50, 19–25. doi: 10.1016/j.alcohol.2015.11.001

Sinha, R. (2001). How does stress increase risk of drug abuse and relapse? *Psychopharmacology (Berl.)* 158, 343–359. doi: 10.1007/s002130100917

Skorzewska Lehner, M., Wislowska-Stanek, A., Turzynska, D., Sobolewska, A., Krzascik, P., et al. (2015). GABAergic control of the activity of the central nucleus of the amygdala in low- and high-anxiety rats. *Neuropharmacoloy* 99, 566–576. doi: 10.1016/j.neuropharm.2015.08.039

Stephens, M. A., and Wand, G. (2012). Stress and the HPA axis: role of glucocorticoids in alcohol dependence. *Alcohol Res.* 34, 468–483.

Sterrenburg, L., Gaszner, B., Boerrigter, J., Santbergen, L., Bramini, M., Roubos, E. W., et al. (2012). Sex-dependent and differential responses to acute restraint stress of corticotropin-releasing factor-producing neurons in the rat paraventricular nucleus, central amygdala, and bed nucleus of the stria terminalis. *J. Neurosci. Res.* 90, 179–192. doi: 10.1002/jnr.22737

Substance Abuse and Mental Health Services (2018). *Key Substance Use and Mental Health indicators in the United States: Results from the 2016 National Survey on Drug Use and Health. Tice P. 2017*. Rockville, MD: Center for Behavioral Health Statistics and Quality, Substance Abuse and Mental Health Services Administration. HHS Publication No. SMA 17-5044, NSDUH series H-52. 1-3-2018. Ref Type: Online Source.

Suzdak, P. D., Schwartz, R. D., Skolnick, P., and Paul, S. M. (1986). Ethanol stimulates gamma-aminobutyric acid receptor-mediated chloride transport in rat brain synaptoneurosomes. *Proc. Natl. Acad. Sci. U.S.A.* 83, 4071–4075. doi: 10.1073/pnas.83.11.4071

Svikis, D. S., Miles, D. R., Haug, N. A., Perry, B., and R. Hoehn-Saric, McLeod, D. (2006). Premenstrual symptomatology, alcohol consumption, and family history of alcoholism in women with premenstrual syndrome. *J. Stud. Alcohol* 67, 833–836. doi: 10.15288/jsa.2006.67.833

Tambour, S., Brown, L. L., and Crabbe, J. C. (2008). Gender and age at drinking onset affect voluntary alcohol consumption but neither the alcohol deprivation effect nor the response to stress in mice. *Alcohol Clin. Exp. Res.* 32, 2100–2106. doi: 10.1111/j.1530-0277.2008.00798.x

Thiele, T. E., van, D. G., and Bernstein, I. L. (1997). Ethanol-induced c-Fos expression in rat lines selected for low and high alcohol consumption. *Brain Res.* 756, 278–282. doi: 10.1016/S0006-8993(97)00228-X

Thorisdottir, I. E., Asgeirsdottir, B. B., Sigurvinsdottir, R., Allegrante, J. P., and Sigfusdottir, I. D. (2017). The increase in symptoms of anxiety and depressed mood among Icelandic adolescents: time trend between 2006 and 2016. *Eur. J. Public Health* 27, 856–861. doi: 10.1093/eurpub/ckx111

Tolin, D. F., and Foa, E. B. (2006). Sex differences in trauma and posttraumatic stress disorder: a quantitative review of 25 years of research. *Psychol. Bull.* 132, 959–992. doi: 10.1037/0033-2909.132.6.959

Uhart, M., Weerts, E. M., McCaul, M. E., Guo, X., Yan, X., Kranzler, H. R., et al. (2013). GABRA2 markers moderate the subjective effects of alcohol. *Addict. Biol.* 18, 357–369. doi: 10.1111/j.1369-1600.2012.00457.x

Valentino, R. J., and Bangasser, D. A. (2016). Sex-biased cellular signaling: molecular basis for sex differences in neuropsychiatric diseases. *Dialogues Clin. Neurosci.* 18, 385–393.

Vollenweider Smith, K. S., Keist, R., and Rudolph, U. (2011). Antidepressant-like properties of alpha2-containing GABA(A) receptors. *Behav. Brain Res.* 217, 77–80. doi: 10.1016/j.bbr.2010.10.009

Watt, M. H., Eaton, L. A., Choi, K. W., Velloza, J., Kalichman, S. C., Skinner, D., et al. (2014). "It's better for me to drink, at least the stress is going away": perspectives on alcohol use during pregnancy among South African women attending drinking establishments. *Soc. Sci. Med.* 116, 119–125. doi: 10.1016/j.socscimed.2014.06.048

Xiao, C., and Ye, J. H. (2008). Ethanol dually modulates GABAergic synaptic transmission onto dopaminergic neurons in ventral tegmental area: role of mu-opioid receptors. *Neuroscience* 153, 240–248. doi: 10.1016/j.neuroscience.2008.01.040

Conflict of Interest Statement: The authors declare that the research was conducted in the absence of any commercial or financial relationships that could be construed as a potential conflict of interest.

frontiers in Genetics

ORIGINAL RESEARCH
published: 04 December 2018
doi: 10.3389/fgene.2018.00513

Estrogen-Dependent Upregulation of *Adcyap1r1* Expression in Nucleus Accumbens Is Associated With Genetic Predisposition of Sex-Specific QTL for Alcohol Consumption on Rat Chromosome 4

John Paul Spence[1], Jill L. Reiter[1], Bin Qiu[2], Hao Gu[2], Dawn K. Garcia[3], Lingling Zhang[2], Tamara Graves[1], Kent E. Williams[1], Paula J. Bice[4], Yi Zou[3], Zhao Lai[4], Weidong Yong[2] and Tiebing Liang[1]**

[1] Department of Medicine, Indiana University School of Medicine, Indianapolis, IN, United States, [2] Comparative Medical Center, Institute of Laboratory Animal Science, Chinese Academy of Medical Sciences & Peking Union Medical College, Beijing, China, [3] Greehey Children's Cancer Research Institute, UT Health San Antonio, San Antonio, TX, United States, [4] Department of Psychology, Southeast Missouri State University, Cape Girardeau, MO, United States

OPEN ACCESS

Edited by:
Kristin Hamre,
The University of Tennessee Health Science Center, United States

Reviewed by:
Camron D. Bryant,
Boston University, United States
Eser Ercil,
Independent researcher, New Haven, CT, United States

***Correspondence:**
Weidong Yong
wyong@cnilas.org
Tiebing Liang
tliang@iu.edu

Specialty section:
This article was submitted to Behavioral and Psychiatric Genetics, a section of the journal Frontiers in Genetics

Received: 07 March 2018
Accepted: 12 October 2018
Published: 04 December 2018

Citation:
Spence JP, Reiter JL, Qiu B, Gu H, Garcia DK, Zhang L, Graves T, Williams KE, Bice PJ, Zou Y, Lai Z, Yong W and Liang T (2018) Estrogen-Dependent Upregulation of Adcyap1r1 Expression in Nucleus Accumbens Is Associated With Genetic Predisposition of Sex-Specific QTL for Alcohol Consumption on Rat Chromosome 4. Front. Genet. 9:513. doi: 10.3389/fgene.2018.00513

Humans show sex differences related to alcohol use disorders (AUD). Animal model research has the potential to provide important insight into how sex differences affect alcohol consumption, particularly because female animals frequently drink more than males. In previous work, inbred strains of the selectively bred alcohol-preferring (P) and non-preferring (NP) rat lines revealed a highly significant quantitative trait locus (QTL) on rat chromosome 4, with a logarithm of the odds score of 9.2 for alcohol consumption. Recently, interval-specific congenic strains (ISCS) were developed by backcrossing the congenic P.NP line to inbred P (iP) rats to further refine the chromosome 4 QTL region. Two ISCS sub-strains, ISCS-A and ISCS-B, were obtained with a narrowed QTL, where the smallest region of overlap consisted of 8.9 Mb in ISCS-B. Interestingly, we found that females from both ISCS lines consumed significantly less alcohol than female iP controls ($p < 0.05$), while no differences in alcohol consumption were observed between male ISCS and iP controls. RNA-sequencing was performed on the nucleus accumbens of alcohol-naïve female ISCS-B and iP rats, which revealed differentially expressed genes (DEG) with greater than 2-fold change that were functionally relevant to behavior. These DEGs included down-regulation of *Oxt*, *Asb4, Gabre, Gabrq*, *Chat, Slc5a7, Slc18a8, Slc10a4,* and *Ngfr*, and up-regulation of *Ttr, Msln, Mpzl2*, *Wnt6, Slc17a7, Aldh1a2,* and *Gstm2*. Pathway analysis identified significant alterations in gene networks controlling nervous system development and function, as well as cell signaling, GABA and serotonin receptor signaling and G-protein coupled receptor signaling. In addition, β-estradiol was identified as the most significant upstream regulator. The expression levels of estrogen-responsive genes that mapped to the QTL interval and have been previously

associated with alcohol consumption were measured using RT-qPCR. We found that expression of the *Adcyap1r1* gene, encoding the pituitary adenylate cyclase-activating polypeptide type 1 (PAC_1) receptor, was upregulated in female ISCS-B compared to female iP controls, while no differences were exhibited in males. In addition, sequence variants in the *Adcyap1r1* promoter region showed a differential response to estrogen stimulation *in vitro*. These findings demonstrate that rat chromosome 4 QTL contains genetic variants that respond to estrogen and are associated with female alcohol consumption.

Keywords: alcohol use disorder, sex-difference, congenic rat model, nucleus accumbens, RNA-seq, *Adcyap1r1*

INTRODUCTION

The development of alcohol use disorders has a strong genetic component. Genetic factors account for more than 50% of the variance in developing alcoholism (Heath et al., 1997; Ducci and Goldman, 2008), and several specific genetic variants are associated with an increased risk for alcoholism (Koss and Goldman, 2000; Dick et al., 2006; Gatti et al., 2010). In addition to genetics, sex-based differences in drug and alcohol use, abuse, and dependence are supported by epidemiological and clinical research (Prescott, 2002; Nolen-Hoeksema, 2004; Ceylan-Isik et al., 2010). Likewise, animal models also display sex-differences in voluntary consumption of drugs and alcohol (Vetter-O'Hagen et al., 2009; Desrivières et al., 2011). However, the mechanisms responsible for sex-specific drinking differences remain largely unknown (Becker and Koob, 2016).

Most sexually dimorphic traits arise through differential gene expression that has different effects on males and females (Dimas et al., 2012; Gershoni and Pietrokovski, 2017). In addition to phenotypic variation that results from the action of sex hormones, gene-by-sex (GxS) interactions involve phenotypic differences that depend on the functional genetic variants (Rawlik et al., 2016). Evidence for sex-specific quantitative traits exist that impact a wide range of complex traits (Karp et al., 2017). Sex-specific quantitative trait loci (QTLs) have also been reported for alcohol preference, ethanol sensitivity, and ethanol locomotor activation in mice and ethanol drinking in rats; however, specific genes mediating these effects have yet to be identified (Melo et al., 1996; Gill et al., 1998; Peirce et al., 1998; Radcliffe et al., 2000; Bice et al., 2006; Vendruscolo et al., 2006; Chesler et al., 2012; DuBose et al., 2013; Vanderlinden et al., 2015)

We and others have used the selectively bred alcohol-preferring (P) and non-preferring (NP) rat model (Li et al., 1991) to investigate the genetic factors involved in alcohol drinking behaviors (Bice et al., 1998; Carr et al., 1998; Liang et al., 2003, 2004; Liang and Carr, 2006). In this model, P rats exhibit several features that are consistent with alcoholism in humans (Cicero, 1979). For example, P rats (1) orally self-administer ethanol in pharmacologically relevant amounts; (2) consume EtOH for its pharmacological effects rather than caloric value or taste; (3) show positive reinforcement; (4) develop tolerance; and (5) exhibit withdrawal symptoms (McBride and Li, 1998; Murphy et al., 2002). QTL analysis of inbred alcohol-preferring/non-preferring (iP/iNP) rats revealed several loci associated with alcohol preference, including a region of chromosome 4 (Chr4) with a LOD score >9.2 (Carr et al., 1998; Bice et al., 2006).

Congenic rat strains were subsequently derived that had transferred the ∼ 130 Mb Chr4 QTL region of the donor strain to the host strain, whereby P.NP designates an iP host rat with the donor iNP Chr4 QTL, and NP.P designates an iNP host rat with the donor iP Chr4 QTL. Alcohol consumption in these reciprocal congenic strains were consistent with the donor strain, such that P.NP rats drank less than P rats and NP.P rats drank more than NP rats (Carr et al., 2006). These and other results confirmed the association of the Chr4 QTL with alcohol consumption, and indicated that multiple loci within this strong QTL may be contributing to the alcohol drinking phenotype (Carr et al., 2006; Spence et al., 2009; Liang et al., 2010). To further refine this Chr4 QTL region, overlapping interval-specific congenic strains (ISCS) were generated by backcrossing the P.NP congenic line with iP rats. This approach resulted in two ISCS lines (Spence et al., 2013). The ISCS-A sub-strain contained ∼ 79 Mb of the NP genomic region between microsatellite markers *D4Mgh16* and *D4Rat173*, while the ISCS-B sub-strain contained ∼ 9 Mb of the NP genomic region between a single nucleotide polymorphism (SNP) in *Snca* and the marker *D4Rat35* (Liang and Carr, 2006; Spence et al., 2013).

Similar to other animal models, female P and iP rats consume more alcohol than the corresponding males (Li et al., 1991; Carr et al., 1998). We hypothesized that a sex-specific QTL existed on rat Chr4 that contributed to the disparate alcohol drinking behavior between males and females. To test this hypothesis, we measured alcohol preference and consumption in male and female P.NP-ISCS rats since they contain a narrowed Chr4 QTL region. To investigate the genetic factors that might be involved in sex-specific drinking phenotypes, we also analyzed transcriptome differences between P.NP-ISCS-B and iP rats in the nucleus accumbens (NAc), a brain region known to play an important role in the reinforcing and rewarding effects of ethanol.

In this study, we report that a sex-specific QTL exists on rat Chr4 that contributes to alcohol consumption. Specifically, we found that replacement of an approximately 9 Mb region of the NP Chr4 locus into the iP genetic background decreased alcohol consumption in female, but not in male ISCS rats when compared to their respective controls. We report that RNA-seq

analysis of NAc from female alcohol-naïve P.NP-ISCS and iP rats identified differentially expressed genes (DEGs) related to neuron function, cell signaling, and behavior. In addition, we found that β-estradiol was predicted to be the top upstream regulator of DEGs. Moreover, promoter SNPs in the Chr4 QTL gene *Acdyap1r1*, which encodes the PAC_1 receptor for the neuropeptide pituitary adenylate cyclase-activating polypeptide (PACAP), responded to estrogen stimulation. These findings indicate that *Acdyap1r1*, a gene previously associated with alcohol abuse in women (Dragan et al., 2017), is a likely candidate gene contributing to female-specific drinking behavior.

MATERIALS AND METHODS

Animals

Rats were bred and maintained at Indiana University School of Medicine. All animals were housed under 12-h light–dark conditions (7:00 am / 7:00 pm) with free access to laboratory rodent chow and water. The animals used for this study included inbred alcohol-preferring (iP) rats (Lumeng et al., 1977; Bice et al., 1998), congenic P.NP strains (Carr et al., 2006), and ISCS-A and -B (Spence et al., 2013). Heterozygous ISCSB-H F1 animals were generated by crossing ISCS-B with iP rats. The experimental protocol used in this study was reviewed and approved by the Indiana University Institutional Animal Care and Use Committee and was carried out in accordance with the NIH Guide for the Care and Use of Laboratory Animals. The animals were maintained in facilities fully accredited by the Association for the Assessment and Accreditation of Laboratory Animal Care (AAALAC).

Alcohol Consumption and Preference in ISCS Sub-Strains

Adult alcohol-naïve male and female rats from the two P.NP-ISCS (A and B strains), ISCSB-H, and iP controls were tested for voluntary alcohol drinking using a 2-bottle free-choice protocol, consisting of 10% ethanol or water for 3 weeks, as described previously (Lumeng et al., 1977; Li et al., 1993). Littermates were included from both ISCS-A and ISCS-B strains when possible. Two experiments were conducted by comparing: 1) ISCS-A (23 males, 22 females) vs. iP controls (10 males, 15 females); and 2) ISCS-B (22 males, 23 females), ISCSB-H (20 males, 18 females), and iP control (23 males, 35 females). Both alcohol consumption and alcohol preference were calculated as was described previously (Li et al., 1991). Body weight, but not food intake, was recorded once a week. To exclude the possibility of a sex difference in taste reactivity, ISCS-B rats (8 females, 7 males) were first tested for saccharin (1.03%) and then for quinine (0.5 μM) intake. Consumption data analyzed by two-way ANOVA followed by Newman-Keuls multiple comparisons test. Results are provided as means and standard error (SE).

RNA Isolation From NAc

Whole brains were extracted from alcohol-naïve adult ISCS-B and iP control rats, and snap frozen in dry ice-bathed isopentane, before brain regions were dissected as previously published (Liang et al., 2004, 2010; Liang and Carr, 2006). The RNA-seq experiment used NAc from female ISCS-B and iP control rats ($N = 3$ for each group). Tissues were stored at −80°C until RNA isolation. RNA was isolated from the NAc using TRIzol, followed by RNeasy mini-column purification (Qiagen, Valencia, CA, United States). RNA purity was measured using a spectrophotometer (Nanodrop 1000) and the 260/280 absorbance ratios were between 1.8 and 2.0. RNA integrity was measured using an Agilent 2100 Bioanalyzer and all samples had RIN >7.

RNA-seq Analysis

Sequencing libraries were constructed using the Illumina TruSeq RNA sample preparation protocol. The resulting libraries were sequenced on an Illumina HiSeq 2000 instrument using a standard single-end 50 bp sequencing protocol. The reads were aligned to the reference *Rattus norvegicus* genome (UCSC Rn 6.0) with TopHat 2 (Trapnell et al., 2010; Kim et al., 2013). No more than 2 mismatches were allowed in the alignment. HTseq was used to count gene expression reads, and DEseq was used to find DEGs after performing median normalization (Anders and Huber, 2010; Anders et al., 2015). DEGs were identified with adjusted $p < 0.05$ for multiple tests by the Benjamini-Hochberg method for controlling false discovery rate (FDR; Benjamini and Hochberg, 1995) and using a cutoff of sequence read rpmk >1. The RNA-seq data is available at GEO[1] with access ID: GSE112399.

IPA and Reactome Pathway Analysis

Two pathway analyses were used in data exploration. Ingenuity Pathway Analysis (IPA), which builds on manually curated content of the Ingenuity Knowledge database, was applied for predicting significant biological mechanisms and pathways (Qiagen[2]). The complete data set containing gene identifiers and corresponding expression values was uploaded into the application. Each identifier was mapped to its corresponding object in Ingenuity's Knowledge Base. An FDR-adjusted *p*-value cutoff of 0.05 was set to identify molecules whose expression was significantly differentially regulated. These molecules, called Network Eligible molecules, were overlaid onto a global molecular network developed from information contained in Ingenuity's Knowledge Base. Networks of Network Eligible Molecules were then algorithmically generated based on their connectivity. The Functional Analysis identified the biological functions and/or diseases that were most significant to the data set. Molecules from the dataset that met the FDR-adjusted *p*-values cutoff of <0.05 and were associated with biological functions and/or diseases in Ingenuity's Knowledge Base were considered for the analysis. Right-tailed Fisher's exact test was used to calculate a *p*-value determining the probability that each biological function and/or disease assigned to that data set is due to chance alone. Canonical pathways analysis identified the pathways from the Ingenuity Pathways Analysis library of

[1]https://www.ncbi.nlm.nih.gov/geo

[2]https://www.qiagenbioinformatics.com/products/ingenuity-pathway-analysis/

canonical pathways that were most significant to the data set. Molecules from the data set that met the FDR-adjusted p-values cutoff of $p < 0.05$ and were associated with a canonical pathway in Ingenuity's Knowledge Base were considered for the analysis. The significance of the association between the data set and the canonical pathway was measured in two ways: (1) A ratio of the number of molecules from the data set that map to the pathway divided by the total number of molecules that map to the canonical pathway is displayed. (2) Fisher's exact test was used to calculate a p-value determining the probability that the association between the genes in the dataset and the canonical pathway is explained by chance alone.

In addition, the *Reactome* Knowledgebase version 62[3] was applied to analyze the molecular interaction details of signal transduction, transport, and other cellular processes (Fabregat et al., 2016). Settings for *Reactome* analysis were DEGs with p-values <0.05 and FC > 2; a total of 212 genes were used for analysis. Pathway hierarchical organization provides *Reactome* pathways overview and highlights parent-child relationships of overrepresented connections in the pathway.

Validation of Candidate Gene Expression

Reverse transcription quantitative PCR (RT-qPCR) was performed using RNA from a separate set of experimental male and female ISCS-B and iP control (N = 6–8) animals than were utilized for RNA-seq. Each PCR assay was conducted using 6–8 biological replicates, and each cDNA sample was amplified in triplicate in qPCR for the same RT reaction. In brief, 1 μg RNA was reverse transcribed using Superscript III reverse-transcription reagent for first-strand cDNA synthesis (Invitrogen) using random primers. Each 50 μl PCR reaction contained cDNA corresponding to 35 ng of total RNA, SYBR Green Real-Time PCR Master mix (Life Sciences), and primers (5 μM). PCR was performed using the ABI PRISM 7300 Sequence Detection System (ThermoFisher), relative mRNA expression levels were normalized to *Gapdh*, and the standard curve method was used for data analysis. *Vector NTI* was used for primer design, and annealing temperatures ranged from 60 to 63°C. The primers used are listed in **Supplementary Table S5**. T-test was used to analyze the data and statistical significance was set at $p < 0.05$.

DNA Sequence Analysis

Genomic DNA was isolated from iP and iNP rats using Gentra Puregene Tissue kit (QIAGEN). PCR primers were designed to amplify the *Adcyap1r1* promoter region up to 2 kb upstream of the transcription start site; primer sequences are listed in **Supplementary Table S5**. PCR products were purified using the GenElute PCR Cleanup Kit (Sigma, St. Louis, MO) and ligated upstream of the luciferase gene in the pGL3-basic vector (Invitrogen). Plasmid DNA was isolated using the QIAprep Spin Miniprep kit, and the cloned *Adcyap1r1* promoter was sequenced using Indiana University sequencing core service. Genomic DNA sequences were aligned to the Rn.6 reference sequence.

[3]www.reactome.org

Transient Transfection and Dual-Luciferase Activity Assays

The P and NP reporter plasmids utilized in this study were constructed as previously described (Liang et al., 2003). Human neuroblastoma SK-N-SH cells (ATCC HTB-11) were cultured in Minimal Essential Medium (Invitrogen) containing 7.5% $NaHCO_3$, 2 mM Glut-max, 0.1 mM non-essential amino acids, 1 mM pyruvate, and 10% FBS (Invitrogen, Carlsbad, CA, United States) at 37°C in a humidified 5% CO_2 incubator. Twenty-four hours before transfection, 5.0×10^4 cells were plated into individual wells of a 24-well plate. Using Tf_x-50 reagent (Promega, Madison, WI, United States), each well was co-transfected with 0.5 μg of the pGL-3 luciferase plasmid plus 4 ng of the CMV Renilla luciferase vector (pRL-CMV, Invitrogen), which was utilized as an internal control for transfection efficiency. The human ER-α expression vector was a kind gift from Dr. Edwin R. Sánchez. The cells were subsequently incubated for 24 h at 37°C and washed with PBS before cell extracts were prepared in passive lysis buffer and assayed for firefly and Renilla luciferase activities using the Dual-Luciferase Reporter Assay System (Promega) in a TD-20/20 Luminometer (Turner BioSystems). The reporter assays were repeated five times in triplicate using plasmids that were independently purified at least twice.

RESULTS

Recessive Sex-Specific QTL Maps to Rat Chromosome 4

We examined whether the narrowed Chr4 QTL in the ISCS-A and ISCS-B sub-strains affected the drinking phenotype by testing alcohol consumption. In most alcohol drinking animal models, females have higher alcohol consumption than male rats, and this same phenotype was observed in control iP rats (**Figure 1**). However, we found that alcohol consumption was similar between males and females of both ISCS rat lines (∼3.5 to 4.5 g EtOH/kg BW/day). When ISCS alcohol consumption was compared to the iP background strain, both female ISCS-A and ISCS-B rats consumed 20–30% less alcohol ($p < 0.05$), while no differences were observed in the male rats (**Figure 1**). Our findings suggest a sex-specific QTL that maps to the overlapping Chr4 region in these two sub-strains between approximately 83.8 and 92.7 Mb (position reference to RGSC-v3.4).

To determine whether female alcohol consumption was a dominant or recessive trait, we tested alcohol consumption in heterozygous offspring of the ISCS-B line since this sub-strain contained the smallest overlapping genomic region. We found female homozygous ISCS-B animals consumed less alcohol than female heterozygous ISCSB-H ($p < 0.05$); however, we found no difference between female homozygous iP control and ISCSB-H. The similarity in alcohol consumption between iP and ISCSB-H indicates that the reduction in female drinking is a recessive trait. Additionally, no difference was detected in alcohol consumption between males of any genotypes (**Supplementary Figure S1**). No

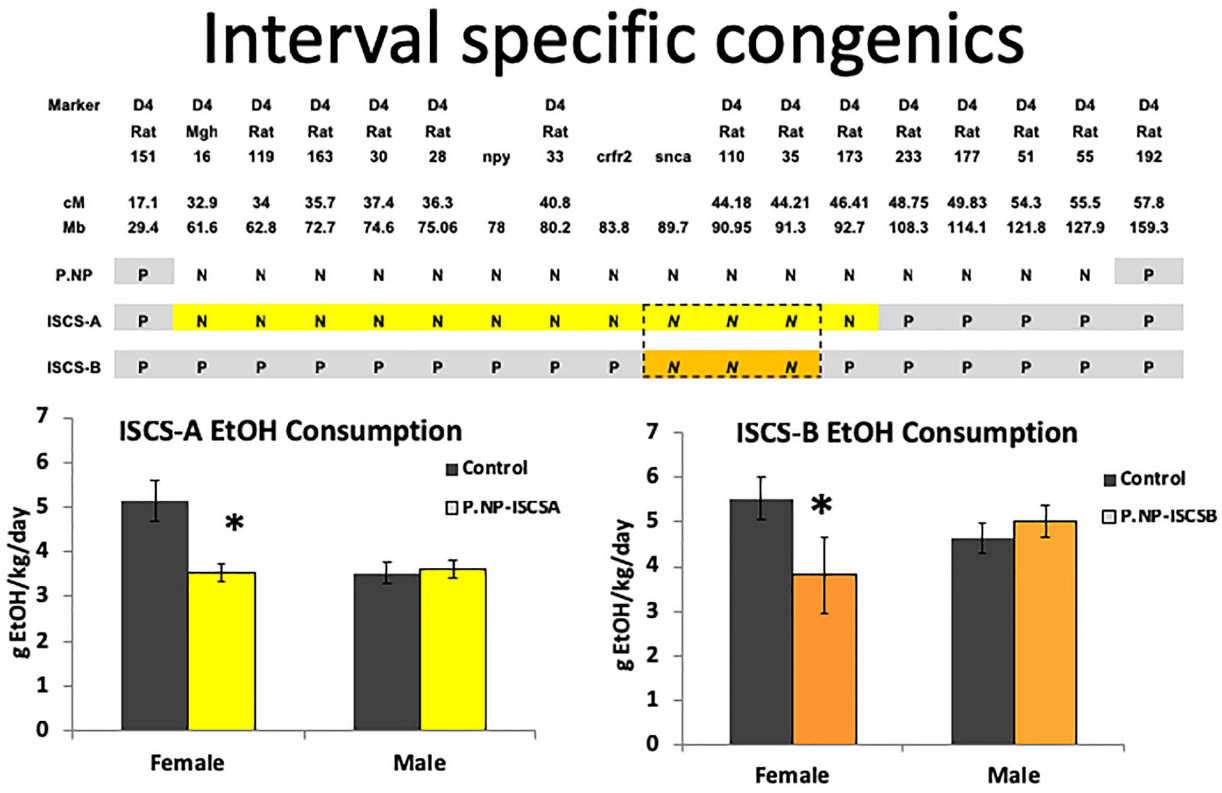

FIGURE 1 | P.NP is the congenic strain with the Chr4 QTL region in P rats replaced by the NP Chr4. Backcrossing P.NP with iP rat resulted in interval-specific congenic strains (ISCS). ISCS-A and ISCS-B shared a narrowed Chr4 QTL between 83.8 and 92.7 Mb (region in dash-lined box). Relative to iP control rats, only females in either ISCS consumed less alcohol; alcohol consumption (gEtOH/Kg/day) was calculated and is shown as mean ± SEM. *indicates $p < 0.05$.

sex differences were observed with either saccharin (adjusted *p*-value = 0.6) or quinine intake (adj $p = 0.56$), which indicates that differences in alcohol consumption were not associated with taste preferences (**Supplementary Figure S2**). Furthermore, alcohol consumption was not associated with body weight since we previously showed that there were no differences in body weight between ISCS-B and iP animals (Spence et al., 2013).

Identification of DEGs in the NAc Between ISCS-B and iP Rats

Since the only genetic differences between ISCS-B and iP rats existed within a minimum 1.79 Mb and maximum 8.9 Mb region of Chr4, we reasoned that genes in this narrowed Chr4 QTL might impact global gene expression in female rats related to alcohol consumption. To identify transcriptome changes, we performed RNA-seq on the NAc of alcohol-naïve female ISCS-B and iP (control) rats. High quality RNA-seq data were generated as documented by the correlation of biological replicates higher than 0.96. The average read count of each sample was more than 42 million with an average of more than 99.9% mapped reads (**Supplementary Table S1**).

We found 759 DEGs with the FDR set at $p < 0.05$; 212 of these DEGs showed FC > 2. The top 30 up- and down-regulated genes with adj $p < 0.05$ in ISCS-B females are listed in **Table 1**. Among the down-regulated genes, some are important for neuron functions: *Oxt* and *Gabre* (Donhoffner et al., 2016). Four genes were involved in the cholinergic system: *Chat*, *Slc5a7*, *Slc18a3*, and *Lhx8*. Other significant down-regulated genes are known to influence neurotransmission, neuron growth, and addiction, including *Ngfr*, *Ntrk1*, and *Ntsr1* (Gehle and Erwin, 1998; Pandey et al., 2017); and the estrogen receptor gene *Esr1* is an important regulator of sex-differences. Among the up-regulated genes, *Wnt6 and Cdh1* are associated with neuron development; other up-regulated DEGs are related to detoxification of drug and alcohol metabolism, such as *Ptgds* and *Gstm2*. Notably, many of the up-regulated DEGs are related to the development and function of the nervous system. The complete list of DEGs with FC > 2 and FDR adj $p < 0.05$ can be found in **Supplementary Table S3**.

To determine the genomic distribution of the DEG identified in the present study, we plotted the negative log-adjusted *p*-values for each DEG by chromosome (**Figure 2**). Of the 212 DEGs with FC > 2 (**Supplementary Table S3**), we found that 13 genes mapped to Chr4, including *Tacr1*, *Chrm2*, *Neurod6*, *Slc13a4,* and *Aqp1*; notably, these genes were differentially expressed and associated with drinking differences. Among the Chr4 DEG, *Tacr1*, which encodes the receptor for tachykinin substance P (also known as neurokinin 1), has been found to be associated

TABLE 1 | Top 30 up- and down-regulated genes.

Gene symbol	Full name	log2 fold change	adj-*p*-value
Top molecules down-regulated			
Oxt	Oxytocin/neurophysin 1 prepropeptide	−8.582	0.019
Tmem212	Transmembrane protein 212	−4.604	0.003
Gabre	Gamma-aminobutyric acid (GABA) A receptor; epsilon	−3.494	0.017
Ngfr	Nerve growth factor receptor	−3.321	0.000
Spata18	Spermatogenesis associated 18	−3.043	0.009
Mir384	microRNA 384	−2.644	0.007
Lhx8	LIM homeobox 8	−2.427	0.000
Wdr63	WD repeat domain 63	−2.308	0.045
Slc18a3	Solute carrier family 18 member A3	−2.164	0.000
Slc5a7	Solute carrier family 5 (sodium/choline cotransporter); member 7	−2.087	0.000
Esr1	Estrogen receptor 1	−2.064	0.013
Chat	Choline O-acetyltransferase	−2.004	0.000
Slc10a4	Solute carrier family 10; member 4	−1.997	0.000
Klhl1	Kelch-like family member 1	−1.989	0.003
St8sia6	ST8 alpha-N-acetyl-neuraminidase alpha-2;8-sialyltransferase 6	−1.964	0.008
Ntrk1	Neurotrophic tyrosine kinase; receptor; type 1	−1.962	0.000
Gpr165	G protein-coupled receptor 165	−1.900	0.001
Zim1	Zinc finger; imprinted 1	−1.853	0.000
Stk32b	Serine/threonine kinase 32B	−1.835	0.000
Ecel1	Endothelin converting enzyme-like 1	−1.733	0.000
Dynlrb2	Dynein light chain roadblock-type 2	−1.722	0.031
Ntsr1	Neurotensin receptor 1	−1.713	0.000
Gbx1	Gastrulation brain homeobox 1	−1.708	0.000
Ppp1r32	Protein phosphatase 1; regulatory subunit 32	−1.682	0.000
Pth2r	Parathyroid hormone 2 receptor	−1.661	0.000
Shh	Sonic hedgehog	−1.625	0.000
Slc27a2	Solute carrier family 27 (fatty acid transporter); member 2	−1.624	0.002
Lrrc34	Leucine rich repeat containing 34	−1.624	0.001
Nkx2-1	NK2 homeobox 1	−1.617	0.001
Gpx3	Glutathione peroxidase 3	−1.608	0.014
Top molecules up-regulated			
Rn5-8s	5.8S ribosomal RNA	2.898	0.019
LOC310926	hypothetical protein LOC310926	2.247	0.001
Mpzl2	myelin protein zero-like 2	1.945	0.000
LOC100134871	beta globin minor gene	1.923	0.037
LOC689064	beta-globin	1.849	0.014
Shisa3	shisa family member 3	1.797	0.001
Ccl9	chemokine (C-C motif) ligand 9	1.783	0.025
Aqp1	aquaporin 1	1.744	0.000
Cxcl10	chemokine (C-X-C motif) ligand 10	1.698	0.034
Wnt6	wingless-type MMTV integration site family; member 6	1.663	0.000
Gstm2	glutathione S-transferase mu 2	1.637	0.011
Osr1	odd-skipped related transciption factor 1	1.550	0.000
RT1-Da	RT1 class II; locus Da	1.545	0.000
Cd74	Cd74 molecule; major histocompatibility complex; class II invariant chain	1.544	0.000
Folr2	folate receptor 2 (fetal)	1.541	0.024
Cdh1	cadherin 1	1.540	0.023
Kcnj13	potassium channel; inwardly rectifying subfamily J; member 13	1.503	0.000
Gjb2	gap junction protein; beta 2	1.494	0.000
Tfap2b	transcription factor AP-2 beta	1.489	0.004

(Continued)

TABLE 1 | Continued

Gene symbol	Full name	log2 fold change	adj-*p*-value
Ptgds	prostaglandin D2 synthase (brain)	1.463	0.000
RGD1305645	similar to RIKEN cDNA 1500015O10	1.457	0.002
Clec10a	C-type lectin domain family 10; member A	1.451	0.000
Cyp1b1	cytochrome P450; family 1; subfamily b; polypeptide 1	1.449	0.010
PCOLCE2	procollagen C-endopeptidase enhancer 2	1.447	0.000
Bhlhe22	basic helix-loop-helix family; member e22	1.440	0.000
Slc22a6	solute carrier family 22 (organic anion transporter); member 6	1.438	0.000
Rln1	relaxin 1	1.423	0.006
Serpinf1	serpin peptidase inhibitor; clade F (alpha-2 antiplasmin; pigment epithelium derived factor); member 1	1.402	0.001
Slfn3	schlafen 3	1.394	0.000
Chrnb3	cholinergic receptor; nicotinic; beta 3 (neuronal)	1.363	0.002

DEG between ISCSB and iP control female rats in the nucleus accumbens with highest fold change and with FDR adjusted $p < 0.05$ are listed.

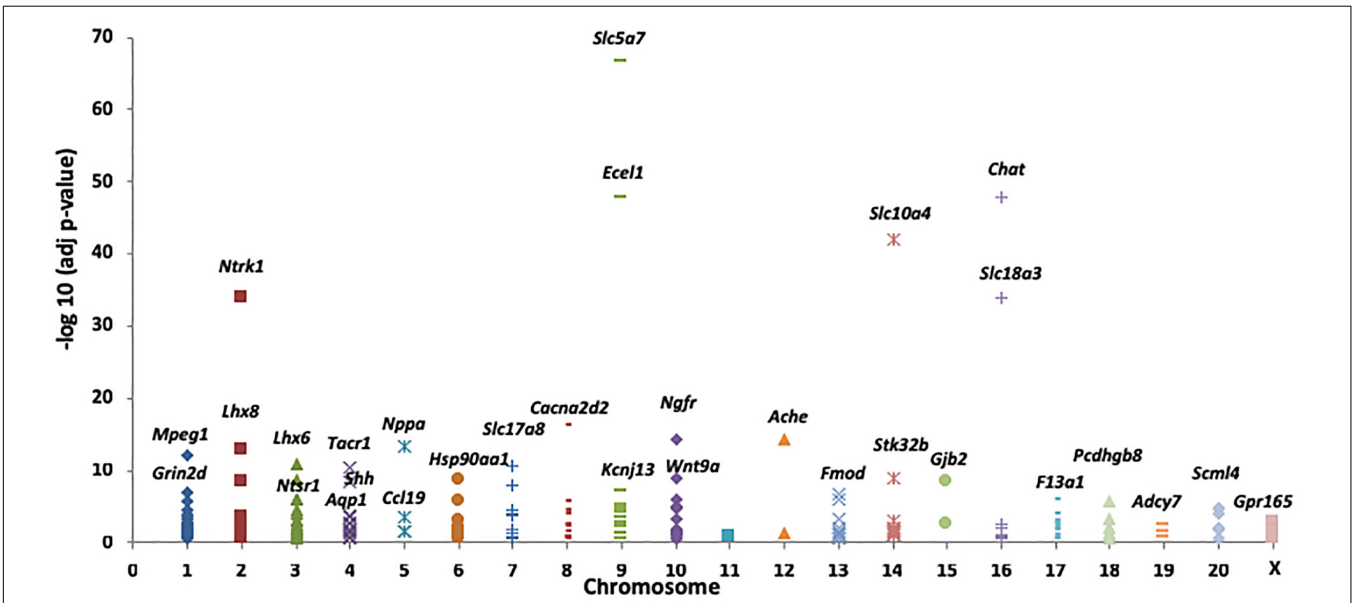

FIGURE 2 | A total of 73 differentially expressed genes (DEG) between female iP and ISCS-B rats possess a fold change >2 with $p < 0.05$. The significance of these genes was plotted by corresponding chromosomes. Genes with the lowest *p*-values for each chromosome are labeled.

with alcohol consumption in both humans and animals (Thorsell et al., 2005; George et al., 2008; Schank et al., 2013).

Networks Associated With DEGs in NAc and Pathway Analysis of *Trans*-Acting Factors That Affect Sex-Specific Gene Expression

We utilized IPA to predict relevant molecular networks, biological functions, and canonical pathways altered between ISCS-B and iP female rats. The input gene list included 790 DEGs with an FDR-adjusted *p*-value cutoff of 0.05 (**Figure 3** and **Supplementary Figure S3**). The most significant networks identified were relevant to axonal guidance signaling, cAMP-mediated signaling, and GABA receptor signaling, which are also important for drinking behavior (**Figure 3**). Genes within these pathways that have been associated with alcohol consumption in previous research studies include *Adcy7*, *Aldh1a2*, *Chrm2*, *Grin2d*, *Nfkb*, *Gsat4*, *Tacr1*, and *Oprm1*. Interestingly, the majority of genes in GABA receptor signaling and glutamate degradation III pathways showed reduced expression, while more genes with increased expression were found in pathways involved in axonal guidance, G-protein coupled receptor signaling, and glutathione-redox reactions (**Figure 3**).

To understand what factors might be driving these DEGs, we used IPA upstream analysis to predict the top transcriptional regulators. The top three upstream regulators were β-estradiol, α-synuclein, and β-catenin. Other additional relevant upstream regulators are included in **Table 2**. Among these predicted upstream regulators, our findings suggest that the hormones β-estradiol, progesterone, as well as dihydrotestosterone, likely contribute to differences in sex-specific gene expression.

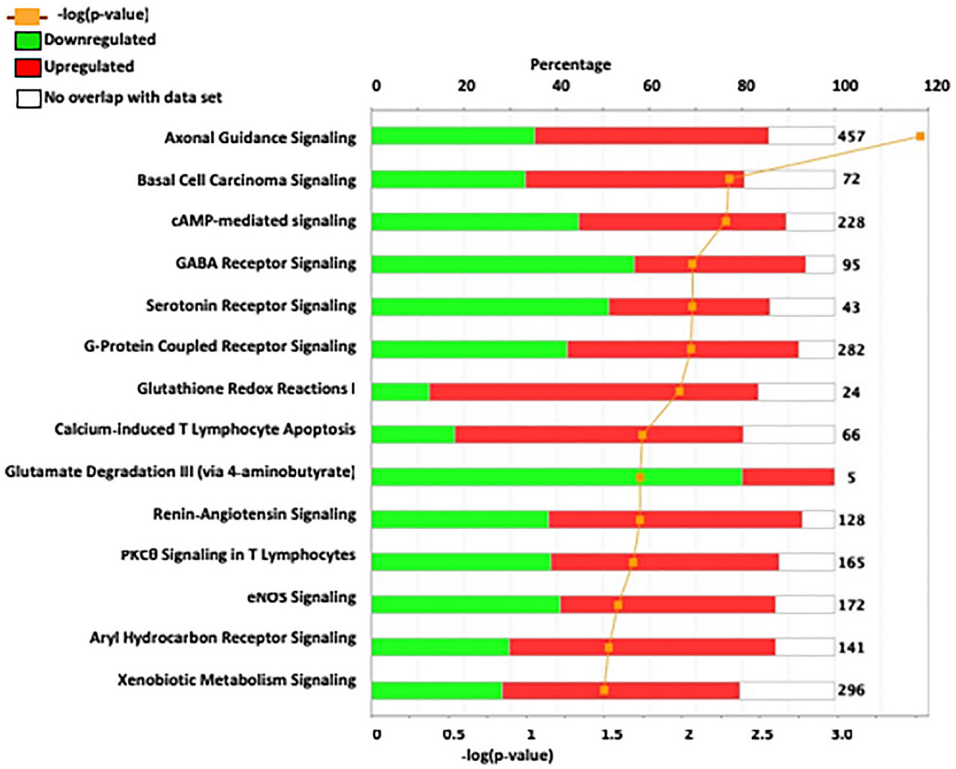

FIGURE 3 | In depth analysis of DEG between ISCS-B and iP using IPA. The most significant IPA canonical pathways are listed on the left. The stacked bar chart reveals the percentage of up-regulated (red) and down-regulated (green) genes within each canonical pathway. The numerical value at the right of each bar represents the total number of genes in the canonical pathways. The secondary x-axis (bottom) represents the -log of *p*-value.

Reactome Pathways and Overrepresented Connections in the Pathway

In addition to IPA analysis, DEGs with *p*-values <0.05, FC > 2 were used as input for *Reactome* data analysis, which is focused on molecular interactions within cells. The results of this analysis showed that the signal transduction pathways involving peptide ligand-binding receptors of class A/1 had the lowest *p*-values, indicating the significance of these interactions (**Figure 4**). We also found interesting regulator effect networks in our dataset. For example, Ngf and Raf1 play roles in dopamine and coordination, and ASCL1, estrogen receptor, and NGF are regulators of cell movement in neurons. More networks can be found in the (**Supplementary Table S4**).

Significant DEGs in NAc Between Males and Females Comparing ISCS-B and iP Rats

To determine whether the DEG identified in female NAc were sex-specific or also were differentially expressed in males, mRNA expression levels of selected DEGs were measured using RT-qPCR in both male and female ISCS-B and iP NAc tissue. The genes selected for measurement either showed a high fold change between the ISCS-B and iP RNA-seq data (e.g., *Lhx8, Ngfr*, *Slc5a7*), or were located in the Chr4 QTL and had been shown to be associated with alcohol consumption (e.g., *Adcyap1r1, Adcy7, Snca*, and *Tacr1*) or were reported

TABLE 2 | Upstream regulators.

Upstream regulator	Full name	Activation *z*-score	*p*-value of overlap
Beta-estradiol	Beta-estradiol	−0.563	1.78E-23
SNCA	α-synuclein	3.667	2.27E-12
CTNNB1	Catenin beta 1	0.807	1.47E-11
Progesterone	Progesterone	1.34	2.95E-11
HTT	Huntingtin	0.808	7.94E-11
CREB1	cAMP responsive element binding protein 1	0.952	1.03E-10
JAK1/2	Janus kinase 1	4.123	1.74E-10
BDNF	Brain derived neurotrophic factor	−1.374	8.24E-10
JUN	Jun proto-oncogene, AP-1 transcription factor subunit	1.345	1.57E-09
IFNG	Interferon gamma	2.602	8.33E-09
Dihydrotestosterone	Dihydrotestosterone	0.89	2.37E-08
ESR1	Estrogen receptor 1	−0.193	3.36E-08

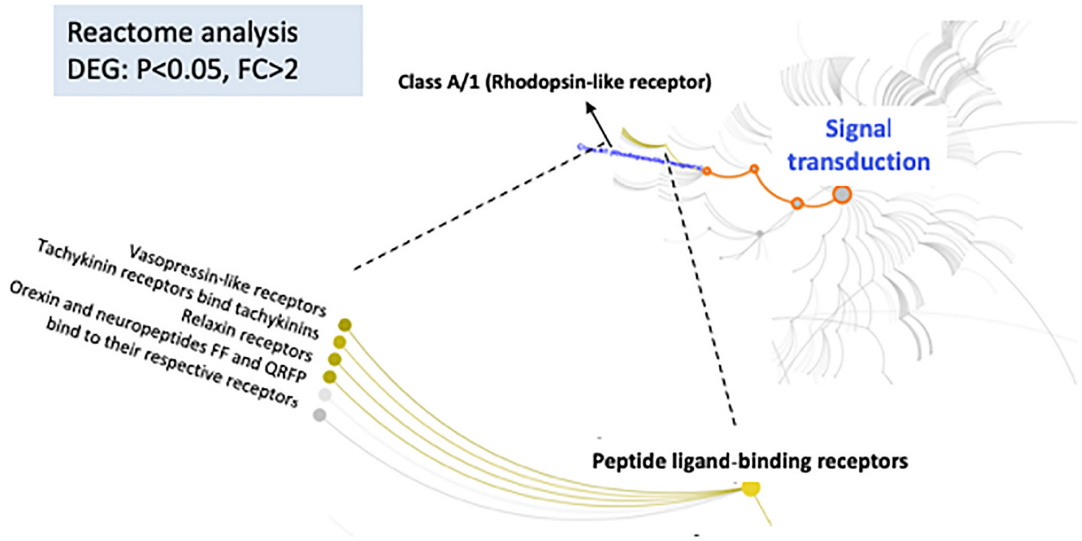

FIGURE 4 | Reactome database was used to analyze DEG relationships organized into biological pathways and processes (https://reactome.org/dev/). It reveals significant alterations in signal transduction pathways between female iP and ISCS-B rats. Color-highlighted edges indicate over-represented interactions.

previously to be differentially expressed between P and NP rats (e.g., *Ppm1K* and *Aqp1*). RT-qPCR was performed using RNA isolated from a different set of ISCS-B and iP rats. **Figure 5** displays the fold-change (ISCS-B/iP ratio) and **Supplementary Table S2** includes relative gene expression levels and *t*-test *p*-values between ISCS-B and iP animals for both males and females. Among these genes, *Chat*, *Lhx8*, *Ngfr*, *Slc18a3*, and *Tacr1* were found to be differentially expressed in both male and female ISCS-B compared to iP rats; however, differential expression of *Adcy7* and *Slc5a7* was observed between ISCS-B and iP males (p = 0.009 and 0.002, respectively), but no differences were found in females. Interestingly, *Nap1l5*, which is a maternally imprinted gene (Smith et al., 2003), was up-regulated in ISCS-B compared to iP females, but not males, which suggests that altered expression might be related to sex-specific differences in epigenetic regulation. Of particular relevance, *Adcyap1r1*, which has been associated with drinking in women (Dragan et al., 2017), was also up-regulated in ISCS-B compared to iP females, but was not significantly different in males (**Figures 6A,B**).

Rat *Adcyap1r1* Promoter Contains Predicted Estrogen-Response Elements

In addition to RNA-seq, we also performed GenBank and literature searches for genes that mapped to the Chr4 interval region and that had evidence of an association with alcohol consumption or response to estrogen. This approach identified several estrogen-responsive genes, including *Adcyap1r1*. Importantly, the *Adcyap1r1* genotype was associated with alcohol abuse in women (Dragan et al., 2017), and it also has been shown to respond to alcohol treatment (Koh et al., 2006). In addition, the human *ADCYAP1R1* gene contains a SNP in an estrogen response element (ERE) that was associated with PTSD

TABLE 3 | Promoter variance in *Adcyap1r1* gene.

	304–314 repeat C	524	532–533	1283	1885–1886
ReqSeq	C (11)	G	-	T	-
iP	C (10)	CGT	-	-	A
iNP	C (13)	G	C insertion	T	G

The nt location reference to 2 kb (designate as + 1) upstream of TSS.

only in females (Ressler et al., 2011). Therefore, we selected this gene for further mechanistic investigation to determine whether an ERE also existed in the rat *Adcyap1r1* promoter, and if any genetic variants existed between iP and iNP strains that might affect estrogen receptor α (ERα) binding. Estrogen receptor binding site prediction was performed using Genomtix[4], which revealed four potential EREs within 2 kb upstream of the *Adcyap1r1* transcription start site (**Figure 6C**), which was designated as + 1. We cloned and sequenced a 2 kb region of the *Adcyap1r1* promoter from genomic DNA of both iP and ISCS-B, which contained the *Adcyap1r1* iNP Chr4 sequence. In addition to confirming the presence of ERE consensus sites, we identified five sequence variants, including two that mapped near predicted EREs at nt 485–494 (#1) and nt 1303–1310 (#4) (**Table 3** and **Figure 6**).

Luciferase Expression of iNP Promoter of *Adcyap1r1* Was Significantly Upregulated by ERα

To evaluate the potential of these genomic variants to act as *cis*-elements in ERα transactivation of *Adcyap1r1* gene expression, we performed *in vitro* dual luciferase promoter assays. The iP and iNP promoter regions of *Adcyap1r1* were cloned into

[4]http://www.genomatix.de/

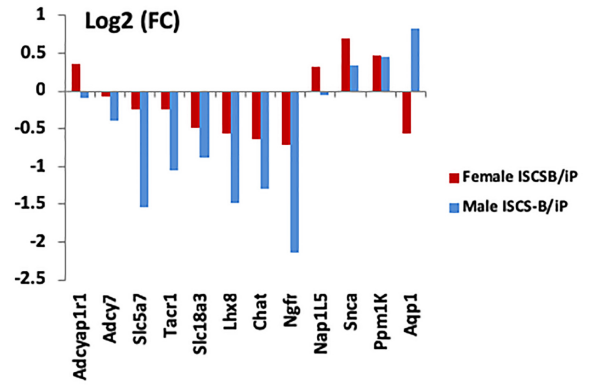

FIGURE 5 | RT-qPCR comparisons of gene expression between male and female iP and ISCS-B rats. *Chat*, *Slc18a3*, *Lhx8*, and *Ngfr* were confirmed to be differentially expressed in both male and female ISCS-B compared to iP rats. *Adcyap1r1* and *Nap1L5* were upregulated in female ISCS-B compared to iP animals, but no difference was found in males.

the pGL3 vector separately, and tested with and without dual ERα expression from the pcDNA vector. When empty pcDNA vector was transfected, the NP promoter showed higher luciferase activity compared to the P promoter. This effect could result from an endogenous estrogen effect or from the action of other transcription factors. As shown in **Figure 6**, luciferase expression was significantly upregulated by ERα, when the *Adcyap1r1* promoter was transcribed from the iNP compared to the iP genome. This result indicated that the iNP variant was more sensitive to ERα binding than the iP variant and suggested that these variants could contribute to the observed sex-differences in alcohol consumption between the iP and iNP strains.

DISCUSSION

Our results revealed a sex-specific QTL for alcohol consumption on rat Chr4 and point to a potential role for the gene *Acdyap1r1* in female-specific alcohol drinking behavior in the P rat model of AUD. Specifically, we identified DEG's in the NAc that were associated with the transferred QTL region in ISCS-B rats. These DEG's were predicted to affect gene networks controlling nervous system development and function, as well as drug metabolism and behavior. Notably, the top predicted upstream regulator of DEG's in female NAc was β-estradiol. Importantly, we found that sequence variants in the *Acdyap1r1* promoter showed differential activation by the estrogen receptor.

Females drink more alcohol than males in most, if not all, selectively bred lines of rodent models for alcohol consumption, including the iP rats used in this study (Li and Lumeng, 1984; Lancaster and Spiegel, 1992; McBride and Li, 1998; Chester et al., 2006). In the present study, we found that when a relatively small region of the iNP genome was substituted in the iP Chr4 QTL region, homozygous female ISCS rats consumed less alcohol (g EtOH/kg BW/day) and they exhibited similar alcohol consumption compared to iP control animals (**Figure 1**); this effect was not detected in their male counterparts. The reduced alcohol consumption in ISCS females was not due to body weight since we previously demonstrated that ISCS-B animals do not differ in body weight from the iP line (Spence et al., 2013). Additionally, because heterozygous female ISCSB-H animals consumed similar amounts of alcohol as iP controls, the sex-specific QTL we identified is a recessive trait.

The sex-specific drinking phenotype identified in the current research suggests that genetic variation from the NP genome within the ISCS-B congenic region likely contributes to decreased alcohol consumption in females in the P and NP model. We previously created the ISCS lines that decreased the background heterogeneity found in the P.NP congenic strain and simultaneously narrowed the QTL region (Spence et al., 2009; Spence et al., 2013; Baud and Flint, 2017). The sole difference within the entire genomes of ISCS-B and iP is a 1.7–8.9 Mb genomic segment, or less than approximately 0.3% of the 2719 Mb rat genome (Jensen-Seaman et al., 2004). Clearly, this ISCS-B genomic region contains variants from the NP donor, which modify gene expression via *cis*-elements or interact with *trans*-acting factors (e.g., estrogen receptor), thereby altering gene networks that significantly affect female alcohol consumption (**Figure 6**). We hypothesized that many interactions exist between genes within this 1.7–8.9 Mb genomic region and genes outside this region, and replacement of this region would result in *trans*-regulation via *cis-acting* elements.

Adcy7 has been associated with female-specific ethanol consumption in mice (Pronko et al., 2010; Cruz et al., 2011; Desrivières et al., 2011). IPA showed that *ADCY7*, *ADCY*, and *Creb* are involved in drug metabolism and behavior. Our finding indicated that the adenylate cyclase (AC) signaling pathway was enriched with genes associated with female alcohol consumption or response to estrogen regulation (**Figure 7**). We emphasize that upregulation of *Adcyap1r1* may affect AC, and downstream genes such as *PAK*, *ERK* and *BDNF*, which could also play important roles in neuron protection.

Hormones affect gene expression at both *cis*- (e.g., in the narrowed Chr4 region) and *trans*- (elsewhere) locations. Through data mining and literature searching, we identified multiple genes in the Chr4 QTL (e.g., *Aqp1*, *Abcg2*, *Adcyap1r1*, *Npy*, and *Snca*) that are regulated by estrogen directly or indirectly. Bioinformatics analysis also predicted upstream regulators of the DEGs which indicated that sex hormones are likely to play an important role (**Table 2**). Hormones, such as β-estradiol, target multiple DEGs, including *Tacr1* on Chr4, and *Chat*, *Nts*, *Nupr1*, *Ogn*, *Ttr*, and *Oprm1* on other chromosomes. Importantly, all these genes have relatively high fold change between ISCS-B and iP rats. In addition, β-estradiol is also predicted to target *Aldh1a2* and affect alcohol metabolism. *Esr1* encoding the estrogen receptor α is significantly decreased in ISCS-B NAc. Interestingly, β-estradiol is a regulator of the *Chat* and *Tacr1* genes.

We hypothesized that the sex-dependent differences in gene expression were related to promoter variants between

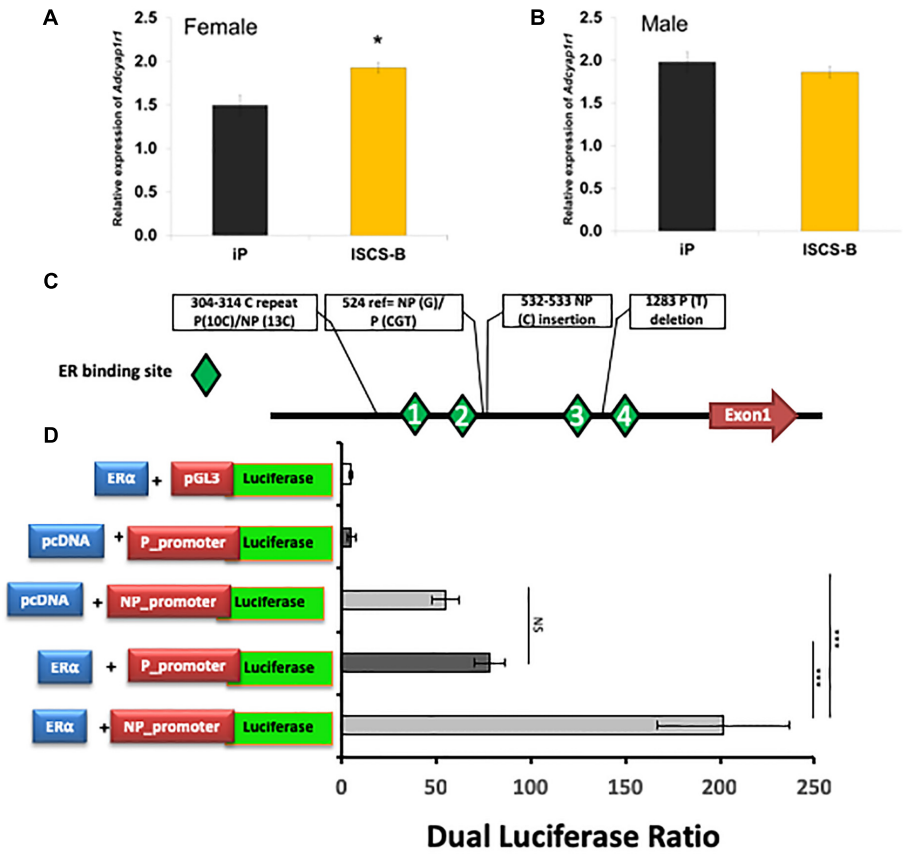

FIGURE 6 | (A) *Adcyap1r1* expression is increased in female ISCS-B relative to iP rats. **(B)** Male ISCS-B rats demonstrate no significant difference from iP in *Adcyap1r1* expression. **(C)** A schematic of the *Adcyap1r1* promoter sequence demonstrating ER binding sites and polymorphisms between iP and iNP. **(D)** ERα transactivation of both variants of the *Adcyap1r1* promoter enhanced luciferase activity, but the iNP promoter exhibited significantly more luciferase activity than iP.

the iP and ISCS-B lines, altering the binding affinity for *trans-acting* factors (e.g., estrogen receptor) involved in gene transcription (**Figure 8**). We show that genetic variants in the *Adcyap1r1* promoter respond to estrogen stimulation, thereby providing one possible mechanism for sex-specific differences in alcohol consumption. In humans, *ADCYAP1R1* has been associated with female alcohol consumption (Dragan et al., 2017). Pituitary adenylyl cyclase-activating polypeptide (ADCYAP)-ADCYAP1R1 pathway is regulated by estrogen and is involved in abnormal fear responses underlying PTSD (Ramikie and Ressler, 2016). Our finding that SNPs in the promoter region of the NP *Adcyap1r1* allele are more sensitive to estrogen stimulation *in vitro* suggests that alcohol consumption is mediated, in part, by estrogen regulation of ADCYAP1R1 in the P and NP model, providing a potential explanation for why alcohol consumption was decreased in female ISCS lines. Moreover, ADCYAP was found to be co-localized with ChAT in nerve fibers (Drescher et al., 2006) and it is possible that *Adcyap1r1* could also interact with ChAT, thereby providing a potential mechanism for how increased *ADCYAP1R1* expression might promote neuroprotection (**Figure 7**). In addition, pathway analysis showed an increase of glutathione-redox reactions I, conveying a similar neuroprotection function.

In this research, we observed that genes related to cholinergic function were reduced more than 4-fold in ISCS-B relative to iP, including *Chat*, *Slc18a3*, *Slc5a7*, and LIM homeobox 8. Consistent with our findings, previous studies found higher expression of *Chat*, *Slc18a3*, and *Slc5a7* in the NAc shell of adult P rats compared to NP rats (McBride et al., 2013). Further, cocaine treatment and withdrawal are also associated with increased *ChAT*, *Slc5a7*, and *Slc18a3* expression in the NAc (Eipper-Mains et al., 2013). Others also have reported that alcohol consumption reduces ChAT in NAc, resulting in fewer basal forebrain cholinergic neurons (Jamal et al., 2007; Coleman et al., 2011; Pereira et al., 2014). Thus, the cholinergic neuron function in the NAc deserves further investigation with regard to its involvement in female drinking. Another significant finding is the down-regulation of *Ngfr* and *Lhx8*, resulting in alterations of *Ntrk1*, which might regulate downstream MAPK signaling and Wnt (**Figure 7**).

We speculate that a potential mechanism for sex-dependent differences in gene expression is that promoter variants between the iP and ISCS-B lines alter the binding affinity for *trans-acting* factors, such as estrogen receptor (**Figure 8**), resulting in different levels of mRNA expression between female ISCS-B and iP controls. Because two

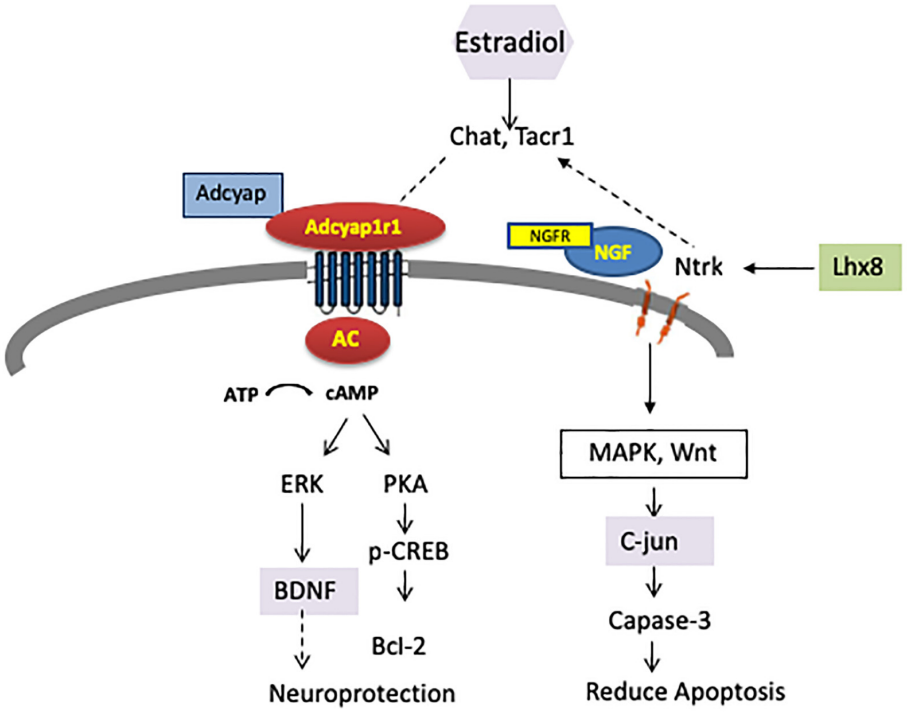

FIGURE 7 | DEGs were enriched in two pathways which affect neuron function and are also regulated by estrogen receptor (ER). Adenylate cyclase (AC) and downstream signaling affecting neuroprotection was upregulated, while NtrK, Ngfr, and Lhx8 signaling affecting apoptosis were downregulated.

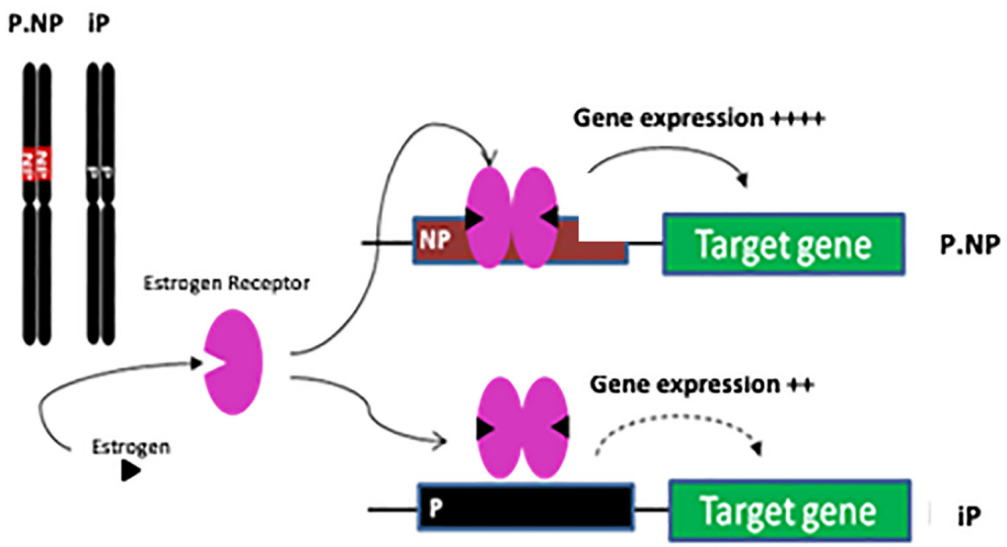

FIGURE 8 | Schematic of genetic and estrogen receptor interaction affecting gene expression. The only difference between congenic P.NP and iP is on Chr4 region. Compared with P genomic sequence, the genetic difference in NP is proposed to lead to stronger binding of estrogen receptor in promoters of targeted genes resulting in increased gene expression.

interrelated pathways were found to be enriched for genes associated with female alcohol consumption or response to estrogen regulation (**Figure 7**), we further speculate that upregulation of *Adcyap1r1* may affect adenylyl cyclase signaling resulting in neuron protection and downregulation of *Ntrk* and *Ngf* signaling resulting in reduced apoptosis. These data suggest that AC and cholinergic function may play important roles in female alcohol consumption.

Additionally, BDNF, C-jun and estradiol are all significant upstream regulators that affect DEG expression and are functionally important in these pathways. Together, these findings demonstrate a potential role for estrogen in the upregulation of *Adcyap1r1* expression that is associated with a sex-specific QTL for alcohol consumption on rat chromosome 4.

AUTHOR CONTRIBUTIONS

TL along with JPS, JLR, and WY designed the research and wrote the manuscript. JPS, TG, KEW, and PJB performed the animal model development, alcohol consumption test, and molecular analysis in the research. WY along with BQ, HG, and LZ performed cloning and transient transfection. DKG and ZL executed the RNA-seq. YZ along with TL, WY, and JPS analyzed the data. All authors have read and given final approval for the manuscript.

FUNDING

This research was supported by grants from CAMS Innovation Fund for Medical Sciences (CIFMS) (2017-I2M-3-015), the National Science Foundation of China (Nos. 81700751 and 2013CB945001), the National Institutes of Health NIH/NIAAA, R01 AA10707, P60AA007611, and R24AA015512. We appreciate the funding from Biomedical Research Grant of the Indiana University School of Medicine that allowed us to initiate this research.

ACKNOWLEDGMENTS

We would like to express our appreciation to Michelle Johnson and Judy Powers who provided technical support, Dr. Lucinda Carr, Dr. Lawrence Lumeng, and Indiana Alcohol Research Center, for their support in initiating this long-term project and providing useful discussion of this research.

SUPPLEMENTARY MATERIAL

The Supplementary Material for this article can be found online at: https://www.frontiersin.org/articles/10.3389/fgene.2018.00513/full#supplementary-material

FIGURE S1 | Female ISCS-B rats demonstrated less consumption than iP and ISCSB-H. Males demonstrated no differences between strains. Female heterozygotes (ISCSB-H) showed a similar level of alcohol consumption when compared to iP controls.

FIGURE S2 | Female and male ISCS-B rats exhibited similar consumption of either saccharin or quinine indicating no taste difference between sexes.

FIGURE S3 | Differentially expressed genes were plotted by gene expression and fold change. The top five Ingenuity Pathway Analysis networks, diseases and bio functions are listed.

TABLE S1 | RNA-seq reads of each sample.

TABLE S2 | Gene expression in the nucleus accumbens of both male and female rats using RT-qPCR.

TABLE S3 | Differentially expressed gene list.

TABLE S4 | Significant top regulator effect networks.

TABLE S5 | List of primer sequences.

REFERENCES

Anders, S., and Huber, W. (2010). Differential expression analysis for sequence count data. *Genome Biol.* 11:R106. doi: 10.1186/gb-2010-11-10-r106

Anders, S., Pyl, P. T., and Huber, W. (2015). HTSeq–a python framework to work with high-throughput sequencing data. *Bioinformatics* 31, 166–169. doi: 10.1093/bioinformatics/btu638

Baud, A., and Flint, J. (2017). Identifying genes for neurobehavioural traits in rodents: progress and pitfalls. *Dis. Model Mech.* 10, 373–383. doi: 10.1242/dmm.027789

Becker, J. B., and Koob, G. F. (2016). Sex differences in animal models: focus on addiction. *Pharmacol. Rev.* 68, 242–263. doi: 10.1124/pr.115.011163

Benjamini, Y., and Hochberg, Y. (1995). Controlling the false discovery rate: a practical and powerful approach to multiple testing. *J. R. Stat. Soc.* 57, 289–290.

Bice, P., Foroud, T., Bo, R., Castelluccio, P., Lumeng, L., Li, T. K., et al. (1998). Genomic screen for QTLs underlying alcohol consumption in the P and NP rat lines. *Mamm. Genome* 9, 949–955. doi: 10.1007/s003359900905

Bice, P. J., Foroud, T., Carr, L. G., Zhang, L., Liu, L., Grahame, N. J., et al. (2006). Identification of QTLs influencing alcohol preference in the High Alcohol Preferring (HAP) and Low Alcohol Preferring (LAP) mouse lines. *Behav. Genet.* 36, 248–260. doi: 10.1007/s10519-005-9019-6

Carr, L. G., Foroud, T., Bice, P., Gobbett, T., Ivashina, J., Edenberg, H., et al. (1998). A quantitative trait locus for alcohol consumption in selectively bred rat lines. *Alcohol. Clin. Exp. Res.* 22, 884–887. doi: 10.1111/j.1530-0277.1998.tb03883.x

Carr, L. G., Habegger, K., Spence, J. P., Liu, L., Lumeng, L., and Foroud, T. (2006). Development of congenic rat strains for alcohol consumption derived from the alcohol-preferring and nonpreferring rats. *Behav. Genet.* 36, 285–290. doi: 10.1007/s10519-005-9021-z

Ceylan-Isik, A. F., McBride, S. M., and Ren, J. (2010). Sex difference in alcoholism: who is at a greater risk for development of alcoholic complication? *Life Sci.* 87, 133–138. doi: 10.1016/j.lfs.2010.06.002

Chesler, E. J., Plitt, A., Fisher, D., Hurd, B., Lederle, L., Bubier, J. A., et al. (2012). Quantitative trait loci for sensitivity to ethanol intoxication in a C57BL/6Jx129S1/SvImJ inbred mouse cross. *Mamm. Genome* 23, 305–321. doi: 10.1007/s00335-012-9394-2

Chester, J. A., de Paula Barrenha, G., DeMaria, A., and Finegan, A. (2006). Different effects of stress on alcohol drinking behaviour in male and female mice selectively bred for high alcohol preference. *Alcohol Alcohol.* 41, 44–53. doi: 10.1093/alcalc/agh242

Cicero, T. (1979). "A critique of animal analogues of alcoholism," in *Biochemistry and Pharmacology of Ethanol*, Vol. 2, eds E. Majchrowicz and E. P. Noble (New York, NY: Plenum Press), 533–560.

Coleman, L. G. Jr., He, J., Lee, J., Styner, M., and Crews, F. T. (2011). Adolescent binge drinking alters adult brain neurotransmitter gene expression, behavior, brain regional volumes, and neurochemistry in mice. *Alcohol. Clin. Exp. Res.* 35, 671–688. doi: 10.1111/j.1530-0277.2010.01385.x

Cruz, M. T., Bajo, M., Maragnoli, M. E., Tabakoff, B., Siggins, G. R., and Roberto, M. (2011). Type 7 adenylyl cyclase is involved in the ethanol and CRF sensitivity of GABAergic synapses in mouse central amygdala. *Front. Neurosci.* 4:207. doi: 10.3389/fnins.2010.00207

Desrivières, S., Pronko, S. P., Lourdusamy, A., Ducci, F., Hoffman, P. L., Wodarz, N., et al. (2011). Sex-specific role for adenylyl cyclase type 7 in alcohol dependence. *Biol. Psychiatry* 69, 1100–1108. doi: 10.1016/j.biopsych.2011.01.037

Dick, D. M., Bierut, L., Hinrichs, A., Fox, L., Bucholz, K. K., Kramer, J., et al. (2006). The role of GABRA2 in risk for conduct disorder and alcohol and

drug dependence across developmental stages. *Behav. Genet.* 36, 577–590. doi: 10.1007/s10519-005-9041-8

Dimas, A. S., Nica, A. C., Montgomery, S. B., Stranger, B. E., Raj, T., Buil, A., et al. (2012). Sex-biased genetic effects on gene regulation in humans. *Genome Res.* 22, 2368–2375. doi: 10.1101/gr.134981.111

Donhoffner, M. E., Goings, S. P., Atabaki, K., and Wood, R. I. (2016). Intracerebroventricular oxytocin self-administration in female rats. *J. Neuroendocrinol.* 28. doi: 10.1111/jne.12416

Dragan, W. L., Czerski, P. M., and Dragan, M. (2017). PAC1 receptor (ADCYAP1R1) genotype and problematic alcohol use in a sample of young women. *Neuropsychiatr. Dis. Treat.* 13, 1483–1489. doi: 10.2147/NDT.S137331

Drescher, M. J., Drescher, D. G., Khan, K. M., Hatfield, J. S., Ramakrishnan, N. A., Abu-Hamdan, M. D., et al. (2006). Pituitary adenylyl cyclase-activating polypeptide (PACAP) and its receptor (PAC1-R) are positioned to modulate afferent signaling in the cochlea. *Neuroscience* 142, 139–164. doi: 10.1016/j.neuroscience.2006.05.065

DuBose, C. S., Chesler, E. J., Goldowitz, D., and Hamre, K. M. (2013). Use of the expanded panel of BXD mice narrow QTL regions in ethanol-induced locomotor activation and motor incoordination. *Alcohol. Clin. Exp. Res.* 37, 170–183. doi: 10.1111/j.1530-0277.2012.01865.x

Ducci, F., and Goldman, D. (2008). Genetic approaches to addiction: genes and alcohol. *Addiction* 103, 1414–1428. doi: 10.1111/j.1360-0443.2008.02203.x

Eipper-Mains, J. E., Kiraly, D. D., Duff, M. O., Horowitz, M. J., McManus, C. J., Eipper, B. A., et al. (2013). Effects of cocaine and withdrawal on the mouse nucleus accumbens transcriptome. *Genes Brain Behav.* 12, 21–33. doi: 10.1111/j.1601-183X.2012.00873.x

Fabregat, A., Sidiropoulos, K., Garapati, P., Gillespie, M., Hausmann, K., Haw, R., et al. (2016). The reactome pathway knowledgebase. *Nucleic Acids Res.* 44, D481–D487. doi: 10.1093/nar/gkv1351

Gatti, D. M., Zhao, N., Chesler, E. J., Bradford, B. U., Shabalin, A. A., Yordanova, R., et al. (2010). Sex-specific gene expression in the BXD mouse liver. *Physiol. Genomics* 42, 456–468. doi: 10.1152/physiolgenomics.00110.2009

Gehle, V. M., and Erwin, V. G. (1998). Common quantitative trait loci for alcohol-related behaviors and CNS neurotensin measures: voluntary ethanol consumption. *Alcohol. Clin. Exp. Res.* 22, 401–408. doi: 10.1097/00000374-199804000-00016

George, D. T., Gilman, J., Hersh, J., Thorsell, A., Herion, D., Geyer, C., et al. (2008). Neurokinin 1 receptor antagonism as a possible therapy for alcoholism. *Science* 319, 1536–1539. doi: 10.1126/science.1153813

Gershoni, M., and Pietrokovski, S. (2017). The landscape of sex-differential transcriptome and its consequent selection in human adults. *BMC Biol.* 15:7. doi: 10.1186/s12915-017-0352-z

Gill, K., Desaulniers, N., Desjardins, P., and Lake, K. (1998). Alcohol preference in AXB/BXA recombinant inbred mice: gender differences and gender-specific quantitative trait loci. *Mamm. Genome* 9, 929–935. doi: 10.1007/s003359900902

Heath, A. C., Bucholz, K. K., Madden, P. A., Dinwiddie, S. H., Slutske, W. S., Bierut, L. J., et al. (1997). Genetic and environmental contributions to alcohol dependence risk in a national twin sample: consistency of findings in women and men. *Psychol. Med.* 27, 1381–1396. doi: 10.1017/S0033291797005643

Jamal, M., Ameno, K., Ikuo, U., Kumihashi, M., Wang, W., and Ijiri, I. (2007). Ethanol and acetaldehyde: in vivo quantitation and effects on cholinergic function in rat brain. *Novartis Found. Symp.* 285, 137–141, discussion 141–144, 198–199.

Jensen-Seaman, M. I., Furey, T. S., Payseur, B. A., Lu, Y., Roskin, K. M., Chen, C. F., et al. (2004). Comparative recombination rates in the rat, mouse, and human genomes. *Genome Res.* 14, 528–538. doi: 10.1101/gr.1970304

Karp, N. A., Mason, J., Beaudet, A. L., Benjamini, Y., Bower, L., Braun, R. E., et al. (2017). Prevalence of sexual dimorphism in mammalian phenotypic traits. *Nat. Commun.* 8:15475. doi: 10.1038/ncomms15475

Kim, D., Pertea, G., Trapnell, C., Pimentel, H., Kelley, R., and Salzberg, S. L. (2013). TopHat2: accurate alignment of transcriptomes in the presence of insertions, deletions and gene fusions. *Genome Biol.* 14:R36. doi: 10.1186/gb-2013-14-4-r36

Koh, P. O., Won, C. K., and Ho, J. H. (2006). Ethanol decreases the expression of pituitary adenylate cyclase activating polypeptide in rat testes. *J. Vet. Med. Sci.* 68, 635–637. doi: 10.1292/jvms.68.635

Koss, M. P., and Goldman, D. (2000). Genetic factors and alcoholism. *Am. J. Public Health* 90:1799. doi: 10.2105/AJPH.90.11.1799

Lancaster, F. E., and Spiegel, K. S. (1992). Sex differences in pattern of drinking. *Alcohol* 9, 415–420. doi: 10.1016/0741-8329(92)90041-8

Li, T. K., and Lumeng, L. (1984). Alcohol preference and voluntary alcohol intakes of inbred rat strains and the National Institutes of Health heterogeneous stock of rats. *Alcohol. Clin. Exp. Res.* 8, 485–486. doi: 10.1111/j.1530-0277.1984.tb05708.x

Li, T. K., Lumeng, L., and Doolittle, D. P. (1993). Selective breeding for alcohol preference and associated responses. *Behav. Genet.* 23, 163–170. doi: 10.1007/BF01067421

Li, T. K., Lumeng, L., Doolittle, D. P., and Carr, L. G. (1991). Molecular associations of alcohol-seeking behavior in rat lines selectively bred for high and low voluntary ethanol drinking. *Alcohol Alcohol. Suppl.* 1, 121–124.

Liang, T., and Carr, L. G. (2006). Regulation of alpha-synuclein expression in alcohol-preferring and – non preferring rats. *J. Neurochem.* 99, 470–482. doi: 10.1111/j.1471-4159.2006.04111.x

Liang, T., Habegger, K., Spence, J. P., Foroud, T., Ellison, J. A., Lumeng, L., et al. (2004). Glutathione S-transferase 8-8 expression is lower in alcohol-preferring than in alcohol-nonpreferring rats. *Alcohol. Clin. Exp. Res.* 28, 1622–1628. doi: 10.1097/01.ALC.0000145686.79141.57

Liang, T., Kimpel, M. W., McClintick, J. N., Skillman, A. R., McCall, K., Edenberg, H. J., et al. (2010). Candidate genes for alcohol preference identified by expression profiling in alcohol-preferring and -nonpreferring reciprocal congenic rats. *Genome Biol.* 11:R11. doi: 10.1186/gb-2010-11-2-r11

Liang, T., Spence, J., Liu, L., Strother, W. N., Chang, H. W., Ellison, J. A., et al. (2003). alpha-Synuclein maps to a quantitative trait locus for alcohol preference and is differentially expressed in alcohol-preferring and –nonpreferring rats. *Proc. Natl. Acad. Sci. U.S.A.* 100, 4690–4695. doi: 10.1073/pnas.0737182100

Lumeng, L., Hawkins, T. D., and Li, T. (1977). "New strains of rats with alcohol preference and nopreference," in *Alcohol and Aldehyde Metabolizing System*, Vol. III, eds R. G. Thurman, J. R. Williamson, H. Drott, and B. S. Chance (New York, NY: Academic Press), 537–544. doi: 10.1016/B978-0-12-691403-0.50056-2

McBride, W. J., Kimpel, M. W., McClintick, J. N., Ding, Z. M., Hyytia, P., Colombo, G., et al. (2013). Gene expression within the extended amygdala of 5 pairs of rat lines selectively bred for high or low ethanol consumption. *Alcohol* 47, 517–529. doi: 10.1016/j.alcohol.2013.08.004

McBride, W. J., and Li, T. K. (1998). Animal models of alcoholism: neurobiology of high alcohol-drinking behavior in rodents. *Crit. Rev. Neurobiol.* 12, 339–369. doi: 10.1615/CritRevNeurobiol.v12.i4.40

Melo, J. A., Shendure, J., Pociask, K., and Silver, L. M. (1996). Identification of sex-specific quantitative trait loci controlling alcohol preference in C57BL/ 6 mice. *Nat. Genet.* 13, 147–153. doi: 10.1038/ng0696-147

Murphy, J. M., Stewart, R. B., Bell, R. L., Badia-Elder, N. E., Carr, L. G., McBride, W. J., et al. (2002). Phenotypic and genotypic characterization of the Indiana University rat lines selectively bred for high and low alcohol preference. *Behav. Genet.* 32, 363–388. doi: 10.1023/A:1020266306135

Nolen-Hoeksema, S. (2004). Gender differences in risk factors and consequences for alcohol use and problems. *Clin. Psychol. Rev.* 24, 981–1010. doi: 10.1016/j.cpr.2004.08.003

Pandey, S., Badve, P. S., Curtis, G. R., Leibowitz, S. F., and Barson, J. R. (2017). Neurotensin in the posterior thalamic paraventricular nucleus: inhibitor of pharmacologically relevant ethanol drinking. *Addict. Biol.* doi: 10.1111/adb.12546 [Epub ahead of print].

Peirce, J. L., Derr, R., Shendure, J., Kolata, T., and Silver, L. M. (1998). A major influence of sex-specific loci on alcohol preference in C57Bl/6 and DBA/2 inbred mice. *Mamm. Genome* 9, 942–948. doi: 10.1007/s003359900904

Pereira, P. A., Neves, J., Vilela, M., Sousa, S., Cruz, C., and Madeira, M. D. (2014). Chronic alcohol consumption leads to neurochemical changes in the nucleus accumbens that are not fully reversed by withdrawal. *Neurotoxicol. Teratol.* 44, 53–61. doi: 10.1016/j.ntt.2014.05.007

Prescott, C. A. (2002). Sex differences in the genetic risk for alcoholism. *Alcohol Res. Health* 26, 264–273.

Pronko, S. P., Saba, L. M., Hoffman, P. L., and Tabakoff, B. (2010). Type 7 adenylyl cyclase-mediated hypothalamic-pituitary-adrenal axis responsiveness: influence of ethanol and sex. *J. Pharmacol. Exp. Ther.* 334, 44–52. doi: 10.1124/jpet.110.166793

Radcliffe, R. A., Bohl, M. L., Lowe, M. V., Cycowski, C. S., and Wehner, J. M. (2000). Mapping of quantitative trait loci for hypnotic sensitivity to ethanol in crosses

derived from the C57BL/6 and DBA/2 mouse strains. *Alcohol. Clin. Exp. Res.* 24, 1335–1342. doi: 10.1111/j.1530-0277.2000.tb02101.x

Ramikie, T. S., and Ressler, K. J. (2016). Stress-related disorders, pituitary adenylate cyclase-activating peptide (PACAP)ergic system, and sex differences. *Dialogues Clin. Neurosci.* 18, 403–413.

Rawlik, K., Canela-Xandri, O., and Tenesa, A. (2016). Evidence for sex-specific genetic architectures across a spectrum of human complex traits. *Genome Biol.* 17:166. doi: 10.1186/s13059-016-1025-x

Ressler, K. J., Mercer, K. B., Bradley, B., Jovanovic, T., Mahan, A., Kerley, K., et al. (2011) Post-traumatic stress disorder is associated with PACAP and the PAC1 receptor. *Nature* 470, 492–497. doi: 10.1038/nature09856

Schank, J. R., Tapocik, J. D., Barbier, E., Damadzic, R., Eskay, R. L., Sun, H., et al. (2013). Tacr1 gene variation and neurokinin 1 receptor expression is associated with antagonist efficacy in genetically selected alcohol-preferring rats. *Biol. Psychiatry* 73, 774–781. doi: 10.1016/j.biopsych.2012.12.027

Smith, R. J., Dean, W., Konfortova, G., and Kelsey, G. (2003). Identification of novel imprinted genes in a genome-wide screen for maternal methylation. *Genome Res.* 13, 558–569. doi: 10.1101/gr.781503

Spence, J. P., Lai, D., Shekhar, A., Carr, L. G., Foroud, T., and Liang, T. (2013). Quantitative trait locus for body weight identified on rat chromosome 4 in inbred alcohol-preferring and -nonpreferring rats: potential implications for neuropeptide Y and corticotrophin releasing hormone 2. *Alcohol* 47, 63–67. doi: 10.1016/j.alcohol.2012.10.005

Spence, J. P., Liang, T., Liu, L., Johnson, P. L., Foroud, T., Carr, L. G., et al. (2009). From QTL to candidate gene: a genetic approach to alcoholism research. *Curr. Drug Abuse Rev.* 2, 127–134. doi: 10.2174/1874473710902020127

Thorsell, A., Slawecki, C. J., Khoury, A., Mathe, A. A., and Ehlers, C. L. (2005). Effect of social isolation on ethanol consumption and substance P/neurokinin expression in Wistar rats. *Alcohol* 36, 91–97. doi: 10.1016/j.alcohol.2005.07.003

Trapnell, C., Williams, B. A., Pertea, G., Mortazavi, A., Kwan, G., van, Baren MJ, et al. (2010). Transcript assembly and quantification by RNA-Seq reveals unannotated transcripts and isoform switching during cell differentiation. *Nat. Biotechnol.* 28, 511–515. doi: 10.1038/nbt.1621

Vanderlinden, L. A., Saba, L. M., Bennett, B., Hoffman, P. L., and Tabakoff, B. (2015). Influence of sex on genetic regulation of "drinking in the dark" alcohol consumption. *Mamm. Genome* 26, 43–56. doi: 10.1007/s00335-014-9553-8

Vendruscolo, L. F., Terenina-Rigaldie, E., Raba, F., Ramos, A., Takahashi, R. N., and Mormede, P. (2006). Evidence for a female-specific effect of a chromosome 4 locus on anxiety-related behaviors and ethanol drinking in rats. *Genes Brain Behav.* 5, 441–450. doi: 10.1111/j.1601-183X.2005.00177.x

Vetter-O'Hagen, C., Varlinskaya, E., and Spear, L. (2009). Sex differences in ethanol intake and sensitivity to aversive effects during adolescence and adulthood. *Alcohol Alcohol.* 44, 547–554. doi: 10.1093/alcalc/agp048

Conflict of Interest Statement: The authors declare that the research was conducted in the absence of any commercial or financial relationships that could be construed as a potential conflict of interest.

frontiers in Genetics

ORIGINAL RESEARCH
published: 04 December 2018
doi: 10.3389/fgene.2018.00602

Ethanol's Effect on *Coq7* Expression in the Hippocampus of Mice

*Diana Zhou[1†], Yinghong Zhao[2†], Michael Hook[1†], Wenyuan Zhao[1], Athena Starlard-Davenport[1], Melloni N. Cook[1,3], Byron C. Jones[1], Kristin M. Hamre[4] and Lu Lu[1]**

[1] Department of Genetics, Genomics and Informatics, The University of Tennessee Health Science Center, Memphis, TN, United States, [2] Department of Neurology, Affiliated Hospital of Nantong University, Nantong, China, [3] Department of Psychology, The University of Memphis, Memphis, TN, United States, [4] Department of Anatomy and Neurobiology, The University of Tennessee Health Science Center, Memphis, TN, United States

Coenzyme Q (CoQ) is a well-studied molecule, present in every cell membrane in the body, best known for its roles as a mitochondrial electron transporter and a potent membrane anti-oxidant. Much of the previous work was done *in vitro* in yeast and more recent work has suggested that CoQ may have additional roles prompting calls for a re-assessment of its role using *in vivo* systems in mammals. Here we investigated the putative role of Coenzyme Q in ethanol-induced effects *in vivo* using BXD RI mice. We examined hippocampal expression of *Coq7* in saline controls and after an acute ethanol treatment, noting enriched biologic processes and pathways following ethanol administration. We also identified 45 ethanol-related phenotypes that were significantly correlated with *Coq7* expression, including six phenotypes related to conditioned taste aversion and ethanol preference. This analysis highlights the need for further investigation of *Coq7* and related genes *in vivo* as well as previously unrecognized roles that it may play in the hippocampus.

Keywords: ethanol, Coenzyme Q, oxidative stress, hippocampus, mouse models, genetics, genomics

OPEN ACCESS

Edited by:
Elizabeth A. Thomas, The Scripps Research Institute, United States

Reviewed by:
Camron D. Bryant, Boston University, United States
Marvin Rafael Diaz, Binghamton University, United States

***Correspondence:**
Lu Lu
lulu@uthsc.edu

† These authors have contributed equally to this work as co-first authors

Specialty section:
This article was submitted to Behavioral and Psychiatric Genetics, a section of the journal Frontiers in Genetics

Received: *04 June 2018*
Accepted: *16 November 2018*
Published: *04 December 2018*

Citation:
Zhou D, Zhao Y, Hook M, Zhao W, Starlard-Davenport A, Cook MN, Jones BC, Hamre KM and Lu L (2018) Ethanol's Effect on Coq7 Expression in the Hippocampus of Mice. Front. Genet. 9:602. doi: 10.3389/fgene.2018.00602

INTRODUCTION

Coenzyme Q (CoQ or ubiquinol) is a lipophilic molecule present in every cell membrane in the body (Crane, 2001; Turunen et al., 2004). It is best known for its roles as a mitochondrial electron transporter and a potent membrane anti-oxidant (Ernster and Dallner, 1995; Bentinger et al., 2007). CoQ is made up of a benzoquinone ring with an isoprenoid side chain (containing 6–10 units) conserved across species from yeast (as CoQ_6), to mice (as CoQ_7), to humans (as CoQ_{10}) (Lenaz, 1985). CoQ production in any species is the result of a complex biosynthesis process involving 10 to 15 or more genes (depending on the species) encoding a series of enzymes and non-enzymatic proteins, many of which belong to the *Coq* family of genes (*Coq 1 – Coq 10A/B*) (Acosta et al., 2016, see their **Table 1** and **Figure 1** for a complete list). Despite this molecule being characterized and isolated nearly 60 years ago (Festenstein et al., 1955; Wolf et al., 1958; Crane et al., 1989), it continues to remain relevant through ongoing investigations that are fine-tuning its roles in bioenergetics and anti-oxidant defense.

Much of the early genetic work regarding CoQ stemmed from submitochondrial fraction studies (Mellors and Tappel, 1966; Landi et al., 1984) and yeast *Saccharomyces cerevisiae* (González-Mariscal et al., 2014), which highlighted CoQ biosynthesis as necessary for mitochondrial antioxidant defense, with less CoQ production resulting in impaired defenses and increased presence of anti-oxidant molecules. But ongoing work has revealed CoQ's role as an anti-oxidant to be more complex than previously thought. *In vitro* studies using CoQ deficient skin fibroblasts

showed severe (<20% of normal) and mild (>60%) CoQ deficiency did not increase reactive oxygen species (ROS) production while moderate deficiency (30–50%) markedly increased ROS production (Quinzii et al., 2008, 2010). Recent *in vivo* studies in CoQ knockout mouse models have been more equivocal, finding that CoQ deficiency does not always directly correspond with ROS production or tissue dysfunction (Quinzii et al., 2013; Licitra and Puccio, 2014; Wang et al., 2015; Luna-Sánchez et al., 2015). This has led some researchers to emphasize the need for better characterization of CoQ's roles *in vivo* using mammalian models vs. studies *in vitro* or using yeast (Wang and Hekimi, 2016).

In the current study, we use a systems genetics approach to examine the relationship between acute ethanol effects and hippocampal *Coq7* expression in a well characterized genetic population of BXD Recombinant Inbred (RI) mice derived from the C57BL/6J (B6) and DBA/2J (D2) inbred strains, furthering our understanding of CoQ biosynthesis regulation *in vivo*. Currently, there is little evidence connecting *Coq7* and regulation of ethanol responses. However, ethanol metabolism into acetaldehyde is a well understood source of oxidative stress in the brain, causing lipid peroxidation and other oxidative damage to brain tissue (Hipolito et al., 2007; Hernández et al., 2016). This metabolic damage is thought to be warded off by increased gene expression of endogenous anti-oxidants, such as superoxide dismutase (Reddy et al., 1999; Enache et al., 2008). *Coq7* (also known as *mclk-1*) encodes a hydroxylase (coq7p) involved in one of the final steps of CoQ synthesis, conversion of demethoxyubiquinone (DMQ) to CoQ (Acosta et al., 2016). This step in biosynthesis is thought to be the regulated step in CoQ biosynthesis (Marbois and Clarke, 1996; Padilla et al., 2009; Martín-Montalvo et al., 2013; Lohman et al., 2014), making it a prime target to explore how endogenous CoQ production changes in response to acute oxidative stress. Additional evidence suggesting that *Coq7* is important in alcohol responses comes from a study in HXB/BXH RI rats where *Coq7* has been proposed as a candidate gene for alcohol dependency and consumption (Tabakoff et al., 2009).

Previous studies from our lab have shown that gene expression in the hippocampus is particularly sensitive to the effects of acute ethanol (1.8 g/kg) (Urquhart et al., 2016; Baker et al., 2017). Others have also shown that acute ethanol (2.0 g/kg) produces brain region-specific changes in gene expression, including in the hippocampus (Kerns et al., 2005). Here, we demonstrate a positive relationship between acute ethanol ingestion and *Coq7* expression in hippocampus. We also map an expression quantitative trait locus (eQTL) for *Coq7* in BXD RI mice as well as identify pathways associated with *Coq7* and its correlated genes. Through this, we aim to better characterize *Coq7* as a vital gene in the oxidative stress response caused by brain ethanol metabolism.

MATERIALS AND METHODS

BXD Strain and Database Description

The BXD RI mouse strains were derived by crossing the parental strains B6 and D2. The F1 progeny were subsequently intercrossed followed by inbreeding to fix parental genotypes at each locus. The BXD mice are a densely phenotyped and genotyped family and have been used as a genetic reference panel for identifying the genetic basis of phenotypes and diseases, including molecular expression phenotypes, as well as for identifying pathways regulating gene expression. For this study, the dataset of Hippocampus Consortium M430v2 (Jun06) RMA that we generated previously (Overall et al., 2009) was used for genetic mapping, transcript measurement of which was taken from the hippocampus of 67 BXD strains, the parental B6 and D2 strains, and reciprocal F1 hybrids (B6D2F1 and D2B6F1). Detailed information on the strain, sex, age of each animal can be accessed from http://genenetwork.org/webqtl/main.py?FormID=sharinginfo&GN_AccessionId=110. This data set has been uploaded into Gene Expression Omnibus (GEO) with accession number GSE84767 where the data can be downloaded.

Ethanol Treatment

The BXD parental strains B6 and D2 mice were used for acute ethanol treatment. Ten mice per strain (2∼3 mice per sex) including both males and females at 2–4 months old were divided into two groups: (1) saline group: given an isovolumetric IP injection of saline and (2) ethanol group: treated with an IP injection of 2.0 g/kg i.p., ethanol (12.5% v/v). The dose of 2.0 g/kg of ethanol was chosen to allow for comparisons with other studies in mice seeking to produce genetically based ethanol-sensitive behaviors (Cunningham and Noble, 1992; Cunningham and Prather, 1992; Cunningham, 1995; Risinger and Cunningham, 1995, 1998). Twenty-four hours after treatment, these mice were sacrificed for tissue harvest (Cook et al., 2015).

Tissue Harvest

The B6 and D2 mice treated with ethanol or saline were anesthetized with an overdose of avertin (1.25% 2,2,2-tribromoethanol and 0.8% tert-pentyl alcohol in water; 0.8–1.0 ml, i.p.) until they were immobile, a period of less than 2 min. After this time mice were sacrificed by cervical dislocation. The hippocampi were harvested according to previously described methods (Lu et al., 2001). The left and right hippocampi were pooled and stored in RNAlater overnight at 4°C, then kept at −80°C until RNA extraction.

RNA Extraction

RNA was extracted from the hippocampus using RNA STAT-60 (protocols can be found at Tel-Test[1]) as per the manufacturer's instructions. A spectrophotometer (Nanodrop Technologies[2]) was used to measure RNA concentration and purity, and the Agilent 2100 Bioanalyzer was used to evaluate RNA integrity. To pass quality control, the RNA integrity values needed to be greater than 8. The majority of samples had values between 8 and 10.

Gene Expression

The Affymetrix GeneChip™ Mouse Transcriptome Array 1.0 (MTA 1.0) was used to generate gene expression data, from

[1]www.tel-test.com

[2]http://www.nanodrop.com

B6 and D2 mice treated with ethanol or saline, according to the manufacturers' protocol. Affymetrix Expression Console Software was used to identify and remove outlier arrays, and normalize raw data in CEL files using the Robust Multichip Array (RMA) method (Pan et al., 2011). The expression data were then re-normalized using a modified *Z* score described in a previous publication (Bolstad et al., 2003). We calculated the log base 2 of the normalized values, computed *Z* scores for each array, multiplied the *Z* scores by 2, and added an offset of 8 units to each value. This transformation yields a set of *Z*-like scores for each array that have a mean of 8, a variance of 4, and standard deviation of 2. The advantage of this modified *Z* score is that a twofold difference in expression corresponds approximately to a 1 unit change.

Quantitative RT-PCR

Total RNA from 10 hippocampi per treatment group (both B6 and D2 mice) was used for a quantitative RT-PCR experiment. The gene-specific probe and primer sets for *Coq7* (upstream 5′-tttggaccatagctgcattg-3′, downstream 5′-tgaggcctcttccatactctg-3′) were deduced using Universal Probe Library Assay Design software[3]. *Coq7* mRNA levels were detected and analyzed on a LightCycler 480 System (Roche, Indianapolis, IN, Unites States[3]) under the following cycling conditions: 1 cycle at 95°C for 5 min and then 40 cycles at 95°C for 10 s, 60°C for 30 s, and 72°C for 10 s. The PCR mix contained 0.2 μl of 10 μM primers, 0.1 μl of 10 μM Universal library probe, 5 μl of LC 480 master mix (2×), 2 μl of template cDNA, and RNase-free water to 10 μl. TATA box-binding protein (TBP) was selected as the endogenous quantity control. The relative gene expression of *Coq7* was analyzed with the ΔΔCT method with TBP used as the reference gene for normalization. *Coq7* expression (fold change) in each ethanol treated mouse relative to average of the corresponding control mice was calculated as: Fold Change = 2^−[ΔCT(*Coq7* in each ethanol treated mouse) - (Mean of ΔCT of control mice)].

Statistical Analysis

The *Coq7* gene expression data from saline or alcohol treatment in B6 and D2 mice were evaluated using the analysis of covariance (ANCOVA) with treatment, strain, and sex as factors, and adjusted for age and body weight.

Phenotype QTL and Expression QTL (eQTL) Mapping and SNP Analysis

We performed phenotype QTL and eQTL analyses using the WebQTL module on GeneNetwork[4] according to our published methods (Chesler et al., 2005). The genome-wide efficient mixed model association algorithm (GEMMA) was used to identify potential eQTLs regulating *Coq7* expression levels and phenotype QTLs near the *Coq7* locus, and to estimate the significance at each location using known genotypic data for those sites. Each of these analyses produced a likelihood ratio statistic (LRS) score, providing us with a quantitative measure of confidence of linkage between the observed phenotypes or expression level of *Coq7* and known genetic markers. The significance of the QTL and eQTLs were calculated using more than 2000 permutations tests. Loci were considered statistically significant if genome-wide $p < 0.05$. Sequence variability between B6 and D2 was then determined using the Sanger mouse SNP database[5].

Gene Function Analysis

Prior to gene function analysis, co-expression and literature correlation were performed to filter a list of transcripts correlated with *Coq7* gene expression in the ethanol and saline groups. Co-expression analysis was performed on GeneNetwork. *Coq7* probe

[3]https://www.roche-applied-science.com

[4]www.genenetwork.org

[5]https://www.sanger.ac.uk/sanger/Mouse_SnpViewer/rel-1303

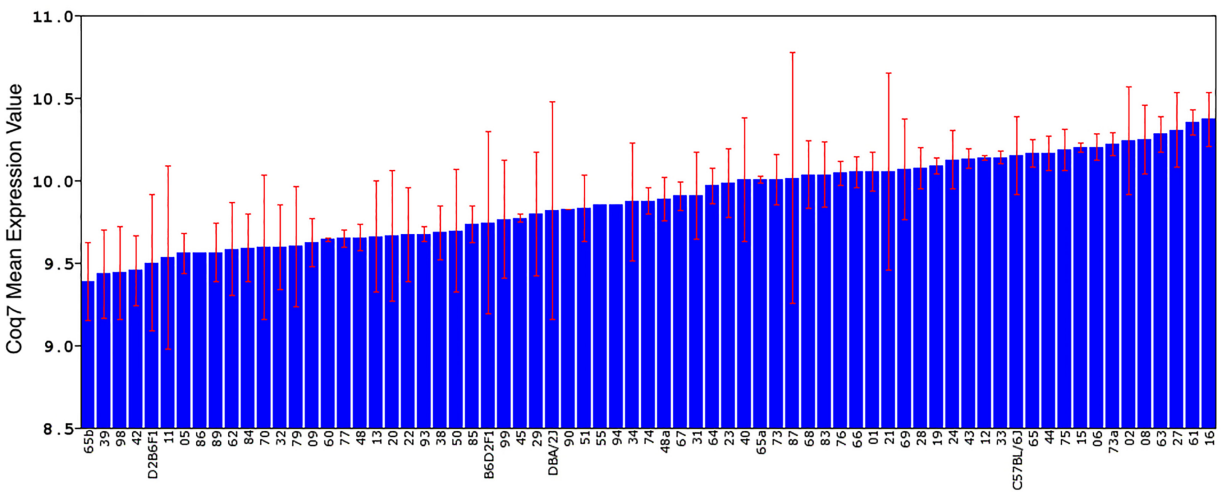

FIGURE 1 | Differential expression of *Coq7* across BXD RI strains rank ordered by expression level. The standard deviation and mean expression of *Coq7* in each strain is shown across the parental DBA/2J and C57BL/6J strains, F1 hybrids, and 67 BXD strains. The *x*-axis represents the mouse strain, while the *y*-axis shows the mean gene expression using the log2 scale.

TABLE 1 | The single nucleotide polymorphisms (SNPs) in the UTR and coding area of *Coq7* gene.

Chr	Position	Gene	dbSNP	B6	D2	function
7	118509846	Coq7	–	T	C	synonymous_variant
7	118509921	Coq7	rs32487665	T	C	synonymous_variant
7	118510146	Coq7	rs32487669	C	T	stop_gained
7	118525104	Coq7	–	C	T	3_prime_utr_variant
7	118525149	Coq7	rs32485072	T	A	3_prime_utr_variant
7	118525163	Coq7	–	T	C	3_prime_utr_variant
7	118525817	Coq7	rs46657874	C	G	splice_region_variant
7	118525833	Coq7	–	G	A	synonymous_variant
7	118525836	Coq7	–	A	G	synonymous_variant
7	118525851	Coq7	rs13472501	A	G	synonymous_variant
7	118529595	Coq7	rs13459101	G	A	synonymous_variant

set expression was compared to all probe sets on the MTA 1.0 array. Criterion for significant co-expression included average $\log_2$ probe set expression greater than 7.0, as well as a significant correlation with *Coq7*, indicated by a Pearson product correlation value ($p < 0.05$). We further filtered *Coq7* co-expressed probe sets in the ethanol and saline groups by performing literature correlations using the Semantic Gene Organizer to find the potential biological correlation between *Coq7* and other genes (Homayouni et al., 2004). Genes with higher correlation values ($r > 0.3$) were selected for further analysis. The top 500 genes with significant co-expression ($p < 0.05$) and literature correlations ($r > 0.45$) for the ethanol and saline data sets were then selected and uploaded to Webgestalt[6] for gene function analyses (Zhang et al., 2005). Enrichment of biological function in the top 500 *Coq7* ethanol and saline co-expression data sets was determined using the hypergeometric test. The *p*-values from the hypergeometric test were automatically adjusted to account for multiple comparisons using the Benjamini and Hochberg correction (Benjamini and Hochberg, 1995). Categories with an adjusted *p*-value of less than 0.05 indicated that the set of submitted genes was significantly over-represented in those categories.

[6]http://bioinfo.vanderbilt.edu/webgestalt/

Phenotype Correlation

We used the BXD phenotype database in our GeneNetwork website[4] to find alcohol phenotypes highly correlated (Pearson product correlation, $p < 0.05$) with expression of the *Coq7* probe set in hippocampus from naïve BXD mice (Hippocampus Consortium M430v2 (Jun06) RMA data set).

RESULTS

Coq7 Expression Variance Across BXD Mice and Heritability

Only one probe set in the Affymetrix M430 dataset represents the *Coq7* gene (1415556_at), which targets the last five coding exons. *Coq7* expression (log2 scale) varied widely between BXD strains, with a fold-change of 2.57 (**Figure 1**). BXD65b had the lowest expression (9.38 ± 0.24), and BXD16 had the highest expression (10.70 ± 0.16). There is also a 1.26-fold difference in *Coq7* transcript abundance between B6 (10.15 ± 0.23) and D2 (9.81 ± 0.66).

eQTL Mapping and Sequence Variants of Coq7

The Affymetrix M430 database was used for eQTL mapping. *Coq7* is located on chromosome 7 at 118.53 Mb, and a significant eQTL modulating the expression of this gene with a likelihood ratio statistics (LRS) of 81 was mapped to the *Coq7* gene locus

TABLE 2 | ANOVA analysis of *Coq7* expression in the hippocampus.

Source	df	Sums of Squares	Mean Square	*F*-ratio	*P*-value
Intercept	1	1123.54	1123.54	3839480	<0.0001
Treatment	1	0.003281	0.003281	11.213	0.0286
Strain	1	0.000225	0.000225	0.7684	0.4302
Treatment*Strain	1	0.001315	0.001315	4.4951	0.1013
Sex	1	0.000281	0.000281	0.9592	0.3828
Treatment*sex	1	0.013775	0.013775	47.073	0.0024
Strain*Sex	1	0.000037	0.000037	0.12496	0.7416
Age	1	0.000455	0.000455	1.5543	0.2805
Treatment*Age	1	0.001535	0.001535	5.2472	0.0838
Strain*Age	1	0.001828	0.001828	6.2477	0.0668
Sex*Age	1	0.001784	0.001784	6.097	0.069
Body Weight (Wt)	1	0.002022	0.002022	6.9113	0.0583
Treatment*BodyWt	1	0.000328	0.000328	1.1205	0.3495
Strain*BodyWt	1	0.000149	0.000149	0.50948	0.5148
Sex*BodyWt	1	0.000631	0.000631	2.1555	0.216
Age*BodyWt	1	0.001043	0.001043	3.5626	0.1321
Error	4	0.001171	0.000293		
Total	19	0.039494			

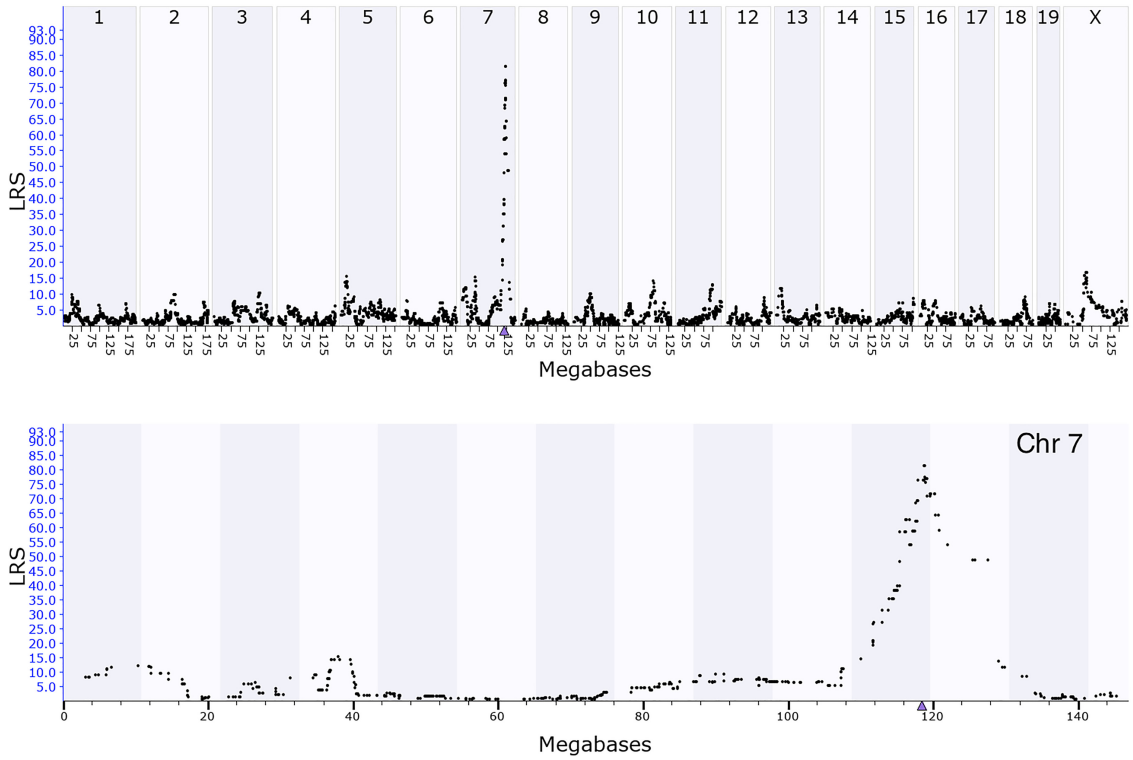

FIGURE 2 | GEMMA eQTL mapping for *Coq7* expression in hippocampus. The *x*-axis represents positions on the mouse genome in megabases (Mb), while the *y*-axis represents the likelihood ratio statistic scores (LRS), a measurement of the linkage between expression of *Coq7* and inheritance of B6 and D2 alleles at different regions of the genome. Top panel shows interval mapping for the whole mouse genome, indicating a significant eQTL at chromosome 7. Bottom panel shows a close-up view of chromosome 7 in which the peak of eQTL was around 119 Mb of chromosome 7 where *Coq7* is located (triangle).

(**Figure 2**). This indicates that *Coq7* is *cis*-regulated, meaning one or more sequence variants affecting its expression is located within or near the gene itself. Using the open access sequence data resources at Sanger[5], we identified 140 SNPs in *Coq7* between the BXD parental strains B6 and D2. Eleven SNPs are located at 3′-UTR and coding area (**Table 1**) including one stop gain variance that could have strong downstream effect. The rest of them are located at non-coding area. All SNPs are listed in **Supplementary Table 1**. In addition, we identified 42 indels in *Coq7* between the BXD parental strains (**Supplementary Table 2**), with two of them being frameshift variants that could also have a strong downstream effect.

Expression Differences of *Coq7* Between Saline and Ethanol Groups

We used the Affymetrix MTA datasets to analyze the effect of alcohol on the expression of *Coq7* in the hippocampal tissue of B6 and D2 mice using an ANOVA with treatment, strain and sex as the between subject factors. The average of *Coq7* expression in the saline group was 7.46 ± 0.01 (log2 scale), while the average for the ethanol group was 7.52 ± 0.01 (log2 scale), indicating an increase in expression after ethanol treatment. ANCOVA analysis showed a significant effect of ethanol treatment on *Coq7* transcript abundance (P = 0.029) and also interaction of ethanol treatment and sex significantly effects on *Coq7* transcript abundance (P = 0.002) (**Table 2**). For B6 strain, the average of Coq7 expression in the ethanol group was 7.53 ± 0.04 (log2 scale), while the average for the saline group was 7.46 ± 0.03 (log2 scale). For D2 strain, the average of Coq7 expression in the ethanol group was 7.51 ± 0.05 (log2 scale), while the average for the saline group was 7.47 ± 0.03 (log2 scale). The T-test analysis showed a significant effect of ethanol treatment on *Coq7* transcript abundance in the B6 strain (P = 0.0234), not in the D2 strain (P = 0.2454).

qRT-PCR Validation

Coq7 expression was validated using RT-PCR. The RT-PCR results showed significantly increased expression of *Coq7* (F = 11.77, P = 0.027) after ethanol treatment. This was consistent with the results from microarray analysis. In addition, we also found significant strain differences between B6 and D2 (F = 9.326, P = 0.038), and sex difference between males and females (F = 11.788, P = 0.027).

Gene Ontology Analysis

We used the top 500 transcripts co-expressed with *Coq7* from both saline and ethanol group to perform gene ontology (GO) analysis. For the saline-treated group, significant biological processes included "ATP metabolic process," "mitochondrion organization," "electron transport chain," and "ubiquinone

TABLE 3 | Significant pathways for the Saline group.

Pathway name	# of genes	raw *P*-value	adj *P*-value
Electron Transport Chain	24	1.29E-19	6.97E-18
TCA Cycle	13	1.61E-14	4.35E-13
Amino Acid metabolism	19	8.53E-13	1.54E-11
Oxidative phosphorylation	13	9.11E-11	1.23E-09
Glycolysis and Gluconeogenesis	12	1.22E-10	1.32E-09
Kennedy pathway	6	1.58E-07	1.42E-06
Fatty Acid Biosynthesis	6	1.94E-05	0.0001
One carbon metabolism and related pathways	6	0.0004	0.0027
PPAR signaling pathway	8	0.0005	0.003
Nucleotide Metabolism	4	0.0006	0.0032
One Carbon Metabolism	5	0.001	0.0042
Folic Acid Network	4	0.0009	0.0042
Proteasome Degradation	6	0.0011	0.0042
selenium	4	0.001	0.0042
Glutathione and one carbon metabolism	4	0.0045	0.0159
mRNA processing	18	0.0047	0.0159
Acetylcholine Synthesis	2	0.0078	0.0248
Urea cycle and metabolism of amino groups	3	0.0091	0.0273
Triacylglyceride Synthesis	3	0.0103	0.0293
Glutathione metabolism	3	0.0116	0.0313

biosynthetic process" (**Supplementary Table 3**). For the ethanol treated group, 54 enriched GO biological processes categories reached significance (**Supplementary Table 4**). Many of the categories in the ethanol group overlapped with those in the saline group, but all of the ATP metabolic and mitochondrial function related categories were no longer significant. Instead, several new enriched categories including serine metabolic process, behavior and cognition show up.

Gene pathway enrichment analysis for the saline-treated group revealed 21 related pathways (adj $P < 0.05$, **Table 3**), while the ethanol-treated group revealed six related pathways (adj $P < 0.05$, **Table 4**). The top enriched pathway in the saline group including "Electron Transport Chain" and "Oxidative phosphorylation" are not shared with the ethanol group. A pathway of interest unique to the ethanol group is "Oxidative stress."

Phenotype Correlation Analysis

We performed correlational analyses with phenotypes archived in the GeneNetwork database to identify ethanol-related behaviors correlated with *Coq7* ($p < 0.05$) expression in the hippocampus. We found 45 ethanol-related phenotypes significantly correlated with *Coq7* expression (**Supplementary Table 5**), most of which are related to ethanol consumption, ethanol response, ethanol preference, and body temperature after ethanol treatment; some of which are mapped near *Coq7* location. For example, one phenotype (record ID 10496, ethanol response) has a significant QTL with a LRS of 13.8 ($P < 0.05$) on chromosome 7 at 114∼119 Mb (**Figure 3**) where *Coq7* is located.

DISCUSSION

Currently, mechanisms through which ethanol affects *Coq7* and ubiquinone are unknown and previous studies analyzing *Coq7* and ethanol are lacking. To this end, we attempted to elucidate the relationship between ethanol and expression of *Coq7* in the hippocampus of BXD mice by identifying genes and biological pathways that may link the two. *Coq7* is variably expressed in naïve hippocampal tissue from BXD RI strains and is *cis*-regulated, making it an excellent candidate

TABLE 4 | Significant pathways for the Ethanol group.

Pathway name	# of genes	raw *P*-value	adj *P*-value
One carbon metabolism and related pathways	7	4.62E-05	0.0027
mRNA processing	20	0.0008	0.0155
Cytoplasmic Ribosomal Proteins	7	0.0008	0.0155
Oxidative Stress	4	0.0021	0.0305
Glutathione and one carbon metabolism	4	0.0043	0.0416
Myometrial Relaxation and Contraction Pathways	9	0.0042	0.0416

for study as a modifier of gene expression or biological phenotypes (Ciobanu et al., 2010). We found that there are multiple SNPs and Indels in *Coq7*, which may be responsible for its differential expression in the hippocampal tissues across BXD strains. This also suggests that one or more polymorphism may affect *Coq7* expression and play a role in gene regulation (Kunugi et al., 2001; Jablonski et al., 2005). Furthermore, we found increased expression of *Coq7* following acute ethanol injection and identified 45 ethanol-related phenotypes correlated with *Coq7*, supporting its likely involvement in ethanol responses (**Supplementary Table 5**). These findings included six phenotypes related to conditioned taste aversion and ethanol preference. It has been previously proposed that *Coq7* may play a role in alcohol consumption (Tabakoff et al., 2009), aligning with the result of our phenotypic analysis. While this phenotypic alignment is interesting, it should be noted that our experiment did not directly test ethanol consumption behaviors before and after ethanol injection, limiting how generalizable this result may be. Future direct observation of changes in ethanol preferences following ethanol injection or a period of oral consumption would likely be worthwhile.

Comparison of functional enrichment analysis results between our treatment groups may hold insight into why *Coq7* was upregulated following ethanol injection. In the saline treatment group, we found processes related to cellular metabolism and ATP generation (**Supplementary Table 3**). Presumably, when proteins needed to break down energy substrates are expressed, *Coq7* is also expressed. This is unsurprising considering CoQ's role in the electron transport chain as an electron shuttle, representing a lynchpin of the final step of ATP generation following metabolism. Conversely, these metabolic functions were largely insignificant in the ethanol treatment group's analysis, suggesting a less prominent role. This may well be representative of ethanol's effect on the mitochondria, which has been shown to decrease respiratory rates and the rate of ATP synthesis following chronic exposure (Thayer and Rubin, 1979; Manzo-Avalos and Saavedra-Molina, 2010). This notion was further corroborated by pathway enrichment analysis, which found pathways such "Electron Transport Chain," "TCA cycle," "Amino Acid Cycle," "Oxidative phosphorylation," and "Glycolysis and Gluconeogenesis" associated with the saline treated group (**Table 3**), but not the ethanol treatment group.

The ethanol group uniquely had "Oxidative Stress" as a significantly enriched gene pathway (**Table 4**). Notably, three of the four genes in this gene pathway encode proteins contributing to anti-oxidant enzymes: *Sod2* (superoxide dismutase, Azadmanesh and Borgstahl, 2018), *Gclc* (glutamate-cysteine ligase, a catalyst for glutathione synthesis; Lu, 2009, 2013), and *Txnrd1* (thioredoxin reductase 1; Turanov et al., 2010). While all three are well-established anti-oxidants, previous work on their interactions with ethanol vary greatly. Superoxide dismutase (SOD) is perhaps best studied but also the most controversial. SOD activity in the murine brain following ethanol exposure has been shown to increase (Somani et al., 1996; Enache et al., 2008; Reis et al., 2017), remain unchanged (Gönenç et al., 2005) and decrease (Ledig et al., 1981) under various conditions. The other two genes are less well characterized. *Gclc* mRNA expression shown to be induced by ethanol in rat liver and brain (Lu et al., 1999; Narasimhan et al., 2011) and *Txnrd1* has not been as well studied in terms of ethanol-induced stress.

However, a recent paper by Casañas-Sánchez et al. (2016) found all three of these genes, as well as many other anti-oxidant genes, to have increased expression in hippocampal derived HT22 cells following acute, sub-toxic ethanol exposure. To explain its result, this paper emphasized the growing understanding of ROS as second messengers, capable of influencing gene expression (D'Autréaux and Toledano, 2007; Kaspar et al., 2009; Schieber and Chandel, 2014). These findings have been pioneered in the growing field of "redox biology," which heavily emphasizes a more nuanced understanding of the impact of ROS. Current work suggests that varying levels of ROS production (so called "basal," "low," "intermediate," and "high" oxidative stress) cause different cellular reactions (Lushchak, 2014; Sies, 2015). Casañas-Sánchez et al. (2016) reasoned that low levels of ethanol increased the level of oxidative stress, as ethanol

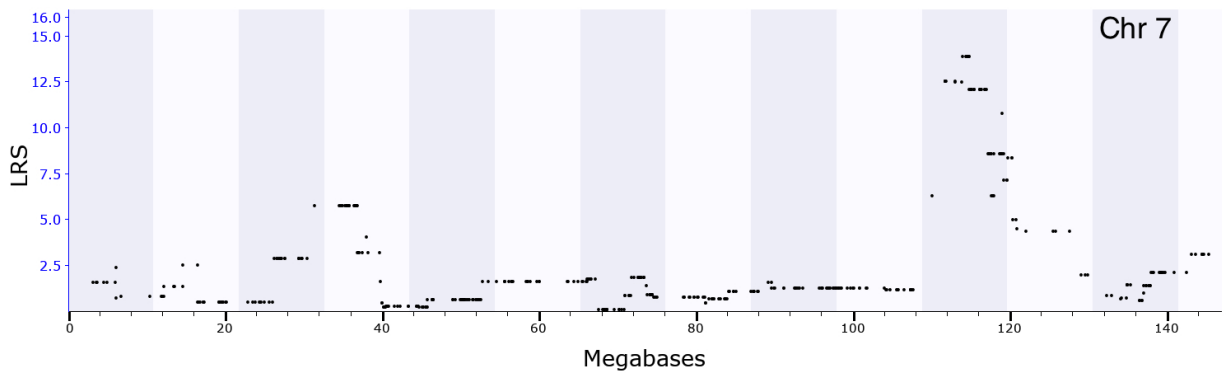

FIGURE 3 | GEMMA QTL mapping for locomotion behavior after ethanol injection (2 g/kg). The *x*-axis represents a position on the mouse genome in megabases (Mb), while the y-axis gives the likelihood ratio statistic scores (LRS). The mapping result showed that the peak of QTL was around 114∼119 Mb of chromosome 7.

is a well-documented potent producer of ROS by virtue of its metabolism (Lieber, 1976; Zakhari, 2006; Das and Vasudevan, 2007), resulting in beneficial mitohormetic anti-oxidant gene expression.

This phenomenon may similarly be occurring in our study, as evidenced by the induction of *Coq7* and the phenotypic shift to oxidative stress protection in the ethanol treatment group. It may be that CoQ is unimportant as an anti-oxidant under basal or low-level oxidative stress, as seen in CoQ knockout mouse studies, but is induced under heightened oxidative stress levels alongside other well-known anti-oxidants. The variation of *Coq7* expression in BXD RI mice could result in variation in this inducible response, accounting for differences in how individual strains of BXDs react to ethanol ingestion. Tabakoff et al. (2009) argue that several of their identified "alcohol consumption genes" could theoretically modulate GABA release from the hypothalamus to areas like the ventral tegmental area, ultimately affecting downstream reward behaviors through a variety of molecular mechanisms (see their **Figure 3**). Logically, the variation in genetic expression among individuals or under different conditions may end up modulating behavior. While Tabakoff mentions *Coq7* as an identified "ethanol consumption gene," they do not outline how it might affect GABA release in this way. With the idea of ROS as signaling molecules in mind, variation in *Coq7* expression (or other anti-oxidant defenses) could limit or permit ROS signaling, potentially altering critical neurologic signaling pathways related to reward-seeking behavior, similar to those proposed by Tabakoff et al. (2009). How these alterations would occur is still a matter of investigation. Work has examined some of the intracellular mechanisms by which ROS can affect plasticity and signaling in the hippocampus, mainly through induction of long-term potentiation (LTP). This induction seems to be through ROS acting as a second messenger, inducing phosphorylation of established LTP effectors such as PKC, ERK, and CamKII (Malinow et al., 1989; Klann et al., 1998; Kishida et al., 2005). For recent reviews on the topic, please see Beckhauser et al. (2016) and Oswald et al. (2018). However, there has been little investigation into ROS's effect on motivational circuitry. While further work is needed, ethanol-induced oxidative stress may represent a worthwhile line of inquiry to better understand hippopcampal cellular responses to heightened oxidative stress *in vivo* and their downstream effects on neurotransmission and behavior.

In sum, we analyzed the effect of ethanol on the expression of *Coq7* using a systems genetic approach. We identified an eQTL showing variability in *Coq7* expression in BXD RI mice and found its expression to be increased following ethanol treatment. We also uncovered several pathways and genes which may interact with *Coq7* to regulate the ethanol response. Based on this and previous reports, *Coq7* may act as an inducible anti-oxidant at heightened levels of oxidative stress, aligning both with previous work and current questions on this ubiquitous molecule. Further research into the specific interactions between *Coq7* and identified genes may elucidate their relationships and shed light on how *Coq7* affects mitochondria following acute ethanol consumption.

ETHICS STATEMENT

All animal work was conducted in accordance with of and procedures approved by the Institutional Animal Care and Use Committees at The University of Tennessee Health Science Center and University of Memphis following NIH guidelines.

AUTHOR CONTRIBUTIONS

DZ provided the primary analysis and primary writing for the manuscript. YZ provided the primary interpretation of experiment and primary writing for the manuscript. MH provided the primary writing, editing, literature review, and for the manuscript and data interpretation of experiment. WZ provided the analysis and RT-PCR experiment. AS-D, MC, AD, and BJ provided the final editing and critique of manuscript. KH provided the primary experiment, final editing and critique of the manuscript. LL provided the procedure, planning, funding, and oversight for experiment as well as final editing and critique of manuscript.

FUNDING

This study was supported by National Institutes of Health grants R01AA021951 (LL, BJ) and U01AA014425 (LL), and Internal New Grant Support Funding (E073239005) from the University of Tennessee Health Science Center (LL).

ACKNOWLEDGMENTS

The authors thank Dr. Robert Williams for his financial support, bioinformatics support, and experiment design.

SUPPLEMENTARY MATERIAL

The Supplementary Material for this article can be found online at: https://www.frontiersin.org/articles/10.3389/fgene.2018.00602/full#supplementary-material

REFERENCES

Acosta, M. J., Fonseca, L. V., Desbats, M. A., Cerqua, C., Zordan, R., Trevisson, E., et al. (2016). Coenzyme Q biosynthesis in health and disease. *Biochim. Biophys. Acta* 1857, 1079–1085. doi: 10.1016/j.bbabio.2016.03.036

Azadmanesh, J., and Borgstahl, G. E. (2018). A review of the catalytic mechanism of human manganese superoxide dismutase. *Antioxidants* 7:E25. doi: 10.3390/antiox7020025

Baker, J. A., Li, J., Zhou, D., Yang, M., Cook, M. N., Jones, B. C., et al. (2017). Analyses of differentially expressed genes after exposure to acute stress, acute

ethanol, or a combination of both in mice. *Alcohol* 58, 139–151. doi: 10.1016/j.alcohol.2016.08.008

Beckhauser, T. F., Francis-Oliveira, J., and De Pasquale, R. (2016). Reactive oxygen species: physiological and physiopathological effects on synaptic plasticity: supplementary issue: brain plasticity and repair. *J. Exp. Neurosc.* 10(Suppl. 1), 23–48. doi: 10.4137/JEN.S39887

Benjamini, Y., and Hochberg, Y. (1995). Controlling the false discovery rate: a practical and powerful approach to multiple testing. *J. R. Stat. Soc. Ser. B* 57, 289–300.

Bentinger, M., Brismar, K., and Dallner, G. (2007). The antioxidant role of coenzyme Q. *Mitochondrion* 7, S41–S50. doi: 10.1016/j.mito.2007.02.006

Bolstad, B. M., Irizarry, R. A., Åstrand, M., and Speed, T. P. (2003). A comparison of normalization methods for high density oligonucleotide array data based on variance and bias. *Bioinformatics* 19, 185–193. doi: 10.1093/bioinformatics/19.2.185

Casañas-Sánchez, V., Pérez, J. A., Quinto-Alemany, D., and Díaz, M. (2016). Sub-toxic ethanol exposure modulates gene expression and enzyme activity of antioxidant systems to provide neuroprotection in hippocampal HT22 cells. *Front. Physiol.* 7:312. doi: 10.3389/fphys.2016.00312

Chesler, E. J., Lu, L., Shou, S., Qu, Y., Gu, J., Wang, J., et al. (2005). Complex trait analysis of gene expression uncovers polygenic and pleiotropic networks that modulate nervous system function. *Nat. Genet.* 37, 233–242. doi: 10.1038/ng1518

Ciobanu, D. C., Lu, L., Mozhui, K., Wang, X., Jagalur, M., Morris, J. A., et al. (2010). Detection, validation, and downstream analysis of allelic variation in gene expression. *Genetics* 184, 119–128. doi: 10.1534/genetics.109.107474

Cook, M. N., Baker, J. A., Heldt, S. A., Williams, R. W., Hamre, K. M., and Lu, L. (2015). Identification of candidate genes that underlie the QTL on chromosome 1 that mediates genetic differences in stress-ethanol interactions. *Physiol. Genom.* 47, 308–317. doi: 10.1152/physiolgenomics.00114.2014

Crane, F., Hatefi, Y., Lester, R., and Widmer, C. (1989). Isolation of a quinone from beef heart mitochondria. 1957. *Biochim. Biophys. Acta* 1000, 362–363.

Crane, F. L. (2001). Biochemical functions of coenzyme Q10. *J. Am. Coll. Nutr.* 20, 591–598. doi: 10.1080/07315724.2001.10719063

Cunningham, C. L. (1995). Localization of genes influencing ethanol-induced conditioned place preference and locomotor activity in BXD recombinant inbred mice. *Psychopharmacology* 120, 28–41. doi: 10.1007/BF02246142

Cunningham, C. L., and Noble, D. (1992). Conditioned activation induced by ethanol: role in sensitization and conditioned place preference. *Pharmacol. Biochem. Behav.* 43, 307–313. doi: 10.1016/0091-3057(92)90673-4

Cunningham, C. L., and Prather, L. K. (1992). Conditioning trial duration affects ethanol-induced conditioned place preference in mice. *Anim. Learn. Behav.* 20, 187–194. doi: 10.3758/BF03200416

Das, S. K., and Vasudevan, D. (2007). Alcohol-induced oxidative stress. *Life Sci.* 81, 177–187. doi: 10.1016/j.lfs.2007.05.005

D'Autréaux, B., and Toledano, M. B. (2007). ROS as signalling molecules: mechanisms that generate specificity in ROS homeostasis. *Nat. Rev. Mol. Cell Biol.* 8, 813–824. doi: 10.1038/nrm2256

Enache, M., Van Waes, V., Vinner, E., Lhermitte, M., Maccari, S., and Darnaudéry, M. (2008). Impact of an acute exposure to ethanol on the oxidative stress status in the hippocampus of prenatal restraint stress adolescent male rats. *Brain Res.* 1191, 55–62. doi: 10.1016/j.brainres.2007.11.031

Ernster, L., and Dallner, G. (1995). Biochemical, physiological and medical aspects of ubiquinone function. *Biochim. Biophys. Acta* 1271, 195–204. doi: 10.1016/0925-4439(95)00028-3

Festenstein, G., Heaton, F., Lowe, J., and Morton, R. (1955). A constituent of the unsaponifiable portion of animal tissue lipids (λmax. mμ.). *Biochem. J.* 59, 558–566. doi: 10.1042/bj0590558

Gönenç, S., Uysal, N., Açikgöz, O., and Kayatekin, B. (2005). Effects of melatonin on oxidative stress and spatial memory impairment induced by acute ethanol treatment in rats. *Physiol. Res.* 54, 341–348.

González-Mariscal, I., García-Testón, E., Padilla, S., Martín-Montalvo, A., Viciana, T. P., Vazquez-Fonseca, L., et al. (2014). The regulation of coenzyme q biosynthesis in eukaryotic cells: all that yeast can tell us. *Mol. Syndromol.* 5, 107–118. doi: 10.1159/000362897

Hernández, J. A., López-Sánchez, R. C., and Rendón-Ramírez, A. (2016). Lipids and oxidative stress associated with ethanol-induced neurological damage. *Oxid. Med. Cell. Longev.* 2016:1543809. doi: 10.1155/2016/1543809

Hipolito, L., Sanchez, M., Polache, A., and Granero, L. (2007). Brain metabolism of ethanol and alcoholism: an update. *Curr. Drug Metab.* 8, 716–727. doi: 10.2174/138920007782109797

Homayouni, R., Heinrich, K., Wei, L., and Berry, M. W. (2004). Gene clustering by latent semantic indexing of MEDLINE abstracts. *Bioinformatics* 21, 104–115. doi: 10.1093/bioinformatics/bth464

Jablonski, M. M., Dalke, C., Wang, X., Lu, L., Manly, K. F., Pretsch, W., et al. (2005). An ENU-induced mutation in Rs1h causes disruption of retinal structure and function. *Mol. Vis.* 11, 569–581.

Kaspar, J. W., Niture, S. K., and Jaiswal, A. K. (2009). Nrf2: INrf2 (Keap1) signaling in oxidative stress. *Free Radic. Biol. Med.* 47, 1304–1309. doi: 10.1016/j.freeradbiomed.2009.07.035

Kerns, R. T., Ravindranathan, A., Hassan, S., Cage, M. P., York, T., Sikela, J. M., et al. (2005). Ethanol-responsive brain region expression networks: implications for behavioral responses to acute ethanol in DBA/2J versus C57BL/6J mice. *J. Neurosci.* 25, 2255–2266. doi: 10.1523/JNEUROSCI.4372-04.2005

Kishida, K. T., Pao, M., Holland, S. M., and Klann, E. (2005). NADPH oxidase is required for NMDA receptor-dependent activation of ERK in hippocampal area CA1. *J. Neurochem.* 94, 299–306. doi: 10.1111/j.1471-4159.2005.03189.x

Klann, E., Roberson, E. D., Knapp, L. T., and Sweatt, J. D. (1998). A role for superoxide in protein kinase C activation and induction of long-term potentiation. *J. Biol. Chem.* 273, 4516–4522. doi: 10.1074/jbc.273.8.4516

Kunugi, H., Ishida, S., Akahane, A., and Nanko, S. (2001). Exon/intron boundaries, novel polymorphisms, and association analysis with schizophrenia of the human synaptic vesicle monoamine transporter (SVMT) gene. *Mol. Psychiatry* 6, 456–460. doi: 10.1038/sj.mp.4000895

Landi, L., Cabrini, L., Sechi, A. M., and Pasquali, P. (1984). Antioxidative effect of ubiquinones on mitochondrial membranes. *Biochem. J.* 222, 463–466. doi: 10.1042/bj2220463

Ledig, M., M'Paria, J.-R., and Mandel, P. (1981). Superoxide dismutase activity in rat brain during acute and chronic alcohol intoxication. *Neurochem. Res.* 6, 385–390. doi: 10.1007/BF00963853

Lenaz, G. (1985). *Coenzyme Q: Biochemistry, Bioenergetics, and Clinical Applications of Ubiquinone*. Hoboken, NJ: John Wiley & Sons Incorporated.

Licitra, F., and Puccio, H. (2014). An overview of current mouse models recapitulating coenzyme q10 deficiency syndrome. *Mol. Syndromol.* 5, 180–186. doi: 10.1159/000362942

Lieber, C. S. (1976). The metabolism of alcohol. *Sci. Am.* 234, 25–33. doi: 10.1038/scientificamerican0376-25

Lohman, D. C., Forouhar, F., Beebe, E. T., Stefely, M. S., Minogue, C. E., Ulbrich, A., et al. (2014). Mitochondrial COQ9 is a lipid-binding protein that associates with COQ7 to enable coenzyme Q biosynthesis. *Proc. Natl. Acad. Sci. U.S.A.* 111, E4697–E4705. doi: 10.1073/pnas.1413128111

Lu, L., Airey, D. C., and Williams, R. W. (2001). Complex trait analysis of the hippocampus: mapping and biometric analysis of two novel gene loci with specific effects on hippocampal structure in mice. *J. Neurosci.* 21, 3503–3514. doi: 10.1523/JNEUROSCI.21-10-03503.2001

Lu, S. C. (2009). Regulation of glutathione synthesis. *Mol. Aspects Med.* 30, 42–59. doi: 10.1016/j.mam.2008.05.005

Lu, S. C. (2013). Glutathione synthesis. *Biochim. Biophys. Acta* 1830, 3143–3153. doi: 10.1016/j.bbagen.2012.09.008

Lu, S. C., Huang, Z. Z., Yang, J. M., and Tsukamoto, H. (1999). Effect of ethanol and high-fat feeding on hepatic γ-glutamylcysteine synthetase subunit expression in the rat. *Hepatology* 30, 209–214. doi: 10.1002/hep.510300134

Luna-Sánchez, M., Díaz-Casado, E., Barca, E., Tejada, M. Á., Montilla-García, Á., Cobos, E. J., et al. (2015). The clinical heterogeneity of coenzyme Q10 deficiency results from genotypic differences in the Coq9 gene. *EMBO Mol. Med.* 7, 670–687. doi: 10.15252/emmm.201404632

Lushchak, V. I. (2014). Free radicals, reactive oxygen species, oxidative stress and its classification. *Chem. Biol. Interact.* 224, 164–175. doi: 10.1016/j.cbi.2014.10.016

Malinow, R., Schulman, H., and Tsien, R. W. (1989). Inhibition of postsynaptic PKC or CaMKII blocks induction but not expression of LTP. *Science* 245, 862–866. doi: 10.1126/science.2549638

Manzo-Avalos, S., and Saavedra-Molina, A. (2010). Cellular and mitochondrial effects of alcohol consumption. *Int. J. Environ. Res. Public Health* 7, 4281–4304. doi: 10.3390/ijerph7124281

Marbois, B. N., and Clarke, C. F. (1996). The COQ7 gene encodes a protein in Saccharomyces cerevisiae necessary for ubiquinone biosynthesis. *J. Biol. Chem.* 271, 2995–3004. doi: 10.1074/jbc.271.6.2995

Martín-Montalvo, A., González-Mariscal, I., Pomares-Viciana, T., Padilla-López, S., Ballesteros, M., Vazquez-Fonseca, L., et al. (2013). The phosphatase Ptc7 induces coenzyme Q biosynthesis by activating the hydroxylase Coq7 in yeast. *J. Biol. Chem.* 288, 28126–28137. doi: 10.1074/jbc.M113.474494

Mellors, A., and Tappel, A. L. (1966). The inhibition of mitochondrial peroxidation by ubiquinone and ubiquinol. *J. Biol. Chem.* 241, 4353–4356.

Narasimhan, M., Mahimainathan, L., Rathinam, M. L., Riar, A. K., and Henderson, G. I. (2011). Overexpression of Nrf2 protects cerebral cortical neurons from ethanol-induced apoptotic death. *Mol. Pharmacol.* 80, 988–999. doi: 10.1124/mol.111.073262

Oswald, M. C., Garnham, N., Sweeney, S. T., and Landgraf, M. (2018). Regulation of neuronal development and function by ROS. *FEBS Lett.* 592, 679–691. doi: 10.1002/1873-3468.12972

Overall, R. W., Kempermann, G., Peirce, J., Lu, L., Goldowitz, D., Gage, F. H., et al. (2009). Genetics of the hippocampal transcriptome in mouse: a systematic survey and online neurogenomics resource. *Front. Neurosci.* 3:55. doi: 10.3389/neuro.15.003.2009

Padilla, S., Tran, U., Jimenez-Hidalgo, M., Lopez-Martin, J., Martin-Montalvo, A., Clarke, C., et al. (2009). Hydroxylation of demethoxy-Q6 constitutes a control point in yeast coenzyme Q6 biosynthesis. *Cell. Mol. Life Sci.* 66, 173–186. doi: 10.1007/s00018-008-8547-7

Pan, Y., Balazs, L., Tigyi, G., and Yue, J. (2011). Conditional deletion of Dicer in vascular smooth muscle cells leads to the developmental delay and embryonic mortality. *Biochem. Biophys. Res. Commun.* 408, 369–374. doi: 10.1016/j.bbrc.2011.02.119

Quinzii, C. M., Garone, C., Emmanuele, V., Tadesse, S., Krishna, S., Dorado, B., et al. (2013). Tissue-specific oxidative stress and loss of mitochondria in CoQ-deficient Pdss2 mutant mice. *FASEB J.* 27, 612–621. doi: 10.1096/fj.12-209361

Quinzii, C. M., López, L. C., Gilkerson, R. W., Dorado, B., Coku, J., Naini, A. B., et al. (2010). Reactive oxygen species, oxidative stress, and cell death correlate with level of CoQ10 deficiency. *FASEB J.* 24, 3733–3743. doi: 10.1096/fj.09-152728

Quinzii, C. M., López, L. C., Von-Moltke, J., Naini, A., Krishna, S., Schuelke, M., et al. (2008). Respiratory chain dysfunction and oxidative stress correlate with severity of primary CoQ10 deficiency. *FASEB J.* 22, 1874–1885. doi: 10.1096/fj.07-100149

Reddy, S., Husain, K., Schlorff, E., Scott, R., and Somani, S. (1999). Dose response of ethanol ingestion on antioxidant defense system in rat brain subcellular fractions. *Neurotoxicology* 20, 977–987.

Reis, R., Charehsaz, M., Sipahi, H., Ekici, A. I. D., Macit, Ç, Akkaya, H., et al. (2017). Energy drink induced lipid peroxidation and oxidative damage in rat liver and brain when used alone or combined with alcohol. *J. Food Sci.* 82, 1037–1043. doi: 10.1111/1750-3841.13662

Risinger, F. O., and Cunningham, C. L. (1995). Genetic differences in ethanol-induced conditioned taste aversion after ethanol preexposure. *Alcohol* 12, 535–539. doi: 10.1016/0741-8329(95)00040-2

Risinger, F. O., and Cunningham, C. L. (1998). Ethanol-induced conditioned taste aversion in BXD recombinant inbred mice. *Alcoholism* 22, 1234–1244. doi: 10.1111/j.1530-0277.1998.tb03904.x

Schieber, M., and Chandel, N. S. (2014). ROS function in redox signaling and oxidative stress. *Curr. Biol.* 24, R453–R462. doi: 10.1016/j.cub.2014.03.034

Sies, H. (2015). Oxidative stress: a concept in redox biology and medicine. *Redox Biol.* 4, 180–183. doi: 10.1016/j.redox.2015.01.002

Somani, S., Husain, K., Diaz-Phillips, L., Lanzotti, D., Kareti, K., and Trammell, G. (1996). Interaction of exercise and ethanol on antioxidant enzymes in brain regions of the rat. *Alcohol* 13, 603–610. doi: 10.1016/S0741-8329(96)00075-4

Tabakoff, B., Saba, L., Printz, M., Flodman, P., Hodgkinson, C., Goldman, D., et al. (2009). Genetical genomic determinants of alcohol consumption in rats and humans. *BMC Biol.* 7:70. doi: 10.1186/1741-7007-7-70

Thayer, W. S., and Rubin, E. (1979). Effects of chronic ethanol intoxication on oxidative phosphorylation in rat liver submitochondrial particles. *J. Biol. Chem.* 254, 7717–7723.

Turanov, A. A., Kehr, S., Marino, S. M., Yoo, M.-H., Carlson, B. A., Hatfield, D. L., et al. (2010). Mammalian thioredoxin reductase 1: roles in redox homoeostasis and characterization of cellular targets. *Biochem. J.* 430, 285–293. doi: 10.1042/BJ20091378

Turunen, M., Olsson, J., and Dallner, G. (2004). Metabolism and function of coenzyme Q. *Biochim. Biophys. Acta* 1660, 171–199. doi: 10.1016/j.bbamem.2003.11.012

Urquhart, K. R., Zhao, Y., Baker, J. A., Lu, Y., Yan, L., Cook, M. N., et al. (2016). A novel heat shock protein alpha 8 (Hspa8) molecular network mediating responses to stress-and ethanol-related behaviors. *Neurogenetics* 17, 91–105. doi: 10.1007/s10048-015-0470-0

Wang, Y., and Hekimi, S. (2016). Understanding ubiquinone. *Trends Cell Biol.* 26, 367–378. doi: 10.1016/j.tcb.2015.12.007

Wang, Y., Oxer, D., and Hekimi, S. (2015). Mitochondrial function and lifespan of mice with controlled ubiquinone biosynthesis. *Nat. Commun.* 6:6393. doi: 10.1038/ncomms7393

Wolf, D. E., Hoffman, C. H., Trenner, N. R., Arison, B. H., Shunk, C. H., Linn, B. O., et al. (1958). Coenzyme QI Structure studies on the coenzyme Q group. *J. Am. Chem. Soc.* 80:4752.

Zakhari, S. (2006). Overview: How is alcohol metabolized by the body? *Alcohol Res. Health* 29, 245–255.

Zhang, B., Kirov, S., and Snoddy, J. (2005). WebGestalt: an integrated system for exploring gene sets in various biological contexts. *Nucleic Acids Res.* 33(Suppl. 2), W741–W748. doi: 10.1093/nar/gki475

Conflict of Interest Statement: The authors declare that the research was conducted in the absence of any commercial or financial relationships that could be construed as a potential conflict of interest.

frontiers in Genetics

REVIEW
published: 09 January 2019
doi: 10.3389/fgene.2018.00695

Crosstalk of Genetic Variants, Allele-Specific DNA Methylation, and Environmental Factors for Complex Disease Risk

Huishan Wang[1,2], *Dan Lou*[1] *and Zhibin Wang*[1,3]*

[1] *Laboratory of Human Environmental Epigenome, Department of Environmental Health and Engineering, Bloomberg School of Public Health, Johns Hopkins University, Baltimore, MD, United States,* [2] *Li Ka Shing Faculty of Medicine, The University of Hong Kong, Pokfulam, Hong Kong,* [3] *State Key Laboratory of Biocatalysis and Enzyme Engineering, School of Life Sciences, Hubei University, Wuhan, China*

Over the past decades, genome-wide association studies (GWAS) have identified thousands of phenotype-associated DNA sequence variants for potential explanations of inter-individual phenotypic differences and disease susceptibility. However, it remains a challenge for translating the associations into causative mechanisms for complex diseases, partially due to the involved variants in the noncoding regions and the inconvenience of functional studies in human population samples. So far, accumulating evidence has suggested a complex crosstalk among genetic variants, allele-specific binding of transcription factors (ABTF), and allele-specific DNA methylation patterns (ASM), as well as environmental factors for disease risk. This review aims to summarize the current studies regarding the interactions of the aforementioned factors with a focus on epigenetic insights. We present two scenarios of single nucleotide polymorphisms (SNPs) in coding regions and non-coding regions for disease risk, via potentially impacting epigenetic patterns. While a SNP in a coding region may confer disease risk via altering protein functions, a SNP in non-coding region may cause diseases, via SNP-altering ABTF, ASM, and allele-specific gene expression (ASE). The allelic increases or decreases of gene expression are key for disease risk during development. Such ASE can be achieved via either a "SNP-introduced ABTF to ASM" or a "SNP-introduced ASM to ABTF." Together with our additional in-depth review on insulator CTCF, we are convinced to propose a working model that the small effect of a SNP acts through altered ABTF and/or ASM, for ASE and eventual disease outcome (named as a "SNP intensifier" model). In summary, the significance of complex crosstalk among genetic factors, epigenetic patterns, and environmental factors requires further investigations for disease susceptibility.

Keywords: allele-specific DNA methylation (ASM), single nucleotide polymorphisms (SNPs), allele-specific gene expression (ASE), genetic variants, regional "autosomal chromosome inactivation (ACI)", quantitative trait locus (QTL), allele-specific binding of transcription factors (ABTFs), SNP intensifier model

OPEN ACCESS

Edited by:
Feng C. Zhou,
Indiana University Bloomington, United States

Reviewed by:
Amy C. Lossie,
National Institutes of Health (NIH), United States
Cuncong Zhong,
University of Kansas, United States

***Correspondence:**
Zhibin Wang
zwang47@jhu.edu

Specialty section:
This article was submitted to Behavioral and Psychiatric Genetics, a section of the journal Frontiers in Genetics

Received: *08 March 2018*
Accepted: *12 December 2018*
Published: *09 January 2019*

Citation:
Wang H, Lou D and Wang Z (2019) Crosstalk of Genetic Variants, Allele-Specific DNA Methylation, and Environmental Factors for Complex Disease Risk. Front. Genet. 9:695. doi: 10.3389/fgene.2018.00695

INTRODUCTION

Genetic variants identified from genome-wide association studies (GWAS) promise to uncover the understanding of inter-individual differences in phenotypes and the risk of complex diseases. One hypothesis is that the susceptibility of an individual to a complex disease is due to the interaction of genetic variants with environmental factors acting through epigenetic mechanisms. Therefore, understanding the complex crosstalk among genetic variation, environmental exposure, and epigenetic patterns is essential for unraveling the etiology of common disease. This review aims to illustrate potential mechanisms for the crosstalk of genetic factors, epigenetic patterns, and allelic binding of transcriptional factors (ABTF), as well as the crosstalk with environmental exposure for disease susceptibility. We begin the review with a basic and brief, but hopefully necessary introduction on the fundamental insights of epigenetic mechanisms (DNA methylation and histone modifications) in the regulation of gene transcription, because both DNA methylation and histone modifications are linked with genetic variants and environmental exposure for disease or complex traits in many burgeoning reports (detailed below). We then describe the crosstalk among different factors (including genetic variation, epigenetic variation, gene expression, and environmental factors) for complex disease risk. We complement the aforementioned broad topics with an in-depth summary on the crosstalk among insulator CTCF, genetic variation, and epigenetic variation in disease or complex traits. This subtopic is currently of high interest in the biomedical arena because of CTCF's pleiotropic roles in biology. CTCF helps shape the high-order genome organization (e.g., "4D nucleosome" program), acts as a tumor suppressor (Kemp et al., 2014), and plays an important role in complex traits. To better envision the underlying mechanisms, we selectively discuss the most relevant investigations regardless of the disease investigated. That is, we did not focus on one type of complex diseases, because a relevant functional study may not be available if we restrain our references to one disease. Hence, with such selection, we may unintentionally overlook many important reports within a given disease. In cases where the expected or hypothesized mechanism may not have been thoroughly addressed, we try to provide a diagram to aid our illustration. We will start our review with brief information on epigenetic background.

EPIGENETIC MECHANISMS INVOLVED IN TRANSCRIPTIONAL REGULATION

DNA Methylation Patterns: Establishment, Maintenance, and Functional Roles

DNA methylation patterns are established and maintained by three DNA methyltransferases (Dnmts), namely Dnmt1, Dnmt3a, and Dnmt3b, in both the mouse and human genomes (Bestor, 2000). In a simplified "two-step" model, it is the role of Dnmt3a and Dnmt3b, which initiate methylation of globally hypomethylated genomic DNA (after implantation) to establish methylation patterns during early embryonic development (Okano et al., 1999). Afterwards, via coupling with DNA replication machinery, Dnmt1 faithfully copies methylation information from the parental strands to the daughter strands during DNA replication (Jones and Liang, 2009; Jurkowska et al., 2011). Because of this copying role, Dnmt1 is referred to as the "maintenance methyltransferase," whereas Dnmt3a and Dnmt3b are called the "de novo methyltransferases." In support of this model, Dnmt3a and Dnmt3b have high activity toward unmethylated DNA, while Dnmt1 shows low activity toward unmethylated DNA and prefers hemi-methylated DNA (Jeltsch, 2006; Jurkowska et al., 2011).

However, with the recent availability of base-resolution methylome data for Dnmt knockout cells, this "two-step" model seems oversimplified (Li et al., 2015). Our data demonstrate that in the absence of Dnmt1, Dnmt3a and Dnmt3b can still maintain symmetrical methylation of CpG dinucleotides (where a cytosine nucleotide is followed by a guanine nucleotide linearly along 5′ to 3′ direction) to some degree. In addition, the presence of Dnmt1 alone allows cells to maintain the methylation levels of retrotransposon long terminal repeats (LTRs) in Dnmt double knockout cells ($Dnmt3a^{-/-}/3b^{-/-}$), at levels comparable to wild type cells. In $Dnmt1^{-/-}$, the presence of only two *de novo* methyltransferases (Dnmt3a and Dnmt3b) still enables embryonic stem cells to retain methylation at retrotransposon long interspersed nuclear elements (LINEs). Therefore, Dnmt1 is required for methylation of LTRs, whereas Dnmt3a and Dnmt3b are necessary for LINE methylation (**Figure 1**) (Li et al., 2015). Collectively, it is more accurate to state that the concerted actions of three Dnmt enzymes are required for the maintenance and establishment of DNA methylation patterns in the mouse genome. While at the last stage of publishing this review, a new report suggests that Dnmt1 does have de novo methyltransferase activity (Li et al., 2018).

The unexpected division of labor between maintenance Dnmt1 and *de novo* Dnmt3a and Dnmt3b for retrotransposons is informative for deeper mechanistic insights in future investigations. In early epidemiological studies, the methylation levels of LINEs or Alu sequences in the human/mouse genome were assumed to represent global DNA methylation changes. Though the assumption was largely untested (Nelson et al., 2011), LINE or Alu methylation has been used as a biomarker for environmental exposure or a diseased state. For example, in a recent cohort study that examined the association between DNA methylation of pre-diagnostic leukocyte and gastric cancer risk, it was reported that the latter was inversely associated with Alu methylation. Intriguingly, LINE methylation was not associated with gastric cancer risk (Gao et al., 2012). The association of Alu but not LINE methylation with gastric cancer risk is in line with other distinct mechanisms in control of different classes of retrotransposons (Li et al., 2015). Presumably, the mechanism for Alu methylation was affected in gastric cancer, but the mechanism for LINE methylation was not. In an effort to assess Alu (LINE not investigated) methylation from peripheral blood DNA of healthy donors and patients with alcohol use disorders, Kim and colleagues found that Alu methylation levels are significantly higher in the latter than the former (Kim et al., 2016). The underlying mechanism for the aforementioned

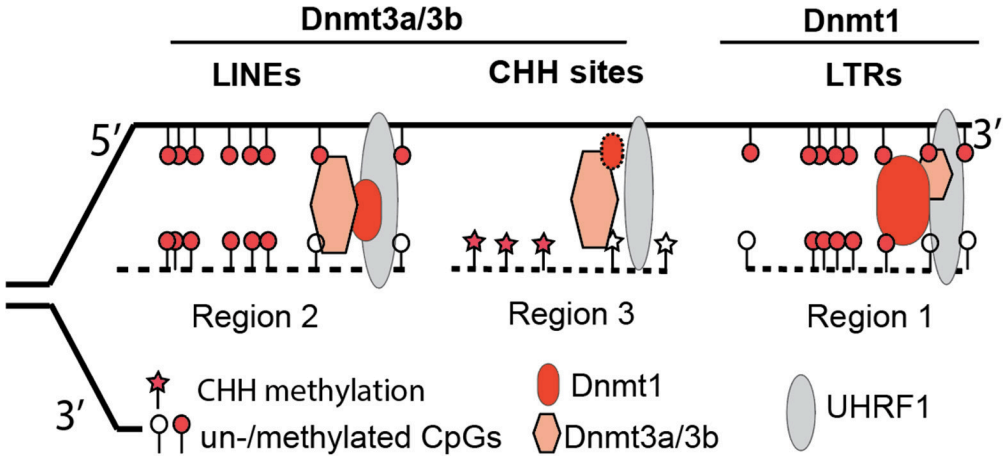

FIGURE 1 | A revised model illustrating the complementary and concerted actions from Dnmt3a/3b *de novo* activity and Dnmt1 maintenance activity at three representative genomic regions. Via interacting with proteins such as UHRF1 at replication forks, Dnmt1 plays a dominant role in retaining methylation at retrotransposon LTRs (region 1), whereas Dnmt3a/3b are mainly responsible for methylation at retrotransposon LINEs (region 2) or genomic regions with CHH (H = A, T, or C) sites (region 3). The loss of Dnmt3a/3b or Dnmt1 results in hypomethylated retrotransposon LTRs or LINEs. The size of each symbol represents the degree of importance for protein factors in maintaining methylation patterns in particular genomic regions, with the bigger symbol being the more important in maintenance.

associations, however, remains to be determined. In the agouti viable yellow (A^{vy}) mouse studies, methylation of CpG sites within a LTR retrotransposon is vulnerable (hypomethylated) to environmental insults, including Bisphenol A (BPA), folate, and alcohol (Dolinoy, 2008; Kaminen-Ahola et al., 2010). Because LTR's methylation depends on Dnmt1 (Li et al., 2015), it may imply that Dnmt1-dependent methylation activity is more sensitive to environmental exposure. It is also worth mentioning that Dnmt1 is highly expressed in most somatic tissues, whereas Dnmt3a and Dnmt3b are not. In summary, depending on exposure-alteration of Dnmt1 or Dnmt3a/3b, the LINE or LTR methylation level should be selected accordingly, in order to represent global DNA methylation changes in cells.

Methylation of CpG sites can occur in the transcribed regions of genes (either silenced or expressed) (Lister et al., 2009), suggesting that the alteration of DNA methylation patterns may not affect the expression of a large number of genes. Indeed, recent investigations demonstrate that global DNA hypomethylation did not alter the transcriptome as drastically as previously expected (Blattler et al., 2014; Li et al., 2015). In contrast to methylation changes in a global fashion in *Dnmt*-knockout cells, environmental exposure including BPA exposure seems to change methylation patterns only at specific genomic loci (Dolinoy et al., 2007; Kundakovic et al., 2015). Therefore, if the environmental exposure-altered methylation has an important impact on gene transcription, we expect that the CpG sites bearing the altered methylation must play critical roles in gene regulation, such as CpG sites within enhancers or binding motif of critical transcriptional factors (TF) or the imprinting control regions (ICRs).

Histone Modification for Permissive or Inhibitive Transcription

Another layer of epigenetic mechanisms for the regulation of gene expression is posttranslational modifications (PTMs) of histone tails. To date, there are a few hundred distinct histone tail modifications, including histone acetylation, methylation, and phosphorylation (Strahl and Allis, 2000; Tan et al., 2011). The former two have been known for decades to possess roles in gene transcription, and several representative histone acetylation and methylation marks have been actively pursuing by the community for many years (Allfrey et al., 1964; Barski et al., 2007; Wang et al., 2008). For example, the ENCODE project selects eight histone marks out of many potential histone acetylations and methylations: H3K4me1 (H3 lysine 4 monomethylation), H3K4me2, H3K4me3, H3K9ac (H3 lysine 9 acetylation), H3K27ac, H3K36me3, H3K9me3, and H3K27me3 (Yue et al., 2014). The former six are active histone marks in association with expressed genes, whereas the latter two are repressive marks in association with silent genes. Except H3K36me3 at gene bodies, the remaining seven histone marks can be enriched at promoters and enhancers (Dai and Wang, 2014).

Each histone mark demonstrates useful and maybe distinct information, but they can also share overlapping information (Wang et al., 2008). Seven marks can be present at promoters and/or enhancers, but each mark may better serve a particular application. H3K4me3, H3K9ac, and H3K27ac are enriched at promoters or transcription start sites of active genes (Wang et al., 2008). Similarly, H3K4me1, H3K9ac, and H3K27ac are enriched at enhancers, with H3K27ac particularly enriched at active enhancers (Creyghton et al., 2010). One active mark (out of the former five) and one inactive mark (either H3K9me3 or H3K27me3) can be used to predict bivalent promoters (Bernstein et al., 2006; Roh et al., 2006). Among potential combinations, H3K27me3 and H3K4me3 are popularly chosen for testing promoter bivalency. In addition to these popularly analyzed histone acetylations and methylations, many more new histone marks have been recently identified (Tan et al., 2011) and their roles in gene transcription and biological pathways

are less clear (Goudarzi et al., 2016). Recently, even one of the well-characterized histone acetylation marks, H3K27ac, was shown to have an unexpected suppressing role. In contrast to the transcriptional activation of H3K27ac at enhancers and promoters, age-related up-regulated genes contain hyper H3K27ac in gene bodies, acting to suppress the overexpression of inflammaging genes (Cheng et al., 2018). In addition, the expression changes of these age-related genes can be predicted by gene body H3K27ac level. It seems that histone marks have the potential to reflect the aging stage or disease conditions.

INTERACTIONS OF GENETIC VARIANTS AND EPIGENETIC PATTERNS FOR COMPLEX DISEASE RISK

A common SNP is defined as a single base change in a DNA sequence that occurs among a significant proportion (≥1%) of a population (Lockwood et al., 2014). SNPs may reside in coding regions or non-coding regions. Contrary to the common belief, it is estimated that about 90% of GWAS-associated genetic variants reside in non-coding regions (Welter et al., 2014; Farh et al., 2015). While variants in coding regions may confer disease risk through altered protein sequences and, therefore, altered protein functions, variants in non-coding regions (usually enhancers) contribute to disease susceptibility through changing gene transcription and non-coding RNAs (Hrdlickova et al., 2014). These genetic variants might engage in crosstalk with sequence-specific transcription factors and epigenetic patterns (including DNA methylation) (McVicker et al., 2013), thereby impacting the transcription of genes locally or remotely.

Genetic Variants in Coding Regions for Disease Susceptibility via Altering Epigenetic Patterns

There are at least two scenarios, including SNPs within epigenetic enzymes and SNPs in TFs (**Figure 2**), that lead to the altered epigenetic patterns for increased disease risk. SNPs within epigenetic enzymes (including DNMTs and histone modifying enzymes) may potentially alter their functions, thereby subsequently changing epigenetic patterns in a genome-wide fashion. SNPs in TFs may impact the function of TFs' binding to DNA or its recruitment of epigenetic enzymes, thereby changing epigenetic patterns indirectly (Khandanpour et al., 2012).

SNPs in DNA methyltransferases have been reported in association with complex diseases. For example, polymorphisms in three DNMTs with methylation activity (DNMT1, DNMT3A, and DNMT3B) and in one DNMT without methylation activity (DNMT3L) are associated with an increased risk of schizophrenia (Saradalekshmi et al., 2014). Though many SNPs reside inside non-coding regions, at least one of them (rs2228611, within DNMT1 exon) has been found to be significantly associated with schizophrenia at genotypic and allelic levels in a South Indian population. SNPs in DNMT1 (exonic rs16999593) and DNMT3A (intronic rs1550117) may contribute to the gastric cancer risk, according to a recent meta-analysis (Li et al., 2016). Polymorphism rs1550117 of DNMT3A has been shown in association with the late-onset Alzheimer's disease. Specifically, patients with an AA genotype showed a 2.08-fold risk when compared to patients with a GG genotype (Ling et al., 2016). When investigating the imprinting disorder Beckwith-Wiedemann syndrome, Dagar and colleagues screened variants within the DNMT1 coding region and identified three patients (out of 53 examined) who contained three rare missense variants: rs138841970: C>T, rs150331990: A>G, and rs757460628: G>A; encoding NP_001124295 p.Arg136Cys, p.His1118Arg, and p.Arg1223His, respectively (Dagar et al., 2018). Using the DNMT1 binding as a surrogate for DNMT1 enzymatic activity, GFP-tagged DNMT1 fusion proteins with site-directed mutation show a reduced binding affinity (40-70%) of variants compared to that of the wild-type DNMT1. While it would be more informative to validate the expected DNA demethylation with bisulfite sequencing in three patients, the report at least provides a reasonable support for an association between variants in DNMT1 and increased disease risk (Dagar et al., 2018).

SNPs in histone-modifying enzymes and/or cofactors are also associated with complex disease susceptibility. GWAS from the GABRIEL Consortium (a multidisciplinary study of genetic and environmental causes of asthma) identified significant SNPs within histone-modifying enzymes in asthmatic patients, including histone deacetylases (HDAC4, HDAC7, HDAC9) and H3 lysine 36 demethylases (KDM4C, KDM2A) (Moffatt et al., 2010; Kidd et al., 2016). A focused summary of SNPs and mutations within histone lysine methyltransferases (KMTs) and histone lysine demethylases (KDMs) (Van Rechem and Whetstine, 2014) listed a few SNPs in coding regions of KMTs and KDMs in association with diseases. In contrast, the less frequent mutations or the deletion of KMTs and KDMs seem to be associated with more diseases. Although the variations in coding regions are expected to affect protein stability,

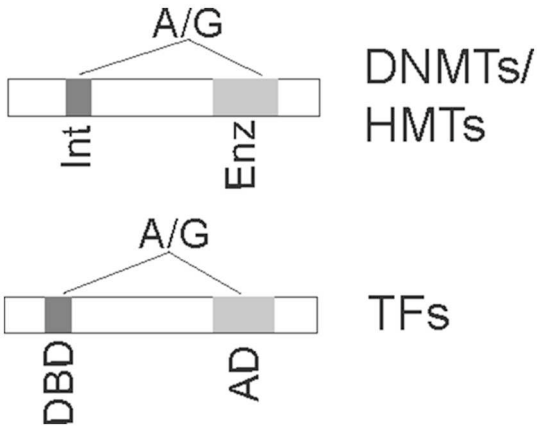

FIGURE 2 | SNPs in critical domains of coding regions of epigenetic enzymes (**Top**) or transcription factors (**Bottom**) for disease risk are depicted. SNPs illustrated in the top panel may change the enzymatic activities if in enzymatic domain (Enz) or may change the interacting domain (Int) for interaction with other proteins, resulting in altered epigenetic marks. SNPs in the bottom panel will either abolish the DNA-binding domain (DBD) to target consensus sequences or impair activation domain (AD) for recruitment of epigenetic enzymes, thereby altering epigenetic patterns at target genes.

folding, ligand-binding, and/or post-translational modification, it remains unclear how these SNPs impact the function of DNMTs and histone-modifying enzymes.

SNPs within coding regions of DNA-binding TFs can also potentially impact epigenetic patterns (**Figure 2**). These variants have an indirect effect, compared to the direct effect of SNP-altering epigenetic enzymes. The human growth factor independence 1 (GFI1), a DNA-binding transcription repressor, is important for hematopoietic stem cell and B and T cell differentiation. About 3 to 7% of white subjects contain GFI136N, which impairs binding to target genes such as *HOXA9*, resulting in elevated histone H3K4me2 signals and thereby promoting gene transcription. Compared with the GFI136S genotype, people with GFI136N have an increased risk (60%) for acute myeloid leukemia (Khandanpour et al., 2012). In one early cited report, identified common SNPs that have a potential impact on DNA binding of zinc finger TFs are unlikely to alter gene transcription in trans (Lockwood et al., 2014). However, Lockwood et al.'s results also suggest that large-scale analyses might offer a different conclusion, as in the case of GFI1.

Genetic Variants in Non-coding Regions for Complex Disease Risk via Crosstalk With DNA Methylation Status and/or TF Binding for Shaping Chromatin Structure

As aforementioned, about 90% of GWAS-identified genetic variants reside within the non-coding regions (Farh et al., 2015). SNPs in non-coding regions may impact gene function via several mechanisms. Intronic SNPs may affect splicing and/or mRNA stability, and studies have shown that an intronic SNP (rs910083-C) within *DNMT3B* is associated with an increased risk of nicotine dependence and squamous cell lung carcinoma. Though the mechanism is yet unclear, this SNP is associated with hypermethylation of about 252 bp upstream of the *DNMT3B* gene (Hancock et al., 2017). SNPs affecting the TFs' binding sites can predispose disease susceptibility by impacting the associated TFs' regulatory pathways (**Figure 3**), partially because SNPs at conserved residues within the consensus sequences for TFs can decrease or even abolish the binding of these TFs or because SNPs generate a new binding site for TFs. For example, the SNP A>C within the *Hcn2* locus for an allele-specific metal responsive element of metal regulatory transcription factor 1 (MTF1) (Martos et al., 2017). Hence, SNPs in this category could alter merely the DNA sequence, or, if they alter or generate CpG dinucleotides, they could simultaneously alter both the consensus sequence and its DNA methylation.

Accumulating evidence suggests that GWAS-identified and disease risk-associated genetic variants may largely confer their impacts by changing the expression of neighboring genes (Kilpinen et al., 2013; McVicker et al., 2013; Soldner et al., 2016; Allen et al., 2017; Gallagher et al., 2017; Li X. et al., 2017). Such changes may act through variant-disrupted motifs that eliminate or introduce the TF binding as described above. In our opinion, two TFs—ZFP57 and CTCF—are particularly intriguing to work with because of their known potential to impact chromatin in a global fashion (Ong and Corces, 2014; Riso et al., 2016). Both

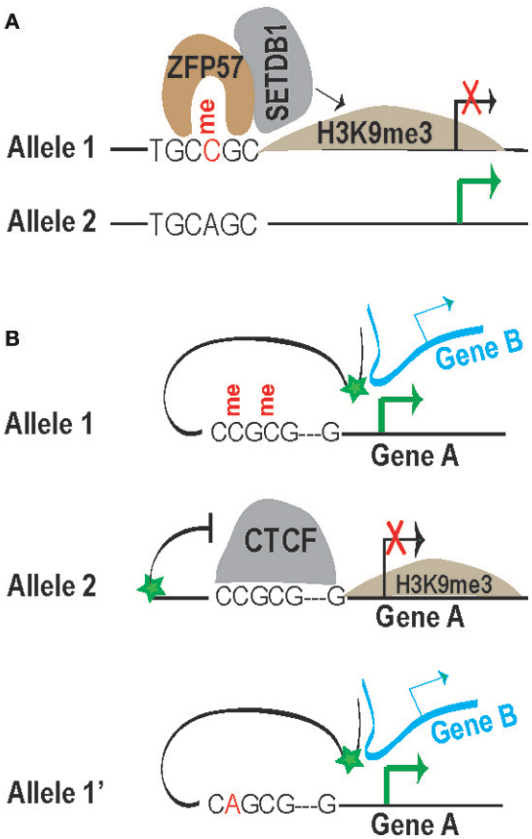

FIGURE 3 | Illustration of methyl-CpG-dependent recruitment of ZFP57 **(A)** and methyl-CpG-sensitive binding of CTCF **(B)** for control of gene transcription. **(A)** CpG methylation within the motif is required for ZFP57 binding and subsequent recruitment of SETDB1 for the establishment of H3K9me3 locally. An SNP change of C to A abolishes ZFP57 binding. Without ZFP57/SETDB1-mediated repressive H3K9me3, genes in this allele 2 will be expressed. **(B)** In allele 1, the methylated CTCF motif prevents CTCF binding, thereby allowing upstream enhancers (green star) to access the transcription start sites (TSSs) for activation of gene A from the same chromosome and of gene B from a different chromosome. In allele 2, CTCF binds to the unmethylated motif, preventing enhancers to access the TSS of gene A for gene activation. In allele 1′, the SNP A replacing C will affect the binding of CTCF; therefore, allele 1′ will have a similar consequence to allele 1. Note that the enhancer may act to a different gene, such as gene such as gene B (top and bottom panel).

are DNA-binding TFs, and polymorphisms at different residues within their binding motifs seem to carry different weight with TF binding. In addition, these two TFs represent two distinct classes of TFs in terms of the impact of methylation status on their recruitments. That is, methylation is required for the binding of ZFP57 (Quenneville et al., 2011), while methylation prevents the binding of CTCF (Bell and Felsenfeld, 2000).

Methylation-Sensitive CTCF

CTCF biology

The insulator CTCF is an intriguing TF with potential roles for altering chromatin in a genome-wide fashion (Phillips and Corces, 2009; Ong and Corces, 2014). CTCF may also

serve as a pioneer TF to shape local chromatin for recruiting additional TFs to their target sites (Tehranchi et al., 2016). In contrast to ZFP57, which is dependent upon methylation for binding, hypomethylation of the consensus sequence CCGCGNGGNGGCAG is critical for CTCF binding (Bell and Felsenfeld, 2000; Kim et al., 2007; Cuddapah et al., 2009). One essential role of CTCF is to block the spread of chromatin structure to the opposite side of a CTCF binding site (barrier) or to block the enhancer activity toward a promoter (Cuddapah et al., 2009; Phillips and Corces, 2009). The prototypical role of insulation has been revealed by investigation of CTCF at the imprinted *H19*/*Igf2* locus (Bell and Felsenfeld, 2000). *H19* and *Igf2* are located on the opposite side of CTCF-bound regions and there are a few enhancers downstream of the *H19* gene. CTCF binding motifs show allelic methylation, thereby dictating allelic CTCF binding. CTCF cannot bind to the methylated motifs of the paternal allele, allowing enhancers to access the paternal *Igf2* gene for activation. In contrast, CTCF binds to the unmethylated motifs of the maternal allele, thereby blocking enhancer access of *Igf2*, but allowing access of *H19* for stimulation. Experimental mutations to abolish CTCF binding affect imprinted expression within the locus (Singh et al., 2012).

CTCF's insulation is not limited to imprinted loci and is expected to act in a three dimensional fashion, presumably because enhancers can loop with multiple loci to regulate genes on the same or even different chromosome(s) (Spilianakis et al., 2005). **Figure 3B** presents a simplified cartoon to show the enhancer-blocking activity of CTCF in crosstalk with SNPs. In Allele 1, allelically methylated CpG sites prevent CTCF binding, enabling the enhancer to interact with gene A from the same chromosome and gene B from a different chromosome for stimulation. In Allele 2, the unmethylated motif allows CTCF insulation, thereby blocking the enhancer's access to stimulate gene A and, hence, keeping gene A silenced. A SNP change from C to A will potentially alter the conserved residues (illustrated in Allele 1′) and perhaps also the methylation status, preventing, or enabling CTCF insulation. Depending on the "conserveness" affected, the SNPs or mutations may reduce or even completely abolish CTCF binding to its motifs (Li W. et al., 2017), eventually affecting its insulation effect.

CTCF, genetic variation, and gene expression changes

Having briefly summarized CTCF insulation, we then did an in-depth examination of genetic variants within CTCF-binding motifs and their crosstalk with ABTF and ASMs in terms of impact on human health. Given the diverse functions of CTCF in transcription, imprinting, and X-chromosome inactivation (Phillips and Corces, 2009; Ong and Corces, 2014), it is not surprising that investigations begin to reveal the associations of these genetic variants with diseases or complex traits (**Table 1**) by impacting the allelic binding of CTCF. Among many reports (**Table 1**), several thorough investigations have presented their detailed insights of CTCF's allelic binding through long-range chromatin interactions that affect gene expression and, therefore, disease risks. Like ZFP57, CTCF's insulation or regulation of long-range chromatin interaction is not limited to ICRs of imprinted loci, but also applies to regular genomic regions (exemplified below).

For example, severe human influenza was reported in association with SNP rs34481144 A/G in the 5′ UTR of a regular *IFITM3* gene (not imprinted) that encodes antiviral protein IFITM3 for inhibition of viral entry (Allen et al., 2017). IFITM3 in memory $CD8^+$ T cells promotes the adaptive immunity for antiviral resistance. Functional studies have revealed that the risk allele A decreases the binding of interferon regulatory factor 3 (IRF3) but increases the binding of CTCF. The latter is expected to impact the expression of *IFITM3*-neighboring genes via its insulation activity. Authors also demonstrate that increased methylation at rs3448114 blocks the binding of CTCF, thereby enhancing the expression of *IFITM3*. These investigations exemplify our proposed "SNP intensifier" model; a tiny difference at one residue (A/G, with the former disrupting a CpG site) is intensified via changing allelic DNA methylation, thereby affecting CTCF affinity and altering the expression of neighboring genes for disease risk (Allen et al., 2017). While this line of study has been limited to *in vitro* assays and would be much improved with *in vivo* confirmation of CRISPR/cas9-altered SNP A/G, the presented results are agreeable and consistent with the model presented later in section Conclusion, Challenges, and Perspectives.

Another example is the investigation of birth weight of babies conceived through assisted reproductive technology (ART) that was related to the imprinted locus. In ART, fresh embryo transfer-derived newborns are associated with low birth weight, while newborns derived from frozen embryo transfer are associated with increased birth weight (Marjonen et al., 2018). The underlying mechanism remains largely unknown. ART is expected to increase imprinting defects (Eroglu and Layman, 2012); therefore, the *IGF2*/*H19* locus, with its role in normal placental and embryonic growth, was selected for characterization. As described above, the *IGF2*/*H19* locus is regulated by an ICR that bears seven CTCF-binding motifs. In placentas from women who have used ART, a SNP rs10732516 A/G within the sixth binding motif (CCGCGc/tGGNGGCAG or complementary strand CTGCCNCCa/gCGCGG) of CTCF results in allele-specific demethylation on the paternal allele of rs10732516 paternal A/maternal G genotype, but not on the paternal G/maternal A genotype (Marjonen et al., 2018). The SNP allele A would interrupt the first CpG site of the complementary strand sequence CTGCCNCCa/gCGCGG and is associated with hypomethylation. It seems that the first CpG site might carry more weight in controlling DNA methylation status than do the following two CpG sites. These investigations also lack the expression status of *H19* and *IGF2* among genotypes (A/A, A/G, and G/G) for further mechanistic analysis. Fresh embryo transfer-derived newborns with the G/G genotype have shown an increased birth weight and larger head circumference when compared to the parameters of the A/A genotype (Marjonen et al., 2018).

The same group above has also examined SNP rs10732516 at the *IGF2*/*H19* locus for the consequences of prenatal alcohol

TABLE 1 | The crosstalk among CTCF, genetic variants, epigenetic variation in complex diseases or traits. (N/A, not available).

Complex traits or diseases	Loci	Mechanism			Key results and/or model suggested	References
		Genetic variants	Epigenetic variation	ABTF		
Asthma	ORMDL3	Yes	Yes	Yes	A SNP (rs4065275) in an enhancer within the 1st intron of *ORMDL3* promotes CTCF binding, whereas another SNP (rs12936231) downstream of the enhancer impairs CTCF binding. SNPs therefore alters three-dimentional organization in the asthma-risk allele to facilitate the expression of ORMDL3, which inhibits IL-2 production.	Schmiedel et al., 2016; Bérubé et al., 2017
Birth weight	H19/IGF2	Yes	Yes	N/A	A SNP rs10732516 A/G within the sixth binding motif of CTCF within the ICR results in allele-specific demethylation in paternal allele of rs10732516 paternal A/maternal G genotype. Allelic binding of CTCF is expected.	Marjonen et al., 2018
Cerebellum weight (CW)	H19/IGF2	Yes	Yes	Yes	DNA methylation at CTCF-binding site 3 within ICR explains ∼25% of the CW variation; Genetic variation of the ICR in strong association with CW in a parental-origin dependent fashion.	Pidsley et al., 2012
Dementia	TMEM106B	Yes	Yes	Yes	The risk allele of rs1990620 increases the recruitment of CTCF, thereby leading to haplotype-specific effects on three-dimentional chromatin interactions and thus increased *TMEM106B* expression. The latter increases cytotoxicity for risk of neurodegeneration.	Gallagher et al., 2017
Influenza	IFITM3	Yes	Yes	Yes	A SNP (rs34481144) in the 5′ UTR of antiviral IFITM3 gene renders the risk allele with lower TF IRF3 binding but higher CTCF binding, thereby altering expression correlations among *IFITM3*-neighboring genes. The risk allele also disrupts a CpG site that is under differential methylation in CD8+ T cell subsets.	Allen et al., 2017
Lung cancer	DAGLA	Yes	N/A	N/A	A SNP within CTCF binding site inside an intron of *DAGLA* was significantly associated with increased risk of lung cancer	Dai et al., 2015
Lynch syndrome	MLH1	Yes			A SNP rs143969848 (G>A) within CTCF motif, part of an enhancer and also upstream of *MLH1* transcription start site, disrupts enhancing activity and MLH1 expression.	Liu et al., 2018
Mental illness	3p22 (TRANK1)	Yes		Yes	The risk allele of SNP rs9834970 shows lower baseline expression of *TRANK1* that may further alter genes important for neurodevelopment/differentiation. While the role of rs9834970 unknown, a nearby SNP rs906482 alters CTCF binding and the allele with increased CTCF binding is the risk allele of rs9834970.	Jiang et al., 2018
Osteoporosis	SOST	Yes		Yes	Four SNPs within the locus of *SOST* (negative regulator of bone formation and positive regulator of bone resorption). Among them, the SNP rs1230399 shows FOXA1 binding activity, resulting a T allele-specific activation; the SNP rs1107748 renders C allele transcriptional enhancer activity through a CTCF binding site; Variant rs75901553 C >T abolishes the binding site of miR-98-5p that is negative responsive to parathyroid hormone.	Ye et al., 2018
Osteoporosis	1p36.12 (LINC00339)	Yes		Yes	A SNP rs6426749 functions as a distal allele-specific enhancer stimulating the expression of a lncRNA	Chen et al., 2018
Type 2 diabetes	TF binding Sites	Yes	N/A	N/A	SNPs within motifs of CTCF, EP300, FOXA1/2, HNF4A, and TCF7L2 are associated with T2D from computational analyses	Cheng et al., 2017

exposure, which is known to affect development of the fetal nervous system and to restrict fetal head growth (Treit et al., 2016). Investigators found that alcohol exposure decreases the hypermethylation of the paternal allele of rs10732516 paternal A/maternal G genotype in placentas (Marjonen et al., 2017).

Additional reports listed in **Table 1**, including rs1990620 within the *TMEM106B* locus in association with neurodegeneration, support the "SNP intensifier" working model (presented later) (Gallagher et al., 2017). Lastly, CTCF is linked with intellectual disability (Bastaki et al., 2017; Hori et al., 2017). Altogether, a change of one residue (for example, C to A in **Figure 3**) may abolish or introduce the allelic recruitment of CTCF (and its associated insulation or long-range chromatin interactions), thereby causing a change from biallelic to monoallelic (or vice versa) expression of genes, and thus the copy numbers of the mRNA of related genes are altered.

Additional methylation-sensitive TFs

Many additional TFs—including bHLH, bZIP, and ETS family members—are also inhibited by methyl-CpG (Yin et al., 2017). Therefore, any SNPs that change these TFs' consensus motifs and/or result in methyl-CpG (e.g., "AG" becoming methylation-prone "CG") have the potential to alter the binding of these TFs and, subsequently, to alter these TFs-controlled genes. Future investigations in these similar TFs will certainly be promising.

Methylation-Dependent ZFP57

The DNA-binding transcription factor ZFP57 only binds to the methylated TGCCGC hexanucleotide and, subsequently, recruits cofactor KAP1 and DNMTs, as well as SETDB1 (Quenneville et al., 2011). The recruited SETDB1, as a histone-modifying enzyme, is expected to establish H3K9me3 heterochromatin mark around ZFP57-targeted sites (**Figure 3A**) (Anvar et al., 2016). In addition, polymorphisms at CpG dinucleotides will not only change the consensus residue, but also change the methylation status (namely CpG-SNP), which may impact TF binding more severely. The A replacing the C in Allele 2 will change the consensus residue and methylation status (**Figure 3A**). Indeed, when AT replaced the fourth and fifth residues CG, the resulting oligonucleotide (mut1) was shown to lose both the consensus sequence and its methylation status. When TGC was changed to GAG, the resulting oligonucleotide (mut2) only altered consensus sequences, but still maintained the methyl-CpG. Intriguingly, the mut1 probe did not compete as well as the mut2 probe, at least in electrophoresis shift assays (Quenneville et al., 2011), suggesting that the methylation status may be more critical than the consensus sequence for ZFP57 binding.

While the association of methylated TGCCGC in H3K9me3 patterns was initially investigated in imprinting control regions (ICRs) of imprinted loci (Quenneville et al., 2011), regular genomic regions are expected to have similar ZFP57-associated H3K9me3. In other words, so long as genomic loci contain the TGCCGC sequences, these loci are potentially subjected to ZFP57/SETDB1-regulated H3K9me3. Therefore, SNPs at ZFP57 motifs are expected to play a role beyond imprinted genes (Anvar et al., 2016). Because ZFP57-mediated H3K9me3 signal distribution seems to have a relatively long range, any alterations of TGCCGC sequences could potentially affect the transcription of multiple genes within the region.

The effect of SNPs within the ZFP57 motifs on disease risk remains to be determined in human populations. Our literature search was relatively futile in this aspect; however, a few reports indeed linked methylation QTLs to expression changes of ZFP57 in disease/traits, including post-traumatic stress disorder (Rutten et al., 2018), metabolic trait (Volkov et al., 2016), and psychosis (Rivollier et al., 2017). Compared to the extensive studies of SNPs within CTCF binding motifs for complex traits/diseases (which burgeoned only in the past 2 to 3 years) (**Table 1**), we expect more upcoming reports to show the effect of SNPs within ZFP57 binding motifs on disease risk because these SNPs seem to abnormally alter allelic expression of genes (Anvar et al., 2016). From F1 hybrid ES cells between C57BL/6 and Cast/EiJ, genetic variants with disruption of ZFP57 consensus motif and methylation status are linked to monoallelic expression of neighboring genes (Strogantsev et al., 2015). Note: Allelic increases or decreases of gene expression are key for CTCF-involved disease risk (**Figure 4**).

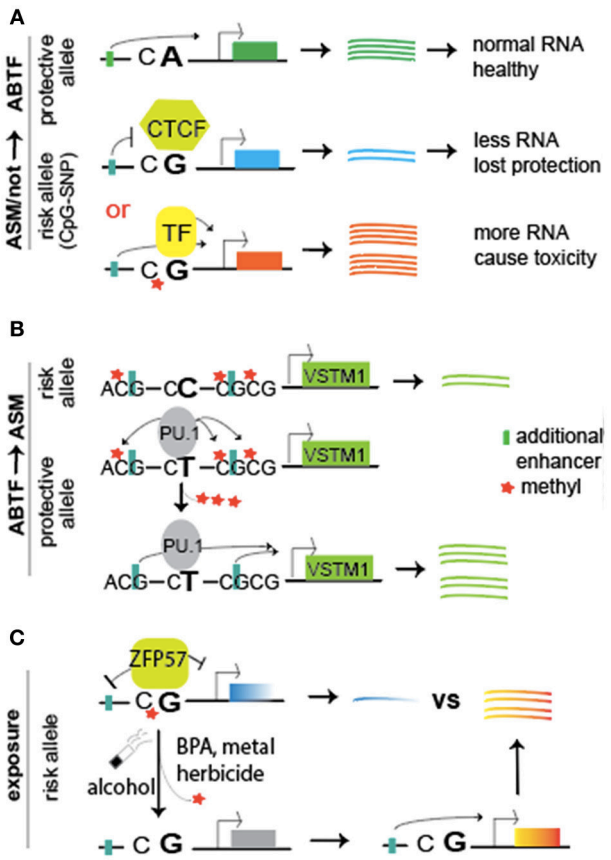

FIGURE 4 | A working model of "SNP intensifier via allele-specific binding of TFs," either having a crosstalk or not with allele-specific methylation. **(A)** Compared to the protective allele with CA dinucleotides (Top), the risk allele bears a CG site that can be maintained in unmethylated (Middle) or methylated (Bottom) status. The former may result in methylation-sensitive recruitment of transcription factors such as insulator CTCF, preventing an upstream enhancer to stimulate gene transcription for less RNA copies. Therefore, less RNA transcripts may be not good enough to provide necessary protective roles like the protective allele. In contrast, the methylated status may recruit methylation-dependent active TFs (or repressors) for stimulation of gene transcription, resulting in more RNA copies and thereby causing toxicity to the cells. Note the change from CA on protective allele to CG on risk allele, introducing a CpG-SNP. **(B)** Illustrate a model of SNP-resulted ABTF (e.g., protective T allele recruiting PU.1) that initiates the Tet-mediated demethylation of neighboring CG sites on the allele it binds (Kumar et al., 2017). Such demethylation may relieve the inhibitory role of methyl group on enhancers for stimulation of gene transcription. In contrast, the risk C allele does not recruit PU.1 for demethylation. **(C)** Introduce the crosstalk with exposure. The methyl-CpG site (e.g., within a binding motif of ZFP57) is sensitive to environmental exposure (alcohol, BPA, cigarette smoke, herbicides, and metals). The resulting demethylation eliminates methyl-CpG-dependent binding of TFs (such as ZFP57), thereby abolishing ZFP57′s repression of genes. The simulated expression from upstream enhancers leads to allelic imbalance for disease risk. In all cases **(A–C)**, the total RNA copies were altered, resulting in a disastrous dosage effect for disease risk.

In summary, this section presents the mechanistic insights of SNP-resulted allele-specific methylation that facilitates the allelic binding of TFs such as ZFP57 (**Figure 4A**, bottom panel) and of SNP-resulted motifs (unmethylated) for insulator CTCF (**Figure 4A**, middle panel). In both cases, ABTFs play a key role in allelic regulation of gene transcript. In the following section, we will review SNP-resulted ABTF, thereby leading to the subsequent ASMs and potential ASE (**Figure 4B**).

GENETIC VARIANTS IN SHAPING ALLELE-SPECIFIC DNA METHYLATIONS (ASMS) AND POTENTIAL ALLELE-SPECIFIC GENE EXPRESSION (ASE) FOR DISEASE RISK

Unexpected ASMs and ASE for Autosomal Genes in the Human or Mouse Genome

It is worth presenting genetic variants in shaping ASMs (separately from the above section Interactions of Genetic Variants and Epigenetic Patterns for Complex Disease Risk). In this section, we envision the underlying mechanism for ASMs and ASE. Traditionally, both ASM and ASE are considered as the phenomena of genomic imprinting and X chromosome inactivation (XCI). However, more recent reports have started to unveil unexpected allelic asymmetries of many non-imprinted autosomal genes in the mammalian genome (Klengel et al., 2013; Izzi et al., 2016).

Increasing evidence shows that both the human and mouse genomes contain hundreds or even thousands of ASMs (Cheung et al., 2017). Originally aimed to identify unknown imprinted genes, one study identified many unexpected ASMs from genomic loci outside of known imprinted regions in several human tissues (Kerkel et al., 2008). Further investigations demonstrate that these ASMs are tissue-specific and individual-specific, suggesting genetic background in affecting ASMs (Yang et al., 2010). Looking at two mouse strains (C57BL/6 and BALB/c) and their F1 hybrid offspring, investigators focused on 181 large genomic intervals with an approach based on methyl-CpG immunoprecipitation and locus-wide tilling arrays, identifying several hundreds of differentially methylated regions and strain-specific methylation patterns controlled by *cis*-acting polymorphisms (Schilling et al., 2009). Regarding the identification of unknown imprinted loci in the mouse genome, our group has developed a computational approach based on the feature of monoallelic hyper- or hypomethylation at ICRs to scan the base-resolution DNA methylomes from the mouse ES cell J1 line (Li et al., 2015; Martos et al., 2017) that identified more than 2,000 regions showing bimodal methylation patterns. These regions are potentially associated with monoallelic methylation. In the subsequent validation, we generated four independent hybrid ES lines (from a reciprocal cross between 129S1/SvlmJ and Cast/EiJ or between C57BL/6NJ and Cast/EiJ) and confirmed the ASM of the *Hcn2*/*Polrmt* locus—that is, within this locus, the Cast allele with a SNP C is always hypomethylated (i.e., independent of parental origin), whereas the 129 allele or the C57 allele with a SNP A is always hypermethylated. Intriguingly, the SNP C renders the Cast allele a new motif for metal regulator transcription factor MTF1 (Martos et al., 2017).

Do Non-imprinted ASMs Control ASE?

The extent to which the non-imprinted ASMs control allelic gene expression, remains to be defined. Because imprinted ASMs control ASE, one would expect the similar control of ASMs for the allelic expression of genes on autosomes. Indeed, reports support that ASMs are at least one of the factors to cause allelic imbalance of gene expression.

1. **Genetic variants-resulting demethylation of one allele for ASM and ASE.** This class of variant regulation is initially featured by SNP-facilitated ABTF, which initiates allelic demethylation for ASM and ASE (**Figure 4B**). In other words, ABTF leads to ASM. One example is an atopic dermatitis-associated SNP rs612529 T/C in the promoter of *VSTM1* that encodes SIRL-1. It turns out that the protective T allele facilitates the recruitment of transcription factors YY1 and PU.1 (Kumar et al., 2017). YY1 can either activate or repress gene transcription, depending on the context in which it binds (Gordon et al., 2006), whereas PU.1 seems to demethylate its target genes through Tet2 demethylation (de la Rica et al., 2013). Indeed, the neighboring CpG sites of the PU.1 binding site on the protective T allele, as compared to those of the risk C allele, are hypomethylated in monocytes, thereby leading to allelic upregulation of gene transcripts. The risk C allele does not recruit PU.1, resulting in the low expression of SIRL-1 in monocytes. The latter leads to a higher risk for manifestation of an inflammatory skin disease (Kumar et al., 2017). Another example is the allele-specific demethylation of long-range enhancers of the *FKBP5* (FK506 binding protein 5) gene, which increases the susceptibility of developing stress-related psychiatric disorders in adulthood (Klengel et al., 2013). FKBP5 is an important regulator of the glucocorticoid receptor complex that is involved in the stress hormone system. Exposure to early childhood abuse is associated with demethylation of the enhancer on the risk allele (with the AA genotype), bringing the enhancer through long-range interaction to transcription machinery for allelically increased transcript of *FKBP5*. The latter results in a long-term malfunction of the stress hormone system and a genome-wide impact on the function of immune cells (Klengel et al., 2013). The third example is growth differentiation factor 5 (GDF5), a ligand of the TGF-beta superfamily of proteins, essential for normal skeletal development. In the 5′ UTR of the *GDF5* gene, a C-to-T SNP rs144383 is a risk factor for osteoarthritis of the knee. Methylation of a highly conserved CpG site (4 bp upstream of rs144383 and part of SP1 and SP3 motif) affects allele-specific binding of repressor SP1 and SP3, thereby attenuating the repressive effect of SP1 and SP3 proteins and resulting in allelic expression of *GDF5* (Reynard et al., 2014). This ABTF of SP1 and SP3 may exemplify how the above mentioned MTF1 predisposed the hypomethylation of Cast allele within the *Hcn2* locus in our studies. Presumably, this MTF1 predisposes the Cast allele for

Tet proteins for demethylation; however, the extent to which the ABTF predisposes allelic hypomethylation remains to be determined (Martos et al., 2017). Working on chromosome 21 in leukocytes from healthy individuals, investigations also show that the genetic variation among individuals affects ASMs, thereby leading to ASE (Zhang et al., 2009). In acute lymphoblastic leukemia, ASE for 470 SNPs within 400 genes was detected. The level of ASE varies from a 1.4-fold overexpression of one allele to strictly monoallelic expression. Further investigation suggests that ASE is associated with promoter CpG site methylation (Milani et al., 2009).

2. **Genetic variants-resulting methylation of one allele for ASM and ASE.** In contrast to the demethylation of one allele for ASMs mentioned above, genetic variant-related methylation of one allele can also lead to ASMs and potential ASE. For example, the SNP rs12041331 has been linked to cardiovascular disease and platelet reactivity (Izzi et al., 2016). The major G allele of rs12041331 (leading to a CpG-SNP within the intron of the *PEAR1* locus) is linked to a higher transcript level than the minor A allele in endothelial cells and platelets. The resulting CpG site of GG carriers is fully methylated in leukocytes. Intriguingly, this methylated CpG site of the G allele recruits more nuclear proteins than does the unmethylated A allele. However, the authors did not characterize these nuclear proteins (Izzi et al., 2016); otherwise, their insights would be clearer. Based on our summary above, it is reasonable to expect a similar binding of TFs like ZFP57 to the methylated CpG site. That is, methylation-dependent recruitment of c-Jun and/or ATF3 (resulted due to CpG-SNP on the G allele) may understand the higher *PEAR1* expression and risk. More recent reports linking ASMs to disease or complex traits include the SNP rs174537-regulated ASM at the *FADS* gene locus for long-chain polyunsaturated fatty acid biosynthesis (Rahbar et al., 2018) and ASMs of susceptibility genes for inflammatory bowel disease (Chiba et al., 2018).

Is Dosage Effect the Key for Disease Risk?

Imprinting disorders have been linked to abnormal biallelic expression or biallelic silencing of imprinted genes in contrast to monoallelic expression (Bartolomei, 2009; Weksberg, 2010). The dosage effect is certainly key for imprinting disorders. As for non-imprinted loci with ASMs and/or ASE, we expect a similar role. Allelic imbalance—a hallmark of cancer—has been known to contribute to cancers for many years. For example, monoallelic expression of cancer-related genes, including *TP53* and *IDH1*, seems to be in association with tumor aggressiveness and progression (Walker et al., 2012). The ASE of *BRCA1* and, to a lesser extent, of *BRCA2*, contributes to an increased risk for breast cancer (Chen et al., 2008). ASE is also observed in acute lymphoblastic leukemia, as described above (Milani et al., 2009). Our thorough examinations including insulator CTCF-involved diseases/traits (examples in **Table 1**) and other TFs-mediated traits/diseases (described above) demonstrate the causative increase or decrease of gene transcripts of one allele. In the authors' opinion, this is a dosage effect, like imprinting disorders for complex traits or diseases.

VULNERABILITY OF GENETIC VARIANT-INFLUENCED ASMS AND/OR ASE IN RESPONSE TO ENVIRONMENTAL FACTORS FOR DISEASE RISK

The extent to which these genetic variants-influenced ASMs and ASE are vulnerable to environmental factors remains to be determined. However, we may learn from previous investigations on imprinted ASMs, as both imprinted ASMs and genetic variants-influenced (or non-imprinted) ASMs share the feature of mono-allelicity. Since there is no backup from the complementary allele, the mono-allelicity of methylation, presumably, is the cause for vulnerability. It is, therefore, reasonable to expect that ASMs (both imprinted and non-imprinted) are vulnerable to exposure.

The imprinted ASMs at ICRs, the key for imprinted gene expression, are known to be vulnerable to environmental exposures, including BPA and cadmium, as they can alter the allelic expression of imprinted genes and, consequently, increase disease susceptibility (Heijmans et al., 2008; Susiarjo et al., 2013; Van de Pette et al., 2017; Cowley et al., 2018). Indeed, in response to cadmium exposure, ASMs at ICRs do show a higher sensitivity to cadmium when compared to other loci in newborn cord blood and maternal blood (Cowley et al., 2018). As for alcohol use disorder, prenatal alcohol exposure alters one ASM of the *H19*/*Igf2* locus, thereby causing about a 1.5-fold decrease of *Igf2* transcripts (Downing et al., 2011). The ASMs of imprinted loci, including *Dio3,* and *H19*/*Igf2*, are susceptible to fetal alcohol exposure, thereby changing the allelic expression of *Dio3* and *Igf2* (Haycock and Ramsay, 2009; Tunc-Ozcan et al., 2016, 2018). Lastly, calorie restriction can also alter imprinted *Igf2* expression in a sex-dependent manner. In rats, moderate calorie restriction during gestational days 8 through 21 of Sprague-Dawley dams (F0) increases the adult hippocampal *Igf2* transcripts in F1 females, and in these F1 females-produced (in cross with naïve male Brown Norway) F2 offspring (Harper et al., 2014). Although it was not fully investigated as to whether calorie restriction altered ASM within the *H19*/*Igf2* locus for this intergenerational increase of *Igf2* in female offspring, similar treatment with maternal vitamin D depletion has suggested changes in DNA methylation (Xue et al., 2016).

With the established vulnerability of imprinted ASMs to exposure, the non-imprinted ASMs are expected to behave similarly. As exemplified above, the risk allele (AA carrier) of the *FKBP5* locus is indeed vulnerable to child abuse exposure (Klengel et al., 2013). With social or mental stress, the oxytocin receptor gene (*OXTR*) SNP rs53576 (G-A) is expected to be associated with social behavior. Investigations demonstrate that prenatal mental stress exposure is linked to child autistic traits, but not related to *OXTR* methylation across the rs53575 G allele homozygous children or A allele holder (Rijlaarsdam et al., 2017). Though not clear about the allelic sensitivity to

mental stress from the investigation, the *OXTR* methylation levels were positively in association with social problems for the G allele homozygous children (but not the A allele carriers). Using five human cell types for 50 treatments, Luca and colleagues identified 1,455 genes with ASE and 215 genes with gene-by-environment (GxE) interactions (Moyerbrailean et al., 2016). More importantly, exposure-perturbed genes showed a 7-fold increased odds of being reported in GWAS. Almost half of 215 genes showing GxE interactions are associated with complex traits, as revealed by GWAS. These results are consistent with the idea that genes with ASE are vulnerable to exposure. Additional evidence regarding alcohol use disorder also supports this idea. In rats, drinking alcohol affects the ASE of about 300 genes, as reported recently from Zhou and colleagues (Lo et al., 2018). This affection is expected through the crosstalk among genetic variants, epigenetic patterns, and alcohol exposure.

CONCLUSION, CHALLENGES, AND PERSPECTIVES

Accumulating evidence supports that the GWAS-identified variants in non-coding regions are implicated in complex human diseases or traits, an implication that involves an extensive crosstalk among SNPs, ASMs, and ABTFs for impacting ASE (**Figures 4A,B**), as well as environmental exposure-altering ASMs and ABTFs (**Figure 4C**), thereby rendering a person more susceptible to diverse diseases. Exposure to environmental factors (bisphenol A, metal, herbicides), alcohol, and cigarette smoke has been demonstrated to affect chromatin structure (DNA methylation and histone modifications), thereby potentially altering ASMs and ABTFs (Cowley et al., 2018; Meehan et al., 2018; Pathak and Feil, 2018; Strakovsky and Schantz, 2018; Zhu et al., 2018). With more investigations of the crosstalk of SNP-TFs-allelic expression changes and of SNP-insulator CTCF-allelic expression changes, which have burgeoned only in the past 2 years (**Table 1**), it becomes clearer that the signal of a small change at one residue (i.e., SNP) is intensified by introducing or abolishing allelic DNA methylation, thereby impacting the allelic recruitment or abolishment of TFs. The allele-specificity of TFs eventually increases or decreases transcript copies from one allele, and the resulting changes of dosage seem to be the key for disease risk (**Figure 4**). We thus coin this working model as the "SNP intensifier."

A future challenge is to provide more evidence to elucidate this mechanism of variants contributing to human disease susceptibility and inter-individual phenotypic differences. In regard to the elucidation, several roadblocks must first be cleared and a better standard must be established, including the quick characterization of all GWAS-associated genetic variants in affecting epigenetic patterns and gene transcription, and the conclusive determination of each variant's role in complex human disease susceptibility. More specifically, we should seek to identify all SNPs-resulted ASMs or methylation QTLs in a cost-effective and high throughput manner, characterize the chronic effect of slightly increased RNA transcripts of a gene for disease risk, and integrate layers of information from variants, ASMs/ASE, and exposure for deeper mechanistic insights.

The community certainly needs an integrated system for biological analyses of data from layers of genetic variants, epigenetic patterns, and expression QTL (eQTL). Intriguingly, a summary data-based Mendelian Randomization (SMR) method was recently developed (Zhu et al., 2016). The method of SMR borrows the concept of Mendelian Randomization (MR) analysis, which uses a genetic variant (e.g., a SNP) as an instrumental variable to assess the putative causative effect of an exposure (e.g., gene expression level) on an outcome (e.g., diseased phenotype). Because the variance in a phenotype explained by a single genetic variant, or the expression change of a single gene, is likely to be very small, a limitation of MR analysis is the requirement of an extremely large sample size. To overcome this limitation, Zhu et al. used the summary-level data (for instance, effect sizes or test statistics) available from the very large-scale GWAS and eQTL studies (Zhu et al., 2016). With SMR analyses, investigators integrated summary-level GWAS data on up to 339,224 individuals and eQTL data on 5,311 individuals for the identification of 126 genes in association with five human complex traits. Out of these 126 genes, *TRAF1* and *ANKRD55* were found to be associated with rheumatoid arthritis, and *SNX19* and *NMRAL1* were found to be associated with schizophrenia. Using the SMR approach, an independent group identified DNA methylation sites in association with GWAS-identified variants for multiple complex traits out of more than 40 traits examined (Hannon et al., 2017) and showed the potential role of genetic variants in the *RNASET2* locus in association with eQTL and mQTL (methylation quantitative trait locus) for Crohn's disease. Similarly, the group that first reported the SMR method also integrated the summary-level data of mQTL with that of GWAS and eQTL (Wu et al., 2018) and revealed pleiotropic associations between 7,858 DNA methylation sites and 2,733 genes, which can be regarded as a map of the methylome to the transcriptome. Further analyses identified 149 DNA methylation sites and 66 genes showing pleiotropic associations with 12 complex traits. Wu et al. hypothesize a mechanism whereby a genetic variant impacts complex disease by way of genetic modulation of transcription through DNA methylation.

Characterization of genetic variant-influenced ASMs remains a challenge as well. Not surprisingly, these ASMs show tissue specificity (Do et al., 2016; Marzi et al., 2016). Therefore, the cost-effective identification of all ASMs in different tissues is needed. With tissue specificity, methylation status of CpGs within a given ASM can be changed during cell development, and differentiation. For example, our data demonstrate that HCN2 ASM seems to exist in embryonic stem cells, but that CpG sites of unmethylated allele were methylated in differentiated neural progenitor cells and neurons (Martos et al., 2017). In addition, the characterization of vulnerability of each ASM, from different tissues to different environmental stresses, is also critical for understanding the complex human diseases. Lastly, the current method to analyze DNA methylation for large cohort studies relies on an array-based approach that is limited to low resolution, and

there is an urgent need for an alternative sequencing-based method for efficient screening of hundreds or thousands of samples.

Due to the accompanied ethnic issues of human samples, animal studies are required to solve the mystery of the detailed mechanistic insights. For example, animal studies are needed for exploration of the effect of chronic and even subtle changes of one allele. F1 hybrid mice, between two strains of rat or mouse, have many more SNPs (for example, up to 25 million SNPs between mouse strains 129 and Cast) for insights (Schilling et al., 2009; Lossie et al., 2014; Lo et al., 2016; Martos et al., 2017). The interactions between genetic variants and disease susceptibility may be tested via different crossing strategies in the Diversity Outbred mouse population and the Collaborative Cross inbred stains (French et al., 2018), another hot topic that will not be described in detail in this review.

While the mechanistic insights gained through the extensive hard work above have brought the community closer to our ultimate goal of finding opportunities for the intervention and prevention of human diseases, at least one investigation has shown encouraging results in this regard. Administration of thyroxin (T4) or metformin to neonatal rats after fetal alcohol exposure was shown to reverse the expression changes of *Dio3* and *Igf2* and to alleviate the fear memory deficit that was triggered by fetal alcohol exposure (Tunc-Ozcan et al., 2018). This reverse encourages the exploration of drugs for potential intervention.

Finally, the evidence from our own studies suggests the existence of ASMs that are independent of SNPs (Martos et al., 2017) in mouse embryonic stem cells that were generated from an inbred mouse strain 129 (i.e., no SNPs between two alleles). To understand the significance and mechanism of these random ASMs, we envision a similar mechanism to XCI and propose a hypothesis of regional "autosomal chromosome inactivation (ACI)" (Martos et al., 2017). However, the significance and impact of ACI on human health remains a mystery.

AUTHOR CONTRIBUTIONS

HW, DL, and ZW prepared the manuscript. HW and DL contribute significantly in terms of literature reading, summarizing, and presenting.

ACKNOWLEDGMENTS

The laboratory of ZW at Johns Hopkins was supported by U.S. National Institutes of Health (R01ES25761, U01ES026721 opportunity fund, and R21ES028351) and Johns Hopkins Catalyst Award. ZW also thanks Dr. Jian Yang at the University of Queensland for the critical reading of the manuscript, and sincerely apologizes to fellow investigators whose important contributions were not directly referenced due to space and reference limitations.

REFERENCES

Allen, E. K., Randolph, A. G., Bhangale, T., Dogra, P., Ohlson, M., Oshansky, C. M., et al. (2017). SNP-mediated disruption of CTCF binding at the IFITM3 promoter is associated with risk of severe influenza in humans. *Nat. Med.* 23, 975–983. doi: 10.1038/nm.4370

Allfrey, V. G., Faulkner, R., and Mirsky, A. E. (1964). Acetylation and methylation of histones and their possible role in the regulation of Rna synthesis. *Proc. Natl. Acad. Sci. U.S.A.* 51, 786–794. doi: 10.1073/pnas.51.5.786

Anvar, Z., Cammisa, M., Riso, V., Baglivo, I., Kukreja, H., Sparago, A., et al. (2016). ZFP57 recognizes multiple and closely spaced sequence motif variants to maintain repressive epigenetic marks in mouse embryonic stem cells. *Nucleic Acids Res.* 44, 1118–1132. doi: 10.1093/nar/gkv1059

Barski, A., Cuddapah, S., Cui, K., Roh, T. Y., Schones, D. E., Wang, Z., et al. (2007). High-resolution profiling of histone methylations in the human genome. *Cell* 129, 823–837. doi: 10.1016/j.cell.2007.05.009

Bartolomei, M. S. (2009). Genomic imprinting: employing and avoiding epigenetic processes. *Genes Dev.* 23, 2124–2133. doi: 10.1101/gad.1841409

Bastaki, F., Nair, P., Mohamed, M., Malik, E. M., Helmi, M., Al-Ali, M. T., et al. (2017). Identification of a novel CTCF mutation responsible for syndromic intellectual disability - a case report. *BMC Med. Genet.* 18:68. doi: 10.1186/s12881-017-0429-0

Bell, A. C., and Felsenfeld, G. (2000). Methylation of a CTCF-dependent boundary controls imprinted expression of the Igf2 gene. *Nature* 405, 482–485. doi: 10.1038/35013100

Bernstein, B. E., Mikkelsen, T. S., Xie, X., Kamal, M., Huebert, D. J., Cuff, J., et al. (2006). A bivalent chromatin structure marks key developmental genes in embryonic stem cells. *Cell* 125, 315–326. doi: 10.1016/j.cell.2006.02.041

Bérubé, S., Al Tuwaijri, A., Kohan-Ghadr, H. R., Elzein, S., Farias, R., Berube, J., et al. (2017). Role of DNA methylation in expression control of the IKZF3-GSDMA region in human epithelial cells. *PLoS ONE* 12:e0172707. doi: 10.1371/journal.pone.0172707

Bestor, T. H. (2000). The DNA methyltransferases of mammals. *Hum. Mol. Genet.* 9, 2395–2402. doi: 10.1093/hmg/9.16.2395

Blattler, A., Yao, L., Witt, H., Guo, Y., Nicolet, C. M., Berman, B. P., et al. (2014). Global loss of DNA methylation uncovers intronic enhancers in genes showing expression changes. *Genome Biol.* 15:469. doi: 10.1186/s13059-014-0469-0

Chen, X., Weaver, J., Bove, B. A., Vanderveer, L. A., Weil, S. C., Miron, A., et al. (2008). Allelic imbalance in BRCA1 and BRCA2 gene expression is associated with an increased breast cancer risk. *Hum. Mol. Genet.* 17, 1336–1348. doi: 10.1093/hmg/ddn022

Chen, X. F., Zhu, D. L., Yang, M., Hu, W. X., Duan, Y. Y., Lu, B. J., et al. (2018). An osteoporosis risk SNP at 1p36.12 acts as an allele-specific enhancer to modulate LINC00339 expression via long-range loop formation. *Am. J. Hum. Genet.* 102, 776–793. doi: 10.1016/j.ajhg.2018.03.001

Cheng, H., Xuan, H., Green, C. D., Han, Y., Sun, N., Shen, H., et al. (2018). Repression of human and mouse brain inflammaging transcriptome by broad gene-body histone hyperacetylation. *Proc. Natl. Acad. Sci. U.S.A.* 115, 7611–7616. doi: 10.1073/pnas.1800656115

Cheng, M., Liu, X., Yang, M., Han, L., Xu, A., and Huang, Q. (2017). Computational analyses of type 2 diabetes-associated loci identified by genome-wide association studies. *J. Diabetes* 9, 362–377. doi: 10.1111/1753-0407.12421

Cheung, W. A., Shao, X., Morin, A., Siroux, V., Kwan, T., Ge, B., et al. (2017). Functional variation in allelic methylomes underscores a strong genetic contribution and reveals novel epigenetic alterations in the human epigenome. *Genome Biol.* 18:50. doi: 10.1186/s13059-017-1173-7

Chiba, H., Kakuta, Y., Kinouchi, Y., Kawai, Y., Watanabe, K., Nagao, M., et al. (2018). Allele-specific DNA methylation of disease susceptibility genes in Japanese patients with inflammatory bowel disease. *PLoS ONE* 13:e0194036. doi: 10.1371/journal.pone.0194036

Cowley, M., Skaar, D. A., Jima, D. D., Maguire, R. L., Hudson, K. M., Park, S. S., et al. (2018). Effects of cadmium exposure on dna methylation at imprinting control regions and genome-wide in mothers and newborn children. *Environ. Health Perspect.* 126:037003. doi: 10.1289/EHP2085

Creyghton, M. P., Cheng, A. W., Welstead, G. G., Kooistra, T., Carey, B. W., Steine, E. J., et al. (2010). Histone H3K27ac separates active from poised enhancers and predicts developmental state. *Proc. Natl. Acad. Sci. U.S.A.* 107, 21931–21936. doi: 10.1073/pnas.1016071107

Cuddapah, S., Jothi, R., Schones, D. E., Roh, T. Y., Cui, K., and Zhao, K. (2009). Global analysis of the insulator binding protein CTCF in chromatin barrier regions reveals demarcation of active and repressive domains. *Genome Res.* 19, 24–32. doi: 10.1101/gr.082800.108

Dagar, V., Hutchison, W., Muscat, A., Krishnan, A., Hoke, D., Buckle, A., et al. (2018). Genetic variation affecting DNA methylation and the human imprinting disorder, Beckwith-Wiedemann syndrome. *Clin. Epigenetics* 10:114. doi: 10.1186/s13148-018-0546-4

Dai, H., and Wang, Z. (2014). Histone modification patterns and their responses to environment. *Curr. Envir. Health Rep.* 1, 11–21. doi: 10.1007/s40572-013-0008-2

Dai, J., Zhu, M., Wang, C., Shen, W., Zhou, W., Sun, J., et al. (2015). Systematical analyses of variants in CTCF-binding sites identified a novel lung cancer susceptibility locus among Chinese population. *Sci. Rep.* 5:7833. doi: 10.1038/srep07833

de la Rica, L., Rodríguez-Ubreva, J., García, M., Islam, A. B., Urquiza, J. M., Hernando, H., et al. (2013). PU.1 target genes undergo Tet2-coupled demethylation and DNMT3b-mediated methylation in monocyte-to-osteoclast differentiation. *Genome Biol.* 14:R99. doi: 10.1186/gb-2013-14-9-r99

Do, C., Lang, C. F., Lin, J., Darbary, H., Krupska, I., Gaba, A., et al. (2016). Mechanisms and disease associations of haplotype-dependent allele-specific DNA methylation. *Am. J. Hum. Genet.* 98, 934–955. doi: 10.1016/j.ajhg.2016.03.027

Dolinoy, D. C. (2008). The agouti mouse model: an epigenetic biosensor for nutritional and environmental alterations on the fetal epigenome. *Nutr. Rev.* 66 (Suppl. 1), S7–S11. doi: 10.1111/j.1753-4887.2008.00056.x

Dolinoy, D. C., Huang, D., and Jirtle, R. L. (2007). Maternal nutrient supplementation counteracts bisphenol A-induced DNA hypomethylation in early development. *Proc. Natl. Acad. Sci. U.S.A.* 104, 13056–13061. doi: 10.1073/pnas.0703739104

Downing, C., Johnson, T. E., Larson, C., Leakey, T. I., Siegfried, R. N., Rafferty, T. M., et al. (2011). Subtle decreases in DNA methylation and gene expression at the mouse Igf2 locus following prenatal alcohol exposure: effects of a methyl-supplemented diet. *Alcohol* 45, 65–71. doi: 10.1016/j.alcohol.2010.07.006

Eroglu, A., and Layman, L. C. (2012). Role of ART in imprinting disorders. *Semin. Reprod. Med.* 30, 92–104. doi: 10.1055/s-0032-1307417

Farh, K. K., Marson, A., Zhu, J., Kleinewietfeld, M., Housley, W. J., Beik, S., et al. (2015). Genetic and epigenetic fine mapping of causal autoimmune disease variants. *Nature* 518, 337–343. doi: 10.1038/nature13835

French, J. E., Gatti, D. M., Morgan, D. L., Kissling, G. E., Shockley, K. R., Knudsen, G. A., et al. (2018). Erratum: "diversity outbred mice identify population-based exposure thresholds and genetic factors that influence benzene-induced genotoxicity". *Environ. Health Perspect.* 126:069003. doi: 10.1289/EHP3950

Gallagher, M. D., Posavi, M., Huang, P., Unger, T. L., Berlyand, Y., Gruenewald, A. L., et al. (2017). A dementia-associated risk variant near TMEM106B alters chromatin architecture and gene expression. *Am. J. Hum. Genet.* 101, 643–663. doi: 10.1016/j.ajhg.2017.09.004

Gao, Y., Baccarelli, A., Shu, X. O., Ji, B. T., Yu, K., Tarantini, L., et al. (2012). Blood leukocyte Alu and LINE-1 methylation and gastric cancer risk in the Shanghai Women's Health Study. *Br. J. Cancer* 106, 585–591. doi: 10.1038/bjc.2011.562

Gordon, S., Akopyan, G., Garban, H., and Bonavida, B. (2006). Transcription factor YY1: structure, function, and therapeutic implications in cancer biology. *Oncogene* 25, 1125–1142. doi: 10.1038/sj.onc.1209080

Goudarzi, A., Zhang, D., Huang, H., Barral, S., Kwon, O. K., Qi, S., et al. (2016). Dynamic competing histone H4 K5K8 acetylation and butyrylation are hallmarks of highly active gene promoters. *Mol. Cell* 62, 169–180. doi: 10.1016/j.molcel.2016.03.014

Hancock, D. B., Guo, Y., Reginsson, G. W., Gaddis, N. C., Lutz, S. M., Sherva, R., et al. (2017). Genome-wide association study across European and African American ancestries identifies a SNP in DNMT3B contributing to nicotine dependence. *Mol. Psychiatry* 23, 1–9. doi: 10.1038/mp.2017.193

Hannon, E., Weedon, M., Bray, N., O'Donovan, M., and Mill, J. (2017). Pleiotropic effects of trait-associated genetic variation on dna methylation: utility for refining GWAS loci. *Am. J. Hum. Genet.* 100, 954–959. doi: 10.1016/j.ajhg.2017.04.013

Harper, K. M., Tunc-Ozcan, E., Graf, E. N., Herzing, L. B., and Redei, E. E. (2014). Intergenerational and parent of origin effects of maternal calorie restriction on Igf2 expression in the adult rat hippocampus. *Psychoneuroendocrinology* 45, 187–191. doi: 10.1016/j.psyneuen.2014.04.002

Haycock, P. C., and Ramsay, M. (2009). Exposure of mouse embryos to ethanol during preimplantation development: effect on DNA methylation in the h19 imprinting control region. *Biol. Reprod.* 81, 618–627. doi: 10.1095/biolreprod.108.074682

Heijmans, B. T., Tobi, E. W., Stein, A. D., Putter, H., Blauw, G. J., Susser, E. S., et al. (2008). Persistent epigenetic differences associated with prenatal exposure to famine in humans. *Proc. Natl. Acad. Sci. U.S.A.* 105, 17046–17049. doi: 10.1073/pnas.0806560105

Hori, I., Kawamura, R., Nakabayashi, K., Watanabe, H., Higashimoto, K., Tomikawa, J., et al. (2017). CTCF deletion syndrome: clinical features and epigenetic delineation. *J. Med. Genet.* 54, 836–842. doi: 10.1136/jmedgenet-2017-104854

Hrdlickova, B., de Almeida, R. C., Borek, Z., and Withoff, S. (2014). Genetic variation in the non-coding genome: involvement of micro-RNAs and long non-coding RNAs in disease. *Biochim. Biophys. Acta* 1842, 1910–1922. doi: 10.1016/j.bbadis.2014.03.011

Izzi, B., Pistoni, M., Cludts, K., Akkor, P., Lambrechts, D., Verfaillie, C., et al. (2016). Allele-specific DNA methylation reinforces PEAR1 enhancer activity. *Blood* 128, 1003–1012. doi: 10.1182/blood-2015-11-682153

Jeltsch, A. (2006). On the enzymatic properties of Dnmt1: specificity, processivity, mechanism of linear diffusion and allosteric regulation of the enzyme. *Epigenetics* 1, 63–66. doi: 10.4161/epi.1.2.2767

Jiang, X., Detera-Wadleigh, S. D., Akula, N., Mallon, B. S., Hou, L., Xiao, T., et al. (2018). Sodium valproate rescues expression of TRANK1 in iPSC-derived neural cells that carry a genetic variant associated with serious mental illness. *Mol. Psychiatry* doi: 10.1038/s41380-018-0207-1. [Epub ahead of print].

Jones, P. A., and Liang, G. (2009). Rethinking how DNA methylation patterns are maintained. *Nat. Rev. Genet.* 10, 805–811. doi: 10.1038/nrg2651

Jurkowska, R. Z., Jurkowski, T. P., and Jeltsch, A. (2011). Structure and function of mammalian DNA methyltransferases. *Chembiochem* 12, 206–222. doi: 10.1002/cbic.201000195

Kaminen-Ahola, N., Ahola, A., Maga, M., Mallitt, K. A., Fahey, P., Cox, T. C., et al. (2010). Maternal ethanol consumption alters the epigenotype and the phenotype of offspring in a mouse model. *PLoS Genet.* 6:e1000811. doi: 10.1371/journal.pgen.1000811

Kemp, C. J., Moore, J. M., Moser, R., Bernard, B., Teater, M., Smith, L. E., et al. (2014). CTCF haploinsufficiency destabilizes DNA methylation and predisposes to cancer. *Cell Rep.* 7, 1020–1029. doi: 10.1016/j.celrep.2014.04.004

Kerkel, K., Spadola, A., Yuan, E., Kosek, J., Jiang, L., Hod, E., et al. (2008). Genomic surveys by methylation-sensitive SNP analysis identify sequence-dependent allele-specific DNA methylation. *Nat. Genet.* 40, 904–908. doi: 10.1038/ng.174

Khandanpour, C., Krongold, J., Schütte, J., Bouwman, F., Vassen, L., Gaudreau, M. C., et al. (2012). The human GFI136N variant induces epigenetic changes at the Hoxa9 locus and accelerates K-RAS driven myeloproliferative disorder in mice. *Blood* 120, 4006–4017. doi: 10.1182/blood-2011-02-334722

Kidd, C. D., Thompson, P. J., Barrett, L., and Baltic, S. (2016). Histone modifications and Asthma. The interface of the epigenetic and genetic landscapes. *Am. J. Respir. Cell Mol. Biol.* 54, 3–12. doi: 10.1165/rcmb.2015-0050TR

Kilpinen, H., Waszak, S. M., Gschwind, A. R., Raghav, S. K., Witwicki, R. M., Orioli, A., et al. (2013). Coordinated effects of sequence variation on DNA binding, chromatin structure, and transcription. *Science* 342, 744–747. doi: 10.1126/science.1242463

Kim, D. S., Kim, Y. H., Lee, W. K., Na, Y. K., and Hong, H. S. (2016). Effect of alcohol consumption on peripheral blood Alu methylation in Korean men. *Biomarkers* 21, 243–248. doi: 10.3109/1354750X.2015.1134661

Kim, T. H., Abdullaev, Z. K., Smith, A. D., Ching, K. A., Loukinov, D. I., Green, R. D., et al. (2007). Analysis of the vertebrate insulator protein CTCF-binding sites in the human genome. *Cell* 128, 1231–1245. doi: 10.1016/j.cell.2006.12.048

Klengel, T., Mehta, D., Anacker, C., Rex-Haffner, M., Pruessner, J. C., Pariante, C. M., et al. (2013). Allele-specific FKBP5 DNA demethylation mediates gene-childhood trauma interactions. *Nat. Neurosci.* 16, 33–41. doi: 10.1038/nn.3275

Kumar, D., Puan, K. J., Andiappan, A. K., Lee, B., Westerlaken, G. H., Haase, D., et al. (2017). A functional SNP associated with atopic dermatitis controls cell type-specific methylation of the VSTM1 gene locus. *Genome Med.* 9:18. doi: 10.1186/s13073-017-0404-6

Kundakovic, M., Gudsnuk, K., Herbstman, J. B., Tang, D., Perera, F. P., and Champagne, F. A. (2015). DNA methylation of BDNF as a biomarker of early-life adversity. *Proc. Natl. Acad. Sci. U.S.A.* 112, 6807–6813. doi: 10.1073/pnas.1408355111

Li, H., Li, W., Liu, S., Zong, S., Wang, W., Ren, J., et al. (2016). DNMT1, DNMT3A and DNMT3B polymorphisms associated with gastric cancer risk: a systematic review and meta-analysis. *EBioMed.* 13, 125–131. doi: 10.1016/j.ebiom.2016.10.028

Li, W., Shang, L., Huang, K., Li, J., Wang, Z., and Yao, H. (2017). Identification of critical base pairs required for CTCF binding in motif M1 and M2. *Protein Cell* 8, 544–549. doi: 10.1007/s13238-017-0387-5

Li, X., Kim, Y., Tsang, E. K., Davis, J. R., Damani, F. N., Chiang, C., et al. (2017). The impact of rare variation on gene expression across tissues. *Nature* 550, 239–243. doi: 10.1038/nature24267

Li, Y., Zhang, Z., Chen, J., Liu, W., Lai, W., Liu, B., et al. (2018). Stella safeguards the oocyte methylome by preventing de novo methylation mediated by DNMT1. *Nature* 564, 136–140. doi: 10.1038/s41586-018-0751-5

Li, Z., Dai, H., Martos, S. N., Xu, B., Gao, Y., Li, T., et al. (2015). Distinct roles of DNMT1-dependent and DNMT1-independent methylation patterns in the genome of mouse embryonic stem cells. *Genome Biol.* 16:115. doi: 10.1186/s13059-015-0685-2

Ling, C., Fangyu, D., Wanhua, H., Kelong, C., Zhimin, W., Yuting, Z., et al. (2016). DNMT3A rs1550117 Polymorphism is associated with late-onset alzheimer's disease in a Chinese population. *Am. J. Alzheimers. Dis. Other Demen.* 31, 278–281. doi: 10.1177/1533317515603688

Lister, R., Pelizzola, M., Dowen, R. H., Hawkins, R. D., Hon, G., Tonti-Filippini, J., et al. (2009). Human DNA methylomes at base resolution show widespread epigenomic differences. *Nature* 462, 315–322. doi: 10.1038/nature08514

Liu, Q., Thoms, J. A. I., Nunez, A. C., Huang, Y., Knezevic, K., Packham, D., et al. (2018). Disruption of a−35 kb enhancer impairs CTCF binding and MLH1 expression in colorectal cells. *Clin. Cancer Res.* 24, 4602–4611. doi: 10.1158/1078-0432.CCR-17-3678

Lo, C. L., Lossie, A. C., Liang, T., Liu, Y., Xuei, X., Lumeng, L., et al. (2016). High resolution genomic scans reveal genetic architecture controlling alcohol preference in bidirectionally selected rat model. *PLoS Genet.* 12:e1006178. doi: 10.1371/journal.pgen.1006178

Lo, C. L., Lumeng, L., Bell, R. L., Liang, T., Lossie, A. C., Muir, W. M., et al. (2018). CIS-acting allele-specific expression differences induced by alcohol and impacted by sex as well as parental genotype of origin. *Alcohol. Clin. Exp. Res.* 42, 1444–1453. doi: 10.1111/acer.13776

Lockwood, S. H., Guan, A., Yu, A. S., Zhang, C., Zykovich, A., Korf, I., et al. (2014). The functional significance of common polymorphisms in zinc finger transcription factors. *G3* 4, 1647–1655. doi: 10.1534/g3.114.012195

Lossie, A. C., Muir, W. M., Lo, C. L., Timm, F., Liu, Y., Gray, W., et al. (2014). Implications of genomic signatures in the differential vulnerability to fetal alcohol exposure in C57BL/6 and DBA/2 mice. *Front. Genet.* 5:173. doi: 10.3389/fgene.2014.00173

Marjonen, H., Auvinen, P., Kahila, H., Tšuiko, O., Kõks, S., Tiirats, A., et al. (2018). rs10732516 polymorphism at the IGF2/H19 locus associates with genotype-specific effects on placental DNA methylation and birth weight of newborns conceived by assisted reproductive technology. *Clin. Epigenetics* 10:80. doi: 10.1186/s13148-018-0511-2

Marjonen, H., Kahila, H., and Kaminen-Ahola, N. (2017). rs10732516 polymorphism at the IGF2/H19 locus associates with a genotype-specific trend in placental DNA methylation and head circumference of prenatally alcohol-exposed newborns. *Human Reprod. Open* 2017, 1–12. doi: 10.1093/hropen/hox014

Martos, S. N., Li, T., Ramos, R. B., Lou, D., Dai, H., Xu, J. C., et al. (2017). Two approaches reveal a new paradigm of 'switchable or genetics-influenced allele-specific DNA methylation' with potential in human disease. *Cell Discov.* 3:17038. doi: 10.1038/celldisc.2017.38

Marzi, S. J., Meaburn, E. L., Dempster, E. L., Lunnon, K., Paya-Cano, J. L., Smith, R. G., et al. (2016). Tissue-specific patterns of allelically-skewed DNA methylation. *Epigenetics* 11, 24–35. doi: 10.1080/15592294.2015.1127479

McVicker, G., van de Geijn, B., Degner, J. F., Cain, C. E., Banovich, N. E., Raj, A., et al. (2013). Identification of genetic variants that affect histone modifications in human cells. *Science* 342, 747–749. doi: 10.1126/science.1242429

Meehan, R. R., Thomson, J. P., Lentini, A., Nestor, C. E., and Pennings, S. (2018). DNA methylation as a genomic marker of exposure to chemical and environmental agents. *Curr. Opin. Chem. Biol.* 45, 48–56. doi: 10.1016/j.cbpa.2018.02.006

Milani, L., Lundmark, A., Nordlund, J., Kiialainen, A., Flaegstad, T., Jonmundsson, G., et al. (2009). Allele-specific gene expression patterns in primary leukemic cells reveal regulation of gene expression by CpG site methylation. *Genome Res.* 19, 1–11. doi: 10.1101/gr.083931.108

Moffatt, M. F., Gut, I. G., Demenais, F., Strachan, D. P., Bouzigon, E., Heath, S., et al. (2010). A large-scale, consortium-based genomewide association study of asthma. *N. Engl. J. Med.* 363, 1211–1221. doi: 10.1056/NEJMoa0906312

Moyerbrailean, G. A., Richards, A. L., Kurtz, D., Kalita, C. A., Davis, G. O., Harvey, C. T., et al. (2016). High-throughput allele-specific expression across 250 environmental conditions. *Genome Res.* 26, 1627–1638. doi: 10.1101/gr.209759.116

Nelson, H. H., Marsit, C. J., and Kelsey, K. T. (2011). Global methylation in exposure biology and translational medical science. *Environ. Health Perspect.* 119, 1528–1533. doi: 10.1289/ehp.1103423

Okano, M., Bell, D. W., Haber, D. A., and Li, E. (1999). DNA methyltransferases Dnmt3a and Dnmt3b are essential for *de novo* methylation and mammalian development. *Cell* 99, 247–257. doi: 10.1016/S0092-8674(00)81656-6

Ong, C. T., and Corces, V. G. (2014). CTCF: an architectural protein bridging genome topology and function. *Nat. Rev. Genet.* 15, 234–246. doi: 10.1038/nrg3663

Pathak, R., and Feil, R. (2018). Environmental effects on chromatin repression at imprinted genes and endogenous retroviruses. *Curr. Opin. Chem. Biol.* 45, 139–147. doi: 10.1016/j.cbpa.2018.04.015

Phillips, J. E., and Corces, V. G. (2009). CTCF: master weaver of the genome. *Cell* 137, 1194–1211. doi: 10.1016/j.cell.2009.06.001

Pidsley, R., Dempster, E., Troakes, C., Al-Sarraj, S., and Mill, J. (2012). Epigenetic and genetic variation at the IGF2/H19 imprinting control region on 11p15.5 is associated with cerebellum weight. *Epigenetics* 7, 155–163. doi: 10.4161/epi.7.2.18910

Quenneville, S., Verde, G., Corsinotti, A., Kapopoulou, A., Jakobsson, J., Offner, S., et al. (2011). In embryonic stem cells, ZFP57/KAP1 recognize a methylated hexanucleotide to affect chromatin and DNA methylation of imprinting control regions. *Mol. Cell* 44, 361–372. doi: 10.1016/j.molcel.2011.08.032

Rahbar, E., Waits, C. M. K., Kirby, E. H. Jr., Miller, L. R., Ainsworth, H. C., Cui, T., et al. (2018). Allele-specific methylation in the FADS genomic region in DNA from human saliva, CD4+ cells, and total leukocytes. *Clin. Epigenetics* 10:46. doi: 10.1186/s13148-018-0480-5

Reynard, L. N., Bui, C., Syddall, C. M., and Loughlin, J. (2014). CpG methylation regulates allelic expression of GDF5 by modulating binding of SP1 and SP3 repressor proteins to the osteoarthritis susceptibility SNP rs143383. *Hum. Genet.* 133, 1059–1073. doi: 10.1007/s00439-014-1447-z

Rijlaarsdam, J., van IJzendoorn, M. H., Verhulst, F. C., Jaddoe, V. W., Felix, J. F., Tiemeier, H., et al. (2017). Prenatal stress exposure, oxytocin receptor gene (OXTR) methylation, and child autistic traits: the moderating role of OXTR rs53576 genotype. *Autism Res.* 10, 430–438. doi: 10.1002/aur.1681

Riso, V., Cammisa, M., Kukreja, H., Anvar, Z., Verde, G., Sparago, A., et al. (2016). ZFP57 maintains the parent-of-origin-specific expression of the imprinted genes and differentially affects non-imprinted targets in mouse embryonic stem cells. *Nucleic Acids Res.* 44, 8165–8178. doi: 10.1093/nar/gkw505

Rivollier, F., Chaumette, B., Bendjemaa, N., Chayet, M., Millet, B., Jaafari, N., et al. (2017). Methylomic changes in individuals with psychosis, prenatally exposed to endocrine disrupting compounds: lessons from diethylstilbestrol. *PLoS ONE* 12:e0174783. doi: 10.1371/journal.pone.0174783

Roh, T. Y., Cuddapah, S., Cui, K., and Zhao, K. (2006). The genomic landscape of histone modifications in human T cells. *Proc. Natl. Acad. Sci. U.S.A.* 103, 15782–15787. doi: 10.1073/pnas.0607617103

Rutten, B. P. F., Vermetten, E., Vinkers, C. H., Ursini, G., Daskalakis, N. P., Pishva, E., et al. (2018). Longitudinal analyses of the DNA methylome in deployed military servicemen identify susceptibility loci for post-traumatic stress disorder. *Mol. Psychiatry* 23, 1145–1156. doi: 10.1038/mp.2017.120

Saradalekshmi, K. R., Neetha, N. V., Sathyan, S., Nair, I. V., Nair, C. M., and Banerjee, M. (2014). DNA methyl transferase (DNMT) gene polymorphisms could be a primary event in epigenetic susceptibility to schizophrenia. *PLoS ONE* 9:e98182. doi: 10.1371/journal.pone.0098182

Schilling, E., El Chartouni, C., and Rehli, M. (2009). Allele-specific DNA methylation in mouse strains is mainly determined by cis-acting sequences. *Genome Res.* 19, 2028–2035. doi: 10.1101/gr.095562.109

Schmiedel, B. J., Seumois, G., Samaniego-Castruita, D., Cayford, J., Schulten, V., Chavez, L., et al. (2016). 17q21 asthma-risk variants switch CTCF binding and regulate IL-2 production by T cells. *Nat. Commun.* 7:13426. doi: 10.1038/ncomms13426

Singh, P., Lee, D. H., and Szabó, P. E. (2012). More than insulator: multiple roles of CTCF at the H19-Igf2 imprinted domain. *Front. Genet.* 3:214. doi: 10.3389/fgene.2012.00214

Soldner, F., Stelzer, Y., Shivalila, C. S., Abraham, B. J., Latourelle, J. C., Barrasa, M. I., et al. (2016). Parkinson-associated risk variant in distal enhancer of alpha-synuclein modulates target gene expression. *Nature* 533, 95–99. doi: 10.1038/nature17939

Spilianakis, C. G., Lalioti, M. D., Town, T., Lee, G. R., and Flavell, R. A. (2005). Interchromosomal associations between alternatively expressed loci. *Nature* 435, 637–645. doi: 10.1038/nature03574

Strahl, B. D., and Allis, C. D. (2000). The language of covalent histone modifications. *Nature* 403, 41–45. doi: 10.1038/47412

Strakovsky, R. S., and Schantz, S. L. (2018). Impacts of bisphenol A (BPA) and phthalate exposures on epigenetic outcomes in the human placenta. *Environ. Epigenet.* 4:dvy022. doi: 10.1093/eep/dvy022

Strogantsev, R., Krueger, F., Yamazawa, K., Shi, H., Gould, P., Goldman-Roberts, M., et al. (2015). Allele-specific binding of ZFP57 in the epigenetic regulation of imprinted and non-imprinted monoallelic expression. *Genome Biol.* 16:112. doi: 10.1186/s13059-015-0672-7

Susiarjo, M., Sasson, I., Mesaros, C., and Bartolomei, M. S. (2013). Bisphenol a exposure disrupts genomic imprinting in the mouse. *PLoS Genet.* 9:e1003401. doi: 10.1371/journal.pgen.1003401

Tan, M., Luo, H., Lee, S., Jin, F., Yang, J. S., Montellier, E., et al. (2011). Identification of 67 histone marks and histone lysine crotonylation as a new type of histone modification. *Cell* 146, 1016–1028. doi: 10.1016/j.cell.2011.08.008

Tehranchi, A. K., Myrthil, M., Martin, T., Hie, B. L., Golan, D., and Fraser, H. B. (2016). Pooled ChIP-seq links variation in transcription factor binding to complex disease risk. *Cell* 165, 730–741. doi: 10.1016/j.cell.2016.03.041

Treit, S., Zhou, D., Chudley, A. E., Andrew, G., Rasmussen, C., Nikkel, S. M., et al. (2016). Relationships between head circumference, brain volume and cognition in children with prenatal alcohol exposure. *PLoS ONE* 11:e0150370. doi: 10.1371/journal.pone.0150370

Tunc-Ozcan, E., Harper, K. M., Graf, E. N., and Redei, E. E. (2016). Thyroxine administration prevents matrilineal intergenerational consequences of *in utero* ethanol exposure in rats. *Horm. Behav.* 82, 1–10. doi: 10.1016/j.yhbeh.2016.04.002

Tunc-Ozcan, E., Wert, S. L., Lim, P. H., Ferreira, A., and Redei, E. E. (2018). Hippocampus-dependent memory and allele-specific gene expression in adult offspring of alcohol-consuming dams after neonatal treatment with thyroxin or metformin. *Mol. Psychiatry* 23, 1643–1651. doi: 10.1038/mp.2017.129

Van de Pette, M., Abbas, A., Feytout, A., McNamara, G., Bruno, L., To, W. K., et al. (2017). Visualizing changes in Cdkn1c expression links early-life adversity to imprint mis-regulation in adults. *Cell Rep.* 18, 1090–1099. doi: 10.1016/j.celrep.2017.01.010

Van Rechem, C., and Whetstine, J. R. (2014). Examining the impact of gene variants on histone lysine methylation. *Biochim. Biophys. Acta* 1839, 1463–1476. doi: 10.1016/j.bbagrm.2014.05.014

Volkov, P., Olsson, A. H., Gillberg, L., Jørgensen, S. W., Brøns, C., Eriksson, K. F., et al. (2016). A genome-wide mQTL analysis in human adipose tissue identifies genetic variants associated with DNA methylation, gene expression and metabolic traits. *PLoS ONE* 11:e0157776. doi: 10.1371/journal.pone.0157776

Walker, E. J., Zhang, C., Castelo-Branco, P., Hawkins, C., Wilson, W., Zhukova, N., et al. (2012). Monoallelic expression determines oncogenic progression and outcome in benign and malignant brain tumors. *Cancer Res.* 72, 636–644. doi: 10.1158/0008-5472.CAN-11-2266

Wang, Z., Zang, C., Rosenfeld, J. A., Schones, D. E., Barski, A., Cuddapah, S., et al. (2008). Combinatorial patterns of histone acetylations and methylations in the human genome. *Nat. Genet.* 40, 897–903. doi: 10.1038/ng.154

Weksberg, R. (2010). Imprinted genes and human disease. *Am. J. Med. Genet. C Semin. Med. Genet.* 154C, 317–320. doi: 10.1002/ajmg.c.30268

Welter, D., MacArthur, J., Morales, J., Burdett, T., Hall, P., Junkins, H., et al. (2014). The NHGRI GWAS Catalog, a curated resource of SNP-trait associations. *Nucleic Acids Res.* 42, D1001–D1006. doi: 10.1093/nar/gkt1229

Wu, Y., Zeng, J., Zhang, F., Zhu, Z., Qi, T., Zheng, Z., et al. (2018). Integrative analysis of omics summary data reveals putative mechanisms underlying complex traits. *Nat. Commun.* 9:918. doi: 10.1038/s41467-018-03371-0

Xue, J., Schoenrock, S. A., Valdar, W., Tarantino, L. M., and Ideraabdullah, F. Y. (2016). Maternal vitamin D depletion alters DNA methylation at imprinted loci in multiple generations. *Clin. Epigenetics* 8:107. doi: 10.1186/s13148-016-0276-4

Yang, H. H., Hu, N., Wang, C., Ding, T., Dunn, B. K., Goldstein, A. M., et al. (2010). Influence of genetic background and tissue types on global DNA methylation patterns. *PLoS ONE* 5:e9355. doi: 10.1371/journal.pone.0009355

Ye, W., Wang, Y., Mei, B., Hou, S., Liu, X., Wu, G., et al. (2018). Computational and functional characterization of four SNPs in the SOST locus associated with osteoporosis. *Bone* 108, 132–144. doi: 10.1016/j.bone.2018.01.001

Yin, Y., Morgunova, E., Jolma, A., Kaasinen, E., Sahu, B., Khund-Sayeed, S., et al. (2017). Impact of cytosine methylation on DNA binding specificities of human transcription factors. *Science* 356:eaaj2239. doi: 10.1126/science.aaj2239

Yue, F., Cheng, Y., Breschi, A., Vierstra, J., Wu, W., Ryba, T., et al. (2014). A comparative encyclopedia of DNA elements in the mouse genome. *Nature* 515, 355–364. doi: 10.1038/nature13992

Zhang, Y., Rohde, C., Reinhardt, R., Voelcker-Rehage, C., and Jeltsch, A. (2009). Non-imprinted allele-specific DNA methylation on human autosomes. *Genome Biol.* 10:R138. doi: 10.1186/gb-2009-10-12-r138

Zhu, Y., Li, Y., Lou, D., Gao, Y., Yu, J., Kong, D., et al. (2018). Sodium arsenite exposure inhibits histone acetyltransferase p300 for attenuating H3K27ac at enhancers in mouse embryonic fibroblast cells. *Toxicol. Appl. Pharmacol.* 357, 70–79. doi: 10.1016/j.taap.2018.08.011

Zhu, Z., Zhang, F., Hu, H., Bakshi, A., Robinson, M. R., Powell, J. E., et al. (2016). Integration of summary data from GWAS and eQTL studies predicts complex trait gene targets. *Nat. Genet.* 48, 481–487. doi: 10.1038/ng.3538

Conflict of Interest Statement: ZW is a consultant of Shandong Bio-focus Gene-tech Co. Ltd.

The remaining authors declare that the research was conducted in the absence of any commercial or financial relationships that could be construed as a potential conflict of interest.

Advantages of publishing in Frontiers

OPEN ACCESS
Articles are free to read for greatest visibility and readership

FAST PUBLICATION
Around 90 days from submission to decision

HIGH QUALITY PEER-REVIEW
Rigorous, collaborative, and constructive peer-review

TRANSPARENT PEER-REVIEW
Editors and reviewers acknowledged by name on published articles

Frontiers
Avenue du Tribunal-Fédéral 34
1005 Lausanne | Switzerland

Visit us: www.frontiersin.org
Contact us: frontiersin.org/about/contact

REPRODUCIBILITY OF RESEARCH
Support open data and methods to enhance research reproducibility

DIGITAL PUBLISHING
Articles designed for optimal readership across devices

FOLLOW US
@frontiersin

IMPACT METRICS
Advanced article metrics track visibility across digital media

EXTENSIVE PROMOTION
Marketing and promotion of impactful research

LOOP RESEARCH NETWORK
Our network increases your article's readership